

# **Helicopter Control Law Design Using Eigenstructure Assignment**

Stuart James Griffin

D.Phil.

The University of York  
Department of Electronics

September 18, 1997

# Abstract

Helicopters are inherently unstable, very non-linear and highly cross-coupled, and therefore must be augmented with feedback control to reduce the pilot workload to an acceptable level. Single-input single-output loop-at-a-time techniques form the orthodox approach to control law design. However, with increasing demands on the control law and the advent of helicopter fly-by-wire, these techniques are seen to be inadequate. While multivariable techniques form the natural successor, practitioners have been slow to embrace them. Discouraged by their abstract nature and perceived inadequacies such as lack of visibility and limited influence on the control law structure.

This thesis develops an output feedback eigenstructure assignment technique with the purpose of meeting the needs of practising engineers. It begins by reviewing some basic helicopter flight dynamics and pays particular attention to producing a linearisation of the non-linear dynamics. The applicable handling qualities specifications are examined and a visible link between the British specification (Def-Stan 00-970) and a desired eigenstructure is developed. A new approach to eigenstructure assignment theory is presented and applied to a derive two stage assignment technique. Several extensions to the two stage technique are developed, these include multistage assignment, retro assignment and a novel projection technique that better enables the designer to meet the assignment goals. A technique that allows a trade-off between eigenvalue and eigenvector design goals is also presented and shown to have an analytical solution for the case of real eigenvalues.

Eigenstructure assignment has no inherent mechanism for ensuring robustness. Therefore a post-assignment robustness improvement algorithm is developed. The algorithm attempts to preserve performance while improving either a time domain or singular value robustness measure. The complete design methodology is applied to the development of an attitude command control law for the hover case and good results are shown. While helicopter control laws are the motivating application, both the eigenstructure assignment and robustness improvement techniques are generic.

# Contents

<b>Abstract</b>	<b>i</b>
<b>Acknowledgements</b>	<b>xiii</b>
<b>Nomenclature</b>	<b>xiv</b>
<b>Abbreviations</b>	<b>xix</b>
<b>1 Introduction</b>	<b>1</b>
1.1 Development of Helicopter Fly-by-Wire . . . . .	2
1.2 The Practice-Theory Gap . . . . .	5
1.2.1 Design Visibility . . . . .	6
1.2.2 Controller Structure . . . . .	7
1.2.3 Control Theory . . . . .	8
1.3 Multivariable Techniques . . . . .	8
1.4 Thesis Overview . . . . .	9
1.5 References . . . . .	10
<b>2 The Helicopter</b>	<b>13</b>
2.1 Flight Mechanics . . . . .	13
2.1.1 The Main Rotor . . . . .	15
2.1.2 Equations of Motion . . . . .	20
2.1.3 Static Stability . . . . .	22
2.2 Computer Simulation and Trim . . . . .	23
2.2.1 Computer Simulation . . . . .	23
2.2.2 Trim . . . . .	25
2.3 Linearisation . . . . .	27
2.3.1 Numerical Methods . . . . .	28
2.3.2 Higher Order Approximations . . . . .	34
2.4 Modal Analysis . . . . .	39

2.4.1	Normalisation . . . . .	40
2.4.2	Model Reduction . . . . .	44
2.4.3	The System Zeros . . . . .	48
2.5	Flight Control . . . . .	50
2.5.1	Auto-Stabilisation Equipment . . . . .	51
2.5.2	A Conventional Control Law . . . . .	53
2.6	Summary . . . . .	56
2.7	References . . . . .	57
<b>3</b>	<b>Handling Qualities</b>	<b>58</b>
3.1	Introduction . . . . .	58
3.2	The ADS 33 . . . . .	60
3.3	The Def-Stan 00-970 Vol. 2 Part 6 . . . . .	65
3.4	Discussion . . . . .	69
3.5	Handling Qualities and Control Law Design . . . . .	71
3.5.1	An Ideal Eigenstructure . . . . .	72
3.5.2	Ideal Roll and Pitch Eigenvalue Locations . . . . .	74
3.5.3	Ideal Heave and Yaw Eigenvalue Locations . . . . .	83
3.5.4	Ideal Eigenvectors . . . . .	85
3.6	Summary . . . . .	89
3.7	References . . . . .	89
<b>4</b>	<b>Feedback Design for Performance</b>	<b>91</b>
4.1	Introduction . . . . .	91
4.2	The State Feedback Problem . . . . .	92
4.3	Projection With Eigenvalue Trade-off . . . . .	95
4.3.1	Introduction . . . . .	95
4.3.2	The Problem . . . . .	95
4.3.3	The Solution . . . . .	97
4.4	Practical Implementation . . . . .	102
4.4.1	Trivial Extension to Output Feedback . . . . .	104
4.5	The Output Feedback Problem . . . . .	105
4.5.1	The Protection Method . . . . .	106
4.5.2	Parametric Methods . . . . .	107
4.5.3	Two Stage Assignment . . . . .	118
4.5.4	Retro Assignment . . . . .	128
4.5.5	Multistage Assignment . . . . .	137
4.5.6	Assignment with Simple Projection . . . . .	142

4.5.7	Assignment with Sympathetic Projection . . . . .	144
4.5.8	Assignment with Iterative Projection . . . . .	147
4.5.9	Assignment with Projection and Eigenvalue Trade-off . . . . .	150
4.5.10	Eigenstructure Assignment and Similarity Transforms . . . . .	152
4.5.11	Gain Suppression . . . . .	154
4.6	Direct Assignment of the Modal Coupling Matrices . . . . .	157
4.7	Dynamic Compensation . . . . .	163
4.7.1	The Augmented System Method . . . . .	163
4.7.2	The Observer Method . . . . .	166
4.8	Summary and Further Work . . . . .	169
4.8.1	Summary . . . . .	169
4.8.2	Further Work . . . . .	169
4.9	References . . . . .	170
<b>5</b>	<b>Robustness</b>	<b>175</b>
5.1	Introduction . . . . .	175
5.2	Eigenstructure Assignment and Robustness . . . . .	177
5.3	An Outline of the Robustness Improvement Algorithm . . . . .	179
5.4	Robustness Measures . . . . .	180
5.4.1	The Time Domain Robustness Measure . . . . .	180
5.4.2	The Singular Value Robustness Measure . . . . .	184
5.5	Robustness Measure Gradient Functions . . . . .	198
5.5.1	Numerical Perturbation . . . . .	200
5.5.2	Analytic Gradients for the Time Domain Robustness Measure . . . . .	202
5.5.3	Analytic Gradients for the Singular Value Robustness Measure. . . . .	211
5.6	Mitigation of Performance Degradation . . . . .	218
5.6.1	Eigenvector Protection . . . . .	218
5.6.2	Eigenvalue Protection . . . . .	223
5.7	Further Work . . . . .	223
5.7.1	Development of the Robustness Improvement Algorithm . . . . .	224
5.7.2	Extension to Performance Robustness . . . . .	225
5.8	References . . . . .	226
<b>6</b>	<b>Design Example</b>	<b>230</b>
6.1	A State Feedback Control Law . . . . .	230
6.2	An Output Feedback Control Law . . . . .	247
6.3	Summary . . . . .	284

---

<b>7</b>	<b>Conclusions and Further Work</b>	<b>285</b>
7.1	Conclusions . . . . .	285
7.2	Contributions . . . . .	287
7.3	Further Work . . . . .	288
<b>A</b>	<b>Helicopter Linearisation at Hover</b>	<b>291</b>
A.1	The State Space Description . . . . .	291
A.2	The Reduced Order Model State Space Description . . . . .	293
<b>B</b>	<b>Supporting Mathematics</b>	<b>296</b>
B.1	Proof of Matrix Lemma 4.5.3 . . . . .	296
B.2	Guaranteed Real Gain Matrix Proof . . . . .	300
B.3	Proof that the Retro-Stage Offers No Additional DoF . . . . .	302
B.4	References . . . . .	304
<b>C</b>	<b>Polynomial Matrices</b>	<b>305</b>
C.1	Calculation of the Allowed Eigenvector Subspace . . . . .	305
C.2	Evaluation of the Eigenvector Cost Function . . . . .	309
C.3	References . . . . .	316

# List of Figures

2.1.1	A plan view of a rotor disk. . . . .	14
2.1.2	A typical swash plate assembly. . . . .	15
2.1.3	A single blade with flapping hinge. . . . .	17
2.1.4	Conventional body fixed axis set for a helicopter. . . . .	21
2.2.5	A typical simulation structure. . . . .	24
2.3.6	Vertical velocity response of a linear (Jacobian only) and non-linear helicopter model at hover for a 1 and 10 feet/s perturbation in forward velocity. . . . .	32
2.3.7	Plots of the change in various state derivatives against roll rate ( $p$ ) for a non-linear helicopter model at hover. . . . .	33
2.3.8	Plots of the change in various state derivatives against roll rate ( $p$ ) for a second order model (Jacobian + Hessian) of a helicopter at hover. . . . .	37
2.3.9	Vertical velocity response of a linear (Jacobian only), Hessian (Jacobian + Hessian) and non-linear helicopter model at hover for s 1 and 10 feet/s perturbation in forward velocity. . . . .	38
2.4.10	The root locus of a Lynx model over the speed range 0-160 knots (The lower plot depicts the origin of the upper plot). . . . .	39
2.4.11	Simplified helicopter dynamics in hover (see Equation (2.4.80)). . . . .	47
2.5.12	A simple control law. . . . .	52
2.5.13	Typical auto-stabilisation equipment. . . . .	52
2.5.14	The Westland Helicopters EH101 actuation system. . . . .	54
2.5.15	A control law structure suitable for standard auto-stabilisation equipment. . . . .	55
3.1.1	A conceptual model of the pilot as a controller. . . . .	59
3.2.2	Gain and phase bandwidth definitions. . . . .	62
3.2.3	Bandwidth criteria for target acquisition and tracking (pitch and roll). . . . .	63
3.2.4	Handling Qualities criteria for the Mid-term response. . . . .	64
3.3.5	A typical transient response in roll, pitch or yaw to a pulse input. . . . .	66
3.5.6	An s-plane interpretation of the Def-Stan short term stability criteria. . . . .	79
3.5.7	An s-plane interpretation of the Def-Stan short term stability criteria plus the ADS 33 bandwidth and damping ratio loci and the ideal point $\lambda_{t2}$ . . . . .	82

4.7.1	The augmented system . . . . .	164
4.7.2	An observer and controller . . . . .	166
5.4.1	Input multiplicative uncertainty with constant output feedback . . . . .	184
5.4.2	The general single loop structure. . . . .	186
5.4.3	Single loop structure for input multiplicative uncertainty. . . . .	186
5.4.4	Equivalent transformed single loop systems. . . . .	195
5.6.5	A geometric interpretation of performance protection. . . . .	222
5.6.6	An illustrative geometric interpretation of performance protection. . . . .	222
6.1.1	Roll attitude response (top) to a lateral and pitch attitude response (bottom) to a longitudinal pulse input of 10% for one second of an 8 <sup>th</sup> order linear helicopter model at hover with state feedback control. . . . .	232
6.1.2	On and off axis attitude responses (roll and pitch) to a 10% one second lateral (top) and longitudinal (bottom) pulse input for an 8 <sup>th</sup> order linear helicopter model at hover with state feedback control. . . . .	233
6.1.3	Yaw rate response (top) to a one second 10% pulse and heave velocity (bottom) induced by a 10% step input for an 8 <sup>th</sup> order linear helicopter model with state feedback control. . . . .	234
6.1.4	Roll attitude response (top) to a lateral and pitch attitude response (bottom) to a longitudinal pulse input of 10% for one second of a 12 <sup>th</sup> order linear helicopter model at hover with state feedback control. . . . .	235
6.1.5	Roll attitude response (top) to a lateral and pitch attitude response (bottom) to a longitudinal pulse input of 10% for one second of a 12 <sup>th</sup> order linear helicopter model at hover with a revised state feedback control law. . . . .	236
6.1.6	Roll attitude response (top) to a lateral and pitch attitude response (bottom) to a longitudinal pulse input of 10% for one second of an 8 <sup>th</sup> order linear helicopter model at hover with a robustified state feedback control law employing performance protection. . . . .	239
6.1.7	Roll attitude response (top) to a lateral and pitch attitude response (bottom) to a longitudinal pulse input of 10% for one second of an 8 <sup>th</sup> order linear helicopter model at hover with a robustified state feedback control law <i>not</i> employing performance protection. . . . .	240
6.1.8	On and off axis attitude responses (roll and pitch) to a 10% one second lateral (top) and longitudinal (bottom) pulse input for an 8 <sup>th</sup> order linear helicopter model at hover with robustified feedback control employing performance protection. . . . .	241
6.1.9	On and off axis attitude responses (roll and pitch) to a 10% one second lateral (top) and longitudinal (bottom) pulse input for an 8 <sup>th</sup> order linear helicopter model at hover with robustified feedback control <i>not</i> employing performance protection. . . . .	242
6.1.10	Yaw rate response (top) to a one second 10% pulse and heave velocity (bottom) induced by a 10% step input for an 8 <sup>th</sup> order linear helicopter model with robustified state feedback control produced employing performance protection. . . . .	243



6.1.11	Yaw rate response (top) to a one second 10% pulse and heave velocity (bottom) induced by a 10% step input for an 8 <sup>th</sup> order linear helicopter model with robustified state feedback control produced <i>without</i> performance protection. . . . .	244
6.1.12	Linear velocity responses ( $u, v, w$ ) to a one second 10% pulse for an 8 <sup>th</sup> order linear helicopter model with robustified state feedback control produced with performance protection. . . . .	245
6.1.13	Linear velocity responses ( $u, v, w$ ) to a one second 10% pulse for an 8 <sup>th</sup> order linear helicopter model with robustified state feedback control produced <i>without</i> performance protection. . . . .	246
6.2.14	Roll attitude response (top) to a lateral and pitch attitude response (bottom) to a longitudinal pulse input of 10% for one second of an 8 <sup>th</sup> order linear helicopter model at hover with an output feedback control law synthesized according to option <i>one</i> of Table 6.2.5. . . . .	251
6.2.15	On and off axis attitude responses (roll and pitch) to a 10% one second lateral (top) and longitudinal (bottom) pulse input for an 8 <sup>th</sup> order linear helicopter model at hover with an output feedback control law synthesized according to option <i>one</i> of Table 6.2.5. . . . .	252
6.2.16	Linear velocity responses ( $u, v, w$ ) to a one second 10% pulse for an 8 <sup>th</sup> order linear helicopter model with an output feedback control law synthesized according to option <i>one</i> of Table 6.2.5. . . . .	253
6.2.17	Yaw rate response (top) to a one second 10% pulse and heave velocity (bottom) induced by a 10% step input for an 8 <sup>th</sup> order linear helicopter model with output feedback control synthesized according to option <i>one</i> of Table 6.2.5. . . . .	254
6.2.18	Roll attitude response (top) to a lateral and pitch attitude response (bottom) to a longitudinal pulse input of 10% for one second of an 8 <sup>th</sup> order linear helicopter model at hover with an output feedback control law synthesized according to option <i>three</i> of Table 6.2.5. . . . .	256
6.2.19	On and off axis attitude responses (roll and pitch) to a 10% one second lateral (top) and longitudinal (bottom) pulse input for an 8 <sup>th</sup> order linear helicopter model at hover with an output feedback control law synthesized according to option <i>three</i> of Table 6.2.5. . . . .	257
6.2.20	Linear velocity responses ( $u, v, w$ ) to a one second 10% pulse for an 8 <sup>th</sup> order linear helicopter model with an output feedback control law synthesized according to option <i>three</i> of Table 6.2.5. . . . .	258
6.2.21	Yaw rate response (top) to a one second 10% pulse and heave velocity (bottom) induced by a 10% step input for an 8 <sup>th</sup> order linear helicopter model with an output feedback control synthesized according to option <i>three</i> of Table 6.2.5. . . . .	259
6.2.22	Roll attitude response (top) to a lateral and pitch attitude response (bottom) to a longitudinal pulse input of 10% for one second of an 8 <sup>th</sup> order linear helicopter model at hover with an output feedback control law synthesized using the iterative projection algorithm of Section 4.5.8. . . . .	261
6.2.23	Yaw rate response (top) to a one second 10% pulse and heave velocity (bottom) induced by a 10% step input for an 8 <sup>th</sup> order linear helicopter model at hover with an output feedback control synthesized using the iterative projection algorithm of Section 4.5.8. . . . .	262

6.2.24	On and off axis attitude responses (roll and pitch) to a 10% one second lateral (top) and longitudinal (bottom) pulse input for an 8 <sup>th</sup> order linear helicopter model at hover with an output feedback control law synthesized using the iterative projection algorithm of Section 4.5.8. . . . .	263
6.2.25	Linear velocity responses ( $u, v, w$ ) to a one second 10% pulse for an 8 <sup>th</sup> order linear helicopter model with an output feedback control law synthesized using the iterative projection algorithm of Section 4.5.8. . . . .	264
6.2.26	Roll attitude response (top) to a lateral and pitch attitude response (bottom) to a longitudinal pulse input of 10% for one second of an 8 <sup>th</sup> order linear helicopter model at hover with an output feedback control law synthesized using an iterative projection algorithm employing eigenvalue trade-off. . . . .	266
6.2.27	On and off axis attitude responses (roll and pitch) to a 10% one second lateral (top) and longitudinal (bottom) pulse input for an 8 <sup>th</sup> order linear helicopter model at hover with an output feedback control law synthesized using an iterative projection algorithm employing eigenvalue trade-off. . . . .	267
6.2.28	Yaw rate response (top) to a one second 10% pulse and heave velocity (bottom) induced by a 10% step input for an 8 <sup>th</sup> order linear helicopter model with an output feedback control synthesized using an iterative projection algorithm employing eigenvalue trade-off. . . . .	268
6.2.29	Linear velocity responses ( $u, v, w$ ) to a one second 10% pulse for an 8 <sup>th</sup> order linear helicopter model with an output feedback control law synthesized using an iterative projection algorithm employing eigenvalue trade-off. . . . .	269
6.2.30	Roll attitude response (top) to a lateral and pitch attitude response (bottom) to a longitudinal pulse input of 10% for one second of a 12 <sup>th</sup> order linear helicopter model at hover with an output feedback control law synthesized using an iterative projection algorithm employing eigenvalue trade-off. . . . .	271
6.2.31	Convergence of the robustness improvement algorithm with the singular value based measure for an 8 <sup>th</sup> helicopter model with output feedback control and a bilinear uncertainty structure at the input and output. . . . .	272
6.2.32	Roll attitude response (top) to a lateral and pitch attitude response (bottom) to a longitudinal pulse input of 10% for one second of an 8 <sup>th</sup> order linear helicopter model at hover with an output feedback control law that has been optimised with respect to a singular value based robustness measure. . . . .	274
6.2.33	On and off axis attitude responses (roll and pitch) to a 10% one second lateral (top) and longitudinal (bottom) pulse input for an 8 <sup>th</sup> order linear helicopter model at hover with an output feedback control law that has been optimised with respect to a singular value based robustness measure. . . . .	275
6.2.34	Yaw rate response (top) to a one second 10% pulse and heave velocity (bottom) induced by a 10% step input for an 8 <sup>th</sup> order linear helicopter model with an output feedback control law that has been optimised with respect to a singular value based robustness measure. . . . .	276
6.2.35	Linear velocity responses ( $u, v, w$ ) to a one second 10% pulse for an 8 <sup>th</sup> order linear helicopter model with an output feedback control law that has been optimised with respect to a singular value based robustness measure. . . . .	277

- 
- 6.2.36 Convergence of the robustness improvement algorithm with the time domain measure for an  $8^{th}$  helicopter model with output feedback control and the uncertainty structure of Equation (6.2.15). . . . . 279
- 6.2.37 Roll attitude response (top) to a lateral and pitch attitude response (bottom) to a longitudinal pulse input of 10% for one second of an  $8^{th}$  order linear helicopter model at hover with an output feedback control law that has been optimised with respect to a time domain robustness measure. . . . . 280
- 6.2.38 On and off axis attitude responses (roll and pitch) to a 10% one second lateral (top) and longitudinal (bottom) pulse input for an  $8^{th}$  order linear helicopter model at hover with an output feedback control law that has been optimised with respect to a time domain robustness measure. . . . . 281
- 6.2.39 Yaw rate response (top) to a one second 10% pulse and heave velocity (bottom) induced by a 10% step input for an  $8^{th}$  order linear helicopter model with an output feedback control law that has been optimised with respect to a time domain robustness measure. . . . . 282
- 6.2.40 Linear velocity responses ( $u, v, w$ ) to a one second 10% pulse for an  $8^{th}$  order linear helicopter model with an output feedback control law that has been optimised with respect to a time domain robustness measure. . . . . 283

# List of Tables

1.3.1	A comparison of different multivariable techniques . . . . .	8
2.2.1	Levels of rotorcraft modelling fidelity. . . . .	23
2.3.2	Trim point and validity estimate for a linearisation at hover. . . . .	31
2.4.3	Open loop pole locations taken from linearisations of a non-linear Lynx model at forward speeds of 0, 60 and 120 knots. . . . .	40
2.4.4	State and input normalisation values. . . . .	41
2.4.5	Open loop eigenvectors for a Lynx linearisation at hover. . . . .	42
2.4.6	Transfer function residues for main rotor collective to vertical velocity and tail rotor collective to yaw rate. . . . .	43
2.4.7	Pole locations for the full and reduced order helicopter models at hover. . . . .	45
2.4.8	A comparison of the full system and decoupled subsystem poles. . . . .	45
2.4.9	System poles for a reduced order and then simplified helicopter model at hover. . .	46
2.4.10	System zeros for different output combinations taken from the reduced order helicopter model at hover (not simplified). . . . .	49
2.4.11	System zero directions for the reduced order helicopter model at hover (see Table 2.4.10). . . . .	50
3.1.1	Handling qualities levels of compliance. . . . .	60
3.2.2	Maximum value for LOES in heave. . . . .	64
3.3.3	The Def-Stan 00-970 longitudinal short-term stability handling qualities criteria as defined in Leaflet 601/1 section 4. . . . .	68
4.3.1	Comparison of the least squares eigenvector assignment errors for assignment using simple projection with and without eigenvalue trade-off. . . . .	102
4.5.2	The number of eigenvectors assignable in stages one and two of the two stage assignment technique. . . . .	119
4.5.3	Design freedom in stages one and two of the two stage assignment technique. . . .	120
4.5.4	Degrees of freedom available using retro assignment. . . . .	133
4.5.5	Comparison of the two and three stage design procedures in terms of degrees of freedom and the number of assignable eigenvectors per stage. . . . .	138

---

4.5.6	The least squares eigenvector assignment errors for two and three stage simple projection, sympathetic projection and iterative projection. . . . .	149
4.5.7	The least squares eigenvector assignment errors for eigenvalue trade-off applied inconjunction with: two and three stage simple projection, sympathetic projection and iterative projection. . . . .	152
4.5.8	The resulting eigenvalue locations for the assignments described in Table 4.5.7. . . . .	152
5.4.1	Common open loop uncertainty representations . . . . .	185
5.4.2	Single loop transfer functions for some uncertainty representations . . . . .	187
5.4.3	Gain and phase margins for the uncertainty representations of Table 5.4.1 . . . . .	193
6.1.1	Desired eigenvalue locations for a helicopter in hover (see Section 3.5.2) . . . . .	230
6.1.2	Multivariable gain and phase margins at the input and output of an 8 <sup>th</sup> order linear helicopter model with the initial state feedback control law. . . . .	237
6.1.3	Multivariable gain and phase margins at the input and output of an 8 <sup>th</sup> order linear helicopter model with input robustness optimised (singular value measure) control laws employing zero and 50% performance protection. . . . .	237
6.2.4	The change in key linear velocity stability derivatives due to state feedback. . . . .	247
6.2.5	A list of some of the multistage assignment possibilities for a six output, four input, eighth order helicopter model. . . . .	248
6.2.6	Centre locations and radii used for the output feedback control law synthesis with eigenvalue trade-off. . . . .	265
6.2.7	Eigenvalue locations for the closed loop helicopter system using a control law synthesised with eigenvalue trade-off. . . . .	265
6.2.8	Multivariable gain and phase margins at the input and output of the closed loop helicopter system using a control law synthesised with eigenvalue trade-off. . . . .	270
6.2.9	Multivariable gain and phase margins at the input and output of the closed loop helicopter system using a control law that has been optimised with respect to a singular value based robustness measure. . . . .	273
6.2.10	Multivariable gain and phase margins at the input and output of the closed loop helicopter system using a control law that has been optimised with respect to a time domain robustness measure. . . . .	278

# Acknowledgements

I am extremely grateful to GKN Westland Helicopters Ltd for their financial and technical support especially Dr P. Taylor who's keen insight into the 'real engineering problem' provided the impetus for this work. I'd like to thank Jill Dean and my parents for their support and encouragement throughout my DPhil but especially during the write-up. I must also thank my friends and fellow students, in particular Steve Baines, Steve Lawes, Jonathan Elphick, Ralph Stroph, Mikel Miaza, Alan Gee and Rob Davies. Finally, I'm grateful to Mr T. Clarke for supervising this project and for his advice and enthusiasm.

# Nomenclature

<b>BOLD</b>	upper case indicates matrices
<b>bold</b>	lower case indicates vectors
$(\cdot)^T$	transpose of $(\cdot)$
$(\cdot)^*$	conjugate transpose of $(\cdot)$
$(\cdot)^{-1}$	inverse of $(\cdot)$
$(\cdot)^\dagger$	pseudo or Moore Penrose inverse of $(\cdot)$
$(\cdot)^\perp$	the complement space of $(\cdot)$
$\circ$	the Hadamard product
$(a, b)$	range $a < \cdot < b$
$[a, b)$	range $a \leq \cdot < b$
$ \cdot $	modulus or absolute value
$\ \cdot\ _n$	vector $p$ -norm
$\forall$	for all
$\beta$	blade flap angle
$\Delta(s)$	model uncertainty transfer function matrix
$\Delta_A$	set of allowed uncertainty structures
$\Delta_A$	error associated with state space A-matrix
$\Delta_B$	error associated with state space B-matrix
$\Delta_C$	error associated with state space C-matrix
$\Delta_D$	error associated with state space D-matrix
$\delta$	Dirac impulse
$\delta_{ij}$	the Kronecker delta
$\epsilon_a$	absolute error tolerance
$\epsilon_p$	proportional error tolerance
$j$	unit of imaginary numbers ( $\sqrt{-1}$ )
$\nabla_\eta$	a vector operator that differentiates with respect to the elements of $\eta$
$\Lambda$	a diagonal matrix of system eigenvalues
$\Lambda_D$	a matrix of desired eigenvalue locations
$\Lambda_{D1}$	a matrix of desired eigenvalue locations for stage one
$\Lambda_{D2}$	a matrix of desired eigenvalue locations for stage two
$\lambda_i$	the $i^{th}$ eigenvalue
$\lambda_{a_i}$	set of allowed values for the $i^{th}$ eigenvalue
$\lambda_{d_i}$	the $i^{th}$ desired eigenvalue location
$\lambda_{o_i}$	optimum value for the $i^{th}$ eigenvalue
$\sigma_i$	the $i^{th}$ singular value
$\bar{\sigma}$	maximum singular value
$\underline{\sigma}$	minimum singular value

$\rho(\mathbf{X})$	spectral radius or maximum eigenvalue of $\mathbf{X}$
$\mu(\mathbf{X})$	the structured singular value of $\mathbf{X}$
$\phi$	roll angle in the body axis set
$\theta$	pitch angle in the body axis set
$\theta_0$	main rotor collective pitch angle
$\theta_t$	tail rotor collective pitch angle
$\psi$	yaw angle in the body axis set or blade azimuth angle
$\Omega$	angular velocity of rotor blades
$\omega$	frequency in radians
$\omega_r$	flapping resonant frequency
$\tau_p$	phase delay
$\zeta$	damping factor
$\mathbf{A}$	state space A-matrix
$\bar{\mathbf{A}}$	state space A-matrix for a system with protected eigenvalues
$\hat{\mathbf{A}}$	state space A-matrix for an augmented system
$\mathbf{A}_{CL}$	state space A-matrix of the closed loop system
$A_1$	lateral cyclic coefficient
$a_{1s}$	rotor lateral cyclic state
$\mathbf{B}$	state space B-matrix
$\bar{\mathbf{B}}$	state space B-matrix for a system with protected eigenvalues
$\hat{\mathbf{B}}$	state space B-matrix for an augmented system
$B_1$	longitudinal cyclic coefficient
$\mathbf{b}_i$	a single state space input vector corresponding to the $i^{th}$ input
$b_{1s}$	rotor longitudinal cyclic state
$\mathbb{C}$	the set of all complex numbers
$\mathbb{C}^n$	an $n$ dimensional vector of complex numbers
$\mathbb{C}^{n \times m}$	an $n \times m$ matrix of complex numbers
$\mathbf{C}$	state space C-matrix
$\bar{\mathbf{C}}$	state space C-matrix for a system with protected eigenvalues
$\hat{\mathbf{C}}$	state space C-matrix for an augmented system
$\mathcal{C}(s)$	mode controllability subspace for the eigenvalue location $s$
$\mathbf{c}_i$	a single state space output row vector corresponding to the $i^{th}$ output
$\mathbf{D}$	state space D-matrix or diagonal scaling matrix
$\hat{\mathbf{D}}$	state space D-matrix for an augmented system
$\mathbf{d}$	an optimisation descent direction
$\det(\cdot)$	determinant of a matrix
$\text{diag}(\cdot)$	a diagonal matrix
$\mathbf{e}_r$	approximation error
$\mathbf{F}$	a block diagonal matrix of right design vectors
$F_x$	total force along $x$ -axis
$F_y$	total force along $y$ -axis
$F_z$	total force along $z$ -axis
$\mathbf{f}_i$	the $i^{th}$ right design vector
$\mathbf{f}_{o,i}$	optimum $i^{th}$ right design vector
$\mathbf{G}$	a block diagonal matrix of left design vectors
$\mathbf{G}(s)$	MIMO transfer function matrix
$\mathbf{G}_o(s)$	a nominal open loop system
$g(s)$	a SISO transfer function
$\mathbf{g}_i$	the $i^{th}$ left design vector



<b>H</b>	a Hessian matrix
<b>Hc</b>	a matrix of concatenated Hessian vectors ( <b>h</b> )
<b>h</b>	Hessian matrix expanded as a vector by stacking its columns
<b>h</b>	height
$\dot{h}$	rate of change of height
$h'$	flapping hinge offset
$h(t)$	Heaviside or unit step function
$\text{Im}(x)$	the imaginary part of $x$
<b>I</b>	the identity matrix
$I_r$	moment of inertia of rotor blade
$I_{xx}$	moment of inertia of body about $x$ axis
$I_{xy}$	product of inertia in the plane $xy$
$I_{yy}$	moment of inertia of body about $y$ axis
$I_{zz}$	moment of inertia of body about $z$ axis
$J_c$	cost function for a constrained optimisation
$J_u$	cost function for an unconstrained optimisation
$\ker(\mathbf{X})$	the null space of $\mathbf{X}$
<b>K</b>	matrix of static feedback gains
<b>K(s)</b>	feedback controller
$\mathbf{L}_j$	$\text{range}(\mathbf{L}_j^T)$ spans the allowed left eigenvector subspace
<b>Lc</b>	$\text{range}(\mathbf{Lc}^T)$ spans the allowed mode controllability subspace
<b>L</b>	roll moment in body axis set
$L_p$	change in roll moment due to a change in roll rate
$L_q$	change in roll moment due to a change in pitch rate
$L_u$	change in roll moment due to a change in forward speed
$L_v$	change in roll moment due to a change in sideslip velocity
$\Omega(s)$	the allowed left eigenvector subspace for the eigenvalue location $s$
<b>M(s)</b>	Single loop transfer function matrix
$\mathbf{M}_j$	$\text{range}(\mathbf{M}_j^T)$ spans the output space associated with the allowed left eigenvector subspace
<b>M</b>	pitch moment in body axis set
$M_p$	change in pitch moment due to a change in roll rate
$M_q$	change in pitch moment due to a change in pitch rate
$M_u$	change in pitch moment due to a change in forward speed
$m$	number of outputs or vehicle mass
$\tilde{m}$	number of outputs for a reduced system
<b>N</b>	yaw moment in body axis set
$N_r$	change in yaw moment due to a change in yaw rate
$N_p$	change in yaw moment due to a change in roll rate
$N_u$	change in yaw moment due to a change in forward speed
$\Omega(s)$	mode observability subspace for the eigenvalue location $s$
$\mathbf{P}_i$	$\text{range}(\mathbf{P}_i)$ spans the input space associated with allowed right eigenvector subspace
<b>P(s)</b>	a polynomial matrix where $\text{range}(\mathbf{P}(s))$ spans the input space associated with allowed right eigenvector subspace for the eigenvalue location $s$
$\mathcal{P}_X$	a projector on to the space $\text{range}(\mathbf{X})$
$p$	roll rate in the body axis set
$\mathbf{Q}_i$	$\text{range}(\mathbf{Q}_i)$ spans the allowed right eigenvector subspace
<b>Q(s)</b>	a polynomial matrix where $\text{range}(\mathbf{Q}(s))$ spans the allowed right eigenvector subspace for eigenvalue location $s$

$Q_0$	range( $Q_0$ ) spans the allowed mode observability subspace
$q$	pitch rate in the body axis set
$R$	positive definite weighting matrix
$R$	total length of a rotor blade
$Re(x)$	the real part of $x$
$\mathcal{R}(s)$	the allowed right eigenvector subspace for the eigenvalue location $s$
$r$	number of inputs or yaw rate in the body axis set or distance along a blade
$\bar{r}$	number of inputs for a reduced system
$r_i$	the $i^{th}$ residue
rank( $X$ )	size of the largest non-singular minor of $X$
range( $X$ )	the space spanned by the columns of the matrix $X$
$s_i$	number of eigenvalues assigned in stage $i$
sup( $\cdot$ )	supremum
$S$	a matrix with columns equal to an assigned set of input vectors
$S_1$	a matrix with columns equal to a subset of the input vectors
$S(s)$	feedback system sensitivity function
$T$	a matrix with rows equal to an assigned set of output vectors
$T_2$	a matrix with columns equal to a subset of the output vectors
$T$	total lift generated by a blade
$T_{01}$	time of the first zero crossing as specified by the Def-Stan 00-970
$T_{02}$	time of the second zero crossing as specified by the Def-Stan 00-970
$T_{11}$	time taken for the response to decay to 10 percent of its peak value as specified by the Def-Stan 00-970
$T_{30}$	time taken for the response to decay to 30 percent of its peak value as specified by the Def-Stan 00-970
$T_F$	maximum time permitted to reach the specified steady state error as specified by the Def-Stan 00-970
trace( $\cdot$ )	the trace matrix norm
$U$	a unitary matrix
$U$	speed normal to a blade
$u$	state space input vector
$u$	forward velocity in the body axis set
$u(t)$	time domain system input
$V$	a matrix of right eigenvectors
$V_1$	a matrix with columns equal to a subset of the right eigenvectors
$V_D$	a matrix with columns equal to the desired right eigenvectors
$V_{D1}$	a matrix with columns equal to a subset of the desired right eigenvectors
$V_{O1}$	a matrix with columns equal to a set of assigned mode observability vectors
$V_f$	total velocity
$v_i$	the $i^{th}$ right eigenvector
$v$	side velocity in the body axis set
vec( $X$ )	a vector produced by stacking the columns of $X$
$W$	a matrix with rows equal to the left eigenvectors
$W_2$	a matrix with rows equal to a subset of the left eigenvectors
$W_D$	a matrix with rows equal to the desired left eigenvectors
$W_{D2}$	a matrix with rows equal to a subset of the desired left eigenvectors
$W_{C2}$	a matrix with rows equal to a set of assigned mode controllability vectors
$w_j$	the $j^{th}$ left eigenvector
$w$	vertical velocity in the body axis set

---

$\mathbf{X}_N$	state normalisation transform
$X_\theta$	change forward force due to a change in pitch attitude
$X_F$	permitted steady state error as specified by the Def-Stan 00-970
$\mathbf{x}$	state space, state vector
$\dot{\mathbf{x}}$	derivative of the state vector
$\mathbf{x}_h$	cross-product state vector
$x_1$	maximum value of the first overshoot as specified by the Def-Stan 00-970
$x_2$	maximum value of the second overshoot as specified by the Def-Stan 00-970
$\mathbf{Y}_N$	input normalisation transform
$Y_\phi$	change side force due to a change in roll attitude
$\mathbf{y}$	state space output vector
$\mathbf{y}_e$	truncation error
$y_1$	response build-up after 0.5s as specified by the Def-Stan 00-970
$y(t)$	system output
$Z_w$	change in vertical force due to a change in vertical velocity

# Abbreviations

ACAH	Attitude Command Attitude Hold
ACT	Active Control Technology.
ADMU	Actuator Drive and Monitor Units.
ADOCS	Advanced Digital/Optical Control System.
ADS	Aeronautical Design Standard.
AFCS	Automatic Flight Control System.
ASE	Automatic Stabilisation Equipment
ATTHeS	Advanced Technology Testing Helicopter System.
BIBO	Bounded Input Bounded Output
BW	Bandwidth
CAA	Civil Aviation Authority
CACSD	Computer Aided Control System Design.
CPU	Central Processing Unit.
CSAS	Control and Stability Augmentation System.
DFP	Davidon Fletcher Powell
DH	Direction Hold
FAA	Federal Aviation Authority
FBL	Fly-by-Light.
FBW	Fly-by-Wire.
FCC	Flight Control Computer.
FFT	Fast Fourier Transform.
FPCC	Flight Propulsion Control Coupling
GA	Genetic Algorithm
GM	Gain Margin
HH	Height Hold
HLH	Heavy Lift Helicopter.
LHP	Left Half Plane; referring to the complex $s$ -plane.
LOES	Low Order Equivalent System
LQG	Linear Quadratic Gaussian.
LQR	Linear Quadratic Regulator.
LMI	Linear Matrix Inequalities
LTR	Loop Transfer Recovery.
MFD	Matrix Fraction Description
MIMO	Multiple Input Multiple Output.
MTE	Mission Task Element
OFE	Operation Flight Envelope
PIO	Pilot Induced Oscillation
PM	Phase Margin

---

QFT	Quantitative Feedback Theory
RC	Rate Command
RHP	Right Half Plane; referring to the complex $s$ -plane.
SAS	Stability Augmentation System
SISO	Single Input Single Output.
SRM	Step Response Model
SSV	Structured Singular Value
SVD	Singular Value Decomposition
TAGS	Tactical Aircraft Guidance System.
TBA	To Be Advised
TRC	Translational Rate Command
TPP	Tip Path Plane
UCE	Usable Cue Environment

# Chapter 1

## Introduction

### Contents

---

1.1	Development of Helicopter Fly-by-Wire . . . . .	2
1.2	The Practice-Theory Gap . . . . .	5
1.3	Multivariable Techniques . . . . .	8
1.4	Thesis Overview . . . . .	9
1.5	References . . . . .	10

---

All high performance aircraft employ feedback control to achieve the desired level of performance, handling and stability [BDG94]. Helicopters are inherently unstable, highly cross-coupled and very non-linear [Pad96, Pro90]. Hence feedback control is particularly important. Conventional feedback control implementations consist of three main components: sensors to measure body rates and attitudes, analogue or digital hardware to realise the control law and limited authority actuators to apply the control output. To the best of author's knowledge all the control laws currently flying on commercial helicopters have been designed using a single-input-single-output (SISO) loop-at-a-time technique [Tay97]. This technique involves pairing the inputs and outputs, then applying classical frequency domain or root locus ideas to design an independent control law for each loop. While SISO loop-at-a-time techniques are established and proven in practice, they do have some drawbacks. For instance:

- Despite the independent control laws cross-coupling in the helicopter will cause the feedback loops to interact, often to the extent that closing one loop forces a re-design of other loops. This leads to a labour-intensive, and thus costly, design process.
- Using the gain and phase margins of the individual feedback loops to estimate the robustness of the system as a whole has been shown to be dangerously misleading [DS81].

From a control theory perspective, the use of SISO techniques is ill-suited to what is clearly a multi-input multi-output (MIMO) problem.

Multivariable techniques promise to overcome many of the problems of their SISO counterparts. Increasing demands for cost efficient design and improved performance are forcing an examination of these techniques. Perhaps the single most important factor driving the move towards multivariable techniques is the advent of full authority fly-by-wire (FBW) systems.

## 1.1 Development of Helicopter Fly-by-Wire

Fly-by-wire describes aircraft in which the mechanical links between the pilot controls and the control surfaces have been replaced by electrical connections<sup>1</sup>. The two major benefits of FBW are weight reduction, due to omission of the mechanical control runs, and the ability to use a full authority Automatic Flight Control System (AFCS). By inserting a computational component between the pilot and the airframe a full authority AFCS opens up a number of opportunities [Bal94, BDG94, LDDK94]:

- Reduced pilot workload through improved handling qualities.
- Increased airframe design freedom, due to gust and manoeuvre load reduction, greater tolerance of airframe instabilities and an enhanced ability to accommodate body flexure modes.
- Command limiting and improved handling will enable an extended operational flight envelope with a more consistent response throughout the envelope.
- Greater subsystem integration, leading to; more complex autopilot modes, better fuel economy and less vibration [RN94].
- Improved decoupling, by moving mechanical decoupling and mixing components into the control system.
- The ability to use side-stick configurations for further weight and space saving.
- The ability to define alternative interpretations of pilot commands.
- Improved gust and turbulence rejection for a more stable hover platform and better ride quality.

With the increased authority of the control law comes increased responsibility, both in terms of safety and handling. For instance, since the pilot will apply all control commands through the AFCS, its performance will, now more than ever, determine the vehicle handling. The design engineer will need a precise understanding of the piloting requirements in order to avoid inadvertently introducing new handling problems.

Fully exploiting the opportunities of FBW presents some significant engineering challenges, especially in the areas of fault tolerance, control law design and handling qualities. Despite the engineering challenge, the lure of such an array of benefits has prompted helicopter manufacturers to investigate fly-by-wire. Boeing undertook the first research programme in the late '60s with the Tactical

---

<sup>1</sup>Optical connections may also be employed this is sometimes called Fly-by-Light (FBL).

Aircraft Guidance System (TAGS) [LDDK94]. This incorporated a full authority controller and a side-stick inceptor. Between '71 and '74 Boeing continued development of FBW systems with the Boeing 347 Heavy Lift Helicopter (HLH) demonstrator. This was a twin rotor helicopter and its full authority AFCS demonstrated Level 1 handling qualities plus an impressive precision hover. In the early 80s Boeing initiated the Advanced Digital/Optical Control System (ADOCS) programme. This involved modifying a Black Hawk UH60 with FBW and side-stick controls. It was used for an extensive investigation into handling qualities and control law design issues [TFMT89, Tis87]. In 1991 Boeing's research into FBW culminated in the US military choosing a Boeing-Sikorsky partnership to develop a new scout/attack helicopter, the Comanche RAH-66. The Comanche is based on results of the ADOCS programme and incorporates a full authority FBW AFCS, an optical data bus, a side-stick inceptor and integrated full authority engine management [LDDK94, Har96]. In January 1996 the Comanche made its maiden flight [Har96], although the Congressional Budget Office (CBO) have cast doubts on the future of the Comanche [McD96]. As well as Boeing, McDonnell Douglas/Bell have also developed a FBW system, called the Advanced Digital Flight Control System (ADFCS). This has been implemented on a AH-64 Apache AV05 and has demonstrated good handling qualities [Pad96].

In Europe, progress has been slower. Two important milestones are the GKN Westland Helicopter's EH101 and the Eurocopter NH90. The EH101 is not FBW, but it is the first European helicopter with a wholly digital AFCS and the first helicopter in the world to attain simultaneous flight certification from the Federal Aviation Authority (FAA) and Civil Aviation Authority (CAA) in Britain and Italy [Har96]. A fully digital AFCS and civil certification of safety critical software is an important step towards FBW. The NH90 [Fla96] will have FBW control. A prototype<sup>2</sup> made its maiden flight in December 95. The DLR Institute für Flugmeckanik installed FBW controls on a BO105. The helicopter was known as the Advanced Technology Testing Helicopter System (ATThES) and used as a variable stability platform for the investigation of handling qualities. It was not intended as a basis for the development of FBW technology. For instance, due to very limited fault tolerance it relied on a second pilot for safety.

The progression of the helicopter industry towards FBW has far reaching implications for control law design, some of which are highlighted below:

- Improved handling qualities with command interpretation will require *more sophisticated control laws*.
- Integration with subsystems and the need for more sensor data to implement load reduction and suppression of flexure modes will increase the number inputs and outputs. This will lead to *larger control laws*.
- The combination of composite materials and bearing-less rotor heads will produce lower frequency, more excitable, flexure and rotor modes. It is likely these modes will couple with the

---

<sup>2</sup>The NH90 prototypes are believed to have mechanical backup [Elp96].



rigid body dynamics, especially when high bandwidth control laws are used. Mode coupling will make *control law design more difficult*.

- The increased dependence upon the control law to meet performance goals and the growing impact of the airframe and rotor designs on the control law solution, will require the control law design to be initiated earlier as a parallel task that forms an *integral part of the vehicle design*.
- Multi-mode AFCSs will be needed for mission tailored handling qualities this will require more control laws. Furthermore, gain scheduling will be needed to maintain performance across the flight envelope and extend it into non-linear regions. Each schedule implies an additional control law. Thus an *increased number of control laws* will be needed.
- The complete AFCS will use switching logic and scheduling algorithms to combine all the control laws. Efficient integration will place constraints on the *control law structure*. For instance, scheduling a large number of gains or changing structure between schedules introduces implementation complexity and consumes processing resources. Hence, a possible constraint may be to prescribe the controller structure and number of gains.
- For both good robustness and improved response decoupling a *cross-coupled control law*<sup>3</sup> will be required. This has implications, not only for the control law structure, but also for the fault tolerant approach [Elp96]. Conventionally, decoupled control laws are implemented in channels and, in case of failure, replicated as lanes. Cross-coupled control laws are not readily compatible with such an approach and, faced with this problem, some developers have adopted alternative architectures. For instance, the Boeing Comanche and NASA X29 [CBBB94] both employ a hierarchical approach where failure causes reversion to simpler control laws and, for the extremely unstable X29, the final backup is implemented in analogue hardware.
- The need for greater agility will require higher bandwidth control laws with special attention paid to the response poise and sensitivity. This will *further complicate the control design process*.
- The lack of a mechanical backup ensures that the full authority AFCS and its control laws will be subject to very close scrutiny during the certification process. Since exhaustive testing is not possible, it will be incumbent upon the manufacturers to demonstrate that their control law design approach produces control laws that are absolutely safe. Constructing a convincing argument will, to some extent, depend on the concepts on which the design approach is based and the *visibility of the design process* as a whole. *Robustness* will also have an important role to play in demonstrating safety. The magnitude of this problem should not be underestimated and it is pertinent to point out that none of the rotorcraft FBW developments to-date have been for the civil market.

---

<sup>3</sup>The Comanche AFCS uses a fully populated decoupling matrix that is scheduled with forward speed [LDDK94].

- A multi-objective approach to control law design will be needed to achieve the array of benefits that a full authority AFCS can bring. Inevitably, objectives will have to be traded-off and the design process should make the *trade-offs evident* and facilitate *fast design iterations*.

Consideration of the above points, in particular robustness, fast design iterations, increased complexity, difficulty and size, indicates that SISO loop-at-a-time techniques will be inadequate for the next generation of helicopters. Large sophisticated, cross-coupled control laws are needed to exploit the opportunities of FBW. Only multivariable techniques can deliver this.

Development of a civil FBW aircraft is a tremendous engineering challenge and to mitigate the risk, manufacturers may wish to develop intermediate aircraft, as a stepping stone. One approach may be to use MIMO techniques to develop control laws for the existing limited authority, decoupled SISO architectures. Unfortunately, other than a shorter development time, this approach is unlikely to offer much performance improvement over its well refined SISO predecessors. An alternative intermediate step would be a limited authority, cross-coupled control law. This would offer some performance improvement and the opportunity to develop and certify a fault tolerant harness suitable for FBW whilst having the reassurance of limited authority.

Helicopters have a relatively long product life. For instance, aircraft designed in the sixties, such as the Lynx and Sea-King, are still popular today. This factor may force manufacturers to reject an intermediate step and move directly to fly-by-wire. FBW does not preclude the possibility of a core or backup analogue control system and this may prove necessary to ease certification and reduce the risk associated with a FBW design.

While offering many benefits, MIMO techniques do introduce their own problems; some of which have lead to a *practice-theory gap*.

## 1.2 The Practice-Theory Gap

Although, MIMO techniques offer many benefits their popularity among practitioners does not reflect this. For instance, Blight *et al* [BDG94] state:

*'It is well-known that post-1960 developments in control theory have seen relatively little application in production aircraft designs.'*

There are a number reasons why practitioners have not embraced multivariable techniques, Blight *et al* [BDG94] highlight four key deficiencies as issues:

1. *Control problems that actually require modern multivariable methods for their solution.*
2. *Easy-to-use software to perform modern methods.*
3. *Education in the benefits and use of new methods.*

#### 4. Research to close the practice-theory gap.

Issue one will, without question, be satisfied by future rotorcraft AFCS requirements and attention is focused on issue four. It is the author's belief that, while there are perceived inadequacies with multivariable methods the motivation to develop software tools and educate engineers will be severely abated. Perhaps the two perceived inadequacies that have contributed most significantly to the practice-theory gap are visibility and controller structure.

### 1.2.1 Design Visibility

With existing SISO loop-at-a-time techniques the design engineer starts with an initial design, evaluates its performance then adjusts gain values or adds compensator elements until the desired performance is achieved. A positive side effect of this, labour-intensive, approach is that the engineer will understand the function of each compensator element and the effect of varying gain values.

The design parameters used by multivariable techniques are no longer the gains themselves, but alternative quantities such as positive definite weighting matrices or transfer functions for shaping frequency responses. The controller is synthesised from the design parameters using a complex mathematical process that obscures the link between the design parameters and the individual gain values. The final controller generally resists meaningful interpretation in terms of familiar SISO elements and the effect of changing gain values is difficult to reason.

The loss of functional visibility has practical implications beyond the reluctance of engineers to relinquish their low level understanding. For instance, control law design is normally based on linear models, but is ultimately applied to a non-linear plant. In order to maintain the desired performance the controller will invariably require adjustment or *tuning* [MMS88]. Conventionally, gain value adjustments are made based on experience and the engineer's low level understanding. The same approach is difficult to apply with controllers designed using multivariable techniques since the effect of gain value changes is poorly understood and the number of gains is often much larger. Loss of visibility also has implications for certification [HGS95] where manufactures will have to demonstrate that their control laws are completely safe. While they can argue that their multivariable design technique is established and based on sound theory, ultimately, the manufacturer is left with a large complex control law, that resists a deeper explanation of how it works.

There is an inherent conflict between visibility and multivariable techniques. For instance, it is unlikely that any technique will offer the speed and convenience of a synthesised controller and also offer a full SISO interpretation without going through at least some of the rigour of a SISO design.

Synthesised controllers are ill suited to gain based visibility but are better suited and more able to offer visibility in terms of their natural design parameters. Visibility of this form implies the design parameters should have a clear link with both the design objectives and the final performance. Manness and Murray-Smith [MMS92] state:

*Even when the system is well understood, the use of multivariable control methods is fraught with difficulties due to the complexity of the dynamics and the complicated form of the design objective to be met, and the interaction of these aspects of the controller design.*

From this statement it is clear that if the design parameters have no visible link to the dynamics or the objectives then they will introduce an abstraction that will hinder an already difficult design process. It will be important to know how the design parameters relate to competing objectives if design trade-offs are to be evident and an effective compromise found.

Meaningful design parameters should allow tuning to be conducted by reworking the initial design, which is preferable to adjusting gain values directly. Since once the controller gain values are altered, continued development using the original synthesis technique is unlikely to be possible<sup>4</sup>. For tuning by reworking the initial design to be effective the design approach must support fast design iterations. Computationally exorbitant optimisations<sup>5</sup> are best avoided.

While meaningful design parameters will not significantly help certification they do go along way to increasing design visibility.

## 1.2.2 Controller Structure

Using conventional SISO loop-at-a-time techniques the controller is built up block by block. The engineer has complete control over the controller structure and can trade-off performance against configuration.

On the other hand, synthesis based multivariable techniques generally only offer a fixed-gain state feedback solution or an observer based output feedback solution [DGKF89]. In practice, state feedback can rarely be used and an observer must be implemented. The observer generally has a prescribed structure and dynamic order equal to the plant model. The engineer is thus faced with implementing a high order dynamic controller while having minimal influence over its structure. Model reduction techniques [Moo81, AL89] can be used to simplify the controller but their effectiveness depends on the application and they offer no assistance in manipulating the controller structure.

Fixed structure high order control laws have practical drawbacks. For instance, the control law must be combined with switching logic to be incorporated into the AFCS. The inability to manipulate the control law structure will hamper integration and is likely to result in switching entire control laws which is computationally expensive and thus undesirable. Gain scheduling presents a similar problem where an increased number of gains will have to be updated.

Generally, large control laws are undesirable since they require more computational resources, are cumbersome to integrate and are less visible. For instance, an appropriate SISO interpretation is more

---

<sup>4</sup>Very few design approaches support the reverse mapping of gain values back to design parameters.

<sup>5</sup>Parallel processing can be used to execute computationally exorbitant optimisations in practical time scales [Dav94, Law94].

likely to be found for a low order control law.

### 1.2.3 Control Theory

Gain scheduling and control law switching are widely accepted techniques. However, there is very little theoretical foundation for these techniques and issues such as maintained stability and bumpless transfer must be addressed using non-linear simulation and *ad hoc* solutions. While multivariable techniques do not particularly introduce new problems they do compound existing ones, since their emphasis on design through synthesis with a single set of design parameters accentuates the need for a more complete theoretical framework [HG93, Hyd95].

## 1.3 Multivariable Techniques

Before deciding to apply eigenstructure assignment, several techniques were investigated and considered [Gri94, MGMS90]. An important factor in guiding the decision was the nature of the design objectives to be met. The current British military specification for handling qualities is the Def-Stan 00-970 [Pit89]. This has received much less attention than its new US counterpart, the ADS 33 [AVS89]. However, it remains the focus of British manufacturers, such as GKN Westland Helicopters Ltd [Tay94] and has consequently been adopted for this work. The Def-Stan uses time domain parameters to define the criteria most pertinent to control law design. Thus a key consideration has been how visibly the design parameters related to both the design objectives and time domain performance. Table 1.3.1 provides a very terse comparison of  $\mathcal{H}_\infty$  [Kwa93], the Linear Quadratic Gaussian (LQG) with Loop Transfer Recovery (LTR) [SA87], eigenstructure assignment, Quantitative Feedback Theory (QFT) [Hor82] and quasi-classical techniques such as the Characteristic Locus and the Inverse Nyquist Array [Mac89].

	Robustness	Design parameter visibility	Design influence on controller structure	Fast design iterations
$\mathcal{H}_\infty$	X	-	-	X
LQR/LTR	X	-	-	X
Eigenstructure assignment	-	X	X	X
QFT	X	-	X	-
Quasi-Classical Techniques	-	-	X	-

Table 1.3.1: A comparison of different multivariable techniques

Eigenstructure assignment is the only technique that addresses the two issues important to narrowing the practice-theory gap: design parameter visibility and controller structure. The eigenstructure can

not only be related to the design objectives but, through its clear links with the time domain response [ASC83], it can also be related to the final performance. Working with the eigenstructure has further benefits. It is a natural representation for the system dynamics, and its analysis is an established branch of aeronautical engineering [Pro90]. Thus the eigenstructure facilitates a free flow of information between analysis and design, by allowing both control engineers and aerodynamicists to work with familiar concepts. This should aid an integrated approach to vehicle design.

Eigenstructure assignment does not inherently encompass dynamic compensation but simple extensions have been developed [Kim75] that give complete control over the dynamic compensator order and some ability to determine its structure through the choice of input/output variables. The facility to design low order compensators, that are more amenable to a SISO interpretation, should go some way to addressing functional visibility.

Eigenstructure assignment is a very flexible and visible technique that offers great potential in meeting the demands of helicopter control law design. It provides access to all the available design freedom and a range of *add-ons* have been developed [SSA94] to exploit this. These include techniques to prescribe the structure of the control law, deal with time delays and reduce gain magnitudes. The drawback of eigenstructure assignment is that it has no inherent mechanism for ensuring robustness and can assign a robust solution as easily as a catastrophically unrobust one. Robustness must be addressed using a post-assignment optimisation which will usually involve a trade-off with performance. Other researchers [GL90, HMMS90, Fav94] have also decided the benefits of eigenstructure assignment outweigh the robustness drawback and have achieved considerable success with the approach.

The choice of multivariable technique does not have a single correct answer: diverse techniques can yield similar performing controllers. In fact, manufacturers may well adopt different approaches since factors such as in-house expertise, availability and cost of software, compatibility with existing design approaches and the target market (civil/military) will also be important.

It is the author's thesis that eigenstructure assignment harnessed in a suitable design methodology is an appropriate and effective means of developing helicopter control laws. The remainder of this thesis attempts to develop such a methodology.

## 1.4 Thesis Overview

To produce a more accessible document an effort has been made to write self-contained chapters. As a result each chapter has its own introduction, summary, suggestions for further work, references, and places the work in context as it is described. A brief outline of the chapters follows.

Chapter 2 is an overview of the helicopter, since an understanding of its dynamics is essential background for any serious attempt at control law design. It includes a simple description of the system dynamics and flight mechanics, an outline of how to produce a computer simulation and trim it, development of a novel linearisation approach and higher order approximations, modal analysis for the

hover case and an overview of a conventional AFCS and its implementation.

In order to meet the design objectives the handling qualities requirements must be understood. Chapter 3 introduces handling qualities in general then describes the two currently most important handling qualities specifications. Criteria from the British specification (Def-Stan 00-970) are the used to develop an ideal eigenstructure.

Chapter 4 details the eigenstructure assignment approach. It begins with the state feedback case and develops an extension that allows eigenvalue and eigenvector design objectives to be traded-off. The output feedback problem is then introduced. Previous approaches are described along with supporting theory, and fundamental limits are established. From this theoretical basis a two stage assignment technique is derived. This forms the core technique for a host of extensions which include, retro assignment, multistage assignment, sympathetic projection, iterative projection and others. The extensions represent a set of tools that will enable the engineer to make best use of the available design freedom. It is then argued that assignment of eigenvectors in the state space is only of value when state space is aligned with the output space i.e. the states have physical significance. A general technique for assignment in the input/output spaces is developed. This involves assigning the modal coupling matrices. Dynamics compensation using an augmented system or an observer approach is then described. Finally, some topics for further work are discussed.

Any credible control law design approach must consider robustness. Chapter 5 presents two techniques for post-assignment robustness improvement. The techniques use broadly the same algorithm but are based on different robustness measures; a time domain measure and a singular value based measure. The focus of both techniques is to improve robustness with minimal degradation in performance. The chapter concludes with a summary and suggestions for further work.

Chapter 6 presents a helicopter control law design example. An attitude command controller is designed for the hover case. Different design approaches are explored and some design trade-offs are highlighted. The overall results are very promising and certainly indicate the potential of this technique.

Chapter 7 draws together the results from the previous chapters and suggests how they might be combined into a single practical and complete design methodology. This chapter also lists the significant contributions of this work and highlights a few of the most important topics for further work.

## 1.5 References

- [AL89] BDO Anderson and Y Lui. Controller reduction: Concepts and approaches. *IEEE Trans. on Automatic Control*, 34(8):802–812, August 1989.
- [ASC83] AN Andry, EY Shapiro, and JC Chung. Eigenstructure assignment for linear systems. *IEEE Trans. on Aerospace and Electronic Systems*, 19(5):711–727, September 1983.
- [AVS89] AVSCOM. Handling qualities requirements for military rotorcraft. Army Aeronautical Design Standard ADS33c, US Army Aviation Systems Command, 4300 Goodfellow Boulevard, St. Louis Missouri, August 1989.
- [Bal94] DEH Balmford. Some reflections on trends in rotorcraft technology and configurations - into the 21st century. *Aeronautical Journal*, pages 113–126, April 1994.

- [BDG94] JD Blight, RL Dailey, and D Gangsaas. Practical control law design for aircraft using multivariable techniques. *Int. Journal of Control*, 59(1):93–137, January 1994.
- [CBBB94] R Clarke, JJ Burken, JT Bosworth, and JE Bauer. X-29 flight control system: Lessons learned. *Int. Journal of Control*, 59(1):199–219, 1994.
- [Dav94] R Davies. *Robust Eigenstructure Assignment for Flight Control Applications*. DPhil, University of York, Heslington, York, YO1 5DD, England, 1994.
- [DGKF89] JC Doyle, K Glover, PP Khargonekar, and BA Francis. State-space solutions to standard  $\mathcal{H}_\epsilon$  and  $\mathcal{H}_\infty$  control problems. *IEEE Trans. on Automatic Control*, 34(8):831–847, August 1989.
- [DS81] JC Doyle and G Stein. Multivariable feedback design: Concepts for a classical/modern synthesis. *IEEE Trans. on Automatic Control*, 26(1):4–16, February 1981.
- [Elp96] JR Elphick. *Fault Tolerance in Rotorcraft Digital Flight Control Systems*. DPhil, University of York, Department of Electronics, Heslington, York, YO1 5DD, England, January 1996.
- [Fav94] C Favre. Fly by wire for commercial aircraft: The airbus experience. *Int. Journal of Control*, 59(1):139–157, January 1994.
- [Fla96] ME Rhett Flater. NH90 achieves first flight. *Vertiflite*, 42(2):8–10, March 1996.
- [GL90] WL Garrad and E Low. Eigenspace design of helicopter flight control systems. Technical report DAAL03-86-K-0056, Department of Aerospace Engineering and Mechanics, University of Minnesota., November 1990.
- [Gri94] SJ Griffin. The application of modern control techniques to the rotorcraft flight control problem. M.Phil/D.Phil Transfer Report, The Department of Electronics, The University of York, UK, December 1994.
- [Har96] J Harse. AHS Technical Committee Highlights II: Aircraft design. *Vertiflite*, 42(3):44–52, May 1996.
- [HG93] RA Hyde and K Glover. The application of scheduled  $\mathcal{H}_\infty$  controllers to a VSTOL aircraft. *IEEE Trans. on Automatic Control*, 38(7):1021–1039, July 1993.
- [HGS95] RA Hyde, K Glover, and GT Shanks. VSTOL first flight of an  $\mathcal{H}_\infty$  control law. *Computing and Control Engineering Journal*, 6(1):11–16, February 1995.
- [HMMS90] G Hughes, MA Manness, and DJ Murray-Smith. Eigenstructure assignment for handling qualities in helicopter flight control law design. In *Proceedings of the 16<sup>th</sup> Annual European Rotorcraft Forum*, pages III.10.2.1–12, Glasgow, Scotland, UK, September 1990. Royal Aeronautical society.
- [Hor82] I Horowitz. Quantative feedback theory. *IEE Proceedings D*, 129(6):215–226, November 1982.
- [Hyd95] RA Hyde.  *$\mathcal{H}_\infty$  Aerospace Control Design A VSTOL Flight Application*. Advances in Industrial Control Series. Springer-Verlag, 1995.
- [Kim75] H Kimura. Pole assignment by gain output feedback. *IEEE Trans. on Automatic Control*, 20:509–516, August 1975.
- [Kwa93] H Kwakernaak. Robust control and  $\mathcal{H}_\infty$ -optimization: Tutorial paper. *Automatica*, 29(2):255–273, 1993.
- [Law94] ST Lawes. *Real-Time Helicopter Modelling Using Transputers*. DPhil, University of York, Heslington, York, YO1 5DD, England, September 1994.
- [LDDK94] KH Landis, JM Davis, C Dabuno, and JF Keller. Advanced flight control technology achievements at boeing helicopters. *Int. Journal of Control*, 59(1):263–290, February 1994.
- [Mac89] JM Maciejowski. *Multivariable Feedback Design*. Electronic Systems Engineering. Addison Wesley, 1989.
- [McD96] RL McDaniel. A close look at an analysis of us army helicopter programs. *Vertiflite*, 42(2):30–31, March 1996.
- [MGMS90] MA Manness, JJ Gribble, and Murray-Smith. Multivariable methods for helicopter control law design: A review. In *Proceedings of the 16<sup>th</sup> Annual European Rotorcraft Forum*, pages III.5.2.1–14, Glasgow, Scotland, UK, September 1990. Royal Aeronautical society.
- [MMS88] MA Manness and DJ Murray-Smith. Paper 67: A technique for the tuning of helicopter flight control systems. In *Fourteenth European Rotorcraft Forum*, pages 67–1–67–12, Milan, Italy, September 1988.
- [MMS92] MA Manness and DJ Murray-Smith. Aspects of multivariable flight control law design for helicopters using eigenstructure assignment. *Journal of The American Helicopter Society*, 37(3):18–32, July 1992.
- [Moo81] BC Moore. Principal component analysis in linear systems: Controllability, observability, and model reduction. *IEEE Trans. on Automatic Control*, 26(1):17–32, February 1981.
- [Pad96] GD Padfield. *Helicopter Flight Dynamics*. Blackwell Science Ltd, 1996.
- [Pit89] B Pitkin. Flight and ground handling qualities. Military Defence Specification DEF-STAN 00-970, Ministry of Defence, September 1989.
- [Pro90] RW Prouty. *Helicopter Performance Stability, and Control*. Robert E. Krieger Publishing Company, 1990.



- 
- [RN94] SM Rock and K Neighbors. Integrated flight/propulsion control for helicopters. *Journal of The American Helicopter Society*, pages 34–43, July 1994.
- [SA87] G Stein and M Athans. The LQG/LTR procedure for multivariable feedback control design. *IEEE Trans. on Automatic Control*, 32(2):105–114, February 1987.
- [SSA94] KM Sobel, EY Shapiro, and AN Andry. Eigenstructure assignment. *Int. Journal of Control*, 59(1):13–37, 1994.
- [Tay94] P Taylor. -. Flight Systems Engineer, Westland Helicopters Plc, Yeovil, UK; Personal Communications, 1994.
- [Tay97] P Taylor. Personal Communications, 1997. Chief Handling Qualities Engineer, GKN Westland Helicopters Ltd, Yeovil, Summerset, UK.
- [TFMT89] MB Tischler, JW Fletcher, PM Morris, and GT Tucker. Application of flight control system methods to an advanced combat aircraft. Technical Memorandum NASA TM-101054, Ames Research Center, Ames Research Center, MS 211-2, Moffett Field, CA 94035, July 1989.
- [Tis87] MB Tischler. Digital control of highly augmented combat rotorcraft. Technical Memorandum NASA TM-88346, Ames Research Center, Moffett Field, CA 9403, May 1987.

# Chapter 2

## The Helicopter

### Contents

---

2.1	Flight Mechanics . . . . .	13
2.2	Computer Simulation and Trim . . . . .	23
2.3	Linearisation . . . . .	27
2.4	Modal Analysis . . . . .	39
2.5	Flight Control . . . . .	50
2.6	Summary . . . . .	56
2.7	References . . . . .	57

---

Any worthwhile attempt at helicopter control law design must be based on a sound understanding of the system dynamics. Hence this chapter gives a rudimentary overview of the helicopter dynamics. In practice, engineers employ computer simulations, trim algorithms and linearisations. This chapter describes the fundamentals of these tools and develops a novel approach to linearisation. A useful insight into the system dynamics can be gained from modal analysis of linearisations. Such an analysis is presented for the hover case. In an effort to learn from previous experience a conventional flight control law is examined.

### 2.1 Flight Mechanics

In its most primitive analysis, helicopter flight is merely a demonstration of Newton's third law. That is, accelerating a large mass of air downwards must produce an equal and opposing force that lifts the helicopter. The simplicity of this fundamental principle disguises the many problems that engineers have had to overcome in making the helicopter a viable vehicle. First, it was necessary to stop the fuselage from spinning by adding a tail rotor or, for tandem configurations, ensuring the second rotor spins in the opposite direction. Then the problems of directing the vehicle around the sky must be solved. Intuitively, one might control the vertical acceleration by varying the main rotor speed,

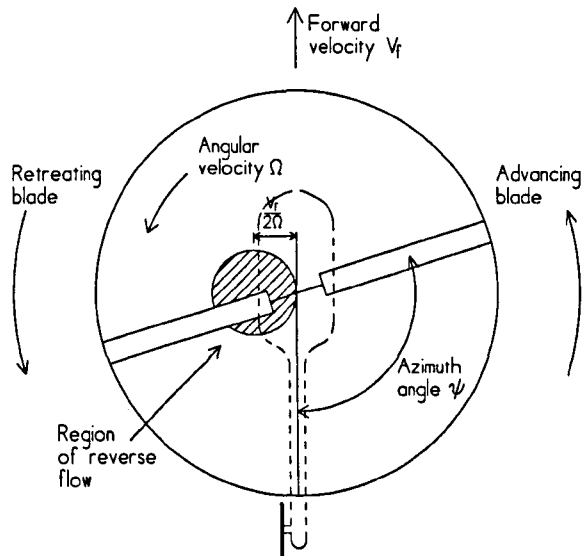


Figure 2.1.1: A plan view of a rotor disk.

however, this is not feasible. Since the large angular momentum of the rotor would require an immense torque to induce a respectable rate of change in angular velocity. Instead the pilot uses the *main rotor collective* to vary the collective pitch ( $\theta_0$ ) of the rotor blades and thus the amount of thrust developed. The blade pitching motion is often called *feathering* and is accomplished through of pitch bearing or feathering hinge.

A similarly, elegant solution is employed to provide directional control. By using the *lateral and longitudinal cyclic* controls, the pilot can vary the angle of incidence of the rotor blades as a function of their angular position. This provides control over the distribution of lift across the rotor disk and effectively enables the main rotor thrust to be directed. Angular position or azimuth of the blades ( $\psi$ ) is defined according to Figure 2.1.1. The blade pitch ( $\theta$ ) is described by:

$$\theta = \theta_0 - A_1 \cos \psi - B_1 \sin \psi \quad (2.1.1)$$

Where  $\theta_0$  is the collective pitch,  $\psi$  is the blade azimuth,  $A_1$  is the *lateral cyclic coefficient* and  $B_1$  is the *longitudinal cyclic coefficient*.

Equation (2.1.1) shows that the blade pitch is composed of both a fixed and a harmonic component. The cyclic rotor controls are represented by the longitudinal and lateral cyclic coefficients and examination of Equation (2.1.1) shows that rotor controls are phased by  $90^\circ$ . That is, the lateral coefficient determines the differential thrust in the longitudinal axis and conversely for longitudinal coefficient. The reason for this will be explained in Section 2.1.1.

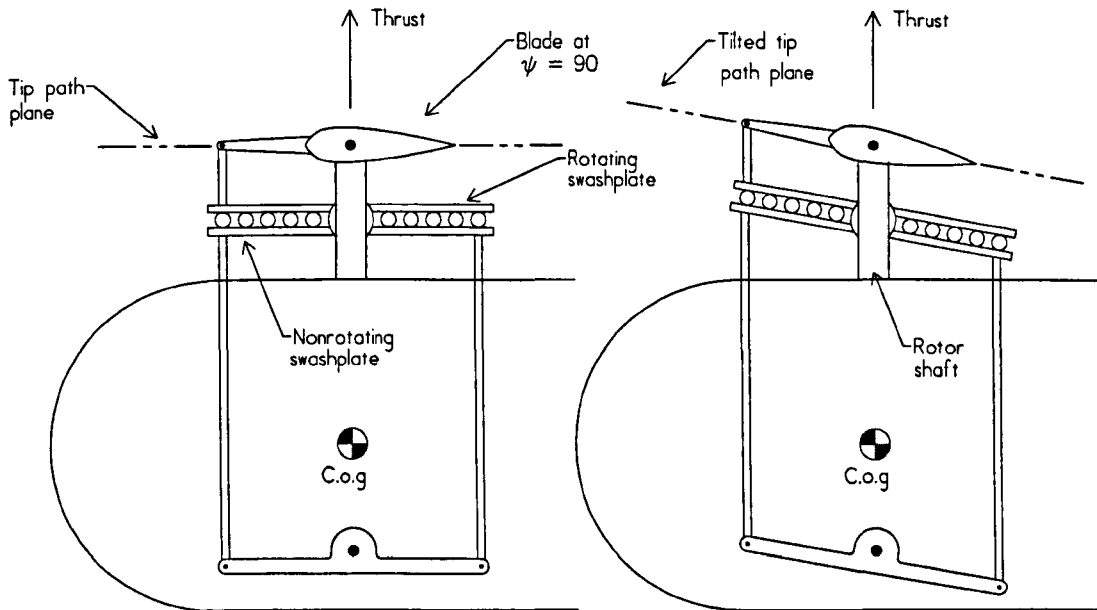


Figure 2.1.2: A typical swash plate assembly.

In the cockpit, the pilot has a collective lever and cyclic stick. These are generally connected to a *swash-plate* assembly. This transfers the body-fixed controls to the rotating rotor system. It consists of both a fixed and a rotating plate. The rotating plate is connected to the blades and determines their pitch. The swash-plate is moved vertically to provide collective control and tilted to provide cyclic control. A typical arrangement is shown in Figure 2.1.2.

The pilot also has two foot pedals to control the tail rotor collective ( $\theta_t$ ). Depressing the left or right pedal decreases or increases the tail rotor thrust and is used to balance the main rotor torque reaction or control heading and side slip at low speeds.

### 2.1.1 The Main Rotor

The main rotor dominates the helicopter behaviour and dynamics, since it provides the lift, propulsion and the majority of the directional control. The specification of the main rotor will determine important performance limits for the vehicle as a whole; for instance, the maximum forward velocity. During forward flight, the air velocity normal to the rotor blade varies as function of the blade angular position. The forward airspeed ( $V_f$ ) combines the motion of the advancing blade to give an increased net air flow ( $U$ ). Equally, the retreating blade suffers a reduced net air flow. A simple analysis shows that the air speed normal to the blade ( $U$ ) is:

$$U = \Omega r + V_f \sin \psi \quad (2.1.2)$$

Where  $\Omega$  is the angular velocity of the rotor blades and  $r$  is the radial position along the blade.

The reduced air flow over the retreating blade gives rise a region where there is no net forward air flow, this is known as the *region of reverse flow*. At the boundary of the reverse flow region the air speed normal to the blade will equal zero. Thus:

$$0 = \Omega r + V_f \sin(\psi) \quad (2.1.3)$$

$$= \Omega r^2 (\sin(\psi)^2 + \cos(\psi)^2) + r V_f \sin(\psi) \quad (2.1.4)$$

Hence:

$$\left(\frac{V_f}{2\Omega}\right)^2 = \left(r \sin(\psi) + \frac{V_f}{2\Omega}\right)^2 + (r \cos(\psi))^2 \quad (2.1.5)$$

Examination of Equation (2.1.5) shows that the reverse flow region describes a circle whose radius ( $\frac{V_f}{2\Omega}$ ) grows with increasing forward velocity ( $V_f$ ). At high forward velocities the majority of the retreating blade lift is generated near the tip of the blade, which must adopt a high angle of incidence to generate enough lift. Eventually the forward velocity is limited by the point at which the retreating blade *stalls* i.e. the angle incidence becomes so large that the blade experiences very high drag and a rapid loss of lift. Modern helicopters use advanced rotor tip designs that delay the onset of stall and thus increase the helicopter's maximum forward velocity<sup>1</sup>.

If the blades were to rotate with fixed incidence, the cyclic variation in air velocity would cause a corresponding variation in lift. As a consequence the roots of the blades would suffer excessive oscillatory stresses and a large portwards rolling moment would develop. One method of removing these undesirable effects, which has been widely adopted since first employed by Juan de la Cierva in 1923, is to allow the blades to *flap* up and down on hinges mounted near the rotor head. Clearly, the flap hinge relieves stresses at the root of the blade. However, it also significantly reduces the portwards rolling moment. This is because the advancing blade experiences a greater air speed causing it rise; thereby reducing the air incident angle (or angle of attack), thus generating less lift. The result is a more symmetric distribution of lift across the rotor disk at the expense of a reduction in average lift.

The periodic flapping changes the radial position of the blade elements, which by the conservation of angular momentum, must experience an in-plane acceleration, know as a *Coriolis force*. A second,

---

<sup>1</sup>Using an advanced tip design [Sed90] fitted to a Lynx, GKN Westlands Helicopters Ltd. set the helicopter world speed record (249 mph) in 1986.

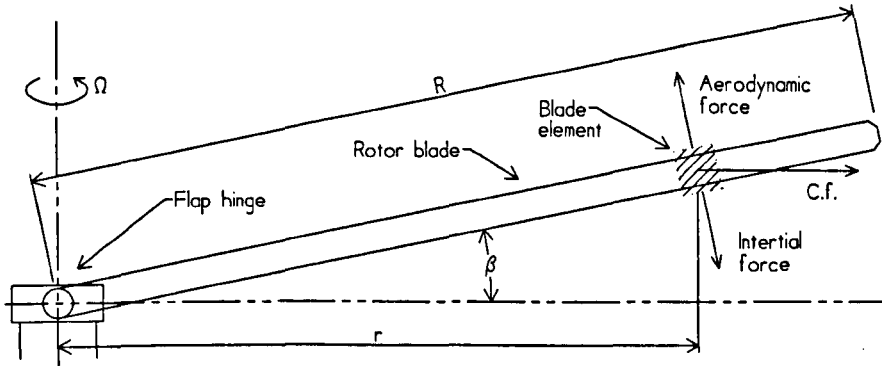


Figure 2.1.3: A single blade with flapping hinge.

*lag* hinge is generally added to accommodate in-plane motion resulting from the Coriolis force. The lag hinge is mounted outside and perpendicular to the flap hinge. Rotor heads employing flap and lag hinges are called articulated heads. The flapping motion is aerodynamically well damped, leading to small flapping angles ( $< 10^\circ$ ). The same is not true for the lead-lag motion. This often requires a mechanical damper which, through its actions, limits the oscillation amplitude. Whilst flapping contributes significantly to the performance of the rotor, the lead-lag motion has little effect. It is therefore instructive to perform a simple analysis of the flapping motion as follows.

Consider the blade element of spanwise length  $dv$  depicted in Figure 2.1.3. The forces on the element, normal to the blade, can be expressed as a sum of blade inertia ( $r\ddot{\beta} m dr$ ), centrifugal force ( $\sin(\beta) r\Omega^2 m dr$ ), blade weight ( $\cos(\beta)gm dr$ ) and thrust ( $dT$ ). The resulting moment about the flap hinge is:

$$dT = r^2 \ddot{\beta} m dr + \sin(\beta) r^2 \Omega^2 m dr + r \cos(\beta) gm dr \quad (2.1.6)$$

Where  $m dr$  is the mass of the blade element,  $\beta$  is the flapping angle, and  $g$  is acceleration due to gravity.

Using the small angle approximation and integrating over the blade span gives:

$$\int_0^R dT dr = \ddot{\beta} \int_0^R mr^2 dr + \Omega^2 \beta \int_0^R mr^2 dr + \frac{g}{r} \int_0^R mr^2 dr \quad (2.1.7)$$

Substituting for the blade moment of inertia is  $I_r = \int_0^R mr^2 dr$  and assuming the blade mass per unit length is constant:

$$T = \ddot{\beta}I_r + \Omega^2\beta I_r + \frac{3g}{2R}I_r \quad (2.1.8)$$

Where  $R$  is the blade length and  $T$  is the total Lift generated by the blade.

Typically, the blade length is  $R \approx 5m$ , the moment of inertia is ( $I_r \approx 10^4 Kgm^2$ ), the angular velocity of the blades is ( $\Omega \approx 30rad/s$ ) and the blade flapping is ( $\beta < 10^\circ$ ). The term due to gravity ( $\frac{3g}{2R} \approx 3$ ) is negligible in comparison to  $\Omega^2$  and  $\ddot{\beta}$  and will therefore be ignored. The residual second order homogeneous differential equation is:

$$0 = \ddot{\beta}I_r + \Omega^2\beta I_r \quad (2.1.9)$$

This equation describes a system with a resonant frequency of  $\Omega$ . Since the lift ( $T$ ) varies periodically with the blade azimuth ( $\psi$ ), the flapping motion is driven at its resonant frequency and the rotor is therefore a system in resonance. The cyclic pitch also drives the rotor at near its resonant frequency and is therefore effective and efficient. As is characteristic of all resonant systems, there is a  $90^\circ$  phase shift between the input and output. This means that, although the maximum lift occur at  $\psi = 90^\circ$ , the maximum displacement occurs at  $\psi = 180^\circ$ . This has implications when applying cyclic control to the rotor. For instance, to tilt the rotor disk laterally, the swash plate must be tilted longitudinally, and vice versa. The rotor lag will also introduce a significant delay into any stabilising feedback loop and must therefore be included during the design. In reality the rotor lag is not exactly  $90^\circ$  but generally slightly lower ( $\approx 80^\circ$ ). This is because Equation (2.1.8) is a vastly over-simplified description of the flapping dynamics, which is exemplified by the lack of a damping term. A more detailed analysis should consider the following additional effects:

1. The variation in lift ( $T$ ) due to: flapping angle ( $\beta$ ), flapping angular rate ( $\dot{\beta}$ ), cyclic control ( $A_1, B_1, \theta_0$ ), blade azimuth ( $\psi$ ) and other variables. In fact, it is the  $\dot{\beta}$  term that provides the aerodynamic damping.
2. Aerodynamic drag. The rotor blade aerofoil shape will generate drag as well as lift.
3. Inflow dynamics. The lift is also dependent on the motion of air through the rotor disk.
4. Flexibility of rotor blade. A rotor blade will flex along its length, supporting high frequency standing waves and twist.
5. The lagging motion and its mechanical damping.
6. The coupling of the body motions into the blade motion.

7. Variations in the rotor angular velocity. This requires calculation of the main rotor torque and modelling of the power plant and governor systems.

More detailed analysis [Pad96, p. 34] shows that the rotor dynamics will generally reach steady state in one revolution ( $\approx 20\text{rad/s}$ ). Due to the large mass of the vehicle, the rotor dynamics are considerably quicker than the body dynamics which are limited to oscillatory motions of  $\approx 4\text{rad/s}$ .

Since the steady state flapping is periodic it can be described as a Fourier series:

$$\beta = a_0 - \sum_{n=1}^{\infty} a_n \cos(n\psi) - \sum_{n=1}^{\infty} b_n \sin(n\psi) \quad (2.1.10)$$

This is generally truncated to a first order approximation which is known as the tip path plane (TPP) representation or a disk model, due to the direct physical interpretation of the Fourier coefficients. For instance  $a_1$ ,  $b_1$  are the longitudinal and lateral flapping angles and  $a_0$  is the residual blade angle due to the weight of the helicopter, or *coning angle*.

Often mechanical and performance constraints make it necessary to offset the flapping hinges a small distance ( $\frac{h'}{R} \approx 3\% - 4\%$ ) from the centre of rotation. Equation (2.1.11) shows that the hinge offset increases the resonant frequency and hence causes a slight reduction in phase lag.

$$\omega_r = \left(1 + \frac{3h'}{2R}\right)^{\frac{1}{2}} \Omega \quad (2.1.11)$$

Where  $h'$  is the flapping hinge offset distance and  $\omega_r$  the nominal resonant frequency.

Some modern helicopter designs employ hingeless rotors that replace the flapping and lag hinges with flexible elements made of advanced composite materials. The primary motive behind hingeless rotors is the production of a more compact rotor head that reduces parasitic drag. However, hingeless rotors bring a collection of desirable and objectionable side effects. For instance, a hingeless rotor can exert a larger direct moment and thus increases control power<sup>2</sup>. On the other hand they have a tendency to cause instability at high speeds. The flapping behaviour of hingeless rotors does not differ significantly from articulated rotors. Often the coning angle and flapping angles are very similar. In fact, for analysis purposes, hingeless rotors are often approximated as articulated rotors with a large offset distance ( $\frac{h'}{R} \approx 10\% - 15\%$ ). This approximation and Equation (2.1.11) reveal that hingeless rotors have a resonant frequency higher than  $\Omega$  and thus a phase lag less  $90^\circ$ .

<sup>2</sup>Control power is a measure of the pilots ability to induce moments on the airframe.



## 2.1.2 Equations of Motion

The contribution of the fuselage and empennage to the helicopter dynamics can be analysed using conventional fixed wing techniques. That is, the fuselage motion is dictated by the equations of motion and aerodynamic forces. Using the body-fixed axis set, illustrated in Figure 2.1.4, the equations of motion can be stated as follows:

$$F_x = m(\dot{u} + qw - rv) \quad (2.1.12)$$

$$F_y = m(\dot{v} - pw + ru) \quad (2.1.13)$$

$$F_z = m(\dot{w} + pv - qu) \quad (2.1.14)$$

$$L = \dot{p}I_{xx} - \dot{r}I_{xz} + qr(I_{zz} - I_{yy}) - pqI_{xz} \quad (2.1.15)$$

$$M = \dot{q}I_{yy} + pr(I_{xx} - I_{zz}) - r^2I_{xz} + p^2I_{xz} \quad (2.1.16)$$

$$N = \dot{r}I_{zz} - \dot{p}I_{xz} + pq(I_{yy} - I_{xx}) + qrI_{xz} \quad (2.1.17)$$

Where  $F_x$ ,  $F_y$  and  $F_z$  are the external linear forces defined according to Figure 2.1.4 and are due to gravity, propulsion and aerodynamics. The terms  $u$ ,  $v$  and  $w$  denote the linear velocities;  $L$ ,  $M$  and  $N$  denote the external angular moments; and  $p$ ,  $q$  and  $r$  denote the angular velocities and the sense of all the terms is defined according to Figure 2.1.4.  $I_{xx}$ ,  $I_{yy}$  and  $I_{zz}$  are moments of inertia about the indicated axes. Finally,  $I_{xz}$  is the product of inertia in the  $xz$  plane.  $I_{yz}$  and  $I_{xy}$  are assumed to equal zero due to the symmetry of the fuselage.

The equations of motion reveal a coupling between roll and yaw due to the product of inertia  $I_{xz}$ . Such cross-coupling is typical of all helicopters and is not confined to just the roll and yaw axes. The main rotor is, in principle, a large gyroscope and will precess in an orthogonal direction to an applied torque. Hence roll and pitch motions are also coupled. This effect is more noticeable if the rotor is able to exert a large direct moment on the fuselage, due to a considerable flap hinge offset or a hingeless rotor. It is also typical for the controls to induce moments in more than one axis. For instance, a change in tail rotor thrust will principally induce a moment in yaw, but since the tail rotor is not centred on the  $x$  axis, a roll moment and side slip velocity will also arise.

The aerodynamic forces exerted by the fuselage are characterised by the total velocity, angle of attack and side slip angle. However, the conventional definition of the sideslip and attack angles must be modified to include the main rotor downwash. This is most accurately incorporated using wind tunnel data, since the interaction between the main rotor downwash and the fuselage is too complicated to be reliably predicted mathematically. Wind tunnel data is required to calculate the fuselage and empennage lift, drag and pitch moments at a given angle of attack, as well as the yaw moment, roll moment and side force due to a specified side slip angle.

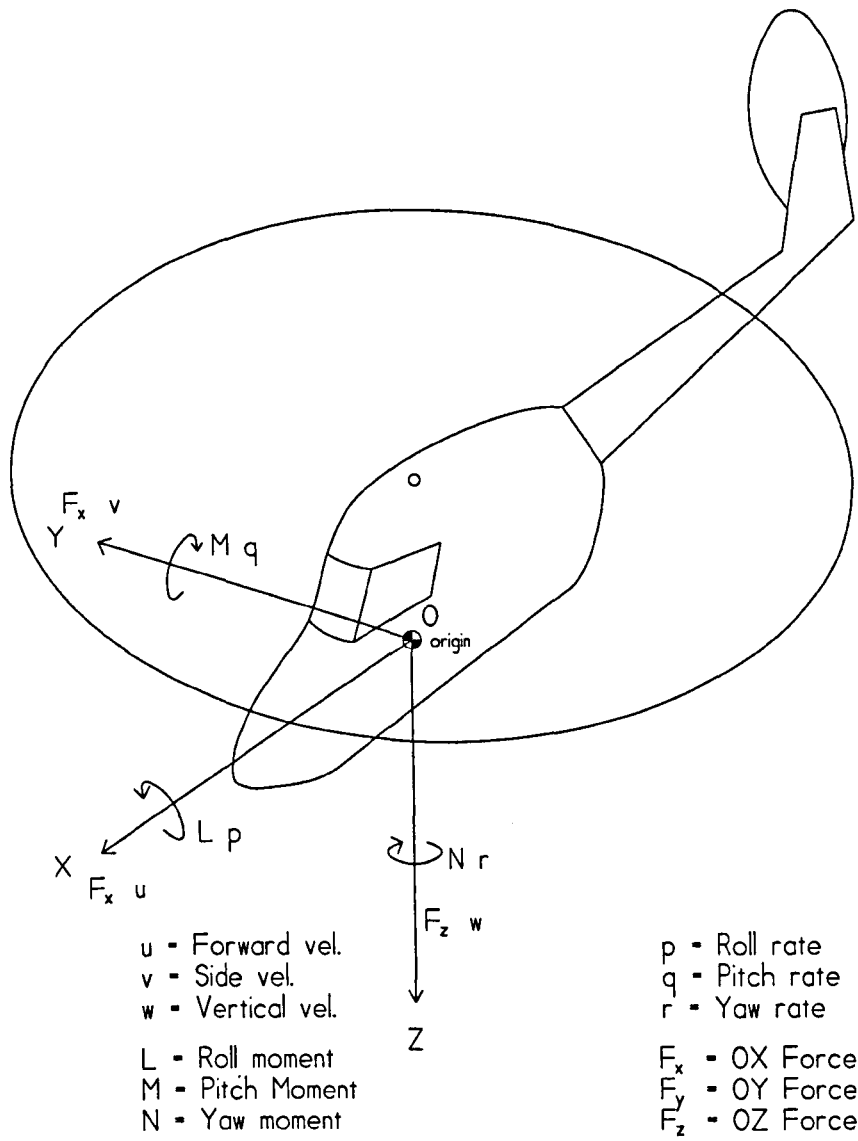


Figure 2.1.4: Conventional body fixed axis set for a helicopter.

For a more detailed analysis of helicopter dynamics, the reader is referred to Bramwell [Bra76], Johnson [Joh80], Prouty [Pro90] and Padfield [Pad96].

### 2.1.3 Static Stability

Static stability [McI90] refers to the ability of a vehicle initially to generate restoring forces when perturbed from an equilibrium. The term static stability is peculiar to the field of aeronautical engineering. A statically stable vehicle may still produce divergent oscillations and thus be dynamically unstable.

To perform an analysis of a vehicle's static stability it generally suffices to apply simple physical arguments. This simple analysis accentuates the dominant features of the vehicles dynamic behaviour and is thus worthwhile. A cursory analysis of the helicopter response to some key perturbations is described below:

**Stability in angle of attack** A vertical gust will cause a uniform increase in the angle of attack of the main rotor, which will increase the main rotor thrust and flapping motion. The increased flapping induces a nose-up pitching moment that is destabilising, since it further increases the angle of attack.

**Stability in forward speed** An incremental perturbation in forward speed will again increase flapping and thus induce a nose pitching moment. This moment is stabilising since it tilts the main rotor thrust rearwards, thus opposing the increase in forward speed. It is interesting to note that in hover, the restoring moment usually leads to dynamic instability which is damped during forward flight by the tail plane.

**Stability in roll and pitch** A disturbance in roll or pitch will cause the main rotor to precess in an orthogonal direction. The precession excites the flapping dynamics which due to the  $90^\circ$  phase lag tilts the rotor tip path plane (TTP) in a direction that opposes the original disturbance. The main rotor therefore possesses static stability in roll and pitch. However, in forward flight the asymmetric distribution of lift leads to considerable coupling between roll and pitch axes.

**Stability due to side slip** A disturbance in side slip rotates the direction of maximum flapping and thus tilts the TTP in the direction that opposes the original disturbance generating a stabilising roll moment.

**Stability in Yaw** The tail rotor and, during forward flight, the vertical fin give the helicopter a degree of *weather cock* stability. A portwards disturbance in yaw will increase the tail rotor incidence and therefore the tail rotor thrust. The additional thrust is statically stabilising as it opposes the original disturbance.

This crude analysis gives a flavour of the stability of the helicopter. However, further analysis requires additional tools such as computer simulation and linearisation.

## 2.2 Computer Simulation and Trim

For a thorough assessment of helicopter stability, one should solve the non-linear differential equations describing the vehicle dynamics, then apply stability criteria, such as bounded input bounded output (BIBO) analysis. However, even a simple mathematical description of the helicopter will involve non-linear differential equations with time-varying coefficients that draw on a substantial pool of numerical data. Deriving explicit solutions for these equations is an impossible task. The widely accepted alternative is to use a combination of computer simulation and linearisation.

### 2.2.1 Computer Simulation

Computer simulation is an immensely important tool in the field of aeronautical engineering, and finds wide application beyond stability analysis. Typical applications include vehicle design, prediction of operational limits, vibration analysis, flight controller design, piloted simulation for training, handling qualities assessment and as a source of linearisations. Padfield [Pad96, p. 90] suggests that a simulation should offer no more fidelity than is required and identifies three discrete levels of helicopter model complexity as shown in Table 2.2.1.

Level	Description	Application
One	A quasi-static rotor head, with analytically integrated loads and aerodynamics based on momentum theory and linear inflow assumptions.	Low bandwidth control, parametric trends for performance and flying qualities studies near trim.
Two	A rotor with flapping DoFs numerically integrated loads, non-linear inflow dynamics and modelling of other aerodynamic artifacts.	Medium bandwidth control, parametric trends for performance and flying qualities studies up to the OFE.
Three	A rotor with flapping and structural DoFs, numerically integrated loads and a full 3D non-linear wake analysis.	Rotor design, prediction of rotor limits and vibration analysis.

Table 2.2.1: Levels of rotorcraft modelling fidelity.

The mathematical description of a helicopter can ultimately be expressed in the following generic form:

$$\dot{\mathbf{x}} = \mathbf{f}(\mathbf{x}, \mathbf{u}, t) \quad (2.2.18)$$

Where  $\mathbf{f}(\mathbf{x}, \mathbf{u}, t)$  is a vector of functions thus  $\left[ f_1(\mathbf{x}, \mathbf{u}, t), \dots, f_n(\mathbf{x}, \mathbf{u}, t) \right]^T$ ,  $\mathbf{x}$  is the state vector,  $\mathbf{u}$  is the input vector and  $t$  denotes time. Typical definitions of the state and input vectors, for a simple

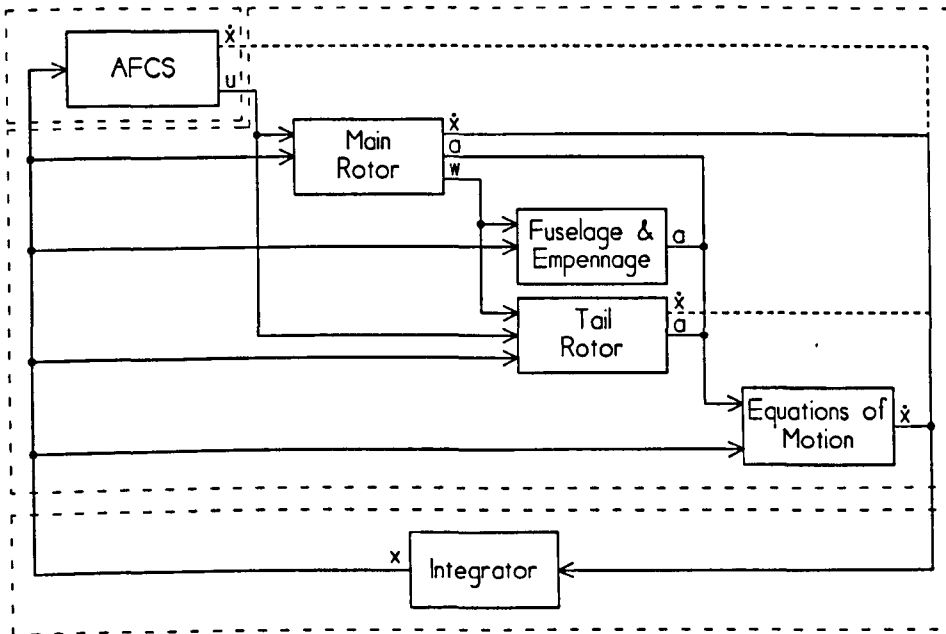


Figure 2.2.5: A typical simulation structure.

model, are:

$$\mathbf{x}^T \triangleq [u, v, w, p, q, r, \phi, \theta, \psi, a_{1s}, b_{1s}] \tag{2.2.19}$$

$$\mathbf{u}^T \triangleq [A_1, B_1, \theta_0, \theta_t] \tag{2.2.20}$$

Where  $u, v, w, p, q, r, \theta_0, \theta_t, A_1, B_1$  are as defined in Section 2.1,  $\phi, \theta, \psi$  are the roll attitude, pitch attitude and heading respectively<sup>3</sup> and  $a_{1s}, b_{1s}$  are longitudinal and lateral flapping angles.

The established approach to computer simulation is forward numerical integration of Equation (2.2.18).

The helicopter is a complex arrangement of interacting subsystems. Thus, in practice, it serves to decompose the simulation into its physical subsystems. This approach leads to a more visible and maintainable simulation. It also allows the physical concurrency to be mapped on to parallel hardware for high fidelity real time simulation [Law94]. Figure 2.2.5 depicts a typical simulation structure. An outline functional description of the individual subsystems is given as follows:

**The Flight Control System** implements the feedback control system. It receives state information

<sup>3</sup>The body attitudes  $\phi, \theta, \psi$  are also known as the Euler angles.

from which it derives sensor outputs. The sensor outputs are processed by the controller to produce incremental adjustments to the vehicle controls. If a dynamic controller is implemented then the subsystem will also produce state derivatives that must be integrated.

**The Main Rotor** is the most complex subsystem. Its inputs are the system state and the cyclic and collective controls. With these it calculates the main rotor inflow, the forces and moments developed by the rotor and the resulting wake. It will generally output state derivatives associated with its own degrees of freedom. Various levels of complexity may be implemented from a full blade element model with 3D wake and inflow analysis, to a static disk model.

**The Fuselage and Empennage** subsystem receives state and wake information and generally uses wind tunnel data to calculate the forces and moments developed. To provide a continuous estimate the wind tunnel data must be interpolated. Linear interpolation is often employed. However, this can introduce discontinuities. In practice best results are obtained using a smooth interpolation method such as cubic spline [PTVF92].

**The Tail Rotor** is fed the system state, tail rotor collective and wake information. Using similar, but generally simpler, techniques to the main rotor it calculates the moments and forces developed. It may also output state derivatives.

**Equations of Motions.** At this point the forces and moments are summed and the equation of motion are solved for the linear and angular accelerations.

**Integration.** A numerical technique is used to integrate the state derivatives to produce the new system state. The numerical technique should be chosen to suit the characteristics of the system [PTVF92].

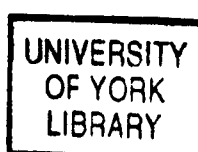
A simulation with the structure outlined above was employed in this work [Coo92]. For expedience the simulation was incorporated in Matlab [Mat92] as a Mex file [Mat94].

Repeated integration using the simulation structure described above will produce time history data, however, the simulation must be started with a sensible set of initial control inputs and state values. Generally, a simulation model will be released from a trim condition.

### 2.2.2 Trim

A pilot's principal task while flying is to maintain a desired flight condition by holding the forces and moments about the three airframe axes at equilibrium. When equilibrium is achieved the helicopter is said to be *trimmed*. Common trim conditions are:

**Hover** All resultant forces, moments and translational velocities are zero. To hold this trim condition the helicopter will have to adopt starboard roll attitude to balance the tail rotor thrust and often



a nose-up pitch attitude to accommodate the main rotor shaft tilt<sup>4</sup> and an aft centre of gravity.

**Straight and level flight** again all angular and linear accelerations are zero and the forward velocity is constant. At low speeds the pilot will trim for zero side slip and accept a small roll attitude. However, as speed increases ( $V_f > 50 \text{ knots}$ ) the pilot will adopt a 'wings level' attitude and endure a small side slip angle.

**Co-ordinated turn** The helicopter turns with a fixed bank angle while holding all linear accelerations and pitch rate at zero. Roll and yaw rate are adjusted via the tail rotor thrust such that the fuselage side force is zero. This ensures passengers and pilot are not swept from side to side as the helicopter turns.

**Steady climb** the helicopter is trimmed to a fixed climb angle and rate.

Mathematically, a trim condition is a set of constraints that, when applied to the equations of motion and flapping equations, enables the control angles ( $\theta_0, \theta_t, A_1, B_1$ ) and other parameters to be determined. For a unique solution to a given trim condition the number of constraints must equal the number of variables.

Using the state ( $\mathbf{x}$ ) and input ( $\mathbf{u}$ ) definitions given above, the constraints for the hover conditions are:

$$\text{Hover} \quad \begin{cases} u = 0 & p = 0 & \dot{u} = 0 & \dot{p} = 0 & \dot{a}_{1s} = 0 \\ v = 0 & q = 0 & \dot{v} = 0 & \dot{q} = 0 & \dot{b}_{1s} = 0 \\ w = 0 & r = 0 & \dot{w} = 0 & \dot{r} = 0 & \end{cases} \quad (2.2.21)$$

Note there are fourteen constraints and fourteen variables<sup>5</sup>. Thus the trim condition may be uniquely defined. The first six constraints are trivially met by setting the appropriate state variable to zero. The remaining constraints can be met using any non-linear equation solver. However, in practice, Newton-Raphson has proved effective. This involves calculating the Jacobian<sup>6</sup> of  $[\dot{u}, \dot{v}, \dot{w}, \dot{p}, \dot{q}, \dot{r}, \dot{a}_{1s}, \dot{b}_{1s}]$  with respect to the unconstrained variables  $[\phi, \theta, a_{1s}, b_{1s}, \theta_0, \theta_t, A_1, B_1]$  and then iterating [Arf85].

The trim constraints for straight and level flight at an air speed of  $V_f$  are:

$$\text{Level Flight} \quad \begin{cases} u = \sqrt{V_f^2 - v^2} \cos(\theta) & p = 0 & \dot{u} = 0 & \dot{p} = 0 & \dot{a}_{1s} = 0 \\ & q = 0 & \phi = 0 & \dot{v} = 0 & \dot{q} = 0 & \dot{b}_{1s} = 0 \\ w = \sqrt{V_f^2 - v^2} \sin(\theta) & r = 0 & \dot{w} = 0 & \dot{r} = 0 & \end{cases} \quad (2.2.22)$$

<sup>4</sup>The main rotor is usually tilted so that the cabin floor will be level at cruise velocity ( $\approx 80$  knots). This does have the drawback that the main rotor torque reaction couples into roll.

<sup>5</sup>Heading ( $\psi$ ) is ignored since it affects no other state.

<sup>6</sup>The Euler angle derivatives are not considered since if  $p, q, r$  are zero these are necessarily zero.

The algorithm outlined above was employed, in Matlab, to trim the non-linear simulation model. It typically trimmed the model in six iterations and reduced the state derivatives to within machine precision ( $10^{-10}$ ) of zero.

The facility to trim a model is not just important for initialising simulations. A trim condition is also a vital pre-requisite for generating a linearisation of a non-linear model.

## 2.3 Linearisation

A linearisation is a first order Taylor approximation of a non-linear analytic function. This is a locally valid representation for non-linear differential equations providing, the linearisation is made around an equilibrium state ( $\dot{\mathbf{x}} = \mathbf{0}$ ) or trim condition. The locality for which a linearisation is an acceptable approximation depends on the characteristics of the system. Strong non-linearities, such as the fuselage force and moment functions, quickly degrade the approximation. Thus, linearisations of helicopters are only representative for small perturbations from the equilibrium state.

Let  $\mathbf{x}_0$  and  $\mathbf{u}_0$  denote an equilibrium state ( $0 = f_i(\mathbf{x}_0, \mathbf{u}_0)$ ) and  $\mathbf{x}$  and  $\mathbf{u}$  denote perturbations from the equilibrium then the full Taylor series [Arf85] is:

$$f_i(\mathbf{x}_0 + \mathbf{x}, \mathbf{u}_0 + \mathbf{u}) = \sum_{n=0}^{\infty} \frac{1}{n!} (\mathbf{x} \cdot \nabla_{\mathbf{x}} + \mathbf{u} \cdot \nabla_{\mathbf{u}})^n f_i(\mathbf{x}_0, \mathbf{u}_0) \quad (2.3.23)$$

The first order approximation is:

$$f_i(\mathbf{x}_0 + \mathbf{x}, \mathbf{u}_0 + \mathbf{u}) \approx f_i(\mathbf{x}_0, \mathbf{u}_0) + (\mathbf{x} \cdot \nabla_{\mathbf{x}} + \mathbf{u} \cdot \nabla_{\mathbf{u}}) f_i(\mathbf{x}_0, \mathbf{u}_0) \quad (2.3.24)$$

Applying the steady state assumption gives:

$$f_i(\mathbf{x}_0 + \mathbf{x}, \mathbf{u}_0 + \mathbf{u}) \approx (\mathbf{x} \cdot \nabla_{\mathbf{x}} + \mathbf{u} \cdot \nabla_{\mathbf{u}}) f_i(\mathbf{x}_0, \mathbf{u}_0) \quad (2.3.25)$$

If  $\boldsymbol{\varepsilon}^T = [\varepsilon_1, \dots, \varepsilon_n]$  then  $\nabla_{\boldsymbol{\varepsilon}}$  is the vector differential operator defined thus  $\nabla_{\boldsymbol{\varepsilon}} = \left[ \frac{\partial}{\partial \varepsilon_1}, \dots, \frac{\partial}{\partial \varepsilon_n} \right]$ . Using the function of vectors  $\mathbf{f}(\mathbf{x}, \mathbf{u})$  Equation (2.3.25) can be written in the standard state space form:

$$\dot{\mathbf{x}} = (\nabla_{\mathbf{x}} \mathbf{f}(\mathbf{x}_0, \mathbf{u}_0)) \mathbf{x} + (\nabla_{\mathbf{u}} \mathbf{f}(\mathbf{x}_0, \mathbf{u}_0)) \mathbf{u} \quad (2.3.26)$$

By convention:



$$\mathbf{A}^{n \times n} \triangleq \nabla_{\mathbf{x}} \mathbf{f}(\mathbf{x}_0, \mathbf{u}_0) = \begin{bmatrix} \frac{\partial f_1}{\partial x_1} & \dots & \frac{\partial f_1}{\partial x_n} \\ \vdots & \ddots & \vdots \\ \frac{\partial f_n}{\partial x_1} & \dots & \frac{\partial f_n}{\partial x_n} \end{bmatrix} \quad (2.3.27)$$

$$\mathbf{B}^{n \times r} \triangleq \nabla_{\mathbf{u}} \mathbf{f}(\mathbf{x}_0, \mathbf{u}_0) = \begin{bmatrix} \frac{\partial f_1}{\partial u_1} & \dots & \frac{\partial f_1}{\partial u_r} \\ \vdots & \ddots & \vdots \\ \frac{\partial f_n}{\partial u_1} & \dots & \frac{\partial f_n}{\partial u_r} \end{bmatrix} \quad (2.3.28)$$

Hence:

$$\dot{\mathbf{x}} = \mathbf{A}\mathbf{x} + \mathbf{B}\mathbf{u} \quad (2.3.29)$$

The usefulness of linearisations in stability analysis is a result of *Liaphonov's linearisation theorem* [Vid93], which states that, under certain conditions, it is valid to draw conclusions about the non-linear system stability from the behaviour of a linearisation. The sufficient conditions are that the system be in steady-state, that  $\mathbf{f}(\mathbf{x}, \mathbf{u})$  be continuously differentiable and the elements of  $\mathbf{A}$  are bounded.

Linearisations have many benefits beyond stability analysis. They provide access to the wealth of linear systems theory and are thus a vital tool in control law design. Analysis of linearised dynamics and examination of the individual derivatives can offer an intuitive and tractable insight into the functioning of a complex non-linear system. For small perturbations linearisations offer a computationally light method of simulating the system behaviour. Furthermore, the steady state assumption is likely to be valid for the majority of the helicopter flight path since the pilot will strive to hold the helicopter in trim.

However, for any comprehensive analysis of helicopter dynamics, it is vital that linearisation is backed-up with a full non-linear computer simulation which has been validated against actual flight data. Simulation is the only sure way of assessing behaviour to large perturbations and stability away from trim. The importance of an accurate computer simulation is accentuated when reduced order linear models are used. Since these often ignore the potentially destabilising dynamics associated with sensors and actuators [Tho93].

### 2.3.1 Numerical Methods

In theory, a linearisation can be calculated analytically by evaluating the partial derivatives indicated in Equation (2.3.27) and Equation (2.3.28). However, in practice, the system equations often do not lend themselves to differentiation. It may also occur that the analytical solution does not yield the best results in terms of model fidelity.

The widely accepted solution is to apply numerical techniques. Two distinct approaches are often employed [Pad96]; identification and perturbation methods.

Identification methods [SCM96] generally attempt to find a linear system that best approximates a given set of time history input-output data. This approach has the advantage that it may be applied to measurement data from real systems and that it inherently attempts to accommodate non-linearities. However, it is clearly impossible for a linear system of any order to portray hard non-linearities such as saturation and hysteresis, which can often overwhelm an identification algorithm. Multivariable identification techniques are very complex and are, in themselves, a considerable topic of research. Therefore they were not applied in this work.

Perturbation methods are based on the definition of the partial derivative:

$$\frac{\partial f(x_0)}{\partial x} = \lim_{\delta \rightarrow 0} \frac{f(x_0 + \delta) - f(x_0)}{\delta} \quad (2.3.30)$$

From the above it is clear that a good approximation to the partial derivative can be calculated using a suitably small perturbation ( $\delta$ ) and a difference equation as follows:

$$\frac{\partial f(x_0)}{\partial x} \approx \frac{f(x_0 + \delta) - f(x_0)}{\delta} \quad (2.3.31)$$

Thus a straightforward approach to calculating a linearisation is to perturb each state and input independently and perform a difference calculation as illustrated below:

$$\mathbf{A} \approx \left[ \frac{1}{\delta} (\mathbf{f}(x_0 + \delta \mathbf{e}_1, \mathbf{u}_0) - \mathbf{f}(x_0, \mathbf{u}_0)), \dots, \frac{1}{\delta} (\mathbf{f}(x_0 + \delta \mathbf{e}_n, \mathbf{u}_0) - \mathbf{f}(x_0, \mathbf{u}_0)) \right] \quad (2.3.32)$$

Where  $\mathbf{e}_i$  is an all zero vector of equal length to  $\mathbf{x}_0$  except the  $i^{th}$  element is unity.

However, there is a dearth of theory [Wig92] supporting numerical perturbation. Selection of perturbation size and estimates of the linearisation accuracy are often based on heuristics [Sug94, Rah93, TA93]. Taylor and Antoniotti [TA93] suggest that the perturbation size should be selected as a compromise between round off error and truncation error. As the perturbation size is reduced errors will eventually begin to increase due to finite precision arithmetic or round off error. Equally, as the perturbation size is increased non-linearities will cause the errors to increase. This increase can be attributed to truncation of the Taylor series. While the technique of Taylor and Antoniotti will find a good approximation to the partial derivative, it may still produce a poor approximation of the system, since the perturbation size used to calculate the partial derivatives may be vastly different from that used in subsequent simulation and controller synthesis.

The quality of the linearisation has direct implications for the controller synthesis, since a poor

match at this stage will yield a controller that is unlikely to perform adequately on the real plant. Even an ideal linearisation process must throw away considerable information about the system non-linearities: information that is often needed later to form an uncertainty model so that the controller may function on the real plant. To address these issues a new linearisation algorithm was developed. Its aim were:

- To produce to a representative linearisation.
- To estimate the valid region of the linearisation.
- To produce an uncertainty model associated with the linearisation.

The basic principle behind the algorithm is to calculate the maximum deviation from the trim point such that the function displays acceptably linear behaviour. To have confidence that the function is displaying linear behaviour, it is necessary to consider several points within the deviation. The most non-linear point is recorded and returned as uncertainty information. The details of the algorithm are described below. For brevity the scalar case is considered.

1. Initialise the perturbation size ( $\delta$ ) and counter ( $i = 1$ ).
2. Evaluate the non-linear function for positive and negative excursions of the current deviation ( $i\delta$ ):

$$y_p(i) = f(x_0 + i\delta, u_0) \quad (2.3.33)$$

$$y_n(i) = f(x_0 - i\delta, u_0) \quad (2.3.34)$$

3. Update the minimum and maximum gradient values of the chord between the function output and the origin.

$$g_{max} = \max \left\{ g_{max}, \frac{y_p(i)}{i\delta}, \frac{y_n(i)}{-i\delta} \right\} \quad (2.3.35)$$

$$g_{min} = \min \left\{ g_{min}, \frac{y_p(i)}{i\delta}, \frac{y_n(i)}{-i\delta} \right\} \quad (2.3.36)$$

4. Calculate the current best fit linear approximation ( $a_e$ ):

$$a_e = \frac{\sum_{k=1}^i y_p(k)(k\delta) + y_n(k)(-k\delta)}{\sum_{k=1}^i (k\delta)^2 + (-k\delta)^2} \quad (2.3.37)$$

State	Trim Value	Valid Range	Unit
$u$	0	5.5	feet/s
$v$	0	2.75	feet/s
$w$	0	8.0	feet/s
$p$	0	0.1719	rad/s
$q$	0	0.1406	rad/s
$r$	0	0.4688	rad/s
$\theta$	-0.0572	0.0020	rad
$\phi$	0.0596	0.0020	rad
$\psi$	0	33.0	rad
$a_{1s}$	0.0114	33.0	rad
$b_{1s}$	-0.0050	33.0	rad

Table 2.3.2: Trim point and validity estimate for a linearisation at hover.

5. Check that minimum ( $g_{min}$ ) and maximum ( $g_{max}$ ) gradients are acceptably close to the current estimate ( $a_e$ ):

$$g_{max} < a_e(1 + \epsilon_p) + \epsilon_a \quad (2.3.38)$$

$$g_{min} > a_e(1 - \epsilon_p) - \epsilon_a \quad (2.3.39)$$

Where  $\epsilon_p$  and  $\epsilon_a$  are user supplied proportional and absolute error tolerances. If the gradients are acceptable increase the counter ( $i = i + 1$ ) if the gradients are unacceptable reset the counter ( $i = 1$ ) and decrease the perturbation size  $\delta = \frac{\delta}{2}$ .

6. If the counter is equal to the maximum counter value ( $i_{max}$ ) then stop else go to step two.

To generalise the algorithm to the multivariable case it is only necessary to repeat the process for each partial derivative. A Matlab implementation of the above algorithm was used to linearise the non-linear simulation model. Typical values for  $\epsilon_p$ ,  $\epsilon_a$  and  $i_{max}$  are  $\epsilon_p = 0.01$ ,  $\epsilon_a = 0.01$  and  $i_{max} = 10$ . While it is difficult to offer a formal justification for the algorithm, in practice it has proved a useful tool. Appendix A.1 contains a linearisation of a non-linear helicopter model in hover. It also presents the associated uncertainty information, which was calculated as follows:

$$\Delta a_e = \max \{g_{max} - a_e, a_e - g_{min}\} \quad (2.3.40)$$

The valid perturbation sizes and trim point information are shown in Table 2.3.2.

The validity estimates for the heading ( $\psi$ ) and the flapping angles ( $a_{1s}$ ,  $b_{1s}$ ) are unrealistically large. This is because heading does not effect any other state and is often ignored in the dynamic analysis

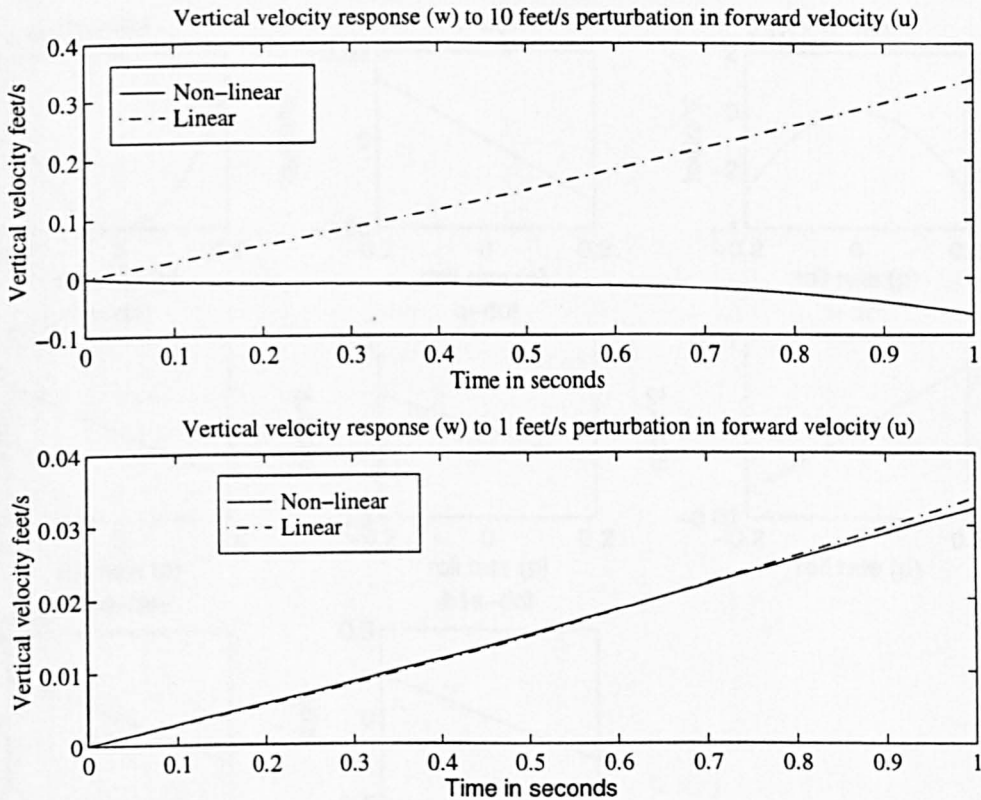


Figure 2.3.6: Vertical velocity response of a linear (Jacobian only) and non-linear helicopter model at hover for a 1 and 10 feet/s perturbation in forward velocity.

of helicopters. During the hover the retreating and advancing blades experience the same air speed. Thus the flapping dynamics are not excited and the response to changes in flapping angle is linear. While the model's portrayal of this situation is accurate, the situation itself is artificial, since it implies that the flapping angles can be adjusted independently and that the body dynamics remain in the hover state during the flapping angle excursion.

The validity estimates for the other states do provide a useful indicator for the maximum deviation in the state variable for which the linearised model is representative. For instance, Figure 2.3.6 shows the response in vertical velocity ( $w$ ) to perturbations in forward speed of 1 and 10 feet/s. These represent perturbations beyond and within the valid range indicated in Table 2.3.2.

From Figure 2.3.6 we see that the linearisation shows good fidelity for the 1 feet/s perturbation but almost immediate divergence for the 10 feet/s perturbation. The first column of  $\Delta A$  in Appendix A.1 is the uncertainty associated with perturbations in forward velocity. It shows that the maximum uncertainty (0.0110) is associated with the vertical velocity derivative ( $\Delta A_{3,1}$ ) and indeed vertical velocity does show the worst response.

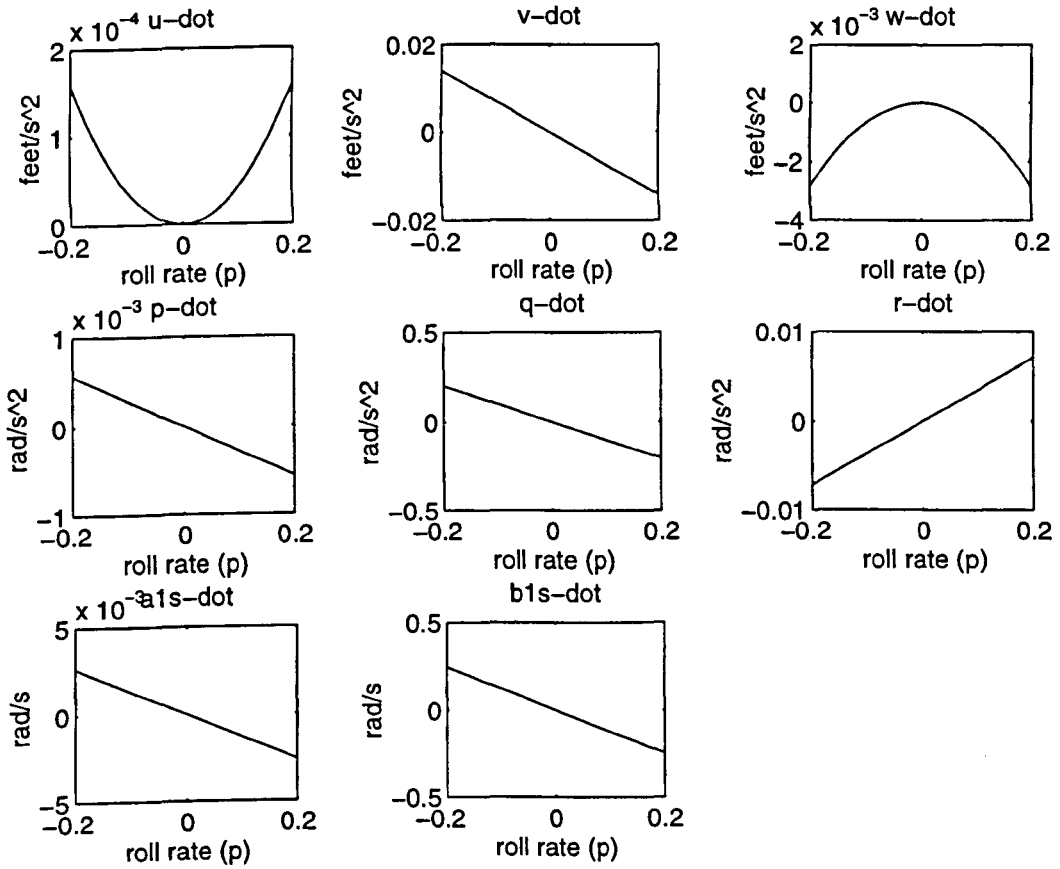


Figure 2.3.7: Plots of the change in various state derivatives against roll rate (p) for a non-linear helicopter model at hover.

Comparison of the uncertainty matrix ( $\Delta A$ ) with the linearised system matrix ( $A$ ) shows that it sometimes occurs that a zero element in the system matrix has considerable uncertainty associated with it. For instance, consider the change in vertical acceleration ( $\dot{w}$ ) due to roll rate (p), element (3, 4), we note that:

$$A_{3,4} = 0.0 \tag{2.3.41}$$

$$\Delta A_{3,4} = 0.0110 \tag{2.3.42}$$

Figure 2.3.7 shows the variation in  $\dot{w}$  as function of roll rate (p). The function is clearly even and thus can not be approximated by an odd function such as a linear expression. Thus the linearisation algorithm has correctly indicated a non-linearity.

Even functions are not uncommon at equilibrium points as illustrated by the graph of  $\dot{u}$  against  $p$  in Figure 2.3.7 and the inability of a linearisation to portray the even component of functions is a fundamental limitation.

### 2.3.2 Higher Order Approximations

A potential method for improving the fidelity of an equilibrium point representation is to use a higher order Taylor approximation. A drawback of a higher order representation is that the number of coefficients required by the representation increases rapidly. For instance, a first order representation requires  $n^2$  coefficients while a second order representation requires  $n^3$ , although the symmetry of the solution allows this figure to be reduced to  $\frac{n^3+n^2}{2}$ .

A second order approximation can faithfully represent even functions. It uses second order derivative information, often expressed as a Hessian:

$$\mathbf{H}_k^{n \times n} = \begin{bmatrix} \frac{\partial^2 f_k}{\partial x_1^2} & \cdots & \frac{\partial^2 f_k}{\partial x_1 \partial x_n} \\ \vdots & \ddots & \vdots \\ \frac{\partial^2 f_k}{\partial x_n \partial x_1} & \cdots & \frac{\partial^2 f_k}{\partial x_n^2} \end{bmatrix} \quad (2.3.43)$$

If the rows of  $\mathbf{A}$  are denoted  $\mathbf{A}^T = [\mathbf{a}_1^T, \dots, \mathbf{a}_n^T]$  then a second order system approximation is:

$$\dot{x}_k \approx \mathbf{a}_k \mathbf{x} + \frac{\mathbf{x}^T \mathbf{H}_k \mathbf{x}}{2} \quad k = 1 \dots n \quad (2.3.44)$$

The Hessian can be calculated directly using numerical perturbation. However, this involves evaluating the difference between two gradients that are themselves numerical estimates and thus may be prone to round off errors. One alternative is to use a polynomial interpolation based approach [GL96, p. 184]. Let  $h_k(i, j)$  denote the  $ij^{\text{th}}$  element of  $\mathbf{H}_k$  for  $i \neq j$  and  $ij^{\text{th}}$  element of  $\frac{\mathbf{H}_k}{2}$  for  $i = j$  then Equation (2.3.44) may re-expressed as:

$$\dot{x}_k \approx \mathbf{a}_k \mathbf{x} + \sum_{i=1}^n \sum_{j=i}^n h_k(i, j) x_i x_j \quad k = 1 \dots n \quad (2.3.45)$$

Using the following definitions:

$$\begin{aligned} \mathbf{xh}^T &= \left[ x_1 \begin{bmatrix} x_1, \dots, x_n \end{bmatrix}, x_2 \begin{bmatrix} x_2, \dots, x_n \end{bmatrix}, \dots, x_n \begin{bmatrix} x_n \end{bmatrix} \right] \\ \mathbf{h}_k &= \left[ \begin{bmatrix} h_k(1,1), \dots, h_k(1,n) \end{bmatrix}, \begin{bmatrix} h_k(2,2), \dots, h_k(2,n) \end{bmatrix}, \dots, \begin{bmatrix} h_k(n,n) \end{bmatrix} \right] \end{aligned} \quad (2.3.46)$$

Equation (2.3.45) may be written more compactly as:

$$\dot{x}_k \approx \mathbf{a}_k \mathbf{x} + \mathbf{h}_k \mathbf{xh} \quad k = 1 \dots n \quad (2.3.47)$$

A further definition:

$$\mathbf{HC}^T = \left[ \mathbf{h}_1, \dots, \mathbf{h}_n \right] \quad (2.3.48)$$

enables the second order representation to be expressed in a multivariable format:

$$\dot{\mathbf{x}} \approx \mathbf{Ax} + \mathbf{HC} \mathbf{xh} \quad (2.3.49)$$

Estimation of the combined Hessian ( $\mathbf{HC}$ ) can be reduced to a standard least squares problem as follows:

$$\dot{\mathbf{x}} \approx \mathbf{Ax} + \mathbf{HC} \mathbf{xh} \quad (2.3.50)$$

$$\mathbf{f}(\mathbf{x}_0 + \mathbf{x}, \mathbf{u}_0) - \mathbf{Ax} \approx \mathbf{HC} \mathbf{xh} \quad (2.3.51)$$

Letting  $\mathbf{y}_e = \mathbf{f}(\mathbf{x}_0 + \mathbf{x}, \mathbf{u}_0) - \mathbf{Ax}$  denote the truncation error. Then:

$$\mathbf{y}_e \approx \mathbf{HC} \mathbf{xh} \quad (2.3.52)$$

Thus we wish to find the combined Hessian ( $\mathbf{HC}$ ) that best approximates the truncation error ( $\mathbf{y}_e$ ). A good estimate of the combined Hessian ( $\mathbf{HC}$ ) will require a set of truncation errors that have been systematically produced. The algorithm employed in this work is outlined as follows:

1. Initialise the counter ( $i = 1$ ), declare the empty matrices  $\mathbf{X}_H$ ,  $\mathbf{Y}_E$  and set initial perturbation size ( $\delta$ ).
2. Positively perturb the state  $x_i$  alone. Form  $\mathbf{x}$ ,  $\mathbf{xh}$  and calculate  $\mathbf{y}_e = \mathbf{f}(\mathbf{x}_0 + \mathbf{x}, \mathbf{u}_0) - \mathbf{Ax}$ .



Append  $\mathbf{x}_h$  to  $\mathbf{X}_H$  and  $\mathbf{y}_e$  to  $\mathbf{Y}_E$  thus:

$$\mathbf{X}_H = \begin{bmatrix} \mathbf{X}_H & \mathbf{x}_h \end{bmatrix} \quad (2.3.53)$$

$$\mathbf{Y}_E = \begin{bmatrix} \mathbf{Y}_E & \mathbf{y}_e \end{bmatrix} \quad (2.3.54)$$

3. Positively perturb  $x_i$  and also perturb  $x_j$   $j = i + 1 \dots n$  both positively and negatively. For each perturbation form  $\mathbf{x}$ ,  $\mathbf{x}_h$ ,  $\mathbf{y}_e$  and update  $\mathbf{X}_H$  and  $\mathbf{Y}_E$ .
4. Repeat steps two and three, continuing to update  $\mathbf{X}_H$  and  $\mathbf{Y}_E$ , but perturb  $x_i$  *negatively*.
5. If  $i = n$  go to step six else increment  $i$  and go to step two.
6. Calculate the combined Hessian ( $\mathbf{H}_C$ ) as follows:

$$\mathbf{H}_C = \mathbf{Y}_E (\mathbf{X}_H)^\dagger \quad (2.3.55)$$

7. Check the approximation error ( $\mathbf{e}_r$ ):

$$\mathbf{e}_r = \mathbf{Y}_E - \mathbf{H}_C \mathbf{X}_H \quad (2.3.56)$$

if the error is larger than the user input tolerance decrease the perturbation size ( $\delta$ ), reset  $\mathbf{X}_H$ ,  $\mathbf{Y}_E$ ,  $i = 1$  and go to step two, else end.

The basic algorithm outlined above may be extended to maximise the perturbation size of each state individually. Figure 2.3.8 depicts a second order estimate of the state derivatives as a function of roll rate. Comparison with Figure 2.3.7 shows the Hessian system to produce a good approximation of the non-linear response.

Figure 2.3.9 displays the linear, Hessian and nonlinear system response for a one feet/s and ten feet/s perturbation in forward velocity. It shows that for the small perturbation both the linear and Hessian systems show good fidelity. For the large perturbation the Hessian system is a better approximation than the linear system but still diverges from the non-linear response.

Generally, for deviations near the equilibrium point the Hessian system does show improved or equal fidelity to the linear response. However, if the response diverges significantly from the trim point then the quadratic contribution from the Hessian matrix increases disproportionately, and the response rapidly loses fidelity. The Hessian system is relatively straightforward to generate and although non-linear itself, it is more amenable to non-linear control theory, such as non-linear inverse dynamics [SC94], than the full non-linear model.

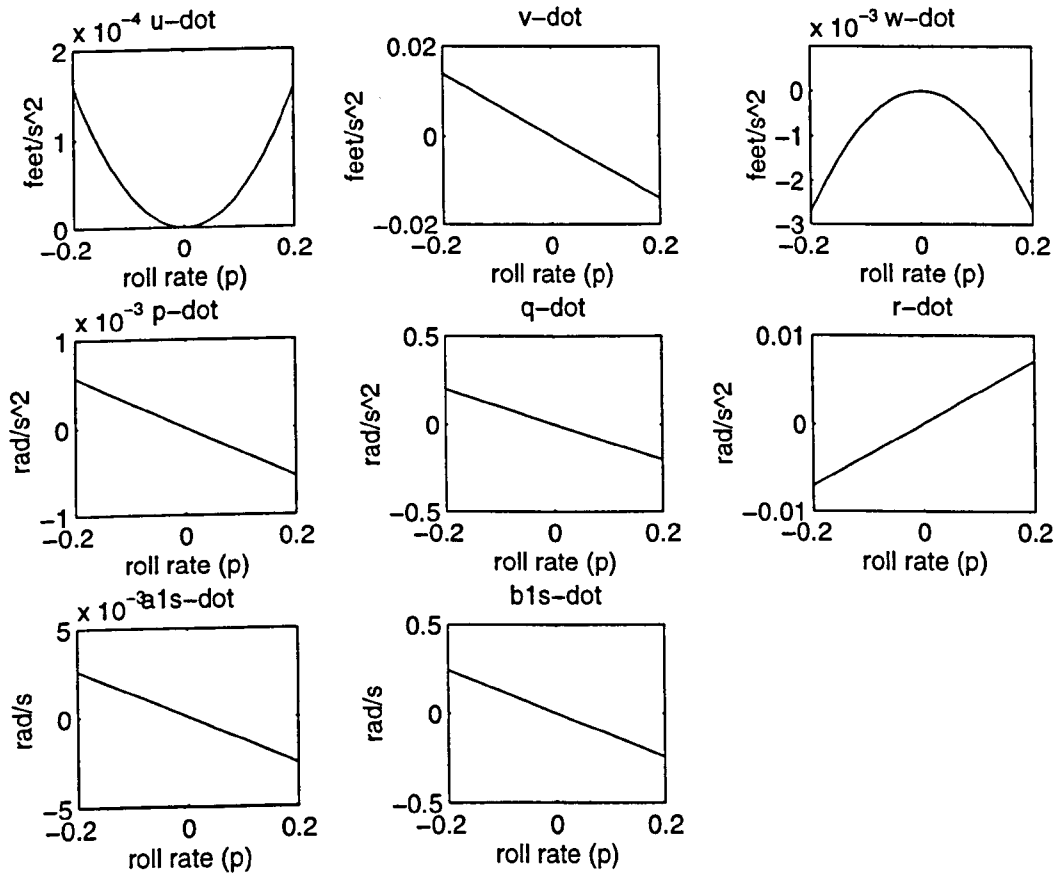


Figure 2.3.8: Plots of the change in various state derivatives against roll rate ( $p$ ) for a second order model (Jacobian + Hessian) of a helicopter at hover.

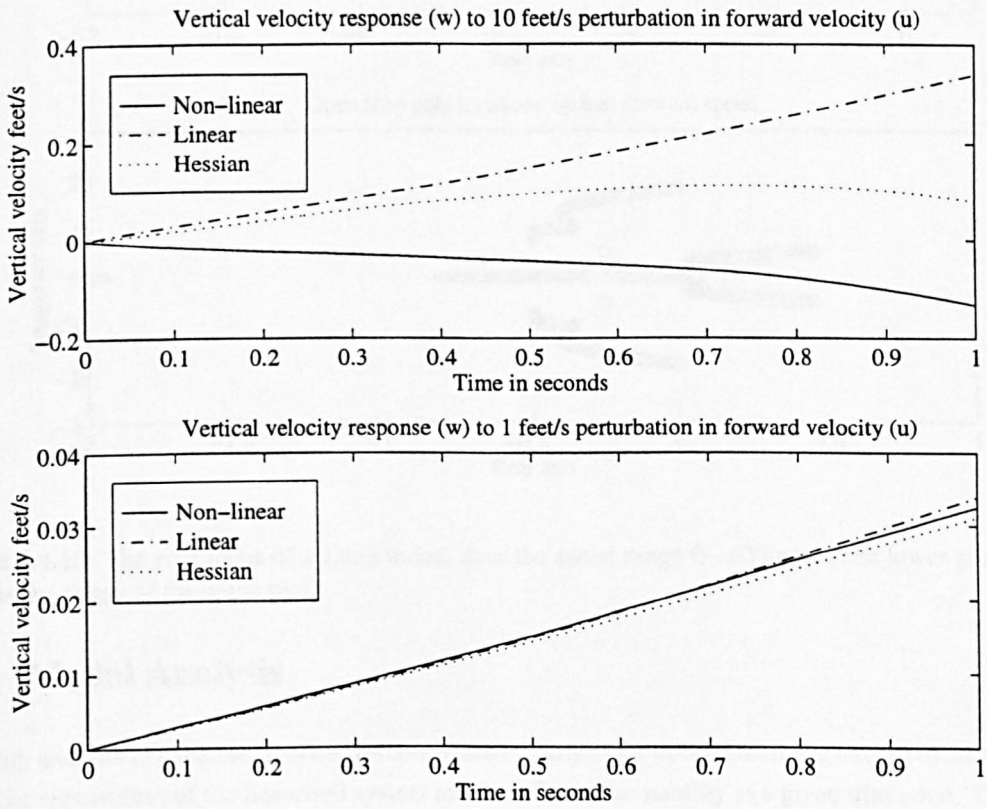


Figure 2.3.9: Vertical velocity response of a linear (Jacobian only), Hessian (Jacobian + Hessian) and non-linear helicopter model at hover for 1 and 10 feet/s perturbation in forward velocity.

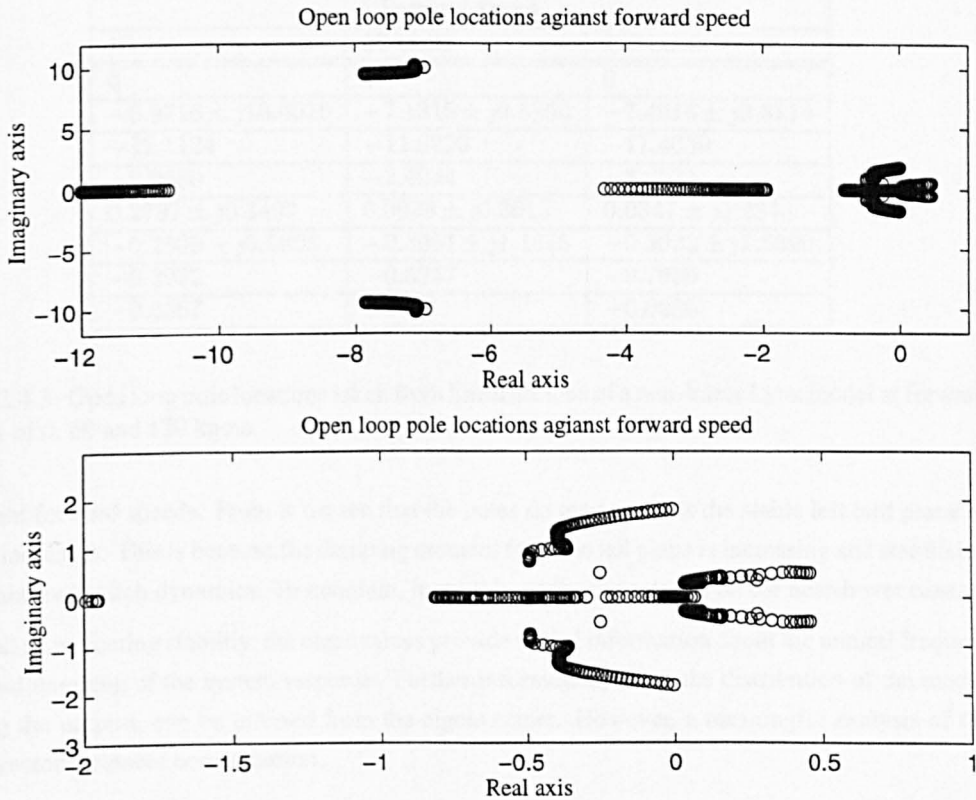


Figure 2.4.10: The root locus of a Lynx model over the speed range 0-160 knots (The lower plot depicts the origin of the upper plot).

## 2.4 Modal Analysis

Stability analysis of linearised models has contributed greatly to the understanding of aircraft dynamics. The eigenvalues of the linearised system matrix indicate the stability at a given trim point. To assess stability over a range of trim conditions, a linearisation is calculated at each trim point and its stability examined. This technique is most commonly used to examine the stability variation with forward speed.

Figure 2.4.10 depicts the system pole locations over a speed range<sup>7</sup> of 0 to 160 knots. It shows that the pole locations vary significantly with speed. This is because the character of the helicopter dynamics change with speed. In the hover, flapping dynamics are not excited and tail plane and fin contribute little to the system dynamics. As speed increases the empennage contribution increases and flapping is excited, leading to a more asymmetric response. Table 2.4.3 displays the pole locations at three

<sup>7</sup>The helicopter is trimmed to zero side slip over the entire speed range.

Forward Speed		
Hover	60 knots	120 knots
0	0	0
$-6.9716 \pm j10.0016$	$-7.1315 \pm j9.6800$	$-7.4916 \pm j9.5114$
-12.1124	-11.9220	-11.4039
-2.0680	-2.4044	-3.0631
$0.2797 \pm j0.3497$	$0.0929 \pm j0.3615$	$0.0347 \pm j0.2844$
$-0.2509 \pm j0.5005$	$-0.3961 \pm j1.1615$	$-0.3023 \pm j1.5390$
-0.2972	-0.5257	-0.7909
-0.3367	0.0150	-0.0280

Table 2.4.3: Open loop pole locations taken from linearisations of a non-linear Lynx model at forward speeds of 0, 60 and 120 knots.

different forward speeds. From it we see that the poles do tend towards the stable left half plane as speed increases. This is because the damping moment from the tail plane is increasing and stabilising the main rotor pitch dynamics. To maintain, focus this work concentrates on the near-hover case.

As well as indicating stability, the eigenvalues provide useful information about the natural frequencies and damping of the system response. Further information, about the distribution of the modes among the outputs, can be inferred from the eigenvectors. However, a meaningful analysis of the eigenvectors requires normalisation.

### 2.4.1 Normalisation

Examination of the right eigenvectors can reveal which modes will be predominately observed in each state. If the states have physical significance, the mode distribution can give insightful information about the underlying dynamics. If the states do not have physical significance, the mode observability matrix ( $\mathbf{CV}$ ) should be used instead. Note that  $\mathbf{V} = [\mathbf{v}_1, \dots, \mathbf{v}_n]$  denotes a matrix of right eigenvectors ( $\mathbf{v}_k$ ).

For a fair evaluation of mode dominance the states must be normalised [GLP89a, Web92]. This normalisation is has no formal mathematical basis but is a subjective process that allows states with different physical units to be compared. Different engineering approaches can be taken:

- Use the maximum value indicated in the Handling Qualities specification.
- Use values found in normal operating conditions. Note that the values should be deviations from trim.

Ultimately, normalisation depends on the pilot perception: would a 1.0 feet/s oscillation in forward velocity be more or less noticeable than a 0.02 rad/s oscillation in roll rate? Table 2.4.4 shows the normalisation values used in this work.

State	Value	State	Value	Input	Value
u	5 ft/s	$\theta$	0.1 rad	$\theta_0$	0.02 rad
v	5 ft/s	$\phi$	0.1 rad	$\theta_t$	0.035 rad
w	5 ft/s	$\psi$	0.1 rad	$A_1$	0.02 rad
p	0.1 rad/s	$a_{1,s}$	0.025 rad	$B_1$	0.035 rad
q	0.1 rad/s	$b_{1,s}$	0.025 rad		
r	0.1 rad/s				

Table 2.4.4: State and input normalisation values.

Normalisation is applied by re-defining the state and input vectors. Let us define two normalisation transforms.

$$\mathbf{X}_N = \text{diag}(5, 5, 5, 0.1, 0.1, 0.1, 0.1, 0.1, 0.1, 0.025, 0.025) \quad (2.4.57)$$

$$\mathbf{Y}_N = \text{diag}(0.02, 0.035, 0.02, 0.035) \quad (2.4.58)$$

The transformed states and inputs are:

$$\mathbf{x} = \mathbf{X}_N \mathbf{x}_n \quad (2.4.59)$$

$$\mathbf{u} = \mathbf{Y}_N \mathbf{u}_n \quad (2.4.60)$$

Thus the state space representation is transformed as follows:

$$\dot{\mathbf{x}} = \mathbf{A}\mathbf{X}_N \mathbf{x}_n + \mathbf{B}\mathbf{Y}_N \mathbf{u}_n \quad (2.4.61)$$

$$\mathbf{X}_N \mathbf{x}_n = \mathbf{A}\mathbf{X}_N \mathbf{x}_n + \mathbf{B}\mathbf{Y}_N \mathbf{u}_n \quad (2.4.62)$$

$$\dot{\mathbf{x}}_n = \mathbf{X}_N^{-1} \mathbf{A}\mathbf{X}_N \mathbf{x}_n + \mathbf{X}_N^{-1} \mathbf{B}\mathbf{Y}_N \mathbf{u}_n \quad (2.4.63)$$

The open loop right eigenvectors are shown in Table 2.4.5. From them, it can be seen that the eigenvalue at the origin is associated solely with the heading and is known as the heading integration mode. We also see that the two first order modes at -12.11 and -2.07 are predominately associated with roll and pitch respectively. They are subsidence modes and are manifest as follows. An angular rate in one axis will cause the rotor to precess in the orthogonal axis this excites the flapping dynamics which causes the disk to tilt opposing the original angular rate. The two remaining first order modes (-0.30, -0.34) are definitely linked with the yaw dynamics and further analysis will show that they are predominately associated with the heave and yaw subsidence modes. The fast complex mode

Output	Open Loop Right Eigenvectors			
Modes	0	$-6.97 \pm j10.00$	$-12.11$	$-2.07$
$u$	0.00	$0.00 \pm j0.00$	-0.01	0.15
$v$	0.00	$0.00 \pm j0.00$	0.00	-0.04
$w$	0.00	$0.00 \pm j0.00$	0.00	0.01
$p$	0.00	$-0.13 \pm j0.89$	-0.45	-0.16
$q$	0.00	$-0.10 \pm j0.02$	0.26	-0.80
$r$	0.00	$-0.02 \pm j0.16$	-0.08	0.00
$\phi$	0.00	$0.07 \pm j - 0.03$	0.04	0.08
$\theta$	0.00	$0.01 \pm j0.01$	-0.02	0.39
$\psi$	<b>1.00</b>	$0.01 \pm j - 0.01$	0.01	-0.02
$a_{1s}$	0.00	$0.08 \pm j - 0.05$	<b>-0.84</b>	0.34
$b_{1s}$	0.00	<b><math>-0.26 \pm j - 0.27</math></b>	0.13	0.20
Modes	$0.28 \pm j0.35$	$-0.25 \pm j0.50$	$-0.30$	$-0.34$
$u$	$-0.15 \pm j0.12$	$0.14 \pm j - 0.04$	-0.04	0.05
$v$	$0.15 \pm j0.44$	$0.07 \pm j0.40$	-0.06	0.07
$w$	$-0.01 \pm j0.03$	$0.00 \pm j0.02$	0.01	0.06
$p$	$-0.16 \pm j0.01$	$0.11 \pm j - 0.14$	-0.02	0.03
$q$	$0.02 \pm j0.05$	$0.03 \pm j0.04$	-0.01	0.01
$r$	$0.25 \pm j0.20$	$0.38 \pm j - 0.11$	0.28	-0.32
$\phi$	$-0.17 \pm j0.29$	$-0.34 \pm j - 0.09$	0.02	-0.03
$\theta$	$0.14 \pm j0.03$	$0.02 \pm j - 0.12$	-0.02	0.02
$\psi$	<b><math>0.68 \pm j - 0.15</math></b>	<b><math>-0.47 \pm j - 0.51</math></b>	<b>-0.96</b>	<b>0.94</b>
$a_{1s}$	$-0.04 \pm j0.01$	$0.02 \pm j - 0.03$	0.00	0.01
$b_{1s}$	$-0.01 \pm j - 0.01$	$-0.01 \pm j - 0.01$	0.00	0.00

Table 2.4.5: Open loop eigenvectors for a Lynx linearisation at hover.

$(-6.97 \pm j10.00)$  is the regressive flapping mode. It is well damped ( $\zeta = 0.57$ ) but is coupled into the roll dynamics.

Examination of the right eigenvector which, in this case, is the same as the mode observability matrix, gives half of the available information, that is how, the modes couple into the states. The reciprocal information of how the modes are excited by the inputs can be found by examining the mode controllability matrix ( $\mathbf{WB}$ ). Note, that  $\mathbf{W}^T = [\mathbf{w}_1^T, \dots, \mathbf{w}_n^T]$  denotes a matrix of left eigenvectors ( $\mathbf{w}_k$ ). The two pieces of information can be combined. This leads to *residue analysis*. Suppose that the system transfer function matrix is  $\mathbf{G}(s)$  and the  $ij^{th}$  element is denoted  $g_{ij}(s)$ . The transfer function matrix may be expressed in dyadic form as follows:

$$\mathbf{G}(s) = \sum_{k=1}^n \frac{\mathbf{Cv}_k \mathbf{w}_k \mathbf{B}}{s - \lambda_k} \quad (2.4.64)$$

Mode	$\theta_0 \mapsto w$	$\theta_t \mapsto r$
0.00	0.00	0.00
$-6.97 \pm j10.00$	$0.00 \pm j0.00$	$-0.03 \pm j0.02$
-12.11	0.00	-0.00
-2.07	0.00	-0.00
$0.28 \pm j0.35$	$0.01 \pm j0.00$	$-0.11 \pm j0.10$
$-0.25 \pm j0.50$	$0.00 \pm j0.01$	$-0.26 \pm j0.02$
-0.30	-0.17	-1.57
-0.34	-1.06	-0.45

Table 2.4.6: Transfer function residues for main rotor collective to vertical velocity and tail rotor collective to yaw rate.

Let the input (**B**) and output (**C**) matrices be decomposed as follows:

$$\mathbf{B} = [\mathbf{b}_1, \dots, \mathbf{b}_r] \quad (2.4.65)$$

$$\mathbf{C} = [\mathbf{c}_1^T, \dots, \mathbf{c}_m^T] \quad (2.4.66)$$

The individual transfer functions may be expressed as:

$$g_{ij}(s) = \sum_{k=1}^n \frac{\tau_k}{s - \lambda_k} \quad (2.4.67)$$

where  $\tau_k$  is a residue and is equal to:

$$\tau_k = \mathbf{c}_i \mathbf{v}_k \mathbf{w}_k \mathbf{b}_j \quad (2.4.68)$$

Examination of the residues can reveal which mode is dominant in a particular transfer functions. For instance, consider main rotor collective ( $\theta_0$ ) to vertical velocity ( $w$ ) and tail rotor collective ( $\theta_t$ ) to yaw rate ( $r$ ). Then, Table 2.4.6 clearly shows that 0.34 is the dominant heave mode and 0.30 is the dominant yaw mode. This information could not be easily deduced from the eigenvectors alone.

While much information can be gained from the modal structure, for greater engineering insight it is useful to develop a model that just expresses the quintessential dynamics.



## 2.4.2 Model Reduction

The heading state affects no other modes and can thus be simply truncated from the model. If we assume that the flapping dynamics are much faster than the body dynamics, we may residualise the flapping dynamics. Suppose the state space system is partitioned as follows:

$$\begin{bmatrix} \dot{x}_1 \\ \dot{x}_2 \end{bmatrix} = \begin{bmatrix} A_{11} & A_{12} \\ A_{21} & A_{22} \end{bmatrix} \begin{bmatrix} x_1 \\ x_2 \end{bmatrix} + \begin{bmatrix} B_1 \\ B_2 \end{bmatrix} u \quad (2.4.69)$$

$$y = \begin{bmatrix} C_1 & C_2 \end{bmatrix} \begin{bmatrix} x_1 \\ x_2 \end{bmatrix} \quad (2.4.70)$$

If the flapping angles ( $a_{1s}$ ,  $b_{1s}$ ) are associated with  $x_2$  then steady state flapping implies  $\dot{x}_2 = 0$ . Thus:

$$0 = A_{21}x_1 + A_{22}x_2 + B_2u \quad (2.4.71)$$

$$x_2 = -A_{22}^{-1}A_{21}x_1 - A_{22}^{-1}B_2u \quad (2.4.72)$$

Substituting  $x_2$  back into the system matrices gives:

$$\dot{x}_1 = (A_{11} - A_{12}A_{22}^{-1}A_{21})x_1 + (B_1 - A_{12}A_{22}^{-1}B_2)u \quad (2.4.73)$$

$$y = (C_1 - C_2A_{22}^{-1}A_{21})x_1 - (C_2A_{22}^{-1}B_2)u \quad (2.4.74)$$

Finally, to summarise the reduced order system is:

$$\hat{A} = A_{11} - A_{12}A_{22}^{-1}A_{21} \quad (2.4.75)$$

$$\hat{B} = B_1 - A_{12}A_{22}^{-1}B_2 \quad (2.4.76)$$

$$\hat{C} = C_1 - C_2A_{22}^{-1}A_{21} \quad (2.4.77)$$

$$\hat{D} = C_2A_{22}^{-1}B_2 \quad (2.4.78)$$

After truncation and residualisation the system is eighth order. Whilst the order is only reduced by three, the number of system matrix coefficients is almost halved, offering considerable simplification. Appendix A.2 contains the state space matrices for the reduced order system.

Table 2.4.7 compares the eigenvalues of the reduced order system with the original eleventh order system.

System Eigenvalues	
Eleventh Order	Eighth Order
0	
$-6.9716 \pm j10.0016$	
-12.1124	-9.2980
-2.0680	-1.9464
$0.2797 \pm j0.3497$	$0.2749 \pm j0.3505$
$-0.2509 \pm j0.5005$	$-0.2574 \pm j0.5037$
-0.2972	-0.2982
-0.3367	-0.3376

Table 2.4.7: Pole locations for the full and reduced order helicopter models at hover.

The correspondence between the eigenvalues is very good except for the roll subsidence mode ( $-9.298$ ). This is to be expected since the roll mode is coupled into flapping dynamics. Once the system has been reduced to a more manageable size, it is instructive to relate the system matrix coefficients to the system modes. One approach [Pad96, p. 329] [Pro90] is to apply simplifying assumptions, such as decoupled longitudinal and lateral dynamics, to produce simple subsystems, where the relationship between the modes and coefficients is easily derived. This approach does offer considerable physical insight but often breaks down for helicopters because the cross-coupling effects are too strong to neglect. For instance, Table 2.4.8 compares the eigenvalues for the longitudinal ( $u, w, q, \theta$ ) and lateral ( $v, p, r, \phi$ ) subsystems. Some modes, such as the roll subsidence and heave modes, are still recognisable but, generally, the decoupled approximation is poor.

System Eigenvalues		
Full Model	Longs.	Lats.
-9.2980		-9.7509
-1.9464	-1.7226	
$0.2749 \pm j0.3505$	$0.0836 \pm j0.5345$	
$-0.2574 \pm j0.5037$		$-0.0364 \pm j0.4153$
-0.2982		-0.1424
-0.3376	-0.3234	

Table 2.4.8: A comparison of the full system and decoupled subsystem poles.

An alternative approach is use a sensitivity analysis to simplify the model. Coefficients that do not have a significant effect on the eigenstructure are eliminated and the resulting structure is analysed. The basic algorithm is outlined as follows:

1. Initialise the counter  $k = 1$  and  $l = 1$ .
2. Calculate the sensitivity of each element ( $a_{ij}$ ) of the system matrix ( $\mathbf{A}$ ) with respect to the eigenvalue  $\lambda_k$  and multiply it by the respective element of  $\mathbf{A}$ .

$$S_{ij} = \left| a_{ij} \frac{\partial \lambda}{\partial a_{ij}} \right| \tag{2.4.79}$$

3. Reset the counter  $l = 1$ .
4. Select the  $l$  largest values of  $S_{ij}$  and form an system matrix ( $A_k$ ) with only the corresponding elements  $a_{ij}$ .
5. If no eigenvalue of  $A_k$  is acceptably close to  $\lambda_k$  then increment  $l$  and go to step four.
6. If  $k$  is not equal to  $n$  increment  $k$  and go to step two else form a simplified system matrix that is the union of all  $A_k$ .

The simplified system matrix is shown below, it is not recommended to use this system matrix for simulation or design but only as an analysis tool.

$$As = \begin{bmatrix} 0 & 0 & 0 & 0 & 0 & 0 & 0 & -32.1 \\ 0 & 0 & 0 & 0 & 0 & 0 & 32.1 & 0 \\ 0 & 0 & -0.32 & 0 & 0 & 0 & 0 & 0 \\ 0.17 & -0.056 & 0 & -9.71 & 4.51 & 0 & 0 & 0 \\ 0.016 & 0 & 0 & -0.79 & -1.52 & 0 & 0 & 0 \\ 0.030 & 0 & 0 & -1.71 & 0 & -0.22 & 0 & 0 \\ 0 & 0 & 0 & 1.00 & 0 & 0 & 0 & 0 \\ 0 & 0 & 0 & 0 & 1.00 & 0 & 0 & 0 \end{bmatrix} \tag{2.4.80}$$

Table 2.4.9 compares the eigenvalues with the full system matrix. While there is certainly some mismatch, this very simple model does capture the essentials of the system dynamics.

System Eigenvalues	
Reduced Model	Simple Model
-9.2980	-9.2759
-1.9464	-1.9541
$0.2749 \pm j0.3505$	$0.2494 \pm j0.3648$
$-0.2574 \pm j0.5037$	$-0.2508 \pm j0.4432$
-0.2982	-0.2208
-0.3376	-0.3230

Table 2.4.9: System poles for a reduced order and then simplified helicopter model at hover.

Figure 2.4.11 illustrates the simplified system and allows some key stability derivative to be identified, as follows:

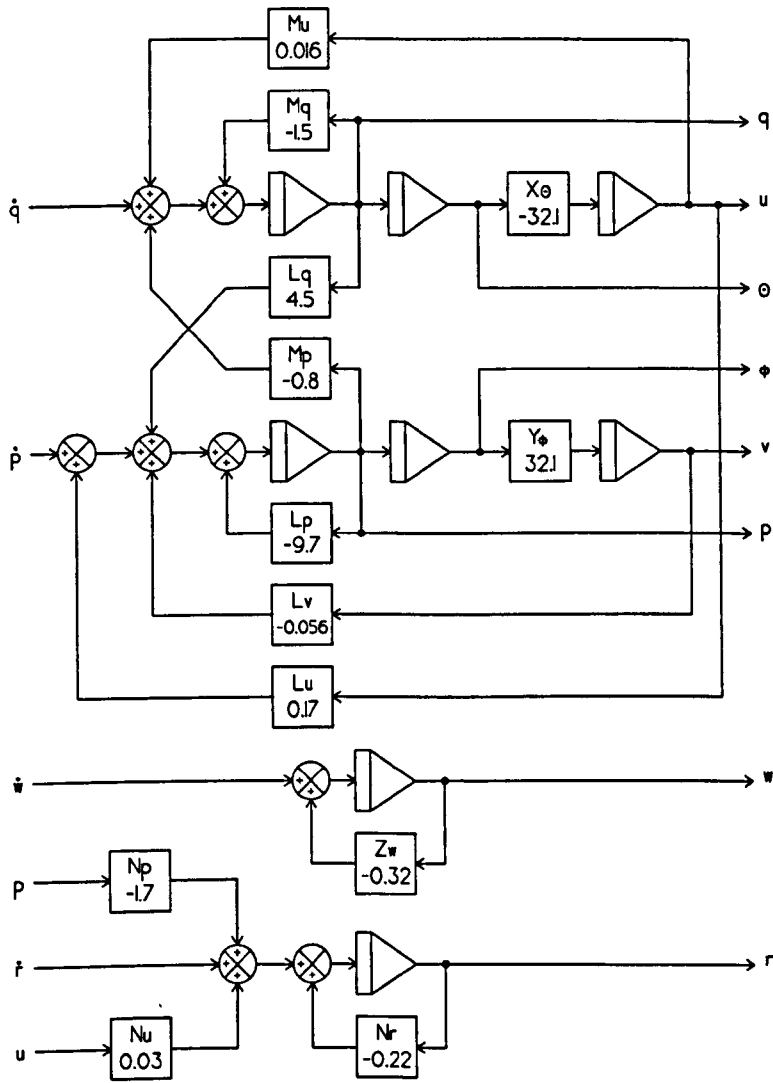


Figure 2.4.11: Simplified helicopter dynamics in hover (see Equation (2.4.80)).

- The damping derivatives  $L_p$  ( $-9.7$ ) and  $M_q$  ( $-1.5$ ) are dominant in determining the roll and pitch subsidence modes.
- The cross-coupling derivatives,  $L_q$  ( $4.5$ ) and  $M_p$  ( $-0.79$ ) are fundamental to the helicopter dynamics. They are pre-dominantly due to the response phasing of the flapping dynamics not being exactly equal to  $90^\circ$ . In this case the modelled helicopter has a hingeless rotor with a large effective hinge offset. This leads to a response phase of approximately  $76^\circ$ . Thus the flapping dynamics will not just oppose the pitch and roll motion but also induce a moment in the orthogonal axis. The ratio of the derivatives is in proportion to the relative moments of inertia for the roll and pitch axes, about 1 to 6. The low moment of inertia in the roll axis makes this axis susceptible to main rotor and other cross-couplings.
- The damping derivative  $Z_w$  ( $-0.32$ ) dominates the heave dynamics. This is because change in vertical velocity alters the main rotor inflow which causes the main rotor thrust to oppose and thus damp the vertical motion.
- The damping  $N_r$  ( $-0.22$ ) is important in damping the yaw dynamics. At hover this is mainly manifest as the yaw rate changing the tail rotor inflow and thus the tail rotor thrust damping the yaw motion. However, as forward speed increases, the fin will become more effective and conventional weathercock stability will begin to prevail.
- The force derivatives  $X_\theta$  ( $-32.1$ ) and  $Y_\phi$  ( $32.1$ ) are due to changes in the body attitudes causing the main rotor thrust vector to be tilted.
- The derivatives  $M_u$  ( $0.79$ ) and  $L_v$  ( $-2.8$ ) are due to changes in velocity exciting the flapping dynamics, which causes *flapback* and thus a body moment. These derivatives are very important to dynamic stability in hover.
- The cross-coupling derivatives  $L_u$ ,  $N_p$  and  $N_u$  stem from different physical sources.  $L_u$  is due to the main rotor coning causing differential changes in incidence for a perturbation in forward velocity.  $N_u$  is due to changes in main rotor torque generating yaw moments and  $N_p$  is due to the product of inertia  $I_{xz}$ .

### 2.4.3 The System Zeros

A complete modal analysis of the open loop helicopter should also examine the system zeros [MK76, SK76, Mac72, Ros70]. The invariant zeros are the values of  $s$  for which the matrix:

$$\begin{bmatrix} s\mathbf{I} - \mathbf{A} & \mathbf{B} \\ \mathbf{C} & \mathbf{0} \end{bmatrix} \quad (2.4.81)$$

loses rank. They can be computed using numerically stable algorithms [END82]. For a fully controllable-observable system these are also the transmission zeros. Using an output matrix equal to  $\mathbf{C} = \mathbf{I}_8$  the reduced order system of Appendix A.2 is found to have no transmission zeros.

It is also insightful to consider transmission zeros with respect to subsets of the inputs and outputs. The simplified system of Figure 2.4.11 illustrates that the states  $u$ ,  $\theta$ ,  $q$  and  $v$ ,  $\phi$ ,  $p$  are predominantly related by simple integration. This can be expected to introduce some near-origin zeros in the appropriate outputs. For instance, suppose that the relationship between forward speed ( $u$ ) and longitudinal cyclic ( $B_1$ ) is:

$$\frac{u(s)}{B_1} = \frac{n(s)}{d(s)} \quad (2.4.82)$$

then for the simplified system the relationship to pitch attitude ( $\theta$ ) and rate ( $q$ ) is:

$$\frac{\theta(s)}{B_1} = \frac{s n(s)}{d(s)} \quad \frac{q(s)}{B_1} = \frac{s^2 n(s)}{d(s)} \quad (2.4.83)$$

A dual argument applies to the lateral channel. The transmission zeros of the reduced order system with respect to all outputs, except the linear velocities ( $u$ ,  $v$ ), are shown in Table 2.4.10. It can be seen that two near-origin zeros are present due to the phase relationship between the linear velocities and the body attitudes. Table 2.4.10 also shows that additionally removing the system attitudes introduces two further near-origin zeros due to the phase relationship between the attitudes and rates.

Outputs	Zeros			
	$p, q, r, \theta, \phi, w$	-0.0039	-0.0020	--
$p, q, r, w$	-0.0039	-0.0020	0.0000	0.0000

Table 2.4.10: System zeros for different output combinations taken from the reduced order helicopter model at hover (not simplified).

The zero directions ( $\mathbf{x}_z$ ) are defined as:

$$\mathbf{0} = \begin{bmatrix} z\mathbf{I} - \mathbf{A} & \mathbf{B} \\ \mathbf{C} & \mathbf{0} \end{bmatrix} \begin{bmatrix} \mathbf{x}_z \\ \mathbf{u}_z \end{bmatrix} \quad (2.4.84)$$

where  $z$  is a system zero. They give information about the orientation of the state and input vectors when a transmission zero blocks all output. Table 2.4.11 shows that the zero directions for the helicopter system zeros.

State/Input	Zeros			
<i>Zero</i>	-0.0039	-0.0020	0.0000	0.0000
<i>u</i>	0.0000	-0.7101	0.3341	-0.8832
<i>v</i>	0.9818	-0.6709	-0.9072	-0.3768
<i>w</i>	0.0000	0.0000	0.0000	0.0000
<i>p</i>	0.0000	0.0000	0.0000	0.0000
<i>q</i>	0.0000	0.0000	0.0000	0.0000
<i>r</i>	0.0000	0.0000	0.0000	0.0000
$\phi$	0.0000	0.0000	-0.0064	0.0002
$\theta$	0.0000	0.0000	-0.0011	0.0028
$A_1$	0.1099	0.1598	-0.2121	0.2500
$B_1$	0.0002	-0.0789	0.0369	-0.0980
$\theta_0$	0.0000	-0.0177	0.0082	-0.0221
$\theta_t$	0.1546	-0.1168	-0.1378	-0.0733

Table 2.4.11: System zero directions for the reduced order helicopter model at hover (see Table 2.4.10).

The zero directions clearly show that  $-0.0039$  is the lateral channel zero and  $-0.0020$  is the longitudinal channel zero which is seen to be strongly coupled in the lateral channel, this is due to the derivative  $L_u$ . Less information can be discerned from the zeros at  $0.0000$  since they are repeated and the zero directions span a two dimensional subspace.

From the preceding modal analysis we can see that the helicopter is highly cross-coupled and has an unstable raw airframe. It is thus a very difficult vehicle to fly and, in practice, a flight control system is required to aid the pilot.

## 2.5 Flight Control

Flying a helicopter without the assistance of a stability augmentation system (SAS) or automatic flight control system (AFCS) is a taxing task for any pilot, since the pilot must apply his own agency to stabilise the airframe. As the basic flying task demands a high pilot workload, this limits the other mission-related tasks that the pilot can reasonably be expected to accomplish. Fortunately, even a very simple SAS structure [McI90] can stabilise the airframe and bring the pilot workload down to a comfortable level. However, it should be appreciated that the purpose of the SAS is not merely to stabilise but rather to make the helicopter fly in a way that most assists the pilot. For instance, the SAS may even introduce a slow unstable mode because the pilot finds this characteristic desirable. The properties of a good SAS are defined by Handling Qualities Specifications. Handling Qualities are concerned with the pilot's perception of how the helicopter flies and Chapter 3 will look at them in some detail.

The AFCS is a complicated and challenging system to develop since it must resolve a wide range of

implementation and control problems. Some of the requirements on a modern AFCS are listed below:

- Alleviation of disturbances such as gusts and turbulence while not impeding pilot commands. Also to provide good ride comfort and fuel economy.
- Be fully integrated with the navigation system, mission management computer, engine management system and sensor units.
- Must be fault tolerant, incorporating self verification, multiple redundant systems and limited authority.
- Should provide a range of autopilot functions from simple heading, height and speed hold to more complicated functions such as auto-land and course following. All transitions between autopilot functions should be smooth and all possible contentions must be fail-safe, innocuously resolved and easily overridden by the pilot.
- Finally the system must implement control laws that attain the required flying qualities throughout the flight envelope. This may require scheduling of several control laws.

This work focuses on control law design. The requirements above show that this is only one element of the complete AFCS. The minimal control law that will stabilise a helicopter requires both attitude and rate feedback [Pad96, Hoh88] as illustrated below:

$$A_{1s} = k_p p + k_\phi (\phi - \phi_r) \quad (2.5.85)$$

$$B_{1s} = k_q q + k_\theta (\theta - \theta_r) \quad (2.5.86)$$

$$\theta_t = k_r r \quad (2.5.87)$$

Where  $k_p$ ,  $k_\phi$ ,  $k_q$ ,  $k_\theta$  and  $k_r$  are the feedback gains,  $\phi_r$  and  $\theta_r$  are offset values that the pilot adjusts to establish a new trim datum.

An alternative control law that does not require offset inputs is shown in Figure 2.5.12.

This control law uses only rate feedback, but generates attitude feedback by integrating the rate signal. A *leaky* integration is employed, so that persistent attitude errors will decay to zero and thereby allow the pilot to establish a new trim datum.

Modern control laws are generally more complicated than those outlined above and require a range of equipment to be implemented as part of a modern AFCS.

### 2.5.1 Auto-Stabilisation Equipment

Figure 2.5.13 is a schematic illustration of some typical auto-stabilisation equipment found in the lateral and longitudinal channels of a modern helicopter. The key components are described as follows:



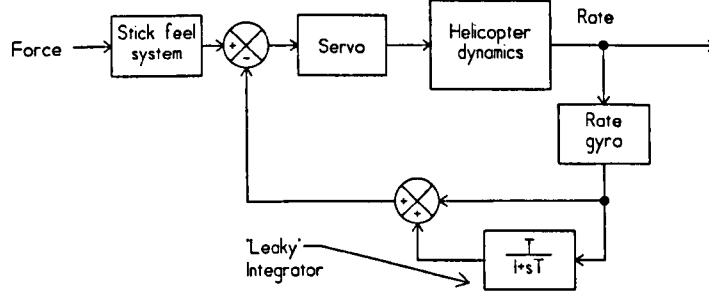


Figure 2.5.12: A simple control law.

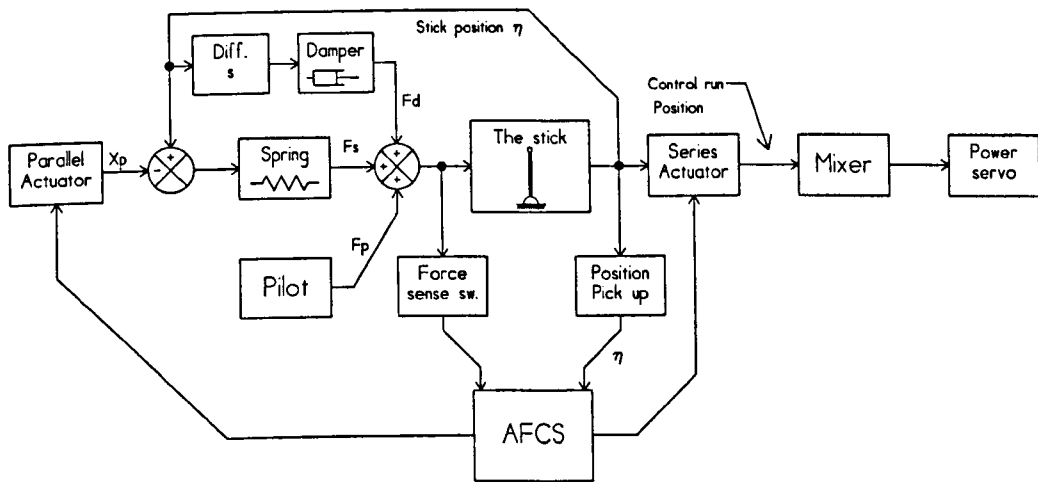


Figure 2.5.13: Typical auto-stabilisation equipment.

**The stick** is used by the pilot to command cyclic pitch. It is directly connected to the power servos via the control runs.

**The series actuators** are inserted in the control runs and change length to operate the power servos. They are generally fast acting electrical actuators with a typical bandwidth of 30Hz. For safety they have limited authority, usually  $\pm 10\%$ . They are operated by the SAS and provide the small control adjustments required to maintain trim and stability.

**The parallel actuator** is an electrical servo with a very slow response. It is connected to the stick via a spring and thus determines current stick datum. The actuator is operated in at least three ways:

1. by the autopilot to execute turn commands by moving the stick.

2. by the pilot directly using the *beep* button to fix a new stick datum after a change in trim condition.
3. by the SAS to centre the series actuators so that they can exploit their full travel.

The parallel actuator has full authority but its slow motion and spring connection ensure that it is easily overridden. Thus the parallel actuator systems driving it are not safety critical.

**The mixer** is effectively the orientation of power servos on the swash plate. An angle is chosen that minimises the cross-coupling between longitudinal and lateral pilot commands.

**The spring** centres the stick and forms part of the artificial stick feel system by exerting a force for the pilot to oppose. In theory the spring should be tightened as forward speed increases. However, in practice, the small speed range of the helicopter makes this an unnecessary embellishment.

**The power servos** are hydraulic jacks that move the swash plate. They exhibit a much slower dynamic response than the series actuator and are often modelled as a dominant first order lag.

**The damper** may be included as part of the artificial stick feel system to resist rapid stick movement and ensure the stick centres without overshoot. The tactile cues provided by the stick feel system are important for handling qualities.

**The force sense switch** is open when the pilot makes large stick movements. It is used to disengage the attitude feedback so that pilot commands are not opposed by the SAS and also to enable the pilot to demand a rate response.

As well as the equipment outlined above, mechanical interlinks are generally employed to provide some decoupling of the pilot commands. For instance, adjustment of the collective lever may also move the longitudinal cyclic and tail rotor collective control runs. This mitigates the coupling of main rotor collective into yaw and pitch, due to the torque reaction and increased flapping.

The Westland Helicopters EH101 actuation system is shown in Figure 2.5.14, with the aircraft body removed. This diagram clearly shows the dual pilot controls, the parallel and series actuators, the main rotor power servos and the mechanical control runs, which pass under the pilot seats and behind their backs.

## 2.5.2 A Conventional Control Law

A control law suitable for the ASE described above is shown in Figure 2.5.15. The control law uses a gyro to measure attitude which is passed through a band limited differentiator ( $T_1, T_3 \approx 0.05\text{sec}$ ) to provide attitude and rate feedback. The attitude and rate feedback gains are denoted  $K_\theta, K_{\dot{\phi}_1}, K_{\dot{\phi}_2}$  and  $K_{\dot{\theta}}, K_{\dot{\phi}}$  respectively. For large pilot commands the force sense logic disengages the attitude feedback giving the pilot rate command. But the roll axis still requires some attitude feedback to

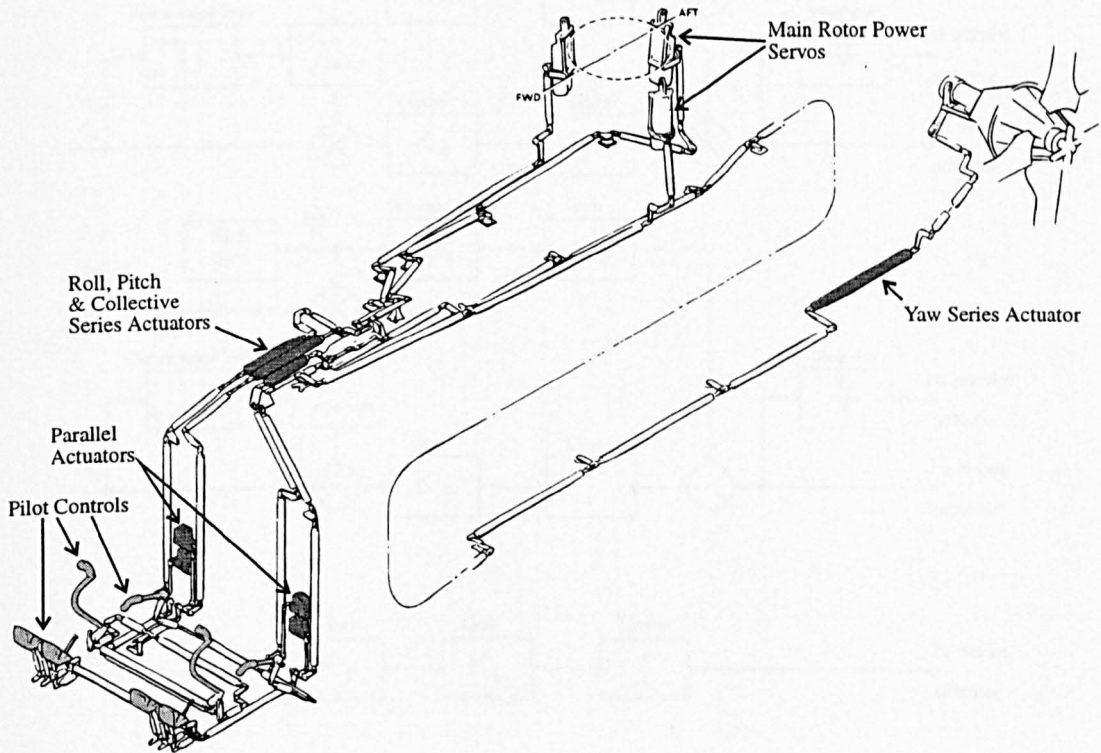


Figure 2.5.14: The Westland Helicopters EH101 actuation system.

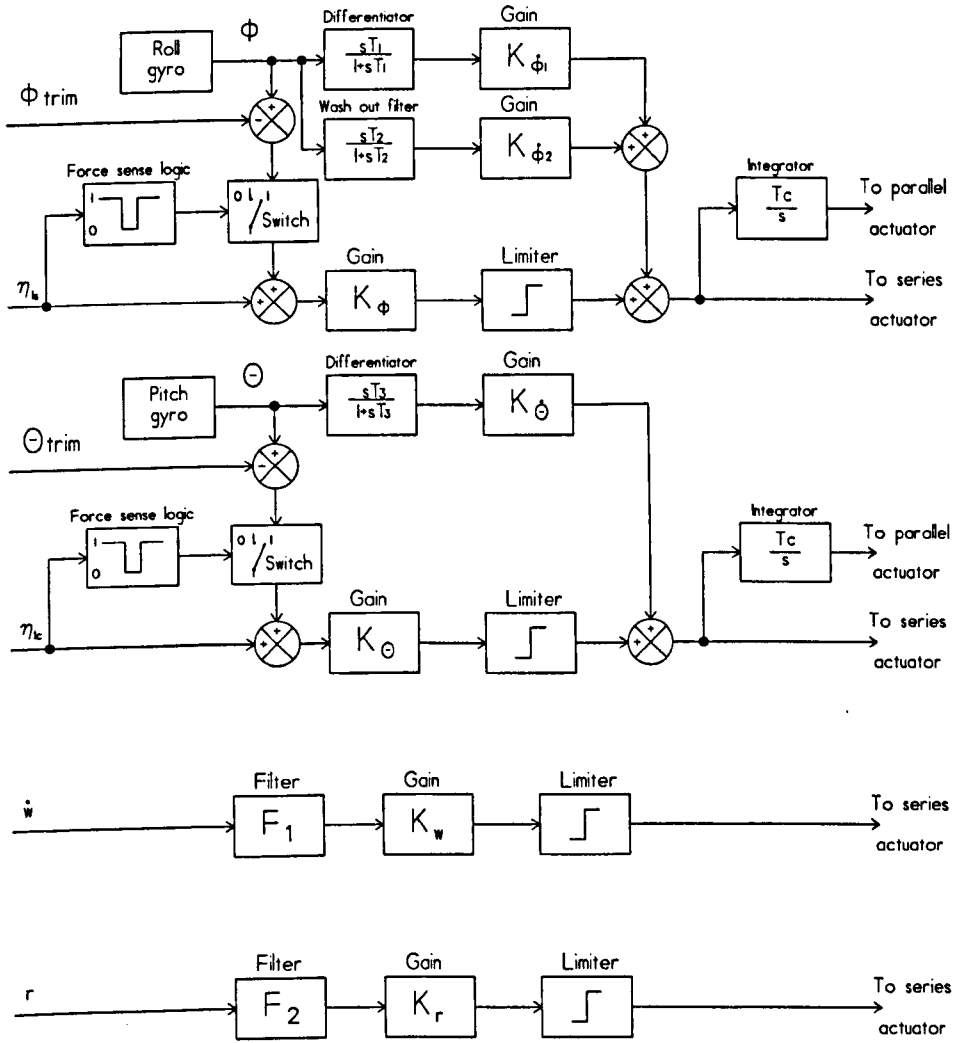


Figure 2.5.15: A control law structure suitable for standard auto-stabilisation equipment.

maintain stability thus a wash-out filter ( $T_2 \approx 2.0\text{sec}$ ) is employed to feedback some roll attitude. The wash-out filter ensures the fed back roll attitude does not oppose the pilot commands.

Feeding the stick position ( $\eta_{1s}, \eta_{1c}$ ) into the control law may seem unnecessary since it already has a direct actuation path via the control runs. However, the stick input ensures that small stick movements are not opposed by the control law and provides attitude command. In some implementations, pre-compensation is applied to the stick input this is, generally, to stop pilot induced oscillations (PIO). It is interesting to note that, regardless of the attitude attained by a large stick input, centring the stick will return the helicopter to the original datum set by the attitude offset values ( $\theta_{trim}, \phi_{trim}$ ). This behaviour is quite different from the conventional fixed wing system where centring the stick will cause the attained attitude to be held. The integrator connected to the parallel actuators has a long time constant and will act to centre the series actuators by adjusting the stick datum.

The heave and yaw channels are much simpler employing only rate feedback. However, a filter network ( $F_1, F_2$ ) may be employed to provide some lead-lag compensation or low pass filtering.

Development of the AFCS typically requires 100's of man years to achieve flight certification since each step must be conducted in accordance with a strict quality regime. Development of an exclusively digital system is a particularly arduous task as large amounts of expensive safety critical software must be written. The SAS control law may be implemented in either software or hardware<sup>8</sup>. It has therefore been suggested [Tay97] that a more cost effective approach is to provide the basic safety critical stabilisation in analogue hardware and the remaining autopilot functions in software.

## 2.6 Summary

This chapter introduces helicopter dynamics and some common analysis tools such as computer simulation, trim, modal decomposition and linearisation. Linearisations form the basis of control law design and a poor linearisation is likely to propagate through the design process to yield a poor controller. Therefore a novel algorithm is developed that produces a representative linearisation and useful error data. Higher order approximations are also briefly considered and shown to offer potential. Modal analysis is an important part of flight dynamics and especially relevant to control law design using eigenstructure assignment. A detailed analysis of the hover case is conducted, the results of which are later used to guide the construction of an ideal eigenstructure.

Some of the work covered in this chapter presents interesting topics for further work. For instance a theoretical basis for the linearisation algorithm could be developed, higher order approximations could be further investigated and the modal analysis could be repeated for different forward speeds.

---

<sup>8</sup>Establishing the reliability and fail safe operation of hardware is much simpler and cheaper than for software [Elp96].

## 2.7 References

- [Arf85] G Arfken. *Mathematical Methods for Physicists*. Academic Press, Inc., 3rd edition, 1985.
- [Bra76] ARS Bramwell. *Helicopter Dynamics*. Edward Arnold, 1976.
- [Coo92] CJ Cooper. Helicopter modelling on the mip's. Final year project report, University of York, Department of Electronics, Heslington, York, Y01 5DD, England, 1992.
- [Elp96] JR Elphick. *Fault Tolerance in Rotorcraft Digital Flight Control Systems*. DPhil, University of York, Department of Electronics, Heslington, York, Y01 5DD, England, January 1996.
- [END82] A Enmami-Naeini and P Van Dooren. Computation of zeros of linear multivariable systems. *Automatica*, 18(4):415–430, 1982.
- [GL96] GH Golub and CF Van Loan. *Matrix Computations*. John Hopkins University Press, 3rd edition, 1996.
- [GLP89] WL Garrad, E Low, and S Prouty. Design of attitude and rate command systems for helicopters using eigenstructure assignment. *Journal of Guidance, Control and Dynamics*, 12(6):783–791, November 1989.
- [Hoh88] RH Hoh. Dynamic requirements in the new handling qualities specification for U.S. military rotorcraft. In *Helicopter Handling Qualities and Control*, pages 4.1–4.17. The Royal Aeronautical Society, November 1988.
- [Joh80] W Johnson. *Helicopter Theory*. Princeton University Press, 1980.
- [Law94] ST Lawes. *Real-Time Helicopter Modelling Using Transputers*. DPhil, University of York, Heslington, York, Y01 5DD, England, September 1994.
- [Mac72] AGJ Macfarlane. A survey of some recent results in linear multivariable feedback theory. *Automatica*, 8:455–492, 1972.
- [Mat92] The MathWorks, Inc, 24 Prime Park Way, Natick, Mass. 01760. *MATLAB Reference Guide*, October 1992.
- [Mat94] The MathWorks, Inc, South Natick, MA 01760. *Matlab: External Interface Guide*, November 1994.
- [McI90] D Mclean. *Automatic Flight Control Systems*. Systems and Control Engineering. Prentice Hall International, 1990.
- [MK76] AGJ MacFarlane and N Karcaniias. Poles and zeros of linear multivariable systems: a survey of the algebraic, geometric and complex-variable theory. *Int. Journal of Control*, 24(1):33–74, 1976.
- [Pad96] GD Padfield. *Helicopter Flight Dynamics*. Blackwell Science Ltd, 1996.
- [Pro90] RW Prouty. *Helicopter Performance Stability, and Control*. Robert E. Krieger Publishing Company, 1990.
- [PTVF92] W.H. Press, S.A. Teukolsky, W.T. Vetterling, and B. P. Flannery. *Numerical Recipes in C: The art of scientific computing*. Cambridge, 1992.
- [Rah93] A Rahooh. Linearization of nonlinear systems using the microcomputer. *Computers In Education Journal*, 3(3):52–59, 1993.
- [Ros70] HH Rosenbrock. *State Space and Multivariable Theory*. Thomas Nelson and Sons Ltd, 1970.
- [SC94] XD Sun and T Clarke. Advanced aircraft flight control using non-linear inverse dynamics. *IEE Proceedings D*, 141(6), November 1994.
- [SCM96] XD Sun, T Clarke, and MA Maiza. A toolbox for minimal state space model realisation. *IEE Proceedings D*, 143(2):152–158, March 1996.
- [Sed90] J Seddon. *Basic Helicopter Aerodynamics*. BSP professional Books, 1990.
- [SK76] U Shaked and N Karcaniias. The use of zeros and zero-directions in model reduction. *Int. Journal of Control*, 23(1):113–135, 1976.
- [Sug94] N Sugiyama. Derivation of system matrices from nonlinear dynamic simulation of jet engines. *Journal of Guidance, Control and Dynamics*, 17(6):1320–1326, November 1994.
- [TA93] JH Taylor and AJ Antoniotti. Linearization algorithm for computer-aided control engineering. *IEEE Control Systems*, 13(2):59–64, April 1993.
- [Tay97] P Taylor. Personal Communications, 1997. Chief Handling Qualities Engineer, GKN Westland Helicopters Ltd, Yeovil, Summerset, UK.
- [Tho93] CR Thornhill. Helicopter flight control. Final year project report, University of York, 1993.
- [Vid93] M Vidyasagar. *Nonlinear Systems Analysis*. Prentice Hall International, Inc., 2nd edition, 1993.
- [Web92] K Webers. Control of a single-rotor helicopter using eigenstructure assignment. Control Research Group Technical Report, University of York, Heslington, York, Y01-5DD, England, September 1992.
- [Wig92] B Wigdorowitz. Application of linearization analysis. *Journal of Guidance, Control and Dynamics*, 15(3):746–750, May 1992.

# Chapter 3

## Handling Qualities

### Contents

---

3.1 Introduction . . . . .	58
3.2 The ADS 33 . . . . .	60
3.3 The Def-Stan 00-970 Vol. 2 Part 6 . . . . .	65
3.4 Discussion . . . . .	69
3.5 Handling Qualities and Control Law Design . . . . .	71
3.6 Summary . . . . .	89
3.7 References . . . . .	89

---

The overriding purpose of any AFCS control law design is to improve handling qualities. Thus a good understanding of the handling qualities requirements is vital for control law design. This chapter presents an overview of the relevant handling qualities requirements and considers them in the context of eigenstructure assignment.

### 3.1 Introduction

It is no great engineering challenge to produce a machine that can propel itself through the air, but to produce a machine with characteristics such that a pilot can control the speed and position in six degrees of freedom, is a tremendous challenge. The major difference between a flying machine and a useful vehicle is handling. Handling qualities have been defined by Cooper and Harper [HC86] as the following:

*‘Those qualities or characteristics of an aircraft that govern the ease and precision with which a pilot is able to perform the tasks required in support of an aircraft role.’*

Handling qualities encompass all aspects of the man machine interface. This includes the cockpit ergonomics, the choice of inceptor and display, for digital systems the presentation and update rate of

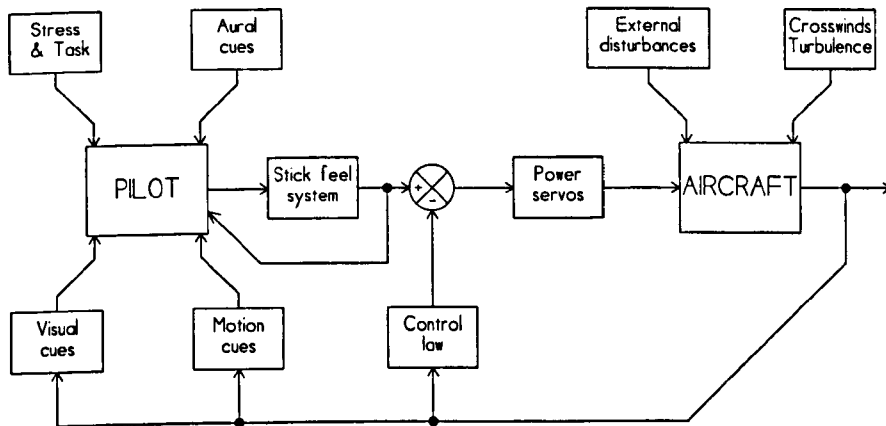


Figure 3.1.1: A conceptual model of the pilot as a controller.

the display, the feel or force feedback from the stick, the field of view, the available autopilot functions and response types and the vehicle response to small, moderate and large amplitude inputs. Any one of these factors can ruin otherwise excellent handling qualities. Good handling qualities are not just a system embellishment, in a critical situation bad handling qualities can culminate in pilot error with disastrous consequences.

Advances in handling qualities have been and still are necessary to increase mission productivity and enable more complex and diverse missions to be undertaken. However, producing a set of criteria that an engineer can apply in order to ensure good handling qualities is a difficult and protracted problem for the following reasons:

- Handling Qualities are subjective. Their ultimate evaluation is based on pilot opinion and one of their aims is to reduce a notional quantity, namely *pilot workload*.
- Analysis of the unpiloted dynamics is not sufficient to guarantee good handling qualities. The pilot can be considered as a highly intricate adaptive controller that augments the dynamics of the helicopter. Thus, only the pilot sees the complete augmented system. As shown in Figure 3.1.1, the pilot can close a variety of loops around the vehicle and AFCS. For instance, adjusting the stick feel system may cause a pilot induced oscillation (PIO) even though the dynamics of the vehicle remain unaltered and could, hypothetically, display a dead beat response.

Handling qualities specifications are therefore the result of protracted studies requiring a large database of information, from ground simulations, test flights and airborne simulations. This is exemplified by the US military standard for helicopter handling qualities MIL-H-8501A which was under revision for some fifteen years. This work has recently culminated in the new ADS 33 specification [AVS89]. All handling qualities specifications measure performance on a 3 level scale as shown in Table 3.1.1



Level	Pilot rating	Definition
1	1-3.5	Clearly adequate.
2	3.5-6.5	Adequate with increased workload or loss of mission effectiveness.
3	6.5-9	Controllable with excessive workload.

Table 3.1.1: Handling qualities levels of compliance.

The handling qualities specifications widely applied in industry are the Ministry of Defence Def-Stan 00-970 Vol. 2 Part 6 [Pit89, Pad96], the MIL-H-8501A [McI90, Pad96] and the Air Design Standard (ADS) 33 [AVS89, HMA<sup>+</sup>85, Key88, Hoh88, Pad96]. The following two sections will present a brief overview of the ADS 33 and Def-Stan 00-970 specifications. Particular attention is paid to the small amplitude dynamic criteria. This is of most relevance for SAS design, not least because of the limited authority of the series actuators. An effort will be made to compare and contrast the specifications because, although different in approach and terminology, fundamentally they show considerable agreement.

### 3.2 The ADS 33

The handling qualities criteria are dependent on an array of parameters. The first section of both specifications is dedicated to categorising the parameters in manner that maintains an intelligent compromise between simplicity and accuracy. The ADS 33 achieves this as follows:

**Mission Task Element (MTE)** are defined as the manoeuvres that form essential ingredients of most missions. MTEs are divided into groups for hover, low-speed (<45 knots) and forward flight (>45 knots). There is no classification of rotorcraft by role or size. This is embodied by the required MTEs. For instance, the target acquisition MTE would not be required for a cargo helicopter.

**Usable Cue Environment (UCE)** defines the quality of the pilot's external view and is measured in 3 levels; 1 is the best and 3 the worst.

**Pilot attention** is defined in two levels fully attended and partially attended. Partially attended implies the pilot undertakes tasks in addition to flight path management (flying).

**Speed range** different criteria apply for speeds above and below 45 knots since the pilot's desired response characteristics will change. For instance, the pilot will not attempt a precision manoeuvre during high speed forward flight.

**Response size** is divided into three categories small, medium and large. This is because the aspects of the response that are important to the pilot depend on the size of the response. For instance,

for small amplitude responses, characteristics such as bandwidth are important whereas, for large amplitude responses, the maximum control power is more relevant.

The specification is applied by considering the speed, UCE, MTE and pilot attention level of interest. For low speeds, where precise manoeuvres are normally conducted and thus the dynamic response is more important, a *response type*, *bandwidth* and *phase delay* are specified. The response type will be one of the following:

**Rate Command (RC)** a fixed stick position commands an appropriate constant rate that diverges for more than four seconds. Rate command may incorporate heading (DH) or height hold (HH).

**Attitude Command Attitude Hold (ACAH)** a fixed stick position commands an appropriate constant body attitude. This is obviously used in conjunction with attitude hold.

**Translational rate command (TRC)** a fixed stick position commands a steady translational rate.

Although rate command is sufficient to achieve level 1 handling qualities for virtually all MTEs in UCE=1. For UCE=2 and divided attention tasks, the additional stability offered by ACAH and other response types is required to compensate for the increased pilot workload. It is important to note that the limited authority of the series actuator dictates that non-rate response types can only be realised for small stick movements. Generally, the situations that require non-rate response types also demand small precise stick movements. However, the advent of full authority, fly-by-wire systems does present the opportunity for novel response types over the full stick range and thus the potential for further, significant reductions in pilot workload.

The bandwidth criteria are *not* specified in terms of the conventional 3 dB point, but defined with respect to the gain and phase margin in the rate or attitude channel of interest, see Figure 3.2.2.

- *Gain bandwidth* is the frequency at which there is 6dBs of gain margin.
- *Phase bandwidth* is the frequency at which there is 45° of phase margin i.e. the phase equals -135°.

For first order systems where the phase is always less than 135° Garrad and Low [GL90, LG93] propose using the pole location as the bandwidth measure. For second order systems:

$$g(s) = \frac{\omega_n^2}{s^2 + 2\zeta\omega_n s + \omega_n^2} \quad (3.2.1)$$

the bandwidth is equal to:

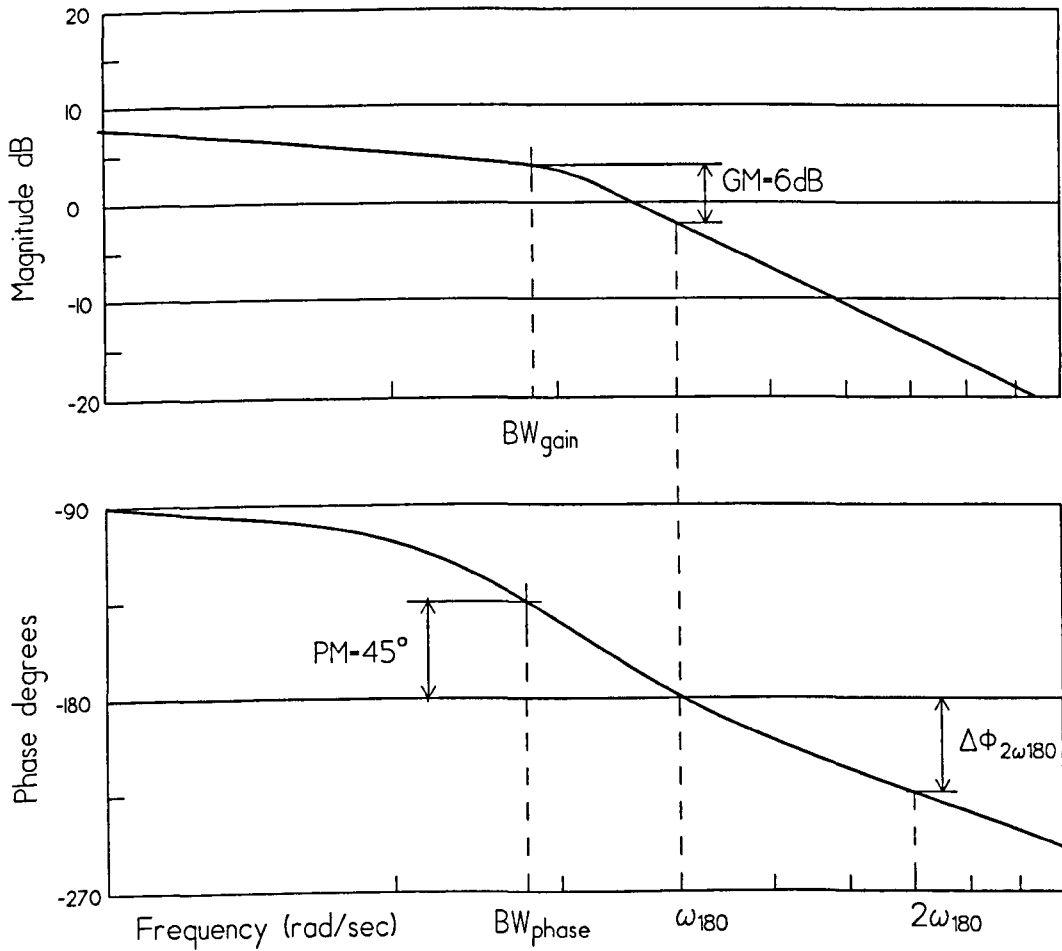


Figure 3.2.2: Gain and phase bandwidth definitions.

$$-135^\circ = \arctan\left(\frac{2\zeta\omega_n\omega}{\omega_n^2 - \omega^2}\right) \quad (3.2.2)$$

$$-1 = \frac{2\zeta\omega_n\omega}{\omega_n^2 - \omega^2} \quad (3.2.3)$$

$$(\omega - \zeta\omega_n)^2 - \zeta^2\omega_n^2 = \omega_n^2 \quad (3.2.4)$$

$$\omega = \omega_n (\zeta + \sqrt{\zeta^2 + 1}) \quad (3.2.5)$$

The rationale behind the bandwidth (BW) definitions is based on the Crossover Model [McR91] of pilot behaviour and measures how ‘tight’ a pure gain pilot can close the attitude loop without threatening stability. The specification requires the lower of the two bandwidth values be used except for

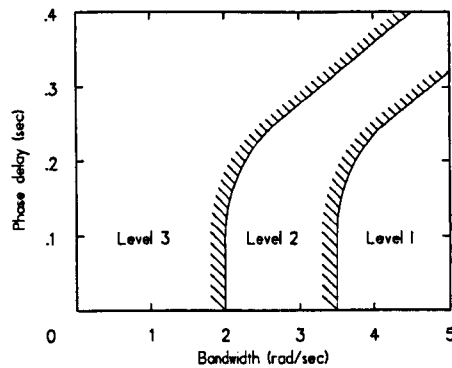


Figure 3.2.3: Bandwidth criteria for target acquisition and tracking (pitch and roll).

ACAH, where only the phase bandwidth applies. The bandwidth values are specified as a function of a second parameter, called *phase delay*. Phase delay is a two point approximation to the phase curve gradient at  $180^\circ$  and is calculated using Equation (3.2.6).

$$\tau_p = \frac{\Delta\Phi_{2\omega_{180}}}{57.3(2\omega_{180})} \quad (3.2.6)$$

Where  $\tau_p$  is the phase delay,  $\omega_{180}$  is frequency at  $180^\circ$  phase,  $2\omega_{180}$  is twice this frequency and  $\Delta\Phi_{2\omega_{180}}$  is the phase change between these frequencies.

Pilot studies have shown that large values of phase delay increase the tendency for pilot induced oscillation (PIO). The specification mitigates this effect by requiring a greater bandwidth value, as illustrated by Figure 3.2.3, which is the requirement for the most demanding MTE, target acquisition. Recent work [BP94] has cast some doubt on the validity of compensating for phase delay with additional bandwidth.

The bandwidth criteria does not directly deal with the system stability. This is specified in terms of damping factor and natural frequency for the *mid-term* response, which is the frequency range just above steady state to just below the bandwidth. The stated criteria are depicted in Figure 3.2.4, which interestingly reveals that extra stability is required in the low frequency response for divided attention tasks.

Medium amplitude responses for roll and pitch are specified in terms of the ratio between the peak rate and attitude traversed i.e.  $\frac{q_{pk}}{\Delta\theta} \frac{p_{pk}}{\Delta\phi}$ . The parameter transforms from being dominated by the channel bandwidth for small changes in attitude to being dominated by the maximum rate for large attitude changes.

Large amplitude manoeuvres are specified as a required minimum angular rate for RC and angular displacements for ACAH.

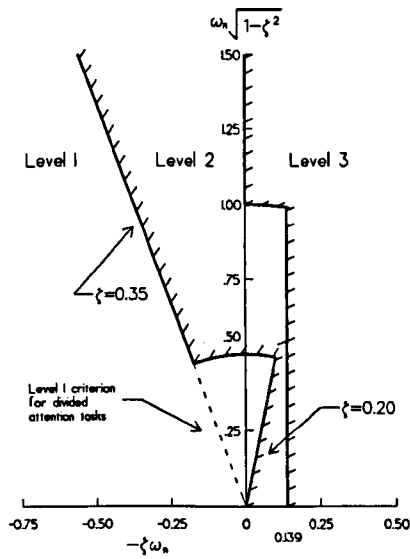


Figure 3.2.4: Handling Qualities criteria for the Mid-term response.

The criteria outlined above apply to the roll, pitch and yaw channels. An alternative approach, based on a Low Order Equivalent System (LOES) is used for the heave channel. A step is applied in heave and the vehicle response ( $\dot{h}$ ) is recorded. Then a nonlinear least squares algorithm is applied to the response data in order to estimate the parameters of the following LOES:

$$\frac{\dot{h}}{\delta_c} = K \frac{e^{-\tau_h s}}{T_h s + 1} \tag{3.2.7}$$

The transfer function is a first order response with time delay. The maximum values for level one and two are shown in Table 3.2.2.

Level	$T_h$ (sec)	$\tau_h$ (sec)
1	5.0	0.20
2	$\infty$	0.30

Table 3.2.2: Maximum value for LOES in heave.

Inter-axis coupling is covered by the global statement:

*'Inputs to achieve a response in one axis should not result in objectionable responses in other axes.'*

As well as this statement, quantitative criteria are stipulated for yaw due to collective, roll due to pitch and pitch due to roll. The guidelines on gust rejection are only pertinent to rotorcraft seeking level 1 compliance and state that the control bandwidth must equal the disturbance rejection bandwidth. This effectively places a severe limitations on the use of a control input pre-filter.

The specification goes on to consider failure states, flight envelopes, visual aids, the behaviour and feel of the primary flying controls, rate of climb, torque response, thrust margin, critical load cases and so on. However, the criteria described above represent those most relevant to SAS design.

### 3.3 The Def-Stan 00-970 Vol. 2 Part 6

At a first glance the Def-Stan appears to resemble the ADS 33 specification. It begins by defining flight envelopes, rotorcraft states and levels of compliance in much the same manner as the ADS 33. However, the description of the terminology below shows that the approaches quickly diverge.

A mission is considered to consist of a continuous set of operational phases. These are divided into non-flight and in-flight phases, the in-flight phases are categorised according to the division of pilot attention and degree of stability verses manoeuvrability required. As described below:

**The active flight phase** implies high pilot involvement in flying, an emphasis on short term dynamics and manoeuvrability. Within this flight phase manoeuvres are delineated as follows:

- i. **Up and away manoeuvring;** flying in open space with pilot commands classified as *aggressive* or *moderate*.
- ii. **Low level, low speed manoeuvring;** precision manoeuvring close to the ground, ship deck, platform, etc.
- iii. **Low level, moderate/high speed manoeuvring;** essentially nap of the earth flying.
- iv. **Low level, low visibility manoeuvring;** pilot involvement in flying is high due to poor visibility including the use of visual aids.

**The attentive flight phase** implies moderate pilot involvement in flying and an emphasis on the short and long term response. This flight phase includes the following manoeuvres.

- i. **Up and away manoeuvring;** with gentle pilot commands.
- ii. **Low level manoeuvring;** using autopilot hover modes where pilot involvement is essentially a preparedness to intervene.

**The passive flight phase** implies low pilot involvement in flying with an emphasis on autopilot control and long term stability. This flight phase is associated with long periods of *hands off* flying.

The definitions above can be considered as the Def-Stan interpretation of MTEs and pilot attention level. The Def-Stan treats response types as follows (Leaflet 600/7 para 2.2):

- i. For active flight phases involving aggressive manoeuvres rate command is preferred.
- ii. For active phases involving precise manoeuvring and most of the attentive flight phase the extra stability offered by attitude command makes this preferable.
- iii. For active phases involving specialised ground reference manoeuvres translational velocity command or even position command may be most suitable.
- iv. For all phases under degraded visual cuing conditions the additional stability of response types other than rate command is likely to be required.

The criteria above show strong coherence with the approach taken by the ADS 33. Both specifications generally require rate command, but compensate for poor visual cuing environments or divided attention tasks by stipulating attitude command. Both specifications also agree that high precision flying and some specialised manoeuvres will need response types other than rate command.

The short-term stability criteria (Leaflet 600/7 para 6.2) are specified in terms of parameters gathered from time history data and cover much the same ground as the ADS 33 small amplitude criteria. Of particular importance is the time history of the transient response to an input pulse of 10% full travel applied for 1 second. A typical output induced by a pulse input is shown in Figure 3.3.5.

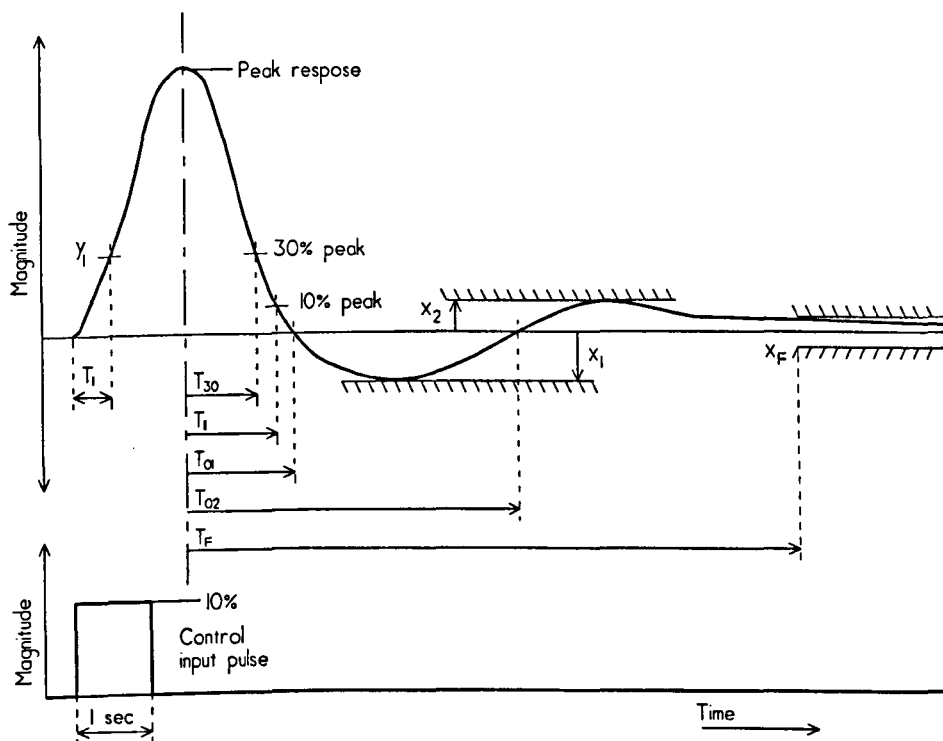


Figure 3.3.5: A typical transient response in roll, pitch or yaw to a pulse input.

The short-term stability parameters are defined with, time referenced from the point at which the *peak response* occurs and magnitude is measured relative to the peak response. All the parameters including the peak response are defined and justified below, also see Figure 3.3.5:

- i. The *peak response* is the maximum value reached by the time response or if the peak occurs before the end of the input pulse it is the value that coincides with the end of the pulse. The peak response is a measure of control responsiveness that must be greater than a minimum value for adequate responsiveness and less than some maximum to avoid over-sensitivity.
- ii. The *initial delay* is the value of the response ( $y_1$ ) at a specified time ( $T_1 = 0.5 \text{ sec}$ )<sup>1</sup> from the *initiation of the control input* and it must be greater than a lower limit (30%). This parameter prevents the control response from exhibiting excessive sluggishness due to delays and lags.
- iii. To avoid *over-sensitivity* the value of  $y_1$  must be less than an upper limit<sup>2</sup>, which is to be advised (TBA). Furthermore the response build up should possess no obtrusive hesitation.
- iv. To achieve the desired stability the transient response must decay rapidly. This is verified using the following parameters:
  - (a) The time taken ( $T_{30}$ ) to decay to less the 30% of the peak value must be less than an upper limit (1 sec for level 1).
  - (b) The minimum value of the first trough ( $x_1$ ) must be less than an upper limit (15% for level 1). The limit is expressed as a percentage of the peak value.
  - (c) The maximum value of the second peak ( $x_2$ ) must be less than an upper limit (10% for level 1).
- v. The accuracy with which the helicopter *returns to the original datum* after the pulse input, is specified as a percentage of the peak value ( $X_F$ ) and must be achieved before  $T_F$  seconds.
- vi. Experience has shown that pilots find a small amount of overshoot desirable. For level 1 handling qualities it is therefore necessary to pass through the original datum. This point ( $T_{01}$ ) must fall between an upper and lower bound, and the second crossing point ( $T_{02}$ ) must be greater than a lower limit. For level 2 compliance this overshoot criterion is replaced with a simpler one. This states that the time ( $T_{11}$ ) at which the response reaches 10% of the peak value must lie between an upper and lower limit. To ensure the overshoot is discernible, the parameter  $x_1$  requires a lower bound in addition to the upper bound. A value of  $\approx 1\%$  was used in practice.

The criteria for the time history parameters are specified with respect to the flight phase, level of compliance and for the active phase the severity of the manoeuvre. The bias of criteria towards the active phase and lack of criteria for the passive phase reflects the significance of the short term dynamics in

<sup>1</sup>This is a provisional value.

<sup>2</sup>In discussions with Barry Pitkin, author of the Def-Stan 00-970, he indicated a value of 70% – 80% was appropriate.



these phases. The reason for no level 3 criteria for aggressive manoeuvres in the active phase is that a pilot is simply unable to embark on such a manoeuvre with severely degraded handling qualities.

The criteria for the longitudinal short term dynamics (Leaflet 601/1 section 4) are summarised in Table 3.3.3. The criteria for the lateral channel (Leaflet 602/1 section 4) are identical except for a slight increase in the required responsiveness. Table 3.3.3 shows that level 2 compliance permits a greater sensitivity, a larger overshoot and a longer settling time. It also reveals that during the active flight phase, level 1 compliance can not be achieved with an attitude response type. Table 3.3.3 displays no direct consideration of the visual conditions and uses a classification based on pilot attention level and manoeuvre type. The reason for this is that the visual conditions affect the pilot attention level and the types of manoeuvre that are appropriate are indirectly considered. For instance, under degraded visual conditions the pilot will only attempt gentle manoeuvres and is thus deemed to be in the attentive flight phase which stipulates the desired attitude command. Using similar reasoning it can be argued that small stick movements i.e. gentle manoeuvres, should invoke attitude command whereas large stick movements (aggressive manoeuvres) should invoke rate command.

Phase	Active				Attentive	
	Aggressive		Moderate		All	
Man. Class						
Level	1	2	1	2	1	2
Response type	Pitch rate	Pitch rate	Pitch rate	Pitch att.	Pitch att.	Pitch att.
Peak response	10-15 °/sec	7-20 °/sec	5-10 °/sec	5° - 10°	4° - 8°	4° - 12°
$T_1$ (sec)	0.5	0.5	0.5	0.5	0.5	0.5
$y_1$ %	30-TBA	30-TBA	30-TBA	30-TBA	30-TBA	30-TBA
$T_{30}$ (sec)	< 1	< 1	< 1	< 1.5	< 1	< 1.5
$x_1$ %	15	20	15	25	10	15
$x_2$ %	10	15	10	15	N/A	N/A
$T_F$ (sec)	3	5	3	5	3	5
$X_F$ %	10	10	10	10	10	10
$T_{01}$ (sec)	1-2	N/A	1-2	N/A	1-2	N/A
$T_{02}$ (sec)	> 2	> 2	> 2	> 2.5	N/A	N/A
$T_{11}$ (sec)	N/A	1 - 2	N/A	1.5 - 3	N/A	1.5 - 3

Table 3.3.3: The Def-Stan 00-970 longitudinal short-term stability handling qualities criteria as defined in Leaflet 601/1 section 4.

The time domain criteria outlined above are applied to the short term dynamics in the roll, pitch and yaw channels. An alternative approach is applied to the heave channel (Leaflet 607/1). The criteria are based around a first order response and specify the minimum time ( $T_1$ ) that a final value ( $X_1$ ) should be reached and a window in which the maximum acceleration should occur. Unfortunately, no quantitative data is given but since ADS 33 also uses a time domain approach based on a first order response, quantitative data can be inferred from this specification.

The specification also considers the long term stability of attitude hold functions (Leaflet 602/2 sec-

tion 3 and Leaflet 601/2 section 3) and requires that the trimmed attitude remains within a fixed tolerance for a minimum stipulated time. Requirements in terms of minimum time constants are stated for inherently slow functions such as air speed control (Leaflet 601/2) and translational velocity control (Leaflets 601/3 and 602/3). It is interesting to note that *no quantitative criteria* are given that might be considered equivalent to the ADS 33 moderate amplitude specification. However, roughly the same ground is covered with the following qualitative statement (Chapter 600 para 10.1.8):

*'Rotorcraft response to control inputs in all channels shall be continuous, progressive and predictable'*

Control margins serve to ensure there is sufficient control power. They are specified as minimum angular rates and attitudes that the pilot can invoke in each channel in a given time and are directly equivalent to the ADS 33 large amplitude requirements.

Interaxis coupling is covered by a global statement (Chapter 600 para 10.1.7) very similar to that stated by the ADS 33:

*'Control inputs in a particular channel or axis shall not result in objectionable rotorcraft responses being generated in other channels or axes, that cannot be contained by relatively small (instinctive) corrections through the appropriate control channel (Leaflet 600/7 para 4).'*

There are no quantitative requirements for coupling between angular rates and attitudes, however, criteria are given for coupling between translational velocities.

### 3.4 Discussion

The ADS 33 is a detailed and stringent specification that contains a myriad of parameters that must be evaluated in order to show compliance. To ease this task and save unnecessary over-design, a more objective approach to the specification will be needed by the manufacture and procurer. For instance, traditionally level one handling qualities are sought in all aspects of the specification. However, it may be more practical through consideration of the vehicle role only to require level 2 for seldom-executed MTEs. With this approach it is likely that some AFCS functions will not be required and thus save considerable expense and development time. A possible candidate for exclusion is TRC.

The most significant difference between the ADS 33 and Def-Stan is their approach to the small amplitude dynamic response. The ADS 33 favours a frequency domain approach based on bandwidth, damping ratio and natural frequency whereas the Def-Stan uses a time domain approach based on the response to small input pulses. The frequency domain criteria lend themselves more readily to many modern design techniques. For instance, the criteria can be used directly in a  $\mathcal{H}_\infty$  based synthesis [YP90], can be converted into ideal simplified transfer functions for  $\mathcal{H}_\infty$  based model match-

ing techniques [SC94] and eigenstructure assignment [GL90]. Furthermore, the use of phase and gain margins affords some measure of the degree of stability. This can be important in avoiding PIO. A drawback of the frequency domain approach is the difficulty in showing compliance. Often non-linearities obscure the mid-term response and identification using pilot applied or automatic frequency sweeps is potentially destructive [Pad96, p. 371] and may be inconclusive. Furthermore, much of the justification for the ADS 33 mid-term response criteria is based on the dutch roll response of fixed wing aircraft [HMA<sup>+</sup>85]. The validity of this is questionable since, for helicopters, such a response is often indiscernible, especially at low speeds. It is because of these drawbacks that the Def-Stan has adopted a time domain approach which it justifies as follows (leaflet 600/7 para 6.1):

*'The response of a particular flight parameter to any disturbance is the summation of a number of periodic and aperiodic modes embracing a range frequency and damping characteristics. The number of such modes is invariably increased with the incorporation of sophisticated stability and control augmentation systems. This mixing of often well damped periodic and aperiodic modes makes it difficult to observe individual modes and meaningfully apply classical frequency and damping factor criteria in stability analyses. Consequently the approach described above has been adopted.'*

Previous time domain criteria have been criticised for using unnatural pilot commands such as step inputs. Pulse inputs form a common element of pilot technique and are often applied in pairs, as control doublets. Another criticism of the time domain approach is that a large number of parameters is needed to assess compliance compared to the single bandwidth parameter required by the ADS 33. While several parameters are required, they are all far simpler to determine than the channel bandwidth. Furthermore, many facets of the vehicle response can lead to objectionable handling so it is perhaps not unnatural that several parameters are required. However, the time domain approach does have its limitations and the Def-Stan concedes that (leaflet 600/7 para 3.4.4):

*'Further criteria, probably based on bandwidth concepts remain to be established to give guidance on avoiding pilot induced oscillations, especially in the case of high control power, highly augmented rotorcraft and in high gain piloting tasks.'*

But equally, initial versions of ADS 33 [HMA<sup>+</sup>85] specification provided time domain criteria for preliminary evaluation. The ADS 33 contains many innovations and a great deal of substantiated quantitative data that is invaluable for design.

In summary, the two specifications display differences in terminology, approach and character. The ADS 33 is a more explicit specification where the procurer will be inclined to relax some requirements. The Def-Stan is a more qualitative specification, providing guidelines that provokes the procurer and manufacturer to agree upon additional performance criteria relevant to the helicopter and its operational role. Finally, it should be appreciated that level one compliance with either specification is not sufficient to demonstrate level one handling qualities, ultimately subjective test pilot evaluation must also be undertaken.

## 3.5 Handling Qualities and Control Law Design

Almost all AFCS control law design begins by determining the design goals from the relevant handling qualities specification. Handling qualities requirements are conceived from the aspect of demonstrating compliance and thus must invariably be converted into an alternative format appropriate for the controller synthesis technique. Poor judgement or a mistake in interpreting the handling qualities requirements will undermine the subsequent design effort. Thus design techniques that facilitate a strong visible link between the interpreted design goals and the original handling qualities requirements, are more likely to succeed and promote confidence in the synthesis technique. Helicopter control law design goals have been formulated in several ways:

1. Direct conversion into frequency domain weighting functions [Tak93b, Gri93, YP90, YP88, WP90, Tak93a]. Both  $\mathcal{H}_\infty$  and  $\mathcal{H}_2$  can be used to shape aspects of the closed loop frequency response. Generally the minimum singular value of key transfers functions such as sensitivity and complementary sensitivity are manipulated using weighting functions [Mac89]. The desired responses are often guided by the ADS 33 bandwidth and damping factor requirements, although, some trial and error is often also necessary.
2. Direct conversion into time domain weighting functions [IS90, Nar69]. The Linear Quadratic Regulator (LQR) uses two positive definite weighting matrices in an integral time domain cost function [AM89], adjusting the matrices alters the system response. Optimal solutions generally have a well damped response, however, trial and error is again often needed to get precisely the desired response.
3. Generation of ideal transfer functions. This is probably the most popular approach and has proved effective. The ideal transfer functions are usually first or second order systems that meet the ADS 33 bandwidth and damping factor criteria. The ideal transfer functions may be used in various controller synthesis techniques, for instance:
  - (i) Model following [OC92, MG94, Hin87]. This technique feeds the error, between the ideal transfer functions and measured vehicle response, into a controller.
  - (ii) Model matching [IC94, WP96, MG93, YI93, SC94]. A controller is designed so that closed loop system will approximate the ideal transfer functions. Minimisation of the approximation error is often formulated as a  $\mathcal{H}_\infty$  control problem. Interestingly, the ideal model may be chosen for its time domain properties, for instance the step response models (SRMs) used by Walker and Postlethwaite [WP96], but the model matching problem is formulated in the frequency domain.
4. Generation of an ideal eigenstructure [MMS92, PMS85, GL90, GLP89a, LG93, CP72, SR75]. This is closely related to the ideal transfer function approach and these representations are sometimes used interchangeably [GL90, GLP89a].

The eigenstructure and ideal transfer approaches both use very simple fully decoupled models that are sometimes called conceptual models [Pad96]. In practice no control law will make a real helicopter achieve the conceptual model. But the conceptual model is not intended to be a realistic design goal. Its purpose is to visibly and unambiguously indicate an aim that will improve the handling qualities. Many researchers have converted the ADS 33 requirements into controller synthesis design goals. However, the Def-Stan does not share the same popularity and, to the author's knowledge, there is no instance in the literature of the Def-Stan requirements being applied to controller synthesis. The design goals used in this work are formulated as an ideal eigenstructure.

### 3.5.1 An Ideal Eigenstructure

Section 2.4 showed that examination of the system eigenstructure is a powerful analysis tool and a well established branch of flight dynamics. A benefit of an ideal eigenstructure is that knowledge and experience from analysis can be directly applied in design. This is particularly useful in ensuring the ideal eigenstructure is plausible. While it may be idealistic, it should not contain any inherent conflicts with the system physics. For instance, an ideal eigenstructure that attempts to decouple angular rate from body attitude is likely to fail due to the kinematic relationship between these variables. Equally, decoupling the linear velocities from the body attitudes or significantly moving the main rotor flapping modes<sup>3</sup> is also fraught with problems.

The ideal eigenstructure has a strong link with the system time response. This is particularly helpful in meeting time domain design goals. Consider the following state space system:

$$\dot{\mathbf{x}} = \mathbf{Ax} + \mathbf{Bu} \quad (3.5.8)$$

$$\mathbf{y} = \mathbf{Cx} \quad (3.5.9)$$

Where the input and output matrices are partitioned as follows:

$$\mathbf{B} = [\mathbf{b}_1, \dots, \mathbf{b}_r] \quad (3.5.10)$$

$$\mathbf{C} = [\mathbf{c}_1^T, \dots, \mathbf{c}_m^T] \quad (3.5.11)$$

Then the time domain solution is [DH95]:

---

<sup>3</sup>The flapping modes may not be influenced since there is no measurement of flapping angle or its derivatives and only first harmonic control of the aerodynamic moment.

$$y_i(t) = \sum_{k=1}^n c_i \mathbf{v}_k e^{\lambda_k t} \mathbf{w}_k \mathbf{x}_0 + \sum_{j=1}^r \sum_{k=1}^n (c_i \mathbf{v}_k) (\mathbf{w}_k \mathbf{b}_j) \int_0^t e^{\lambda_k \tau} u_j(t - \tau) d\tau \quad (3.5.12)$$

Where  $\mathbf{w}_k$  and  $\mathbf{v}_k$  are the left and right eigenvectors associated with  $\lambda_k$  and  $\mathbf{x}_0$  is the initial state vector. Equation (3.5.12) shows that the eigenvalue  $\lambda_k$  determines the decay rate and natural frequency of the mode  $e^{\lambda_k t}$  and terms  $c_i \mathbf{v}_k$ ,  $\mathbf{w}_k \mathbf{b}_j$  and  $\mathbf{w}_k \mathbf{x}_0$  are scalars that determine the magnitude and phase of the response. For instance, suppose an impulse is applied to one input ( $j = 1$ ) and the initial state vector ( $\mathbf{x}_0$ ) is zero. Then the output reduces to:

$$y_i = \sum_{k=1}^n (c_i \mathbf{v}_k) (\mathbf{w}_k \mathbf{b}_1) e^{\lambda_k t} \quad (3.5.13)$$

The contribution of real modes to the output is a simple exponential decay scaled by  $(c_i \mathbf{v}_k) (\mathbf{w}_k \mathbf{b}_1)$ . The following definitions are helpful in understanding the effect of complex modes:

$$a_k + jb_k = (c_i \mathbf{v}_k) (\mathbf{w}_k \mathbf{b}_1) \quad (3.5.14)$$

$$\sigma_k + j\omega_k = \lambda_k \quad (3.5.15)$$

The contribution of a complex mode and its conjugate is:

$$\begin{aligned} (a_k + jb_k)e^{(\sigma_k + j\omega_k)t} + (a_k - jb_k)e^{(\sigma_k - j\omega_k)t} &= e^{\sigma_k t} [a_k (e^{j\omega_k t} + e^{-j\omega_k t}) - b_k (e^{j\omega_k t} - e^{-j\omega_k t})] \\ &= 2\sqrt{a^2 + b^2} e^{\sigma_k t} \cos\left(\omega_k t + \arctan\left(\frac{b_k}{a_k}\right)\right) \end{aligned}$$

It can be seen that the modulus and argument of  $a_k + jb_k$  determine the magnitude and phase of complex modes. The values of  $a_k$  and  $b_k$  depend on the input ( $\mathbf{B}$ ), output ( $\mathbf{C}$ ) matrices and the eigenvectors. By manipulating the eigenvectors ( $\mathbf{v}_k$ ,  $\mathbf{w}_k$ ) or, more directly, the modal coupling vectors ( $\mathbf{C}\mathbf{v}_k$ ,  $\mathbf{w}_k\mathbf{B}$ ) the phase and magnitude and of complex modes can be altered. The phasing of complex modes will determine whether near-frequency modes combine constructively or destructively. Poor phasing can lead to obtrusive peaks or lulls in the response. Hence the argument of complex entries in the eigenvectors or modal coupling matrices should be used to adjust the mode phasing. Equation (3.5.13) shows that the outputs may contain a contribution from all the system modes. Hence an almost universal requirement is to simplify or decouple the response by forcing only one or two modes to appear in each output. This is achieved by manipulating the magnitude of entries in the eigenvectors or modal coupling matrices such that they have a predominantly block diagonal structure.

In addition to decoupling, forcing only one or two modes to appear in each output means fewer eigenvalue parameters will determine the response in each output. This leads to a more visible relationship between the eigenvalues and system response and greatly simplifies selection of ideal eigenvalue locations.

The eigenstructure has a strong link with system transfer function in its partial fraction expanded form. Equation (3.5.16) shows the transfer function in dyadic or partial fraction expanded form.

$$\mathbf{G}(s) = \sum_{k=1}^n \frac{\mathbf{C}\mathbf{v}_k\mathbf{w}_k\mathbf{B}}{s - \lambda_k} \quad (3.5.16)$$

There is a clear link between the eigenvectors or modal coupling matrices and the residue of each mode. Fixing the relative size of different residues may be used to guide the construction of an ideal eigenstructure.

An aim of this work is to produce an ideal eigenstructure that meets the Def-Stan 00-970 short term stability criteria.

### 3.5.2 Ideal Roll and Pitch Eigenvalue Locations

It was decided to characterise the set of second order systems that meet the Def-Stan time domain criteria. A second order system was chosen for the following reasons:

- This is simplest system that will meet the Def-Stan time domain criteria.
- Low order systems have a smooth predictable response which is consistent with the general handling qualities requirements [MMS92].
- Two states are associated with the pitch ( $q, \theta$ ) and roll ( $p, \phi$ ) channels thus for a static feedback solution it is appropriate to consider a second order system.
- Previous work using conceptual model based approaches has shown that low order systems are effective [SC94, GL90, WP90].

Defining an ideal eigenvalue region rather than a single location avoids introducing unnecessary constraints at this early stage in the design. Consider the following second order system:

$$g(s) = \frac{\omega_n^2}{s^2 + 2\zeta\omega_n s + \omega_n^2} \quad (3.5.17)$$

Let us define a pulse of width  $T$ :

$$p(t) = h(t) - h(t - T) \quad (3.5.18)$$

Where  $h(t)$  is the Heaviside step function. Then the system response to a pulse input ( $p(t)$ ) is:

$$y(t) = 1 - \frac{e^{-\zeta\omega_n t}}{\sqrt{1-\zeta^2}} \sin(\omega_d t + \alpha) - \left[ 1 - \frac{e^{-\zeta\omega_n(t-T)}}{\sqrt{1-\zeta^2}} \sin(\omega_d(t-T) + \alpha) \right] h(t-T) \quad (3.5.19)$$

Where:

$$\omega_d = \omega_n \sqrt{1-\zeta^2} \quad (3.5.20)$$

$$\alpha = \arccos(\zeta) = \arctan\left(\frac{\sqrt{1-\zeta^2}}{\zeta}\right) \quad (3.5.21)$$

Assuming an input pulse width ( $T$ ) of one second the Def-Stan indicates that ideally<sup>4</sup> the first peak should occur after the input pulse. For  $t < T$  the derivative of the output is:

$$\frac{\partial y(t)}{\partial t} = \frac{e^{-\zeta\omega_n t}}{\sqrt{1-\zeta^2}} [\zeta\omega_n \sin(\omega_d t + \alpha) - \omega_d \cos(\omega_d t + \alpha)] \quad (3.5.22)$$

a peak implies  $0 = \frac{\partial y(t)}{\partial t}$  thus:

$$0 = \zeta\omega_n \sin(\omega_d t + \alpha) - \omega_d \cos(\omega_d t + \alpha) \quad (3.5.23)$$

$$= \sqrt{\omega_d^2 + (\zeta\omega_n)^2} \sin\left(\omega_d t + \alpha - \arctan\left(\frac{\omega_d}{\zeta\omega_n}\right)\right) \quad (3.5.24)$$

$$= \omega_n \sin(\omega_d t) \quad (3.5.25)$$

Hence the following constraint applies:

$$\boxed{\frac{\pi}{\omega_d} > T} \quad (3.5.26)$$

<sup>4</sup>In fact The Def-Stan 00-970 (Leaflet 600/7 para. 3.4.2) will tolerate a very small peak ( $y_2$ ) before the end of the input pulse.



The Def-Stan references time with respect to the first peak. Hence an initial task is to find the location of this peak. Assuming the peak occurs after  $T$  seconds, the derivative of the output response is:

$$\frac{\partial y(t)}{\partial t} = \frac{e^{-\zeta\omega_n t}}{\sqrt{1-\zeta^2}} \omega_n \sin(\omega_d t) - \frac{e^{-\zeta\omega_n(t-T)}}{\sqrt{1-\zeta^2}} \omega_n \sin(\omega_d(t-T)) \quad (3.5.27)$$

$$= \frac{e^{-\zeta\omega_n t}}{\sqrt{1-\zeta^2}} \omega_n [\sin(\omega_d t) - e^{\zeta\omega_n T} \sin(\omega_d(t-T))] \quad (3.5.28)$$

$$= \frac{e^{-\zeta\omega_n t}}{\sqrt{1-\zeta^2}} \omega_n M [\sin(\omega_d t + \beta)] \quad (3.5.29)$$

Where:

$$\beta = \arctan \left( \frac{e^{\zeta\omega_n T} \sin(\omega_d T)}{1 - e^{\zeta\omega_n T} \cos(\omega_d T)} \right) \quad (3.5.30)$$

$$M = \sqrt{(1 - e^{\zeta\omega_n T} \cos(\omega_d T))^2 + (e^{\zeta\omega_n T} \sin(\omega_d T))^2} \quad (3.5.31)$$

Thus the initial peak occurs at:

$$t_{pk} = \frac{\pi - \beta}{\omega_d} \quad (3.5.32)$$

Comparing Equation (3.5.28) with Equation (3.5.19) we see that for  $t > T$  the response to a pulse ( $p(t)$ ) may be rewritten as:

$$y(t) = \frac{e^{-\zeta\omega_n t}}{\sqrt{1-\zeta^2}} [e^{\zeta\omega_n T} \sin(\omega_d(t-T) + \alpha) - \sin(\omega_d t + \alpha)] \quad (3.5.33)$$

$$= -\frac{e^{-\zeta\omega_n t}}{\sqrt{1-\zeta^2}} M \sin(\omega_d t + \alpha + \beta) \quad (3.5.34)$$

It is clear from Equation (3.5.34) that the first zero crossing occurs at:

$$t_z = \frac{2\pi - \alpha - \beta}{\omega_d} \quad (3.5.35)$$

The Def-Stan (Leaflet 601/1 para 4.2 and Leaflet 602/1 para 4.2) requires the first zero crossing ( $t_z$ ) occurs between one and two seconds after the initial peak ( $t_{pk}$ ) thus  $1 < (t_z - t_{pk}) < 2$  or equivalently:

$$\boxed{1 < \frac{\pi - \alpha}{\omega_d} < 2} \quad (3.5.36)$$

The Def-Stan also stipulates that the second zero crossing ( $T_{02}$ ) should happen two seconds or more after the initial peak thus:

$$\boxed{2 < \frac{2\pi - \alpha}{\omega_d}} \quad (3.5.37)$$

In fact, for this simple second order case, if Equation (3.5.36) is satisfied then Equation (3.5.37) must also be satisfied.

$$1 < \frac{\pi - \alpha}{\omega_d} \quad (3.5.38)$$

From Equation (3.5.21) we see  $\alpha$  is always positive thus:

$$2 < \frac{2\pi - 2\alpha}{\omega_d} < \frac{2\pi - \alpha}{\omega_d} \quad (3.5.39)$$

The ratio between the initial peak and first trough must be less than  $x_1 = 0.15$  (see Table 3.3.3) and ideally greater than  $x_1 = 0.01$ , from Equation (3.5.29) the first trough occurs at:

$$t_{tr} = \frac{2\pi - \beta}{\omega_d} \quad (3.5.40)$$

Thus the ratio is:

$$\frac{y(t_{tr})}{y(t_{pk})} = \frac{\frac{e^{-\zeta\omega_n t_{tr}}}{\sqrt{1-\zeta^2}} M \sin(2\pi - \alpha)}{\frac{e^{-\zeta\omega_n t_{pk}}}{\sqrt{1-\zeta^2}} M \sin(\pi - \alpha)} \quad (3.5.41)$$

since  $-\sin(\theta) = \sin(\pi + \theta)$

$$= -e^{-\zeta\omega_n(t_{tr}-t_{pk})} \quad (3.5.42)$$

$$= -e^{-\frac{\zeta}{\sqrt{1-\zeta^2}}\pi} \quad (3.5.43)$$

Hence the overshoot constraint reduces to a bound in the damping factor ( $\zeta$ ).

$$\boxed{0.01 < e^{-\frac{\zeta}{\sqrt{1-\zeta^2}}\pi} < 0.15} \quad (3.5.44)$$

The Def-Stan constraint on the second peak ( $x_2$ ) may be equally expressed as:

$$\boxed{e^{-\frac{\zeta}{\sqrt{1-\zeta^2}}2\pi} < 0.1} \quad (3.5.45)$$

The Def-Stan specifies that  $T_F = 3$  seconds after the first peak. The steady state error should be less  $X_F = 0.10$  of the initial peak. This can be interpreted as a constraint on the exponential envelope of the pulse response. From Equation (3.5.42) we see:

$$\boxed{e^{-\zeta\omega_n T_F} < 0.1} \quad (3.5.46)$$

The Def-Stan further specifies that the response should decay to less 30% of the peak value within  $T_{30} = 1$  seconds. Starting with Equation (3.5.41) some manipulation yields the following implicit constraint:

$$\boxed{0.3 = \frac{e^{-\zeta\omega_n T_{30}}}{\sqrt{1-\zeta^2}} \sin(\omega_d T_{30} + \alpha)} \quad (3.5.47)$$

To avoid over-sensitivity or sluggishness the Def-Stan specifies the initial build up, that is  $T_1 = 0.5$  seconds from the inception of the pilot command, should lie between 0.30 and 0.75 of the peak response. This constraint is hard to simplify mathematically since it straddles a discrete change in the pilot command. However, some manipulation of Equation (3.5.19) and Equation (3.5.34) gives the following implicit constraint:

$$\boxed{0.3 < \frac{e^{\zeta\omega_n t_{pk}}}{M} \left( 1 - \frac{e^{-\zeta\omega_n T_1}}{\sqrt{1-\zeta^2}} \sin(\omega_d T_1 + \alpha) \right) < 0.75} \quad (3.5.48)$$

The second order system has two degrees of freedom in the complex plane so each constraint can be used to define a line that is a boundary of the allowed region. Most of the constraints can be separated and plotted explicitly. However, both Equation (3.5.47) and Equation (3.5.48) require an implicit

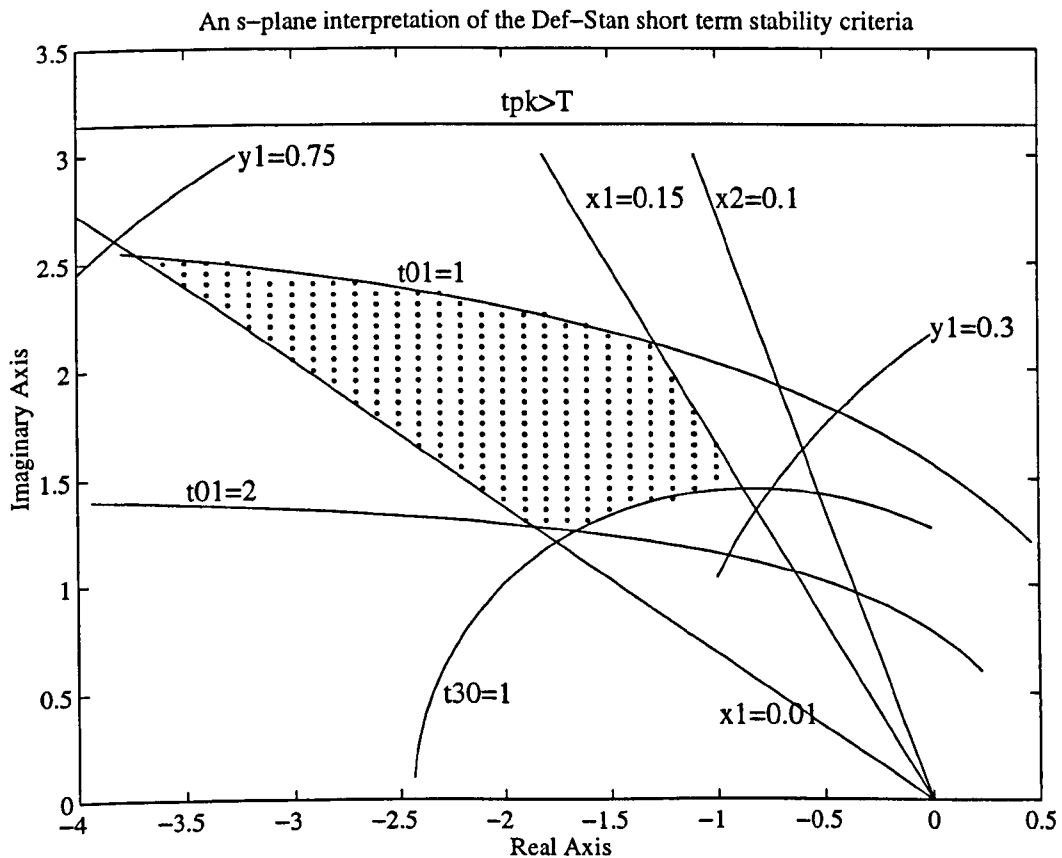


Figure 3.5.6: An s-plane interpretation of the Def-Stan short term stability criteria.

equation solver to be plotted.

The analytical constraints derived above were verified by constructing a second order system for each of many points in the complex plane, simulating the responses to a pulse input and evaluating the handling qualities of these responses. Figure 3.5.6 shows there is a clear correspondence between the analytical constraints and tests points with level one handling qualities. The criteria used to construct Figure 3.5.6 are for the active flight phase (see Table 3.3.3). The region defined by the attentive phase differs in only one respect, the line  $x_1 = 0.15$  swings down to  $x_1 = 0.10$ .

The Def-Stan criteria map to a well defined region in the complex plane, although some constraints are seen to be subsumed by others. This is because second order systems produce a simple linear response that does not exercise all the constraints. The response from a real helicopter would require the additional constraints to be adequately classified. However, in this case, the dominant criteria are easily identified as the first zero crossing  $T_{01}$ , the overshoot criterion  $x_1$  and the thirty percent decay criterion  $T_{30}$ .

While identifying an allowed eigenvalue region maintains flexibility it is also useful to define an ideal location. This can be done from a frequency or time domain perspective. The frequency domain approach simply requires placing a centre point in the allow region. A hand estimated location is:

$$\lambda_f = -1.8 \pm j1.75 \quad (3.5.49)$$

The time domain approach requires identifying a location where the response comfortably meets all the time domain criteria. Any two of the time domain constraints can be used to define a point. However, it is appropriate to use the dominant constraints identified above. Suppose the ideal response achieves a 7.5% overshoot ( $x_1$ ) and a zero crossing ( $T_{01}$ ) one and half seconds after the initial peak. Then from Equation (3.5.44) and Equation (3.5.36):

$$0.075 = e^{-\frac{\zeta}{\sqrt{1-\zeta^2}}\pi} \quad (3.5.50)$$

$$1.5 = \frac{\pi - \alpha}{\omega_d} \quad (3.5.51)$$

Some rearrangement gives:

$$\omega_d = \frac{\pi - \tan\left(\frac{-\pi}{\ln(0.075)}\right)}{1.5} \quad (3.5.52)$$

$$\zeta\omega_n = \frac{-\ln(0.075)}{\pi}\omega_d \quad (3.5.53)$$

which evaluates to the following ideal point:

$$\lambda_{t1} = -1.24 \pm j1.51 \quad (3.5.54)$$

An simpler approach that yields a good engineering approximation is to suppose that the first overshoot (or first trough) occurs two seconds after the initial peak ( $t_{tr} - t_{pk} = 2$ ). This ensures that both the zero crossing criteria are comfortably met and as before a 7.5% overshoot is specified. From Equation (3.5.32), Equation (3.5.40) and Equation (3.5.42):

$$\omega_d = \frac{\pi}{t_{tr} - t_{pk}} \quad (3.5.55)$$

$$\zeta\omega_n = \frac{-\ln(0.075)}{t_{tr} - t_{pk}} \quad (3.5.56)$$

$$(3.5.57)$$

We see that the real and imaginary components are determined by very simple independent equations and evaluation gives:

$$\lambda_{t2} = -1.30 \pm j1.57 \quad (3.5.58)$$

This simple approach can be used to generate an ideal point for the attentive phase criteria. In this phase the criteria are generally the same except the first over shoot must be less than ten percent. Choosing an ideal overshoot of five percent gives the following ideal point:

$$\lambda_{t3} = -1.50 \pm j1.57 \quad (3.5.59)$$

The effect of zeros on the real axis was briefly investigated.

$$g(s) = \frac{\omega_n^2 (s + z)}{s^2 + 2\zeta\omega_n s + \omega_n^2} \quad (3.5.60)$$

Zeros less than -20 from the imaginary axis have no discernible effect on the region defined by the Def-Stan on the complex plane. As the zero moves closer to the imaginary axis the allowed region is progressively cropped from left, each time reducing the maximum response decay rate ( $\zeta\omega_n$ ). For instance, with a zero at -7 the region extends no further left than -2 and with a zero at -3 the allowed region ceases to exist. The effect of a zero on the time response is to accentuate the changes in the pilot command. Responses generally failed the Def-Stan criteria due to an excessive overshoot as the pilot command was removed. This can be explained as follows, the zero can be conceptually moved to the pilot input:

$$y(s) = \frac{\omega_n^2 (s + z)}{s^2 + 2\zeta\omega_n s + \omega_n^2} u(s) \quad (3.5.61)$$

$$y(s) = \frac{\omega_n^2}{s^2 + 2\zeta\omega_n s + \omega_n^2} [(s + z) u(s)] \quad (3.5.62)$$

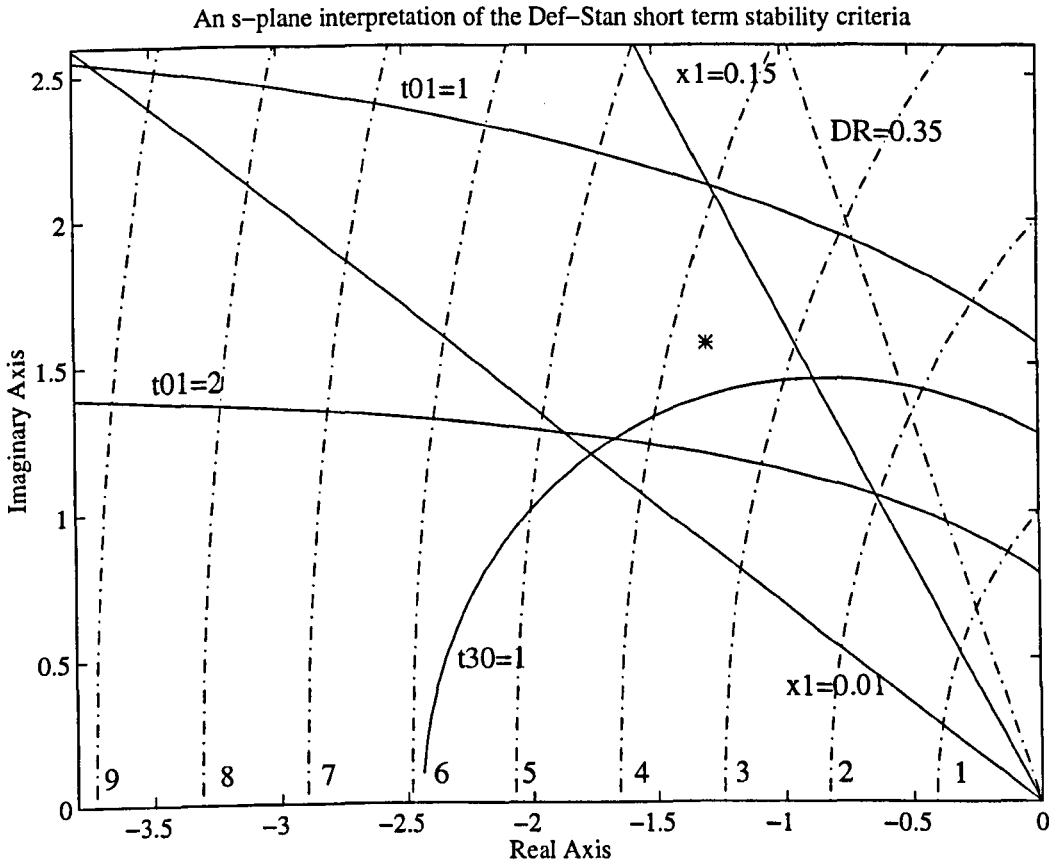


Figure 3.5.7: An s-plane interpretation of the Def-Stan short term stability criteria plus the ADS 33 bandwidth and damping ratio loci and the ideal point  $\lambda_{t2}$ .

The pilot input is now the sum of the original pulse and its derivative, a positive and negative impulse at the pulse transitions. As the zero moves closer to the imaginary axis the relative contribution from the derivative component increases causing a larger overshoot. Systems with a slower response are less effected by this 'derivative kick' hence the allowed region progressively encompasses only the slower systems.

It is worthwhile comparing these results with the ADS 33 criteria. Figure 3.5.7 shows both criteria. The dot-dash lines running from the real axis are the ADS 33 bandwidth criteria (see Equation (3.2.5)). The mid term response damping ratio criterion ( $DR = 0.35$ ) is also indicated as a dot-dash line and the asterisk denotes the approximate ideal point  $\lambda_{t2}$ . Second order systems achieving Def-Stan level one will generally have a bandwidth greater than 3 rad/s. This will meet the ADS 33 level one bandwidth criterion<sup>5</sup> for all MTEs except target acquisition. The Def-Stan permits a

<sup>5</sup> Assuming a phase delay ( $\tau_p$ ) less 0.25 seconds.

minimum damping ratio of 0.52. This is a stricter requirement than the ADS 33 mid term response criterion, which stipulates a minimum of 0.35. The ideal point has a bandwidth of 3.7Hz and a damping ratio of 0.64. This would meet the ADS 33 bandwidth criterion for the most demanding MTE, target acquisition<sup>6</sup>. Despite being specified in different domains, for this case the ADS 33 and Def-Stan show good consistency. While this result, for second order systems, offers some evidence that the specifications are globally consistent, such an extrapolation would be unwise.

### 3.5.3 Ideal Heave and Yaw Eigenvalue Locations

The Def-Stan (Leaflet 603/1 para 4.2) yaw channel requirements are specified using the usual time domain parameters and, except for the peak response, the criteria are equal to those for the roll and pitch channels. However, it is initially planned to use only a static feedback controller and apply rate damping in the yaw channel. Thus only the single real pole associated with the damped yaw response will be assigned. The Def-Stan does offer some guidance for systems exhibiting a first order response in yaw, although it assigns them level two handling qualities. From Table 3.3.3 the response should comply with the sensitivity requirements ( $y_1, T_1$ ) and the 10% decay requirement ( $T_{11} = 1 - 2$ ). These requirements are straightforward to convert into an ideal range for the yaw pole ( $\lambda_y$ ), for instance the 10% decay requirement becomes:

$$\ln(0.1) \leq \lambda_y \leq \frac{\ln(0.1)}{2} \quad (3.5.63)$$

which evaluates as:

$$\boxed{-2.3 \leq \lambda_y \leq -1.2} \quad (3.5.64)$$

The sensitivity requirement ( $y_1, T_1$ ) is:

$$0.3 < \frac{1 - e^{\lambda_y T}}{1 - e^{\lambda_y T_1}} < 0.75 \quad (3.5.65)$$

Where  $T$  is the input pulse width and will coincide with the peak response. This equation reduces to a quadratic, the solution of which reveals:

$$\boxed{-2.2 < \lambda_y} \quad (3.5.66)$$

<sup>6</sup> Assuming a phase bandwidth less than 0.22 seconds.



The ADS 33 specifies the small amplitude yaw response using bandwidth criteria. Garrad and Low [GL90, LG93] suggest that, for first order systems, the bandwidths may be directly interpreted as pole locations. For all MTEs except target acquisition and for phase delays less 0.2 seconds, a bandwidth of  $> 2$  rad/s will achieve level one handling qualities and  $> 0.5$  will achieve level two. Thus for level two compliance the ADS 33 implies the following bound on the yaw pole:

$$-2 < \lambda_y < -0.5 \quad (3.5.67)$$

This shows good agreement with the Def-Stan Criteria. Studies have shown [Pad96, p. 410] that a yaw pole location between -2.2 and -4.1 will meet the ADS 33 level one criteria for the most demanding MTE.

Due to the lack of quantitative guidance in the Def-Stan (Leaflet 607/1 para 4.2) for the desired heave response, criteria will be drawn from the ADS 33. Both specifications assume a single dominant pole ( $\lambda_w$ ) and the ADS 33 requirements (see Table 3.2.2) almost directly specify:

$$\boxed{\lambda_w < -0.2} \quad (3.5.68)$$

The limited authority of the series actuators and strong physical influence of the inflow dynamics mean that the heave pole can not be greatly effected by feedback. Despite this, some researchers [GL90] have attempted to assign some ambitious heave pole locations ( $\lambda_w = -4$ ).

For attitude and rate command response types the poles associated with the linear velocities ( $u, v$ ) may not be significantly influenced by feedback and should instead remain at the location dictated by the system physics. For instance, suppose a helicopter has attitude command. Then the body attitude orientates the thrust vector which, predominantly determines the build-up of the linear velocities. Any attempt to significantly modify the build up of linear velocities will require a change in attitude, which is inconsistent with attitude command.

For translation rate command both specifications require the linear velocities to have a dominant first order response. The ADS 33 requires a time constant of between 2.5 and 5 seconds and the Def-Stan (Leaflet 602/3 para 2.4) requires a settling time of less five seconds.

The two previous sections have demonstrated a clear link between the handling qualities requirements and the ideal system modes. Even for complex requirements with multiple constraints a clear and simple link to the ideal pole location has been established (see Equation (3.5.55) and Equation (3.5.56)). An attempt has been made to produce ideal modes that are consistent with both the Def-Stan and ADS 33 requirements. Specifying the system modes alone is not sufficient to guarantee a good response. One must also consider how they are distributed.

### 3.5.4 Ideal Eigenvectors

Two aims drove the derivation of the ideal eigenvectors:

1. Decoupling the modes into the appropriate outputs.
2. Ensuring the eigenvectors were consistent with the physical relationships between the state variables.

The states were initially divided into four groups; longitudinal ( $u, q, \theta$ ), lateral ( $v, p, \phi$ ), yaw ( $r$ ) and heave ( $w$ ). Each group is fully decoupled from the others and, for the longitudinal and lateral groups, a transfer function approach was used to preserve integral relationship between the states. Consider a longitudinal or lateral third order subsystem. Two poles will be assigned to the system, one complex pole pair ( $\lambda_1, \bar{\lambda}_1$ ) to determine the attitude and rate responses and one real pole ( $\lambda_2$ ) associated with the linear velocity response. The attitude ( $\theta, \phi$ ) is approximately the integral of the rate ( $q, p$ ) and the linear velocity mode ( $\lambda_2$ ) should not be visible in both rate and attitude outputs. All modes will be visible in the linear velocity outputs ( $u, v$ ) since they are related to body attitudes via the linear velocity modes. The preceding description leads to the following ideal transfer functions, which illustrate the longitudinal case:

$$\frac{u}{B_1} = \frac{1}{(s + \lambda_1)(s + \bar{\lambda}_1)(s + \lambda_2)} \quad (3.5.69)$$

$$\frac{q}{B_1} = \frac{s}{(s + \lambda_1)(s + \bar{\lambda}_1)} \quad (3.5.70)$$

$$\frac{\theta}{B_1} = \frac{1}{(s + \lambda_1)(s + \bar{\lambda}_1)} \quad (3.5.71)$$

Suppose the third order subsystem has an input matrix  $Bs = \begin{bmatrix} 0 & 1 & 0 \end{bmatrix}^T$ , output matrix  $Cs = I_3$ , left and right eigenvector matrices denoted  $Ws$  and  $Vs$  and eigenvalue matrix denoted  $\Lambda s$ . Then the subsystem transfer function matrix ( $Gs(s)$ ) may be expressed as:

$$Gs(s) = Cs Vs (sI - \Lambda s)^{-1} Ws Bs \quad (3.5.72)$$

For the longitudinal case, the above is expanded as follows:

$$\begin{bmatrix} u \\ q \\ \theta \end{bmatrix} = \begin{bmatrix} \bar{r}_1 & r_1 & r_4 \\ \bar{r}_2 & r_2 & 0 \\ \bar{r}_3 & r_3 & 0 \end{bmatrix} \begin{bmatrix} \frac{1}{(s+\lambda_1)} & 0 & 0 \\ 0 & \frac{1}{(s+\lambda_1)} & 0 \\ 0 & 0 & \frac{1}{(s+\lambda_2)} \end{bmatrix} \begin{bmatrix} \bar{t}_1 \\ t_1 \\ t_2 \end{bmatrix} B_1 \quad (3.5.73)$$

The zeros in Cs Vs arise because the mode  $\lambda_2$  should not be visible in  $q$  and  $\theta$ . Equation (3.5.73) can be evaluated to give:

$$\frac{u}{B_1} = \frac{\bar{r}_1 \bar{t}_1}{(s + \lambda_1)} + \frac{r_1 t_1}{(s + \bar{\lambda}_1)} + \frac{r_4 t_2}{(s + \lambda_2)} \quad (3.5.74)$$

$$\frac{q}{B_1} = \frac{\bar{r}_2 \bar{t}_1}{(s + \lambda_1)} + \frac{r_2 t_1}{(s + \bar{\lambda}_1)} \quad (3.5.75)$$

$$\frac{\theta}{B_1} = \frac{\bar{r}_3 \bar{t}_1}{(s + \lambda_1)} + \frac{r_3 t_1}{(s + \bar{\lambda}_1)} \quad (3.5.76)$$

By equating coefficients with the numerators of the ideal transfer functions, the eigenvector elements  $r_1, \dots, r_4$  and  $t_1, t_2$  can be calculated, as shown below:

$$\frac{u}{B_1} \quad s^2 : 0 = \bar{r}_1 \bar{t}_1 + r_1 t_1 + r_4 t_2 \quad (3.5.77)$$

$$s^1 : 0 = \bar{r}_1 \bar{t}_1 \lambda_2 + r_1 t_1 \lambda_2 + \bar{r}_1 \bar{t}_1 \bar{\lambda}_1 + r_1 t_1 \lambda_1 + r_4 t_2 \bar{\lambda}_1 + r_4 t_2 \lambda_1 \quad (3.5.78)$$

$$s^0 : 0 \neq \bar{r}_1 \bar{t}_1 \bar{\lambda}_1 \lambda_2 + r_1 t_1 \lambda_1 \lambda_2 + r_4 t_2 \lambda_1 \bar{\lambda}_1 \quad (3.5.79)$$

$$\frac{q}{B_1} \quad s^1 : 0 \neq \bar{r}_2 \bar{t}_1 + r_2 t_1 \quad (3.5.80)$$

$$s^0 : 0 = \bar{r}_2 \bar{t}_1 \bar{\lambda}_1 + r_2 t_1 \lambda_1 \quad (3.5.81)$$

$$\frac{\theta}{B_1} \quad s^1 : 0 = \bar{r}_3 \bar{t}_1 + r_3 t_1 \quad (3.5.82)$$

$$s^0 : 0 \neq \bar{r}_3 \bar{t}_1 \bar{\lambda}_1 + r_3 t_1 \lambda_1 \quad (3.5.83)$$

However, not all the elements can be arbitrarily assigned since the left and right eigenvectors must satisfy:

$$\mathbf{I}_3 = \mathbf{W} \mathbf{s} \mathbf{V} \mathbf{s} \quad (3.5.84)$$

Which can be converted into the following constraints on  $r_1, \dots, r_4$  and  $t_1, t_2$ :

$$\begin{bmatrix} 0 & 1 & 0 \end{bmatrix}^T = \mathbf{C}_s \mathbf{V}_s \mathbf{W}_s \mathbf{B}_s \quad (3.5.85)$$

$$\begin{bmatrix} 0 \\ 1 \\ 0 \end{bmatrix} = \begin{bmatrix} \bar{r}_1 \bar{t}_1 + r_1 t_1 + r_4 t_2 \\ \bar{r}_2 \bar{t}_1 + r_2 t_1 \\ \bar{r}_3 \bar{t}_1 + r_3 t_1 \end{bmatrix} \quad (3.5.86)$$

Examination of Equation (3.5.86) shows that the constraints (3.5.77), (3.5.80) and (3.5.82) will be inherently satisfied. If Equation (3.5.80) is satisfied then it clear that:

$$r_2 = \frac{r_3}{\lambda_1} \quad (3.5.87)$$

will satisfy Equation (3.5.81). It only remains to solve Equation (3.5.78), eliminating  $r_4 t_2$  by substituting Equation (3.5.77), some rearrangement and comparison with Equation (3.5.82) yields:

$$r_1 = \frac{r_3}{(\lambda_2 - \lambda_1)} \quad (3.5.88)$$

Eigenvectors are unique up to scaling therefore, for convenience, let us assume that both  $r_4$  and  $r_3$  are equal to unity. The desired closed loop eigenvectors are:

$$\mathbf{V}_s = \begin{bmatrix} \frac{1}{(\lambda_2 - \lambda_1)} & \frac{1}{(\lambda_2 - \lambda_1)} & 1 \\ \frac{1}{\lambda_1} & \frac{1}{\lambda_1} & 0 \\ 1 & 1 & 0 \end{bmatrix} \quad (3.5.89)$$

We see that the linear velocity mode ( $\lambda_2$ ) will be unobservable in the attitude ( $\theta, \phi$ ) and rate ( $p, q$ ) outputs, which is consistent with the original requirements. In practice, assigning the desired eigenvectors may not ensure that the linear velocity mode is completely unobservable, but this can be achieved by assigning the pole and eigenvector to be coincident with the open loop zero and zero direction (see Section 2.4.3). In fact, the open loop zero directions are encouragingly consistent with the ideal eigenvectors. The use of the open loop zeros has also been proposed by Manness and Murray-Smith [MMS92]. Their motivation was quite different and based on simplifying the system dynamics.

The complete set of ideal eigenvectors may be constructed from the four decoupled blocks as shown below:

$$\begin{bmatrix} u \\ q \\ \theta \\ v \\ p \\ \phi \\ w \\ r \end{bmatrix} = \begin{bmatrix} \frac{1}{(\lambda_u - \lambda_q)} & \frac{1}{(\lambda_u - \lambda_q)} & 1 & 0 & 0 & 0 & 0 & 0 \\ \frac{1}{\lambda_q} & \frac{1}{\lambda_q} & 0 & 0 & 0 & 0 & 0 & 0 \\ 1 & 1 & 0 & 0 & 0 & 0 & 0 & 0 \\ 0 & 0 & 0 & \frac{1}{(\lambda_v - \lambda_p)} & \frac{1}{(\lambda_v - \lambda_p)} & 1 & 0 & 0 \\ 0 & 0 & 0 & \frac{1}{\lambda_p} & \frac{1}{\lambda_p} & 0 & 0 & 0 \\ 0 & 0 & 0 & 1 & 1 & 0 & 0 & 0 \\ 0 & 0 & 0 & 0 & 0 & 0 & 1 & 0 \\ 0 & 0 & 0 & 0 & 0 & 0 & 0 & 1 \end{bmatrix} \quad (3.5.90)$$

Using a different approach Garrad *et al* [GLP89a] present a set of ideal vectors which are broadly consistent with those presented above.

It is important to point out that a key assumption in deriving the desired eigenvectors was the ideal nature of  $C_s$  and  $B_s$ . While we can be sure that  $C_s = I_3$ , it is unlikely that  $B_s = \begin{bmatrix} 0 & 1 & 0 \end{bmatrix}^T$  will be satisfied exactly. For example, the normalised input matrix for the longitudinal and lateral subsystems is:

$$B_{lon} = \begin{bmatrix} 0.26 \\ -6.88 \\ 0.00 \end{bmatrix} B_1 \quad B_{lat} = \begin{bmatrix} 0.15 \\ 26.7 \\ 0.00 \end{bmatrix} A_1 \quad (3.5.91)$$

Matters will be improved by the interlinks which can be considered as a static gain network that decouples the inputs.

The preceding ideal eigenvectors are for small pilot commands, that is pilot stick motions before the force break out point, since they will give attitude command. A natural topic for further work is to derive ideal eigenvectors for rate command. Much of the work required to do this can be drawn from this chapter. For instance, the ideal pole locations for the roll, pitch and yaw rate response will be the same as those derived for the attitude response in Section 3.5.2. However, the pole will be associated purely with angular rate and an additional compensator pole will be needed to form the complex pair. The need for a compensator is consistent with the conventional approach where washed out attitude is often fed back. The attitude response will have a single pole associated with it. This should be determined by the kinematic relationship with the angular rate, since moving this pole by feeding back body attitude will introduce attitude command. The same argument applies to the feed back of the linear velocities which will introduce translation rate command. Since both the attitude and linear velocity modes should not be seen in the rate response, their associated eigenvector and eigenvalues may be placed using the open loop zeros. The heave and yaw eigenvectors and eigenvalues may be assigned as before.

Another interesting topic for further work would be to replace the algebraic technique above with an automated numerical technique. The motivation for this is that the approach above reduces to solving several linear equations, which can be efficiently computed numerically. Ideally, the numerical technique would accept values for the ideal pole locations, the actual system input and output matrices and the desired zero polynomials for key transfer functions. It would produce a set of eigenvectors that, if achieved, would realise the desired zero polynomials. Such a technique would form a useful addition to the eigenstructure assignment technique, allowing ideal eigenvectors to be formulated from a mixture of time domain considerations and zero placement.

### 3.6 Summary

This chapter described the two currently most important rotorcraft handling qualities specifications (the ADS 33 and Def-Stan 00-970) and, in particular, compared and contrasted their approach to the small amplitude dynamic response. The Def-Stan criteria were employed to develop an ideal eigenstructure. This was achieved and a visible link between the requirements and final eigenstructure was demonstrated. It was further shown that the ideal eigenstructure is consistent with the ADS 33 requirements. Some topics for further work have been mentioned these include; construction of a rate command ideal eigenstructure and development of a method for generating eigenvectors that realise a specified zero structure.

### 3.7 References

- [AM89] BDO Anderson and JB Moore. *Optimal Control and Linear Quadratic Methods*. Information and System Sciences Series. Prentice-Hall International Inc., 1989.
- [AVS89] AVSCOM. Handling qualities requirements for military rotorcraft. Army Aeronautical Design Standard ADS33c, US Army Aviation Systems Command, 4300 Goodfellow Boulevard, St. Louis Missouri, August 1989.
- [BP94] CL Blanken and Heinz-Jürgen Pausder. Investigation of the effects of bandwidth and time delay on helicopter roll-axis handling qualities. *Journal of The American Helicopter Society*, pages 24–33, July 1994.
- [CP72] TR Crossley and B Porter. Synthesis of helicopter stabilization systems using modal control theory. *J. Aircraft*, 9(1):3–8, January 1972.
- [DH95] JJ D’Azzo and CH Houpis. *Linear Control System Analysis and Design: Conventional and Modern*. McGraw-Hill Electrical Engineering Series. McGraw-Hill, 4th edition, 1995.
- [GL90] WL Garrad and E Low. Eigenspace design of helicopter flight control systems. Technical report DAAL03-86-K-0056, Department of Aerospace Engineering and Mechanics, University of Minnesota., November 1990.
- [GLP89] WL Garrad, E Low, and S Prouty. Design of attitude and rate command systems for helicopters using eigenstructure assignment. *Journal of Guidance, Control and Dynamics*, 12(6):783–791, November 1989.
- [Gri93] JJ Gribble. Linear quadratic/loop transfer recovery design for a helicopter in low-speed flight. *Journal of Guidance, Control and Dynamics*, 16(4):754–761, July 1993.
- [HC86] RP Harper and GE Cooper. Handling qualities and pilot evaluation. *Journal of Guidance and Dynamics*, 9(5):515–529, September 1986.
- [Hin87] WS Hindson. Implementation and flight-test of a multi-mode rotorcraft flight-control system for single-pilot use in poor visibility. In *Mid-east Region National Specialists’ Meeting in Rotorcraft Flight Controls and Avionics*, pages 1–21, Cherry Hill, New Jersey, October 1987. American Helicopter Society.

- [HMA+85] RH Hoh, DG Mitchell, IL Ashkenas, BL Aponso, SW Ferguson, TJ Rosenthal, DL Key, and CL Blanken. Background information and user's guide for the proposed handling qualities requirements for military rotorcraft. Technical report 1194-3, Systems Technology Inc., 13766 South Hawthorne Boulevard, Hawthorne, California 90250, December 1985.
- [Hoh88] RH Hoh. Dynamic requirements in the new handling qualities specification for U.S. military rotorcraft. In *Helicopter Handling Qualities and Control*, pages 4.1–4.17. The Royal Aeronautical Society, November 1988.
- [IC94] SJ Ingle and R Celi. Effects of higher order dynamics on helicopter flight control law design. *Journal of The American Helicopter Society*, pages 12–23, July 1994.
- [IS90] M Innocenti and C Stanzola. Performance-robustness trade-off of eigenstructure assignment applied to rotorcraft. *Aeronautical Journal*, 94(934):124–131, 1990.
- [Key88] DL Key. A new handling qualities specification for U.S. military rotorcraft. In *Helicopter Handling Qualities and Control*, pages 3.1–3.18. The Royal Aeronautical Society, November 1988.
- [LG93] E Low and WL Garrad. Design of flight control systems to meet rotorcraft handling qualities specifications. *Journal of Guidance, Control and Dynamics*, 16(1):69–78, January 1993.
- [Mac89] JM Maciejowski. *Multivariable Feedback Design*. Electronic Systems Engineering. Addison Wesley, 1989.
- [McI90] D Mclean. *Automatic Flight Control Systems*. Systems and Control Engineering. Prentice Hall International, 1990.
- [McR91] D McRuer. Estimation of pilot ratings via pilot modeling. Technical memorandum, Systems Technology Inc., 13766 S. Hawthorne Blvd., Hawthorne, CA 90250, 1991.
- [MG93] Z Mirfakhraie and WL Garrard. Design of helicopter control system to meet handling quality specification using  $\mathcal{H}_\infty$  techniques. In *AIAA Guidance, Navigation and Control Conference*, pages 1336–1341. AIAA, 1993.
- [MG94] Z Mirfakhraie and WL Garrard. Implicit and explicit model-following helicopter flight controllers. In *AIAA Guidance, Navigation and Control Conference*, pages 1358–1365. AIAA, 1994.
- [MMS92] MA Manness and DJ Murray-Smith. Aspects of multivariable flight control law design for helicopters using eigenstructure assignment. *Journal of The American Helicopter Society*, 37(3):18–32, July 1992.
- [Nar69] RD Murphy K S Narendra. Design of helicopter stabilization systems using optimal control theory. *J. Aircraft*, 6(2):129–136, March 1969.
- [OC92] S Osder and D Caldwell. Design and robustness issues for highly augmented helicopter controls. *Journal of Guidance, Control and Dynamics*, 15(6):1375–1387, November 1992.
- [Pad96] GD Padfield. *Helicopter Flight Dynamics*. Blackwell Science Ltd, 1996.
- [Pit89] B Pitkin. Flight and ground handling qualities. Military Defence Specification DEF-STAN 00-970, Ministry of Defence, September 1989.
- [PMS85] DLK Parry and DJ Murray-Smith. The application of modal control theory to the single rotor helicopter. In *The 11<sup>th</sup> European Rotorcraft Forum*, pages 78–1–78–16, 1985.
- [SC94] XD Sun and T Clarke. Robust  $\mathcal{H}_\infty$ -based implicit model-following control of helicopters. In *IFAC Symposium on Robust Control Design*, pages 249–254. IFAC, September 1994.
- [SR75] S Srinathkumar and RP Rhoten. Eigenvalue/eigenvector control via spectral characterisation: An application to helicopter hover dynamics. In *9<sup>th</sup> ASILOMAR Conference on Circuits Systems and Computers*, pages 605–609, University of Santa Clara Naval Postgraduate School, San Francisco, California, November 1975. IEEE Circuits and Systems Society and IEEE Control Systems Society.
- [Tak93a] MD Takahashi.  $\mathcal{H}_\infty$  helicopter control law design with and without rotor state feedback. In *AIAA Guidance, Navigation and Control Conference*, pages 1323–1335. AIAA, 1993.
- [Tak93b] MD Takahashi. Synthesis and evaluation of an  $\mathcal{H}_2$  control law for a hovering helicopter. *Journal of Guidance, Control and Dynamics*, 16(3):579–584, May 1993.
- [WP90] D Walker and I Postlethwaite. Full authority active control system design for a high performance helicopter. In *Proceedings of the 16<sup>th</sup> Annual European Rotorcraft Forum*, pages III.3.2.1–14, Glasgow, Scotland, UK, September 1990. Royal Aeronautical society.
- [WP96] DJ Walker and I Postlethwaite. Advanced helicopter flight control using two-degree-of-freedom  $\mathcal{H}_\infty$  optimization. *Journal of Guidance, Control and Dynamics*, 19(2):461–468, March 1996.
- [YI93] JS Young and CE Lin. Refined  $\mathcal{H}_\infty$ -optimal approach to rotorcraft flight control. *Journal of Guidance, Control and Dynamics*, 16(2):247–255, April 1993.
- [YP88] A Yue and I Postlethwaite. Robust helicopter control laws for handling qualities enhancement. In *Helicopter Handling Qualities and Control*, pages 14.1–14.17. The Royal Aeronautical Society, November 1988.
- [YP90] A Yue and I Postlethwaite. Improvement of helicopter handling qualities using  $\mathcal{H}_\infty$  optimisation. *IEE Proceedings D*, 137(3):115–129, May 1990.

# Chapter 4

## Feedback Design for Performance

### Contents

---

4.1	Introduction . . . . .	91
4.2	The State Feedback Problem . . . . .	92
4.3	Projection With Eigenvalue Trade-off . . . . .	95
4.4	Practical Implementation . . . . .	102
4.5	The Output Feedback Problem . . . . .	105
4.6	Direct Assignment of the Modal Coupling Matrices . . . . .	157
4.7	Dynamic Compensation . . . . .	163
4.8	Summary and Further Work . . . . .	169
4.9	References . . . . .	170

---

### 4.1 Introduction

This chapter gives an exposition of the current eigenstructure assignment theory and develops some extensions that are generically relevant to practical engineering problems. Although, the impetus for the extensions was to develop tools that support helicopter control law design. The work in this chapter concentrates on achieving performance design goals, robustness is addressed in the following chapter. Initially, the state feedback case is considered which is obviously inappropriate for the helicopter problem, but is theoretically fundamental. From this basis an algorithm is developed that enables a trade-off between eigenvalue and eigenvector design goals. Attention then focuses on the more realistic output feedback case, where a practical and versatile algorithm is developed. Several, enhancements to the basic algorithm are derived; the theme of which is to provide the engineer with the tools to maximally exploit the available design freedom. It is argued that direct assignment of the modal coupling matrices is more appropriate for the output feedback case and a technique that complements the eigenstructure assignment algorithm is developed. Finally, the approach is extended to include to dynamic compensation.



## 4.2 The State Feedback Problem

The state feedback problem can be stated as follows:

Given a state space system  $(\mathbf{A}, \mathbf{B})$  find a real gain matrix  $(\mathbf{K})$  that assigns a desired set of self-conjugate eigenvalues  $\{\lambda_i\}$  and right eigenvectors  $\{\mathbf{v}_i\}$ .

Most of the interest in this problem was initiated after Wonham [Won67] showed that controllability of the pair  $(\mathbf{A}, \mathbf{B})$  was a necessary and sufficient condition to assign a set of arbitrary eigenvalues using state feedback. Early techniques used transformation to controllable canonical form or block Jordan form [PC72, AL67]. These techniques often ignored the freedom offered by multiple input systems or used dyadic controllers [Fal77] to reduce them to equivalent single input systems. The modern topic of eigenstructure assignment began in earnest when Moore [Moo76] illustrated how the extra freedom offered by multiple input systems could be used to place the poles arbitrarily *and* manipulate the closed loop eigenvectors. A summary of this important result is given as follows:

Consider the following state feedback system:

$$\dot{\mathbf{x}} = \mathbf{A}\mathbf{x} + \mathbf{B}\mathbf{u} \quad (4.2.1)$$

$$\mathbf{u} = \mathbf{K}\mathbf{x} \quad (4.2.2)$$

where  $\mathbf{A} \in \mathbb{R}^{n \times n}$ ,  $\mathbf{B} \in \mathbb{R}^{n \times r}$ ,  $\mathbf{K} \in \mathbb{R}^{r \times n}$  and  $\text{rank}(\mathbf{B}) = r$ . The closed loop system matrix is:

$$\mathbf{ACL} = \mathbf{A} + \mathbf{BK} \quad (4.2.3)$$

Let  $(\lambda_i, \mathbf{v}_i)$  be a closed loop eigenvalue and eigenvector pair. Then from the definition of the closed eigenvectors we see:

$$\mathbf{ACL} \mathbf{v}_i = \lambda_i \mathbf{v}_i \quad (4.2.4)$$

$$\mathbf{0} = (\mathbf{A} - \lambda_i \mathbf{I}) \mathbf{v}_i + \mathbf{BK} \mathbf{v}_i \quad (4.2.5)$$

$$\mathbf{0} = \begin{bmatrix} \mathbf{A} - \lambda_i \mathbf{I} & \mathbf{B} \end{bmatrix} \begin{bmatrix} \mathbf{v}_i \\ \mathbf{K} \mathbf{v}_i \end{bmatrix} \quad (4.2.6)$$

Thus a subspace may be calculated in which the closed loop eigenvector and gain-eigenvector product must reside:

$$\ker \left( \begin{bmatrix} \mathbf{A} - \lambda_i \mathbf{I} & \mathbf{B} \end{bmatrix} \right) = \text{range} \left( \begin{bmatrix} \mathbf{Q}_i \\ \mathbf{P}_i \end{bmatrix} \right) \quad (4.2.7)$$

Where  $\ker(\mathbf{X})$  is the null space of  $\mathbf{X}$ . It follows that for some  $\mathbf{f}_i \in \mathbb{C}^{r \times 1}$ :

$$\begin{bmatrix} \mathbf{v}_i \\ \mathbf{K}\mathbf{v}_i \end{bmatrix} = \begin{bmatrix} \mathbf{Q}_i \\ \mathbf{P}_i \end{bmatrix} \mathbf{f}_i \quad (4.2.8)$$

Equation (4.2.8) demonstrates the necessity for a closed loop eigenvector associated with the eigenvalue  $\lambda_i$  to be a member of  $\text{range}(\mathbf{Q})$ . Moore [Moo76] shows that eigenvectors may be arbitrarily selected from  $\text{range}(\mathbf{Q})$  providing conditions C1 to C3 below, are met:

- C1 Selected  $\mathbf{v}_i$  are linearly independent.
- C2  $\mathbf{v}_i = \text{conj}(\mathbf{v}_k)$  whenever  $\lambda_i = \bar{\lambda}_k$ .
- C3 The eigenvalues  $\lambda_i$  should be distinct<sup>1</sup>.

Where the operator  $\text{conj}(\mathbf{X})$  produces the matrix  $\mathbf{X}$  with each element complex conjugated.

Moore also illustrates the practical relevance of being able to select the closed loop eigenvectors through their direct influence on the system time response. Many researchers developed this approach further, often using least squares projection [ASC83, SC81, SS85a, SS85b, SSA94] to achieve eigenvectors as close as possible to a desired set  $\{\mathbf{v}_d\}$ . This approach has proved particularly applicable to aerospace problems [Far89, GLP89a, SS91, SC92]. Other researchers used the extra design freedom to reduce the sensitivity of the closed loop eigenvalues to perturbation in the closed loop system matrix. It was shown by [Wil65, Gil84] that eigenvalue sensitivity is at a minimum when the eigenvectors are orthogonal. That is

$$\mathbf{V}\mathbf{V}^* = \mathbf{I} \quad (4.2.9)$$

Where  $\mathbf{V}$  is the closed loop modal matrix and defined as  $\mathbf{V} = [\mathbf{v}_1, \dots, \mathbf{v}_n]$ .

Algorithms for assigning near-orthogonal eigenvectors were developed by [KND85, OO89, BN89, BP91, Bur90]. These algorithms also form the basis for numerically stable pole placement [GLLT92].

<sup>1</sup>This condition was introduced by Moore [Moo76] to simplify the exposition and later removed by Porter and D'Azzo [PD78] who show how to assign general block Jordan forms.

Solutions for the gain matrix that express the eigenvector design freedom as a set of independent free parameters (parametric solutions) were developed by [FO82, FO83]. Initial solutions required that the open loop and closed loop eigenvalues should not coincide, this was later overcome [FT84]. O'Reilly and Fahmy [OF85] also explored the amount of design freedom available and showed it to depend on the exact Jordan form that is assigned. Minimal parametric solutions form the basis for many optimisation approaches: [Rop83, Dua92a]. The approaches of Fahmy and O'Reilly [FO83] and Moore [Moo76] were unified in the work of Duan [Dua93, Dua94, Dua92b]. Duan showed both solutions to be a special case of a more general approach. Some basic properties of state feedback are listed below:

- If a system is controllable then state feedback may arbitrarily assign the closed loop poles [Won67].
- The right eigenvectors of uncontrollable modes may be manipulated by state feedback [Moo76], but not the left.
- If  $\text{rank}(\mathbf{B}) = r$  the right eigenvectors may be selected from a subspace of dimension at least  $r$ .
- State feedback may alter the observability [SK76] of a system but not the controllability [Bro91, p. 446].
- The invariant and transmission zeros are unaffected by state feedback [MK76, SK76].

In the remainder of this chapter  $\mathbf{A}$ ,  $\mathbf{B}$ ,  $\mathbf{C}$  will denote a state space triple. Where  $\mathbf{A} \in \mathbb{R}^{n \times n}$ ,  $\mathbf{B} \in \mathbb{R}^{n \times r}$  and  $\mathbf{C} \in \mathbb{R}^{m \times n}$ . It is assumed the matrices  $\mathbf{B}$  and  $\mathbf{C}$  are full rank. The rank assumption eliminates consideration of redundant inputs and outputs. If  $\mathbf{B}$  or  $\mathbf{C}$  is rank deficient then an input or output may be constructed from other inputs or outputs. Although, this may have practical implications from a theoretical point of view a redundant input exerts no new influence over the plant and may be ignored. Equally, a redundant output provides no new feedback information and is also ignored.

Chapter 3 demonstrated that eigenvector assignment will form an important part of any flight control law design using eigenstructure assignment, since orthogonalisation alone will be insufficient to meet the design goals. This statement is further supported by the fact that all the notable applications of eigenstructure assignment to flight control law design have used projection-based techniques [GL90, MMS92]. With this in mind it is worthwhile trying to maximally exploit the design freedom with which one is able to assign eigenvectors.

## 4.3 Projection With Eigenvalue Trade-off

### 4.3.1 Introduction

Most eigenstructure assignment algorithms to-date do not permit the designer to trade-off the desired eigenvalues and eigenvectors [SSA94, DH88]. It is clear from Equation (4.2.7) that the eigenvalue location determines the allowed eigenvector subspace (range ( $\mathbf{Q}$ )) and thus affects how well the desired eigenvector can be approximated.

It is also true that most aircraft specifications do not require exact pole placement, but will be satisfied by a value within a desired region [Dav94, Dep80]. In Section 3.5.2 it was demonstrated that the Def-Stan 00-970 effectively specifies a well defined region in the complex plane and thus eigenvalue trade-off is appropriate for helicopter control law design.

Other researchers [WCY91, LH92, PMS85] have developed techniques that enable eigenvalue trade-off. However, in these cases the trade-off is part of a large optimisation that manipulate weighting matrices or the gain matrix directly. The approach taken here is to consider the trade-off between the eigenvalue location and the associated eigenvector. To perform the trade-off one firsts needs a relative figure of merit for a given eigenvalue location and allowed eigenvector subspace. The merit of an allowed eigenvector subspace is measured by how closely a vector within the subspace can approximate a desired eigenvector, in a least squares sense. Two approaches are used to measure the merit of an eigenvalue location. The first costs the distance from an ideal point and the second defines an allowed region for the eigenvalue. The eigenvalue figures of merit lead to an unconstrained and a constrained optimisation respectively. In both cases only the eigenvalue location is optimised. This technique forms a logical extension to the popular projection method [ASC83, SC81, SS85a, SS85b, SSA94, Far89]. A more rigorous statement of the problem is given below:

### 4.3.2 The Problem

Consider the state feedback system of Equation (4.2.1). By definition the closed loop eigenvector ( $\mathbf{V}$ ) and eigenvalue ( $\mathbf{\Lambda}$ ) matrices satisfy:

$$\mathbf{V}^{-1} (\mathbf{A} + \mathbf{BK}) \mathbf{V} = \mathbf{\Lambda} \quad (4.3.10)$$

Where the columns of  $\mathbf{V}$  are the closed loop eigenvectors ( $\mathbf{v}_i$ ):

$$\mathbf{V} = [\mathbf{v}_1, \dots, \mathbf{v}_n] \quad (4.3.11)$$

and principal diagonal of the matrix  $\mathbf{\Lambda}$  contains the closed loop eigenvalues ( $\lambda_i$ ):

$$\Lambda = \text{diag}(\lambda_1, \dots, \lambda_n) \quad (4.3.12)$$

For the unconstrained optimisation problem the objective is to find the feedback gain  $\mathbf{K}$  which minimises the cost function below:

$$J_u = \|\mathbf{V}_D - \mathbf{V}\|_F^2 + \|\Lambda_D - \Lambda\|_F^2 \quad (4.3.13)$$

Where  $\mathbf{V}_D$  is a matrix of the desired eigenvectors ( $\mathbf{v}_{d_i}$ ):

$$\mathbf{V}_D = [\mathbf{v}_{d_1}, \dots, \mathbf{v}_{d_n}] \quad (4.3.14)$$

the matrix  $\Lambda_D$  has a principal diagonal equal to the desired eigenvalues ( $\lambda_{d_i}$ ):

$$\Lambda_D = \text{diag}(\lambda_{d_1}, \dots, \lambda_{d_n}) \quad (4.3.15)$$

$\|\cdot\|_F$  is the matrix Frobenius Norm. The constrained optimisation problem is formulated as:

$$J_c = \|\mathbf{V}_D - \mathbf{V}\|_F^2 \quad \text{subject to} \quad \Lambda \in \Lambda_A \quad (4.3.16)$$

Where  $\Lambda_A$  is the set of all allowed eigenvalue locations. The following assumptions are made:

- A1  $\mathbf{V}_D, \Lambda_D$  must form a self-conjugate set.
- A2 The spectrum of  $\Lambda_D$  must be distinct.
- A3 The pair  $(\mathbf{A}, \mathbf{B})$  must be controllable.
- A4 The matrix  $\mathbf{V}$  must satisfy  $\det(\mathbf{V}) \neq 0$ .

Assumption A3 may be ignored if one only considers a controllable subsystem. Assumption A2 has been introduced to simplify this exposition. It may also be removed, but this will result in a more complicated technique. Assumption A4 ensures that the assigned eigenvectors are linearly independent.

### 4.3.3 The Solution

The cost functions of Equation (4.3.13) can be broken down into  $n$  independent optimisation problems by considering each column independently. The unconstrained problem becomes:

$$Ju = \sum_{i=1}^n Ju_i \quad (4.3.17)$$

$$Ju_i = \|\mathbf{v}_d \mathbf{a}_i - \mathbf{v}_i\|_2^2 + |\lambda_d \mathbf{a}_i - \lambda_i|^2 \quad i = 1 \dots n \quad (4.3.18)$$

Where  $\|\cdot\|_2$  is the vector 2-norm or Euclidean norm and  $|\cdot|$  is the modulus operator. The constrained problem becomes:

$$Jc = \sum_{i=1}^n Jc_i \quad (4.3.19)$$

$$Jc_i = \|\mathbf{v}_d \mathbf{a}_i - \mathbf{v}_i\|_2^2 \quad \text{subject to} \quad \lambda_i \in \lambda_{\mathbf{a}_i} \quad (4.3.20)$$

Where  $\lambda_{\mathbf{a}_i}$  is the set of allowed eigenvalue locations for  $\lambda_i$ .

The next step is to remove the dependence of the cost function on the vector  $\mathbf{v}_i$ . This is achieved by describing the allowed eigenvector subspace from which  $\mathbf{v}_i$  is selected as a function of the eigenvalue location ( $s$ ). A basis for the subspace is formed whereby each element of the matrix is a polynomial function of the eigenvalue location.

Consider the polynomial matrix  $\mathbf{N}(s)$  of maximum and full rank that satisfies:

$$\mathbf{0} = \begin{bmatrix} \mathbf{A} - s\mathbf{I} & \mathbf{B} \end{bmatrix} \mathbf{N}(s) \quad (4.3.21)$$

$\mathbf{N}(s)$  can be compatibly partitioned with respect to Equation (4.3.21), as follows:

$$\mathbf{N}(s) = \begin{bmatrix} \mathbf{Q}(s) \\ \mathbf{P}(s) \end{bmatrix} \quad (4.3.22)$$

Where  $\mathbf{Q}(s)$  is a polynomial matrix with columns that spans the closed loop eigenvector subspace

for a given eigenvalue location ( $s$ ). Methods for calculating  $\mathbf{N}(s)$  are discussed in Appendix C.1. By introducing a design vector  $\mathbf{f}_i$ , that selects a specific eigenvector from the allowed subspace, the cost function  $J_{u_i}$  may now be expressed as follows:

$$J_{u_i} = \|\mathbf{v}_{d_i} - \mathbf{Q}(s) \mathbf{f}_i\|_2^2 + |\lambda_{d_i} - s|^2 \quad (4.3.23)$$

and similarly for the constrained case:

$$J_{c_i} = \|\mathbf{v}_{d_i} - \mathbf{Q}(s) \mathbf{f}_i\|_2^2 \quad \text{subject to} \quad s \in \lambda_{a_i} \quad (4.3.24)$$

Examination of the cost function shows that the minimisation may be performed in two stages. First, solve for the optimum design vector ( $\mathbf{f}_i$ ) as a function of the eigenvalue location ( $s$ ), then find the optimum eigenvalue location. Mathematically, the unconstrained problem becomes

$$J_{u_i} = \min_{\mathbf{f}_i, s} \left[ \|\mathbf{v}_{d_i} - \mathbf{Q}(s) \mathbf{f}_i\|_2^2 + |\lambda_{d_i} - s|^2 \right] \quad (4.3.25)$$

$$= \min_s \left[ \min_{\mathbf{f}_i} \left( \|\mathbf{v}_{d_i} - \mathbf{Q}(s) \mathbf{f}_i\|_2^2 \right) + |\lambda_{d_i} - s|^2 \right] \quad (4.3.26)$$

and the constrained problem becomes:

$$J_{c_i} = \min_{s \in \lambda_{a_i}} \left[ \min_{\mathbf{f}_i} \left( \|\mathbf{v}_{d_i} - \mathbf{Q}(s) \mathbf{f}_i\|_2^2 \right) \right] \quad (4.3.27)$$

The first optimisation is a standard least squares problem [Bro91, p. 222] and has an analytical solution. The solution produces a function for the optimum design vector, denoted  $\mathbf{f}_{o_i}$ , as a function of eigenvalue location ( $s$ ).

$$\mathbf{f}_{o_i} = \mathbf{Q}(s)^\dagger \mathbf{v}_{d_i} \quad (4.3.28)$$

Where  $(\cdot)^\dagger$  is the pseudo inverse and  $(\cdot)^*$  is the conjugate transpose. If  $\mathbf{Q}(s)$  is full rank<sup>2</sup> then the solution can be expressed as follows:

---

<sup>2</sup>  $\mathbf{Q}(s)$  will be full rank if  $\mathbf{B}$  is full rank.

$$\mathbf{f}_{o_i} = \left( (\mathbf{Q}(s)^* \mathbf{Q}(s))^{-1} \mathbf{Q}(s)^* \right) \mathbf{v}_{d_i} \quad (4.3.29)$$

The optimum design vector ( $\mathbf{f}_{o_i}$ ) can be substituted into Equation (4.3.23) to calculate the minimum value of the cost function as follows:

$$J_{u_i} = \mathbf{v}_{d_i}^* \left[ \mathbf{I} - \mathbf{Q}(s) (\mathbf{Q}(s)^* \mathbf{Q}(s))^{-1} \mathbf{Q}(s)^* \right] \mathbf{v}_{d_i} + |\lambda_{d_i} - s|^2 \quad (4.3.30)$$

and equally for the constrained case:

$$J_{c_i} = \mathbf{v}_{d_i}^* \left[ \mathbf{I} - \mathbf{Q}(s) (\mathbf{Q}(s)^* \mathbf{Q}(s))^{-1} \mathbf{Q}(s)^* \right] \mathbf{v}_{d_i} \quad \text{subject to } s \in \lambda_{a_i} \quad (4.3.31)$$

A second optimisation is conducted over the eigenvalue location. For the case of assigning real eigenvalues both the unconstrained and the constrained optimisation problems can be solved analytically. Since, in both cases, the cost function evaluates to a rational polynomial in  $s$ . The set of all stationary points ( $\lambda_u, \lambda_c$ ) can be found by differentiation and solution of the resulting numerator polynomial. The set of stationary points for the unconstrained problem is defined as:

$$\lambda_u = \left\{ s : 0 = \frac{\partial J_{u_i}}{\partial s} \right\} \quad (4.3.32)$$

and equally for the constrained case:

$$\lambda_c = \left\{ s : 0 = \frac{\partial J_{c_i}}{\partial s} \right\} \quad (4.3.33)$$

To solve the unconstrained problem one must evaluate all the extrema and select the global minimum ( $\lambda_{o_i}$ ).

$$\lambda_{o_i} = \left\{ s : \min_{s \in \lambda_u} J_{u_i}(s, \mathbf{f}_{o_i}) \right\} \quad (4.3.34)$$

For the constrained problem one must only evaluate the extrema within the allowed region and the values at the boundaries of the allowed region, the global minimum is selected from this set.



$$\lambda_{o_i} = \left\{ s : \min_{s \in \lambda_c} J_{c_i}(s, \mathbf{f}_{o_i}), s \in \lambda_{a_i} \right\} \quad (4.3.35)$$

Unfortunately, for the complex case an analytic solution has not yet been found and numerical techniques must be applied. The fundamental difficulty is that the complex case is a problem in two variables, the real and imaginary parts of  $s$ . The extrema occur when the partial derivatives with respect to both the real and imaginary part are zero. This requires the simultaneous solution of two non-linear equations in two unknowns which, unlike the single variable case, does not have a general solution.

The drawback of numerical optimisation is that it is not guaranteed to find the global minimum. However, generally for both the unconstrained and constrained problems, numerical techniques do converge on the global minimum. For the unconstrained case this is because costing the distance from an ideal point forces the global minimum to be near the ideal point, which thus forms a natural starting point for the optimisation. The constrained problem usually converges to a solution on the region boundary for, generally, there is no minimum within the region. Thus the chances of there being two minima and the algorithm converging to the wrong one are slim.

To set up the unconstrained optimisation problem for an algorithm such as Nelder Mead [Wal75, Gra95] it is only required to represent  $s$  as two real variables rather than one complex variable. The constrained optimisation requires a little more setting up, as the allowed regions must be described by a set of inequalities. In most cases it suffices to describe the allowed region as a circle or rectangle, both of which are simple to express as inequality constraints.

Once the optimal eigenvalue locations ( $\lambda_{o_i}$ ) have been found one proceeds to calculate the gain matrix. Using the optimal eigenvalue locations ( $\lambda_{o_i}$ ) the corresponding design vectors  $\mathbf{f}_{o_i}$  are calculated (see Equation (4.3.28)). These are used to form the matrices  $\mathbf{S}$  and  $\mathbf{V}$  as shown below:

$$\mathbf{V} = \left[ \mathbf{Q}(\lambda_{o_1})\mathbf{f}_{o_1}, \dots, \mathbf{Q}(\lambda_{o_n})\mathbf{f}_{o_n} \right] \quad (4.3.36)$$

$$\mathbf{S} = \left[ \mathbf{P}(\lambda_{o_1})\mathbf{f}_{o_1}, \dots, \mathbf{P}(\lambda_{o_n})\mathbf{f}_{o_n} \right] \quad (4.3.37)$$

The gain matrix is given by the formula below:

$$\mathbf{K} = \mathbf{S}\mathbf{V}^{-1} \quad (4.3.38)$$

Equation (4.3.38) reveals the necessity for assumption A4. The closed loop system matrix is:

$$\mathbf{A}_{CL} = \mathbf{A} + \mathbf{BK} = \mathbf{V}\mathbf{\Lambda}\mathbf{V}^{-1} \quad (4.3.39)$$

**Example 4.3.1**

The following example uses the linearised lateral dynamics of the Flight Propulsion Control Coupling (FPCC) fixed-wing aircraft [SSA94, SL89] to demonstrate the benefit of eigenvalue trade-off over basic projection. It should be noted that a helicopter model has not been employed because the large size of the model would produce a cumbersome example that obscures the demonstration. Furthermore, state feedback is not appropriate to the helicopter problem and thus, later, this technique will be extended to the output feedback case.

$$\begin{bmatrix} \dot{x}_1 \\ \dot{x}_2 \\ \dot{x}_3 \\ \dot{x}_4 \\ \dot{x}_5 \end{bmatrix} = \begin{bmatrix} -0.340 & 0.0517 & 0.001 & -0.997 & 0 \\ 0 & 0 & 1 & 0 & 0 \\ -2.69 & 0 & -1.15 & 0.738 & 0 \\ 5.91 & 0 & 0.138 & -0.506 & 0 \\ -0.34 & 0.0517 & 0.001 & 0.0031 & 0 \end{bmatrix} \begin{bmatrix} x_1 \\ x_2 \\ x_3 \\ x_4 \\ x_5 \end{bmatrix} + \begin{bmatrix} 0.0755 & 0 \\ 0 & 0 \\ 4.48 & 5.22 \\ -5.03 & 0.0998 \\ 0.0755 & 0 \end{bmatrix} \begin{bmatrix} \delta_r \\ \delta_a \end{bmatrix}$$

Where  $x_1$  is side slip angle (*deg*),  $x_2$  is bank angle (*deg*),  $x_3$  is roll rate (*deg/s*),  $x_4$  is yaw rate (*deg/s*),  $x_5$  is flight-path angle (*deg*),  $\delta_r$  is rudder (*deg*) and  $\delta_a$  is aileron deflection (*deg*). The desired eigenvectors and eigenvalues are:

$$\begin{array}{ccc} \lambda_{d_{1,2}} = -2 \pm j2 & \lambda_{d_{3,4}} = -3 \pm j2 & \lambda_{d_5} = -0.5 \\ \mathbf{vd}_{1,2} = \begin{bmatrix} \star \\ 0 \\ 0 \\ 1 \\ 0 \end{bmatrix} \pm j \begin{bmatrix} 1 \\ 0 \\ 0 \\ \star \\ 0 \end{bmatrix} & \mathbf{vd}_{3,4} = \begin{bmatrix} 0 \\ \star \\ 1 \\ 0 \\ 0 \end{bmatrix} \pm j \begin{bmatrix} 0 \\ 1 \\ \star \\ 0 \\ 0 \end{bmatrix} & \mathbf{vd}_5 = \begin{bmatrix} \star \\ 0 \\ 0 \\ 0 \\ 1 \end{bmatrix} \end{array}$$

Where  $\star$  denotes 'do not care'. The above system and desired eigenstructure were used to perform simple projection. To measure the success of the projection, the norm of the projection error ( $e_i$ ) was calculated.

$$e_i = \|\mathbf{vd}_i - \mathbf{Q}(\lambda_{o_i})\mathbf{f}_{o_i}\|_2^2 \quad (4.3.40)$$

The same problem was reformulated with allowed eigenvalue regions rather than locations. The regions were defined as circles around the original desired eigenvalue locations with a radius of 20% of the eigenvalue modulus. Again the projection error was calculated and the results are compared in Table 4.3.1.

The results show that a significant reduction in projection error was achieved for all eigenvalues. It is worth noting that for all the eigenvalues the optimum eigenvalue location occurred on the region

Method	$\lambda_{d_{1,2}}$	$\lambda_{d_{3,4}}$	$\lambda_{d_5}$
Basic Projection			
Eigenvalue	$-2.000 + j2.000$	$-3.000 + j2.000$	-0.500
Proj. Error	0.1202	0.0249	0.4420
T.off Projection			
Eigenvalue	$-2.482 + j1.704$	$-3.720 + j2.037$	-0.400
Proj. Error	0.0890	0.0188	0.2285
Error red.(%)	25.99	24.44	48.30

Table 4.3.1: Comparison of the least squares eigenvector assignment errors for assignment using simple projection with and without eigenvalue trade-off.

boundary. The projection method with eigenvalue trade-off is more computationally intensive but not excessively. For the example above, the standard approach took 0.05s to execute on a Pentium 133 with Matlab 4.2c and the trade-off approach took 0.39s on the same system.

## 4.4 Practical Implementation

This section considers some of the practical issues of using the eigenvalue trade-off approach. One of the first issues is the decision between a constrained or unconstrained optimisation. If there are hard limits for the eigenvalue locations in the design specification then a constrained optimisation is the obvious choice. However, the situation is often not so clear cut and one must consider the relative merits of the approaches. The constrained approach is more visible which the introduction identified as a key issue in the design of helicopter control laws. The designer knows within bounds where the eigenvalues will be and can directly influence their location. But the fixed boundaries of the constrained approach can mask a potentially desirable trade-off. For instance, a small relaxation of the boundaries may offer a big improvement in the solution. The unconstrained approach would make this potential improvement more evident. But has the drawback that the designer does not have direct control over the eigenvalue locations and may even obtain an unstable solution. In general the designer will have to adjust the weighting of eigenvalue cost term to reach the most desirable compromise. If instability is unacceptable then it is a simple matter to add a stability constraint to an otherwise unconstrained problem. In fact the optimisation is easily augmented such that stability is guaranteed.

As illustrated above the facility to weight different parts of the cost function will form an important part of any practical implementation. The example further shows that weighting individual eigenvector elements is desirable. This can be achieved by transforming the problem and presents no increase in mathematical difficulty. Consider the unweighted least squares problem:

$$\|\mathbf{v}_{d_i} - \mathbf{Q}(s) \mathbf{f}_i\|^2 = (\mathbf{v}_{d_i} - \mathbf{Q}(s) \mathbf{f}_i)^* (\mathbf{v}_{d_i} - \mathbf{Q}(s) \mathbf{f}_i) \quad (4.4.41)$$

the addition of a positive definite matrix  $\mathbf{R}$  produces the weighted problem:

$$\|\mathbf{v}_{d_i} - \mathbf{Q}(s) \mathbf{f}_i\|_{\mathbf{R}}^2 = (\mathbf{v}_{d_i} - \mathbf{Q}(s) \mathbf{f}_i)^* \mathbf{R} (\mathbf{v}_{d_i} - \mathbf{Q}(s) \mathbf{f}_i) \quad (4.4.42)$$

A positive definite matrix may be factorised as  $\mathbf{R} = \mathbf{R}^{\frac{1}{2}} (\mathbf{R}^{\frac{1}{2}})^*$  thus the weighted problem can be expressed as the original problem transformed.

$$\|\mathbf{R}^{\frac{1}{2}} \mathbf{v}_{d_i} - \mathbf{R}^{\frac{1}{2}} \mathbf{Q}(s) \mathbf{f}_i\|^2 = (\mathbf{v}_{d_i} - \mathbf{Q}(s) \mathbf{f}_i)^* \mathbf{R}^{\frac{1}{2}} (\mathbf{R}^{\frac{1}{2}})^* (\mathbf{v}_{d_i} - \mathbf{Q}(s) \mathbf{f}_i) \quad (4.4.43)$$

Generally,  $\mathbf{R}$  is a diagonal matrix that weights individual residuals and may contain zeros if certain elements are to be ignored (see example above).

For the case of assigning real eigenvalues evaluation of the analytic solution will involve the manipulation of polynomial matrices. The first step is to solve for  $\mathbf{N}(s)$ :

$$\mathbf{0} = \begin{bmatrix} \mathbf{A} - s\mathbf{I} & \mathbf{B} \end{bmatrix} \mathbf{N}(s) \quad (4.4.44)$$

Appendix C.1 gives a detailed description of different approaches to solving this equation. Once a solution to Equation (4.4.44) has been found, the next step is to calculate the eigenvector cost function:

$$J_{V_i} = \mathbf{v}_{d_i}^* \left[ \mathbf{I} - \mathbf{Q}(s) (\mathbf{Q}(s)^* \mathbf{Q}(s))^{-1} \mathbf{Q}(s)^* \right] \mathbf{v}_{d_i} \quad (4.4.45)$$

Appendix C.2 describes methods of evaluating the above expression some of which obviate the need to solve Equation (4.4.44). Appendix C.2 also details some interesting properties of expressions with the structure above.

Symbolic evaluation of Equation (4.4.45) is not trivial but need only be performed once for a given open loop system. Subsequent optimisation can make repeated use of the result.

For the case of assigning complex eigenvalues the techniques described make use of complex arith-

metic. However, conversion to all real arithmetic is easily accomplished<sup>3</sup> and the optimisation need only be performed for one eigenvalue of each conjugate pair<sup>4</sup>.

#### 4.4.1 Trivial Extension to Output Feedback

Unfortunately, for most systems state feedback is impractical, since it assumes that all the states are measurable. This further implies that all the states have physical significance. The dual scenario of 'output injection' is equally impractical for this assumes that each state may be affected by a separate input. Early practitioners [ASC83, Bro91] sought simple extensions to the more general output feedback case. Porter [Por77] derives conditions when a state feedback solution may be factorised into an output feedback one. That is:

$$\mathbf{K} = \mathbf{K}_o \mathbf{C} \quad (4.4.46)$$

Where  $\mathbf{K}$  is the state feedback gain and  $\mathbf{K}_o$  is the output feedback gain resulting from the factorisation.

Other researchers [ASC83, Bro91] augmented the state feedback approach with an output matrix  $\mathbf{C} \in \mathbb{R}^{m \times n}$ . This provides a simple but limited extension to output feedback, the allowed subspace equation becomes:

$$\mathbf{0} = [\mathbf{A} - \lambda_i \mathbf{I}, \mathbf{B}] \begin{bmatrix} \mathbf{v}_i \\ \mathbf{K} \mathbf{C} \mathbf{v}_i \end{bmatrix} \quad (4.4.47)$$

By analogy with state feedback case we can calculate the gain matrix as follows:

$$\mathbf{V} = [\mathbf{Q}_1 \mathbf{f}_1, \dots, \mathbf{Q}_p \mathbf{f}_p] \quad (4.4.48)$$

$$\mathbf{S} = [\mathbf{P}_1 \mathbf{f}_1, \dots, \mathbf{P}_p \mathbf{f}_p] \quad (4.4.49)$$

$$\mathbf{K} = \mathbf{S}(\mathbf{C}\mathbf{V})^\dagger \quad (4.4.50)$$

However, to recover the gain matrix from  $\mathbf{S}$  it is necessary that  $p \leq m$ . Thus clearly this technique only permits a maximum of  $m$  eigenvalues to be assigned. The remaining eigenvalues will adopt arbitrary values and may be unstable. The eigenvectors are selected from a space of minimum dimension  $r$ . This is confirmed in the following lemma of Srinathkumar:

<sup>3</sup>Lemma 4.5.4 indicates how to achieve an all real arithmetic.

<sup>4</sup>The other eigenvalue must be the conjugate.

**Lemma 4.4.1 Srinathkumar [Sri78]**

For the system  $(A, B, C)$   $\max(m, r)$  eigenvalues can be assigned. In addition,  $\max(m, r)$  left or right eigenvectors can be partially assigned with  $\min(m, r)$  entries in each vector arbitrarily chosen.

◇◇

This Lemma is easily misconstrued and one may falsely believe that no more than  $\max(m, r)$  eigenvalues can be assigned. In fact, it is often possible to assign more eigenvalues but the corresponding eigenvectors are subject to more constraints than simply lying in the allowed subspace.

## 4.5 The Output Feedback Problem

The output feedback problem may be stated as follows:

Given the state space system  $(A, B, C)$  defined earlier find a real gain matrix  $(K)$  that assigns a desired set of self-conjugate eigenvalues  $\{\lambda_{d_i}\}$  and eigenvectors  $\{v_{d_i}\}$ .

Although, the problem is a very simple extension to the state feedback case, the solution is not. Early investigations of the problem concentrated on finding conditions for complete pole assignment. An important result was independently presented by both Kimura [Kim75] and Davison *et al* [DW75].

**Theorem 4.5.1 Kimura [Kim75] Theorem 3**

If the system  $(A, B, C)$  is both controllable and observable and satisfies  $m + r > n$  then it is pole-assignable, i.e., for any given  $\{\lambda_{d_i}\}$  there exist  $K$  such that  $\lambda(A + BKC)$  is in arbitrary neighbourhood of  $\{\lambda_{d_i}\}$ . ◇◇

The fundamental nature of the condition  $m + r > n$  will become apparent throughout this chapter. Theorem 4.5.1 indicates that exact pole assignment is not always possible, Fletcher and Magni [FM87, Fle87, Mag87] derive the precise conditions for when assignment fails. The conditions are highly pathological and thus of little practical consequence. Some other fundamental properties of output feedback are listed below:

- Controllability and observability are invariant under output feedback [Bro91].
- The invariant and transmission zeros can not be altered by output feedback [MK76].
- The right eigenvectors associated with uncontrollable and the left eigenvectors associated with unobservable modes may be manipulated by output feedback.
- As the output feedback gains are increased the closed loop poles tend to the system transmission zeros [Mac72].

### 4.5.1 The Protection Method

The first approach to complete pole assignment used protection methods [Sri78, DW75]. The underlining principle is initially to assign a subset of the poles and protect these poles by augmenting the system so that the assigned poles are either uncontrollable or unobservable, then assign the remaining poles by calculating an output feedback gain for the augmented system. The initial poles are protected since uncontrollable and unobservable modes are invariant under output feedback. Lemma 4.5.2 is fundamental to this approach.

#### Lemma 4.5.2

Given  $A \in \mathbb{R}^{n \times n}$  and  $\{v_i, \lambda_i\}$  that satisfy  $Av_i = \lambda_i v_i$ . If  $X \in \mathbb{R}^{n \times n}$  is such that  $Xv_j = 0$  where  $j \subset \{1 \dots n\}$  then  $\{v_j, \lambda_j\}$  are eigenvalues and vectors of  $A + X$ .  $\diamond\diamond$

A brief outline of the resulting protection method is described as follows. For simplicity it is assumed, without loss of generality, that a limiting case of  $m + r = n + 1$  applies and that  $m = \max(m, r)$ ,  $m = \text{rank}(C)$ ,  $r = \text{rank}(B)$ .

1. First, find  $K_1$  such that  $m - 1$  eigenvalues are assigned. This is always possible for a controllable observable triple  $(A, B, C)$  since Davison and Chatterjee [DC71] show that  $\max(m, r)$  poles may be assigned.
2. Calculate a matrix  $X$  such that  $XC[v_1, \dots, v_{m-1}] = 0$  where  $v_i$  are the right eigenvectors associated with the eigenvalues assigned in the previous step. Form a reduced system as follows

$$\tilde{C} = XC \quad (4.5.51)$$

$$\tilde{A} = A + BK_1C \quad (4.5.52)$$

The reduced system will have one output and  $m - 1$  unobservable modes corresponding to those assigned in the previous step.

3. Find a gain matrix  $K_2$  that assigns the remaining  $n - m + 1$  poles of the reduced system. This is always possible since re-invoking the result of Davison and Chatterjee [DC71] indicates that  $\max(1, r)$  poles may be assigned and in this case  $r = n - m + 1$ .
4. The final gain matrix is equal to  $K_1 + K_2X$ .

A generalisation to systems with more inputs than outputs and thus protection of left eigenvectors is straightforward. Fahmy and O'Reilly [FO88a] present a more detailed treatment of the protection method and consider when the method fails. This method illustrates the importance of the condition  $m + r > n$ . We note stage one assigns  $\max(m, r) - 1$  poles, stage two can assign a maximum of  $\min(m, r)$  thus complete assignment requires that:

$$\max(m, r) - 1 + \min(m, r) \geq n \quad (4.5.53)$$

or equivalently:

$$m + r > n \quad (4.5.54)$$

## 4.5.2 Parametric Methods

In the state feedback case all possible solutions were conveniently parameterised by the allowed right eigenvector subspace. However, the extension to output feedback in Section 4.4.1 demonstrates that, in the output feedback case, only a subset of the allowed right eigenvector subspace is available to assign a given set of poles. To parameterise this subset, it is necessary to consider the dual left eigenvector subspace, as defined below:

$$\mathcal{L}(s) = \{\mathbf{w} \in \mathbb{C}^{1 \times n} : (\mathbf{A} - s\mathbf{I})^T \mathbf{w}^T \in \text{range}(\mathbf{C}^T)\} \quad (4.5.55)$$

or

$$\mathcal{L}(s)^T = \text{range}(\mathbf{L}^T) \quad \text{where } \mathbf{L} \text{ satisfies } \begin{bmatrix} \mathbf{L} & \mathbf{M} \end{bmatrix} \begin{bmatrix} \mathbf{A} - s\mathbf{I} \\ \mathbf{C} \end{bmatrix} = \mathbf{0} \quad (4.5.56)$$

A complementary definition of the right eigenspace is:

$$\mathcal{R}(s) = \{\mathbf{v} \in \mathbb{C}^{n \times 1} : (\mathbf{A} - s\mathbf{I})\mathbf{v} \in \text{range}(\mathbf{B})\} \quad (4.5.57)$$

or from Equation (4.2.7)

$$\mathcal{R}(s) = \text{range}(\mathbf{Q}) \quad \text{where } \mathbf{Q} \text{ satisfies } \begin{bmatrix} \mathbf{A} - s\mathbf{I} & \mathbf{B} \end{bmatrix} \begin{bmatrix} \mathbf{Q} \\ \mathbf{P} \end{bmatrix} = \mathbf{0} \quad (4.5.58)$$

Some fundamental properties of the allowed eigenvector subspaces are listed below:

- If  $(\mathbf{A}, \mathbf{B})$  is a controllable pair then  $\dim(\mathcal{R}(s)) = r$  for all  $s$ .



- If  $(\mathbf{A}, \mathbf{C})$  are an observable pair then  $\dim(\mathcal{L}(s)) = m$  for all  $s$ .
- The null space of the individual subspaces are:

$$\mathbf{0} = \mathcal{L}(s)(\mathbf{A} - s\mathbf{I})\mathbf{B}^\perp \quad (4.5.59)$$

$$\mathbf{0} = \mathfrak{R}(s)^T(\mathbf{A} - s\mathbf{I})^T \ker(\mathbf{C}) \quad (4.5.60)$$

Where  $\dim$  is the dimension of the subspace and  $\mathbf{B}^\perp$  is a matrix of maximum and full rank that satisfies  $\mathbf{B}^T \mathbf{B}^\perp = \mathbf{0}$ .

The importance of the allowed eigenvector subspaces to the output feedback problem is illustrated by the following pole assignment Theorem 4.5.2 of Kimura [Kim77] which parameterises all possible closed loop eigenvector combinations that will assign a complete set of poles for an arbitrary system.

**Theorem 4.5.2 Kimura [Kim77]**

*A self-conjugate set  $\{\lambda_{d_i}\}$  is pole assignable if and only if there exists  $\mathbf{v}_i \in \mathfrak{R}(\lambda_{d_i})$  and  $\mathbf{w}_j \in \mathcal{L}(\lambda_{d_j})$  such that:*

*C1  $(\mathbf{v}_i, i = 1 \dots n)$  are linearly independent and  $\lambda_{d_i} = \bar{\lambda}_{d_k}$  implies  $\mathbf{v}_i = \bar{\mathbf{v}}_k$ .*

*C2  $(\mathbf{w}_j, j = 1 \dots n)$  are linearly independent and  $\lambda_{d_j} = \bar{\lambda}_{d_k}$  implies  $\mathbf{w}_j = \bar{\mathbf{w}}_k$ .*

*C3  $\mathbf{w}_j \mathbf{v}_i = 0$  for all  $i \neq j$ .*

◇◇

The first two conditions ensure the gain matrix is real and are equivalent to those for the state feedback case. The third condition is often called the orthogonality condition, it introduces some clear contrasts with the state feedback case.

1. Parameterisation of the allowed eigenvectors is no longer just dependent on the associated eigenvalue and open loop system.
2. The parameterisation is non-linear and can not be expressed by independent subspaces.

The additional complexity described in the two points above has impeded the application of projection methods to the output feedback problem.

From the definition of left and right eigenvectors the necessity of condition C3 is clear. However, it is not intuitive that this condition should be the principal part of a necessary and sufficient condition for the existence of a gain matrix. A new and simple proof is given as follows:

**Proof**

Let  $\mathbf{v}_i \in \mathfrak{R}(\lambda_{d_i})$  and  $\mathbf{V} = [\mathbf{v}_1, \dots, \mathbf{v}_n]$ , where  $\mathbf{v}_i$  satisfy condition C1 of Theorem 4.5.2. By the definition of  $\mathfrak{R}(\lambda_i)$  there exists some  $\mathbf{S} \in \mathbb{C}^{r \times n}$  such that:

$$[(A - \lambda_{d_1}I)v_1, \dots, (A - \lambda_{d_n}I)v_n] = B[z_1, \dots, z_n] \quad (4.5.61)$$

$$AV - V\Lambda_D = BS \quad (4.5.62)$$

$$A - V\Lambda_D V^{-1} = BSV^{-1} \quad (4.5.63)$$

where  $\Lambda_D = \text{diag}[\lambda_{d_1}, \dots, \lambda_{d_n}]$  is a diagonal matrix of the desired eigenvalue set,  $z_i \in \mathbb{C}^{1 \times 1}$  is column vector that selects a vector from the column space of  $B$  and  $S = [z_1, \dots, z_n]$  is the concatenation of these vectors.

The term  $V\Lambda_D V^{-1}$  is the closed loop system matrix (**ACL**). Examination of Equation (4.5.63) shows that for a gain matrix ( $K$ ) to exist it is necessary that  $BSV^{-1}$  can be factorised into  $BKC$ .

Let  $w_j \in \mathcal{L}(\lambda_{d_j})$  and  $W^T = [w_1^T, \dots, w_n^T]$  where  $w_j$  satisfy condition C2 of Theorem 4.5.2. Equally, by the definition of  $\mathcal{L}(\lambda_{d_j})$  there exists some  $T \in \mathbb{C}^{n \times m}$  such that:

$$[(A - \lambda_{d_1}I)^T w_1^T, \dots, (A - \lambda_{d_n}I)^T w_n^T] = [z_1^T, \dots, z_n^T] \quad (4.5.64)$$

$$WA - \Lambda_D W = TC \quad (4.5.65)$$

$$A - W^{-1}\Lambda_D W = W^{-1}TC \quad (4.5.66)$$

Where  $\Lambda_D$  is as defined above but in this instance  $z_i \in \mathbb{C}^{1 \times m}$  is row vector that selects a vector from the row space of  $C$  and  $T^T = [z_1^T, \dots, z_n^T]$ .

The term  $W^{-1}\Lambda_D W$  is also the closed loop system matrix (**ACL**). Again, examination Equation (4.5.66) shows that for a gain matrix ( $K$ ) to exist it is necessary that  $W^{-1}TC$  can be factorised into  $BKC$ .

It is therefore required that Equation (4.5.63) and Equation (4.5.66) can be consistently factorised, a sufficient condition for which is that they are equal:

$$W^{-1}TC = BSV^{-1} \quad (4.5.67)$$

In which case either term may be factorised into  $BKC$  and the closed loop right/left eigenvectors of  $A + BKC$  are the columns of  $V$  and the rows  $W$  respectively.

Substituting Equation (4.5.63) and Equation (4.5.66) into Equation (4.5.67) and rearranging gives:

$$W^{-1}\Lambda_D W = V\Lambda_D V^{-1} \quad (4.5.68)$$

$$\Lambda_D (WV) = (WV)\Lambda_D \quad (4.5.69)$$

Finally, there exists a non-zero solution for an arbitrary choice of  $\Lambda_D$  if and only if  $WV$  is diagonal or equivalently

$$w_j v_i = 0 \quad \text{for all } i \neq j \quad (4.5.70)$$

◇◇

The original proof of Kimura [Kim77] required that the desired eigenvalue set  $\{\lambda_{d_i}\}$  should not have elements coincident with either the open loop eigenvalues or other elements in the set. Fletcher [Fle80] points out these requirements are superfluous and indeed the proof given above does not require them. However, it is worth noting that Theorem 4.5.2 precludes assignment of generalised eigenvectors since these are not generally within the sets  $\mathcal{L}(\lambda)$  and  $\mathcal{R}(\lambda)$ . Assignment of general Jordan structures is tackled by Fahmy and O'Reilly [FO88b]. Some researchers [BFP78, Fle80] developed assignment algorithms based on explicitly meeting the conditions of Theorem 4.5.2. This primarily involves meeting the orthogonality condition.

Once a set of eigenvectors that comply with Theorem 4.5.2 are found, the relevant gain matrix can be calculated by factorising  $S$  or  $T$  of Equation (4.5.62) and Equation (4.5.65) the solution is:

$$K = S(CV)^\dagger = (WB)^\dagger T \quad (4.5.71)$$

If the eigenvectors alone are available the gain matrix may be calculated from the closed loop system matrix ( $A_{CL}$ ) as follows:

$$K = B^\dagger (A_{CL} - A)C^\dagger \quad (4.5.72)$$

Where closed loop system matrix is given by  $A_{CL} = W^{-1}\Lambda_D W$  or  $A_{CL} = V\Lambda_D V^{-1}$ .

Equation (4.5.72) is also presented by Fletcher *et al* [FKKN85], but the pseudo inverse is expressed as a singular value decomposition. Fletcher *et al* [FKKN85] go on to show that the gain matrix may be calculated using using a subset of the left and right eigenvectors, the importance of which is illustrated in the next section.

Condition C3 of Theorem 4.5.2 may be expressed as a single matrix equation. This representation is more compact and useful when attempting to meet Condition C3 using optimisation approaches. Recall that the allowed subspaces are spanned by the range of the matrices  $Q$  and  $L$ . Thus the closed loop eigenvectors selected from the allowed subspaces may be expressed as follows:

$$\mathbf{v}_i = \mathbf{Q}_i \mathbf{f}_i \quad (4.5.73)$$

$$\mathbf{w}_j = \mathbf{g}_j \mathbf{L}_j \quad (4.5.74)$$

Where  $\mathbf{f}_i \in \mathbb{C}^{r \times 1}$  is a column vector of right design parameters and  $\mathbf{g}_i \in \mathbb{C}^{1 \times m}$  is a row vector of left design parameters.

It is clear that the left and right modal matrices are given by:

$$\mathbf{V} = [\mathbf{Q}_1 \mathbf{f}_1, \dots, \mathbf{Q}_n \mathbf{f}_n] \quad (4.5.75)$$

$$\mathbf{W}^T = [\mathbf{L}_1^T \mathbf{g}_1^T, \dots, \mathbf{L}_n^T \mathbf{g}_n^T] \quad (4.5.76)$$

To express Condition C3 as a single matrix equation the following definitions are required:

$$\mathbf{F} = \begin{bmatrix} \mathbf{f}_1 & 0 & \dots & 0 \\ 0 & \mathbf{f}_2 & & \vdots \\ \vdots & & \ddots & \vdots \\ 0 & \dots & \dots & \mathbf{f}_n \end{bmatrix} \quad (4.5.77)$$

$$\mathbf{Q}_T = [\mathbf{Q}_1, \mathbf{Q}_2, \dots, \mathbf{Q}_n] \quad (4.5.78)$$

and

$$\mathbf{G} = \begin{bmatrix} \mathbf{g}_1 & 0 & \dots & 0 \\ 0 & \mathbf{g}_2 & & \vdots \\ \vdots & & \ddots & \vdots \\ 0 & \dots & \dots & \mathbf{g}_n \end{bmatrix} \quad (4.5.79)$$

$$\mathbf{L}_T^T = [\mathbf{L}_1^T, \mathbf{L}_2^T, \dots, \mathbf{L}_n^T] \quad (4.5.80)$$

Applying the definitions above it can be seen that:

$$\mathbf{V} = \mathbf{Q}_T \mathbf{F} \quad (4.5.81)$$

$$\mathbf{W} = \mathbf{G} \mathbf{L}_T \quad (4.5.82)$$

Thus Condition C3 may be expressed as:

$$\mathbf{G} \mathbf{L} \mathbf{T} \mathbf{Q} \mathbf{T} \mathbf{F} = \mathbf{I} \quad (4.5.83)$$

In fact the condition above differs slightly from that of Theorem 4.5.2 since eigenvectors products must be scaled to equal one. However, it is clear that any set of eigenvectors that meet Theorem 4.5.2 condition C3 can be transformed to meet the condition above. An interesting property of Equation (4.5.83) is that:

$$(\mathbf{F}\mathbf{G})\mathbf{L}\mathbf{T}\mathbf{Q}\mathbf{T}(\mathbf{F}\mathbf{G}) = \mathbf{F}\mathbf{G} \quad (4.5.84)$$

which implies that the product  $\mathbf{F}\mathbf{G}$  is a generalised inverse of the product  $\mathbf{L}\mathbf{T}\mathbf{Q}\mathbf{T}$  [BIG74].

### Reduced Orthogonality Conditions

The orthogonality condition of Theorem 4.5.2 requires that  $2n$  eigenvectors are specified to assign  $n$  poles. This is excessive since the protection method shows that assigning  $n$  eigenvectors is sufficient to place  $n$  poles. This observation motivates the following reduced orthogonality condition.

#### Theorem 4.5.3

*The set  $\{\lambda_{d_i}\}$  is pole assignable if there exists  $\mathbf{w}_i \in \mathcal{L}(\lambda_{d_i})$  and  $\mathbf{v}_j \in \mathcal{R}(\lambda_{d_j})$  such that:*

$$C1 \text{ rank} \left( \mathbf{C} \begin{bmatrix} \mathbf{v}_1, \dots, \mathbf{v}_p \end{bmatrix} \right) = p \text{ and } \lambda_{d_i} = \bar{\lambda}_{d_k} \text{ implies } \mathbf{v}_i = \bar{\mathbf{v}}_k$$

$$C2 \text{ rank} \left( \mathbf{B}^T \begin{bmatrix} \mathbf{w}_{p+1}^T, \dots, \mathbf{w}_n^T \end{bmatrix} \right) = n - p \text{ and } \lambda_{d_j} = \bar{\lambda}_{d_k} \text{ implies } \mathbf{w}_j = \bar{\mathbf{w}}_k$$

$$C3 \mathbf{w}_j \mathbf{v}_i = 0 \text{ for all } i = 1 \dots p; j = (p+1) \dots n$$

◇◇

#### Proof

The main part of the proof closely follows that of Theorem 4.5.2 and seeks conditions for a consistent factorisation of two matrices. The following Lemma forms an essential part of the proof.

#### Lemma 4.5.3 (See Appendix B.1 for the proof.)

*Let  $\mathbf{K} \in \mathbb{C}^{r \times m}$ ,  $\mathbf{X} \in \mathbb{C}^{m \times x}$ ,  $\mathbf{S}_1 \in \mathbb{C}^{r \times x}$ ,  $\mathbf{Y} \in \mathbb{C}^{y \times r}$  and  $\mathbf{T}_2 \in \mathbb{C}^{y \times m}$ , where  $m \geq x$  and  $r \geq y$ . Then the matrix equations:*

$$\mathbf{K}\mathbf{X} = \mathbf{S}_1 \quad (4.5.85)$$

$$\mathbf{Y}\mathbf{K} = \mathbf{T}_2 \quad (4.5.86)$$

have a consistent solution for  $\mathbf{K}$  if all the following conditions hold.

$$C1 \text{ rank } (\mathbf{X}) = x$$

$$C2 \text{ rank } (\mathbf{Y}) = y$$

$$C3 \mathbf{T}_2 \mathbf{X} = \mathbf{Y} \mathbf{S}_1$$

The general solution for  $\mathbf{K}$  is then:

$$\mathbf{K} = \mathbf{Y}^\dagger \mathbf{T}_2 + \mathbf{S}_1 \mathbf{X}^\dagger - \mathbf{Y}^\dagger \mathbf{Y} \mathbf{S}_1 \mathbf{X}^\dagger + (\mathbf{I} - \mathbf{Y}^\dagger \mathbf{Y}) \mathbf{Z} (\mathbf{I} - \mathbf{X} \mathbf{X}^\dagger) \quad (4.5.87)$$

or equivalently:

$$\mathbf{K} = \mathbf{Y}^\dagger \mathbf{T}_2 + \mathbf{S}_1 \mathbf{X}^\dagger - \mathbf{Y}^\dagger \mathbf{T}_2 \mathbf{X} \mathbf{X}^\dagger + (\mathbf{I} - \mathbf{Y}^\dagger \mathbf{Y}) \mathbf{Z} (\mathbf{I} - \mathbf{X} \mathbf{X}^\dagger) \quad (4.5.88)$$

where  $\mathbf{Z} \in \mathbb{C}^{y \times x}$  is a free parameter matrix that characterises the complete set of solutions.

◇◇

Let  $\mathbf{v}_i \in \mathfrak{R}(\lambda_{d_i})$  and  $\mathbf{V}_1 = [\mathbf{v}_1, \dots, \mathbf{v}_p]$ , where  $\mathbf{v}_i$  satisfies condition C1 of Theorem 4.5.3. By the definition of  $\mathfrak{R}(\lambda_{d_j})$  there exists some  $\mathbf{S}_1 \in \mathbb{C}^{r \times p}$  such that:

$$[(\mathbf{A} - \lambda_{d_1} \mathbf{I}) \mathbf{v}_1, \dots, (\mathbf{A} - \lambda_{d_p} \mathbf{I}) \mathbf{v}_p] = \mathbf{B} [\mathbf{z}_1, \dots, \mathbf{z}_p] \quad (4.5.89)$$

$$\mathbf{A} \mathbf{V}_1 - \mathbf{V}_1 \mathbf{\Lambda} \mathbf{D}_1 = \mathbf{B} \mathbf{S}_1 \quad (4.5.90)$$

Where  $\mathbf{\Lambda} \mathbf{D}_1 = \text{diag}(\lambda_{d_1}, \dots, \lambda_{d_p})$  is a diagonal matrix and the values along the main diagonal form a self-conjugate subset of the desired eigenvalues. The vector  $\mathbf{z}_i \in \mathbb{C}^{r \times 1}$  is a column vector that selects a vector from the column space of  $\mathbf{B}$  and  $\mathbf{S}_1 = [\mathbf{z}_1, \dots, \mathbf{z}_p]$  is the concatenation of these vectors.

To assign  $\mathbf{V}_1$  as right eigenvectors we require that  $\mathbf{S}_1$  can be factorised into  $\mathbf{K} \mathbf{C} \mathbf{V}_1$ .

Let  $\mathbf{w}_j \in \mathfrak{L}(\lambda_{d_j})$  and  $\mathbf{W}_2^T = [\mathbf{w}_{p+1}^T, \dots, \mathbf{w}_n^T]$ . Equally,  $\mathbf{w}_j$  satisfies condition C2 of Theorem 4.5.3. By the definition of  $\mathfrak{L}(\lambda_{d_j})$  there exists some  $\mathbf{T}_2 \in \mathbb{C}^{(n-p) \times m}$  such that:

$$\left[ (\mathbf{A} - \lambda_{d_{p+1}} \mathbf{I})^T \mathbf{w}_1^T, \dots, (\mathbf{A} - \lambda_{d_n} \mathbf{I})^T \mathbf{w}_n^T \right] = \left[ \mathbf{z}_{p+1}^T, \dots, \mathbf{z}_n^T \right] \quad (4.5.91)$$

$$\mathbf{W}_2 \mathbf{A} - \mathbf{\Lambda} \mathbf{D}_2 \mathbf{W}_2 = \mathbf{T}_2 \mathbf{C} \quad (4.5.92)$$

Where  $\Lambda D_2 = \text{diag}(\lambda_{d_{p+1}}, \dots, \lambda_{d_n})$  is a diagonal matrix and the values along the main diagonal are the remaining unassigned desired eigenvalues. The vector  $\mathbf{z}_i \in \mathbb{C}^{1 \times m}$  is a row vector that selects a vector from the row space of  $\mathbf{C}$  and  $\mathbf{T}_2^T = [\mathbf{z}_{n-p}^T, \dots, \mathbf{z}_n^T]$ .

To assign  $\mathbf{W}_2$  as left eigenvectors we require that  $\mathbf{T}_2$  can be factorised into  $\mathbf{W}_2 \mathbf{B} \mathbf{K}$ .

Thus to assign both  $\mathbf{V}_1$  and  $\mathbf{W}_2$  we require a consistent solution to matrix Equation (4.5.93) and Equation (4.5.94).

$$\mathbf{K}(\mathbf{C}\mathbf{V}_1) = \mathbf{S}_1 \quad (4.5.93)$$

$$(\mathbf{W}_2 \mathbf{B})\mathbf{K} = \mathbf{T}_2 \quad (4.5.94)$$

Applying conditions C1 and C2 of Lemma 4.5.3 to the above equations dictates that:

$$\text{rank}(\mathbf{C}\mathbf{V}_1) = p \quad (4.5.95)$$

$$\text{rank}(\mathbf{W}_2 \mathbf{B}) = n - p \quad (4.5.96)$$

Equation (4.5.95) and Equation (4.5.96) are tantamount to restating conditions C1 and C2 of Theorem 4.5.3 and are thus guaranteed to be satisfied.

Finally, condition C3 of Lemma 4.5.3 requires that:

$$\mathbf{T}_2 \mathbf{C}\mathbf{V}_1 = \mathbf{W}_2 \mathbf{B}\mathbf{S}_1 \quad (4.5.97)$$

Post-multiplying Equation (4.5.92) with  $\mathbf{V}_1$  and pre-multiplying Equation (4.5.90) with  $\mathbf{W}_2$  allows Equation (4.5.97) to be expressed as follows:

$$\mathbf{W}_2 \mathbf{T}_2 \mathbf{C}\mathbf{V}_1 = \mathbf{W}_2 \mathbf{B}\mathbf{S}_1 \mathbf{V}_1 \quad (4.5.98)$$

$$\mathbf{W}_2 \mathbf{A}\mathbf{V}_1 - \Lambda D_2 \mathbf{W}_2 \mathbf{V}_1 = \mathbf{W}_2 \mathbf{A}\mathbf{V}_1 - \mathbf{W}_2 \mathbf{V}_1 \Lambda D_1 \quad (4.5.99)$$

$$\Lambda D_2 \mathbf{W}_2 \mathbf{V}_1 = \mathbf{W}_2 \mathbf{V}_1 \Lambda D_1 \quad (4.5.100)$$

Thus  $\mathbf{W}_2 \mathbf{V}_1$  must be found that satisfies Equation (4.5.100), for general  $\Lambda D_1, \Lambda D_2$ . A little deliberation reveals the only solution is the trivial case  $\mathbf{W}_2 \mathbf{V}_1 = \mathbf{0}$  or equivalently:

$$\mathbf{w}_j \mathbf{v}_i = 0 \quad \text{for all } i = 1 \dots p; j = (p+1) \dots n \quad (4.5.101)$$

◇◇

Condition C3 of Theorem 4.5.3 involves the orthogonality of only  $n$  eigenvectors and is thus considerably simpler than Theorem 4.5.2. It is worth discussing the implications of conditions C1 and C2. The rank constraint of condition C1 has two implications. First, it ensures that the assigned modes are observable and thus embodies the fundamental fact that observability can not be altered by output feedback. The rank condition also dictates that a maximum of  $m$  right eigenvectors may be assigned. The rank constraint of condition C2 has complementary implications, that is, ensuring controllability and dictating that no more than  $r$  left eigenvectors may be assigned. At first inspection Theorem 4.5.3 would seem to imply that  $r$  left and  $m$  right eigenvectors may be assigned simultaneously. Thus for complete pole assignment it appears that it is only necessary to satisfy  $m + r \geq n$ . However, the following argument will reveal that while this is technically possible it is computationally very difficult to achieve.

Suppose condition C1 is satisfied and  $\max(m, r) = m$ . For complete pole assignment a minimum of  $n - r$  right eigenvectors ( $\mathbf{v}_i$ ) are selected. Condition C3 indicates that  $\mathbf{w}_j$  must lie in the left null space of  $\mathbf{v}_i$ . That is:

$$\mathbf{w}_j [\mathbf{v}_1, \dots, \mathbf{v}_{n-r}] = 0. \quad (4.5.102)$$

Assignable  $\mathbf{w}_j$  must also belong to  $\mathcal{L}(\lambda_{d_j})$ . Thus to satisfy both requirements the vectors must lie in the following intersection

$$\mathbf{w}_j^T \in \ker \left( [\mathbf{v}_1, \dots, \mathbf{v}_{n-r}]^T \right) \cap \mathcal{L}(\lambda_{d_j})^T \quad (4.5.103)$$

An intersection space is only guaranteed if the combined dimension of the subspaces is greater than that of their resident vector space. In this case the dimensions are:

$$\dim \left( \ker \left( [\mathbf{v}_1, \dots, \mathbf{v}_{n-r}]^T \right) \right) = r \quad (4.5.104)$$

$$\dim (\mathcal{L}(\lambda_{d_j})^T) = m \quad (4.5.105)$$

Thus complete pole assignment generally requires  $m + r > n$ . However, one may attempt to choose  $\mathbf{v}_i$  such that Equation (4.5.103) is satisfied. This is by no means trivial.

Theorem 4.5.3 can be generalised to accommodate more general cases than even  $n = m + r$ , again, computing eigenvectors that satisfy these conditions is not trivial. This generalisation is achieved by applying a more general version of Lemma 4.5.3 at the appropriate point in the proof of Theorem 4.5.3. For instance, if  $p$  is chosen to equal  $m$  and Lemma B.1.1 of Appendix B.1 is applied.



Then the following extension to Theorem 4.5.3 is readily derived.

**Theorem 4.5.4**

The set  $\{\lambda_{d_i}\}$  is pole assignable if there exists  $\mathbf{w}_i \in \mathcal{L}(\lambda_{d_i})$  and  $\mathbf{v}_j \in \mathcal{R}(\lambda_{d_j})$  such that:

$$C1 \text{ rank} \left( \mathbf{C} \begin{bmatrix} \mathbf{v}_1, \dots, \mathbf{v}_m \end{bmatrix} \right) = m \text{ and } \lambda_{d_i} = \bar{\lambda}_{d_k} \text{ implies } \mathbf{v}_i = \bar{\mathbf{v}}_k$$

$$C2 \text{ rank} \left( \begin{bmatrix} \mathbf{w}_{m+1}^T, \dots, \mathbf{w}_n^T \end{bmatrix} \right) = n - m \text{ and } \lambda_{d_j} = \bar{\lambda}_{d_k} \text{ implies } \mathbf{w}_j = \bar{\mathbf{w}}_k$$

$$C3 \mathbf{w}_j \mathbf{v}_i = 0 \text{ for all } i = 1 \dots m; j = (m+1) \dots n$$

◇◇

Note the lack of an input matrix ( $\mathbf{B}$ ) in condition C2 means the number of left eigenvectors that may be assigned is independent of the number of inputs ( $r$ ).

In similar manner to Theorem 4.5.2, condition C3 of Theorem 4.5.3 and Theorem 4.5.4 may be expressed as a single matrix equation. The following definitions are required:

$$\mathbf{F}_1 = \begin{bmatrix} \mathbf{f}_1 & \mathbf{0} & \dots & \mathbf{0} \\ \mathbf{0} & \mathbf{f}_2 & & \vdots \\ \vdots & & \ddots & \vdots \\ \mathbf{0} & \dots & \dots & \mathbf{f}_p \end{bmatrix} \quad (4.5.106)$$

$$\mathbf{Q}_{\mathbf{T}_1} = [\mathbf{Q}_1, \mathbf{Q}_2, \dots, \mathbf{Q}_p] \quad (4.5.107)$$

and

$$\mathbf{G}_2 = \begin{bmatrix} \mathbf{g}_{p+1} & \mathbf{0} & \dots & \mathbf{0} \\ \mathbf{0} & \mathbf{g}_{p+2} & & \vdots \\ \vdots & & \ddots & \vdots \\ \mathbf{0} & \dots & \dots & \mathbf{g}_n \end{bmatrix} \quad (4.5.108)$$

$$\mathbf{L}_{\mathbf{T}_2}^T = [\mathbf{L}_{p+1}^T, \mathbf{L}_{p+2}^T, \dots, \mathbf{L}_n^T] \quad (4.5.109)$$

Thus condition C3 may be expressed as:

$$\mathbf{G}_2 \mathbf{L}_{\mathbf{T}_2} \mathbf{Q}_{\mathbf{T}_1} \mathbf{F}_1 = \mathbf{0} \quad (4.5.110)$$

Solving Equation (4.5.110) subject to conditions C1 and C2 of Theorem 4.5.4 is fundamental to the output feedback problem and may be formulated as a set of coupled bilinear equations [AP96]. If

one considers the case  $p = m$  then from the dimensions of  $F_1$  and  $G_2$  it is straightforward to show that there are  $m(r - 1) + (n - m)(m - 1)$  free parameters. Equally, the dimensions of the final product  $G_2 L T_2 Q T_1 F_1$  show that there are  $m(n - m)$  equations. Thus a necessary condition for a general solution is:

$$m(r - 1) + (n - m)(m - 1) \geq m(n - m) \quad (4.5.111)$$

$$mr \geq n \quad (4.5.112)$$

Clearly, this necessary condition is more general than  $m + r > n$  and considerable research has been conducted to find sufficient conditions that approach this necessary condition. Early, efforts [BP70, RH78] often resulted in conditions that were expressed in terms of controllability and observability indices [Kai80, Kou81]. The proofs were generally constructive, thus allowing a controller to be calculated. However, the calculations were often *ad hoc* and the results only applied to the pole placement case. In a slightly reformulated problem it was shown [BB81] that, for the case of complex gain matrices,  $mr \geq n$  is a sufficient condition for complete pole assignment. However, for the practical case of real gain matrices it has been shown [WH78] that  $mr \geq n$  is not a sufficient condition. More recently, it has been shown [Wan92, RSW95] that  $mr > n$  is a sufficient condition for complete pole assignment. Although, these results show that assignment is possible, they offer very little indication how a desired assignment may be achieved. Considerable further research will be needed to develop solutions to the more relaxed  $mr > n$  condition, especially if the solutions are to offer a parametric format that allows complete pole assignment and partial eigenvector assignment. It is important to note that the reason we consider the case  $m + r > n$  is not because of a fundamental limit. But because it allows us to meet condition C3 of Theorem 4.5.3 using linear techniques or equivalently to reduce Equation (4.5.110) to a set of linear equation. For example, consider the case  $p = m$  and suppose that values for  $g_j$   $j = m + 1 \dots n$  are arbitrarily chosen, it then remains to solve:

$$0 = G_2 L T_2 Q_i f_i \quad i = 1 \dots m \quad (4.5.113)$$

Since the dimensions of  $G_2 L T_2 Q_i$  are  $(n - m) \times r$ , it follows that Equation (4.5.113) may be solved using standard linear techniques if  $n - m < r$  or equivalently  $m + r > n$ .

The eigenstructure assignment techniques described in the remainder of this chapter all operate by requiring  $m + r > n$ , assigning some of the design vectors ( $f$ ,  $g$ ) and then using linear techniques to calculate the remaining design vectors ( $g$ ,  $f$ ). In the example above two stages were employed; first assigning  $g_j$  then calculating  $f_i$ . However, more than two stages may be employed. This leads to multi-stage techniques which can have practical advantage. It is possible to generate a solution to Equation (4.5.110) and still have some design freedom available in which case a retro-assignment

technique may be employed.

Other researchers [Kim75, Kim77, RO87, RO89, FKKN85, AP96] have presented similar reduced orthogonality conditions. The first can be traced back to the seminal paper of Kimura [Kim75]. This result required that  $p = m$  and that the desired eigenvalue set be  $m$ -decomposable, that is contain a subset of  $m$  self-conjugate values. The technique Kimura [Kim77] presents for generating vectors that meet the conditions is somewhat convoluted. This situation is improved by Roppenecker and O'Reilly [RO87, RO89], who present a simpler technique by expressing the condition directly in terms of eigenvectors selected from the allowed subspaces. But they add the restriction that the desired eigenvalues must not coincide with the open loop set, and a further restriction that one eigenvalue of the  $m$ -decomposable set must be real. Fletcher *et al* [FKKN85] present the result in a new format. It is not obvious how to use this format and they do not consider how to generate vectors that comply with their conditions.

In the following section Theorem 4.5.3 and Lemma 4.5.3 are almost directly utilised to form an eigenstructure assignment technique.

### 4.5.3 Two Stage Assignment

The two stage assignment technique is based on Theorem 4.5.3 and Lemma 4.5.3. Before proceeding with the details of the technique, it is worth outlining the procedure.

The first stage begins by selecting a set of  $s_1$  left or right eigenvectors from the allowed subspace. The eigenvectors are chosen to meet the relevant condition of Theorem 4.5.3 (either C1 or C2). It is always possible to select a set of such eigenvectors.

The second stage entails selecting a set of  $s_2$  dual eigenvectors. These eigenvectors are subject to more restrictions than those of the first stage, for they must reside in the appropriate allowed subspace, and in order to meet condition C3 Theorem 4.5.3, must be orthogonal to the first stage eigenvector set. The subspace of eigenvectors that comply with both restrictions is calculated and from this subspace the eigenvectors are selected. These vectors must also meet the appropriate condition of Theorem 4.5.3 (C1 or C2).

Finally, the gain matrix is calculated using the result of Lemma 4.5.3. For complete pole assignment  $n$  eigenvectors must be assigned and consequently it is necessary that:

$$s_1 + s_2 = n \quad (4.5.114)$$

The two stage technique will now be considered in detail. It will be assumed that  $m + r > n$  and thus complete pole assignment using linear techniques is generally possible.

### Design Procedure

First, decide whether to assign left or right eigenvectors in stage one. This decision is dominated by two factors: the number of eigenvectors that can be assigned and the distribution of the design freedom. Table 4.5.2 shows how the number of eigenvectors that can be assigned depends on whether left or right eigenvectors are assigned first.

	Right first	Left first
Stage 1	$m - 1 \geq s_1 \geq n - r$	$r - 1 \geq s_1 \geq n - m$
Stage 2	$r \geq s_2 \geq n - m + 1$	$m \geq s_2 \geq n - r + 1$

Table 4.5.2: The number of eigenvectors assignable in stages one and two of the two stage assignment technique.

Conditions can arise that force the decision to assign left or right eigenvectors in stage one. Consider the following situation:

- C1 All eigenvalues in the desired set are complex.
- C2 The system dimensions satisfy  $n = m + r - 1$ .

In this case only one column of Table 4.5.2 will be available. This is because, in both stages, one and two a self-conjugate set of eigenvalues must be assigned. Thus to assign all complex eigenvalues both  $s_1$  and  $s_2$  must be even numbers. But if  $n = m + r - 1$  then the ranges in Table 4.5.2 reduce to single values and for only one column of Table 4.5.2 will both  $s_1$  and  $s_2$  be even numbers. It is guaranteed that, even under these circumstances, one column will always be available. This can be seen by noting the diagonal entries of Table 4.5.2 differ by one. This situation does not arise very often in practice and thus these conditions are not overly restrictive.

Generally, more design freedom is available in stage one. This is because stage two is subject to the additional restrictions imposed by the orthogonality condition. It is, naturally, recommended that the engineer exploits the additional design freedom available in stage one. For instance, if it is important that a closed loop eigenvector has a specific structure or is orthogonal to some specified vectors for disturbance decoupling [ZSA90]. Then this eigenvector should be assigned in stage one, where the additional design freedom means that the desired structure is most likely to be achieved. In situations with competing design goals it may pay to experiment with assigning left or right eigenvectors in stage one. Table 4.5.3 shows the design freedom available in stages one and two, when assigning left or right eigenvectors first. 'Design freedom' may be interpreted as either the number of eigenvector elements that may be arbitrarily chosen or the dimension of the subspace minus one, from which the eigenvectors are chosen.

Table 4.5.3 and Table 4.5.2 show that the design freedom and the freedom to choose the number of eigenvalues assigned in each stage are almost entirely prescribed by the relative number of states to

Design Freedom	Right first	Left first
Stage 1	$r - 1$	$m - 1$
Stage 2	$m - 1 - s_1$	$r - 1 - s_1$

Table 4.5.3: Design freedom in stages one and two of the two stage assignment technique.

inputs and outputs.

To avoid verbosity in the remainder of this section it will be assumed that right eigenvectors are assigned in stage one.

### Stage One

Let the subset of desired eigenvalues to be assigned in stage one be denoted by:

$$\Lambda_{D1} = \text{diag}(\lambda_{d_1}, \dots, \lambda_{d_{s_1}}) \quad (4.5.115)$$

Calculate the allowed right eigenvector subspace associated with each eigenvalue. This can be achieved using numerically stable code such as SVD and QR [GL83] to calculate the null space indicated in Equation (4.5.116):

$$\mathbf{0} = \begin{bmatrix} \mathbf{A} - \lambda_{d_i} \mathbf{I} & \mathbf{B} \end{bmatrix} \begin{bmatrix} \mathbf{Q}_i \\ \mathbf{P}_i \end{bmatrix} \quad \text{for all } i = 1 \dots s_1 \quad (4.5.116)$$

Select the closed loop right eigenvectors  $\mathbf{v}_i$  from  $\text{range}(\mathbf{Q}_i)$ , this may be accomplished using a design vector  $\mathbf{f}_i \in \mathbb{C}^{r \times 1}$  as follows:

$$\mathbf{v}_i = \mathbf{Q}_i \mathbf{f}_i \quad (4.5.117)$$

Form the following matrices

$$\mathbf{V}_1 = \begin{bmatrix} \mathbf{Q}_1 \mathbf{f}_1, \dots, \mathbf{Q}_{s_1} \mathbf{f}_{s_1} \end{bmatrix} \quad (4.5.118)$$

$$\mathbf{S}_1 = \begin{bmatrix} \mathbf{P}_1 \mathbf{f}_1, \dots, \mathbf{P}_{s_1} \mathbf{f}_{s_1} \end{bmatrix} \quad (4.5.119)$$

Selected  $\mathbf{v}_i$  must comply with condition C1 of Theorem 4.5.3. In practice the condition C1 is no

more than a technical detail and rarely causes a problem. Furthermore, it is guaranteed that a vector meeting the condition exists [Sri78]. The rank part of condition C1 may be equivalently stated as:

$$\text{range}(\mathbf{V}_1) \cap \ker(\mathbf{C}) = \emptyset \quad (4.5.120)$$

Where  $\emptyset$  is the empty set<sup>5</sup>. When condition C1 fails calculating the intersection space of Equation (4.5.120) reveals the offending direction. If left eigenvectors are assigned in stage one then the allowed left eigenvector subspaces are calculated as follows:

$$\mathbf{0} = \begin{bmatrix} \mathbf{L}_i & \mathbf{M}_i \end{bmatrix} \begin{bmatrix} \mathbf{A} - \lambda_{d_i} \mathbf{I} \\ \mathbf{C} \end{bmatrix} \quad \text{for all } i = 1 \dots s_1 \quad (4.5.121)$$

and the closed loop left eigenvectors ( $\mathbf{w}_i$ ) may be selected from the row space of  $\mathbf{L}_i$  using a design vector ( $\mathbf{g}_i \in \mathbb{C}^{1 \times m}$ ):

$$\mathbf{w}_i = \mathbf{g}_i \mathbf{L}_i \quad (4.5.122)$$

The following concatenated vectors should also be formed:

$$\mathbf{W}_1^T = \begin{bmatrix} \mathbf{L}_1^T \mathbf{g}_1^T, \dots, \mathbf{L}_{s_1}^T \mathbf{g}_{s_1}^T \end{bmatrix} \quad (4.5.123)$$

$$\mathbf{T}_1^T = \begin{bmatrix} \mathbf{M}_1^T \mathbf{g}_1^T, \dots, \mathbf{M}_{s_1}^T \mathbf{g}_{s_1}^T \end{bmatrix} \quad (4.5.124)$$

Condition C2 of Theorem 4.5.3 may also be equivalently expressed as an intersection condition:

$$\text{range}(\mathbf{W}_1^T) \cap \ker(\mathbf{B}^T) = \emptyset \quad (4.5.125)$$

Having selected  $s_1$  right eigenvectors proceed to stage two, as follows.

### Stage Two

Let the subset of desired eigenvalues to be assigned in stage two be denoted by:

<sup>5</sup>This is slight abuse of notation;  $\emptyset$  may include the null vector.

$$\Lambda D_2 = \text{diag}(\lambda_{d_{s_1+1}}, \dots, \lambda_{d_n}) \quad (4.5.126)$$

The left eigenvectors ( $\mathbf{w}_j$ ) must both reside in the allowed subspace  $\mathcal{L}(\lambda_{d_j})$  and be orthogonal to the stage one right eigenvectors ( $\mathbf{V}_1$ ). Mathematically, this is expressed by the following intersection condition:

$$\mathbf{w}_j^T \in \ker(\mathbf{V}_1^T) \cap \mathcal{L}(\lambda_{d_j})^T \quad \text{for all } j = (s_1 + 1) \dots n \quad (4.5.127)$$

The intersection subspace can be calculated by augmenting Equation (4.5.121) as follows:

$$\mathbf{0} = \begin{bmatrix} \mathbf{L}_j & \mathbf{M}_j \end{bmatrix} \begin{bmatrix} \mathbf{V}_1 & \mathbf{A} - \lambda_{d_j} \mathbf{I} \\ \mathbf{0} & \mathbf{C} \end{bmatrix} \quad \text{for all } j = (s_1 + 1) \dots n \quad (4.5.128)$$

The complementary augmented matrix for assigning right eigenvectors in stage two is shown below:

$$\mathbf{0} = \begin{bmatrix} \mathbf{A} - \lambda_{d_j} \mathbf{I} & \mathbf{B} \\ \mathbf{W}_1 & \mathbf{0} \end{bmatrix} \begin{bmatrix} \mathbf{Q}_j \\ \mathbf{P}_j \end{bmatrix} \quad \text{for all } j = (s_1 + 1) \dots n \quad (4.5.129)$$

Select  $s_2 = n - s_1$  left eigenvectors  $\mathbf{w}_j$  from the row space of  $\mathbf{L}_j$ , this can again be accomplished using a design vector  $\mathbf{g}_j \in \mathbb{C}^{1 \times (m-s_1)}$  as follows:

$$\mathbf{w}_j = \mathbf{g}_j \mathbf{L}_j \quad (4.5.130)$$

Form the following matrices

$$\mathbf{W}_2^T = \begin{bmatrix} \mathbf{L}_{s_1+1}^T \mathbf{g}_{s_1+1}^T, \dots, \mathbf{L}_n^T \mathbf{g}_n^T \end{bmatrix} \quad (4.5.131)$$

$$\mathbf{T}_2^T = \begin{bmatrix} \mathbf{M}_{s_1+1}^T \mathbf{g}_{s_1+1}^T, \dots, \mathbf{M}_n^T \mathbf{g}_n^T \end{bmatrix} \quad (4.5.132)$$

The selected  $\mathbf{w}_j$  must meet condition C2 of Theorem 4.5.3 which may be expressed as follows:

$$\text{range}(\mathbf{W}_2^T) \cap \ker(\mathbf{B}^T) = \emptyset \quad (4.5.133)$$

$$\left[ \ker(\mathbf{W}_2) \cup \text{range}(\mathbf{B}) \right]^\perp = \emptyset \quad (4.5.134)$$

$$\left[ \text{range}(\mathbf{V}_1) \cup \text{range}(\mathbf{B}) \right]^\perp = \emptyset \quad (4.5.135)$$

Thus if  $\begin{bmatrix} \mathbf{V}_1 & \mathbf{B} \end{bmatrix}$  is full rank then the left eigenvectors ( $\mathbf{W}_2$ ) will comply with condition C2 of Theorem 4.5.3. Interestingly, Equation (4.5.135) allows the stage two eigenvector to be checked against condition C2 before they are even selected. In fact, the check can be made at the end of stage one when the stage one eigenvectors themselves are checked against condition C1.

Equation (4.5.128) expresses the orthogonality condition and allowed subspace in a lucid way. However, it is not the most efficient means of calculating the intersection of two null spaces [GL83, p. 583].

### Gain Matrix Calculation

Finally, calculate the gain matrix using the formula below:

$$\mathbf{K} = (\mathbf{W}_2 \mathbf{B})^\dagger \mathbf{T}_2 + \mathbf{S}_1 (\mathbf{C}\mathbf{V}_1)^\dagger - (\mathbf{W}_2 \mathbf{B})^\dagger \mathbf{T}_2 \mathbf{C}\mathbf{V}_1 (\mathbf{C}\mathbf{V}_1)^\dagger \quad (4.5.136)$$

This completes the two stage assignment procedure.

The gain matrix equation is taken directly from Lemma 4.5.3 with the free parameter matrix ( $\mathbf{Z}$ ) set to zero. To the author's knowledge the only instance of a similar gain equation was presented in a proof by Fletcher *et al* [FKKN85]. Their derivation is quite different and independent from that of Lemma 4.5.3. Fletcher *et al* [FKKN85] do not combine the equation with an assignment technique or consider how to use the free parameter.

Although, the terms of Equation (4.5.136) may be complex, conditions C1 and C2 of Theorem 4.5.3 ensure the gain matrix is always real. The proof supporting this statement may be found in Appendix B.2.

Two stage assignment can be conducted using all real arithmetic. The following simple Lemma illustrates how this may be achieved:

#### Lemma 4.5.4

*Let  $\mathbf{X}$  and  $\mathbf{Y}$  be two complex matrices conformable for multiplication, the product  $\mathbf{X}\mathbf{Y}$  satisfies:*



$$\begin{bmatrix} \operatorname{Re}(\mathbf{XY}) \\ \operatorname{Im}(\mathbf{XY}) \end{bmatrix} = \begin{bmatrix} \operatorname{Re}(\mathbf{X}) & -\operatorname{Im}(\mathbf{X}) \\ \operatorname{Im}(\mathbf{X}) & \operatorname{Re}(\mathbf{X}) \end{bmatrix} \begin{bmatrix} \operatorname{Re}(\mathbf{Y}) \\ \operatorname{Im}(\mathbf{Y}) \end{bmatrix} \quad (4.5.137)$$

◇◇

The preceding lemma should be applied to Equations (4.5.116), (4.5.121), (4.5.128) and (4.5.129). The gain matrix may also be calculated using only real arithmetic. A technique for doing this is easily inferred from the proof in Appendix B.2. However, most modern numerical software packages are capable of complex arithmetic [Eat94, Mat92].

#### Example 4.5.2

The following is a numerical example to illustrate the two stage approach. Arbitrary matrices have been employed since a helicopter based example would be cumbersome to present and obscure the illustration. Consider the following unstable controllable-observable system:

$$\dot{\mathbf{x}} = \begin{bmatrix} 1 & 2 & -3 & 5 \\ 0 & 3 & -1 & 7 \\ 5 & 8 & 1 & -9 \\ 2 & 6 & 3 & 8 \end{bmatrix} \mathbf{x} + \begin{bmatrix} 1 & 0 & 2 \\ 2 & 3 & 7 \\ 9 & -2 & 1 \\ 5 & 2 & 4 \end{bmatrix} \mathbf{u} \quad (4.5.138)$$

$$\mathbf{y} = \begin{bmatrix} 7 & 3 & 0 & 2 \\ 1 & -1 & 0 & 1 \\ 2 & 3 & 1 & 2 \end{bmatrix} \quad (4.5.139)$$

We note that with four states ( $n = 4$ ), three inputs ( $r = 3$ ) and three outputs ( $m = 3$ ) that complete assignment is possible. Let us assign two right eigenvectors in stage one ( $s_1 = 2$ ) with locations of  $(-1, -2)$  and two left eigenvectors in stage two ( $s_2 = 2$ ) with locations of  $(-3, -4)$ .

Using Equation (4.5.116) the allowed right eigenvector subspaces are calculated as follows:

$$\mathbf{Q}_1 = \begin{bmatrix} -0.7869 & 0 & 0 \\ 0.2676 & -0.0991 & -0.7106 \\ -0.2613 & -0.2731 & 0.0068 \\ 0.0850 & -0.0360 & 0.0608 \end{bmatrix} \quad \mathbf{Q}_2 = \begin{bmatrix} 0.6651 & 0 & 0 \\ -0.2202 & -0.1259 & -0.7039 \\ 0.3822 & -0.2746 & 0.0131 \\ -0.1173 & -0.0483 & 0.0154 \end{bmatrix}$$

Applying the following simple design vectors:

$$\mathbf{f}_1 = \begin{bmatrix} 1 \\ 0 \\ 0 \end{bmatrix} \quad \mathbf{f}_2 = \begin{bmatrix} 0 \\ 1 \\ 0 \end{bmatrix} \quad (4.5.140)$$

the selected right eigenvectors are:

$$\mathbf{V}_1 = \begin{bmatrix} -0.7869 & 0 \\ 0.2676 & -0.1259 \\ -0.2613 & -0.2746 \\ 0.0850 & -0.0483 \end{bmatrix} \quad (4.5.141)$$

and the corresponding input vectors are:

$$\mathbf{S}_1 = \begin{bmatrix} 0.3039 & 0.3725 \\ -0.2919 & 0.8026 \\ -0.2369 & -0.3514 \end{bmatrix} \quad (4.5.142)$$

The left eigenvector subspaces are calculated using Equation (4.5.128). However, since there are two right eigenvectors and only three outputs the subspace has one dimension and thus there are no degrees of freedom with which to select the left eigenvectors. The left eigenvectors subspaces are:

$$\mathbf{L}_3 = \begin{bmatrix} 0.0060 & 0.0782 & -0.0015 & -0.1952 \end{bmatrix} \quad (4.5.143)$$

$$\mathbf{L}_4 = \begin{bmatrix} 0.0080 & 0.0762 & -0.0037 & -0.1773 \end{bmatrix} \quad (4.5.144)$$

and again the corresponding output vectors are:

$$\mathbf{T}_2 = \begin{bmatrix} -0.2365 & 0.6529 & 0.6881 \\ -0.2376 & 0.6949 & 0.6507 \end{bmatrix} \quad (4.5.145)$$

Evaluating Equation (4.5.136) gives the following gain matrix:

$$\mathbf{K} = \begin{bmatrix} 0.4221 & -1.4721 & -0.9173 \\ -0.0290 & 1.2579 & -0.9231 \\ -0.4864 & 1.6741 & 0.9507 \end{bmatrix} \quad (4.5.146)$$

Below, the closed loop system ( $A_{CL} = A + BKC$ ) is expressed in modal form, that is  $A_{CL} = V\Lambda W$ , to verify the assignment.

$$V = \begin{bmatrix} 0.7869 & 0.0000 & 421.7761 & 295.0693 \\ -0.2676 & 0.1259 & -114.4853 & -143.5863 \\ 0.2613 & 0.2746 & 590.3653 & 430.0502 \\ -0.0850 & 0.0483 & -42.5622 & -51.7691 \end{bmatrix} \quad (4.5.147)$$

$$\Lambda = \begin{bmatrix} -1.00 & 0 & 0 & 0 \\ 0 & -2.00 & 0 & 0 \\ 0 & 0 & -3.00 & 0 \\ 0 & 0 & 0 & -4.00 \end{bmatrix} \quad (4.5.148)$$

$$W = \begin{bmatrix} 1.0367 & -13.3751 & -0.5831 & 38.1620 \\ -1.4299 & -36.2028 & 1.6270 & 105.7775 \\ 0.0060 & 0.0782 & -0.0015 & -0.1952 \\ -0.0080 & -0.0762 & 0.0037 & 0.1773 \end{bmatrix} \quad (4.5.149)$$

From the modal form the assigned eigenvalues and eigenvectors are easily recognised.

### Degrees of Freedom

This section considers how much design freedom two stage assignment offers and how it is distributed between the two stages. The contents of Table 4.5.2 and Table 4.5.3 are also derived. Consider stage one assignment of right eigenvectors. Condition C1 of Theorem 4.5.3 implicitly dictates that  $s_1 \leq m$ . However, this condition is superseded by one imposed in stage two. Consider the augmented matrix in Equation (4.5.128). Inspection of its dimensions  $(n + m) \times (n + s_1)$  shows that a solution to Equation (4.5.128) will only generally exist if:

$$s_1 \leq (m - 1) \quad (4.5.150)$$

Condition C2 of Theorem 4.5.3 dictates:

$$s_2 \leq r \quad (4.5.151)$$

and complete assignment requires that:

$$s_1 + s_2 = n \quad (4.5.152)$$

Combining these inequalities indicates how many eigenvectors may be assigned in stage one when assigning right eigenvectors first:

$$m - 1 \geq s_1 \geq n - r \quad (4.5.153)$$

Substituting  $s_1 = n - s_2$  into the previous inequality indicates how many eigenvectors may be assigned in stage two:

$$r \geq s_2 \geq n - m + 1 \quad (4.5.154)$$

The two inequalities represent the first column of Table 4.5.2 and a dual argument for the case of assigning left eigenvectors first generates the second column of Table 4.5.2.

The entries of Table 4.5.3 are derived by considering the dimension of the null spaces from which the eigenvectors are selected. For the case of stage one assignment of right eigenvectors, Equation (4.5.116) shows the stage one null space to have a column dimension of  $r$ . Equally, Equation (4.5.128) shows that the stage two null space will, in general, have a row dimension of  $m - s_1$ . Again, a dual argument holds for stage one assignment of left eigenvectors which generates the second column of Table 4.5.3.

When considering the degrees of freedom (DoF), unity is subtracted from the relevant dimension of the null spaces. Since a one dimensional subspace is a direction, which uniquely describes an eigenvector and thus represents no design freedom. In fact, it is straightforward to verify that the gain equation Equation (4.5.136) will produce the same gain matrix irrespective of eigenvector scaling.

From the first column of Table 4.5.3 (assignment of right eigenvectors first) it can be seen that the total degrees of freedom available for assignment of the eigenvectors is:

$$(r - 1)s_1 + (m - s_1 - 1)s_2 = F_r \quad (4.5.155)$$

Which may be alternatively expressed as:

$$mr - n - (m - s_1)(r - s_2) = F_r \quad (4.5.156)$$

$$mr = F_r + n + (m - s_1)(r - s_2) \quad (4.5.157)$$

The terms in Equation (4.5.157) have the following significance:

- $mr$  is equal to the number gain elements and thus is fundamentally number of free parameters available.
- $n$  is the number of parameters required to assign  $n$  eigenvalues [RO89].
- $F_r$  is the number of degrees of freedom used to assign the eigenvectors.
- $(m - s_1)(r - s_2)$  is a number of, so far unused, free parameters available to assign the eigenvectors.

From the second column of Table 4.5.3 the dual case for assignment of left eigenvectors first, is easily derived:

$$mr - n - (r - s_1)(m - s_2) = F_l \quad (4.5.158)$$

We see that the number of free parameters is the same but the distribution is different. It is interesting to note that if  $r+m$  exceeds  $n$  by two then the term  $(r-s_1)(m-s_2)$  may not evaluate to zero. In which case not all the available degrees of freedom have been used. However, a technique to recover these degrees of freedom in a final and independent assignment stage has been developed. The technique is known as *Retro Assignment*.

#### 4.5.4 Retro Assignment

Retro assignment can only be performed if the previous assignment stage has not made full use of the available design freedom. The previous assignment technique may be a two stage, multi-stage (which is discussed later) or generic technique.

In this section it will be shown that unused design freedom is equivalent to a non-unique gain matrix and that the remaining design freedom is expressed by the free parameter in the gain matrix equation. Retro Assignment involves constructing a reduced system that protects the assigned eigenvectors and expresses the remaining design freedom as a feedback gain. A value for the feedback gain may be calculated using any controller design technique, however, emphasis will be given to eigenstructure assignment.

Equation (4.5.87) of Lemma 4.5.3 shows that the full gain matrix equation can be expressed as follows:

$$\begin{aligned} \mathbf{K} = & (\mathbf{W}_2 \mathbf{B})^\dagger \mathbf{T}_2 + \mathbf{S}_1 (\mathbf{C} \mathbf{V}_1)^\dagger - (\mathbf{W}_2 \mathbf{B})^\dagger \mathbf{T}_2 \mathbf{C} \mathbf{V}_1 (\mathbf{C} \mathbf{V}_1)^\dagger \\ & + \left( \mathbf{I} - (\mathbf{W}_2 \mathbf{B})^\dagger (\mathbf{W}_2 \mathbf{B}) \right) \mathbf{Z} \left( \mathbf{I} - (\mathbf{C} \mathbf{V}_1) (\mathbf{C} \mathbf{V}_1)^\dagger \right) \end{aligned} \quad (4.5.159)$$

Where  $\mathbf{Z} \in \mathbb{R}^{r \times m}$  is the free parameter matrix.

Examination of Equation (4.5.159) shows that the free parameter term will only evaluate to a non-zero matrix if the following conditions hold:

$$\text{C1 } \text{rank}(\mathbf{W}_2 \mathbf{B}) < r \text{ and}$$

$$\text{C2 } \text{rank}(\mathbf{C} \mathbf{V}_1) < m$$

In which case the free parameter matrix ( $\mathbf{Z}$ ) characterises all gain matrix solutions. However, Equation (4.5.159) is not a minimal characterisation<sup>6</sup> and solutions will be repeated. The following observations are key to generating a minimal characterisation:

$$\text{range}(\mathbf{I} - (\mathbf{W}_2 \mathbf{B})^\dagger (\mathbf{W}_2 \mathbf{B})) = \ker(\mathbf{W}_2 \mathbf{B}) \quad (4.5.160)$$

$$\text{range}(\mathbf{I} - (\mathbf{C} \mathbf{V}_1) (\mathbf{C} \mathbf{V}_1)^\dagger) = \ker(\mathbf{V}_1^T \mathbf{C}^T) \quad (4.5.161)$$

Inspection of the above equations shows that a minimal characterisation can be constructed by replacing the matrices adjacent to the free parameter matrix ( $\mathbf{Z}$ ) with matrices whose columns form a minimal basis for the indicated null spaces. Let us define:

$$\text{range}(\mathbf{N} \mathbf{W} \mathbf{B}) = \ker(\mathbf{W}_2 \mathbf{B}) \quad (4.5.162)$$

$$\text{range}(\mathbf{N} \mathbf{C} \mathbf{V}^T) = \ker(\mathbf{V}_1^T \mathbf{C}^T) \quad (4.5.163)$$

Where the columns of  $\mathbf{N} \mathbf{W} \mathbf{B} \in \mathbb{C}^{r \times (r-s_2)}$  form a minimal basis for  $\ker(\mathbf{W}_2 \mathbf{B})$  and the columns of  $\mathbf{N} \mathbf{C} \mathbf{V}^T \in \mathbb{C}^{m \times (m-s_1)}$  are a minimal basis for  $\ker(\mathbf{V}_1^T \mathbf{C}^T)$ . Note that for the generalisation to multistage techniques  $s_1$  and  $s_2$  should be interpreted as the total number of right and left eigenvectors assigned in the previous stages. Then a minimal characterisation [BIG74, p. 77] is given as follows:

<sup>6</sup>Technically, the mapping of  $\mathbf{Z}$  to  $\mathbf{K}$  through Equation (4.5.159) is not bijective.

$$\mathbf{K} = (\mathbf{W}_2 \mathbf{B})^\dagger \mathbf{T}_2 + \mathbf{S}_1 (\mathbf{C} \mathbf{V}_1)^\dagger - (\mathbf{W}_2 \mathbf{B})^\dagger \mathbf{T}_2 \mathbf{C} \mathbf{V}_1 (\mathbf{C} \mathbf{V}_1)^\dagger + \mathbf{N}_{\mathbf{WB}} \mathbf{Z}_2 \mathbf{N}_{\mathbf{CV}} \quad (4.5.164)$$

Where  $\mathbf{Z}_2 \in \mathbb{R}^{(r-s_2) \times (m-s_1)}$  is a minimal free parameter matrix. The dimensions of  $\mathbf{Z}_2$  indicate that a non-unique gain matrix will only exist if:

$$(m - s_1)(r - s_2) > 0 \quad (4.5.165)$$

Recalling Equation (4.5.157) we see that this is the exact condition under which unused design freedom exists. Furthermore, the dimensions of  $\mathbf{Z}_2$  show that all the unused degrees of freedom are available. Examination of exactly how the unused free parameters are manifest reveals how best to utilise them. In this case the gain matrix consists of a fixed part, denoted by  $\mathbf{K}_F$ :

$$\mathbf{K}_F = (\mathbf{W}_2 \mathbf{B})^\dagger \mathbf{T}_2 + \mathbf{S}_1 (\mathbf{C} \mathbf{V}_1)^\dagger - (\mathbf{W}_2 \mathbf{B})^\dagger \mathbf{T}_2 \mathbf{C} \mathbf{V}_1 (\mathbf{C} \mathbf{V}_1)^\dagger \quad (4.5.166)$$

and a variable part denoted by  $\mathbf{K}_Z$ :

$$\mathbf{K}_Z = \mathbf{N}_{\mathbf{WB}} \mathbf{Z}_2 \mathbf{N}_{\mathbf{CV}} \quad (4.5.167)$$

Thus the closed loop matrix ( $\mathbf{A}_{CL}$ ) has the form:

$$\mathbf{A}_{CL} = \mathbf{A} + \mathbf{B} \mathbf{K} \mathbf{C} \quad (4.5.168)$$

$$= (\mathbf{A} + \mathbf{B} \mathbf{K}_F \mathbf{C}) + \mathbf{B} \mathbf{K}_Z \mathbf{C} \quad (4.5.169)$$

$$= (\mathbf{A} + \mathbf{B} \mathbf{K}_F \mathbf{C}) + \mathbf{B} \mathbf{N}_{\mathbf{WB}} \mathbf{Z}_2 \mathbf{N}_{\mathbf{CV}} \mathbf{C} \quad (4.5.170)$$

Inspection of the above shows a reduced system can be constructed as follows:

$$\tilde{\mathbf{A}} = \mathbf{A} + \mathbf{B} \mathbf{K}_F \mathbf{C} \quad (4.5.171)$$

$$\tilde{\mathbf{B}} = \mathbf{B} \mathbf{N}_{\mathbf{WB}} \quad (4.5.172)$$

$$\tilde{\mathbf{C}} = \mathbf{N}_{\mathbf{CV}} \mathbf{C} \quad (4.5.173)$$

$$\tilde{\mathbf{K}} = \mathbf{Z}_2 \quad (4.5.174)$$

The reduced system has less inputs and outputs than the original system. Let  $\tilde{r}$  denote the number of inputs and  $\tilde{m}$  denote the number of outputs. Then:

$$\tilde{r} = r - s_2 \quad (4.5.175)$$

$$\tilde{m} = m - s_1 \quad (4.5.176)$$

Recalling Lemma 4.5.2, we note that if:

$$\tilde{\mathbf{B}}\tilde{\mathbf{K}}\tilde{\mathbf{C}}\mathbf{V}_1 = \mathbf{0} \quad (4.5.177)$$

then the right eigenvectors assigned by  $\mathbf{K}$  are protected for any  $\mathbf{Kz}$ . The definition of  $\mathbf{Ncv}$  given in Equation (4.5.163) dictates that:

$$\tilde{\mathbf{B}}\tilde{\mathbf{K}}\mathbf{Ncv}\mathbf{CV}_1 = \mathbf{0} \quad (4.5.178)$$

Thus the right eigenvectors ( $\mathbf{V}_1$ ) are protected. Equally, the definition of  $\mathbf{NWB}$  given in Equation (4.5.162) dictates that:

$$\mathbf{W}_2\mathbf{BNWB}\tilde{\mathbf{K}}\tilde{\mathbf{C}} = \mathbf{0} \quad (4.5.179)$$

Thus the left eigenvectors ( $\mathbf{W}_2$ ) are also protected. Eigenvector protection has a direct effect on the controllability and observability properties of the reduced system. Consider the product of the closed loop modal matrix and reduced system output matrix:

$$\begin{bmatrix} \mathbf{0}^{\tilde{m} \times s_1} & \mathbf{X}^{\tilde{m} \times s_2} \end{bmatrix} = \tilde{\mathbf{C}} \begin{bmatrix} \mathbf{V}_1 & \mathbf{V}_2 \end{bmatrix} \quad (4.5.180)$$

Clearly, the pair  $(\tilde{\mathbf{A}}, \tilde{\mathbf{C}})$  will have  $s_1$  unobservable modes associated with the right eigenvectors  $\mathbf{V}_1$ . Equally, the input matrix and modal matrix product reveals that:

$$\begin{bmatrix} \mathbf{X}^{s_1 \times \tilde{r}} \\ \mathbf{0}^{s_2 \times \tilde{r}} \end{bmatrix} = \begin{bmatrix} \mathbf{W}_1 \\ \mathbf{W}_2 \end{bmatrix} \tilde{\mathbf{B}} \quad (4.5.181)$$



the pair  $(\tilde{\mathbf{A}}, \tilde{\mathbf{B}})$  will have  $s_2$  uncontrollable modes associated with the left eigenvectors  $\mathbf{W}_2$ .

### Eigenstructure Assignment in the Retro-Stage

Principally, eigenstructure assignment in the retro-stage is the same as eigenstructure structure assignment of the original open loop system. However, it is unlikely that the original open loop system would have the controllability and observability properties of the reduced system and these introduce some interesting quirks.

Since all the poles have now been assigned and are protected, all the remaining design freedom can only be used for the manipulation of eigenvectors. However, half of the eigenvectors are now protected. Hence assignment must focus on the complementary eigenvectors. For instance, if the initial design assigned  $(\mathbf{v}_i, \lambda_{d_i})$  then in the retro-stage it is only possible to assign  $\mathbf{w}_i$ .

Another side effect of the reduced system controllability and observability properties is that the allowed subspaces are inflated. Consider calculating the right eigenvector allowed subspace  $\tilde{\mathbf{Q}}_j$ . From a well known definition of controllability [DeC89] we can see that the uncontrollable modes  $\lambda_{d_j}$  associated with the eigenvectors  $\mathbf{w}_j$  will satisfy:

$$\mathbf{w}_j \left[ \tilde{\mathbf{A}} - \lambda_{d_j} \mathbf{I}, \tilde{\mathbf{B}} \right] = \mathbf{0} \quad \text{for all } j = (s_1 + 1) \dots n \quad (4.5.182)$$

Which implies the following rank equality:

$$\text{rank} \left( \left[ \tilde{\mathbf{A}} - \lambda_{d_j} \mathbf{I}, \tilde{\mathbf{B}} \right] \right) = n - 1 \quad (4.5.183)$$

It is well known [RS70, p. 71] that the size of a the null space is equal to the column dimension, in this case  $n + \tilde{m}$ , minus the rank of the matrix  $(n - 1)$ . Thus the allowed subspace  $\text{range}(\tilde{\mathbf{Q}}_j)$  will satisfy:

$$\left[ \tilde{\mathbf{A}} - \lambda_{d_j} \mathbf{I}, \tilde{\mathbf{B}} \right] \begin{bmatrix} \tilde{\mathbf{Q}}_j \\ \tilde{\mathbf{P}}_j \end{bmatrix} = \mathbf{0} \quad (4.5.184)$$

where  $\tilde{\mathbf{Q}}_j \in \mathbb{C}^{n \times (\tilde{m}+1)}$  and  $\tilde{\mathbf{P}}_j \in \mathbb{C}^{\tilde{m} \times (\tilde{m}+1)}$ . Technically, the rank deficiency of the matrix  $\left[ \tilde{\mathbf{A}} - \lambda_{d_j} \mathbf{I}, \tilde{\mathbf{B}} \right]$  will depend on the geometric multiplicity of the eigenvalue  $\lambda_{d_j}$ . Thus Equation (4.5.183) should read:

$$\text{rank} \left( \left[ \tilde{\mathbf{A}} - \lambda_{d_j} \mathbf{I}, \tilde{\mathbf{B}} \right] \right) = n - g_j \quad (4.5.185)$$

Where  $g_j$  is the geometric multiplicity of  $\lambda_{d_j}$  and thus number of dimensions by which the allowed subspace will swell. An identical argument applies to calculating the left eigenvector allowed subspace ( $\tilde{\mathbf{L}}_j$ ). Assuming that all the closed loop eigenvalues are distinct or  $g_j = 1$ , Table 4.5.4 summarises the number of eigenvectors that may be assigned and the degrees of freedom (DoF) available.

	Right first		Left first	
	No. Assignable	DoF	No. Assignable	DoF
Stage 1	$\bar{s}_1 \leq \bar{m}$	$\bar{r}$	$\bar{s}_1 \leq \bar{r}$	$\bar{m}$
Stage 2	$\bar{s}_2 \leq \bar{r}$	$\bar{m} - \bar{s}_1$	$\bar{s}_2 \leq \bar{m}$	$\bar{r} - \bar{s}_1$

Table 4.5.4: Degrees of freedom available using retro assignment.

Table 4.5.4 is very similar to Table 4.5.2 and Table 4.5.3 and the entries are derived in an almost identical manner. Note that a maximum of  $\bar{m} + \bar{r} - 1$  eigenvectors may be partially assigned. However, it is not necessary to partially assign the maximum number of eigenvectors and one may choose to assign less. For instance, suppose that  $\bar{m} = 2$  and  $\bar{r} = 2$  then the assignment options are:

1. Assign two eigenvectors assigned with two DoF.
2. Assign one eigenvector with two DoF and two eigenvectors with one DoF.

An assignment with one DoF offers limited choice and it may prove preferable to assign two eigenvector with more design freedom.

The gain matrix ( $\tilde{\mathbf{K}}$ ) is calculated using the equation below, this is identical to Equation (4.5.136):

$$\tilde{\mathbf{K}} = (\bar{\mathbf{W}}_1 \bar{\mathbf{B}})^\dagger \bar{\mathbf{T}}_1 + \bar{\mathbf{S}}_2 (\bar{\mathbf{C}} \bar{\mathbf{V}}_2)^\dagger - (\bar{\mathbf{W}}_1 \bar{\mathbf{B}})^\dagger \bar{\mathbf{T}}_1 \bar{\mathbf{C}} \bar{\mathbf{V}}_2 (\bar{\mathbf{C}} \bar{\mathbf{V}}_2)^\dagger \quad (4.5.186)$$

In theory this equation could be augmented with a free parameter term and a further stage of retro assignment undertaken. The final closed loop form is given by:

$$\mathbf{A}_{CL} = \bar{\mathbf{A}} + \bar{\mathbf{B}} \tilde{\mathbf{K}} \bar{\mathbf{C}} \quad (4.5.187)$$

$$\mathbf{A}_{CL} = \mathbf{A} + \mathbf{B} \left( \mathbf{K}_F + \mathbf{N}_{WB} \tilde{\mathbf{K}} \mathbf{N}_{Cv} \right) \mathbf{C} \quad (4.5.188)$$

## Discussion

Examination of the retro-assignment technique indicates that, perhaps, a more general approach is possible. In the current method the assigned eigenvectors are all protected. However, it is possible to construct a reduced system that protects an alternative set of eigenvectors. It is only required that

those eigenvectors are selected to protect all eigenvalues. For instance, suppose that the columns of  $\mathbf{V}\mathbf{x}$  are the right eigenvectors to be protected and the rows of  $\mathbf{W}\mathbf{x}$  are the left eigenvectors associated with remaining unprotected modes. Then any  $\mathbf{N}\mathbf{w}_B$  and  $\mathbf{N}\mathbf{c}_V$  that satisfy:

$$\text{range}(\mathbf{N}\mathbf{w}_B) = \ker(\mathbf{W}\mathbf{x}\mathbf{B}) \quad (4.5.189)$$

$$\text{range}(\mathbf{N}\mathbf{c}_V^T) = \ker(\mathbf{V}\mathbf{x}^T\mathbf{C}^T) \quad (4.5.190)$$

may be used to construct a reduced system as follow:

$$\tilde{\mathbf{B}} = \mathbf{B}\mathbf{N}\mathbf{w}_B \quad (4.5.191)$$

$$\tilde{\mathbf{C}} = \mathbf{N}\mathbf{c}_V\tilde{\mathbf{C}} \quad (4.5.192)$$

However, if eigenstructure assignment is applied in the retro-stage then for any:

$$\text{range}(\mathbf{V}\mathbf{x}) \not\subseteq \text{range}(\mathbf{V}\mathbf{1}) \quad (4.5.193)$$

this approach implies re-assigning the eigenvectors from the previous assignment stage, which could be desirable, if extra *or* alternative design freedom is available in retro-stage. However, in Appendix B.3 it is demonstrated that re-assigning eigenvectors in the retro-stage is futile as it offers no extra DoF.

If the two stage assignment technique is used prior to the retro-stage and it is intended to use eigenstructure assignment in the retro-stage then it is possible to proceed without producing a reduced system. Instead the retro-stage is conducted before calculating the gain matrix of the initial two stage assignment. The method is cursorily described below:

Once stages one and two of the initial design are complete the remaining design freedom can be expressed as allowed subspaces for the unassigned eigenvectors. Consider assignment of right eigenvectors ( $\mathbf{v}_j$ ) in the retro-stage, a maximum of  $m - s_1$  eigenvectors may be selected from the following subspace:

$$\mathbf{v}_j \in \mathfrak{R}(\lambda_{d_j}) \cap \ker \left( \left[ \mathbf{w}_{s_1+1}^T, \dots, \mathbf{w}_{j-1}^T, \mathbf{w}_{j+1}^T, \dots, \mathbf{w}_n^T \right]^T \right) \quad s_1 + 1 \geq j \geq n \quad (4.5.194)$$

Where the eigenvectors must form a self-conjugate set. Equally, if there is still design freedom remaining then left eigenvectors may be selected from:

$$\mathbf{w}_i = \mathcal{L}(\lambda_{d_i}) \cap \ker \left( \left[ \mathbf{v}_1, \dots, \mathbf{v}_{i-1}, \mathbf{v}_{i+1}, \dots, \mathbf{v}_{s_1}, \mathbf{v}_j \right] \right) \quad (4.5.195)$$

Where  $\mathbf{v}_j$ , represents *all* the right vectors assigned in the previous retro stage. Both intersection spaces can be expressed as augmented matrices almost identical to those of Equation (4.5.129) and Equation (4.5.128). The eigenvectors are subject to the same rank constraints as those of stages one and two. One may assign left then right eigenvectors in the retro-stage which, naturally, implies the dual subspaces must be used. The number of eigenvectors that may be assigned can be easily inferred for Table 4.5.4. The gain matrix is calculated using Equation (4.5.136) where  $(\mathbf{V}_1, \mathbf{S}_1)$  and  $(\mathbf{W}_2, \mathbf{T}_2)$  are appropriately augmented with the assignments from retro-stage. Fletcher [Fle80] presented a similar four stage approach for calculating the closed loop eigenvectors.

It has been tacitly assumed that the design freedom available in the retro-stage would be used to further the design goals of the initial design. However, it may be desirable to use the freedom to further alternative design goals. For instance, recalling that:

$$\mathbf{K} = \mathbf{K}_F + \mathbf{NWB} \tilde{\mathbf{K}} \mathbf{NcV} \quad (4.5.196)$$

then  $\tilde{\mathbf{K}}$  could be manipulated to reduce the values in  $\mathbf{K}$  or, if possible, to impose a specific structure by zeroing elements of  $\mathbf{K}$ .

### Summary

Summarising the procedures defined thus far, stage one selects and assigns  $s_1$  right(left) eigenvectors associated with the  $\frac{s_1}{n}$  subset of the desired spectrum. Stage two then assigns  $s_2 = (n - s_1)$  left(right) eigenvectors to complete the spectral assignment. At this point unused design freedom *may* exist. It can be exploited in the retro-stage. Here, a subset of the right(left) eigenvectors *not* assigned in stage one are assigned, similarly for the unassigned left(right) eigenvectors.

#### Example 4.5.3

Returning to Example 4.5.2 we note that, with three inputs and outputs and two eigenvectors assigned in each stage, the condition for retro assignment is satisfied:

$$(m - s_1)(r - s_2) = 1 \quad (4.5.197)$$

It is worth considering how the degrees of freedom were distributed in Example 4.5.2. The nine gain elements determine the available degrees of freedom, four of which were claimed for pole assignment and another four were used to assign the right eigenvectors. The left eigenvectors were prescribed

and used no degrees of freedom. Thus eight of the nine DoF were used and one remains for retro assignment.

The reduced system is constructed below:

$$\dot{\mathbf{x}} = \begin{bmatrix} 0.9895 & 1.4242 & -2.0158 & 7.7431 \\ -1.8822 & -11.3374 & 1.0512 & 18.3557 \\ 3.5858 & 15.8264 & -4.4585 & -27.2666 \\ -0.6589 & -3.4200 & 0.3704 & 4.8064 \end{bmatrix} \mathbf{x} + \begin{bmatrix} 0.9725 \\ 0.6988 \\ 2.5679 \\ 0.2901 \end{bmatrix} \mathbf{u} \quad (4.5.198)$$

$$\mathbf{y} = \begin{bmatrix} 0.2940 & 0.9172 & -0.2540 & -0.9466 \end{bmatrix} \mathbf{x} \quad (4.5.199)$$

The mode observability ( $\mathbf{W}\tilde{\mathbf{B}}$ ) and controllability ( $\tilde{\mathbf{C}}\mathbf{V}$ ) matrices verify the characteristic controllability and observability properties of the reduced system. Employing the modal matrices from Example 4.5.2 we obtain:

$$\tilde{\mathbf{C}}\mathbf{V} = \begin{bmatrix} 0.00 & 0.00 & -90.66 & -105.17 \end{bmatrix} \quad (4.5.200)$$

$$(\mathbf{W}\tilde{\mathbf{B}})^T = \begin{bmatrix} 1.24 & 8.78 & 0.00 & 0.00 \end{bmatrix} \quad (4.5.201)$$

We note that modes  $-1$ ,  $-2$  are unobservable and modes  $-3$ ,  $-4$  are uncontrollable. Continuing with the retro assignment we note from Table 4.5.4 that one complementary eigenvector can be assigned with one DoF. Let us assign the left eigenvector associated with the  $-1$  mode. The allowed left eigenvector subspace is calculated using Equation (4.5.121) and is given below:

$$\tilde{\mathbf{L}}_1 = \begin{bmatrix} -1.0184 & 11.0600 & 0.4200 & -31.2032 \\ 2.0522 & -0.4883 & 0.7562 & -3.0243 \end{bmatrix} \quad (4.5.202)$$

Using a simple design vector ( $\tilde{\mathbf{g}}_1 = \begin{bmatrix} 1 & 0 \end{bmatrix}$ ) the top row is selected as the assigned left eigenvector. The corresponding output vector, which for this single output case is a scalar, as given below:

$$\tilde{\mathbf{M}}_1 = 0.0795 \quad (4.5.203)$$

The feedback gain is calculated using Equation (4.5.136), although for this simple scalar case the formula reduces to:

$$\bar{K} = \frac{\bar{M}_1}{\bar{W}_1 \bar{B}} \quad (4.5.204)$$

$$= -2.1372 \quad (4.5.205)$$

Modal decomposition of the closed loop system  $(\bar{A} + \bar{B}\bar{K}\bar{C})$  verifies the assignment, as shown below:

$$\mathbf{V} = \begin{bmatrix} -0.7869 & 0.00 & -327.5 & 222.2 \\ 0.2676 & -0.1259 & 281.9 & -234.5 \\ -0.2613 & -0.2746 & -124.1 & 153.5 \\ 0.0850 & -0.0483 & 108.9 & -88.30 \end{bmatrix} \quad (4.5.206)$$

$$\mathbf{\Lambda} = \begin{bmatrix} -1.0 & 0 & 0 & 0 \\ 0 & -2.0 & 0 & 0 \\ 0 & 0 & -3.0 & 0 \\ 0 & 0 & 0 & -4.0 \end{bmatrix} \quad (4.5.207)$$

$$\mathbf{W} = \begin{bmatrix} -1.0184 & 11.060 & 0.4200 & -31.203 \\ -0.7759 & -17.7641 & -2.6456 & 40.6215 \\ -0.0060 & -0.0782 & 0.0015 & 0.1952 \\ -0.0080 & -0.0762 & 0.0037 & 0.1773 \end{bmatrix} \quad (4.5.208)$$

Since a retro-stage is not generally available the remainder of this chapter will focus on extensions that enable the engineer to better achieve the design goals in the initial design.

### 4.5.5 Multistage Assignment

It is not necessary to have only two stages in the initial design. We now describe a multi-stage approach that may proceed to the retro-stage if there is residual design freedom.

Any number of stages may be applied providing they result in eigenvectors that meet the conditions of Theorem 4.5.3. When the distribution of design freedom is taken into consideration then it may well be desirable to introduce additional assignment stages.

To illustrate the multistage procedure, let us augment the two stage technique with one additional stage.

In stage one  $s_1$  right eigenvectors are assigned, in stage two  $s_2$  left eigenvectors are assigned and in

stage three a further  $s_3$  right eigenvectors are assigned. In each stage a self-conjugate set of eigenvalues must be placed. Thus a total of  $(s_1 + s_3)$  right eigenvector are assigned and  $s_2$  left eigenvectors. Naturally, for complete pole assignment it is required that:

$$s_1 + s_2 + s_3 = n \tag{4.5.209}$$

The first two stages proceed exactly as described in Section 4.5.3. But stage two now enjoys more design freedom since the selected eigenvectors must be orthogonal to fewer ( $s_1$ ) stage one right eigenvectors. A maximum of  $r - 1$  left eigenvectors may be assigned in stage two. Each is selected with  $m - s_1 - 1$  degrees of freedom. This may be computed using the usual partitioned matrix of Equation (4.5.128).

A third stage is now required to assign the remaining ( $s_3$ ) right eigenvectors which must be orthogonal to the stage two left eigenvectors. The following partitioned matrix may be used:

$$0 = \begin{bmatrix} A - \lambda_{d_k} I & B \\ W_2 & 0 \end{bmatrix} \begin{bmatrix} Q_k \\ P_k \end{bmatrix} \text{ for all } k = (s_1 + s_2 + 1) \dots n \tag{4.5.210}$$

In contrast with stage one, where the right eigenvectors were selected with  $r - 1$  degrees of freedom, the stage three right eigenvectors can only be selected with  $r - s_2 - 1$  degrees of freedom.

Finally, the left and right eigenvectors should be gathered to form single matrices, so that the gain matrix may be calculated using Equation (4.5.136). Table 4.5.5 compares the distribution of design freedom of the three stage and two stage techniques.

	Three stage		Two stage	
	No. Assigned	D.o.F	No. Assigned	D.o.F
Stage 1	$s_1$	$r - 1$	$s_1 + s_3$	$r - 1$
Stage 2	$s_2$	$m - s_1 - 1$	$s_2$	$m - s_1 - s_3 - 1$
Stage 3	$s_3$	$r - s_2 - 1$	-	-

Table 4.5.5: Comparison of the two and three stage design procedures in terms of degrees of freedom and the number of assignable eigenvectors per stage.

Table 4.5.5 shows the addition of an extra stage increases design freedom in stage two at the expense of reduction in stage three. The total eigenvector design freedom ( $F_{r3}$ ) is easily inferred from Table 4.5.5 and comparison with Equation (4.5.158) readily shows the total design freedom is same but has been redistributed:

$$s_1(r-1) + s_2(m-s_1-1) + s_3(r-1-s_2) = F_{r3} \quad (4.5.211)$$

$$mr - n - (m-s_1-s_3)(r-s_2) = F_{r3} \quad (4.5.212)$$

Examination of Equation (4.5.211) shows that retro-assignment may be performed if:

$$(m-s_1-s_3)(r-s_2) > 0 \quad (4.5.213)$$

In general, there may be any number of stages providing that, in all stages prior to the last stage, the total number of left and right eigenvectors assigned is less than  $r$ ,  $m$  respectively. In the last stage the total number of assigned left or right eigenvectors may be increased to equal  $r$ ,  $m$  respectively. A retro-stage may then be conducted if the total number of assigned right eigenvectors is less than  $m$  and the total number of assigned left eigenvectors is also less than  $r$ .

Increasing the number of stages allows the engineer to distribute the design freedom in a manner that reflects the relative importance of the desired closed loop eigenvectors. For instance, the two stage procedure described earlier will often assign right eigenvectors with much more freedom than left. However, it may be required that some left eigenvectors should be assigned with more freedom and that not all the right eigenvectors require so much freedom. In which case a three stage procedure is preferable. In practice it may pay to experiment with the distribution of the design freedom.

Adding more stages can increase numerical inaccuracy, since inaccuracies introduced in one stage will propagate through to later stages. However, in practice, numerical errors are often subsumed by model uncertainty. Fahmy and O'Reilly [FO88a] present a similar multi-stage technique but use a protection method.

#### Example 4.5.4

Let us re-work Example 4.5.2 using a three stage procedure. In stage one we will assign a single right eigenvector, with exactly the direction and eigenvalue  $(-1)$  chosen in Example 4.5.2. In stage two we will assign two left eigenvectors with eigenvalue locations of  $-3$  and  $-4$ . Finally, in stage three, a right eigenvector will be assigned to a location of  $-4$ .

From Example 4.5.2 the first right eigenvector is:

$$\mathbf{v}_1^T = \begin{bmatrix} -0.7869 & 0.2676 & -0.2613 & 0.0850 \end{bmatrix} \quad (4.5.214)$$

The allowed left eigenvector subspaces are calculated using Equation (4.5.128), which is employed exactly as it was in Example 4.5.2. The subspaces are:



$$\mathbf{L}_3 = \begin{bmatrix} -0.0163 & -0.1925 & -0.1495 & -0.0043 \\ 0 & 0.0074 & -0.0613 & -0.2119 \end{bmatrix} \quad (4.5.215)$$

$$\mathbf{L}_4 = \begin{bmatrix} -0.0203 & -0.1938 & -0.1350 & 0.0066 \\ 0 & 0.0000 & -0.0617 & -0.1900 \end{bmatrix} \quad (4.5.216)$$

Compared to Example 4.5.2 the allowed subspaces have an additional dimension this is because the subspaces must only be orthogonal to a single right eigenvector. Let us suppose that the design vectors were employed to select the top and bottom row of  $\mathbf{L}_3$  and  $\mathbf{L}_4$  respectively. Thus the selected left eigenvectors are:

$$\mathbf{W}_2 = \begin{bmatrix} -0.0163 & -0.1925 & -0.1495 & -0.0043 \\ 0 & 0.0000 & -0.0617 & -0.1900 \end{bmatrix} \quad (4.5.217)$$

The corresponding output vectors are:

$$\mathbf{T}_2 = \begin{bmatrix} 0.1382 & -0.8857 & 0.3697 \\ -0.2071 & 0.3811 & 0.8786 \end{bmatrix} \quad (4.5.218)$$

The stage three right eigenvector must be orthogonal to the stage two left eigenvectors ( $\mathbf{W}_2$ ) and thus are calculated using Equation (4.5.210), which is repeated below:

$$\mathbf{0} = \begin{bmatrix} \mathbf{A} - \lambda_{d_2}\mathbf{I} & \mathbf{B} \\ \mathbf{W}_2 & \mathbf{0} \end{bmatrix} \begin{bmatrix} \mathbf{Q}_2 \\ \mathbf{P}_2 \end{bmatrix} \quad (4.5.219)$$

The allowed right eigenvector subspace ( $\mathbf{Q}_2$ ) will be one dimensional and prescribe the eigenvector, as shown below:

$$\mathbf{Q}_2^T = \begin{bmatrix} 0.6558 & -0.3319 & 0.3593 & -0.1168 \end{bmatrix} \quad (4.5.220)$$

The corresponding input vector is:

$$\mathbf{P}_2^T = \begin{bmatrix} -0.2504 & 0.4020 & 0.3045 \end{bmatrix} \quad (4.5.221)$$

To calculate the gain matrix the right eigenvectors and input vectors, from stages one and three must be concatenated, as follows:

$$\mathbf{V}_1^T = \begin{bmatrix} -0.7869 & 0.2676 & -0.2613 & 0.0850 \\ 0.6558 & -0.3319 & 0.3593 & -0.1168 \end{bmatrix} \quad (4.5.222)$$

$$\mathbf{S}_1^T = \begin{bmatrix} 0.3039 & -0.2919 & -0.2369 \\ -0.2504 & 0.4020 & 0.3045 \end{bmatrix} \quad (4.5.223)$$

Equation (4.5.136) can then be applied as usual and for this case the resulting gain matrix is:

$$\mathbf{K} = \begin{bmatrix} 0.4611 & -1.5324 & -1.0544 \\ 0.1870 & 0.1555 & -0.8198 \\ -0.6513 & 2.2959 & 1.1187 \end{bmatrix} \quad (4.5.224)$$

Modal decomposition of the closed loop form confirms the assignment:

$$\mathbf{V} = \begin{bmatrix} 0.7869 & -0.6558 & -108.04 & 111.12 \\ -0.2676 & 0.3319 & 77.86 & -100.93 \\ 0.2613 & -0.3593 & -82.57 & 118.81 \\ -0.0850 & 0.1168 & 26.84 & -33.35 \end{bmatrix} \quad (4.5.225)$$

$$\mathbf{\Lambda} = \begin{bmatrix} -1.00 & 0 & 0 & 0 \\ 0 & -2.00 & 0 & 0 \\ 0 & 0 & -3.00 & 0 \\ 0 & 0 & 0 & -4.00 \end{bmatrix} \quad (4.5.226)$$

$$\mathbf{W} = \begin{bmatrix} 0.9896 & -26.4892 & -5.4100 & 64.1804 \\ -3.0161 & -63.5129 & -20.6710 & 108.5072 \\ 0.0163 & 0.1925 & 0.1495 & 0.0043 \\ 0.00 & 0.00 & 0.0617 & 0.1900 \end{bmatrix} \quad (4.5.227)$$

This example shows how multistage assignment redistributes the design freedom. In Example 4.5.2 the left eigenvectors were prescribed but in the three stage procedure they were selected with one degree of freedom. The penalty for this is that one right eigenvector was prescribed whereas in Example 4.5.2 this was chosen with two DoFs.

So far, attention has focused on the calculation of allowed subspaces and the pole placement prob-

lem. However, an essential step in all the preceding techniques is the selection or calculation of the design vectors. These determine the closed loop eigenvectors and are thus crucial to performance. The following section concentrates on the selection design vectors and the techniques described are relevant to all the preceding approaches.

#### 4.5.6 Assignment with Simple Projection

All the techniques described so far calculate an allowed subspace from which the closed loop eigenvectors must be selected. Least squares projection has proven an expedient means of selecting the closed loop eigenvectors. However, unlike the state feedback case, for the output feedback case, the allowed eigenvector subspaces are no longer independent, but are related by the orthogonality condition. It is wise to take this into consideration.

Consider two stage assignment with initial assignment of right eigenvectors. An allowed subspace  $\mathbf{Q}_i$  is calculated using Equation (4.5.116). A design vector ( $\mathbf{f}_i$ ) selects the closed loop eigenvector. A weighted least squares problem can be formulated by calculating the difference between the selected closed loop eigenvector and a desired eigenvector ( $\mathbf{v}_{d_i}$ ), then minimising the magnitude of this residual or error vector. This is mathematically expressed as follows:

$$J_i = \|\mathbf{v}_{d_i} - \mathbf{Q}_i \mathbf{f}_i\|_{\mathbf{R}}^2 \quad (4.5.228)$$

$$= (\mathbf{v}_{d_i} - \mathbf{Q}_i \mathbf{f}_i)^* \mathbf{R} (\mathbf{v}_{d_i} - \mathbf{Q}_i \mathbf{f}_i) \quad (4.5.229)$$

Where  $\mathbf{R}$  is a positive definite  $n \times n$  matrix which is usually diagonal. If it is desired to weight some residues to zero then the appropriate rows should be removed from  $\mathbf{Q}_i$  and  $\mathbf{v}_{d_i}$  such that the resultant weighting matrix ( $\mathbf{R}$ ) is positive definite. Assume, without loss of generality, that  $\mathbf{Q}_i$  is a minimal basis for the allowed subspace and therefore has full rank. The weighted least squares solution [BIG74, p. 103] is:

$$\mathbf{f}_{o_i} = (\mathbf{R}^{\frac{1}{2}} \mathbf{Q}_i)^{\dagger} \mathbf{v}_{d_i} \quad (4.5.230)$$

$$= (\mathbf{Q}_i^* \mathbf{R} \mathbf{Q}_i)^{-1} \mathbf{Q}_i^* \mathbf{R} \mathbf{v}_{d_i} \quad (4.5.231)$$

Where  $\mathbf{R} = \mathbf{R}^{\frac{1}{2}} (\mathbf{R}^{\frac{1}{2}})^*$  and  $\mathbf{f}_{o_i}$  is the design vector that selects the least squares optimal eigenvector. As well as finding the optimal direction the least squares solution also scales the eigenvector in order to minimise the cost function. The scaling property of the solution causes all the DoF's in the design vector to be used. However, since the eigenvector may adopt any scaling, one DoF is in fact redundant. For complex eigenvalues calculation of the least squares problem, as described above, will require complex arithmetic. However, Lemma 4.5.4 may be applied to formulate an all real problem. This has benefits beyond avoiding complex arithmetic. If it is desired to independently weight the

real and imaginary residuals then an all real problem will facilitate this by separating the real and imaginary parts. For instance an all real version of Equation (4.5.228) is:

$$J_i = \left\| \begin{bmatrix} \mathbf{R}_1^{\frac{1}{2}} & \mathbf{0} \\ \mathbf{0} & \mathbf{R}_2^{\frac{1}{2}} \end{bmatrix} \left( \begin{bmatrix} \text{Re}(\mathbf{v}_{d_i}) \\ \text{Im}(\mathbf{v}_{d_i}) \end{bmatrix} - \begin{bmatrix} \text{Re}(\mathbf{Q}_i) & -\text{Im}(\mathbf{Q}_i) \\ \text{Im}(\mathbf{Q}_i) & \text{Re}(\mathbf{Q}_i) \end{bmatrix} \begin{bmatrix} \text{Re}(\mathbf{f}_i) \\ \text{Im}(\mathbf{f}_i) \end{bmatrix} \right) \right\|^2 \quad (4.5.232)$$

Where  $\mathbf{R}_1$  is a positive definite matrix that weights the real residuals and similarly,  $\mathbf{R}_2$  weights the imaginary residuals. Naturally, a dual least squares problem may be formulated to select the left eigenvectors in either stage one or stage two. Consider the stage two scenario:

$$J_j = \|\mathbf{w}_{d_j} - \mathbf{g}_j \mathbf{L}_j\|_{\mathbf{R}}^2 \quad (4.5.233)$$

$$= (\mathbf{w}_{d_j} - \mathbf{g}_j \mathbf{L}_j) \mathbf{R} (\mathbf{w}_{d_j} - \mathbf{g}_j \mathbf{L}_j)^* \quad (4.5.234)$$

Where  $\mathbf{R}$  is a positive definite weighting matrix,  $\mathbf{g}_j \in \mathbb{C}^{1 \times (m-s_1)}$  is a left design vector,  $\mathbf{w}_{d_j} \in \mathbb{C}^{1 \times n}$  is a desired left eigenvector and  $\mathbf{L}_j \in \mathbb{C}^{(m-s_1) \times n}$  spans the intersection space indicated in Equation (4.5.128) and recalled below:

$$\text{range}(\mathbf{L}_j^T) = \ker(\mathbf{V}_1^T) \cap \mathcal{L}(\lambda_{d_j})^T \quad (4.5.235)$$

Assuming  $\mathbf{L}_j$  is full rank the solution to the least squares problem is:

$$\mathbf{g}_{o_j} = \mathbf{w}_{d_j} \mathbf{R} \mathbf{L}_j^* (\mathbf{L}_j \mathbf{R} \mathbf{L}_j^*)^{-1} \quad (4.5.236)$$

Where  $\mathbf{g}_{o_j}$  selects the optimal left eigenvector.

The orthogonality condition imposed in Equation (4.5.235) can be formulated as part of the least squares problem. In which case the constrained problem is expressed in terms of the allowed left eigenvector subspace ( $\mathcal{L}(\lambda_{d_j})$ ) and assigned right eigenvector matrix ( $\mathbf{V}_1$ ). Let us redefine  $\mathbf{L}_j$  to span the allowed left eigenvector subspace ( $\text{range}(\mathbf{L}_j^T) = \mathcal{L}(\lambda_{d_j})^T$ ), then mathematically:

$$J_j = \|\mathbf{w}_{d_j} - \mathbf{g}_j \mathbf{L}_j\|_{\mathbf{R}}^2 \quad \text{subject to} \quad \mathbf{0} = \mathbf{g}_j \mathbf{L}_j \mathbf{V}_1 \quad (4.5.237)$$

The solution<sup>7</sup> [Mil87, p. 18] to the constrained optimisation problem is:

<sup>7</sup>An alternative solution is given in Equation (5.5.159)

$$\begin{aligned}
\mathbf{g}_{o_j} = & \mathbf{w}_{d_j} \mathbf{R} \mathbf{L}_j^* (\mathbf{L}_j \mathbf{R} \mathbf{L}_j^*)^{-1} - \\
& \mathbf{w}_{d_j} \mathbf{R} \mathbf{L}_j^* (\mathbf{L}_j \mathbf{R} \mathbf{L}_j^*)^{-1} \mathbf{L}_j \mathbf{V}_1 \left[ \mathbf{V}_1^* \mathbf{L}_j^* (\mathbf{L}_j \mathbf{R} \mathbf{L}_j^*)^{-1} \mathbf{L}_j \mathbf{V}_1 \right]^{-1} \mathbf{V}_1^* \mathbf{L}_j^* (\mathbf{L}_j \mathbf{R} \mathbf{L}_j^*)^{-1}
\end{aligned} \tag{4.5.238}$$

Where, as before,  $\text{range}(\mathbf{L}_j^T) = \mathcal{L}(\lambda_{d_j})^T$  and the columns of  $\mathbf{V}_1$  are right eigenvectors assigned in stage one.

### 4.5.7 Assignment with Sympathetic Projection

The eigenvectors assigned in stage one ultimately determine what can be achieved in stage two. This is because the stage two eigenvectors must reside in the left null space of those assigned in stage one. To ensure that stage two is not too heavily influenced by stage one, an additional term may be added to the optimisation. Let us define  $\mathbf{W}_{D2}$  as follows:

$$\mathbf{W}_{D2}^T = \left[ \mathbf{w}_{d_{s_1+1}}^T, \dots, \mathbf{w}_{d_n}^T \right] \tag{4.5.239}$$

Then the augmented problem is:

$$J_i = \|\mathbf{v}_{d_i} - \mathbf{Q}_i \mathbf{f}_i\|_{\mathbf{R}_1}^2 + w_l \|\mathbf{W}_{D2} \mathbf{Q}_i \mathbf{f}_i\|_{\mathbf{R}_2}^2 \quad i = 1 \dots s_1 \tag{4.5.240}$$

Where  $w_l$  weights the left eigenvector term. The purpose of this term is to force the assigned right eigenvectors to be more orthogonal to the desired left eigenvectors. Thus in stage two it is now possible to meet the orthogonality condition and assign directions closer to those of the desired eigenvectors. The success of the assignment may now predominantly depend on the extent to which the allowed subspaces contain the desired directions. The value of  $w_l$  reflects the relative importance of achieving the desired left or right eigenvectors. The weighting matrices  $\mathbf{R}_1$  and  $\mathbf{R}_2$  are positive definite.  $\mathbf{R}_2$  can be used to encourage orthogonality with respect to specific eigenvectors. The solution to the augmented optimisation [BIG74, p. 111] is:

$$\mathbf{f}_{o_i} = \left[ \mathbf{Q}_i^* (\mathbf{R}_1 + w_l \mathbf{W}_{D2}^* \mathbf{R}_2 \mathbf{W}_{D2}) \mathbf{Q}_i \right]^{-1} \mathbf{Q}_i^* \mathbf{R}_1 \mathbf{v}_{d_i} \tag{4.5.241}$$

The dual problem for assignment of left eigenvectors in stage one is:

$$J_i = \|\mathbf{w}_{d_i} - \mathbf{g}_i \mathbf{L}_i\|_{\mathbf{R}_1}^2 + w_r \|\mathbf{g}_i \mathbf{L}_i \mathbf{V}_{D2}\|_{\mathbf{R}_2}^2 \quad i = 1 \dots s_1 \quad (4.5.242)$$

Where  $\mathbf{V}_{D2} = [\mathbf{v}_{d_{s_1+1}}, \dots, \mathbf{v}_{d_n}]$  is the desired right eigenvector matrix,  $\mathbf{L}_i$  is the allowed left eigenvector subspace defined according to Equation (4.5.121) and  $w_r$  is the dual weighting factor. The solution is:

$$\mathbf{g}_{o_i} = \mathbf{w}_{d_i} \mathbf{R}_1 \mathbf{L}_i^* [\mathbf{L}_i (\mathbf{R}_1 + w_r \mathbf{V}_{D2} \mathbf{R}_2 \mathbf{V}_{D2}^*) \mathbf{L}_i^*]^{-1} \quad (4.5.243)$$

In both cases, stage two assignment should use the simple projection of Equation (4.5.230) or its dual. Selection of a suitable compromise value for  $w_l$  or  $w_r$  may require some experimentation, it is recommended that all the eigenvectors  $\mathbf{w}_{d_i}$  and  $\mathbf{v}_{d_i}$  are normalised thus:

$$1 = \|\mathbf{w}_{d_i}\|_2 \quad 1 = \|\mathbf{v}_{d_i}\|_2 \quad (4.5.244)$$

Examination of the behaviour of Equation (4.5.241) for large  $w_l$  indicates an alternative problem formulation is possible. If  $w_l$  is large then the latter term of Equation (4.5.240) will dominate. As depicted below:

$$J_i \approx w_l \|\mathbf{W}_{D2} \mathbf{Q}_i \mathbf{f}_i\|_{\mathbf{R}_2}^2 \quad (4.5.245)$$

This term has two solutions:

1. Trivial case  $\mathbf{f}_i = 0$ .
2. Subspace solution  $\mathbf{f}_i \in \ker(\mathbf{W}_{D2} \mathbf{Q}_i)$ .

We therefore see that solutions for medium values of  $w_l$  represents a compromise in direction and scaling. Since eigenvectors are defined by direction alone it is desirable to reformulate the problem as a compromise in direction only. To this end let  $\mathbf{N}_{\mathbf{v}_{d_i}} \in \mathbb{C}^{(n-1) \times n}$  be full rank and satisfy:

$$\mathbf{0} = \mathbf{N}_{\mathbf{v}_{d_i}} \mathbf{v}_{d_i} \quad (4.5.246)$$

Then an alternative problem formulation is:

$$J_i = \|N_{vd_i} Q_i f_i\|_{R_1}^2 + w_l \|W_{D2} Q_i f_i\|_{R_2}^2 \quad \text{subject to} \quad 1 = \|Q_i f_i\|_2^2 \quad (4.5.247)$$

In the preceding problem the length of an eigenvector is arbitrarily fixed at unity and the direction is a compromise between the ideal eigenvector direction and orthogonality to the desired left eigenvectors. The solution is a generalised eigenvalue problem:

$$\alpha Q_i^* Q_i f_{o_i} = Q_i^* (N_{vd_i}^* R_1 N_{vd_i} + w_l W_{D2}^* R_2 W_{D2}) Q_i f_{o_i} \quad (4.5.248)$$

### Proof

The preceding solution is derived using a straightforward application of matrix calculus. The cost and constraint function expressed with a Lagrange multiplier ( $\alpha$ ) is:

$$J_i = f_i^* Q_i^* (N_{vd_i}^* R_1 N_{vd_i} + w_l W_{D2}^* R_2 W_{D2}) Q_i f_i + \alpha (1 - f_i^* Q_i Q_i^* f_i) \quad (4.5.249)$$

The derivative is:

$$\frac{\partial J_i}{\partial f_i} = 2Q_i^* (N_{vd_i}^* R_1 N_{vd_i} + w_l W_{D2}^* R_2 W_{D2}) Q_i f_i - 2\alpha Q_i^* Q_i f_i \quad (4.5.250)$$

Setting the derivative equal to zero gives:

$$\alpha Q_i^* Q_i f_{o_i} = Q_i^* (N_{vd_i}^* R_1 N_{vd_i} + w_l W_{D2}^* R_2 W_{D2}) Q_i f_{o_i} \quad (4.5.251)$$

Pre-multiplying Equation (4.5.250) by  $f_{o_i}$  shows that  $\alpha$  is equal to the minimum value of the cost function ( $J_{o_i}$ ). ◇◇

Equation (4.5.248) may be readily solved by applying the QZ Method [GL96, p. 375] where the solution is the eigenvector associated with the smallest positive eigenvalue. However, if  $Q_i$  is full rank then the inverse of the product  $(Q_i^* Q_i)$  exists and Equation (4.5.248) may be expressed as standard eigenvalue problem by pre-multiplying with  $(Q_i^* Q_i)^{-1}$ . Since the solution is an eigenvector we see scaling plays no part in the optimisation.

While the preceding optimisation does have the advantage of concentrating solely on the direction of the eigenvector, it does suffer some drawbacks. For instance, the weighting matrix  $R_1$  loses some visibility, for it now determines the degree to which the solution vector is orthogonal to the row dir-

ections of  $N\mathbf{v}_d$ . In practice  $\mathbf{R}_1$  was set to the identity matrix and  $N\mathbf{v}_d$  was calculated as an orthogonal basis.

Both types of sympathetic projection may be applied to multistage assignment, at each stage before the last, the additional term should be present (see Equation (4.5.245)). The term should only contain the remaining unassigned left or right desired eigenvectors. The last stage should use simple projection.

#### 4.5.8 Assignment with Iterative Projection

Iterative projection is a natural extension to the sympathetic projection method described above. It aims to distribute design freedom evenly between left and right eigenvectors.

In both the multistage and two stage methods the design freedom is distributed among the stages in discrete amounts. However, sympathetic projection has illustrated that a stage may sacrifice some of its design freedom to the following stage, by choosing a sub-optimal solution.

The idea behind iterative assignment is that two stages progressively concede design freedom to each other until there is convergence on a set of assignable eigenvectors. The procedure is described as follows:

1. Initially, simple projection is performed on both left and right eigenvectors using the unconstrained allowed subspaces. At this point it is extremely unlikely the assigned vectors will meet the orthogonality condition.
2. The orthogonality of the left and right eigenvectors is checked. If they are acceptably close to orthogonal the procedure stops. Otherwise the orthogonality weightings  $w_l$  and  $w_r$  are increased and the procedure continues to step three.
3. Using either of the sympathetic assignment methods, re-assign the right eigenvectors to a direction that is nearer to orthogonal with the current left eigenvectors. For example, the cost function for the sympathetic approach with scaling would be:

$$J_i = \|\mathbf{v}_d - \mathbf{Q}_i \mathbf{f}_i\|_{\mathbf{R}_1}^2 + w_l \|\mathbf{W}_2 \mathbf{Q}_i \mathbf{f}_i\|_{\mathbf{R}_2}^2 \quad i = 1 \dots s_1 \quad (4.5.252)$$

4. Again, using either of the sympathetic assignment methods, re-assign the left eigenvectors to be closer to orthogonal with the current right eigenvectors. The complementary cost function is:

$$J_j = \|\mathbf{w}_d - \mathbf{g}_j \mathbf{L}_j\|_{\mathbf{R}_1}^2 + w_r \|\mathbf{g}_j \mathbf{L}_j \mathbf{V}_2\|_{\mathbf{R}_2}^2 \quad j = (s_1 + 1) \dots n \quad (4.5.253)$$



5. Return to step two.

The simplest method for checking the eigenvector orthogonality is to form the product  $\mathbf{W}_2 \mathbf{V}_1$  and decide if the values are sufficiently small. Ultimately, poor orthogonality will cause the poles and eigenvectors to be inaccurately assigned. Thus a more rigorous approach is to calculate the closed loop system matrix and decide if the pole locations are acceptable. However, this approach is computationally more intensive. After each assignment it is important to scale the eigenvectors to a fixed length. The asymptotic convergence properties necessitate an appropriate increase of the weightings. To achieve convergence within practical time scales, the orthogonality weightings should be increased geometrically. For example:

$$w_i = 0 + x + xy + xy^2 + xy^3 + \dots \quad (4.5.254)$$

Where  $x$  and  $y$  control the growth of the weighting term, typical values that may form a good starting point, from practical experience are  $x = 0.01$  and  $y = 1.03$ .

Improved results can be achieved by maintaining a separate orthogonality weighting for each eigenvector. When a particular eigenvector has reached acceptable orthogonality its weighting is no longer increased and thus it suffers no further degradation in performance<sup>8</sup>.

An important property of this approach is that it will always converge to orthogonal eigenvectors. To demonstrate this we require the following well known matrix inversion lemma [GL96].

**Lemma 4.5.5**

*If  $\mathbf{A}$ ,  $\mathbf{B}$ ,  $\mathbf{C}$  and  $\mathbf{D}$  have suitable dimensions and  $(\mathbf{A}, \mathbf{C})$  are non-singular then the following identity holds:*

$$(\mathbf{A} + \mathbf{BCD})^{-1} = \mathbf{A}^{-1} - \mathbf{A}^{-1}\mathbf{B}(\mathbf{DA}^{-1}\mathbf{B} + \mathbf{C}^{-1})^{-1}\mathbf{DA}^{-1} \quad (4.5.255)$$

◇◇

Applying Lemma 4.5.5 to the sympathetic assignment solution (Equation (4.5.241)) gives:

---

<sup>8</sup>The eigenvector may still suffer some change in performance since other eigenvectors will continue to change affecting its re-assignment.

$$f_{oi} = [Q_i^* (R_1 + w_l W_{D2}^* R_2 W_{D2}) Q_i]^{-1} Q_i^* R_1 v_{di} \quad (4.5.256)$$

$$\begin{aligned} &= (Q_i^* R_1 Q_i)^{-1} Q_i^* R_1 v_{di} - \\ &\quad (Q_i^* R_1 Q_1)^{-1} Q_i^* W_{D2}^* \left( W_{D2} Q_i (Q_i^* R_1 Q_1)^{-1} Q_i^* W_{D2}^* + \frac{1}{w_l} R_2^{-1} \right)^{-1} \\ &\quad W_{D2} Q_i (Q_i^* R_1 Q_1)^{-1} Q_i^* R_1 v_{di} \end{aligned} \quad (4.5.257)$$

Comparison of Equation (4.5.238) with Equation (4.5.257) shows that as  $w_l$  tends to infinity the solution becomes a constrained projection and is thereby guaranteed to produce orthogonal eigenvectors.

#### Example 4.5.5

This example compares the performance of the different projection techniques using the system given in Example 4.5.2. For convenience, the desired left ( $W_D$ ) and right ( $V_D$ ) eigenvector matrices equal the identity matrix. Performance is measured in terms of the assignment error ( $e_i$ ):

$$e_i = \|v_{di} - v_i\|_2 \quad (4.5.258)$$

$$e_j = \|w_{dj} - w_j\|_2 \quad (4.5.259)$$

Where  $w_{dj}$ ,  $v_{di}$  are the desired left and right eigenvectors and  $w_j$ ,  $v_i$  are the assigned left and right eigenvectors after projection.

Method	First ( $v_1$ ) R-vector	Second ( $v_2$ ) R-vector	First ( $w_3$ ) L-vector	Second ( $w_4$ ) L-vector
Simple Projection				
Right first	0.1842	0.0174	1.0000	0.3969
Left first	0.7550	0.5899	0.7000	0.2402
Three stage	0.1842	0.9158	0.7696	0.2569
Sympathetic Projection				
Right first	0.6833	0.0569	0.9317	0.3762
Iterative Projection				
NA	0.3265	0.0370	0.9487	0.3216

Table 4.5.6: The least squares eigenvector assignment errors for two and three stage simple projection, sympathetic projection and iterative projection.

With simple projection the assignment error is very much determined by the degrees of freedom available for selecting the eigenvector. When the right eigenvectors ( $v_1$ ,  $v_2$ ) are assigned first they are selected with the maximum amount of design freedom (2 DoFs each) and thus achieve their lowest assignment error. Equally, when the left eigenvectors ( $w_3$ ,  $w_4$ ) are assigned first they achieve their

lowest assignment error. Three stage assignment represents a compromise. The first eigenvector ( $\mathbf{v}_1$ ) is assigned with maximum design freedom (2 DoF) and thus achieves a correspondingly low assignment error. The two left eigenvectors ( $\mathbf{w}_3, \mathbf{w}_4$ ) are assigned with one DoF and achieve intermediate assignment errors. The final right eigenvector is prescribed by the previous assignments and has a large assignment error.

Using sympathetic projection the right eigenvectors shun the optimum direction in favour of one that will assist the next stage. Thus their assignment error increases compared to assignment of right eigenvectors first. However, the left eigenvectors can now adopt directions closer to the optimum and their assignment error decreases. For this example a weighting factor of 100 was applied. Interestingly, it can occur that the left eigenvectors suffer an increase in assignment error.

Iterative projection begins with both left and right eigenvectors adopting the optimum solution and then progressively updating their solutions until they are orthogonal. This generally achieves a compromise in the assignment errors. The choice of initial value for the weighting elements can be used to steer the optimisation. A lower value gives less priority to orthogonalisation and the eigenvector will remain closer to the optimum direction. However, it is generally not possible to achieve a prescribed set of assignment errors and trade-offs are inevitable, some of which can be quite discrete in their nature.

#### 4.5.9 Assignment with Projection and Eigenvalue Trade-off

Section 4.3 presented a new algorithm for state feedback eigenstructure assignment that allows trade-off between the eigenvector and eigenvalue approximations. All of the projection methods described above may be coupled with eigenvalue trade-off.

The solution to the projection method is an eigenvector direction that minimises the problem cost function. The cost function is also dependent on the eigenvalue location. Thus the initial minimisation may be nested in a second optimisation which uses the eigenvalue location to further reduce the cost function. The second optimisation may be formulated as either of the constrained or unconstrained problems described in Section 4.3.

While a nested optimisation may appear computationally intensive, for the projection methods described above, the inner optimisation has an analytical solution that can be directly and efficiently calculated. Generally, a numerical method is employed for the outer optimisation. However, under limited circumstances an analytical solution can be calculated. The basic procedure is outlined as follows:

1. Construct a function ( $J_i(s)$ ) that calculates then minimum value of the eigenvector cost function as a function of the eigenvalue location. This will, generally, involve calculating the allowed subspace  $\mathbf{Q}_i$  or  $\mathbf{L}_i$  for the new pole location and then evaluating Equation (4.5.230) or Equation (4.5.241) and using the result to evaluate the cost function.
2. Formulate a constrained optimisation problem:

$$\min_{s \in \lambda_{a_i}} J_i(s) \quad (4.5.260)$$

or an unconstrained optimisation problem:

$$\min J_i(s) + w_v |\lambda_{d_i} - s|^2 \quad (4.5.261)$$

Where  $w_v$  is a weighting term to reflect the relative importance of the eigenvalue/eigenvector requirements and  $\lambda_{a_i}$  is the set of allowed eigenvalue locations. Then solve the minimisation using a numerical approach such as the quasi-newton method [Gra95].

3. Continue the projection method as before.

If real eigenvalues are being assigned with simple projection then steps one and two may be replaced with the analytic procedure described in Section 4.3. In all other cases a numerical optimisation must be used. In the case of iterative projection, steps three and four of the iterative procedure should be replaced with procedure described above. However, since each iteration now solves two nested optimisations the approach may become cumbersome.

Although, this algorithm bears close resemblance to the state feedback case, its does not share the same optimality. That is, it does not find the global minimum of Equation (4.5.262):

$$J = \|\mathbf{V}_{D1} - \mathbf{V}_1\|_F + \|\mathbf{W}_{D2} - \mathbf{W}_2\|_F + \|\Lambda_D - \Lambda\|_F \quad (4.5.262)$$

Where  $\mathbf{V}_{D1} \in \mathbb{C}^{n \times s_1}$ ,  $\mathbf{W}_{D2} \in \mathbb{C}^{s_2 \times n}$  and  $\Lambda_D \in \mathbb{C}^{n \times n}$  are the desired right eigenvectors, left eigenvectors and eigenvalues respectively.  $\mathbf{V}_1 \in \mathbb{C}^{n \times s_1}$ ,  $\mathbf{W}_2 \in \mathbb{C}^{s_2 \times n}$  and  $\Lambda \in \mathbb{C}^{n \times n}$  are the achieved right eigenvectors, left eigenvectors and eigenvalues respectively.

Further development of this approach is possible. For instance, analytic gradient expressions to aid the optimisation could be derived and analytic solutions for the nested optimisation could also be sought.

#### Example 4.5.6

In this example the projection techniques described in Example 4.5.5 are re-worked with eigenvalue trade-off and the assignment errors are compared. All the eigenvalues were confined to a disk centred on their ideal location, the radius was equal to twenty percent of the eigenvalue modulus.

Comparing Table 4.5.7 with Table 4.5.6 reveals that generally eigenvalue trade-off reduces the assignment error. There is only a single exception in the above example, which has been highlighted. Table 4.5.8 shows the final eigenvalue locations and reveals that, in most cases, the solution occurs

Method	First ( $v_1$ ) R-vector	Second ( $v_2$ ) R-vector	First ( $w_3$ ) L-vector	Second ( $w_4$ ) L-vector
Simple Projection				
Right first	0.1643	0.0000	1.0000	0.3772
Left first	0.7474	0.5390	0.6713	0.2244
Three stage	0.1643	0.8848	0.7484	0.2436
Sympathetic Projection				
Right first	0.6453	0.0000	<b>0.9388</b>	0.3518
Iterative Projection				
NA	0.2702	0.0285	0.9482	0.3204

Table 4.5.7: The least squares eigenvector assignment errors for eigenvalue trade-off applied inconjunction with: two and three stage simple projection, sympathetic projection and iterative projection.

Method	Mode 1 ( $\lambda_1$ )	Mode 2 ( $\lambda_2$ )	Mode 3 ( $\lambda_3$ )	Mode 4 ( $\lambda_4$ )
Simple Projection				
Right first	-0.8000	-2.3043	-3.0000	-3.2000
Left first	-0.8000	-2.4000	-2.4000	-3.2000
Three stage	-0.8000	-2.4000	-2.4000	-3.2000
Sympathetic Projection				
Right first	-0.8000	-2.3043	-3.6000	-3.2000
Iterative Projection				
NA	-0.8000	-1.6000	-3.6000	-3.2000

Table 4.5.8: The resulting eigenvalue locations for the assignments described in Table 4.5.7.

on the boundary of the allowed region.

### 4.5.10 Eigenstructure Assignment and Similarity Transforms

It is interesting to consider the affect of similarity transforms on the eigenstructure assignment solution. Suppose a nominal system is transformed by non-singular  $X$  as follows:

$$A \mapsto X^{-1}AX \tag{4.5.263}$$

$$B \mapsto X^{-1}B \tag{4.5.264}$$

$$C \mapsto CX \tag{4.5.265}$$

Calculation of the right eigenvector allowed subspace becomes:

$$0 = \begin{bmatrix} X^{-1}AX - \lambda_i I, & X^{-1}B \end{bmatrix} \begin{bmatrix} Q_i \\ P_i \end{bmatrix} \quad (4.5.266)$$

$$= X^{-1} \begin{bmatrix} AX - \lambda_i X, & B \end{bmatrix} \begin{bmatrix} Q_i \\ P_i \end{bmatrix} \quad (4.5.267)$$

$$(4.5.268)$$

Thus the similarity transform causes the allowed subspaces to suffer the following mappings:

$$Q_i \mapsto X^{-1}Q_i \quad (4.5.269)$$

$$L_i \mapsto L_i X \quad (4.5.270)$$

Assuming fixed left ( $g_j$ ) and right ( $f_i$ ) design vectors, the assigned left and right eigenvector are transformed as follows:

$$V_1 = \begin{bmatrix} X^{-1}Q_1 f_1, \dots, X^{-1}Q_{s_1} f_{s_1} \end{bmatrix} \quad (4.5.271)$$

thus as to be expected:

$$V_1 \mapsto X^{-1}V_1 \quad (4.5.272)$$

Equally, for the left eigenvectors we note:

$$W_2 \mapsto W_2 X \quad (4.5.273)$$

Consider calculation of the gain matrix using Equation (4.5.136). We note that  $V_1$  and  $W_2$  always appear in the products  $CV_1$  and  $W_2 B$ . Thus they suffer the following mapping:

$$CV_1 \mapsto CXX^{-1}V_1 \quad (4.5.274)$$

$$W_2 B \mapsto W_2 XX^{-1}B \quad (4.5.275)$$

Since this mapping has no effect and the matrices  $S_1$  and  $T_2$  are also unaffected by the similarity transform, the gain will be unaltered by the similarity transform.

However, the assumption of fixed design vector is not entirely realistic and it is more usual that the design vectors are calculated using a projection approach. Let us assume that simple projection is applied. Recalling:

$$\mathbf{f}_{o_i} = (\mathbf{Q}_i^* \mathbf{R} \mathbf{Q}_i)^{-1} \mathbf{Q}_i^* \mathbf{R} \mathbf{v}_{d_i} \quad (4.5.276)$$

then the design vector  $\mathbf{f}_{o_i}$  will undergo the following mapping:

$$(\mathbf{Q}_i^* \mathbf{R} \mathbf{Q}_i)^{-1} \mathbf{Q}_i^* \mathbf{R} \mathbf{v}_{d_i} \mapsto \left( (\mathbf{X}^{-1} \mathbf{Q}_i)^* \mathbf{R} (\mathbf{X}^{-1} \mathbf{Q}_i) \right)^{-1} (\mathbf{X}^{-1} \mathbf{Q}_i)^* \mathbf{R} \mathbf{X}^{-1} \mathbf{v}_{d_i} \quad (4.5.277)$$

This mapping will generally affect  $\mathbf{f}_{o_i}$ . Thus all the design vectors will change as the result of a similarity transform. Most eigenstructure assignment methods use projection to calculate the design vectors, and will therefore produce different solutions depending on the system representation. This is undesirable since it begs the question 'what is the most appropriate representation?'. An approach that obviates this problem is direct assignment of the modal coupling matrices.

#### 4.5.11 Gain Suppression

Eigenstructure assignment will generally utilise all the available gains. However, some gains may be eliminated (set to zero) with minimal degradation in performance. This may be attractive, just to obtain a simpler solution or, implementation issues may require eliminating gains to meet a specific controller structure. For instance, helicopters often employ a channel structure, where the feedback to each input must come exclusively from one or two selected outputs. This precludes the use of cross-feed gains and forces the feedback matrix to have a block diagonal structure.

In this section we consider eliminating gains by calculating their sensitivity with respect to the assigned eigenvalues. Other researchers [Rop83, SYL90, SS87, CR86] have presented similar approaches. Consider the closed loop system matrix:

$$\mathbf{A}_{CL} = \mathbf{A} + \mathbf{B} \mathbf{K} \mathbf{C} \quad (4.5.278)$$

Lemma 5.5.1 [Gil84, PC72] shows that the eigenvalue sensitivity satisfies:

$$\frac{\partial \lambda_k}{\partial \alpha} = \frac{1}{\mathbf{w}_k^* \mathbf{v}_k} \mathbf{w}_k^* \frac{\partial \mathbf{A}_{CL}}{\partial \alpha} \mathbf{v}_k \quad (4.5.279)$$

Where  $\mathbf{v}_i$  and  $\mathbf{w}_i$  are the closed loop eigenvectors associated with  $\lambda_i$  and  $\alpha$  is an independent variable.

Application of Lemma 5.5.4 [Gra81] shows that:

$$\frac{\partial \mathbf{ACL}}{\partial \mathbf{K}_{ij}} = \mathbf{BE}_{ij}\mathbf{C} \quad (4.5.280)$$

Where  $\mathbf{K}_{ij}$  is the  $ij^{th}$  element of  $\mathbf{K}$  and  $\mathbf{E}_{ij}$  is an all zero matrix of equal dimensions to  $\mathbf{K}$  except the  $ij^{th}$  element is unity.

Combing these results gives:

$$\frac{\partial \lambda_k}{\partial \mathbf{K}_{ij}} = \frac{\mathbf{w}_k \mathbf{BE}_{ij} \mathbf{C} \mathbf{v}_k}{\mathbf{w}_k \mathbf{v}_k} \quad (4.5.281)$$

Let the columns of  $\mathbf{B}$  and the rows of  $\mathbf{C}$  be denoted:

$$\mathbf{B} = [\mathbf{b}_1, \dots, \mathbf{b}_r] \quad (4.5.282)$$

$$\mathbf{C}^T = [\mathbf{c}_1^T, \dots, \mathbf{c}_m^T] \quad (4.5.283)$$

The solution may be re-expressed as follows:

$$\frac{\partial \lambda_k}{\partial \mathbf{K}_{ij}} = \frac{\mathbf{w}_k \mathbf{b}_i \mathbf{c}_j \mathbf{v}_k}{\mathbf{w}_k \mathbf{v}_k} \quad (4.5.284)$$

$$= \frac{\mathbf{c}_j \mathbf{v}_k \mathbf{w}_k \mathbf{b}_i}{\mathbf{w}_k \mathbf{v}_k} \quad (4.5.285)$$

The solution for the complete gain matrix may therefore be succinctly expressed as:

$$\frac{\partial \lambda_k}{\partial \mathbf{K}} = \frac{(\mathbf{C} \mathbf{v}_k \mathbf{w}_k \mathbf{B})^T}{\mathbf{w}_k \mathbf{v}_k} \quad (4.5.286)$$

With the gradient information to hand one can decide which gain values to zero. Calvo-Ramon [CR86] and Sobel *et al* [SYL90] suggest calculating the average eigenvalue shift:

$$\mathbf{r}_{ij} = \frac{1}{n} \left[ \sum_{k=1}^n \left| \mathbf{K}_{ij} \frac{\partial \lambda_k}{\partial \mathbf{K}_{ij}} \right|^2 \right]^{\frac{1}{2}} \quad (4.5.287)$$



and using this as the basis for a decision. Sobel *et al* [SYL90] extends the approach to include the sensitivity with respect eigenvectors as well. If the number of gains elements ( $rm$ ) is greater than the number of states ( $n$ ) the following nullspace approach may be applied.

Suppose the matrix  $\mathbf{K}$  is to be perturbed by a matrix  $\Delta\mathbf{K}$

$$\mathbf{K}' = \mathbf{K} + \Delta\mathbf{K} \quad (4.5.288)$$

then a first order estimate of the deviation in the  $k^{th}$  eigenvalue is:

$$\delta\lambda_i = \text{vec} \left( \frac{\partial\lambda_k}{\partial\mathbf{K}} \right)^T \text{vec} (\Delta\mathbf{K}) \quad (4.5.289)$$

Where the  $\text{vec}()$  operator constructs a vector from a matrix by stacking the columns. To consider the effect on all the eigenvalues simultaneously the following matrix is constructed:

$$\mathbf{D}\mathbf{K}^T = \left[ \text{vec} \left( \frac{\partial\lambda_1}{\partial\mathbf{K}} \right), \dots, \text{vec} \left( \frac{\partial\lambda_n}{\partial\mathbf{K}} \right) \right] \quad (4.5.290)$$

Then a vector of eigenvalue deviations is calculated as follows:

$$\left[ \delta\lambda_1, \dots, \delta\lambda_n \right]^T = \mathbf{D}\mathbf{K} \text{vec} (\Delta\mathbf{K}) \quad (4.5.291)$$

The matrix  $\mathbf{D}\mathbf{K}$  has dimensions  $n \times rm$  and will have a null space of dimension at least  $rm - n$ . The existence of this null space implies that the gain matrix may be perturbed in a manner that does not effect the pole locations. This immediately implies an alternative approach, whereby the gain matrix is incrementally adjusted using perturbation matrices that do not effect the eigenvalues.

However, although the perturbation matrices have little effect on the eigenvalues they will alter the eigenvectors and thus the system performance. Further work could consider the effect of gain perturbations on the eigenvectors and even the eigenvector assignment errors. The tools for deriving sensitivity functions with respect to the eigenvectors and assignment errors may be found in [Gra81, PC72, SYL90].

## 4.6 Direct Assignment of the Modal Coupling Matrices

One of the main attractions of eigenstructure assignment, over pole placement, is the ability to influence how the modes couple into the states. This is particularly useful when the states have a physical meaning, as is often the case when models are derived by physical argument. For example, most aircraft models fall into this category. Eigenstructure assignment has been successfully used to decouple flight control problems by separating the modes in to the appropriate physical axes [ASC83, GC86].

However, in many models the states do not have physical meaning, but contribute to form outputs that do have physical significance. This is especially true when the model is generated by identification [SCM96], since identification, is only aware of and thus, can only approximate the input-output relationship. In this case, one is more interested in how the modes couple into the outputs and would wish to assign this property directly. This involves assigning the output mode coupling matrix ( $\mathbf{CV}$ ) [Smi91] where  $\mathbf{C}$  is the output matrix and  $\mathbf{V}$  is the matrix of right eigenvectors.

There is also a more fundamental argument why one should want to assign the input and output mode coupling matrices directly. Assigning a right eigenvector is tantamount to altering the relative observability of the associated mode in chosen states. If the design objective is to alter observability then it is more appropriate to assign the mode-observability matrix ( $\mathbf{CV}$ ) [PC72] directly.

In the state feedback case ( $\mathbf{C} = \mathbf{I}$ ) or when the output matrix can be transformed to the following structure by row ordering and scaling only:

$$\mathbf{C} = \begin{bmatrix} \mathbf{I}_m, & \mathbf{0} \end{bmatrix} \quad (4.6.292)$$

It is clear that assigning the right eigenvectors  $\mathbf{V}$  is equivalent to assigning the mode-observability matrix. An output matrix with the structure described above occurs when the states are measurable, which naturally implies they have some physical significance. Thus in many applications where eigenstructure assignment has proved particularly useful [ASC83, GC86, Far89, GLP89b], by equivalence, the mode-observability matrix has been assigned.

Consideration of input mode coupling can be used to construct a dual argument, that it is more appropriate to assign the mode-controllability matrix or input modal coupling matrix ( $\mathbf{WB}$ ) than the left eigenvectors. The mode-controllability matrix determines the degree to which a mode is excited by an input. If one consider the dyadic representation of the closed loop transfer function:

$$\mathbf{G}(s) = \sum_{i=1}^n \frac{\mathbf{Cv}_i \mathbf{w}_i \mathbf{B}}{s - \lambda_{d_i}} \quad (4.6.293)$$

then we can see that the prevalence of a mode in a particularly input output pair is dependent on the product of the appropriate elements of the mode controllability and observability matrices.

In Section 4.5.10 it was demonstrated that the results of projection based eigenstructure assignment will depend on the system representation. A benefit of assigning the modal coupling matrices is that this dependency disappears.

Other researchers [MMS92, ZSA90, Smi91, Whi91] have both tacitly and explicitly assigned the controllability and observability matrices. For instance, the approach of Manness and Murray-Smith [MMS92] uses *the output space* which is tantamount to assigning the mode observability matrix. Equally the method of Zhang *et al* [ZSA90] for suppression of unwanted inputs is equivalent to assigning the mode controllability matrix. Smith [Smi91] and White [Whi91] explicitly advocate use of the mode controllability and observability matrices. White [Whi91] suggests that performance may be evaluated with a different set of outputs to those used for feedback control. This is a useful approach if an output is important to performance but can not be measured.

The remainder of this section describes a technique for directly assigning the modal coupling matrices. The technique forms a natural extension to the eigenstructure assignment techniques presented in Section 4.5.2. The rows or columns of the modal coupling matrices are selected from allowed subspaces. Consider, the closed system:

$$\mathbf{A}_{CL} = \mathbf{A} + \mathbf{BKC} \quad (4.6.294)$$

where  $(\lambda_i, \mathbf{v}_i)$  form a closed loop eigenvalue, eigenvector pair. A basis for the allowed mode observability subspace may be derived from the definition of the closed loop right eigenvectors:

$$(\mathbf{A} + \mathbf{BKC})\mathbf{v}_i = \lambda_i\mathbf{v}_i \quad (4.6.295)$$

$$(\lambda_i\mathbf{I} - \mathbf{A})\mathbf{v}_i = \mathbf{BK}(\mathbf{Cv}_i) \quad (4.6.296)$$

$$\mathbf{Cv}_i = \mathbf{C}(\lambda_i\mathbf{I} - \mathbf{A})^{-1}\mathbf{BK}(\mathbf{Cv}_i) \quad (4.6.297)$$

$$\mathbf{0} = \begin{bmatrix} \mathbf{I}_m, & \mathbf{C}(\mathbf{A} - \lambda_i\mathbf{I})^{-1}\mathbf{B} \end{bmatrix} \begin{bmatrix} \mathbf{Cv}_i \\ \mathbf{KCv}_i \end{bmatrix} \quad (4.6.298)$$

Equation (4.6.298) shows  $\mathbf{Cv}_i$  must be in the range of  $\mathbf{C}(\mathbf{A} - \lambda_i\mathbf{I})^{-1}\mathbf{B}$ . Let  $\mathcal{D}(\lambda)$  denote the allowed mode observability subspace, then it may be defined as:

$$\mathcal{D}(\lambda) = \{ \mathbf{x}_i : \mathbf{x}_i \in \text{range}(\mathbf{C}(\mathbf{A} - \lambda_i\mathbf{I})^{-1}\mathbf{B}) \} \quad (4.6.299)$$

Although, this definition is the most intuitive, it is undefined if  $\lambda_i$  is coincident with an open loop eigenvalue of  $\mathbf{A}$ . However, Equation (4.6.296) can be used to formulate an alternative definition:

$$\mathcal{D}(\lambda) = \{x_i : x_i = \text{range}(Cv_i) | (A - \lambda_i I)v_i \in \text{range}(B)\} \quad (4.6.300)$$

This definition is principally the right eigenspace multiplied by  $C$ . Dual arguments lead to the following definitions of the allowed mode controllability subspace:

$$\mathcal{C}(\lambda) = \{y_i : y_i^T \in \text{range}(C(A - \lambda_i I)^{-1}B)^T\} \quad (4.6.301)$$

and more generally:

$$\mathcal{C}(\lambda) = \{y_i : y_i^T = \text{range}(B^T w_i^T) | (A - \lambda_i I)^T w_i^T \in \text{range}(C^T)\} \quad (4.6.302)$$

The subspaces can be calculated by using the SVD or QR algorithms to generate a minimal basis for  $\text{range}(L_j B)$  or  $\text{range}(CQ_i)$  as appropriate. The above results allow the selection of desired mode coupling vectors, but to assign these vectors a means of calculating a gain matrix must be developed. Let:

$$0 = \begin{bmatrix} I_m, & C(A - \lambda_{d_i} I)^{-1}B \end{bmatrix} \begin{bmatrix} Q_{O_i} \\ P_i \end{bmatrix} \quad (4.6.303)$$

where  $Q_{O_i} \in \mathbb{C}^{m \times r}$  denotes the allowed mode observability subspace associated with the eigenvalue  $\lambda_{d_i}$  and  $P_i$  has its usual meaning. A design vector  $f_i \in \mathbb{C}^{r \times 1}$  may be used to select a mode observability vector from the allowed subspace:

$$V_{O1} = \begin{bmatrix} Q_{O_1} f_1, \dots, Q_{O_p} f_p \end{bmatrix} \quad (4.6.304)$$

$$S_1 = \begin{bmatrix} P_1 f_1, \dots, P_p f_p \end{bmatrix} \quad (4.6.305)$$

Where  $V_{O1}$  and  $S_1$  are matrices of the selected vectors and for a real gain matrix it is required that if  $\lambda_{d_i} = \bar{\lambda}_{d_k}$  then  $f_i = \bar{f}_k$ . Comparison of Equation (4.6.303) with Equation (4.6.298) shows the gain matrix  $K$  must satisfy:

$$KV_{O1} = S_1 \quad (4.6.306)$$

Equally, let:

$$0 = \begin{bmatrix} \mathbf{LC}_j & \mathbf{M}_j \end{bmatrix} \begin{bmatrix} \mathbf{I}_r \\ \mathbf{C}(\mathbf{A} - \lambda_j \mathbf{I})^{-1} \mathbf{B} \end{bmatrix} \quad (4.6.307)$$

where  $\mathbf{LC}_j \in \mathbb{C}^{m \times r}$  denotes the allowed mode controllability subspace associated with the eigenvalue  $\lambda_{d_j}$  and  $\mathbf{M}_j$  has its usual meaning. A design vector  $\mathbf{g}_j \in \mathbb{C}^{1 \times m}$  may be used to select a mode controllability row vector from the allowed row subspace:

$$\mathbf{WC}_2^T = \begin{bmatrix} \mathbf{LC}_{p+1}^T \mathbf{g}_{p+1}^T, \dots, \mathbf{LC}_n^T \mathbf{g}_n^T \end{bmatrix} \quad (4.6.308)$$

$$\mathbf{T}_2^T = \begin{bmatrix} \mathbf{M}_{p+1}^T \mathbf{g}_{p+1}^T, \dots, \mathbf{M}_n^T \mathbf{g}_n^T \end{bmatrix} \quad (4.6.309)$$

Where  $\mathbf{WC}_2$  and  $\mathbf{T}_2$  denote matrices of the selected vectors and to ensure a real gain matrix, whenever  $\lambda_{d_j} = \bar{\lambda}_{d_k}$  then  $\mathbf{g}_j = \bar{\mathbf{g}}_k$ . Thus, by a dual argument the gain matrix must also satisfy:

$$\mathbf{WC}_2 \mathbf{K} = \mathbf{T}_2 \quad (4.6.310)$$

Recalling, Lemma 4.5.3 reveals the following conditions for a gain matrix solution:

$$\text{C1 } \text{rank}(\mathbf{VO}_1) = p$$

$$\text{C2 } \text{rank}(\mathbf{WC}_2) = n - p$$

$$\text{C3 } \mathbf{WC}_2 \mathbf{S}_1 = \mathbf{T}_2 \mathbf{VO}_1$$

If all the conditions are met, the gain matrix is calculated from the following expression:

$$\mathbf{K} = \mathbf{WC}_2^\dagger \mathbf{T}_2 + \mathbf{S}_1 \mathbf{VO}_1^\dagger - \mathbf{WC}_2^\dagger \mathbf{WC}_2 \mathbf{S}_1 \mathbf{VO}_1^\dagger \quad (4.6.311)$$

Which may be augmented with a free parameter term. An assignment technique requires a means of selecting vectors such that they meet condition C3. This may be achieved by rewriting condition C3 as follows:

$$0 = \begin{bmatrix} \mathbf{WC}_2 & \mathbf{T}_2 \end{bmatrix} \begin{bmatrix} \mathbf{S}_1 \\ -\mathbf{VO}_1 \end{bmatrix} \quad (4.6.312)$$

It may now be appended to either of the allowed subspace equations as shown below:

$$\mathbf{0} = \begin{bmatrix} \mathbf{L} & \mathbf{C}_j & \mathbf{M}_j \end{bmatrix} \begin{bmatrix} \mathbf{S}_1 & \mathbf{I}_r \\ -\mathbf{V}\mathbf{O}_1 & \mathbf{C}(\mathbf{A} - \lambda_{d_j}\mathbf{I})^{-1}\mathbf{B} \end{bmatrix} \quad (4.6.313)$$

and

$$\mathbf{0} = \begin{bmatrix} \mathbf{I}_m & \mathbf{C}(\mathbf{A} - \lambda_{d_j}\mathbf{I})^{-1}\mathbf{B} \\ \mathbf{W}\mathbf{C}_2 & -\mathbf{T}_2 \end{bmatrix} \begin{bmatrix} \mathbf{Q}\mathbf{O}_j \\ \mathbf{P}_j \end{bmatrix} \quad (4.6.314)$$

This immediately leads to a two stage assignment technique that is very similar to the eigenvector case described earlier. The stages of the technique are outlined below:

1. Select  $s_1 < r$  mode controllability vectors from the allowed subspace  $\mathcal{C}(\lambda_{d_i})$ . Or  $s_1 < m$  mode observability vectors from the allowed subspace  $\mathcal{D}(\lambda_{d_i})$ . The selected vectors must form conjugate pairs in accordance with their associated eigenvalues. Then construct  $(\mathbf{V}\mathbf{O}_1, \mathbf{S}_1)$  or  $(\mathbf{W}\mathbf{C}_2, \mathbf{T}_2)$  as appropriate.
2. Select  $s_2 \leq m$  mode observability vectors from the augmented subspace Equation (4.6.314). Or select  $s_2 \leq r$  from the augmented subspace Equation (4.6.313). Again, the selected vectors must form conjugate pairs in accordance with their associated eigenvalues. Then construct the complementary  $(\mathbf{W}\mathbf{C}_2, \mathbf{T}_2)$  or  $(\mathbf{V}\mathbf{O}_1, \mathbf{S}_1)$  as appropriate.

Finally, calculate the gain matrix from Equation (4.6.311). Some points to note about this approach are:

- Complete assignment still requires  $m + r > n$ . The number of vectors that may be assigned and the design freedom available may be read from Table 4.5.2 and Table 4.5.3. However, the 'right' should be replaced with mode-observability and 'left' with mode-controllability. Although the subspaces are the same dimension for both eigenvector and mode coupling assignment, the vectors being assigned are generally smaller ( $\max(m, r) < n$ ). Therefore the chances of acceptably approximating the desired vector from within the subspace are higher.
- Unused design freedom may exist after the two stage technique and the free parameter of Equation (4.6.311) can be used to construct a reduced system for a retro stage.
- Multistage assignment is also possible. It is only required that conditions C1 to C3 are met after all the assignment stages. Thus design freedom can be distributed in the same manner as the eigenvector assignment case.

- This technique does not require a state space representation. Providing, the assigned poles are not coincident with the open loop poles, only the transfer function matrix is needed. Consequently, the assignment is independent of similarity transforms applied to the representation. If the transfer function matrix is used then the following simplification is also possible. Let  $G(s) = C(sI - A)^{-1}B$  then

$$0 = \begin{bmatrix} I_m, & -G(s) \end{bmatrix} \begin{bmatrix} G(s) \\ I_r \end{bmatrix} \quad (4.6.315)$$

Examination of Equation (4.6.303) and Equation (4.6.307) shows that the above may be used for calculation of the allowed subspaces.

The design vectors may be determined using simple projection. The minimisation is formulated as follows:

$$J_i = \|\mathbf{v}_{od_i} - \mathbf{Q} \mathbf{O}_i \mathbf{f}_i\|_{\mathbf{R}}^2 \quad (4.6.316)$$

Where  $\mathbf{R}$  is a positive definite weighting matrix and  $\mathbf{v}_{od_i}$  is the desired form for a column of the mode observability matrix. It describes in which outputs the mode  $\lambda_i$  should prevail. The solution is readily given by Equation (4.5.230). Naturally, a dual formulation for simple projection of the mode controllability matrix may also be formulated.

In the same way that the orthogonality condition, necessary for stage two, may be formulated as a projection constraint, it is also possible to incorporate the constraints imposed by Equation (4.6.312) into the optimisation. The constrained problem is:

$$J_j = \|\mathbf{w}_{od_j} - \mathbf{L} \mathbf{C}_j^* \mathbf{g}_j^*\|_{\mathbf{R}}^2 \quad \text{subject to} \quad 0 = \mathbf{g}_j \begin{bmatrix} \mathbf{L} \mathbf{C}_j & \mathbf{M}_j \end{bmatrix} \begin{bmatrix} \mathbf{S}_1 \\ -\mathbf{V} \mathbf{O}_1 \end{bmatrix} \quad (4.6.317)$$

Where  $\mathbf{w}_{od_j}$  is the desired mode controllability row vector and  $\mathbf{S}_1$ ,  $\mathbf{V} \mathbf{O}_1$  are results of stage one assignment. Again, a dual problem for stage two assignment of mode observability vectors is readily formulated.

Unfortunately, the direct assignment technique does not lend itself to sympathetic projection. The purpose of sympathetic projection is to mitigate the effect on stage two of the additional constraints imposed by Equation (4.6.312). This is accomplished by forcing stage one to adopt a solution that is compatible with the ideal solution to stage two. However, this would imply a term of the form:

$$w_l \left\| \begin{bmatrix} \mathbf{W}_{OD} & \mathbf{P}_D \end{bmatrix} \begin{bmatrix} \mathbf{Q}_{O_i} \\ \mathbf{P}_i \end{bmatrix} \mathbf{f}_i \right\|_{\mathbf{R}_2}^2 \quad (4.6.318)$$

While  $\mathbf{W}_{OD}$  is simply constructed from the row vectors  $\mathbf{w}_{odj}$ , Equation (4.6.298) shows that constructing  $\mathbf{P}_D$  would require prior knowledge of the gain matrix. Hence the difficulty of applying sympathetic projection to direct assignment.

Direct assignment may be used in conjunction with iterative projection. The technique follows the procedure outlined in Section 4.5.8, but the projection problem is reformulated as follows:

$$J_i = \|\mathbf{v}_{od_i} - \mathbf{Q}_{O_i} \mathbf{f}_i\|_{\mathbf{R}_1}^2 + w_l \left\| \begin{bmatrix} \mathbf{W}_{C2} & \mathbf{T}_2 \end{bmatrix} \begin{bmatrix} \mathbf{Q}_{O_i} \\ \mathbf{P}_i \end{bmatrix} \mathbf{f}_i \right\|_{\mathbf{R}_2}^2 \quad i = 1 \dots s_1 \quad (4.6.319)$$

The dual problem is:

$$J_j = \|\mathbf{w}_{od_j} - \mathbf{g}_j \mathbf{L}_{C_j}\|_{\mathbf{R}_1}^2 + w_r \left\| \mathbf{g}_j \begin{bmatrix} \mathbf{L}_{C_j} & \mathbf{M}_j \end{bmatrix} \begin{bmatrix} \mathbf{V}_{O2} \\ \mathbf{S}_2 \end{bmatrix} \right\|_{\mathbf{R}_2}^2 \quad j = (s_1 + 1) \dots n \quad (4.6.320)$$

Other techniques such as gain suppression are readily applied to the direct assignment case.

## 4.7 Dynamic Compensation

In this section two methods of implementing dynamic compensation are presented. Dynamic compensation increases the available design freedom and can therefore achieve design goals that are not possible using static feedback alone. For instance, dynamic compensation can be used to achieve complete pole assignment with systems that do not satisfy  $m + r > n$ .

### 4.7.1 The Augmented System Method

Since first proposed by Johnson and Athans [JA70] the the Augmented System Method has proved an expedient and popular [Kim75, SS87, HO87, Han89, Dua93a, SSA94] method of achieving dynamic compensation. The salient features of this method are listed as follows:

- This method generalises static feedback results to dynamic compensation without requiring any new theory.





Where  $u_1$  and  $y_1$  are inputs and outputs of the open loop system. The augmented system has some interesting properties. Consider calculation of the allowed right eigenvector subspace:

$$\left[ \begin{bmatrix} A & 0 \\ 0 & 0 \end{bmatrix} - s \begin{bmatrix} I_n & 0 \\ 0 & I_l \end{bmatrix} \quad \begin{bmatrix} B & 0 \\ 0 & I_l \end{bmatrix} \right] \begin{bmatrix} 0 & Q \\ I_l & 0 \\ 0 & P \\ sI_l & 0 \end{bmatrix} \quad (4.7.325)$$

We see that the portion of the eigenvector associated with the open loop states must be selected from the unaugmented allowed subspace ( $Q$ ) and that the portion associated with the compensator may be arbitrarily assigned. It is readily shown that the same is true for the allowed left eigenvector subspace. The transmission zeros [MK76, KH86] of the augmented system are the same as those for the open loop system, since if:

$$\begin{bmatrix} sI - A & -B \\ C & 0 \end{bmatrix} \quad (4.7.326)$$

is rank deficient then it is readily shown that:

$$\begin{bmatrix} sI - \hat{A} & -\hat{B} \\ \hat{C} & 0 \end{bmatrix} \quad (4.7.327)$$

is also rank deficient. Hence the transmission zeros are invariant under dynamic compensation introduced by the augmented system method.

A drawback of this method is that there is no well developed theory [SS87] for selecting compensator eigenvalues and eigenvectors. However, with a good understanding of the plant the design engineer can apply classical ideas such as washout filters and lead-lag networks.

The augmented system method may be applied in a less generic manner by augmenting the system with a known compensator structure and then applying static feedback techniques. For instance, the augmented system method described above is pure feedback compensation and does not draw any information from the open loop system inputs. However, an additional input matrix ( $B_P$ ) can be added to the usual augmented structure to feed input information into the compensator states.

$$\hat{B} = \begin{bmatrix} B & 0 \\ B_P & I_l \end{bmatrix} \quad (4.7.328)$$



$$\hat{\mathbf{A}} = \begin{bmatrix} \mathbf{A} & \mathbf{0} \\ \mathbf{0} & \mathbf{A} \end{bmatrix} \quad \hat{\mathbf{B}} = \begin{bmatrix} \mathbf{0} & \mathbf{B} \\ \mathbf{I} & \mathbf{B} \end{bmatrix} \quad \hat{\mathbf{C}} = \begin{bmatrix} \mathbf{0} & \mathbf{I} \\ \mathbf{C} & -\mathbf{C} \end{bmatrix} \quad \hat{\mathbf{K}} = \begin{bmatrix} \mathbf{0} & \mathbf{K}_O \\ \mathbf{K}_c & \mathbf{0} \end{bmatrix} \quad (4.7.329)$$

Full state estimation requires a  $n^{th}$  order compensator<sup>9</sup>. However, it may not be required to estimate all the states since some may be measurable or simply not needed. In which case a reduced order observer [Bro91, Kai80] may be employed.

Suppose an open loop system has  $m$  measurable outputs then a similarity transform may be applied such that:

$$\mathbf{x} = \begin{bmatrix} \mathbf{x}_1 \\ \mathbf{x}_2 \end{bmatrix} \quad \mathbf{A} = \begin{bmatrix} \mathbf{A}_{11} & \mathbf{A}_{12} \\ \mathbf{A}_{21} & \mathbf{A}_{22} \end{bmatrix} \quad \mathbf{B} = \begin{bmatrix} \mathbf{B}_1 \\ \mathbf{B}_2 \end{bmatrix} \quad \mathbf{C} = \begin{bmatrix} \mathbf{I}_m & \mathbf{0} \end{bmatrix} \quad (4.7.330)$$

The lower partition indicates how an open loop estimation of  $\mathbf{x}_2$  may be achieved, let  $\mathbf{x}_{e2}$  be the estimated state:

$$\dot{\mathbf{x}}_{e2} = \mathbf{A}_{22}\mathbf{x}_{e2} + (\mathbf{A}_{21}\mathbf{x}_1 + \mathbf{B}_2\mathbf{u}) \quad (4.7.331)$$

For the system above to produce a meaningful estimate corrective feedback will be required. From the upper portion we see  $\mathbf{A}_{12}\mathbf{x}_2$  contributes to the dynamics of  $\mathbf{x}_1$  which are measurable. Thus an error term may be formulated as follows:

$$\mathbf{e} = \mathbf{A}_{12}\mathbf{x}_2 - \mathbf{A}_{12}\mathbf{x}_{e2} \quad (4.7.332)$$

Substituting the equation from the upper partition gives:

$$\mathbf{e} = (\dot{\mathbf{x}}_1 - \mathbf{A}_{11}\mathbf{x}_1 - \mathbf{B}_1\mathbf{u}) - \mathbf{A}_{12}\mathbf{x}_{e2} \quad (4.7.333)$$

The term  $\dot{\mathbf{x}}_1$  is undesirable since it implies differentiating the system output. Fortunately, this problem can be obviated by noting that the error term will be multiplied by a gain ( $\mathbf{K}_O$ ) then integrated. Rather than integrating the term  $\mathbf{K}_O \dot{\mathbf{x}}_1$  one may simply add  $\mathbf{K}_O \mathbf{x}_1$  to the output. Thus

---

<sup>9</sup>In fact full state estimation may be achieved with a  $n - 1$  order compensator [Kai80].

$$\dot{\mathbf{x}}_{e2} = \mathbf{A}_{22}\mathbf{x}_{e2} + (\mathbf{A}_{21}\mathbf{x}_1 + \mathbf{B}_2\mathbf{u}) + \mathbf{K}_O \mathbf{e} \quad (4.7.334)$$

$$= \mathbf{A}_{22}\mathbf{x}_{e2} + (\mathbf{A}_{21}\mathbf{x}_1 + \mathbf{B}_2\mathbf{u}) + \mathbf{K}_O ((\dot{\mathbf{x}}_1 - \mathbf{A}_{11}\mathbf{x}_1 - \mathbf{B}_1\mathbf{u}) - \mathbf{A}_{12}\mathbf{x}_{e2}) \quad (4.7.335)$$

$$= (\mathbf{A}_{22} - \mathbf{K}_O \mathbf{A}_{12})\mathbf{x}_{e2} + (\mathbf{A}_{21} - \mathbf{K}_O \mathbf{A}_{11})\mathbf{x}_1 + (\mathbf{B}_2 - \mathbf{K}_O \mathbf{B}_1)\mathbf{u} + \mathbf{K}_O \dot{\mathbf{x}}_1$$

Let us remove the derivative term ( $\dot{\mathbf{x}}_1$ ) by re-defining the state variable  $\mathbf{x}_{e2} \mapsto \mathbf{z} + \mathbf{K}_O \mathbf{x}_1$ :

$$\begin{aligned} \dot{\mathbf{z}} &= (\mathbf{A}_{22} - \mathbf{K}_O \mathbf{A}_{12})(\mathbf{z} + \mathbf{K}_O \mathbf{x}_1) + (\mathbf{A}_{21} - \mathbf{K}_O \mathbf{A}_{11})\mathbf{x}_1 + (\mathbf{B}_2 - \mathbf{K}_O \mathbf{B}_1)\mathbf{u} \\ &= (\mathbf{A}_{22} - \mathbf{K}_O \mathbf{A}_{12})\mathbf{z} + (\mathbf{A}_{21} - \mathbf{K}_O \mathbf{A}_{11} + \mathbf{A}_{22}\mathbf{K}_O - \mathbf{K}_O \mathbf{A}_{12}\mathbf{K}_O)\mathbf{x}_1 + (\mathbf{B}_2 - \mathbf{K}_O \mathbf{B}_1)\mathbf{u} \end{aligned}$$

Design of the reduced order observer is the same as for the full state case except that the pair  $(\mathbf{A}_{22}, \mathbf{A}_{12})$  are used. Once the reduced order observer has been designed it may be incorporated in an augmented system to facilitate controller design using static feedback techniques.

$$\hat{\mathbf{A}} = \begin{bmatrix} \mathbf{A} & \mathbf{0} \\ (\mathbf{A}_{21} - \mathbf{K}_O \mathbf{A}_{11} + \mathbf{A}_{22}\mathbf{K}_O - \mathbf{K}_O \mathbf{A}_{12}\mathbf{K}_O) & (\mathbf{A}_{22} - \mathbf{K}_O \mathbf{A}_{12}) \end{bmatrix} \quad (4.7.336)$$

$$\hat{\mathbf{B}} = \begin{bmatrix} \mathbf{B} \\ (\mathbf{B}_2 - \mathbf{K}_O \mathbf{B}_1) \end{bmatrix} \quad (4.7.337)$$

$$\hat{\mathbf{C}} = \begin{bmatrix} \mathbf{C} & \mathbf{0} \\ \mathbf{K}_O & \mathbf{I} \end{bmatrix} \quad (4.7.338)$$

It is interesting to note that an observer makes use of both input and output information and is thus both a pre-compensator and a feedback compensator.

This section has developed tools that allow the fixed gain eigenstructure assignment techniques, that have already been developed, to enjoy the additional design freedom offered by dynamic compensation. The observer method allows the designer to achieve near state feedback performance and is useful when the move from state feedback to static output feedback has caused an unrecoverable loss in performance. However, it should be borne in mind that the robustness properties of the state feedback solution are unlikely to be recovered. The augmented system approach is very flexible, but since there is a dearth of theoretical guidance for designing dynamic compensators using eigenstructure assignment. This technique is best combined with a controller strategy appropriate for the given application. The controller strategy may be drawn from past experience, classical compensator approaches and analysis of the observer based solution.

## 4.8 Summary and Further Work

### 4.8.1 Summary

This chapter pulls together a lot of the current eigenstructure assignment theory and presents it in a unified manner. Several novel extensions to the existing theory are developed. These include:

- An eigenvalue trade-off algorithm with an analytical solution for the real eigenvalue case.
- Concise and simplified proofs that facilitate a clear understanding of the fundamentals of eigenstructure assignment.
- A novel gain equation that forms the basis of a versatile eigenstructure assignment algorithm.
- A retro-assignment stage that allows unused design freedom to be recovered.
- The iterative and sympathetic projection algorithms. These allow more control over the distribution of design freedom during the projection process.
- It is argued that direct assignment of the modal coupling matrices is more appropriate for the output feedback case. Theory is developed that facilitates a technique for direct assignment of the modal coupling matrices.

All the extensions are straightforward additions to a basic two stage assignment algorithm.

### 4.8.2 Further Work

Undoubtedly, the most irritating lacuna in the preceding work is the lack of an analytical result to the trade-off algorithm for the case of complex eigenvalues. Much of the work in Appendix C was undertaken in an effort to find an analytical solution for this case and would form a good starting point for further work. The aim of which would be to find a solution or unequivocally establish there is no analytical solution.

For the work in this chapter to be of use to practising engineers it must be supported by reliable quality software. While considerable software has been developed to exercise the algorithms. Further work would be necessary to package the code in a consistent and complete manner. Probably, the most appropriate format for the software would be a toolbox that provides simple commands which can be easily combined to achieve complex designs. This low level approach ensures the engineer always maintains control over the design.

Many controller synthesis problems have been recently re-expressed as linear matrix inequalities (LMI) [SI96]. This has provided a unified approach. It would be interesting to explore if eigenstructure assignment can re-expressed as an LMI and therefore unified with other, traditionally distinct, branches of control theory.

The direct assignment technique does not lend itself to sympathetic projection in its present form. A topic for further work could be to develop an equivalent mechanism for controlling the influence of the first stage on subsequent assignment stages.

The current approach to gain suppression only considered the affect on the eigenvalues. It would be worthwhile to develop extensions that also consider the eigenvectors and even their associated assignment errors. This will provide the engineer with a clearer idea of the likely impact on performance of eliminating a gain. While gain suppression can be useful in simplifying the design this post-design sensitivity analysis is an *ad hoc* way of achieving structural constraints. A challenging topic for further work would be the development of theory that allowed hard structural constraints to be specified from the outset of the design.

For complete assignment, all techniques considered in this chapter must satisfy the constraint:

$$m + r > n \quad (4.8.339)$$

This constraint is imposed not because of a fundamental law, but because it affords a simplification of the problem that allows us to calculate a solution using linear algebra techniques. It has been quite recently shown [Wan92, RSW95] that complete assignment only requires:

$$mr > n \quad (4.8.340)$$

The inefficiency of the current constraint becomes more acute as the order of the system is increased. For example, for a fourth order system both constraints require an equal number of gains, but for a fortieth order system the linear constraint may require as many as ten times more gains. Developing a general solution to the problem of complete pole assignment using output feedback that requires the minimum number of gain elements is a fundamental problem in control theory and certainly worthy of further research.

## 4.9 References

- [AL67] BDO Anderson and DG Luenberger. Design of multivariable feedback systems. *Proc. IEE*, 114(3):395–399, March 1967.
- [AM89] BDO Anderson and JB Moore. *Optimal Control and Linear Quadratic Methods*. Information and System Sciences Series. Prentice-Hall International Inc., 1989.
- [AP96] AT Alexandridis and PN Paraskevopoulos. A new approach to eigenstructure assignment by output feedback. *IEEE Trans. on Automatic Control*, 41(7):1046–1050, July 1996.
- [ASC83] AN Andry, EY Shapiro, and JC Chung. Eigenstructure assignment for linear systems. *IEEE Trans. on Aerospace and Electronic Systems*, 19(5):711–727, September 1983.
- [BB81] RW Brockett and CI Byrnes. Multivariable nyquist criteria, root loci, and pole placement: A geometric viewpoint. *IEEE Trans. on Automatic Control*, 26(1):271–283, February 1981.

- [BFP78] A Bradshaw, LR Fletcher, and B Porter. Synthesis of output-feedback control laws for linear multivariable continuous-time systems. *Int. Journal of Systems Science*, 9(12):1331–1340, 1978.
- [BIG74] A Ben-Israel and NE Greville. *Generalised Inverses: Theory and Applications*. A Wiley-Interscience publication. John Wiley and Sons, Inc., 1974.
- [BN89] R Byers and SG Nash. Approaches to robust pole assignment. *Int. Journal of Control*, 49(1):97–117, 1989.
- [BP70] FM Brasch and JB Pearson. Pole placement using dynamic compensators. *IEEE Trans. on Automatic Control*, 15(1):34–43, February 1970.
- [BP91] SP Burrows and RJ Patton. Design of low-sensitivity, minimum norm and structurally constrained control law using eigenstructure assignment. *Optimal Control Applications and Methods.*, 12:131–140, 1991.
- [Bro91] WL Brogan. *Modern Control Theory*. Prentice Hall International Inc., 3rd edition, 1991.
- [Bur90] SP Burrows. *Robust Control Design Techniques using Eigenstructure Assignment*. PhD thesis, University of York, Heslington, York, England, Y03-5DD, September 1990.
- [CR86] JR Calvo-Ramon. Eigenstructure assignment by output feedback and residue analysis. *IEEE Trans. on Automatic Control*, 31(3):247–249, March 1986.
- [Dav94] R Davies. *Robust Eigenstructure Assignment for Flight Control Applications*. DPhil, University of York, Heslington, York, Y01 5DD, England, 1994.
- [DC71] EJ Davidson and R Chatterjee. A note on pole assignment in linear systems with incomplete state feedback. *IEEE Trans. on Automatic Control*, 16:98–99, February 1971.
- [DeC89] RA DeCarlo. *Linear Systems: A State Variable Approach with Numerical Implementation*. Prentice-Hall, Inc., 1989.
- [Dep80] Department of Defence, Washington, D.C. *Military specifications - flying qualities of piloted airplanes. MIL-F-8785C*, 1980.
- [DH88] JJ D'Azzo and CH Houpis. *Linear Control System Analysis & Design: Conventional and Modern*. McGraw-Hill Electrical Engineering Series. McGraw-Hill, 3rd edition, 1988.
- [Doy78] JC Doyle. Guaranteed margins for LQG regulator. *IEEE Trans. on Automatic Control*, 23(4):756–757, August 1978.
- [DS79] JC Doyle and G Stein. Robustness with observers. *IEEE Trans. on Automatic Control*, 24(4):607–611, August 1979.
- [Dua92a] GR Duan. Simple algorithm for robust pole assignment in linear output feedback. *IEE Proceedings D*, 139(5):465–469, September 1992.
- [Dua92b] GR Duan. Solution to matrix equation  $AV + BW = EVF$  and eigenstructure assignment for descriptor systems. *Automatica*, 28(3):639–643, 1992.
- [Dua93a] GR Duan. Robust eigenstructure assignment via dynamical compensation. *Automatica*, 29(2):469–474, 1993.
- [Dua93b] GR Duan. Solutions of the equation  $AV + BW = VF$  and their application to eigenstructure assignment in linear systems. *IEEE Trans. on Automatic Control*, 38(2):276–280, February 1993.
- [Dua94] GR Duan. Eigenstructure assignment by decentralised output feedback - a complete parametric approach. *IEEE Trans. on Automatic Control*, 39(5):1009–1014, May 1994.
- [DW75] EJ Davison and SH Wang. On pole assignment in linear multivariable systems using output feedback. *IEEE Trans. on Automatic Control*, 20:516–518, August 1975.
- [Eat94] JW Eaton. *Octave*. Department of Chemistry, University of Texas, 1.0 edition, February 1994.
- [Fal77] F Fallside, editor. *Control System Design by Pole-Zero Assignment*. Academic Press, 1977.
- [Far89] J Farineau. Lateral electric flight control laws of civil aircraft based on eigenstructure assignment technique. In *Paper 89-3594, AIAA Guidance Navigation and Control Conference*, pages 1–15, Boston, MA, August 1989. AIAA.
- [FKKN85] LR Fletcher, J Kautsky, KG Kolka, and NK Nichols. Some necessary and sufficient conditions for eigenstructure assignment. *Int. Journal of Control*, 42(6):1457–1468, 1985.
- [Fle80] LR Fletcher. An intermediate algorithm for pole placement by output feedback in linear multivariable control systems. *Int. Journal of Control*, 31(6):1121–1136, 1980.
- [Fle87] LR Fletcher. Exact pole assignment by output feedback part 2. *Int. Journal of Control*, 45(6):2009–2019, 1987.
- [FM87] LR Fletcher and JF Magni. Exact pole assignment by output feedback part 1. *Int. Journal of Control*, 45(6):1995–2007, 1987.



- [FO82] MM Fahmy and J O'Reilly. On eigenstructure assignment in linear multivariable systems. *IEEE Trans. on Automatic Control*, 27(3):690–693, June 1982.
- [FO83] MM Fahmy and J O'Reilly. Eigenstructure assignment in linear multivariable systems - a parametric solution. *IEEE Trans. on Automatic Control*, 28(10):990–994, October 1983.
- [FO88a] MM Fahmy and J O'Reilly. Multistage parametric eigenstructure assignment by output-feedback control. *Int. Journal of Control*, 48(1):97–116, 1988.
- [FO88b] MM Fahmy and J O'Reilly. Parametric eigenstructure assignment by output-feedback control: the case of multiple eigenvalues. *Int. Journal of Control*, 48(4):1519–1535, 1988.
- [FT84] MM Fahmy and HS Tantawy. Eigenstructure assignment via linear state-feedback control. *Int. Journal of Control*, 40(1):161–178, 1984.
- [GC86] VF Gavito and DJ Collins. Application of eigenstructure assignment to design of robust decoupling controllers in MIMO systems. In *AIAA Guidance, Navigation and Control Conference*, pages 828–834. AIAA, 1986.
- [Gil84] EG Gilbert. Conditions for minimizing the norm sensitivity of characteristic roots. *IEEE Trans. on Automatic Control*, 29(7):658–660, July 1984.
- [GL83] GH Golub and CF Van Loan. *Matrix Computations*. John Hopkins University Press, 1983.
- [GL90] WL Garrad and E Low. Eigenspace design of helicopter flight control systems. Technical report DAAL03-86-K-0056, Department of Aerospace Engineering and Mechanics, University of Minnesota., November 1990.
- [GL96] GH Golub and CF Van Loan. *Matrix Computations*. John Hopkins University Press, 3rd edition, 1996.
- [GLLT92] A Grace, AJ Laub, JN Little, and CM Thompson. *Control System Toolbox for use with Matlab*. The Mathworks Inc., 24 Prime Park Way, Natick, Mass., 01760-1500, July 1992.
- [GLP89a] WL Garrad, E Low, and S Prouty. Design of attitude and rate command systems for helicopters using eigenstructure assignment. *Journal of Guidance, Control and Dynamics*, 12(6):783–791, November 1989.
- [GLP89b] WL Garrad, E Low, and S Prouty. Design of attitude and rate command systems for helicopters using eigenstructure assignment. *Journal of Guidance, Control and Dynamics*, 12(6):783–791, Nov.-Dec. 1989.
- [Gra81] A Graham. *Kronecker Products and Matrix Calculus With Applications*. Ellis Horwood Limited, 1981.
- [Gra95] A Grace. *Optimization Toolbox: For Use with Matlab*. The MathWorks Inc., 24 Prime Park Way, Natick, Mass. 01760-1500, April 1995.
- [Han89] Z Han. Eigenstructure assignment using dynamical compensator. *Int. Journal of Control*, 49(1):233–245, 1989.
- [HO87] P Hippe and J O'Reilly. Parametric compensator design. *Int. Journal of Control*, 45(4):1455–1468, 1987.
- [JA70] TL Johnson and M Athans. On the design of optimal constrained dynamic compensators for linear constant systems. *IEEE Trans. on Automatic Control*, 15:658–660, December 1970.
- [Kai80] T Kailath. *Linear Systems*. Prentice-Hall, Inc., 1980.
- [KH86] H Kazerooni and PK Houpt. On the loop transfer recovery. *Int. Journal of Control*, 43(3):981–996, 1986.
- [Kim75] H Kimura. Pole assignment by gain output feedback. *IEEE Trans. on Automatic Control*, 20:509–516, August 1975.
- [Kim77] H Kimura. A further result on the problem of pole assignment by output feedback. *IEEE Trans. on Automatic Control*, 25(3):458–463, June 1977.
- [KND85] J Kautsky, NK Nichols, and P Van Dooren. Robust pole assignment in linear state feedback. *Int. Journal of Control*, 41(5):1129–1155, 1985.
- [Kou81] TG Koussioris. Controllability indices of a system, minimal indices of its transfer function matrix, and their relations. *Int. Journal of Control*, 34(6):612–622, 1981.
- [LH92] BS Liebst and TC Huckabone. An algorithm for robust eigenstructure assignment using the linear quadratic regulator. In *Proceedings of the AIAA Conference on Guidance, Navigation and Control*, pages 896–908. AIAA, August 1992.
- [Lue66] DG Luenberger. Observers for multivariable systems. *IEEE Trans. on Automatic Control*, 11(2):190–197, April 1966.
- [Mac72] AGJ Macfarlane. A survey of some recent results in linear multivariable feedback theory. *Automatica*, 8:455–492, 1972.
- [Mag87] JF Magni. Exact pole assignment by output feedback part 3. *Int. Journal of Control*, 45(6):2021–2033, 1987.
- [Mat92] The MathWorks, Inc, 24 Prime Park Way, Natick, Mass. 01760. *MATLAB Reference Guide*, October 1992.
- [Mil87] KS Miller. *Some Eclectic Matrix Theory*. Robert E Krieger Publishing Co. Inc., 1987.

- [MK76] AGJ MacFarlane and N Karcnias. Poles and zeros of linear multivariable systems: a survey of the algebraic, geometric and complex-variable theory. *Int. Journal of Control*, 24(1):33–74, 1976.
- [MMS92] MA Manness and DJ Murray-Smith. Aspects of multivariable flight control law design for helicopters using eigenstructure assignment. *Journal of The American Helicopter Society*, 37(3):18–32, July 1992.
- [Moo76] BC Moore. On the flexibility offered by state feedback in multivariable systems beyond closed loop eigenvalue assignment. *IEEE Trans. on Automatic Control*, 21:689–692, October 1976.
- [OF85] J O'Reilly and MM Fahmy. The minimum number of degrees of freedom in state feedback control. *Int. Journal of Control*, 41(3):749–768, 1985.
- [OO89] TJ Owens and J O'Reilly. Parametric state-feedback control for arbitrary eigenvalue assignment with minimum sensitivity. *IEE Proceedings D*, 136(6):307–313, November 1989.
- [PC72] B Porter and R Crossley. *Modal Control*. Taylor and Francis Ltd, 1972.
- [PD78] B Porter and JJ D'Azzo. Closed-loop eigenstructure assignment by state feedback in multivariable linear systems. *Int. Journal of Control*, 27(3):482–492, 1978.
- [PMS85] DLK Parry and DJ Murray-Smith. The application of modal control theory to the single rotor helicopter. In *The 11<sup>th</sup> European Rotorcraft Forum*, pages 78–1–78–16, 1985.
- [Por77] B Porter. Eigenvalue assignment in linear multivariable systems by output feedback. *Int. Journal of Control*, 25(3):483–490, 1977.
- [RH78] HH Rosenbrock and GE Hayton. The general problem of pole assignment. *Int. Journal of Control*, 27(6):837–852, 1978.
- [RO87] G Roppenecker and J O'Reilly. Parametric output feedback controller design. In *Proceeding of the 10th IFAC World Congress*, pages 275–280, 1987.
- [RO89] G Roppenecker and J O'Reilly. Parametric output feedback controller design. *Automatica*, 25(2):259–265, 1989.
- [Rop83] G Roppenecker. Minimum norm output feedback design under specified eigenvalue areas. *System and Control Letters*, 3:101–103, July 1983.
- [RS70] HH Rosenbrock and C Storey. *Mathematics of Dynamical Systems*. Thomas Nelson and Sons Ltd, 1970.
- [RSW95] J Rosenthal, JM Schumacher, and JC Willems. Generic eigenvalue assignment by memoryless real output feedback. *System and Control Letters*, 26:253–260, 1995.
- [SC81] EX Shapiro and JC Chung. Application of eigenvalue/eigenvector assignment by constant output feedback to flight control system design. In *Proc. 15th Annual Conf. On Information Science and Systems*, pages 164–169, 1981.
- [SC92] KM Sobel and JR Cloutier. Eigenstructure assignment for the extended medium range air-to-air missile. *Journal of Guidance, Control and Dynamics*, 15(2):529–531, 1992.
- [SCM96] XD Sun, T Clarke, and MA Maiza. A toolbox for minimal state space model realisation. *IEE Proceedings D*, 143(2):152–158, March 1996.
- [SI96] RE Skelton and T Iwasaki. Increased roles of linear algebra in control education. *IEEE Control Systems*, 15(4):76–89, August 1996.
- [SK76] U Shaked and N Karcnias. The use of zeros and zero-directions in model reduction. *Int. Journal of Control*, 23(1):113–135, 1976.
- [SL89] KM Sobel and FJ Lallman. Eigenstructure assignment for the control of highly augmented aircraft. *Journal of Guidance, Control and Dynamics*, 12(3):318–324, May 1989.
- [Smi91] PR Smith. Use of eigenstructure assignment in VSTOL aircraft control law design. In *Proceedings of Control 91 (Edinburgh)*, pages 1028–1034. IEE, 1991.
- [Sri78] S Srinathkumar. Eigenvalue/eigenvector assignment using output feedback. *IEEE Trans. on Automatic Control*, 23(1):79–81, February 1978.
- [SS85a] KM Sobel and EY Shapiro. Eigenstructure assignment: A tutorial - part I theory. In *Proceedings of American Control Conference*, pages 456–460, Boston, Massachusetts, 1985.
- [SS85b] KM Sobel and EY Shapiro. Eigenstructure assignment: A tutorial - part II application. In *Proceedings of American Control Conference*, pages 461–467, Boston, Massachusetts, 1985.
- [SS87] KM Sobel and EY Shapiro. Application of eigenstructure assignment to flight control design: Some extensions. *Journal of Guidance, Control and Dynamics*, 10(1):73–81, January 1987.
- [SS91] KM Sobel and EY Shapiro. An extension to pseudo control strategy with application to an eigenstructure assignment yaw pointing/lateral translation control law. In *proceedings of the 30<sup>th</sup> Conference on Decision and Control*, pages 515–516. IEEE, December 1991.

- [SSA94] KM Sobel, EY Shapiro, and AN Andry. Eigenstructure assignment. *Int. Journal of Control*, 59(1):13–37, 1994.
- [SYL90] KM Sobel, W Yu, and FJ Lallman. Eigenstructure assignment with gain suppression using eigenvalue and eigenvector derivatives. *Journal of Guidance, Control and Dynamics*, 13(6):1008–1013, November 1990.
- [Wal75] GR Walsh. *Methods of Optimization*. John Wiley and Sons, 1975.
- [Wan92] X Wang. Pole placement by static output feedback. *Journal of Mathematical Systems, Estimation, and Control*, 2(2):205–218, 1992.
- [WCY91] RF Wilson, JR Cloutier, and RK Yedavalli. Control design for robust eigenstructure assignment in linear uncertain systems. In *Proceeding of the 30<sup>th</sup> Conference on Decision and Control*, pages 2982–2987, Brighton, England, December 1991. IEEE.
- [WH78] JC Willems and WH Hesselink. Generic properties of the pole placement problem. In *Proceedings of the 7th IFAC World Congress*, pages 1725–1729. IFAC, 1978.
- [Whi91] BA White. Eigenstructure assignment. *Int. Journal of Control*, 53(6):1413–1429, 1991.
- [Wil65] JH Wilkinson. *The algebraic eigenvalue problem*. Oxford University Press, 1965.
- [Won67] WM Wonham. On pole assignment in multi-input controllable linear systems. *IEEE Trans. on Automatic Control*, 12(6):660–665, 1967.
- [ZSA90] Q Zhang, GL Slater, and RJ Allemang. Suppression of undesired inputs of linear systems by eigenspace assignment. *Journal of Guidance, Control and Dynamics*, 13(1):330–336, March 1990.

# Chapter 5

## Robustness

### Contents

---

5.1	Introduction . . . . .	175
5.2	Eigenstructure Assignment and Robustness . . . . .	177
5.3	An Outline of the Robustness Improvement Algorithm . . . . .	179
5.4	Robustness Measures . . . . .	180
5.5	Robustness Measure Gradient Functions . . . . .	198
5.6	Mitigation of Performance Degradation . . . . .	218
5.7	Further Work . . . . .	223
5.8	References . . . . .	226

---

This chapter gives the theoretical basis for a robustness improvement algorithm. The algorithm will improve robustness with respect to either a time domain or singular value based robustness measure. The algorithm employs a gradient based optimisation and analytic expressions for the gradients are derived. Some typical results can be found in Chapter 6.

### 5.1 Introduction

No mathematical system can precisely model a real system. There are always unpredictable inputs and dynamics that form a fundamental limit and in all practical models there will additional behaviour that is approximated or unmodelled [Pad96, p 90]. This means that even if the inputs of a system are known, the output can not be predicted exactly and is subject to some *uncertainty*.

Robustness refers to the ability of a system to tolerate uncertainty. Practical approaches to measuring and improving robustness require a description of the uncertainty and means of deciding if a system is tolerating or has been overcome by the uncertainty. Generally, stability is used as the deciding threshold and it is in the area of stability robustness where most of the useful theoretical results are concentrated. However, it is easy to imagine a situation where performance has degraded to an unacceptable level long before instability sets in. It is thus, in general, more desirable to achieve perform-

ance robustness. Unfortunately, the area of performance robustness is fundamentally more difficult and is consequently less well developed. The fundamental problem is that acceptable performance is; difficult to define, problem dependent and often, once defined, mathematically unsuitable for the development of a robustness theorem. This has hindered the development of a uniform approach to robust performance. However, results have been developed for some specific situations where acceptable performance can be defined by a norm bounded transfer function [PD93, SD91] or as an allowed region for the closed loop spectrum [YA94, YS91, Jua91, Yed93b].

The numerous sources of uncertainty that are present in a helicopter design model make robustness an important issue for helicopter flight control law design. Some of the significant sources of uncertainty are listed as follows:

1. The rotorcraft flight condition, this represents different trim conditions, altitudes, and other parameters associated with the Operational Flight Envelope (OFE). Generally, forward speed is the dominant uncertainty and therefore of most interest.
2. Sensor errors associated with measuring attitudes, rates, accelerations and speed. In fact at low air speeds, speed measurements are so inaccurate that they prohibit effective gain scheduling.
3. Linearisation of non-linearities. Most design will be based around linear models that have been extracted from full non-linear simulations. The linear model rapidly becomes invalid for moderate perturbations and manoeuvres away from trim.
4. The linear model is a time invariant representation of a time varying system. This especially true of the rotor dynamics, where the spinning rotor is represented by a static system.
5. Deliberate reduced order modelling. For convenience and simplicity a reduced order linear and/or non-linear simulation may be used during the design. These models may ignore such things as actuator dynamics, rotor-states, structural modes, etc.
6. Unmodelled dynamics. Even the most precise model will be unable to describe all the system dynamic behaviour, since the high frequency effects are often stochastic or depend on unmeasurable exogenous inputs. Furthermore, the negative phase introduced by these effects is insidious since it can destabilise.
7. The rotorcraft state represents uncertain inputs that will vary from flight to flight. For instance, the c.o.g positions, all-up weight, weather conditions, etc.
8. Controller implementation. Finite precision arithmetic and the computational delay associated with digital realisations of controllers introduce significant uncertainty.
9. Further uncertainty results from manufacturing variation, non-critical component failure, wear and aging.

The uncertainties above can be broadly divided into two groups: unmodelled dynamics and parameter variations. Parameter variations will cause the elements of the state space description to change in a structured way. Uncertainty in the state space description is called either state space parametric uncertainty or more succinctly time domain uncertainty [Yed85, SSA94].

For the following three independent and significant sources of time domain uncertainty some information about the structure can be extracted.

**Flight condition** By comparing state space models for different flight conditions, information about variations in the model and its subsequent eigenstructure can be extracted.

**Rotorcraft state** The stability and control derivatives of the state space model can be expressed as approximate equations derived using physical arguments and written in terms of physical quantities [Pro90]. Error tolerances can be associated with physical quantities and used to calculate a combined tolerance for the state space derivative.

**Linearisation Errors** The errors introduced by linearisation of a non-linear model can be estimated using the algorithm described in Section 2.3.

It is well established that time domain models are a suitable format for flight control problems and it is suggested that robustness should concentrate on time domain uncertainty. Time domain uncertainty forms a natural complement to the state space model, provides the same physical insight and the techniques described above can be used to extract valuable structural information. The drawback of time domain uncertainty is that it does not explicitly accommodate unmodelled dynamics which are an important source of uncertainty and should not be overlooked. However, in some cases robustness to unmodelled dynamics can be re-expressed as time domain uncertainty.

## 5.2 Eigenstructure Assignment and Robustness

Unlike other techniques such as the Linear Quadratic Regulator (LQR) [AM89] or  $\mathcal{H}_\infty$  control [Zam81], Eigenstructure Assignment has no explicit means of guaranteeing robustness margins. But Eigenstructure Assignment does provide access to all the available design freedom and may assign a robust solution as easily as a non-robust solution. It is therefore only required to provide a technique that will steer the assignment towards a robust solution and many such techniques have been developed.

Early techniques reduced the sensitivity of the eigenvalues to perturbations in the system matrix by orthogonalising the eigenvectors [Bur90, MP88, KND85], since Gilbert and Wilkinson show [Gil84, Wil65] that the system eigenvalues are most insensitive when eigenvectors are orthogonal. Strictly speaking these are not robustness techniques since they do not define a class of perturbation for which the system will remain stable or maintain some performance measure. However, some techniques do optimise the condition number of the modal matrix [KND85] and robustness

measures based on the condition number of the closed loop modal matrix have been developed [ND84, YA94, YL86a, SBY89b]. The orthogonalisation techniques also suffer the drawback that all the eigenvector design freedom is used to orthogonalise the eigenvectors with no consideration of how this affects the system response and especially decoupling. For this reason these techniques are best considered as numerically well-conditioned pole placement algorithms [GLLT90, see *place*].

Work on singular value sensitivities [CFL81] led to techniques that improve singular value based robustness measures [Gar89, MN84, NM85, SATC86, Web92]. These techniques assume that a nominal design has been generated. They attempt to improve the robustness of the design by calculating the gradient of the singular value robustness measure with respect to each design parameter. The design parameters are adjusted in a direction that improves the robustness measure. The principal difference between the algorithms is the choice of design parameters. Garg [Gar89] and Sjøgaard-Andersen *et al* [SATC86] assume the nominal design is generated using state feedback eigenstructure assignment and calculate gradients with respect to the desired eigenstructure and design vectors respectively. Mukhopadhyay and Newsom [MN84, NM85] calculate a gradient with respect to the gain elements of the nominal design. This work therefore makes no assumption about how the nominal design is produced and as a result the gradient functions are simpler. A key issue with these improvements techniques is maintaining performance while improving robustness. All the techniques address this problem by starting with a design that is optimised for performance then hoping that adequate robustness can be achieved before performance has degraded too far. In addition, the techniques of Garg [Gar89] and Sjøgaard-Andersen *et al* [SATC86] can be configured to adjust selected design parameters. These techniques also have the advantage that they adjust the parameters used in the original design. Hence the trade-off between performance and robustness is more visible. Robustness improvement techniques based on measures other than the maximum singular value have been developed [Apk88, Apk89, SYP<sup>+</sup>92].

An alternative to the improvement techniques are approaches that combine the robustness and performance goals in a single constrained optimisation [Muk87, PL94, Dav94, YPS91, YS91, WCY91]. These techniques do not generally use analytically derived gradient information since the cost and constraint functions are too complex to differentiate. As this suggests, the optimisation problems are often difficult and novel techniques such as Genetic Algorithms (GA) have been applied [PL94, Dav94]. Again, optimisation techniques based on measures other than the maximum singular value have been developed [YPS91, YS91, WCY91].

Although, the combined optimisation approaches go some way to addressing the problem of achieving robustness and performance goals simultaneously, they do so at the expense of visibility. The author believes the visibility offered by the improvement techniques make them preferable to the combined optimisation approach. Thus the work presented in the remainder of this chapter is a robustness improvement technique which has been developed by the author.

## 5.3 An Outline of the Robustness Improvement Algorithm

The author's robustness improvement algorithm starts with a controller solution that has been optimised for performance. This solution is expressed in terms of optimal eigenvalue locations and design vectors. The design vectors select the best achievable eigenvector directions from the allowed subspaces. Since the solution is optimal and generally unique, it is clear that any adjustment of the eigenvalues or design vectors will create a sub-optimal solution and consequently a degradation in performance. The robustness improvement algorithm will adjust eigenvalues and design vectors thus there is an inevitable trade-off between performance and robustness. The performance robustness trade-off is a common feature of many modern control techniques [IS90, SA87, Kwa93] and it is important that it is presented in a way that makes the trade-off clear to the design engineer.

The robustness improvement algorithm uses the same parameters as the original design; that is, the eigenvalues and design vectors. This is to make the performance robustness trade-off visible. At each step the algorithm selects an adjustment vector that is a compromise between robustness improvement and performance degradation. The algorithm is also constrained to keep the closed loop eigenvalues within specified regions and thereby maintain performance. The basic steps of the algorithm are listed as follows.

1. Produce initial optimal design.
2. Calculate the robustness measure for the current controller.
3. If the robustness measure is acceptable stop else continue.
4. Calculate the gradient of the robustness measure with respect to the design parameters.
5. Calculate the gradient of the performance measure with respect to the design parameters.
6. Select a compromise direction.
7. Perform a line search in the compromise direction to find a cost reduction step.
8. Re-calculate the controller with new design parameters.
9. Go to step 2.

The key features of the algorithm that distinguish it from previous attempts are as follows:

- It is an extension to output feedback eigenstructure assignment.
- It provides an explicit mechanism to maintain performance through the use of compromise directions.
- It uses novel robustness measures.

Before describing the algorithm in detail it is instructive to look at the robustness measures employed and their derivatives.



## 5.4 Robustness Measures

For comparison it was decided to implement the algorithm using two different robustness measures, a time domain measure and a maximum singular value based measure. Either measure would have to be evaluated at step two of the robustness improvement algorithm this would also require specifying an uncertainty structure. Several time domain measures were considered.

### 5.4.1 The Time Domain Robustness Measure

Lypaunov derived conditions [PTS77, PT80, Yed85, YL86b, Lee82, ZK87, KBH88] were rejected due to their conservatism and limited ability to handle structured perturbations. Polynomial derived conditions [GJ81, KBH88, Vic89, Yed93b] were also examined. They are reported to be conservative [Wis92] and cumbersome to calculate. Other less conventional robustness measures were also considered [ND84, TV90, Yed93a].

For the time domain robustness measure it was decided to use the Gronwall Lemma [Vid93, p. 236] derived condition presented by Yu *et al* [YPS91]. The decision was based on the following reasons:

- Published results [YPS91, SBY89a] show the measure to be less conservative than comparable measures [CW87].
- The measure is dependent on the closed loop eigenstructure in an obvious and intuitive way, which lends itself to differentiation.

Consider a nominal state space system ( $\mathbf{A}$ ,  $\mathbf{B}$ ,  $\mathbf{C}$ ) subject to continuous time varying uncertainties described by  $\Delta\mathbf{A}$  and  $\Delta\mathbf{B}$ .

$$\dot{\mathbf{x}}(t) = \mathbf{A}\mathbf{x}(t) + \Delta\mathbf{A}(t)\mathbf{x}(t) + \mathbf{B}\mathbf{u}(t) + \Delta\mathbf{B}\mathbf{u}(t) \quad (5.4.1)$$

$$\mathbf{y}(t) = \mathbf{C}\mathbf{x}(t) \quad (5.4.2)$$

Suppose the absolute value of the maximum variation is bounded by the matrices  $\mathbf{A}_M$  and  $\mathbf{B}_M$  on an element by element basis.

$$\text{abs}(\Delta\mathbf{A}(t)) \leq \mathbf{A}_M \quad (5.4.3)$$

$$\text{abs}(\Delta\mathbf{B}(t)) \leq \mathbf{B}_M \quad (5.4.4)$$

Consider, also an output feedback gain thus

$$\mathbf{u}(t) = \mathbf{K}\mathbf{y}(t) \quad (5.4.5)$$

**Theorem 5.4.1 Theorem 2 Yu *et al* [YPS91]**

Suppose that  $\mathbf{K}$  is such that the nominal closed loop system is stable with a non-defective modal matrix. Then, the uncertain closed loop system is stable for all  $\Delta\mathbf{A}$  and  $\Delta\mathbf{B}$  if,

$$\rho \left( \sum_{i=1}^n \frac{\text{abs}(\mathbf{v}_i \mathbf{w}_i)}{-\text{Re}(\lambda_i(\mathbf{A} + \mathbf{B}\mathbf{K}\mathbf{C})) \text{abs}(\mathbf{w}_i \mathbf{v}_i)} [\mathbf{A}_M + \mathbf{B}_M \text{abs}(\mathbf{K}\mathbf{C})] \right) < 1 \quad (5.4.6)$$

where  $\mathbf{w}_i$  and  $\mathbf{v}_i$  are the left and right closed loop eigenvectors associated with the closed loop eigenvalue  $\lambda_i$ .

◇◇

Equation (5.4.6) has not been reproduced exactly as stated by Yu *et al* [YPS91]. The additional term  $\text{abs}(\mathbf{w}_i \mathbf{v}_i)$  has been added to the denominator. In the original equation this term was omitted since it was tacitly assumed that the eigenvectors were scaled to satisfy  $\mathbf{w}_i \mathbf{v}_i = 1$ . With the following definitions:

$$\mathbf{ACL} = \mathbf{A} + \mathbf{B}\mathbf{K}\mathbf{C} \quad (5.4.7)$$

$$\mathbf{ABM} = \mathbf{A}_M + \mathbf{B}_M \text{abs}(\mathbf{K}\mathbf{C}) \quad (5.4.8)$$

$$\mathbf{V} = [\mathbf{v}_1, \dots, \mathbf{v}_n] \quad (5.4.9)$$

$$\mathbf{W}^T = [\mathbf{w}_1^T, \dots, \mathbf{w}_n^T] \quad (5.4.10)$$

$$\mathbf{\Lambda RE} = \text{diag} \left[ \frac{1}{-\text{Re}(\lambda_1(\mathbf{ACL})) \text{abs}(\mathbf{w}_1 \mathbf{v}_1)}, \dots, \frac{1}{-\text{Re}(\lambda_n(\mathbf{ACL})) \text{abs}(\mathbf{w}_n \mathbf{v}_n)} \right] \quad (5.4.11)$$

Equation (5.4.6) can be more succinctly expressed as:

$$\rho(\text{abs}(\mathbf{M}) \mathbf{\Lambda RE} \text{abs}(\mathbf{W}) \mathbf{ABM}) \leq 1 \quad (5.4.12)$$

Equation (5.4.6) repays closer examination but first some useful matrix properties are needed:

1. Suppose that  $\mathbf{X}$  is a square matrix with simple eigenvalues and that  $(\mathbf{w}_i, \mathbf{v}_i)$  are the left and right eigenvectors of  $\mathbf{X}$  associated with the eigenvalue  $\lambda_i$ . Then the first order sensitivity of the eigenvalue  $\lambda_i$  to perturbations in each element of  $\mathbf{X}$  may be expressed in matrix form as (Porter and Crossley [PC72, p. 22]):

$$\frac{\partial \lambda_i}{\partial \mathbf{A}} = \frac{(\mathbf{v}_i \mathbf{w}_i)^*}{\mathbf{w}_i \mathbf{v}_i} \quad (5.4.13)$$

Thus if nominal  $\mathbf{X}$  is subject to a perturbation such that  $\hat{\mathbf{X}} = \mathbf{X} + \mathbf{E}$  then a first order estimate of the deviation in  $\lambda_i$ , denoted  $\delta \lambda_i$ , is:

$$\delta \lambda_i = \frac{\mathbf{w}_i \mathbf{E} \mathbf{v}_i}{\mathbf{w}_i \mathbf{v}_i} \quad (5.4.14)$$

2. If  $\mathbf{X}$  and  $\mathbf{Y}$  are equal size square matrices composed of non-negative elements and satisfy

$$\mathbf{X} > \mathbf{Y} \geq \mathbf{0} \quad (5.4.15)$$

on an element by element basis. Then the Perron-Frobenius Theorem [Gra87, p. 121] for non-negative matrices shows:

$$\rho(\mathbf{X}) > \rho(\mathbf{Y}) \quad (5.4.16)$$

3. If  $\mathbf{X}$  and  $\mathbf{Y}$  are square matrices composed of non-negative elements then they satisfy the following spectral radius inequality

$$\rho(\mathbf{X}) + \rho(\mathbf{Y}) \geq \rho(\mathbf{X} + \mathbf{Y}) \quad (5.4.17)$$

The inequality can be proved using a straight forward application of *Rayleigh's principle* [Gra87, p. 121] as shown below, although the form below is adapted for the purposes of the proof:

$$\rho(\mathbf{X} + \mathbf{Y}) = \max_{\mathbf{x} \geq \mathbf{0}} \frac{\mathbf{x}^T (\mathbf{X} + \mathbf{Y}) \mathbf{x}}{\mathbf{x}^T \mathbf{x}} = \frac{\mathbf{x}_0^T (\mathbf{X} + \mathbf{Y}) \mathbf{x}_0}{\mathbf{x}_0^T \mathbf{x}_0} \quad (5.4.18)$$

Where  $\mathbf{x}$  is a column vector of appropriate length composed of non-negative elements. Further application of Rayleigh's principle shows:

$$\frac{\mathbf{x}_o^T \mathbf{X} \mathbf{x}_o}{\mathbf{x}_o^T \mathbf{x}_o} \leq \max_{\mathbf{x} \geq 0} \frac{\mathbf{x}^T \mathbf{X} \mathbf{x}}{\mathbf{x}^T \mathbf{x}} = \rho(\mathbf{X}) \quad (5.4.19)$$

$$\frac{\mathbf{x}_o^T \mathbf{Y} \mathbf{x}_o}{\mathbf{x}_o^T \mathbf{x}_o} \leq \max_{\mathbf{x} \geq 0} \frac{\mathbf{x}^T \mathbf{Y} \mathbf{x}}{\mathbf{x}^T \mathbf{x}} = \rho(\mathbf{Y}) \quad (5.4.20)$$

since  $\rho(\mathbf{X})$  and  $\rho(\mathbf{Y})$  are always non-negative, it follows that:

$$\rho(\mathbf{X}) + \rho(\mathbf{Y}) \geq \rho(\mathbf{X} + \mathbf{Y}) \quad (5.4.21)$$

Reference to Equation (5.4.13) shows that the robustness condition (Equation (5.4.6)) is intimately related to the eigenvalue sensitivity.

Matrix property two shows that increasing  $\text{Re}(\lambda_i(\mathbf{ACL}))$  will always improve the robustness measure. This result is intuitive since one would expect that moving the eigenvalues further from the unstable RHP would improve robustness.

Direct application of matrix property three to Equation (5.4.6) produces the following inequality:

$$\rho(\text{abs}(\mathbf{M}) \Delta_{\text{RE}} \text{abs}(\mathbf{W}) \mathbf{A}_{\text{BM}}) < \sum_{i=1}^n \rho \left( \frac{\text{abs}(\mathbf{v}_i \mathbf{w}_i)}{-\text{Re}(\lambda_i(\mathbf{ACL})) \text{abs}(\mathbf{w}_i \mathbf{v}_i)} \mathbf{A}_{\text{BM}} \right) \quad (5.4.22)$$

Which can be simplified by noting

$$\rho \left( \frac{\text{abs}(\mathbf{v}_i \mathbf{w}_i)}{-\text{Re}(\lambda_i(\mathbf{ACL})) \text{abs}(\mathbf{w}_i \mathbf{v}_i)} \mathbf{A}_{\text{BM}} \right) = \rho \left( \frac{\text{abs}(\mathbf{v}_i) \text{abs}(\mathbf{w}_i) \mathbf{A}_{\text{BM}}}{-\text{Re}(\lambda_i(\mathbf{ACL})) \text{abs}(\mathbf{w}_i \mathbf{v}_i)} \right) \quad (5.4.23)$$

$$= \frac{\text{abs}(\mathbf{w}_i) \mathbf{A}_{\text{BM}} \text{abs}(\mathbf{v}_i)}{-\text{Re}(\lambda_i(\mathbf{ACL})) \text{abs}(\mathbf{w}_i \mathbf{v}_i)} \quad (5.4.24)$$

the final inequality thus becomes:

$$\rho(\text{abs}(\mathbf{M}) \Delta_{\text{RE}} \text{abs}(\mathbf{W}) \mathbf{A}_{\text{BM}}) < \sum_{i=1}^n \frac{\left( \frac{\text{abs}(\mathbf{w}_i) \mathbf{A}_{\text{BM}} \text{abs}(\mathbf{v}_i)}{\text{abs}(\mathbf{w}_i \mathbf{v}_i)} \right)}{-\text{Re}(\lambda_i(\mathbf{ACL}))} \quad (5.4.25)$$

Comparison with Equation (5.4.14) shows that the numerator is closely related to the first order estimate of eigenvalue perturbation and may be considered a worst case eigenvalue deviation. The denominator can be interpreted as the the maximum eigenvalue deviation for which stability is guar-

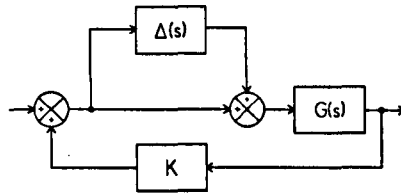


Figure 5.4.1: Input multiplicative uncertainty with constant output feedback

anteed. Thus if any summand is greater than unity, stability can not be guaranteed and the robustness test fails. The numerator is principally dependent on the closed loop eigenvectors and one might seek to improve robustness by decreasing it. This can be achieved by reducing  $\text{abs}(\mathbf{w}_i) \mathbf{A} \mathbf{B} \mathbf{M} \text{abs}(\mathbf{v}_i)$  or increasing  $\text{abs}(\mathbf{w}_i \mathbf{v}_i)$ . Reducing  $\text{abs}(\mathbf{w}_i) \mathbf{A} \mathbf{B} \mathbf{M} \text{abs}(\mathbf{v}_i)$  amounts to selecting eigenvector directions that reduce sensitivity to the given uncertainty structure. Increasing,  $\text{abs}(\mathbf{w}_i \mathbf{v}_i)$  requires making the left and right eigenvectors ( $\mathbf{w}_i$ ,  $\mathbf{v}_i$ ) more co-linear which, if possible, would ultimately lead to the solution of the eigenvalue insensitivity problem that is orthogonal eigenvectors or equivalently unitary  $\mathbf{V}$  and  $\mathbf{W}$ .

Equation (5.4.25) is useful beyond its illustrative properties, since in practice it is a fair approximation of the robustness measure. Examination of the individual summands indicates which parts of the eigenstructure form the dominant contribution to the robustness measure. The individual terms, being much simpler than the original robustness measure, are more easily adjusted to improve robustness.

## 5.4.2 The Singular Value Robustness Measure

Singular value robustness measures are an important part of modern control theory. They refer to techniques where the model uncertainty ( $\Delta(s)$ ) is represented by an unknown transfer function matrix. The techniques calculate the maximum norm that the uncertainty transfer function may realise while still guaranteeing stability. The matrix norm used is, generally, the spectral or Hilbert norm which is equal to the maximum singular value.

Before looking at the details of the robustness measures used in this work it worth outlining some background on singular value robustness tests.

The first step in using a singular value uncertainty bound is to produce an uncertainty representation. An engineer should choose a representation that most accurately accommodates the model error information that is available. For instance, if it is known that the actuators of a plant introduce considerable delay and non-linearity then input multiplicative uncertainty may be considered most appropriate. Some common uncertainty representations are shown in Table 5.4.1.

To assess the impact of the uncertainty on the closed loop system the open loop uncertainty representation must be combined with an appropriate controller structure. For instance, an input multiplicative representation may be combined with a constant output feedback gain as shown in Figure 5.4.1.

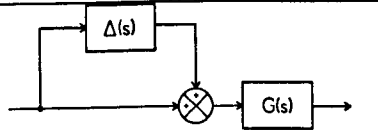
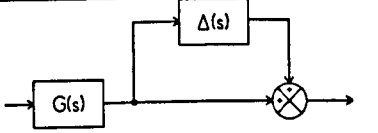
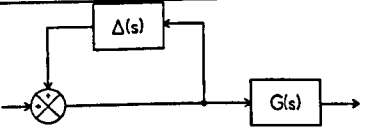
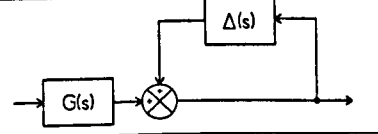
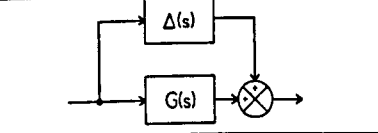
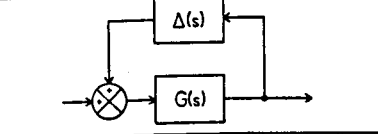
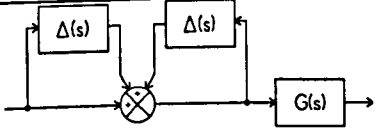
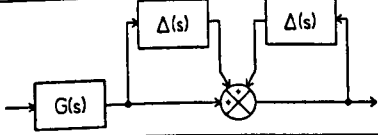
Block representation	Mathematical representation
<b>Input Multiplicative</b>	
	$G(s) = G_o(s)[I + \Delta(s)]$
<b>Output Multiplicative</b>	
	$G(s) = [I + \Delta(s)]G_o(s)$
<b>Input Inverse Multiplicative</b>	
	$G(s) = G_o(s)[I + \Delta(s)]^{-1}$
<b>Output Inverse Multiplicative</b>	
	$G(s) = [I + \Delta(s)]^{-1}G_o(s)$
<b>Feedforward Additive</b>	
	$G(s) = \Delta(s) + G_o(s)$
<b>Feedback Additive</b>	
	$G(s) = G_o(s)[I - \Delta(s)G_o(s)]^{-1}$
<b>Input Bilinear</b>	
	$G(s) = G_o(s)[I - \Delta(s)]^{-1}[I + \Delta(s)]$
<b>Output Bilinear</b>	
	$G(s) = [I - \Delta]^{-1}[I + \Delta]G_o(s)$

Table 5.4.1: Common open loop uncertainty representations

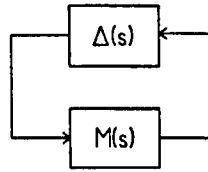


Figure 5.4.2: The general single loop structure.

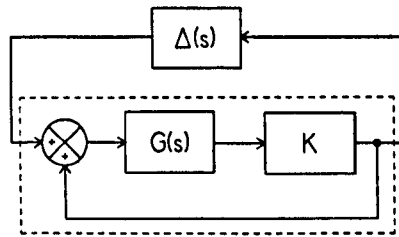


Figure 5.4.3: Single loop structure for input multiplicative uncertainty.

All the uncertainty representations and linear controller structures can be expressed as a single loop structure [Mac89, p. 102], where the uncertainty ( $\Delta(s)$ ) acts as feedback on a single closed loop transfer function ( $M(s)$ ) as illustrated by Figure 5.4.2. It is also possible to represent time domain uncertainty using the same single loop approach [PD89, PD93].

The previous example is no exception and may be converted into a single loop as shown in Figure 5.4.3. In this case the closed loop transfer function ( $M(s) = KG(s)[I + KG(s)]^{-1}$ ) is recognised as the Complementary Sensitivity function. It is often the case that the closed loop transfer function has classical significance [DS81, CFL81, SLH81] and the experience from classical SISO techniques [Bod47, FPEN91] can be brought to bear by using the maximum singular value as a generalisation of vector gain [MSJ79] to the scalar case.

Table 5.4.2 shows the single loop transfer function for each uncertainty representation of Table 5.4.1 while assuming a constant output feedback gain ( $K$ ). The state space representation for the transfer function is also given. In practice, this is the more important form.

In general, the state space and transfer function can be derived by progressively applying simple rules for system interconnection [Mac89, p. 371] [Dai91, p. 15]. Software packages that automate this process have been developed [BPDG93]. However, the user should be aware that finite precision calculations can cause these software packages to accumulate unobservable and uncontrollable dynamics.

Once the single loop structure has been derived then the Multivariable Nyquist Criterion [DW80, MP77] can be used to bound the maximum norm of the uncertainty  $\Delta(s)$  such that the loop is guaranteed to maintain stability.

Transfer function	State space
Input Multiplicative	
$M(s) = \frac{KG(s)[I - KG(s)]^{-1}}{[I - KG(s)]^{-1}KG(s)}$	$\left[ \begin{array}{c c} A + BKC & B \\ \hline KC & 0 \end{array} \right]$
Output Multiplicative	
$M(s) = \frac{G(s)K[I - G(s)K]^{-1}}{[I - G(s)K]^{-1}G(s)K}$	$\left[ \begin{array}{c c} A + BKC & BK \\ \hline C & 0 \end{array} \right]$
Input Inverse Multiplicative	
$M(s) = \frac{[I - KG(s)]^{-1}}{I - KG(s)[I - KG(s)]^{-1}}$	$\left[ \begin{array}{c c} A + BKC & B \\ \hline KC & I \end{array} \right]$
Output Inverse Multiplicative	
$M(s) = \frac{[I - G(s)K]^{-1}}{I - G(s)K[I - G(s)K]^{-1}}$	$\left[ \begin{array}{c c} A + BKC & BK \\ \hline C & I \end{array} \right]$
Feedforward Additive	
$M(s) = \frac{K[I - G(s)K]^{-1}}{[I - KG(s)]K^{-1}}$	$\left[ \begin{array}{c c} A + BKC & BK \\ \hline KC & K \end{array} \right]$
Feedback Additive	
$M(s) = \frac{G(s)[I - KG(s)]^{-1}}{[I - G(s)K]^{-1}G(s)}$	$\left[ \begin{array}{c c} A + BKC & B \\ \hline C & 0 \end{array} \right]$
Input Bilinear	
$M(s) = \frac{[I + KG(s)][I - KG(s)]^{-1}}{[I - KG(s)]^{-1}[I + KG(s)]}$	$\left[ \begin{array}{c c} A + BKC & B \\ \hline 2KC & I \end{array} \right]$
Output Bilinear	
$M(s) = \frac{[I + G(s)K][I - G(s)K]^{-1}}{[I - G(s)K]^{-1}[I + G(s)K]}$	$\left[ \begin{array}{c c} A + BKC & BK \\ \hline 2C & I \end{array} \right]$

Table 5.4.2: Single loop transfer functions for some uncertainty representations



**Theorem 5.4.2 Theorem L1 [DW80]**

The single loop structure of Figure 5.4.2 is stable if and only if

1.  $\det [\mathbf{I} - \Delta(\infty)\mathbf{M}(\infty)] \neq 0$ .
2. The image of  $\det [\mathbf{I} - \Delta(s)\mathbf{M}(s)]$  on the complex plane as 's' traverses the Nyquist Contour encircles the origin  $P_o$  times. Where  $P_o$  is the number of right hand-plane (RHP) poles of  $\Delta(s)\mathbf{M}(s)$ .

◇◇

Theorem 5.4.2 can be developed further by using the relationship between the determinant of a matrix and the product of its eigenvalues, ultimately this idea leads to the Characteristic-locus Method [Mac89, p. 142].

The proof of the Theorem 5.4.2 hinges on the fact that the determinant of the return difference matrix is equal to the ratio of the closed ( $\phi_{cl}(s)$ ) and open ( $\phi_{ol}(s)$ ) loop characteristic polynomials.

$$\det (\mathbf{I} - \Delta(s)\mathbf{M}(s)) = \frac{\phi_{cl}(s)}{\phi_{ol}(s)} \quad (5.4.26)$$

The useful identity of Equation (5.4.26) is easily proved when polynomial matrix fraction descriptions (MFDs) are applied. Let  $\mathbf{N}(s)\mathbf{D}(s)^{-1}$  be a right coprime matrix fraction description of the transfer function product  $\Delta(s)\mathbf{M}(s)$ , then the loop transfer function ( $[\mathbf{I} - \Delta(s)\mathbf{M}(s)]^{-1}$ ) may be expressed as:

$$[\mathbf{I} - \Delta(s)\mathbf{M}(s)]^{-1} = [\mathbf{I} - \mathbf{N}(s)\mathbf{D}(s)^{-1}]^{-1} \quad (5.4.27)$$

$$= \mathbf{D}(s) [\mathbf{D}(s) - \mathbf{N}(s)]^{-1} \quad (5.4.28)$$

Since  $\mathbf{N}(s)$  and  $\mathbf{D}(s)$  are coprime it follows that  $\mathbf{D}(s)$  and  $[\mathbf{D}(s) - \mathbf{N}(s)]$  are also coprime [Mac89, p. 57], [DW80]. Thus  $\det (\mathbf{D}(s) - \mathbf{N}(s))$  is the closed loop characteristic polynomial [Mac89, p. 50], [Kai80, p. 447] and, equally,  $\det (\mathbf{D}(s))$  is the open loop characteristic polynomial.

$$\det [\mathbf{I} - \Delta(s)\mathbf{M}(s)] = \frac{\det [\mathbf{D}(s) - \mathbf{N}(s)]}{\det [\mathbf{D}(s)]} = \frac{\phi_{cl}(s)}{\phi_{ol}(s)} \quad (5.4.29)$$

The Multivariable Nyquist Criterion is necessary and sufficient for internal stability [Mac89, p. 56], [DFT92, p. 36], [GL, p. 39]; that is, all bounded inputs not only promote bounded outputs but also bounded internal signals.

Derivation of an upper limit on the norm bounded uncertainty proceeds by assuming that  $\Delta(s)\mathbf{M}(s)$

is stable. This is justified as follows:

1. Stabilisation is often a purpose of feedback. Hence the nominal transfer function  $M(s)$  will be stable.
2. It is unlikely the unmodelled dynamics represented by the uncertainty  $\Delta(s)$  are unstable for if they were, their divergent behaviour would dominate the system response and dominant dynamics should be included in the nominal model.

With the stability assumption in place, it clear that the characteristic locus of the nominal system, subject to no uncertainty, makes zero encirclements of the origin. As the size of the uncertainty (in a norm-bounded sense) is increased, in general, the potential for instability will increase until the system becomes unstable. At the transition between stability and instability the system will have poles on the  $j\omega$  axis and the characteristic locus will pass through the origin. Mathematically the transition point implies:

$$\det(\mathbf{I} - \Delta(s)M(s)) = 0 \quad \text{for some } s = j\omega \quad (5.4.30)$$

Thus if the uncertainty  $\Delta(s)$  is norm bounded such that Equation (5.4.30) is never satisfied then stability is guaranteed. The following well known matrix property achieves this:

Let  $\mathbf{X}$  be non-singular and  $\mathbf{Y}$  be an equal size arbitrary matrix. Then:

$$\underline{\sigma}(\mathbf{X}) > \bar{\sigma}(\mathbf{Y}) \quad (5.4.31)$$

implies that  $\mathbf{X} + \mathbf{Y}$  is non-singular [GL, p. 34], [LCL+81, Wis92] or:

$$\det(\mathbf{X} + \mathbf{Y}) \neq 0 \quad (5.4.32)$$

Thus, referring to Equation (5.4.30), stability is guaranteed if:

$$\underline{\sigma}(\mathbf{I}) > \bar{\sigma}(\Delta(s)M(s)) \quad (5.4.33)$$

$$1 > \bar{\sigma}(\Delta(s)M(s)) \quad \text{for all } s = j\omega \quad (5.4.34)$$

Using sub-multiplicative property shared by all induced norms [GL, p. 33] the singular value inequality may be more usefully expressed as follows:

$$1 > \bar{\sigma}(\Delta(s)) \bar{\sigma}(M(s)) \quad \text{for all } s = j\omega \quad (5.4.35)$$

$$\frac{1}{\bar{\sigma}(M(s))} > \bar{\sigma}(\Delta(s)) \quad \text{for all } s = j\omega \quad (5.4.36)$$

It is also possible to use the Small Gain Theorem [GL, p. 98], [Dai91, p. 47]. This leads to a more general normed space operator approach where norms other than the maximum singular value may be applied [Saf82].

Although, singular value bounds are useful, to practising engineers they are often seen as abstract quantities that lack engineering 'feel'. Many researchers address this problem by using the induced norm property of the maximum singular value [GL83, p. 449]. This enables the maximum singular value to be interpreted as a worst case vector gain [MSJ79] or in physical terms, as the worst case energy amplification [Moo81]. The concept of a frequency dependent vector gain leads to the term 'principal gains' [KP82, PEM81] and a generalisation of SISO frequency domain concepts [Bod47, FPEN91] such as loop shaping to the MIMO case [Mac89, DS81].

Despite this engineering interpretation of singular values, an alternative bound based on insightful and familiar engineering concepts is desirable [BDG94]. The Multivariable Gain and Phase Margins [Dai91, SGLL81, PEM81, SA77, LSA81, SLH81] are such a measure and defined as follows:

**The MIMO Gain Margin (GM)** If each channel of a MIMO system is simultaneously subject to a gain variation of the form  $r$ , then the GM is the real interval  $[G_L, G_U]$  such that the system remains stable for all gain variations satisfying  $G_L \leq r \leq G_U$ . MIMO gain margins are not unique.

**A MIMO Phase Margin (PM)** is the largest interval of phase change  $[-\theta, \theta]$  simultaneously permitted in each channel such that the system will remain stable. The MIMO phase margin is unique.

The MIMO gain and phase margin differ from their SISO counterparts in some important ways. Firstly they bound simultaneous and uncorrelated perturbation in all specified channels. Secondly, both margins may be defined with respect to channels at the input, output or any other point in the feedback loop, and the margins will, in general, vary for each location in the loop. This is not surprising since there is no physical reason why tolerable gain and phase error should be the same at the sensors and actuators.

Exact calculation of the MIMO gain and phase margins is a hard problem which is often described as a 'real  $\mu$  problem'. Fortunately, the more amenable singular values bounds can be used to calculate conservative estimates of the MIMO gain and phase margin. In one way these estimate may be considered superior to the precise gain and phase margins. While MIMO gain and phase margins do consider simultaneous perturbation in multiple channels they are, however, restricted to perturba-

tion of pure gain or phase. The singular value estimates do, as an inherent part of their conservatism, accommodate simultaneous perturbations that are a combination of gain and phase.

To calculate the MIMO gain and phase margins using singular values, we suppose that a perturbation of the form:

$$\mathbf{H} = \text{diag} (r_1 e^{j\phi_1}, \dots, r_k e^{j\phi_k}) \quad (5.4.37)$$

has been inserted into the feedback loop at the relevant point. For instance at the plant input:

$$\mathbf{G}(s) = \mathbf{G}_o(s)\mathbf{H} \quad (5.4.38)$$

Where  $\mathbf{G}_o(s)$  is a nominal plant model,  $\mathbf{H}$  represents uncertainty at the input and  $\mathbf{G}(s)$  is a model of the actual plant.

The gain margin dictates that the system is stable for  $G_L \leq r_i \leq G_U$ ,  $\phi_i = 0$  and the phase margin dictates the system is stable for  $\theta \geq \phi_i \geq -\theta$ ,  $r_i = 1$ . The multiplicative and bilinear uncertainty representations of Table 5.4.1 may also be considered as perturbations that have been inserted in the feedback loop. However, the uncertainty represented using  $\mathbf{H}$  is a subset of that portrayed by  $\Delta$ . This is because  $\mathbf{H}$  is diagonal and does not represent any channel cross-feeds, while on the other hand,  $\Delta$  is full matrix that may adopt any structure and thus encompasses all possible channel cross-feeds. Gain and phase margin estimates based on uncertainty representations using  $\Delta$  are conservative. This is partly, because of their inability to portray the structure of  $\mathbf{H}$  which leads to consideration of a larger class of uncertainty than is required. The gain and phase margins are derived by accepting the conservatism described above and supposing that the plant is equivalently represented using the  $\Delta(s)$  and  $\mathbf{H}$  uncertainty matrices. The simple structure of  $\mathbf{H}$  then allows a bound on  $\bar{\sigma}(\Delta(s))$  to be converted into a bound on  $r_i$  and  $\phi_i$ . For instance, suppose  $\mathbf{H}$  is inserted at the input and the bound for input multiplicative uncertainty is applied, then assuming equivalent representations:

$$\mathbf{G}_o(s)[\mathbf{I} + \Delta(s)] = \mathbf{G}_o(s)\mathbf{H} \quad (5.4.39)$$

thus,

$$\bar{\sigma}(\Delta(s)) = \bar{\sigma}(\mathbf{H} - \mathbf{I}) \quad (5.4.40)$$

and since  $\mathbf{H}$  is diagonal:

$$\bar{\sigma}(\Delta(s)) = \max_{i=1..k} \{ \text{abs}(r_i e^{j\phi_i} - 1) \} \quad (5.4.41)$$

$$\bar{\sigma}(\Delta(s)) = \max_{i=1..k} \left\{ \sqrt{1 - 2r_i \cos(\phi_i) + r_i^2} \right\} \quad (5.4.42)$$

Thus to calculate the gain margin,  $\phi_i$  is assumed to equal zero, and from Equation (5.4.36) stability is maintained if:

$$\frac{1}{\bar{\sigma}(\mathbf{M}(s))} > \bar{\sigma}(\Delta(s)) \quad (5.4.43)$$

$$\frac{1}{\bar{\sigma}(\mathbf{M}(s))} > \max_{i=1..k} \left\{ \sqrt{(r_i - 1)^2} \right\} \quad (5.4.44)$$

$$\frac{1}{\bar{\sigma}(\mathbf{M}(s))} > \{r_i - 1, 1 - r_i\} \quad \text{for all } i = 1..k \quad (5.4.45)$$

Or equivalently:

$$1 - \frac{1}{\bar{\sigma}(\mathbf{M}(s))} < r_i < 1 + \frac{1}{\bar{\sigma}(\mathbf{M}(s))} \quad \text{for all } i = 1..k, s = j\omega \quad (5.4.46)$$

To calculate a bound on the phase margin we assume  $r_i = 1$  and stability is maintained if:

$$\frac{1}{\bar{\sigma}(\mathbf{M}(s))} > \max_{i=1..k} \left\{ \sqrt{2 - 2 \cos(\phi_i)} \right\} \quad (5.4.47)$$

$$\frac{1}{\bar{\sigma}(\mathbf{M}(s))} > \max_{i=1..k} \left\{ \sqrt{4 \sin^2\left(\frac{\phi_i}{2}\right)} \right\} \quad (5.4.48)$$

$$\frac{1}{\bar{\sigma}(\mathbf{M}(s))} > \left\{ 2 \sin\left(\frac{\phi_i}{2}\right), -2 \sin\left(\frac{\phi_i}{2}\right) \right\} \quad (5.4.49)$$

and it follows:

$$2 \sin^{-1} \left( \frac{1}{2\bar{\sigma}(\mathbf{M}(s))} \right) > \phi_i > -2 \sin^{-1} \left( \frac{1}{2\bar{\sigma}(\mathbf{M}(s))} \right) \quad \text{for all } i = 1..k, s = j\omega \quad (5.4.50)$$

Thus, in this case, the gain and phase margins are both dictated by the minimum of:

General formula	Gain margin	Phase margin
Multiplicative Input or Output		
$t > \sqrt{1 - 2r_i \cos(\phi_i) + r_i^2}$	$1 - t < r_i < 1 + t$	$-2 \sin^{-1}(\frac{t}{2}) < \phi_i < 2 \sin^{-1}(\frac{t}{2})$
Inverse Multiplicative Input or Output		
$t > \sqrt{1 - 2\frac{1}{r_i} \cos(\phi_i) + \frac{1}{r_i^2}}$	$\frac{1}{1-t} > r_i > \frac{1}{1+t}$	$-2 \sin^{-1}(\frac{t}{2}) < \phi_i < 2 \sin^{-1}(\frac{t}{2})$
Bilinear Multiplicative Input or Output		
$t > \sqrt{\frac{1-2r_i \cos(\phi_i)+r_i^2}{1+2r_i \cos(\phi_i)+r_i^2}}$	$\frac{1+t}{1-t} > r_i > \frac{1-t}{1+t}$	$-2 \tan^{-1}(t) < \phi_i < 2 \tan^{-1}(t)$

$t = \frac{1}{\sup_{s=j\omega} \bar{\sigma}(M(s))}$  where  $M(s)$  is the appropriate transfer function from Table 5.4.2.

Table 5.4.3: Gain and phase margins for the uncertainty representations of Table 5.4.1

$$\frac{1}{\|M(s)\|_\infty} = \min_{s=j\omega} \frac{1}{\bar{\sigma}(M(s))} \tag{5.4.51}$$

which can be expressed as the reciprocal of a  $\mathcal{H}_\infty$  norm. This minimum value can be used in conjunction with Equation (5.4.42) to calculate margins for combined gain and phase variation.

The same derivation of gain and phase margin can be applied to the inverse multiplicative and bilinear uncertainty representations and Table 5.4.3 summarises the results for these cases.

The singular value bounds assume a single full uncertainty block of complex values. The derivation of the gain and phase margins demonstrated that this can introduce conservatism when the uncertainty has an alternative structure such as diagonal. Unfortunately, structured uncertainty is common. For instance, if more than one uncertainty block is considered then the single loop representation of the system produces a single uncertainty matrix with a block diagonal structure.

The structured singular value ( $\mu$ ) [Doy82, SD91, PD89, PD93] is an extension to the conventional singular value bounds that addresses the problem of structured uncertainty. The structured singular value is defined as follows [PD93, Defn 3.1]:

Let  $M \in \mathbb{C}^{n \times n}$ , and let  $\Delta A$  be set of all matrices that have the prescribed block diagonal structure

$$\Delta A = \{\text{diag}[\delta_1 \mathbf{I}, \dots, \delta_k \mathbf{I}, \Delta_1, \dots, \Delta_h] : \delta_i, \Delta_i \in \mathbb{C}\} \tag{5.4.52}$$

The  $\delta_i \mathbf{I}$  matrices are called a repeated scalar blocks and each  $\mathbf{I}$  may be of arbitrary size. The  $\Delta_i$  matrices are called full blocks. Again, they may be of arbitrary size.

$$\frac{1}{\mu(\mathbf{M})} = \min \{ \bar{\sigma}(\Delta) : \Delta \in \Delta_{\mathbf{A}}, \det(\mathbf{I} - \mathbf{M}\Delta) = 0 \} \quad (5.4.53)$$

Unless no  $\Delta \in \Delta_{\mathbf{A}}$  makes  $\mathbf{I} - \Delta\mathbf{M}$  singular, in which case  $\mu(\mathbf{M}) = 0$

For a frequency  $s = j\omega$  the structured singular value defines the smallest matrix (in term of its maximum singular value), with a specified structure that destabilises the  $\mathbf{M}(s)\Delta(s)$  single loop system. Repeated scalar and full blocks arise naturally when a system with multiple uncertainties is transformed into a single loop system. The repeated scalar blocks represent a single uncertainty variable that affects the system at more than one point and full blocks are simply MIMO uncertainty blocks associated with MIMO system blocks.

In Equation (5.4.52) the SSV is defined as a reciprocal; this may seem unnecessarily convoluted. However, it provides a measure that is consistent with the singular value bounds and allows  $\mu(\mathbf{M})$  to be used in an analogous manner to both  $\bar{\sigma}(\mathbf{M})$  and  $\rho(\mathbf{M})$ . The SSV defines a potentially useful robustness measure, however, to be of practical value an efficient means of calculating  $\mu$  must be available.

Unfortunately, exact computation of the SSV for general block diagonal uncertainty structures can not be achieved in polynomial time [BYDM94]. However, for practical purposes the SSV can be acceptably approximated by optimising upper and lower bounds. Consider two special cases for the uncertainty structure:

1. If  $\Delta = \{\delta\mathbf{I} : \delta \in \mathbb{C}\}$  then  $\mu(\mathbf{M}) = \rho(\mathbf{M})$ . This follows almost directly from the definition of eigenvalues.  $\det[\frac{1}{\delta}\mathbf{I} + \mathbf{M}] = 0 \Rightarrow \frac{1}{\delta} = -\lambda_i(\mathbf{M})$ . For a general uncertainty structure  $(\Delta_{\mathbf{A}})$ ,  $\delta\mathbf{I}$  will describe a subset of the uncertainty and thus  $\rho(\mathbf{M})$  is an optimistic estimate of  $\mu(\mathbf{M})$  or a lower bound.
2. If  $\Delta = \mathbb{C}^{n \times n}$  then  $\mu(\mathbf{M}) = \bar{\sigma}(\mathbf{M})$ . In this case the structure of  $\Delta_{\mathbf{A}}$  has been ignored and result simply reverts back to the unstructured case. Since  $\mathbb{C}^{n \times n}$  is a superset of the general uncertainty structure  $(\Delta_{\mathbf{A}})$ , thus  $\bar{\sigma}(\mathbf{M})$  is a pessimistic estimate of  $\mu(\mathbf{M})$  or an upper bound.

Thus the SSV is bounded as follows:

$$\rho(\mathbf{M}) \leq \mu(\mathbf{M}) \leq \bar{\sigma}(\mathbf{M}) \quad (5.4.54)$$

An estimate of the SSV is calculated by applying transformations that do not affect  $\mu(\mathbf{M})$ , but tighten the upper and lower bounds. When the difference between the upper and lower bounds is sufficiently small then either bound can be used as an acceptable approximation to  $\mu(\mathbf{M})$ , however, generally the upper bound is used since this is a safe over estimate.

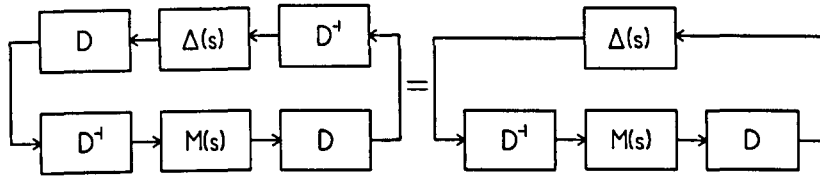


Figure 5.4.4: Equivalent transformed single loop systems.

If  $\mathbf{D}$  is a non-singular diagonal scaling matrix that satisfies  $\mathbf{D}\Delta\mathbf{D}^{-1} = \Delta$  then Figure 5.4.4 illustrates that:

$$\mu(\mathbf{M}) = \mu(\mathbf{DMD}^{-1}) \quad (5.4.55)$$

The  $\mathbf{D}$  scaling may be viewed as a structured similarity transform thus it will affect the upper bound of Equation (5.4.54) but not the lower bound.

Let  $\mathbf{U}$  be a unitary matrix, that is  $\mathbf{U}\mathbf{U}^* = \mathbf{I}$  then the 2-norm preserving property dictates that:

$$\bar{\sigma}(\mathbf{U}\Delta) = \bar{\sigma}(\Delta) \quad (5.4.56)$$

From Equation (5.4.56) and the definition of the SSV:

$$\mu(\mathbf{M}) = \mu(\mathbf{UM}) = \mu(\mathbf{MU}) \quad (5.4.57)$$

Clearly, the norm preserving property of the unitary transform means that it will not affect the upper bound of Equation (5.4.54) but will affect the lower bound. Optimisation of  $\mathbf{U}$  and  $\mathbf{D}$  leads to the following tighter bounds for the SSV:

$$\max_{\mathbf{U}} \rho(\mathbf{UM}) \leq \mu(\mathbf{M}) \leq \inf_{\mathbf{D}} \bar{\sigma}(\mathbf{DMD}^{-1}) \quad (5.4.58)$$

Doyle [Doy82] has shown that the lower bound is an equality:

$$\max \rho(\mathbf{UM}) = \mu(\mathbf{M}) \quad (5.4.59)$$



and that the upper bound is also an equality for three or less blocks. Unfortunately the lower bound is a non-convex optimisation and thus local minima may lead to false estimates of  $\mu$ . On the other hand, the upper bound, is a convex optimisation but for large block problems it may produce a conservative estimate. Practical algorithms for optimising both bounds have been developed [PD89, PD93, BPDG93, FTD91].

The singular value robustness measure used in this work is the SSV upper bound ( $\bar{\sigma}(\mathbf{DMD}^{-1})$ ). This measure is a logical extension to the conventional singular value measures used in previous improvement algorithms [Gar89, MN84, NM85, SATC86, Web92]. However, by exploiting the benefits of the SSV this algorithm can better deal with structured uncertainty. The focus of this work is the improvement of MIMO gain and phase margins which by definition have a diagonal structure. Thus an upper bound on  $\mu$  as an appropriate measure.

The structured singular value can also accommodate time domain uncertainty. Suppose that each element of the system ( $\mathbf{A}$ ) and input ( $\mathbf{B}$ ) matrices is subject to time domain uncertainty. Then the error matrices ( $\Delta\mathbf{A}$ ,  $\Delta\mathbf{B}$ ) of Equation (5.4.1) may be expressed as follows:

$$\Delta\mathbf{A} = \mathbf{L}_A \text{diag}(\delta a_{11}, \delta a_{12}, \dots, \delta a_{nn}) \mathbf{R}_A \quad (5.4.60)$$

$$\Delta\mathbf{B} = \mathbf{L}_B \text{diag}(\delta b_{11}, \delta b_{12}, \dots, \delta b_{nm}) \mathbf{R}_B \quad (5.4.61)$$

For brevity let us assume the system is third order ( $n = 3$ ) with two inputs ( $m = 2$ ), in which case  $\mathbf{L}_A$  and  $\mathbf{R}_A$  have the following structure:

$$\mathbf{L}_A = \begin{bmatrix} 1 & 1 & 1 & 0 & 0 & 0 & 0 & 0 & 0 \\ 0 & 0 & 0 & 1 & 1 & 1 & 0 & 0 & 0 \\ 0 & 0 & 0 & 0 & 0 & 0 & 1 & 1 & 1 \end{bmatrix} \quad (5.4.62)$$

$$\mathbf{R}_A^T = \begin{bmatrix} w_{11} & 0 & 0 & w_{21} & 0 & 0 & w_{31} & 0 & 0 \\ 0 & w_{12} & 0 & 0 & w_{22} & 0 & 0 & w_{32} & 0 \\ 0 & 0 & w_{13} & 0 & 0 & w_{23} & 0 & 0 & w_{33} \end{bmatrix} \quad (5.4.63)$$

The terms  $w_{ij}$  scale the uncertainty on individual elements of the system matrix. An analogous pair of matrices can be constructed to form  $\mathbf{L}_B$  and  $\mathbf{R}_B$ . Let us assume that the system has outputs  $\mathbf{y}$  given by:

$$\mathbf{y} = \mathbf{C}\mathbf{x} \quad (5.4.64)$$

where, for brevity, the output matrix ( $\mathbf{C}$ ) is not subject to uncertainty. The open loop system is:

$$\left[ \begin{array}{c|cc} \mathbf{A} & \mathbf{B} & \mathbf{L}_A & \mathbf{L}_B \\ \hline \mathbf{C} & \mathbf{0} & \mathbf{0} & \mathbf{0} \\ \mathbf{R}_A & \mathbf{0} & \mathbf{0} & \mathbf{0} \\ \mathbf{0} & \mathbf{R}_B & \mathbf{0} & \mathbf{0} \end{array} \right] \quad (5.4.65)$$

Applying a feedback law  $\mathbf{u} = \mathbf{K}\mathbf{y}$  the single loop system ( $\mathbf{M}(s)$ ) becomes:

$$\left[ \begin{array}{c|cc} \mathbf{A} + \mathbf{B}\mathbf{K}\mathbf{C} & \mathbf{L}_A & \mathbf{L}_B \\ \hline \mathbf{R}_A & \mathbf{0} & \mathbf{0} \\ \mathbf{R}_B \mathbf{K}\mathbf{C} & \mathbf{0} & \mathbf{0} \end{array} \right] \quad (5.4.66)$$

The structure of  $\mathbf{L}_A$ ,  $\mathbf{L}_B$  and  $\mathbf{R}_A$ ,  $\mathbf{R}_B$  is easily extended to accommodate systems of arbitrary size systems, the approach can also handle uncertainty in the output ( $\mathbf{C}$ ) and feed-through ( $\mathbf{D}$ ) matrices. A more detailed treatment can be found in [PD89] which also considers correlated perturbations to the system matrix elements. It should be noted that since the matrices of the state space representation contain only real elements, an accurate estimate of the robustness requires the solution of a real- $\mu$  problem.

Robustness to either time domain uncertainty or unmodelled dynamics reduces to calculating  $\mu$  for the appropriated single loop system. It may occur that a time domain and unmodelled dynamics problem yield identical single loop systems and are thus equivalent in the context of  $\mu$ -analysis. Input and output multiplicative uncertainty is an example of such an equivalence. Comparison with Table 5.4.2 shows that if:

$$\mathbf{L}_A = \mathbf{B} \quad (5.4.67)$$

$$\mathbf{R}_A = \mathbf{K}\mathbf{C} \quad (5.4.68)$$

then input multiplicative uncertainty may be equivalently expressed as time domain uncertainty. Suppose that the feedback ( $\mathbf{K}$ ) and input ( $\mathbf{B}$ ) matrices are decompose, as follows:

$$\mathbf{B} = [\mathbf{b}_1, \dots, \mathbf{b}_r] \quad (5.4.69)$$

$$\mathbf{K}^T = [\mathbf{k}_1, \dots, \mathbf{k}_r] \quad (5.4.70)$$

$$(5.4.71)$$

Then an equivalent system error matrix is:

$$\Delta \mathbf{A} = \sum_{i=1}^r \delta_i \mathbf{b}_i \mathbf{k}_i \mathbf{C} \quad (5.4.72)$$

However, to accommodate unmodelled dynamics  $\delta_i$  must be allowed to be complex.

## 5.5 Robustness Measure Gradient Functions

Principally, the robustness improvement algorithm is a specialised optimisation algorithm where the objective function is the robustness measure and the eigenstructure assignment design parameters are the optimised variables. An off-the-shelf optimisation algorithm may be employed to perform robustness improvement, however, development of a specialised algorithm allows it to be carefully tailored to meet the needs of this particular problem.

If a function is continuous and smooth then a gradient based optimisation will generally out perform, algorithms that only evaluate the objective function [Gra89]. Step four of the robustness improvement algorithm, requires derivative information in order to generate a *descent direction* ( $\mathbf{d}$ ). In this section analytical formulae are derived and perturbation techniques are described that enable the derivative information to be calculated. A descent direction is a perturbation on each parameter ( $\delta \mathbf{d}$ ) that will, if sufficiently small, decrease an objective function. Mathematically, this implies:

$$\lim_{\alpha \rightarrow 0} \frac{f(\mathbf{x} + \alpha \mathbf{d}) - f(\mathbf{x})}{\alpha} < 0 \quad (5.5.73)$$

which in the limit may be expressed as:

$$[\nabla f(\mathbf{x})]^T \mathbf{d} < 0 \quad (5.5.74)$$

where  $\mathbf{x}$  is a vector of design parameters,  $f(\mathbf{x})$  is the objective function,  $\alpha$  is a scalar and  $\nabla$  is the vector differential operator [Jef89, p. 516].

The simplest descent direction is the opposite direction to the gradient itself:

$$\mathbf{d} = -\nabla f(\mathbf{x}) \quad (5.5.75)$$

and algorithms that use this direction are known as methods of steepest descent, since the function reduces most rapidly in this direction. Steepest descent algorithms are characterised by initial rapid

reductions in the objective function, but as they approach a minimum they become locked in a cycle of diminishing return; as the function approaches the optimum point, the gradient vanishes and thus so does the direction information.

An alternative descent direction is the Newton Raphson direction [Wal75], which is defined as follows:

$$\mathbf{d} = -\mathbf{H}^{-1}\nabla f(\mathbf{x}) \quad (5.5.76)$$

where  $\mathbf{H}$  is a matrix of second order derivatives known as the Hessian matrix [RS70, p. 160] and since it is positive definite, it follows that  $(\mathbf{d})$  is always a descent direction.

$$-\left[\nabla f(\mathbf{x})\right]^T \mathbf{H}^{-1} \nabla f(\mathbf{x}) < 0 \quad (5.5.77)$$

If  $f(\mathbf{x})$  is a quadratic function then the Newton Raphson direction will find the optimum point in a single step, whereas the steepest descent algorithm will approach the optimum asymptotically. The quadratic function is the simplest function with a strong minimum and objective functions with minima can be reasonably approximated with quadratic functions. Thus, in general, the Newton algorithm will converge faster than the method of steepest descent. The drawback of the Newton Raphson techniques is that calculating and inverting the Hessian can be computationally intensive.

Popular compromises are the quasi-Newton methods. These only require first order gradient information, but use successive gradient measurements to estimate the Hessian matrix. Initially, they start with an estimate:

$$\mathbf{H}_0 = \mathbf{I} \quad (5.5.78)$$

which is progressively updated, using a formula such the Davidon Fletcher Powell formula (DFP) or the Complementary DFP formula [Wal75, Gra95]. If the function is quadratic, then the Hessian estimate  $(\mathbf{H}_k)$  will tend to the actual Hessian and converge on the optimum point in a finite number of steps.

An important part of all the optimisation methods described above is the line search. Once a descent direction has been calculated a step is taken in that direction. For a very small step the objective function is guaranteed to decrease, however, the decrement is likely to be correspondingly small. On the other hand, large steps offer no guarantee of decreasing the function since the descent direction is only valid locally. It is therefore usual to search along the descent direction for a minimum, and thus find the largest step size for which the function monotonically decreases. Different line search

algorithms may be applied. For instance [Wal75], a Fibonacci search, a bisection search or quadratic/cubic interpolation and extrapolation. For quasi-Newton methods an accurate line search is necessary to maintain a positive definite Hessian [Wal75, p. 121].

The method of steepest descent was applied in this work for the following reasons:

- This algorithm does not seek to find the optimum point i.e. the most robust configuration, but instead seeks a point with acceptable robustness. Thus, the initial fast convergence of steepest descent is attractive and the poor performance near the optimal point should be irrelevant.
- The descent direction is altered in order to maintain performance. It is thus potentially fruitless to expend computational effort calculating an optimal direction that will later be adjusted.
- It was decided to start with a simple algorithm and progressively increase complexity as necessary to meet the robustness goals.

Step four of the algorithm may use either of two methods to calculate the function gradients, numerical perturbation and approximate analytic expressions. Numerical perturbation is computationally more intensive and less accurate than analytically derived gradient functions. But is more flexible, since fresh gradient functions do not have to be derived each time the synthesis technique or robustness measure is changed. Let us first consider estimation of the robustness function gradient with respect to eigenvector parameters using the numerical perturbation method.

### 5.5.1 Numerical Perturbation

An important feature of the robustness improvement algorithm is that the optimisation is conducted using the parameters that are input to the controller synthesis algorithm. Naturally, the relationship between the design parameters and the robustness of the final design will largely depend on the controller synthesis algorithm employed. Thus the first step is to choose a controller synthesis algorithm. For the following reasons it was decided to use two stage output feedback assignment.

- The algorithm is simple.
- The algorithm is a good starting point for later extension to multistage or iterative assignment methods.
- Even if the initial design is conducted using an alternative method, robustification using two stage assignment should not cause too much loss of visibility or performance.

For brevity we will assume that right eigenvectors are assigned in stage one and left eigenvectors in stage two. For both stages one and two, the assigned vectors are most succinctly expressed as vectors selected from allowed subspaces by a design vector:

$$\mathbf{v}_i = \mathbf{Q}_i \mathbf{f}_i \quad (5.5.79)$$

$$\mathbf{w}_j = \mathbf{g}_j \mathbf{L}_j \quad (5.5.80)$$

Where  $\mathbf{w}_j$ ,  $\mathbf{v}_i$  are left and right eigenvectors,  $\mathbf{L}_j$ ,  $\mathbf{Q}_i$  are the allowed subspaces and  $\mathbf{g}_j$ ,  $\mathbf{f}_i$  are the associated design vectors.

Clearly, a design vector is only meaningful when taken in conjunction with its corresponding subspace. In principle, numerical perturbation proceeds by perturbing an element of the design vector, while keeping all other elements constant, performing the design algorithm and then noting the change in robustness of the new system. Unfortunately, adjusting the stage one design vectors ( $\mathbf{f}_i$ ) forces re-calculation of the stage two subspaces ( $\mathbf{L}_j$ ). Since the stage two subspaces must satisfy Equation (5.5.81) in order to maintain orthogonality:

$$\mathbf{0} = \mathbf{L}_j [\mathbf{v}_1, \dots, \mathbf{v}_{s1}] \quad (5.5.81)$$

Computation of the new subspace produces a matrix with columns that form an arbitrary basis for the subspace ( $\hat{\mathbf{L}}_j$ ). When the new subspace is used with the old design vectors an arbitrary vector may result. This computational artifact leads to meaningless gradient values. The problem is not restricted to just the gradient calculation. When the optimisation incrementally adjusts the design vectors the synthesis algorithm must be re-run and equally unwanted arbitrary left eigenvectors may result. It is therefore necessary to address this problem.

One obvious approach is to re-calculate design vectors by projecting the desired left eigenvector on to the new subspace.

$$\hat{\mathbf{g}}_j = \mathbf{w}_j (\hat{\mathbf{L}}_j)^\dagger \quad (5.5.82)$$

While for the first iteration of the optimisation this is a sensible approach, in subsequent iterations the design vector should be guided to a new direction that improves robustness. However, repeated re-calculation using the desired eigenvector severely limits the direction in which the design vector may evolve.

The approach adopted is to calculate the new design vector by projecting the old eigenvector on to the new subspace. Using this approach the new eigenvector is as close as possible to the old eigenvector. Thus maintaining continuity between iterations and helping to ensure the dominant changes in direction are due to adjustments made by the optimisation and not simple re-calculation.

In summary gradient calculation using numerical perturbation proceeds as follows:

1. Perturb a specific element of a right design vector ( $\mathbf{f}_i$ ).
2. Calculate the right eigenvectors ( $\mathbf{v}_i$ ).
3. Calculate the new left allowed subspaces ( $\hat{\mathbf{L}}_j$ ).
4. Re-align the left eigenvectors ( $\hat{\mathbf{w}}_j$ ) in the new subspaces ( $\hat{\mathbf{L}}_j$ ) with the old left eigenvectors ( $\mathbf{w}_j$ ).
5. Calculate the gain matrix Equation (4.5.136).
6. Calculate the robustness measure Equation (5.4.6).
7. The gradient is approximated by the change in the robustness measure divided by the perturbation size.

In practice the algorithm uses positive and negative perturbation and compares the resulting gradient values. If the gradient values differ considerably then the perturbation size is reduced. The algorithm deals with complex design vectors by perturbing the real and imaginary parts separately. It should be borne in mind that perturbing a real or imaginary component affects two eigenvectors.

A complementary procedure is used to calculate the gradient with respect to the eigenvalues.

### 5.5.2 Analytic Gradients for the Time Domain Robustness Measure

The numerical perturbation procedure algorithm illustrates the difficulty in deriving analytic expressions for the gradients. For instance, working backwards, the partial derivatives may be calculated as follows:

1. The robustness function with respect to the gain.
2. The gain with respect to the eigenstructure.
3. The eigenstructure with respect to the design vectors (including re-alignment).

The crux of the problem lies with steps two and three where parameters input to the synthesis algorithm (design vectors) are differentiated with respect to its outputs (gain matrix). The synthesis algorithm is sequence of complex functions and thus very awkward to express as a single mathematical function let alone differentiate.

To simplify matters and avoid generating error prone cumbersome expressions that offer no computational saving over numerical perturbation. It was decided to make some simplifying assumptions and derive approximate gradient expressions. A simple mechanism was devised to ensure that the integrity of the optimisation algorithm was not compromised by using approximate data. If the approximate gradients are too inaccurate then the line search will fail to find a step size that reduces the

cost function and the optimisation switches to numerical gradients. On the other hand, if the gradients are sufficiently accurate then the line search will reduce the cost function and the optimisation continues with approximate gradients. The simplifying assumption are:

- A1 The term  $\mathbf{B}_M \text{ abs}(\mathbf{K}\mathbf{C})$  of Equation (5.4.6) is independent of the design parameters or equivalently  $\mathbf{B}_M$  is zero.
- A2 The matrices  $\mathbf{V}$  of Equation (5.4.9) and  $\mathbf{W}$  of Equation (5.4.10) are related solely by the formula  $\mathbf{W} = \mathbf{V}^{-1}$ .

While assumption two is, by the definition of eigenvectors, true it ignores the additional subspace constraints associated with the left eigenvectors as illustrated by Equation (5.5.81).

The derivation proceeds as follows:

**Lemma 5.5.1 Porter and Crossley [PC72, p. 22]**

*Let  $\mathbf{X}$  be a non-defective square matrix, that is a function of an independent variable  $\alpha$ . Then the following holds:*

$$\frac{\partial \rho(\mathbf{X})}{\partial \alpha} = \mathbf{w} \frac{\partial \mathbf{X}}{\partial \alpha} \mathbf{v} \quad (5.5.83)$$

where  $(\mathbf{w}, \mathbf{v})$  are the left and right eigenvectors associated with the largest eigenvalue of  $\mathbf{X}$ .

◇◇

Lemma 5.5.1 may be applied to Equation (5.4.6) as follows:

$$\frac{\partial}{\partial f_{kj}} \left[ \rho \left( \sum_{i=1}^n \frac{\text{abs}(\mathbf{v}_i \mathbf{w}_i)}{-\text{Re}(\lambda_i) \text{abs}(\mathbf{w}_i \mathbf{v}_i)} \mathbf{A}_{BM} \right) \right] = \mathbf{w}_N \frac{\partial}{\partial f_{kj}} \left( \sum_{i=1}^n \frac{\text{abs}(\mathbf{v}_i \mathbf{w}_i)}{-\text{Re}(\lambda_i) \text{abs}(\mathbf{w}_i \mathbf{v}_i)} \mathbf{A}_{BM} \right) \mathbf{v}_N \quad (5.5.84)$$

where the following definitions hold:

$$\lambda_i = \lambda_i(\mathbf{A} + \mathbf{B}\mathbf{K}\mathbf{C}) \quad (5.5.85)$$

$$\mathbf{A}_{BM} = \mathbf{A}_M + \mathbf{B}_M \text{ abs}(\mathbf{K}\mathbf{C}) \quad (5.5.86)$$

and for brevity let us define:



$$\mathbf{N} = \sum_{i=1}^n \frac{\text{abs}(\mathbf{v}_i \mathbf{w}_i)}{-\text{Re}(\lambda_i) \text{abs}(\mathbf{w}_i \mathbf{v}_i)} \mathbf{A}_{\text{BM}} \quad (5.5.87)$$

Then  $(\mathbf{w}_N, \mathbf{v}_N)$  are the left and right eigenvectors associated with the largest eigenvalue of  $\mathbf{N}$  and with a slight abuse of notation  $f_{kj}$  is the  $j^{\text{th}}$  element the  $k^{\text{th}}$  design vector. It is worth remarking that since  $\mathbf{N}$  has non-negative elements,  $(\mathbf{w}_N, \mathbf{v}_N)$  will also be non-negative and are sometimes called the Perron-Frobenius eigenvectors [Hor85].

Assumption two ensures that  $(\mathbf{v}_i, \mathbf{w}_i)$  are appropriately scaled such that  $\text{abs}(\mathbf{w}_i \mathbf{v}_i) = 1$ . Expanding  $\text{abs}(\mathbf{v}_i \mathbf{w}_i)$  gives:

$$\frac{\partial \mathbf{N}}{\partial f_{kj}} = \frac{\partial}{\partial f_{kj}} \left( \sum_{i=1}^n \text{pow} \left( \mathbf{v}_i \mathbf{w}_i \circ \text{conj}(\mathbf{v}_i \mathbf{w}_i), \frac{1}{2} \right) \frac{\mathbf{A}_{\text{BM}}}{-\text{Re}(\lambda_i)} \right) \quad (5.5.88)$$

Where the operator  $\text{pow}(\mathbf{X}, n)$  raises each element of  $\mathbf{X}$  to the power  $n$  and  $\text{conj}(\mathbf{X})$  forms the complex conjugate of each element and 'o' indicates element by element multiplication which is sometimes known as the Hadamard product [HJ91]. Further expansion reveals:

$$\frac{\partial \mathbf{N}}{\partial f_{kj}} = \frac{\partial}{\partial f_{kj}} \left( \sum_{i=1}^n \text{pow} \left( \text{pow}(\text{Re}(\mathbf{v}_i \mathbf{w}_i), 2) + \text{pow}(\text{Im}(\mathbf{v}_i \mathbf{w}_i), 2), \frac{1}{2} \right) \frac{\mathbf{A}_{\text{BM}}}{-\text{Re}(\lambda_i)} \right) \quad (5.5.89)$$

#### Lemma 5.5.2 [Gra81]

Let  $\mathbf{X}$  be an arbitrary matrix that is a function of a variable  $\alpha$ . The following chain rule holds:

$$\frac{\partial}{\partial \alpha} \text{pow}(\mathbf{X}, n) = n \frac{\partial \mathbf{X}}{\partial \alpha} \circ \text{pow}(\mathbf{X}, n-1) \quad (5.5.90)$$

◇◇

For brevity let us define  $\mathbf{X}_i$  as follows:

$$\mathbf{X}_i = \text{pow}(\text{Re}(\mathbf{v}_i \mathbf{w}_i), 2) + \text{pow}(\text{Im}(\mathbf{v}_i \mathbf{w}_i), 2) \quad (5.5.91)$$

then it follows that:

$$\frac{\partial \mathbf{N}}{\partial f_{kj}} = \sum_{i=1}^n \frac{\partial \mathbf{X}_i}{\partial f_{kj}} \circ \frac{1}{2} \text{pow} \left( \mathbf{X}_i, -\frac{1}{2} \right) \frac{\mathbf{A}_{\text{BM}}}{-\text{Re}(\lambda_i)} \quad (5.5.92)$$

Further application of the chain rule can be used to evaluate  $\frac{\partial \mathbf{X}_i}{\partial \mathbf{f}_{kj}}$ :

$$\frac{\partial \mathbf{X}_i}{\partial \mathbf{f}_{kj}} = 2 \frac{\partial}{\partial \mathbf{f}_{kj}} \operatorname{Re}(\mathbf{v}_i \mathbf{w}_i) \circ \operatorname{Re}(\mathbf{v}_i \mathbf{w}_i) + 2 \frac{\partial}{\partial \mathbf{f}_{kj}} \operatorname{Im}(\mathbf{v}_i \mathbf{w}_i) \circ \operatorname{Im}(\mathbf{v}_i \mathbf{w}_i) \quad (5.5.93)$$

Continuing we must calculate  $\frac{\partial}{\partial \mathbf{f}_{kj}} \operatorname{Re}(\mathbf{v}_i \mathbf{w}_i)$  and  $\frac{\partial}{\partial \mathbf{f}_{kj}} \operatorname{Im}(\mathbf{v}_i \mathbf{w}_i)$ , we note that:

$$\frac{\partial}{\partial \mathbf{f}_{kj}} \operatorname{Re}(\mathbf{v}_i \mathbf{w}_i) = \operatorname{Re} \left( \frac{\partial \mathbf{v}_i \mathbf{w}_i}{\partial \mathbf{f}_{kj}} \right) \quad (5.5.94)$$

and equally:

$$\frac{\partial}{\partial \mathbf{f}_{kj}} \operatorname{Im}(\mathbf{v}_i \mathbf{w}_i) = \operatorname{Im} \left( \frac{\partial \mathbf{v}_i \mathbf{w}_i}{\partial \mathbf{f}_{kj}} \right) \quad (5.5.95)$$

For both Equation (5.5.94) and Equation (5.5.95) two cases must be considered; the case  $k = i$  where both  $\mathbf{v}_i$  and  $\mathbf{w}_i$  are dependent on  $\mathbf{f}_{kj}$  and the case  $k \neq i$  where only  $\mathbf{w}_i$  is dependent on  $\mathbf{f}_{kj}$ . Let us first consider the simpler  $k \neq i$  case.

The  $i^{\text{th}}$  left eigenvector ( $\mathbf{w}_i$ ) may be expressed as:

$$\mathbf{w}_i = \mathbf{z}_i [\mathbf{v}_1, \dots, \mathbf{v}_k, \dots, \mathbf{v}_n]^{-1} \quad (5.5.96)$$

where  $\mathbf{z}_k$  is a 1 by  $n$  row vector with all zero elements except the  $i^{\text{th}}$  element which is unity as shown below:

$$\mathbf{z}_i = [0, \dots, 1, \dots, 0] \quad (5.5.97)$$

Thus substituting Equation (5.5.96) into Equation (5.5.94) gives:

$$\mathbf{v}_i \frac{\partial \mathbf{w}_i}{\partial \mathbf{f}_{kj}} = \mathbf{v}_i \mathbf{z}_k \frac{\partial}{\partial \mathbf{f}_{kj}} [\mathbf{v}_1, \dots, \mathbf{v}_k, \dots, \mathbf{v}_n]^{-1} \quad (5.5.98)$$

Further progress requires the following lemma.

**Lemma 5.5.3 [Gra81]**

*Let  $\mathbf{X}$  be a non-singular arbitrary matrix that is a function of a variable  $\alpha$  then it follows:*

$$\frac{\partial \mathbf{X}^{-1}}{\partial \alpha} = -\mathbf{X}^{-1} \frac{\partial \mathbf{X}}{\partial \alpha} \mathbf{X}^{-1} \quad (5.5.99)$$

◇◇

Application of Lemma 5.5.3 on Equation (5.5.98) gives:

$$\frac{\partial \mathbf{v}_i \mathbf{w}_i}{\partial \mathbf{f}_{kj}} = -\mathbf{v}_i \mathbf{z}_i [\mathbf{v}_1, \dots, \mathbf{v}_k, \dots, \mathbf{v}_n]^{-1} \frac{\partial [\mathbf{v}_1, \dots, \mathbf{v}_k, \dots, \mathbf{v}_n]}{\partial \mathbf{f}_{kj}} [\mathbf{v}_1, \dots, \mathbf{v}_k, \dots, \mathbf{v}_n]^{-1} \quad (5.5.100)$$

$$= -\mathbf{v}_i \mathbf{w}_i \frac{\partial [\mathbf{v}_1, \dots, \mathbf{v}_k, \dots, \mathbf{v}_n]}{\partial \mathbf{f}_{kj}} [\mathbf{v}_1, \dots, \mathbf{v}_k, \dots, \mathbf{v}_n]^{-1} \quad (5.5.101)$$

Only the vector  $\mathbf{v}_k$  is dependent on  $\mathbf{f}_{kj}$  thus the derivative with respect to the other vectors is zero.

$$\mathbf{v}_i \frac{\partial \mathbf{w}_i}{\partial \mathbf{f}_{kj}} = -\mathbf{v}_i \mathbf{w}_i \left[ 0, \dots, \frac{\partial \mathbf{v}_k}{\partial \mathbf{f}_{kj}}, \dots, 0 \right] [\mathbf{v}_1, \dots, \mathbf{v}_k, \dots, \mathbf{v}_n]^{-1} \quad (5.5.102)$$

$$= -\mathbf{v}_i \mathbf{w}_i \left[ 0, \dots, \frac{\partial \mathbf{v}_k}{\partial \mathbf{f}_{kj}}, \dots, 0 \right] [\mathbf{w}_1^T, \dots, \mathbf{w}_k^T, \dots, \mathbf{w}_n^T]^T \quad (5.5.103)$$

$$= -\mathbf{v}_i \mathbf{w}_i \frac{\partial \mathbf{v}_k}{\partial \mathbf{f}_{kj}} \mathbf{w}_k \quad (5.5.104)$$

We recall from Equation (5.5.79) that the  $k^{\text{th}}$  right eigenvector ( $\mathbf{v}_k$ ) is selected from an allowed subspace ( $\mathbf{Q}_k$ ) by a design vector ( $\mathbf{f}_k$ ) as follows:

$$\mathbf{v}_k = \mathbf{Q}_k \mathbf{f}_k \quad (5.5.105)$$

The following simple lemma illustrates how to differentiate Equation (5.5.105).

**Lemma 5.5.4 [Gra81]**

Let  $\mathbf{A}$ ,  $\mathbf{X}$ ,  $\mathbf{B}$  be arbitrary matrices that form the following product:

$$\mathbf{Y} = \mathbf{A} \mathbf{X} \mathbf{B} \quad (5.5.106)$$

Then the derivative of  $\mathbf{Y}$  with respect to the  $ij^{\text{th}}$  element of  $\mathbf{X}$  denoted  $\mathbf{X}_{ij}$  is:

$$\frac{\partial \mathbf{Y}}{\partial \mathbf{X}_{ij}} = \mathbf{A} \frac{\partial \mathbf{X}}{\partial \mathbf{X}_{ij}} \mathbf{B} \quad (5.5.107)$$

$$= \mathbf{A} \mathbf{E}_{ij} \mathbf{B} \quad (5.5.108)$$

Where  $\mathbf{E}$  is a matrix of equal dimensions to  $\mathbf{X}$  with all zero elements except the  $ij^{th}$  element which is unity. ◇◇

Application of Lemma 5.5.4 on Equation (5.5.105) and substitution into Equation (5.5.104) gives:

$$\mathbf{v}_i \frac{\partial \mathbf{w}_i}{\partial \mathbf{f}_{kj}} = -\mathbf{v}_i \mathbf{w}_i \mathbf{Q}_k \mathbf{e}_j \mathbf{w}_k \quad (5.5.109)$$

Where  $\mathbf{e}_j$  is a vector of equal dimensions to  $\mathbf{f}_k$  with all zero elements except the  $j^{th}$  element which is equal to unity. The slightly more complex  $k = i$  case requires a matrix calculus product rule as summarised in the following lemma.

**Lemma 5.5.5 [Gra81]**

Let  $\mathbf{UV}$  be the product of two matrices conformal for multiplication and both dependent on a variable  $\alpha$ . Then the following holds:

$$\frac{\partial (\mathbf{UV})}{\partial \alpha} = \frac{\partial \mathbf{U}}{\partial \alpha} \mathbf{V} + \mathbf{U} \frac{\partial \mathbf{V}}{\partial \alpha} \quad (5.5.110)$$

◇◇

Returning to Equation (5.5.94) and applying Lemma 5.5.5, gives:

$$\frac{\partial \mathbf{v}_i \mathbf{w}_i}{\partial \mathbf{f}_{kj}} = \frac{\partial \mathbf{v}_i}{\partial \mathbf{f}_{kj}} \mathbf{w}_i + \mathbf{v}_i \frac{\partial \mathbf{w}_i}{\partial \mathbf{f}_{kj}} \quad (5.5.111)$$

The first term requires differentiation of  $\mathbf{v}_i$  using Lemma 5.5.4 and the derivative of the second term is given directly by Equation (5.5.109). The combined result is illustrated in Equation (5.5.112).

$$\frac{\partial \mathbf{v}_i \mathbf{w}_i}{\partial \mathbf{f}_{kj}} = \mathbf{Q}_k \mathbf{e}_j \mathbf{w}_i - \mathbf{v}_i \mathbf{w}_i \mathbf{Q}_k \mathbf{e}_j \mathbf{w}_k \quad (5.5.112)$$

We are now in a position to construct the complete solution. This involves combining Equations (5.5.84), (5.5.93), (5.5.94), (5.5.95), (5.5.109) and (5.5.112).

$$\begin{aligned} \frac{\partial N}{\partial \mathbf{f}_{kj}} = \mathbf{w}_N \left( \sum_{i=1}^n (\operatorname{Re}(\delta_{ik} \mathbf{Q}_k \mathbf{e}_j \mathbf{w}_k - \mathbf{v}_i \mathbf{w}_i \mathbf{Q}_k \mathbf{e}_j \mathbf{w}_k) \circ \operatorname{Re}(\mathbf{v}_i \mathbf{w}_i) + \right. \\ \left. \operatorname{Im}(\delta_{ik} \mathbf{Q}_k \mathbf{e}_j \mathbf{w}_k - \mathbf{v}_i \mathbf{w}_i \mathbf{Q}_k \mathbf{e}_j \mathbf{w}_k) \circ \operatorname{Im}(\mathbf{v}_i \mathbf{w}_i) \right) \circ \\ \left. \operatorname{pow}(\operatorname{abs}(\mathbf{v}_i \mathbf{w}_i), -1) \frac{\mathbf{ABM}}{-\operatorname{Re}(\lambda_i)} \right) \mathbf{v}_N \end{aligned} \quad (5.5.113)$$

Where  $\delta_{ik}$  is the Kronecker delta which is defined as follows:

$$\delta_{ik} = \begin{cases} 0 & i \neq j, \\ 1 & i = j \end{cases} \quad (5.5.114)$$

Extension to complex design vectors is very straightforward and is accomplished as follows:

1. Since the design vectors must always appear as conjugate pairs, a real component of one design vector will never differ from the real component of its conjugate counterpart and is thus a single variable present in two vectors. The same is, naturally, true for the imaginary components. This has little affect on the derivation until Equation (5.5.98) ( $\mathbf{v}_i \frac{\partial \mathbf{w}_i}{\partial \mathbf{f}_{kj}}$ ) where the left eigenvector ( $\mathbf{w}_i$ ) is dependent on  $\mathbf{f}_{kj}$  in two instances. Let us assume that the design vectors are ordered such that conjugate pairs are adjacent. It follows that:

$$\mathbf{v}_i \frac{\partial \mathbf{w}_i}{\partial \mathbf{f}_{kj}} = -\mathbf{v}_i \mathbf{w}_i \left[ 0, \dots, \frac{\partial \mathbf{v}_k}{\partial \mathbf{f}_{kj}}, \frac{\partial \mathbf{v}_{k+1}}{\partial \mathbf{f}_{kj}}, \dots, 0 \right] [\mathbf{v}_1, \dots, \mathbf{v}_k, \mathbf{v}_{k+1}, \dots, \mathbf{v}_n]^{-1} \quad (5.5.115)$$

$$= -\mathbf{v}_i \mathbf{w}_i \left[ 0, \dots, \frac{\partial \mathbf{v}_k}{\partial \mathbf{f}_{kj}}, \frac{\partial \mathbf{v}_{k+1}}{\partial \mathbf{f}_{kj}}, \dots, 0 \right] [\mathbf{w}_1^T, \dots, \mathbf{w}_k^T, \mathbf{w}_{k+1}^T, \dots, \mathbf{w}_n^T]^T \quad (5.5.116)$$

$$= -\mathbf{v}_i \mathbf{w}_i \left( \frac{\partial \mathbf{v}_k}{\partial \mathbf{f}_{kj}} \mathbf{w}_k + \frac{\partial \mathbf{v}_{k+1}}{\partial \mathbf{f}_{kj}} \mathbf{w}_{k+1} \right) \quad (5.5.117)$$

which upon differentiation gives:

$$\mathbf{v}_i \frac{\partial \mathbf{w}_i}{\partial \mathbf{f}_{kj}} = -\mathbf{v}_i \mathbf{w}_i (\mathbf{Q}_k \mathbf{e}_j \mathbf{w}_k + \mathbf{Q}_{k+1} \mathbf{e}_j \mathbf{w}_{k+1}) \quad (5.5.118)$$

and by noting the two terms in brackets form a conjugate pair we may simplify as follows:

$$\mathbf{v}_i \frac{\partial \mathbf{w}_i}{\partial \mathbf{f}_{kj}} = 2\mathbf{v}_i \mathbf{w}_i \operatorname{Re}(\mathbf{Q}_k \mathbf{e}_j \mathbf{w}_k) \quad (5.5.119)$$

2. The derivative with respect to the imaginary part of a complex design vector ( $\mathbf{f}_{kj}$ ) is based on the following simple result:

$$\frac{\partial \mathbf{f}_k}{\partial \mathbf{f}_{kj}} = j\mathbf{e}_j \quad (5.5.120)$$

Where  $\mathbf{f}_{kj}$  is the imaginary part of the specified design vector element.

All the previous results including the one above are for the real case, however, they can be converted to the imaginary case by replacing all the ' $\mathbf{e}_j$ 's with ' $j\mathbf{e}_j$ '.

### The Time Domain Measure Eigenvalue Gradients

Differentiation with respect to the eigenvalue parameters must take into account that the allowed subspaces are dependent on the eigenvalues locations. Thus adjustment of the eigenvalue locations will also affect the eigenvectors. The simplest formulae that express this dependency are:

$$\mathbf{Q}_i = (\mathbf{A} - \mathbf{I}\lambda_i)^{-1}\mathbf{B} \quad (5.5.121)$$

$$\mathbf{L}_i = \mathbf{C}(\mathbf{A} - \mathbf{I}\lambda_i)^{-1} \quad (5.5.122)$$

Equation (5.5.121) and Equation (5.5.122) lend themselves directly to differentiation. However, they do suffer the limitation that the formulae break down when the closed and open loop eigenvalues are co-incident. With these formulae in mind the derivation of the robustness measure gradient with respect to eigenvalue parameters proceeds as follows. Returning to Equation (5.5.84)

$$\frac{\partial}{\partial \lambda_i} \left[ \rho \left( \sum_{i=1}^n \frac{\operatorname{abs}(\mathbf{v}_i \mathbf{w}_i)}{-\operatorname{Re}(\lambda_i) \operatorname{abs}(\mathbf{w}_i \mathbf{v}_i)} \mathbf{A}_{\text{BM}} \right) \right] = \mathbf{w}_N \frac{\partial}{\partial \lambda_i} \left( \sum_{i=1}^n \frac{\operatorname{abs}(\mathbf{v}_i \mathbf{w}_i)}{-\operatorname{Re}(\lambda_i) \operatorname{abs}(\mathbf{w}_i \mathbf{v}_i)} \mathbf{A}_{\text{BM}} \right) \mathbf{v}_N \quad (5.5.123)$$

and applying the definition given in Equation (5.5.85) and Equation (5.5.86) while invoking assumption A2, gives:

$$\frac{\partial N}{\partial \lambda_k} = \frac{\partial}{\partial \lambda_i} \left( \sum_{i=1}^n \text{abs}(\mathbf{v}_i \mathbf{w}_i) \frac{\mathbf{ABM}}{-\text{Re}(\lambda_i)} \right) \quad (5.5.124)$$

$$= \sum_{i=1}^n \left( \frac{\partial \text{abs}(\mathbf{v}_i \mathbf{w}_i)}{\partial \lambda_k} \frac{\mathbf{ABM}}{-\text{Re}(\lambda_i)} + \text{abs}(\mathbf{v}_i \mathbf{w}_i) \frac{\partial}{\partial \lambda_k} \left( \frac{\mathbf{ABM}}{-\text{Re}(\lambda_i)} \right) \right) \quad (5.5.125)$$

The second term of the sum will evaluate to zero when differentiated with respect to the imaginary part of an eigenvalue. However, for the case  $k = i$ , the real part of an eigenvalue, the expression evaluates as follows:

$$\text{abs}(\mathbf{v}_i \mathbf{w}_i) \frac{\partial}{\partial \lambda_i} \left( \frac{\mathbf{ABM}}{-\text{Re}(\lambda_i)} \right) = \text{abs}(\mathbf{v}_i \mathbf{w}_i) \left( \frac{\mathbf{ABM}}{\text{Re}(\lambda_i)^2} \right) \quad (5.5.126)$$

The first term of Equation (5.5.125) is differentiated using the assumptions of the previous section and the initial derivation follows that of the eigenvector case. Thus:

$$\begin{aligned} \frac{\partial \text{abs}(\mathbf{v}_i \mathbf{w}_i)}{\partial \lambda_i} \frac{\mathbf{ABM}}{-\text{Re}(\lambda_i)} &= \left( 2 \frac{\partial}{\partial \lambda_k} \text{Re}(\mathbf{v}_i \mathbf{w}_i) \circ \text{Re}(\mathbf{v}_i \mathbf{w}_i) + 2 \frac{\partial}{\partial \lambda_k} \text{Im}(\mathbf{v}_i \mathbf{w}_i) \circ \text{Im}(\mathbf{v}_i \mathbf{w}_i) \right) \\ &\quad \circ \frac{1}{2} \text{pow}(\text{abs}(\mathbf{v}_i \mathbf{w}_i), -1) \frac{\mathbf{ABM}}{-\text{Re}(\lambda_i)} \end{aligned} \quad (5.5.127)$$

and examination of Equation (5.5.94) and Equation (5.5.95) and the subsequent derivation reveals:

$$\frac{\partial}{\partial \lambda_k} \text{Re}(\mathbf{v}_i \mathbf{w}_i) = \text{Re} \left( \delta_{ik} \frac{\partial \mathbf{v}_k}{\lambda_k} \mathbf{w}_i - \mathbf{v}_i \mathbf{w}_i \frac{\partial \mathbf{v}_k}{\lambda_k} \mathbf{w}_k \right) \quad (5.5.128)$$

$$\frac{\partial}{\partial \lambda_k} \text{Im}(\mathbf{v}_i \mathbf{w}_i) = \text{Im} \left( \delta_{ik} \frac{\partial \mathbf{v}_k}{\lambda_k} \mathbf{w}_i - \mathbf{v}_i \mathbf{w}_i \frac{\partial \mathbf{v}_k}{\lambda_k} \mathbf{w}_k \right) \quad (5.5.129)$$

Thus it only remains to calculate partial derivative of eigenvectors with respect to the eigenvalues. Recalling Equation (5.5.121), Equation (5.5.79) and applying Lemma 5.5.3:

$$\frac{\partial \mathbf{v}_k}{\partial \lambda_k} = \frac{\partial}{\partial \lambda_k} (\mathbf{A} - \mathbf{I}\lambda_k)^{-1} \mathbf{B}\mathbf{f}_k \quad (5.5.130)$$

$$= -(\mathbf{A} - \mathbf{I}\lambda_k)^{-1} \frac{\partial (\mathbf{A} - \mathbf{I}\lambda_k)}{\partial \lambda_k} (\mathbf{A} - \mathbf{I}\lambda_k)^{-1} \mathbf{B}\mathbf{f}_k \quad (5.5.131)$$

$$= -(\mathbf{A} - \mathbf{I}\lambda_k)^{-1} (-\mathbf{I})(\mathbf{A} - \mathbf{I}\lambda_k)^{-1} \mathbf{B}\mathbf{f}_k \quad (5.5.132)$$

$$= (\mathbf{A} - \mathbf{I}\lambda_k)^{-1} \mathbf{v}_k \quad (5.5.133)$$

Thus the complete solution can now be constructed by backing substituting the preceding results into Equation (5.5.125).

### 5.5.3 Analytic Gradients for the Singular Value Robustness Measure.

To re-cap the singular value robustness measure used in this work is an upper bound on the structured singular value:

$$\mu(\mathbf{M}) \leq \min_{\mathbf{D}} \bar{\sigma}(\mathbf{D}\mathbf{M}\mathbf{D}^{-1}) \quad (5.5.134)$$

The structured singular value is a frequency dependent robustness measure and to improve robustness it is necessary to reduce the peak value across all frequencies. The peak value must be found by searching across a range of frequencies, since  $\mu(\mathbf{M})$  can not be a calculated directly. At each frequency point  $\mu(\mathbf{M})$  must be estimated. This is generally achieved by optimising the  $\mathbf{D}$ -scalings of the singular value upper bound indicated in Equation (5.5.134). Algorithms that perform the peak search and  $\mathbf{D}$ -scaling optimisation have been a keen area of research [FTD91, PD93] and reliable software implementations are now available. This work made use of the  $\mu$ -toolbox from MathWorks [BPDG93].

The robustness improvement algorithm adjusts the design parameters to reduce the singular value upper bound of  $\mu(\mathbf{M})$  that corresponds to the peak frequency.

It is assumed that, for each iteration of the optimisation algorithm, the  $\mathbf{D}$ -scaling remains constant. This ignores the fact that the  $\mathbf{D}$ -scaling is a function of the single loop system ( $\mathbf{M}$ ) and thus a function of the design parameters. However, the relationship between the  $\mathbf{D}$ -scaling and the design parameters can not be expressed in a closed form since the  $\mathbf{D}$ -scaling are the solution to a numerical optimisation. Hence gradient expressions can not be derived. For each iteration of the optimisation, only small adjustments are made to the to the system. Thus the assumption of a constant  $\mathbf{D}$ -scaling is likely to be reasonable. Ultimately, for this technique to be of value it is only necessary for the  $\mathbf{D}$ -scaling to offer benefit over conventional singular value measures where no scaling is applied.

Derivation of analytical gradients for the singular value based measure requires the follows steps:



1. The partial derivative of the maximum singular value with respect to the single loop system matrix (evaluated at the peak frequency) is derived.
2. The partial derivative of the single loop system matrix with respect to the gain matrix is derived.
3. The partial derivatives of the gain matrix with respect to the left and right parameter vectors are derived.
4. The partial derivative of the left design parameters with respect to the right design parameters is derived.

Step one is expressed in the following Lemma.

**Lemma 5.5.6 [MN84]**

Let  $\mathbf{X}$  be a general complex matrix, dependent upon a variable  $\alpha$ , with distinct singular values ( $\sigma_i$ ) and, left and right normalised singular vectors ( $\mathbf{u}_i, \mathbf{v}_i$ ). Which by definition satisfy:

$$\mathbf{X}\mathbf{v}_i = \mathbf{u}_i\sigma_i \quad \mathbf{X}^*\mathbf{u}_i = \mathbf{v}_i\sigma_i \quad (5.5.135)$$

and

$$\mathbf{v}_j^*\mathbf{v}_i = \delta_{ij} \quad \mathbf{u}_j^*\mathbf{u}_i = \delta_{ij} \quad (5.5.136)$$

where  $\delta_{ij}$  is the Kronecker delta. It follows that:

$$\frac{\partial \sigma_i}{\partial \alpha} = \text{Re} \left[ \mathbf{u}_i^* \frac{\partial \mathbf{X}}{\partial \alpha} \mathbf{v}_i \right] \quad (5.5.137)$$

◇◇

Thus, for this case:

$$\frac{\partial}{\partial \mathbf{f}_{kj}} \bar{\sigma}(\mathbf{D}\mathbf{M}(s)\mathbf{D}^{-1}) = \mathbf{u}^* \mathbf{D} \frac{\partial \mathbf{M}(s)}{\partial \mathbf{f}_{kj}} \mathbf{D}^{-1} \mathbf{v} \quad s = j\omega_o \quad (5.5.138)$$

Where  $\mathbf{u}$  and  $\mathbf{v}$  are the singular vectors associated with the maximum singular value ( $\bar{\sigma}$ ) and  $\omega_o$  is the peak frequency.

The precise nature of the solution for Step two depends on the structure of the single loop system. Let us assume that the single loop system has the following state space description:

$$M(s) = \hat{C}(s\mathbf{I} - \hat{\mathbf{A}})^{-1}\hat{\mathbf{B}} + \hat{\mathbf{D}} \quad (5.5.139)$$

The individual matrices will be functions of the gain matrix and thus the design parameters. For brevity let us define:

$$\Phi = (s\mathbf{I} - \hat{\mathbf{A}})^{-1} \quad (5.5.140)$$

differentiation then proceeds as follows:

$$\frac{\partial M(s)}{\partial f_{kj}} = \frac{\partial}{\partial f_{kj}} (\hat{C}\Phi\hat{\mathbf{B}} + \hat{\mathbf{D}}) \quad (5.5.141)$$

$$= \frac{\partial \hat{C}}{\partial f_{kj}} \Phi \hat{\mathbf{B}} + \hat{C} \frac{\partial \Phi}{\partial f_{kj}} \hat{\mathbf{B}} + \hat{C} \Phi \frac{\partial \hat{\mathbf{B}}}{\partial f_{kj}} + \frac{\partial \hat{\mathbf{D}}}{\partial f_{kj}} \quad (5.5.142)$$

$$= \frac{\partial \hat{C}}{\partial f_{kj}} \Phi \hat{\mathbf{B}} + \hat{C} \Phi \frac{\partial \hat{\mathbf{A}}}{\partial f_{kj}} \Phi \hat{\mathbf{B}} + \hat{C} \Phi \frac{\partial \hat{\mathbf{B}}}{\partial f_{kj}} + \frac{\partial \hat{\mathbf{D}}}{\partial f_{kj}} \quad (5.5.143)$$

For example, if robustness to input multiplicative uncertainty is optimised then from Table 5.4.2 the single loop system is as follows:

$$M(s) = \mathbf{K}\mathbf{C}(s\mathbf{I} - \mathbf{A} - \mathbf{B}\mathbf{K}\mathbf{C})^{-1}\mathbf{B} \quad (5.5.144)$$

Again, for brevity let us define:

$$\Phi = (s\mathbf{I} - \mathbf{A} - \mathbf{B}\mathbf{K}\mathbf{C})^{-1} \quad (5.5.145)$$

Substituting this case into the general formula of Equation (5.5.143) gives:

$$\frac{\partial M(s)}{\partial f_{kj}} = \frac{\partial \mathbf{K}\mathbf{C}}{\partial f_{kj}} \Phi \mathbf{B} + \mathbf{K}\mathbf{C} \Phi \frac{\partial (\mathbf{A} + \mathbf{B}\mathbf{K}\mathbf{C})}{\partial f_{kj}} \Phi \mathbf{B} \quad (5.5.146)$$

$$= \frac{\partial \mathbf{K}}{\partial f_{kj}} \mathbf{C} \Phi \mathbf{B} + \mathbf{K}\mathbf{C} \Phi \mathbf{B} \frac{\partial \mathbf{K}}{\partial f_{kj}} \mathbf{C} \Phi \mathbf{B} \quad (5.5.147)$$

All the entries of Table 5.4.2 can be differentiated in a similar manner. Step three involves differentiation of the gain matrix which is a little more involved. The formula for the gain matrix is reproduced

in Equation (5.5.148):

$$\mathbf{K} = (\mathbf{W}_2 \mathbf{B})^\dagger \mathbf{T}_2 + \mathbf{S}_1 (\mathbf{C}\mathbf{V}_1)^\dagger - (\mathbf{W}_2 \mathbf{B})^\dagger \mathbf{T}_2 \mathbf{C}\mathbf{V}_1 (\mathbf{C}\mathbf{V}_1)^\dagger \quad (5.5.148)$$

Differentiation proceeds as follows:

$$\begin{aligned} \frac{\partial \mathbf{K}}{\partial f_{kj}} &= \frac{\partial (\mathbf{W}_2 \mathbf{B})^\dagger}{\partial f_{kj}} \mathbf{T}_2 + (\mathbf{W}_2 \mathbf{B})^\dagger \frac{\partial \mathbf{T}_2}{\partial f_{kj}} + \frac{\partial \mathbf{S}_1}{\partial f_{kj}} (\mathbf{C}\mathbf{V}_1)^\dagger + \mathbf{S}_1 \frac{\partial (\mathbf{C}\mathbf{V}_1)^\dagger}{\partial f_{kj}} \\ &\quad - \frac{\partial (\mathbf{W}_2 \mathbf{B})^\dagger}{\partial f_{kj}} \mathbf{T}_2 \mathbf{C}\mathbf{V}_1 (\mathbf{C}\mathbf{V}_1)^\dagger - (\mathbf{W}_2 \mathbf{B})^\dagger \frac{\partial \mathbf{T}_2}{\partial f_{kj}} \mathbf{C}\mathbf{V}_1 (\mathbf{C}\mathbf{V}_1)^\dagger \\ &\quad - (\mathbf{W}_2 \mathbf{B})^\dagger \mathbf{T}_2 \frac{\partial (\mathbf{C}\mathbf{V}_1)^\dagger}{\partial f_{kj}} (\mathbf{C}\mathbf{V}_1)^\dagger - (\mathbf{W}_2 \mathbf{B})^\dagger \mathbf{T}_2 \mathbf{C}\mathbf{V}_1 \frac{\partial (\mathbf{C}\mathbf{V}_1)^\dagger}{\partial f_{kj}} \end{aligned} \quad (5.5.149)$$

It is apparent from Equation (5.5.149) that differentiation of the gain matrix requires differentiation of the pseudo inverse of a matrix. Fortunately, for assignment to proceed  $\mathbf{W}_2 \mathbf{B}$  and  $\mathbf{C}\mathbf{V}_1$  must be full rank, thus Equation (5.5.150) may be used to represent the pseudo inverse of  $\mathbf{W}_2 \mathbf{B}$  or  $\mathbf{C}\mathbf{V}_1$ .

$$(\mathbf{C}\mathbf{V}_1)^\dagger = ((\mathbf{C}\mathbf{V}_1)^* (\mathbf{C}\mathbf{V}_1))^{-1} (\mathbf{C}\mathbf{V}_1)^* \quad (5.5.150)$$

Differentiation of the pseudo inverse of a matrix using Equation (5.5.150) is summarised in the following Lemma:

**Lemma 5.5.7**

Let  $\mathbf{X} \in \mathbb{C}^{r \times c}$  where  $c < r$  and  $\text{rank}(\mathbf{X}) = c$ . Then the pseudo inverse of  $\mathbf{X}$  may be expressed as:

$$\mathbf{X}^\dagger = (\mathbf{X}^* \mathbf{X})^{-1} \mathbf{X}^* \quad (5.5.151)$$

and the derivative of  $\mathbf{X}$  with respect to an independent variable ( $\alpha$ ) is:

$$\frac{\partial \mathbf{X}^\dagger}{\partial \alpha} = (\mathbf{X}^* \mathbf{X})^{-1} \frac{\partial \mathbf{X}^*}{\partial \alpha} (\mathbf{I} - \mathbf{X} \mathbf{X}^\dagger) - \mathbf{X}^\dagger \frac{\partial \mathbf{X}}{\partial \alpha} \mathbf{X}^\dagger \quad (5.5.152)$$

◇◇

**Proof**

$$\frac{\partial \mathbf{X}^\dagger}{\partial \alpha} = \frac{\partial ((\mathbf{X}^* \mathbf{X})^{-1})}{\partial \alpha} \mathbf{X}^* + (\mathbf{X}^* \mathbf{X})^{-1} \frac{\partial \mathbf{X}^*}{\partial \alpha} \quad (5.5.153)$$

$$= -(\mathbf{X}^* \mathbf{X})^{-1} \frac{\partial (\mathbf{X}^* \mathbf{X})}{\partial \alpha} (\mathbf{X}^* \mathbf{X})^{-1} \mathbf{X}^* + (\mathbf{X}^* \mathbf{X})^{-1} \frac{\partial \mathbf{X}^*}{\partial \alpha} \quad (5.5.154)$$

$$= -(\mathbf{X}^* \mathbf{X})^{-1} \left[ \mathbf{X}^* \frac{\partial \mathbf{X}}{\partial \alpha} + \frac{\partial \mathbf{X}^*}{\partial \alpha} \mathbf{X} \right] (\mathbf{X}^* \mathbf{X})^{-1} \mathbf{X}^* + (\mathbf{X}^* \mathbf{X})^{-1} \frac{\partial \mathbf{X}^*}{\partial \alpha} \quad (5.5.155)$$

$$= (\mathbf{X}^* \mathbf{X})^{-1} \frac{\partial \mathbf{X}^*}{\partial \alpha} (\mathbf{I} - \mathbf{X} \mathbf{X}^\dagger) - \mathbf{X}^\dagger \frac{\partial \mathbf{X}}{\partial \alpha} \mathbf{X}^\dagger \quad (5.5.156)$$

◇◇

Once Lemma 5.5.7 has been applied to Equation (5.5.149) it remains to calculate  $\frac{\partial(\mathbf{CV1})}{\partial \mathbf{f}_{kj}}$ ,  $\frac{\partial(\mathbf{W2B})}{\partial \mathbf{f}_{kj}}$ ,  $\frac{\partial(\mathbf{S1})}{\partial \mathbf{f}_{kj}}$  and  $\frac{\partial(\mathbf{T2})}{\partial \mathbf{f}_{kj}}$ . But since  $\mathbf{CV1}$  and  $\mathbf{S1}$  depend solely on  $\mathbf{f}_i$  and in the dual case,  $\mathbf{W2B}$  and  $\mathbf{T2}$  depend solely on  $\mathbf{g}_i$ . This task reduces to calculating  $\frac{\partial \mathbf{f}_i}{\partial \mathbf{f}_{kj}}$  and  $\frac{\partial \mathbf{g}_i}{\partial \mathbf{f}_{kj}}$ . From the previous derivation it is clear that:

$$\frac{\partial \mathbf{f}_i}{\partial \mathbf{f}_{kj}} = \delta_{ik} \mathbf{e}_j \quad (5.5.157)$$

However, to derive the final Step (4) we must consider how the left eigenvectors are assigned. The left eigenvectors are calculated using a constrained projection.

$$\min_{\mathbf{g}_i} \|\mathbf{w}_i - \mathbf{g}_i \mathbf{L}_i\|_2^2 \quad \text{subject to} \quad \mathbf{0} = \mathbf{g}_i \mathbf{L}_i \mathbf{V}_1 \quad (5.5.158)$$

Where  $\mathbf{w}_i$  is, initially, the desired left eigenvector and subsequently the value from the previous iteration.

The constrained optimisation may be expressed equivalently as a matrix inversion problem [BIG74, p. 112].

$$\begin{bmatrix} \mathbf{g}_i & \mathbf{x}_i \end{bmatrix} \begin{bmatrix} \mathbf{L}_i \mathbf{L}_i^* & \mathbf{L}_i \mathbf{V}_1 \\ \mathbf{V}_1^* \mathbf{L}_i^* & \mathbf{0} \end{bmatrix} = \begin{bmatrix} \mathbf{w}_i \mathbf{L}_i^* & \mathbf{0} \end{bmatrix} \quad (5.5.159)$$

Equation (5.5.159) lends itself directly to differentiation, yielding:

$$\frac{\partial}{\partial \mathbf{f}_{kj}} \begin{bmatrix} \mathbf{g}_i & \mathbf{x}_i \end{bmatrix} = - \begin{bmatrix} \mathbf{L}_i \mathbf{L}_i^* & \mathbf{L}_i \mathbf{V}_1 \\ \mathbf{V}_1^* \mathbf{L}_i^* & \mathbf{0} \end{bmatrix}^{-1} \begin{bmatrix} \mathbf{0} & \mathbf{L}_i \frac{\partial \mathbf{V}_1}{\partial \mathbf{f}_{kj}} \\ \frac{\partial \mathbf{V}_1^*}{\partial \mathbf{f}_{kj}} \mathbf{L}_i^* & \mathbf{0} \end{bmatrix} \begin{bmatrix} \mathbf{L}_i \mathbf{L}_i^* & \mathbf{L}_i \mathbf{V}_1 \\ \mathbf{V}_1^* \mathbf{L}_i^* & \mathbf{0} \end{bmatrix}^{-1} \begin{bmatrix} \mathbf{w}_i \mathbf{L}_i^* & \mathbf{0} \end{bmatrix} \quad (5.5.160)$$

Finally, from the previous derivation we recall that:

$$\frac{\partial \mathbf{V}_1}{\partial \mathbf{f}_{kj}} = \begin{bmatrix} \mathbf{0}, \dots, \mathbf{Q}_k \mathbf{e}_j, \dots, \mathbf{0} \end{bmatrix} \quad (5.5.161)$$

Some computational saving is possible by noting that only part of the matrix inversion solution is required and also, that some entries of the multiplying vector are zero.

The results of Steps one through to four can be combined to produce an analytic estimate of the robustness measure gradient. It is worth noting that this result does not require assumption A2 which was used to derive the time domain measure. However, the penalty for removing this assumption is a considerable increase in the size of the final expression and a corresponding increase in computational load. Using the mathematical techniques described above assumption A2 could be removed from the derivation of the time domain measure gradient functions. However, a similar profusion in the number of equations can be expected.

A small extension to the above derivation is necessary to accommodate the complex case. As noted in the derivation for the time domain measure, the real and imaginary elements must be treated as independent variables present in two vectors. This approach is necessary to ensure the eigenvectors remain in conjugate pairs. Thus, if:

$$\mathbf{f}_{kj} = \alpha + j\beta \quad (5.5.162)$$

then:

$$\frac{\partial \mathbf{V}}{\partial \alpha} = \begin{bmatrix} \mathbf{0}, \dots, \mathbf{Q}_k \mathbf{e}_j, \mathbf{Q}_{k+1} \mathbf{e}_j, \dots, \mathbf{0} \end{bmatrix} \quad (5.5.163)$$

$$\frac{\partial \mathbf{V}}{\partial \beta} = \begin{bmatrix} \mathbf{0}, \dots, j\mathbf{Q}_k \mathbf{e}_j, -j\mathbf{Q}_{k+1} \mathbf{e}_j, \dots, \mathbf{0} \end{bmatrix} \quad (5.5.164)$$

Where it is assumed that the vectors of  $\mathbf{V}$  are ordered such that conjugate pairs are adjacent. Equally,

$$\frac{\partial \mathbf{E}}{\partial \alpha} = [0, \dots, \mathbf{P}_k \mathbf{e}_j, \mathbf{P}_{k+1} \mathbf{e}_j, \dots, 0] \quad (5.5.165)$$

$$\frac{\partial \mathbf{E}}{\partial \beta} = [0, \dots, j\mathbf{P}_k \mathbf{e}_j, -j\mathbf{P}_{k+1} \mathbf{e}_j, \dots, 0] \quad (5.5.166)$$

No other extensions are required to accommodate the complex case.

### The Singular Value Based Measure Eigenvalue Gradients

Compared to the time domain measure, the following eigenvalue gradient functions are less restrictive, since they do not assume the parameter vector is fixed and make no exception for coincident open and closed loop eigenvalues. The effect of adjusting an eigenvalue is that the associated allowed subspace is altered and, as a result, a different eigenvector is assigned. The assignment is succinctly expressed in the following equations:

$$\mathbf{v}_k = \mathbf{Q}_k \mathbf{Q}_k^\dagger \mathbf{v}_{d_k} \quad (5.5.167)$$

$$\mathbf{u}_k = \mathbf{P}_k \mathbf{Q}_k^\dagger \mathbf{v}_{d_k} \quad (5.5.168)$$

The derivatives of the above expressions are

$$\frac{\partial \mathbf{v}_k}{\partial \lambda_k} = \left( \mathbf{Q}_k \frac{\partial (\mathbf{Q}_k^\dagger)}{\partial \lambda_k} + \frac{\partial \mathbf{Q}_k}{\partial \lambda_k} \mathbf{Q}_k^\dagger \right) \mathbf{v}_{d_k} \quad (5.5.169)$$

$$\frac{\partial \mathbf{u}_k}{\partial \lambda_k} = \left( \mathbf{P}_k \frac{\partial (\mathbf{Q}_k^\dagger)}{\partial \lambda_k} + \frac{\partial \mathbf{P}_k}{\partial \lambda_k} \mathbf{Q}_k^\dagger \right) \mathbf{v}_{d_k} \quad (5.5.170)$$

Lemma 5.5.7 shows how  $\frac{\partial (\mathbf{Q}_k^\dagger)}{\partial \lambda_k}$  can be calculated from  $\frac{\partial \mathbf{Q}_k}{\partial \lambda_k}$  and  $\mathbf{Q}_k$ , thus it remains to calculate  $\frac{\partial \mathbf{Q}_k}{\partial \lambda_k}$  and  $\frac{\partial \mathbf{P}_k}{\partial \lambda_k}$ .  $\mathbf{P}$  and  $\mathbf{Q}$  are the solution to the following implicit equation:

$$\begin{bmatrix} \mathbf{A} - \lambda_k \mathbf{I} & \mathbf{B} \end{bmatrix} \begin{bmatrix} \mathbf{Q} \\ \mathbf{P} \end{bmatrix} = \mathbf{0} \quad (5.5.171)$$

differentiation gives:

$$\begin{bmatrix} \mathbf{A} - \lambda_k \mathbf{I} & \mathbf{B} \end{bmatrix} \frac{\partial}{\partial \lambda_k} \begin{bmatrix} \mathbf{Q}_k \\ \mathbf{P}_k \end{bmatrix} + \frac{\partial}{\partial \lambda_k} \begin{bmatrix} \mathbf{A} - \lambda_k \mathbf{I} & \mathbf{B} \end{bmatrix} \begin{bmatrix} \mathbf{Q}_k \\ \mathbf{P}_k \end{bmatrix} = \mathbf{0} \quad (5.5.172)$$

$$\begin{bmatrix} \mathbf{A} - \lambda_k \mathbf{I} & \mathbf{B} \end{bmatrix} \frac{\partial}{\partial \lambda_k} \begin{bmatrix} \mathbf{Q}_k \\ \mathbf{P}_k \end{bmatrix} + \begin{bmatrix} -\mathbf{I} & \mathbf{0} \end{bmatrix} \begin{bmatrix} \mathbf{Q}_k \\ \mathbf{P}_k \end{bmatrix} = \mathbf{0} \quad (5.5.173)$$

$$\begin{bmatrix} \mathbf{A} - \lambda_k \mathbf{I} & \mathbf{B} \end{bmatrix} \begin{bmatrix} \frac{\partial \mathbf{Q}_k}{\partial \lambda_k} \\ \frac{\partial \mathbf{P}_k}{\partial \lambda_k} \end{bmatrix} = \mathbf{Q}_k \quad (5.5.174)$$

Thus the required derivatives are given by the solution to Equation (5.5.174) which may be expressed as follows:

$$\begin{bmatrix} \frac{\partial \mathbf{Q}_k}{\partial \lambda_k} \\ \frac{\partial \mathbf{P}_k}{\partial \lambda_k} \end{bmatrix} = \begin{bmatrix} \mathbf{A} - \lambda_k \mathbf{I} & \mathbf{B} \end{bmatrix}^\dagger \mathbf{Q}_k \quad (5.5.175)$$

To calculate the complete derivative with respect to the eigenvalue, the result above must be used to evaluate Equation (5.5.169) and Equation (5.5.170) and the result must then be back-substituted into the parameter vector gradient functions.

Again, differentiation of complex eigenvalues requires that the real and imaginary parts should be treated as independent parameters that appear in two eigenvalues.

Most of the matrix calculus tools used in the preceding exposition have been collected in Lemma 5.5.1 to Lemma 5.5.7. However, for a more complete and detailed treatment the author strongly recommends the text '*Kronecker Products and Matrix Calculus*' by Alexander Graham [Gra81].

## 5.6 Mitigation of Performance Degradation

So far the robustification algorithm will improve robustness with no regard for the inevitable degradation in performance. It is an aim of this work to provide an algorithm that allows an engineer to choose a compromise between performance and robustness. It is important to appreciate that any attempt to mitigate the degradation in performance will almost certainly come at the expense of impeding the improvement in robustness. In this section the formulae necessary to implement step four and five of the robustness improvement algorithm are described.

### 5.6.1 Eigenvector Protection

The approach taken here is that, each iteration of the optimisation chooses a descent direction that is a compromise between performance protection and robustness improvement. The idea supporting

this approach is that a set of different controllers will achieve acceptable robustness, however, the controllers among this set will vary in performance. The robustness improvement algorithm needs to be guided such that it selects a controller with good performance from among those with acceptable robustness. Thus if, at each iteration, the algorithm improves robustness while minimising the degradation in performance, then the route taken to the acceptably robust controller should lead to a controller with good performance.

Performance is measured in terms of the original design goals, that is, how closely the achieved eigenvectors approximate the desired eigenvectors.

$$\phi = \|\mathbf{v}_{d_k} - \mathbf{Q}_k \mathbf{f}_k\|_2^2 \quad (5.6.176)$$

If the parameter vector  $\mathbf{f}_k$  is incrementally adjusted by  $\Delta \mathbf{f}_k$  then a first order estimate of the degradation in performance can be formulated as follows:

$$\Delta \phi \approx \left( \frac{\partial \phi}{\partial \mathbf{f}_k} \right)^* \Delta \mathbf{f}_k \quad (5.6.177)$$

$$\approx (2\mathbf{Q}_k^* \mathbf{Q}_k \mathbf{f}_k - 2\mathbf{Q}_k^* \mathbf{v}_{d_k})^* \Delta \mathbf{f}_k \quad (5.6.178)$$

Equally, if the robustness measure is denoted  $\gamma$  then the numerical or analytical partial derivatives of the robustness measure  $\left( \frac{\partial \gamma}{\partial \mathbf{f}_k} \right)$  allow the improvement in robustness to be estimated as follows:

$$\Delta \gamma \approx \left( \frac{\partial \gamma}{\partial \mathbf{f}_k} \right)^* \Delta \mathbf{f}_k \quad (5.6.179)$$

Assuming that a steepest descent algorithm is being applied then solely to optimise robustness one would adjust the parameter vector in the opposite direction to the robustness gradient.

$$\Delta \mathbf{f}_k = - \frac{\partial \gamma}{\partial \mathbf{f}_k} \quad (5.6.180)$$

Where  $\Delta \mathbf{f}_k$  would be appropriately scaled. In this implementation the parameter adjustment vector ( $\Delta \mathbf{f}_k$ ) is scaled to a length that is a fixed proportion of the current parameter vector ( $\mathbf{f}_k$ ). The line search algorithm reduces this length until a reduction in the robustness function is achieved.

Let us, for a moment, suppose that the goal of the optimisation is to improve performance. In this case, the optimum direction (in terms of steepest descent) for the parameter vector is the opposite direction to the performance function gradient:



$$\Delta \mathbf{f}_k = -\frac{\partial \phi}{\partial \mathbf{f}_k} \quad (5.6.181)$$

Thus a compromise direction can be formed from a linear combination of the of the robustness and performance function gradients:

$$\Delta \mathbf{f}_k = \left[ -\frac{\partial \phi}{\partial \mathbf{f}_k} \quad -\frac{\partial \gamma}{\partial \mathbf{f}_k} \right] \begin{bmatrix} \alpha \\ \beta \end{bmatrix} \quad (5.6.182)$$

The linear combination must fulfil the following constraints:

- The parameter adjustment vector ( $\Delta \mathbf{f}_k$ ) must be scaled to an appropriate size.
- The primary objective of the optimisation is to improve robustness. Thus the parameter adjustment vector ( $\Delta \mathbf{f}_k$ ) must be a descent direction with respect to robustness. Mathematically, that is:

$$\left( \frac{\partial \gamma}{\partial \mathbf{f}_k} \right)^* \Delta \mathbf{f}_k < 0 \quad (5.6.183)$$

To determine the precise nature of the linear combination some additional mathematical rigour is required. The principle behind the following approach is that a fixed proportion of the robustness descent ( $\Delta \gamma$ ) is sacrificed to mitigate the degradation in performance. Let us assume the parameter adjustment vector must be scaled to a fixed proportion of the current parameter vector, let the proportion be denoted  $p$  and for brevity. Let us define:

$$\nabla \gamma = -\frac{\partial \gamma}{\partial \mathbf{f}_k} \quad (5.6.184)$$

The parameter adjustment vector that achieves the maximum estimated improvement in robustness is:

$$\Delta \mathbf{f}_k = \frac{\nabla \gamma}{\|\nabla \gamma\|_2} p \|\mathbf{f}_k\|_2 \quad (5.6.185)$$

and the maximum estimated reduction in robustness is:

$$\Delta\gamma = \nabla\gamma^* \frac{\nabla\gamma}{\|\nabla\gamma\|_2} p \|\mathbf{f}_k\|_2 \quad (5.6.186)$$

$$= \|\nabla\gamma\|_2 p \|\mathbf{f}_k\|_2 \quad (5.6.187)$$

Let the compromise direction achieve a fixed proportion of the maximum estimated reduction in robustness and let the proportion be denoted by  $q$ . Again, for brevity let us define:

$$\nabla\phi = -\frac{\partial\phi}{\partial\mathbf{f}_k} \quad (5.6.188)$$

Thus the compromise parameter adjustment vector must satisfy:

$$\|\nabla\gamma\|_2 p \|\mathbf{f}_k\|_2 q = \nabla\gamma^* \begin{bmatrix} \nabla\phi & \nabla\gamma \end{bmatrix} \begin{bmatrix} \alpha \\ \beta \end{bmatrix} \quad (5.6.189)$$

and naturally, it must also satisfy the scaling constraint.

$$p \|\mathbf{f}_k\|_2 = \left\| \begin{bmatrix} \nabla\phi & \nabla\gamma \end{bmatrix} \begin{bmatrix} \alpha \\ \beta \end{bmatrix} \right\|_2 \quad (5.6.190)$$

Equation (5.6.190) and Equation (5.6.189) have an insightful geometric interpretation that leads to a simple and intuitive solution. Equation (5.6.189) is the scalar product of two vectors and thus may be expressed as follows:

$$\|\nabla\gamma\|_2 p \|\mathbf{f}_k\|_2 q = \nabla\gamma^* \begin{bmatrix} \nabla\phi & \nabla\gamma \end{bmatrix} \begin{bmatrix} \alpha \\ \beta \end{bmatrix} \quad (5.6.191)$$

$$= \|\nabla\gamma\|_2 \left\| \begin{bmatrix} \nabla\phi & \nabla\gamma \end{bmatrix} \begin{bmatrix} \alpha \\ \beta \end{bmatrix} \right\|_2 \cos(\theta_1) \quad (5.6.192)$$

Where  $\theta_1$  is the angle between the two vectors, substituting Equation (5.6.190) into Equation (5.6.192) gives:

$$\|\nabla\gamma\|_2 p \|\mathbf{f}_k\|_2 q = \|\nabla\gamma\|_2 p \|\mathbf{f}_k\|_2 \cos(\theta_1) \quad (5.6.193)$$

$$q = \cos(\theta_1) \quad (5.6.194)$$

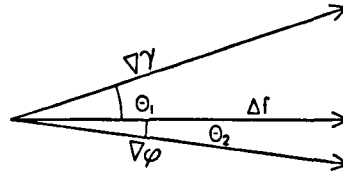


Figure 5.6.5: A geometric interpretation of performance protection.

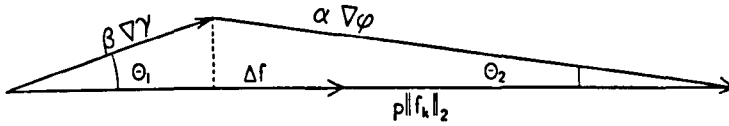


Figure 5.6.6: An illustrative geometric interpretation of performance protection.

We see that  $\theta_1$  is the maximum angle the parameter adjustment angle may deviate from the best estimated robustness improvement direction ( $\nabla\gamma$ ). Figure 5.6.5 illustrates a geometric interpretation of the problem.

From which we can see that the parameter adjustment vector must be constructed from a scaled combination of  $\nabla\gamma$  and  $\nabla\phi$ . Furthermore, the angle between  $\nabla\gamma$  and the parameter adjustment vector ( $\Delta f$ ) is fixed at  $\theta_1$ . Figure 5.6.6 is an equivalent expression of the problem and inspection leads to the following equation:

$$\alpha \|\nabla\phi\| \sin(\theta_2) = \beta \|\nabla\gamma\| \sin(\theta_1) \tag{5.6.195}$$

From Equation (5.6.195) the ratio of  $\alpha$  to  $\beta$  is easily determined and thus the direction of the compromise parameter adjustment vector. It only remains to scale the vector which is achieved as follows:

$$\Delta f_k = \frac{\begin{bmatrix} \nabla\phi & \nabla\gamma \end{bmatrix} \begin{bmatrix} \|\nabla\gamma\| \sin(\theta_1) \\ \|\nabla\phi\| \sin(\theta_2) \end{bmatrix}}{\left\| \begin{bmatrix} \nabla\phi & \nabla\gamma \end{bmatrix} \begin{bmatrix} \|\nabla\gamma\| \sin(\theta_1) \\ \|\nabla\phi\| \sin(\theta_2) \end{bmatrix} \right\|_2} p \|f_k\|_2 \tag{5.6.196}$$

It is a straightforward matter to show that the angles  $\theta_1$  and  $\theta_2$  may be calculated as follows:

$$\theta_1 = \arcsin(\sqrt{1 - q^2}) \tag{5.6.197}$$

and

$$\theta_2 = \arccos\left(\frac{\nabla\phi^*\nabla\gamma}{\|\nabla\phi\|_2\|\nabla\gamma\|_2}\right) - \theta_1 \quad (5.6.198)$$

Occasionally, it may occur that the performance direction ( $\nabla\phi$ ) already subtends the robustness direction ( $\nabla\gamma$ ) at a smaller angle than  $\theta_1$ . In which case, the parameter adjustment vector should equal the performance direction. However, Equation (5.6.196) does not accommodate this scenario and will generate a parameter adjustment vector at the angle  $\theta_1$  regardless. From Equation (5.6.198) it can be seen that this scenario implies that  $\theta_2$  is negative and thus the following simple extension will accommodate this exception:

$$\theta_2 = \begin{cases} \theta_2 & \theta_2 \geq 0, \\ 0 & \theta_2 < 0 \end{cases} \quad (5.6.199)$$

In practice it was observed that, initially,  $\nabla\gamma$  is often very small which may lead to numerically unreliable performance directions. This is because, the initial parameters are optimised for performance and a property of the optimal design is that the derivative of the performance measure with respect to the design parameters will be zero.

Equally, if the robustness optimisation begins to converge before achieving acceptable robustness. As the optimal solution is approached, the robustness improvement direction may become very small and thus numerically unreliable.

## 5.6.2 Eigenvalue Protection

The eigenvalue locations have a significant and usually dominant affect on the system performance. To protect their contribution to performance, a constrained line search is employed. This simply confines each eigenvalue to an allowed region. The allowed regions are formulated as discs around the original desired locations.

## 5.7 Further Work

While the robustness improvement algorithm has proved an effective tool there is certainly scope to develop the algorithm further and investigate alternative approaches. A fundamental limitation of the existing algorithm is that it only improves stability robustness. Although considerable effort is applied to ensure that the robust design achieves good nominal performance, it is only guaranteed that stability will be maintained in the face of the uncertainty. The performance may well become

unacceptable before instability sets in. Thus some possible extensions to performance robustness are indicated.

### 5.7.1 Development of the Robustness Improvement Algorithm

Most of the possible developments listed in this section are natural extensions to the existing algorithm.

1. Currently, a steepest descent algorithm is employed. Unfortunately these algorithms show poor convergence near the optimum point. While it is envisaged that the algorithm should not proceed to the optimum point, since this would indicate a poor compromise between performance and robustness. A Quasi Newton method, such as DFP [Wal75] may improve the convergence of the algorithm, both initially and near the optimum point. However, the Quasi Newton method will also require an improved line search algorithm. The current algorithm successively reduces the step size until a reduction in the cost function is achieved. The Quasi Newton algorithms require a line search that finds the point along the descent direction that not only reduces the cost function but also that minimises the cost function. Common line search algorithms include; bisection, Fibonacci and Gold Section searches, however, interpolation approaches such as Davidon's or Powell's have often proven the most effective [Gra89].
2. The approximate analytical gradients developed for the time domain robustness measure are based on some simplifying assumption. However, the development of the a singular value robustness measure gradients indicates how these assumptions may be removed at the expense of a more complicated final expression. This may represent a worthwhile development if, in other applications, the approximate gradients, prove unreliable.
3. As mentioned in Section 5.6, for initial iterations of the robustness improvement algorithm the performance direction is often numerically unreliable. This could be overcome by using a second order estimate of the performance degradation as shown in Equation (5.7.200).

$$\Delta\phi = (2\mathbf{Q}_k^* \mathbf{Q}_k \mathbf{f}_k - 2\mathbf{Q}_k^* \mathbf{v}_{d_k})^* \Delta\mathbf{f}_k + \Delta\mathbf{f}_k^* (\mathbf{Q}_k^* \mathbf{Q}_k) \Delta\mathbf{f}_k \quad (5.7.200)$$

Where  $\Delta\phi$  is the incremental change in performance,  $\mathbf{Q}_k$  is the allowed eigenvector subspace,  $\mathbf{v}_{d_k}$  is the desired eigenvector,  $\mathbf{f}_k$  is the current parameter vector and  $\Delta\mathbf{f}_k$  is incremental adjustment to the parameter vector.

Although, for initial iterations the first term is small a reliable estimate of the change in performance will be provided by the second quadratic term. However, to incorporate this development it will be necessary to re-work how the compromise direction is calculated.

4. Currently, the improvement of the singular value based measure occurs at a single peak frequency value. It often occurs that there is more than one dominant frequency point and that reducing one peak alone causes the others to increase. Thus a successful optimisation may have to consider more than one peak simultaneously. The robustness improvement algorithm can be easily extended to find more than one peak and the parameter gradient at each peak. However, the resulting optimisation problem is more complicated and may be formulated as a constrained optimisation, where the dominant peak is reduced subject to the parameter adjustment vector being a descent direction with respect to the peaks. Alternatively, the problem may be formulated as a multi-objective minimisation.
5. The singular value based measure used in this work is a straightforward approximation to the structured singular value. However, the structured singular value has been topic of considerable research and several extensions have been developed; for instance, to encompass real [FTD91] and unstable [FP88] uncertainty. These extensions (particularly real uncertainty) could be incorporated into the robustness improvement algorithm. This would require development of new gradient expressions.

### 5.7.2 Extension to Performance Robustness

The structured singular value already provides a method of guaranteeing performance robustness. If the performance criterion can be expressed as a bound on the peak value of a weighted transfer function spectral norm, as would be formulated for an  $\mathcal{H}_\infty$  problem, the uncertainty model may be augmented to include this criterion. In this case, the main loop theorem [PD89, PD93, BPDG93, SD91, DFT92] allows the resultant structured singular value to be bounded such that the performance bound will be satisfied for all variations of the given uncertainty description. This approach to performance robustness does not require any further development of the robustness improvement algorithm. However, it does require that the design goals are re-expressed as frequency domain bounds, which is incongruous with the proposed design methodology, since performance robustness would be achieved with respect to different design goals than those used to synthesise the controller. Furthermore, if the design criterion can be accurately expressed as frequency domain bounds, the original decision to use eigenstructure assignment is undermined.

Two pieces of work have been identified that could form the basis for a performance robustness approach that employs the design goals used by the original controller synthesis.

Apkarian [Apk88] proposes an extension to the structured single value that allows robustness to be formulated in terms of the poles of the system remaining in non-intersection closed regions. At a simplistic level the bound works as follows: the conventional structured single value searches along the  $j\omega$ -axis and indicates if a pole would cross this boundary. Apkarian's extension searches along the contours of the closed regions and consequently indicates if a pole would exit a closed region. A drawback of this extension is that it assumes the uncertainty has poles within the specific closed region. This is equivalent to the conventional assumption that the uncertainty is stable. It would be

a straightforward matter to incorporate Apkarian's extensions into the current robustness improvement algorithm. The peak search routine should be re-written to follow a given contour rather than only searching along the  $j\omega$ -axis.

Yedavalli and Ashokkumar [YA94] develop some singular value based robustness measures, that bound time domain uncertainty such that the poles of the system will remain in specified closed regions. They also extend the work to consider the degree to which the eigenvectors may change direction. This work could be incorporated into the robustness improvement algorithm but would require development of new analytical gradients. A drawback of this approach is that it does not explicitly consider unmodelled dynamics.

## 5.8 References

- [AM89] BDO Anderson and JB Moore. *Optimal Control and Linear Quadratic Methods*. Information and System Sciences Series. Prentice-Hall International Inc., 1989.
- [Apk88] P Apkarian. A helicopter controller design using eigenspace techniques and structured robustness. In *Helicopter Handling Qualities and Control Workshop Proceedings*, pages 13.1–13.13, 4 Hamilton Place, London, W1V 0BQ, November 1988. The Royal Aeronautical Society.
- [Apk89] P Apkarian. Structured stability robustness improvement by eigenspace techniques: A hybrid methodology. *Journal of Guidance, Control and Dynamics*, 12(2):162–168, March 1989.
- [BDG94] JD Blight, RL Dailey, and D Gangsaas. Practical control law design for aircraft using multivariable techniques. *Int. Journal of Control*, 59(1):93–137, January 1994.
- [BIG74] A Ben-Israel and NE Greville. *Generalised Inverses: Theory and Applications*. A Wiley-Interscience publication. John Wiley and Sons, Inc., 1974.
- [Bod47] HW Bode. *Network Analysis and Amplifier Design*. D. Van Nostrand Company Inc., New York, 250 Fourth Avenue, 1947.
- [BPDG93] G Balas, A Packard, JC Doyle, and K Glover.  *$\mu$ -Analysis and Synthesis Toolbox*. The MathWorks Inc., 24 Prime Park Way, Natick, Mass. 01760-1500, July 1993.
- [Bur90] SP Burrows. *Robust Control Design Techniques using Eigenstructure Assignment*. PhD thesis, University of York, Heslington, York, England, YO3-5DD, September 1990.
- [BYDM94] RP Braatz, PM Young, JC Doyle, and M Morari. Computational complexity of  $\mu$  calculation. *IEEE Trans. on Automatic Control*, 39(5):1000–1002, May 1994.
- [CFL81] JB Cruz, JS Freudenberg, and DP Looze. A relationship between sensitivity and stability of multivariable feedback system. *IEEE Trans. on Automatic Control*, 26(1):66–74, February 1981.
- [CW87] BS Chen and CC Wong. Robust linear controller design: Time domain approach. *IEEE Trans. on Automatic Control*, 32(2):161–164, February 1987.
- [Dai91] RL Dailey. Lecture notes for the workshop on  $\mathcal{H}_\infty$  and  $\mu$  methods. 30th IEEE Conf. on decision and control, IEEE, Brighton, December 1991.
- [Dav94] R Davies. *Robust Eigenstructure Assignment for Flight Control Applications*. DPhil, University of York, Heslington, York, YO1 5DD, England, 1994.
- [DFT92] JC Doyle, BA Francis, and AR Tannenbaum. *Feedback Control Theory*. Maxwell Macmillan International, 1992.
- [Doy82] JC Doyle. Analysis of feedback systems with structured uncertainty. *IEE Proceedings D*, 129(6):242–250, November 1982.
- [DS81] JC Doyle and G Stein. Multivariable feedback design: Concepts for a classical/modern synthesis. *IEEE Trans. on Automatic Control*, 26(1):4–16, February 1981.
- [DW80] CA Desoer and YT Wang. On the Generalised Nyquist Stability Criterion. *IEEE Trans. on Automatic Control*, 25(2):187–196, April 1980.

- [FP88] YK Foo and I Postlethwaite. Extensions of the small- $\mu$  for robust stability. *IEEE Trans. on Automatic Control*, 33(2):172–176, February 1988.
- [FPEN91] GF Franklin, JD Powell, and A Emami-Naeini. *Feedback Control of Dynamic Systems*. Addison-Wesley Series in Electrical and Computer Engineering: Control Engineering. Addison-Wesley Publishing Company, 2nd edition, 1991.
- [FTD91] MKH Fan, AL Tits, and JC Doyle. Robustness in the presence of mixed parametric uncertainty and unmodelled dynamics. *IEEE Trans. on Automatic Control*, 36(1):25–38, January 1991.
- [Gar89] S Garg. Stability Robustness Improvement of Direct Eigenspace Assignment Based Feedback Systems Using Singular Value Sensitivities. Technical Report Rep. No. 182302, NASA, Sverdrup Technology, Inc., NASA Lewis Research Group, Cleveland, Ohio, August 1989.
- [Gil84] EG Gilbert. Conditions for minimizing the norm sensitivity of characteristic roots. *IEEE Trans. on Automatic Control*, 29(7):658–660, July 1984.
- [GJ81] S Gutman and EI Jury. A general theory for matrix root-clustering in subregions of the complex plane. *IEEE Trans. on Automatic Control*, 26(4):853–862, August 1981.
- [GL] M Green and DJN Limebeer. Robust linear control. A new book on modern control that is soon to be published.
- [GL83] GH Golub and CF Van Loan. *Matrix Computations*. John Hopkins University Press, 1983.
- [GLLT90] A Grace, AJ Laub, JN Little, and C Thompson. *Control System Toolbox for use with Matlab: User Guide*. The MathWorks, Inc, South Natick, MA 01760, October 1990.
- [Gra81] A Graham. *Kronecker Products and Matrix Calculus With Applications*. Ellis Horwood Limited, 1981.
- [Gra87] A Graham. *Nonnegative Matrices and Applicable Topics in Linear Algebra*. Mathematics and its Applications. Ellis Horwood Limited, Market Cross House, Cooper Street, Chichester, West Sussex, PO19 1EB, England, 1987.
- [Gra89] A Grace. *Computer-Aided Control System Design Using Optimization Methods*. PhD thesis, University of Wales, Bangor, 1989.
- [Gra95] A Grace. *Opimization Toolbox: For Use with Matlab*. The MathWorks Inc., 24 Prime Park Way, Natick, Mass. 01760-1500, April 1995.
- [HJ91] RA Horn and CR Johnson. *Topics in Matrix Analysis*. Cambridge University Press, 1991.
- [Hor85] RA Horn. *Matrix Analysis*. Cambridge University Press, The Pitt Building, Trumpington Street, Cambridge, 1985.
- [IS90] M Innocenti and C Stanzola. Performance-robustness trade-off of eigenstructure assignment applied to rotorcraft. *Aeronautical Journal*, 94(934):124–131, 1990.
- [Jef89] A Jeffrey. *Mathematics for Engineers and Scientists*. Van Nostrand Reinhold (International), 11 New Fetter Lane, London, EC4P 4EE, England, 4th edition, 1989.
- [Jua91] YT Juang. Robust stability and robust assignment of linear systems with structured uncertainty. *IEEE Trans. on Automatic Control*, 36(5):635–637, May 1991.
- [Kai80] T Kailath. *Linear Systems*. Prentice-Hall, Inc., 1980.
- [KBH88] LH Keel, SP Bhattacharyya, and J Howze. Robust control with structured perturbations. *IEEE Trans. on Automatic Control*, 33(1):68–78, January 1988.
- [KND85] J Kautsky, NK Nichols, and P Van Dooren. Robust pole assignment in linear state feedback. *Int. Journal of Control*, 41(5):1129–1155, 1985.
- [KP82] B Kouvaritakis and I Postlethwaite. Principal gains and phases:insensitive robustness measures for assessing the closed-loop stability property. *IEE Proceedings D*, 129(6):233–241, November 1982.
- [Kwa93] H Kwakernaak. Robust control and  $\mathcal{H}_\infty$ -optimization: Tutorial paper. *Automatica*, 29(2):255–273, 1993.
- [LCL+81] NA Lehtomaki, D Castanon, B Levy, G Stein, NR Sandell, and M Athans. Robustness tests utilizing the structure of the modelling error. In *Proceedings of 20th IEEE conference of Decision and Control*, pages 1173–1190, San Diego, CA, December 1981. IEEE.
- [Lee82] WH Lee. Robustness analysis for state space models. Technical Report Report TP-151, Alphatech Inc., 1982.
- [LSA81] NA Lehtomaki, NR Sandell, and M Athans. Robustness results in linear-quadratic gaussian based multivariable control designs. *IEEE Trans. on Automatic Control*, 26(1):75–92, February 1981.
- [Mac89] JM Maciejowski. *Multivariable Feedback Design*. Electronic Systems Engineering. Addison Wesley, 1989.
- [MN84] V Mukhopadhyay and JR Newsom. A multiloop system stability margin using matrix singular values. *Journal of Guidance, Control and Dynamics*, 7(5):582–587, September 1984.



- [Moo81] BC Moore. Principal component analysis in linear systems: Controllability, observability, and model reduction. *IEEE Trans. on Automatic Control*, 26(1):17–32, February 1981.
- [MP77] AGJ MacFarlane and I Postlethwaite. The generalised Nyquist stability criterion and multivariable root loci. *Int. Journal of Control*, 25(1):81–127, 1977.
- [MP88] SK Mudge and RJ Patton. Analysis of the technique of robust eigenstructure assignment with application to aircraft control. *IEE Proceedings D*, 135(4):275–281, July 1988.
- [MSJ79] AGJ MacFarlane and DFA Scott-Jones. Vector gain. *Int. Journal of Control*, 29(1):65–91, 1979.
- [Muk87] V Mukhopadhyay. Stability robustness improvement using constrained optimization techniques. *Journal of Guidance, Control and Dynamics*, 10(2):172–177, March 1987.
- [ND84] NK Nichols and P Van Dooren. Robust pole assignment and optimal stability margins. *Electronic Letters*, 20(16):660–661, August 1984.
- [NM85] JR Newsom and V Mukhopadhyay. A multiloop robust controller design study using singular value gradients. *Journal of Guidance, Control and Dynamics*, 8(4):514–519, July 1985.
- [Pad96] GD Padfield. *Helicopter Flight Dynamics*. Blackwell Science Ltd, 1996.
- [PC72] B Porter and R Crossley. *Modal Control*. Taylor and Francis Ltd, 1972.
- [PD89] A Packard and JC Doyle. Draft excerpts from their forthcoming book on  $\mu$ . It appears the book may never have reached the publishers, 1989.
- [PD93] A Packard and JC Doyle. The complex structured singular value. *Automatica*, 29(1):71–109, 1993.
- [PEM81] I Postlethwaite, JM Edmunds, and AGJ Macfarlane. Principal gains and principal phases in the analysis of linear multivariable feedback systems. *IEEE Trans. on Automatic Control*, 26(1):32–46, February 1981.
- [PL94] RJ Patton and GP Liu. Robust control design via eigenstructure assignment, genetic algorithms and gradient-based optimisation. *IEE Proceedings D*, 141(3):202–207, May 1994.
- [Pro90] RW Prouty. *Helicopter Performance Stability, and Control*. Robert E. Krieger Publishing Company, 1990.
- [PT80] RV Patel and M Toda. Quantitative measures of robustness for multivariable systems. In *Proc. Joint Automat. Contr. Conf.*, pages paper TP8–A, San Francisco, Ca, 1980.
- [PTS77] RV Patel, M Toda, and B Sridhar. Robustness of linear-quadratic state feedback designs in the presence of system uncertainty. *IEEE Trans. on Automatic Control*, 22:945–949, 1977.
- [RS70] HH Rosenbrock and C Storey. *Mathematics of Dynamical Systems*. Thomas Nelson and Sons Ltd, 1970.
- [SA77] MG Safonov and M Athans. Gain and phase margin for multiloop LQG regulators. *IEEE Trans. on Automatic Control*, 22(2):173–178, April 1977.
- [SA87] G Stein and M Athans. The LQG/LTR procedure for multivariable feedback control design. *IEEE Trans. on Automatic Control*, 32(2):105–114, February 1987.
- [Saf82] MG Safonov. Stability margins of diagonally perturbed multivariable feedback systems. *IEE Proceedings D*, 126(6):251–256, November 1982.
- [SATC86] P S $\phi$ gaard-Andersen, E Trostmann, and F Conrad. A singular value sensitivity approach to robust eigenstructure assignment. In *Proc. of 25th Conference on Decision and Control*, pages 121–126. IEEE, December 1986.
- [SBY89a] KM Sobel, SS Banda, and HH Yeh. Robust control for linear systems with structured state space uncertainty. *Int. Journal of Control*, 50(5):1991–2004, 1989.
- [SBY89b] KM Sobel, SS Banda, and HH Yeh. Structured state space robustness with connection to eigenstructure assignment. In *Proceeding of the American Control Conference*, pages 966–973, Pittsburgh PA, June 1989. American Automatic Control Council.
- [SD91] G Stein and JC Doyle. Beyond singular values and loop shapes. *Journal of Guidance, Control and Dynamics*, 14(1):5–16, January 1991.
- [SGLL81] NR Sandell, SW Gully, WH Lee, and NA Lehtomaki. Multivariable stability margins for vehicle flight control systems. In *Proceedings of the IEEE Conference on Decision and Control*, pages 1479–1483, New York, 1981. IEEE.
- [SLH81] MG Safonov, AJ Laub, and GL Hartman. Feedback properties of multivariable systems: The role of the return difference matrix. *IEEE Trans. on Automatic Control*, 26(1):47–65, February 1981.
- [SSA94] KM Sobel, EY Shapiro, and AN Andry. Eigenstructure assignment. *Int. Journal of Control*, 59(1):13–37, 1994.
- [SYP+92] KM Sobel, W Yu, JE Piou, JR Cloutier, and R Wilson. Robust eigenstructure assignment with structured state-space uncertainty and unmodelled dynamics. *International Journal of Systems Science*, 23(5):565–788, 1992.

- [TV90] A Tesi and A Vicino. Robust stability of state-space models with structured uncertainties. *IEEE Trans. on Automatic Control*, 25(2):191–195, February 1990.
- [Vic89] A Vicino. Robustness of pole locations in perturbed systems. *Automatica*, 25(1):109–113, 1989.
- [Vid93] M Vidyasagar. *Nonlinear Systems Analysis*. Prentice-Hall Int., 1993.
- [Wal75] GR Walsh. *Methods of Optimization*. John Wiley and Sons, 1975.
- [WCY91] RF Wilson, JR Cloutier, and RK Yedavalli. Control design for robust eigenstructure assignment in linear uncertain systems. In *Proceeding of the 30<sup>th</sup> Conference on Decision and Control*, pages 2982–2987, Brighton, England, December 1991. IEEE.
- [Web92] K Webers. Control of a single-rotor helicopter using eigenstructure assignment. Control Research Group Technical Report, University of York, Heslington, York, Y01-5DD, England, September 1992.
- [Wil65] JH Wilkinson. *The algebraic eigenvalue problem*. Oxford University Press, 1965.
- [Wis92] KA Wise. Comparison of six robustness tests evaluating missile autopilot robustness to uncertain aerodynamics. *Journal of Guidance, Control and Dynamics*, 15(4):861–869, July 1992.
- [YA94] RK Yedavalli and CR Ashokkumar. Eigenstructure perturbation in disjointed domains for linear systems with structured uncertainty. In *Proceedings of the AIAA Conference on Guidance and Control*, pages 358–367. AIAA, May 1994.
- [Yed85] RK Yedavalli. Perturbation bounds for robust stability in linear state space models. *Int. Journal of Control*, 42(6):1507–1517, 1985.
- [Yed93a] RK Yedavalli. Flight control application of new stability robustness bounds for linear uncertain systems. *Journal of Guidance, Control and Dynamics*, 16(6):1032–1037, November 1993.
- [Yed93b] RK Yedavalli. Robust Root Clustering for Linear Uncertain Systems Using Generalized Lyapunov Theory. *Automatica*, 29(1):237–240, 1993.
- [YL86a] RK Yedavalli and Z Liang. Reduced conservatism in stability robustness bounds by state transformation. *IEEE Trans. on Automatic Control*, 31(9):863–865, September 1986.
- [YL86b] RK Yedavalli and Z Liang. Reduced Conservatism in Stability Robustness Bounds by State Transformation. *IEEE Trans. on Automatic Control*, 31(9):863–865, 1986.
- [YPS91] W Yu, JE Piou, and KM Sobel. Robust eigenstructure assignment for the extended range air to air missile. In *Proceeding of the 30<sup>th</sup> Conference on Decision and Control*, pages 2976–2981, Brighton, England, December 1991. IEEE.
- [YS91] W Yu and KM Sobel. Robust eigenstructure assignment with structured state space uncertainty. *Journal of Guidance, Control and Dynamics*, 14(30):621–628, May 1991.
- [Zam81] G Zames. Feedback and optimal sensitivity: Model reference transformations, multiplicative seminorms, and approximate inverses. *IEEE Trans. on Automatic Control*, 26(2):301–320, April 1981.
- [ZK87] K Zhou and PP Khargonekar. Stability robustness for linear state-space models with structured uncertainty. *IEEE Trans. on Automatic Control*, 32(7):621–623, July 1987.

# Chapter 6

## Design Example

### Contents

---

6.1 A State Feedback Control Law . . . . .	230
6.2 An Output Feedback Control Law . . . . .	247
6.3 Summary . . . . .	284

---

This chapter presents a design example for attitude stabilisation of a Lynx helicopter in hover. The example is not intended as a definitive solution but illustrates some of the tools and techniques described in this Thesis.

### 6.1 A State Feedback Control Law

Although state feedback is not realistic for helicopter control law design it does have a role to play in the development of the more practical fixed gain output feedback solution. The state feedback solution illustrates the best that one can *hope* to achieve with output feedback. If an acceptable state feedback solution can not be found then progression to output feedback is pointless and one should instead re-examine the synthesis technique and design objectives.

The initial state feedback solution is derived using simple projection and fixed eigenvalue locations. At this stage, it is hoped that more powerful techniques are not necessary to achieve the design goals. The desired eigenstructure derived in Section 3.5.4 was employed with the following ideal eigenvalue locations:

$\lambda_p$	$\lambda_v$	$\lambda_q$	$\lambda_u$	$\lambda_w$	$\lambda_r$
$-1.5 \pm j1.6$	$-0.004$	$-1.5 \pm j1.6$	$-0.002$	$-0.33$	$-1.75$

Table 6.1.1: Desired eigenvalue locations for a helicopter in hover (see Section 3.5.2)

The velocity eigenvalue locations ( $\lambda_v, \lambda_u$ ) were chosen to coincide with the open loop zeros. The heave mode ( $\lambda_w$ ) is left at its open loop location and the yaw mode ( $\lambda_r$ ) is the mid point of the criterion given in Equation (3.5.64). The open loop system is given in Appendix A.2 and the resulting gain matrix is:

$$\mathbf{x} = \begin{bmatrix} u & v & w & p & q & r & \phi & \theta \end{bmatrix}$$

$$\begin{bmatrix} A_1 \\ B_1 \\ \theta_0 \\ \theta_t \end{bmatrix} = \begin{bmatrix} -0.0013 & 0.0004 & 0 & 0.0525 & -0.0361 & -0.0002 & -0.0383 & -0.0034 \\ 0.0008 & 0 & -0.0001 & -0.0398 & 0.0743 & 0.0058 & -0.0015 & 0.2450 \\ 0 & 0 & 0 & 0 & 0.0007 & -0.0002 & 0.0062 & -0.0052 \\ 0.0001 & 0.0011 & 0.0004 & -0.0576 & 0.0154 & 0.1911 & -0.0807 & 0.0103 \end{bmatrix}$$

The gain values are generally small. This is often a good indication of a sensible feedback solution. The roll and pitch response to a 10% one second pulse in the longitudinal and lateral channels is shown in Figure 6.1.1, along with a template that illustrates the Def-Stan handling qualities criteria (see Section 3.3). Starting from left to right the criteria depicted by the template are:

1. The gate at 0.5s represents the initial delay and over-sensitivity criteria ( $y_1$ ).
2. The rising vertical line, which coincides with peak response, indicates the minimum value of the peak response. For a larger amplitude response the maximum value is shown as a horizontal line.
3. The gate one second after the peak response this embodies the 30% decay criteria ( $T_{30}$ ).
4. The coincident drop in the lower bound represents the first trough ( $x_1$ ) and steady state settling criteria ( $X_F$ ).
5. The descending vertical line serves to check that a zero crossing occurs in the 1-2 second window after the peak response ( $T_{01}$ ).
6. Finally the lower upper bound also represents the steady state settling criteria ( $T_F, X_F$ ).

A new template must be calculated for each response since most of the gates are defined relative the peak value and time. The applied handling qualities criteria are for the attentive phase because the helicopter is in the hover and the control law provides attitude command (see Section 3.3). Different criteria are required for the roll and pitch channels, although in this case the only difference is the bounds for the peak response value. Unless otherwise indicated the template described above will be applied to the appropriate output responses. Returning to Figure 6.1.1 we see that the responses pass comfortably between the all the gates and thus clearly meet the level one handling qualities criteria.

The cross-coupling into off-axis rates and attitudes is minimal. In both cases the off-axis rates were less than 0.5 deg/s and the attitudes less than 0.1 degrees. Figure 6.1.2 depicts the on-axis and off-axis attitude responses to the lateral and longitudinal stick inputs applied previously.

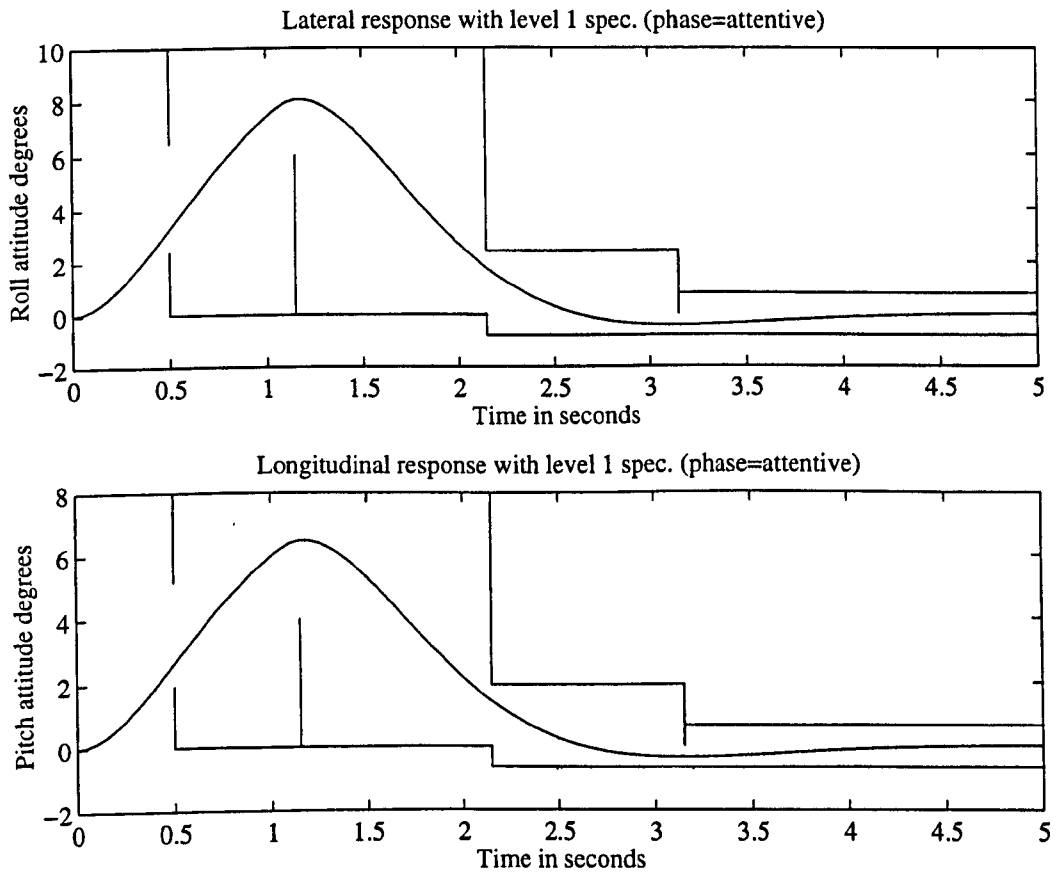


Figure 6.1.1: Roll attitude response (top) to a lateral and pitch attitude response (bottom) to a longitudinal pulse input of 10% for one second of an 8<sup>th</sup> order linear helicopter model at hover with state feedback control.

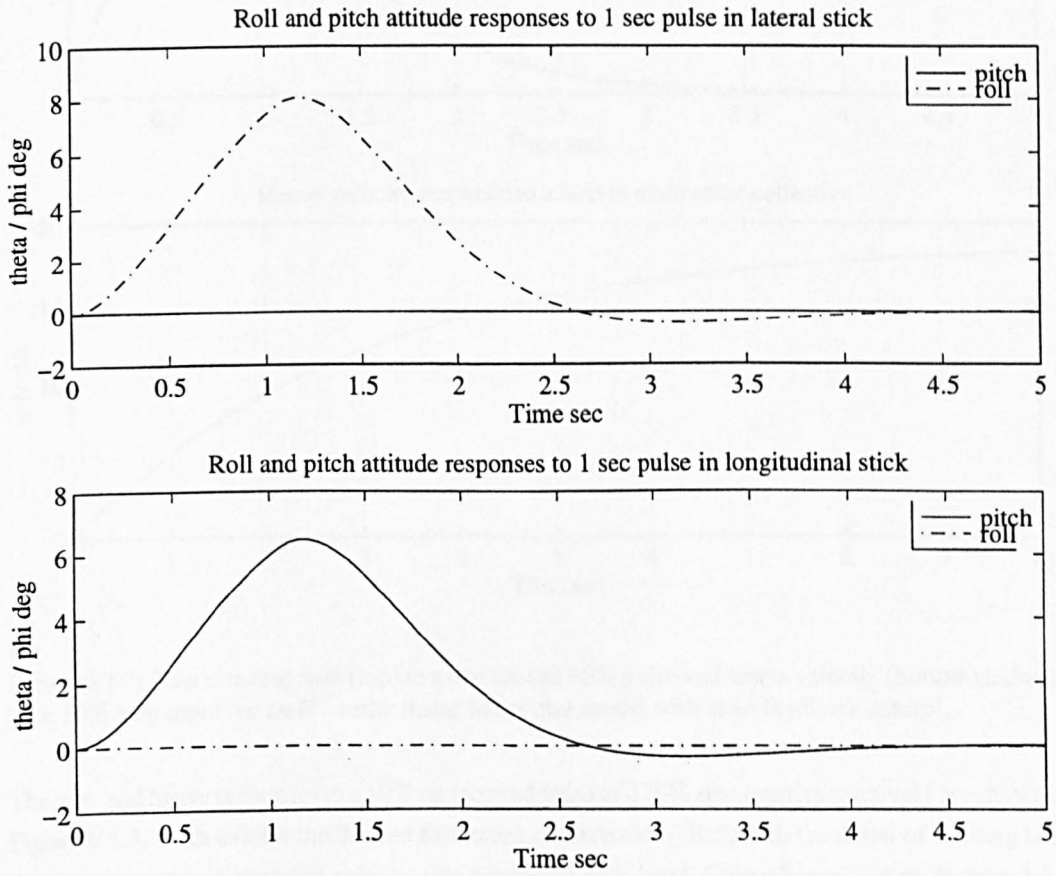


Figure 6.1.2: On and off axis attitude responses (roll and pitch) to a 10% one second lateral (top) and longitudinal (bottom) pulse input for an 8<sup>th</sup> order linear helicopter model at hover with state feedback control.

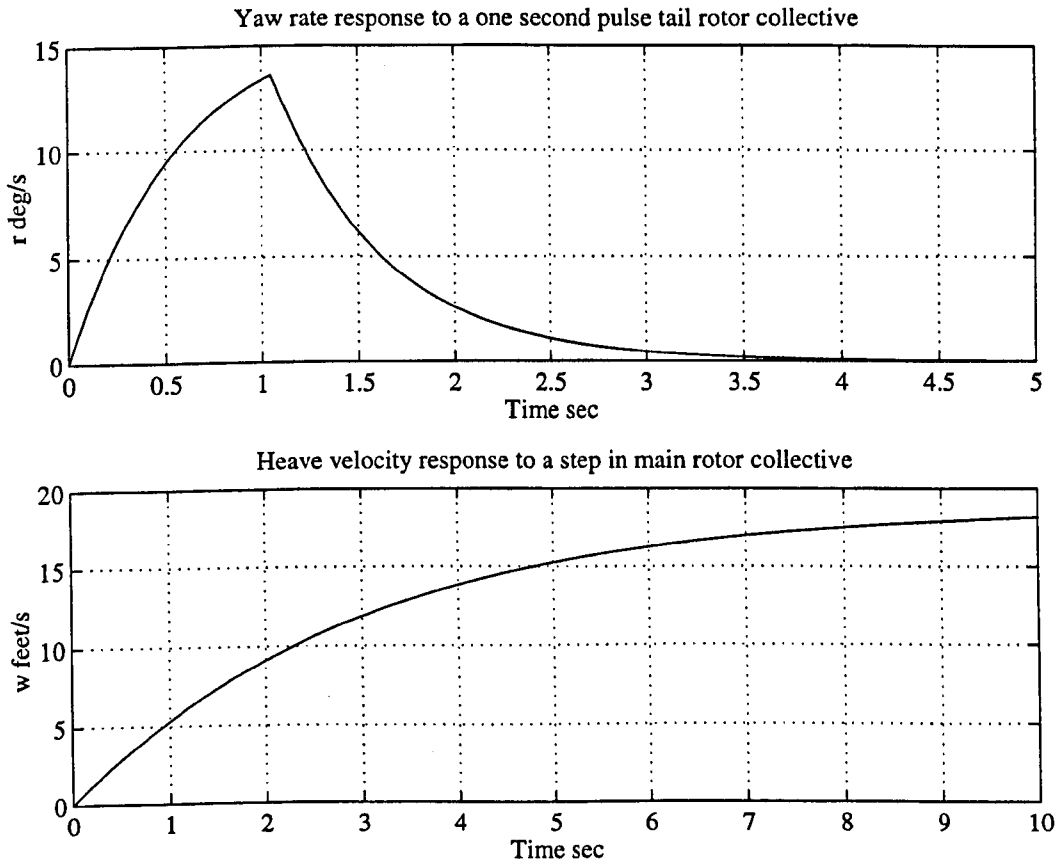


Figure 6.1.3: Yaw rate response (top) to a one second 10% pulse and heave velocity (bottom) induced by a 10% step input for an 8<sup>th</sup> order linear helicopter model with state feedback control.

The yaw and heave responses to a 10% one second pulse and 10% step input respectively are shown in Figure 6.1.3. Both exhibit the desired first order characteristic. Before the addition of heading hold the yaw response is aimed to achieve rate command with level 2 compliance. From Section 3.5.3 we recall that the peak response should be between  $5 - 20^\circ/s$ , greater than 30% at 0.5s and have decayed to 10% peak value between 1 – 2s after the peak response. Inspection shows that the yaw response achieves all these criteria. The criteria for the heave response were drawn from the ADS 33 (see Section 3.2 and Section 3.5.3) and stipulate that the response should have a time constant less than 5 seconds and initial delay less than 0.2 seconds. The response shown in Figure 6.1.3 has no initial delay and a time constant of  $\approx 2.8s$  thus clearly meets the level one criteria.

The results from the state feedback controller are very good. However, this simplified problem uses the reduced 8<sup>th</sup> order model and full feedback information. Thus it may be expected to give good results. To promote confidence in the solution it is worth checking performance with the full 12<sup>th</sup> or-

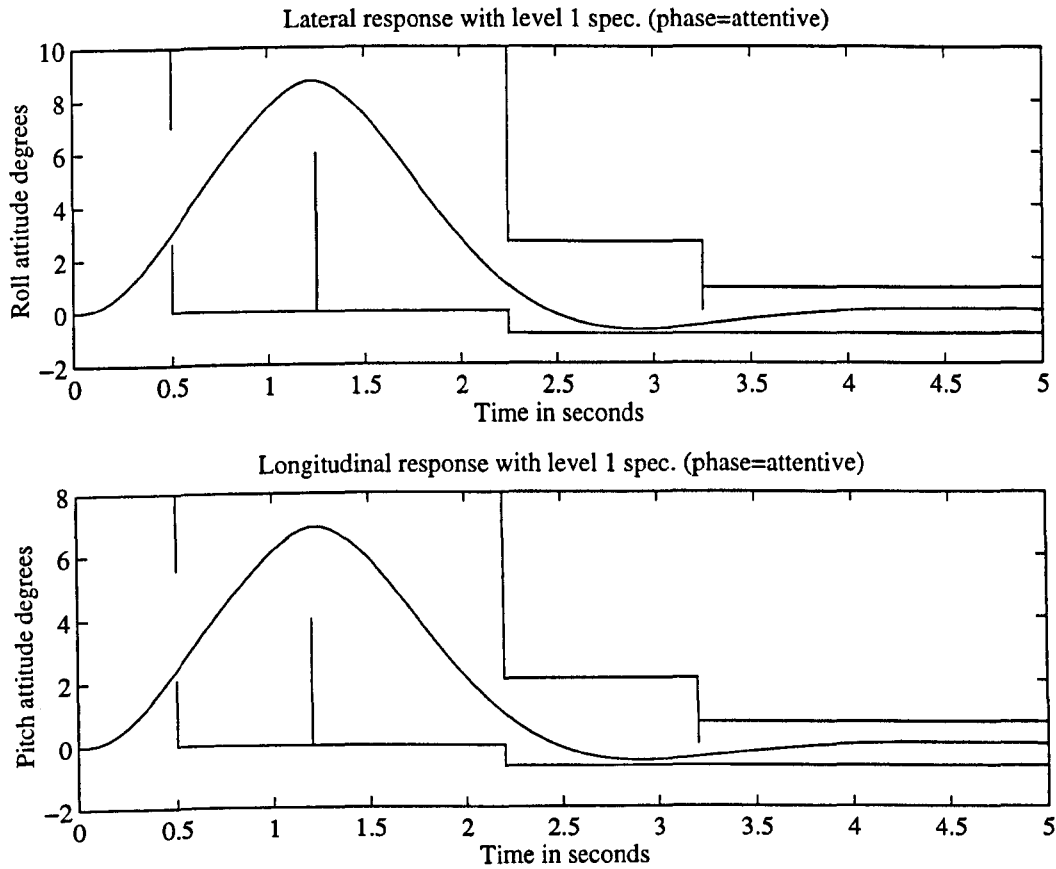


Figure 6.1.4: Roll attitude response (top) to a lateral and pitch attitude response (bottom) to a longitudinal pulse input of 10% for one second of a 12<sup>th</sup> order linear helicopter model at hover with state feedback control.

der model. Figure 6.1.4 shows the lateral and longitudinal responses to a one second pulse with the usual Def-Stan template. The rotor dynamics can be seen to have introduced some initial delay, reduced the system damping and increased the response frequency. Despite these effects the responses still meet the Level one criteria.

In Section 3.5.2 it was established that the response damping was dependent on the real part of the complex eigenvalues. Thus moving the eigenvalues to the left should increase the damping and improve the response. Figure 6.1.5 shows the lateral and longitudinal responses for the pole locations of  $1.7 \pm j1.6$ . The responses show improved damping, which demonstrates a visible link between performance and the desired eigenstructure.

So far no attention has been paid to robustness. The multivariable gain and phase margins are given in Table 6.1.2, they show that the nominal state feedback solution offers very poor robustness.



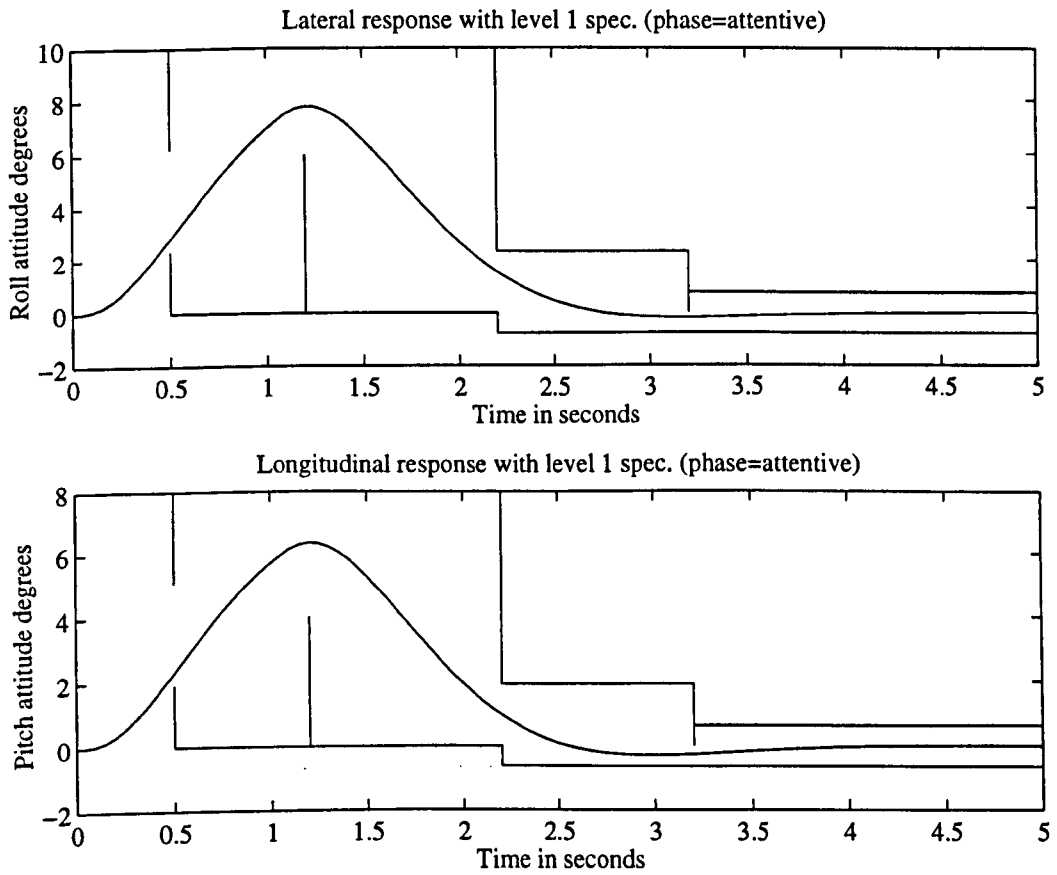


Figure 6.1.5: Roll attitude response (top) to a lateral and pitch attitude response (bottom) to a longitudinal pulse input of 10% for one second of a 12<sup>th</sup> order linear helicopter model at hover with a revised state feedback control law.

	Input	Output
Gain Margin	-0.25 dB, 0.25dB	-0.24 dB, 0.24dB
Phase Margin	-1.6°, 1.6°	-1.5°, 1.5°

Table 6.1.2: Multivariable gain and phase margins at the input and output of an 8<sup>th</sup> order linear helicopter model with the initial state feedback control law.

It is instructive to apply the robustness improvement algorithm to the initial state feedback solution, since this will establish an upper limit that any output feedback solution is very unlikely to exceed. It also provides a good opportunity to demonstrate the performance protection properties of the robustness improvement algorithm. For expedience<sup>1</sup>, the input gain and phase margins are optimised using the bilinear uncertainty structure. An initial optimisation was performed using no performance protection other than confining the eigenvalues to disks with radius of 0.1 centred around the assigned locations. The optimisation was then repeated with the algorithm set to sacrifice fifty percent of robustness improvement to eigenvector performance protection (see Section 5.6).

	Without protection		With protection	
	Input	Output	Input	Output
Gain Margin	-4.53 dB, 3.73 dB	-1.18 dB, 1.17 dB	-3.18 dB, 3.18 dB	-3.18dB, 2.55 dB
Phase Margin	-23.45°, 23.45°	-7.26°, 7.26°	-20.54°, 20.54°	-17.65°, 17.65°

Table 6.1.3: Multivariable gain and phase margins at the input and output of an 8<sup>th</sup> order linear helicopter model with input robustness optimised (singular value measure) control laws employing zero and 50% performance protection.

Table 6.1.3 shows that, as expected, the optimisation without protection achieves better input robustness margins and in fact reduced  $\mu$  to a value of 4.84. The input margins achieved by the optimisation with protection are comparable and correspond to a value for  $\mu$  of 5.52. Interestingly, the algorithm with protection achieves better output margins. This may be because the algorithm without protection is more focused on input robustness.

The gain matrix for the solution with protection is:

<sup>1</sup>The computational time to estimate the structured singular value increases with the number of uncertainty blocks. An input based optimisation uses four uncertainty blocks whereas an output based one will use eight.

$$\mathbf{x} = \begin{bmatrix} u & v & w & p & q & r & \phi & \theta \end{bmatrix}$$

$$\begin{bmatrix} A_1 \\ B_1 \\ \theta_0 \\ \theta_t \end{bmatrix} = \begin{bmatrix} -0.0013 & 0.0003 & 0 & 0.0500 & -0.0362 & -0.0007 & -0.0440 & -0.0040 \\ 0.0005 & 0 & 0 & -0.0385 & 0.0773 & 0.0085 & 0.0002 & 0.2536 \\ 0 & 0 & 0 & -0.0021 & 0.0011 & -0.0001 & 0.0051 & -0.0044 \\ 0.0002 & 0.0006 & 0.0004 & -0.0871 & 0.0159 & 0.1871 & -0.1608 & -0.0007 \end{bmatrix}$$

and equally, the gain matrix for the solution without protection is:

$$\mathbf{x} = \begin{bmatrix} u & v & w & p & q & r & \phi & \theta \end{bmatrix}$$

$$\begin{bmatrix} A_1 \\ B_1 \\ \theta_0 \\ \theta_t \end{bmatrix} = \begin{bmatrix} -0.004 & 0.4401 & -0.1495 & 61.33 & -44.99 & 0.000 & -60.48 & -0.4230 \\ -0.0843 & -0.0055 & -0.0097 & -0.070 & -17.46 & 0.354 & 32.064 & -54.60 \\ -0.0277 & 0.0211 & -0.0001 & 0.000 & -0.6628 & 0.8193 & 1.836 & -1.914 \\ -0.2836 & 0.0315 & -0.0767 & 16.56 & 6.627 & -15.07 & 10.28 & 0.000 \end{bmatrix}$$

Figure 6.1.6 and Figure 6.1.7 show the roll and pitch attitude responses, along with the usual Def-Stan template, of the robustified state feedback control law with and without performance protection. The response for the algorithm with protection is noticeably better although, as expected, both responses have suffered some degradation due to robustification.

Figure 6.1.8 and Figure 6.1.9 show the on-axis and off-axis attitude responses that accompany Figures 6.1.7 and 6.1.6. The plots demonstrate that performance protection has done a lot to preserve the decoupling action of the controller.

Figure 6.1.10 and Figure 6.1.11 show the yaw and heave response, to a one second pulse and step input respectively. The heave response is largely unaffected by robustification. The yaw response has degraded due to robustification but considerably less so for the solution produced by algorithm with performance protection.

Although the response of the linear velocities is not explicitly specified for the attitude command response type, examination of these responses is important and helpful in evaluating the performance of the control law. Figure 6.1.12 and Figure 6.1.13 show the linear velocity responses that accompany Figures 6.1.7 and 6.1.6. The plots confirm that performance protection is effective in preserving the general decoupling properties of the controller.

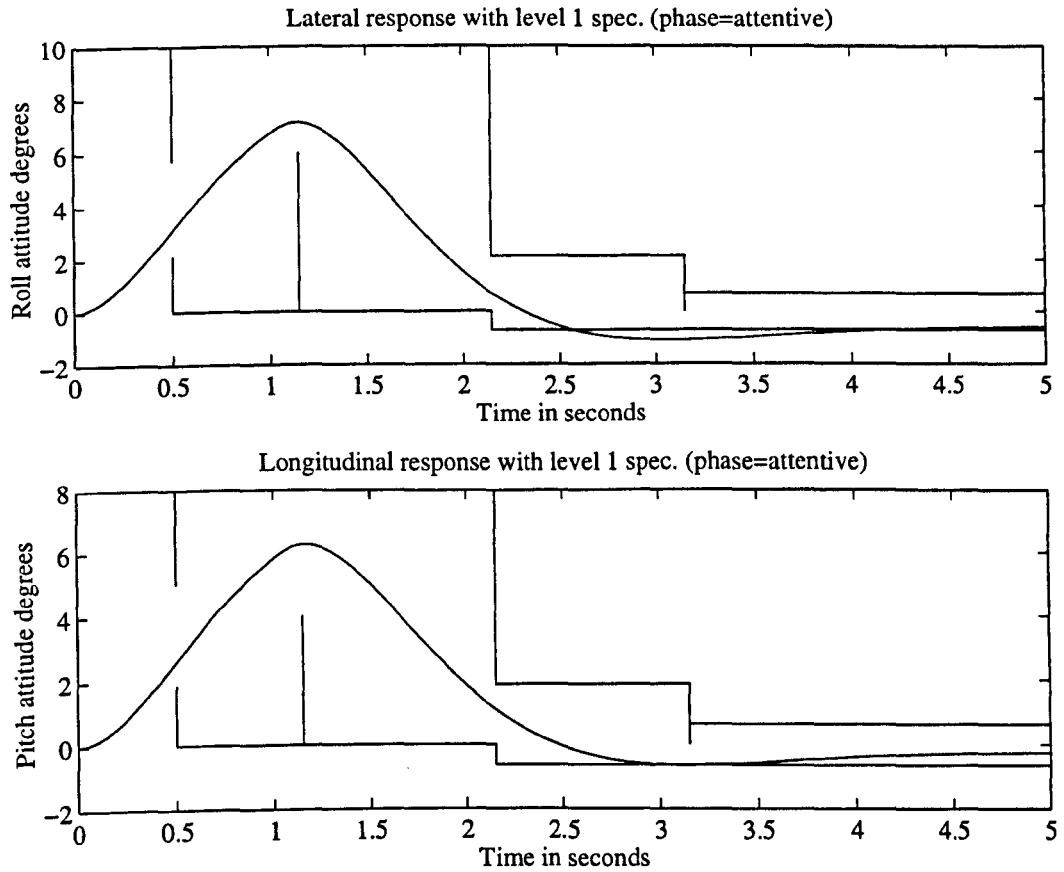


Figure 6.1.6: Roll attitude response (top) to a lateral and pitch attitude response (bottom) to a longitudinal pulse input of 10% for one second of an 8<sup>th</sup> order linear helicopter model at hover with a robustified state feedback control law employing performance protection.

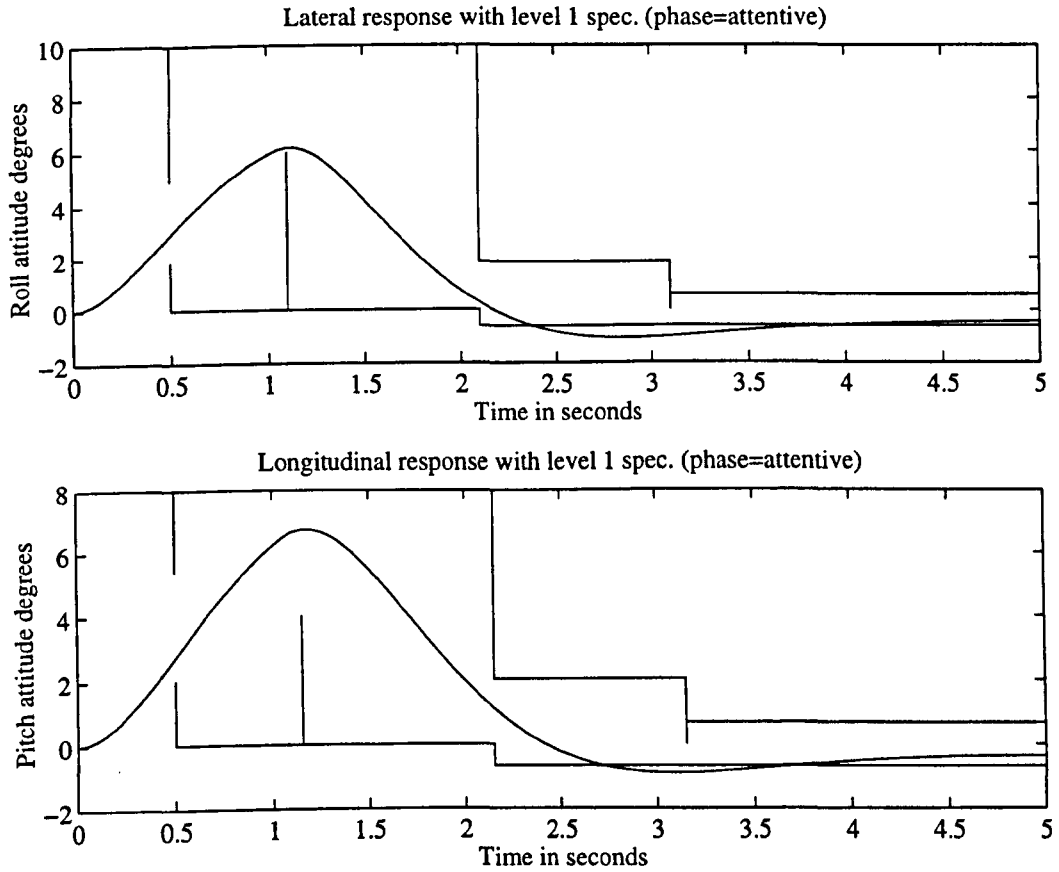


Figure 6.1.7: Roll attitude response (top) to a lateral and pitch attitude response (bottom) to a longitudinal pulse input of 10% for one second of an 8<sup>th</sup> order linear helicopter model at hover with a robustified state feedback control law *not* employing performance protection.

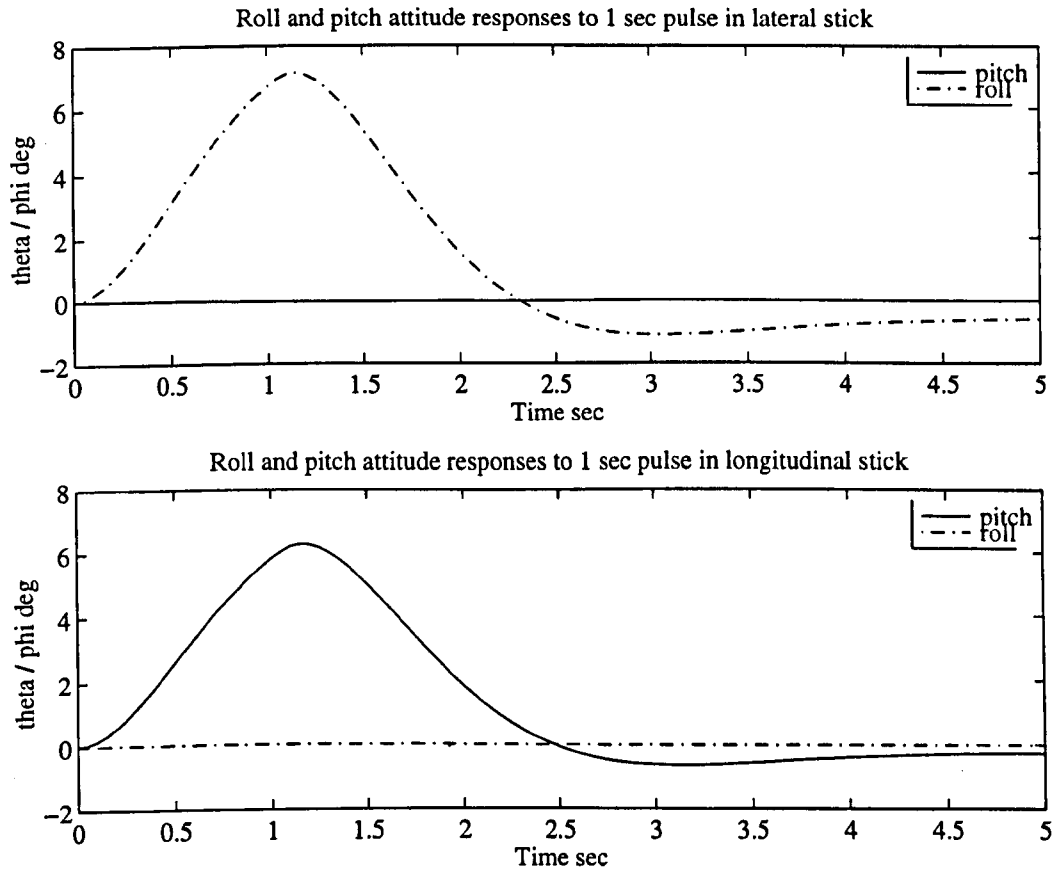


Figure 6.1.8: On and off axis attitude responses (roll and pitch) to a 10% one second lateral (top) and longitudinal (bottom) pulse input for an 8<sup>th</sup> order linear helicopter model at hover with robustified feedback control employing performance protection.

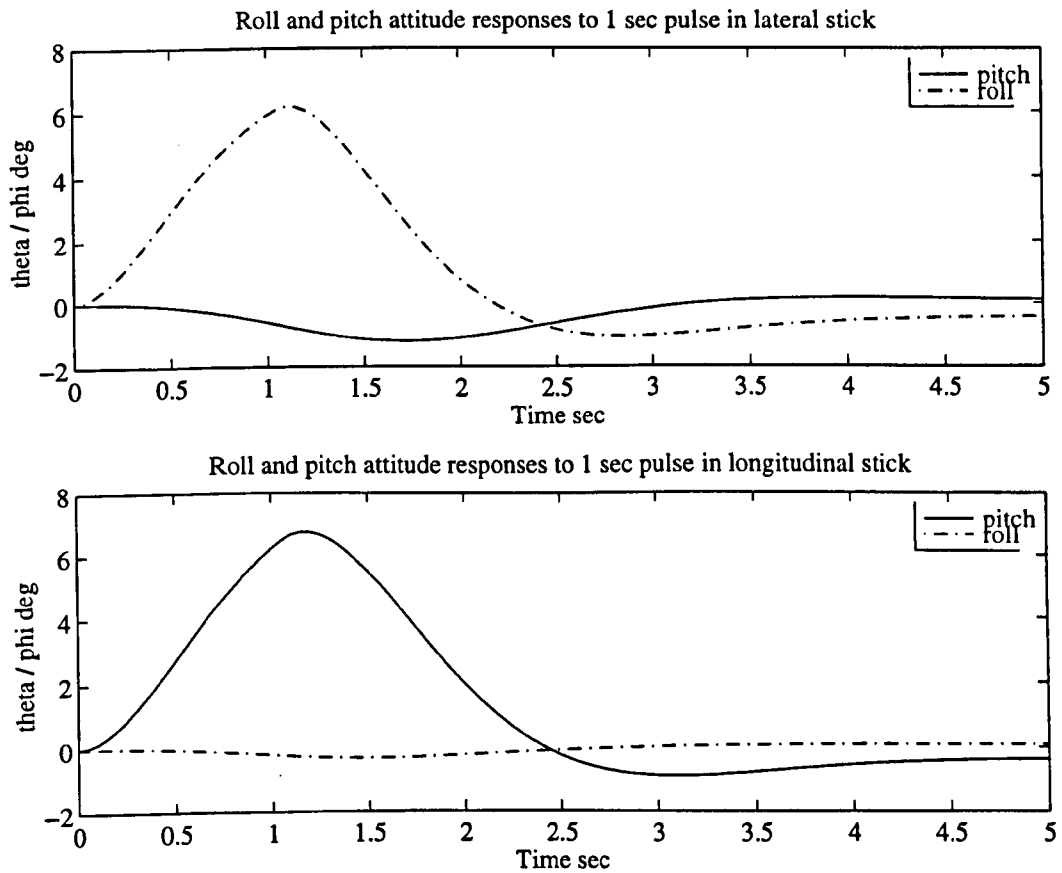


Figure 6.1.9: On and off axis attitude responses (roll and pitch) to a 10% one second lateral (top) and longitudinal (bottom) pulse input for an 8<sup>th</sup> order linear helicopter model at hover with robustified feedback control *not* employing performance protection.

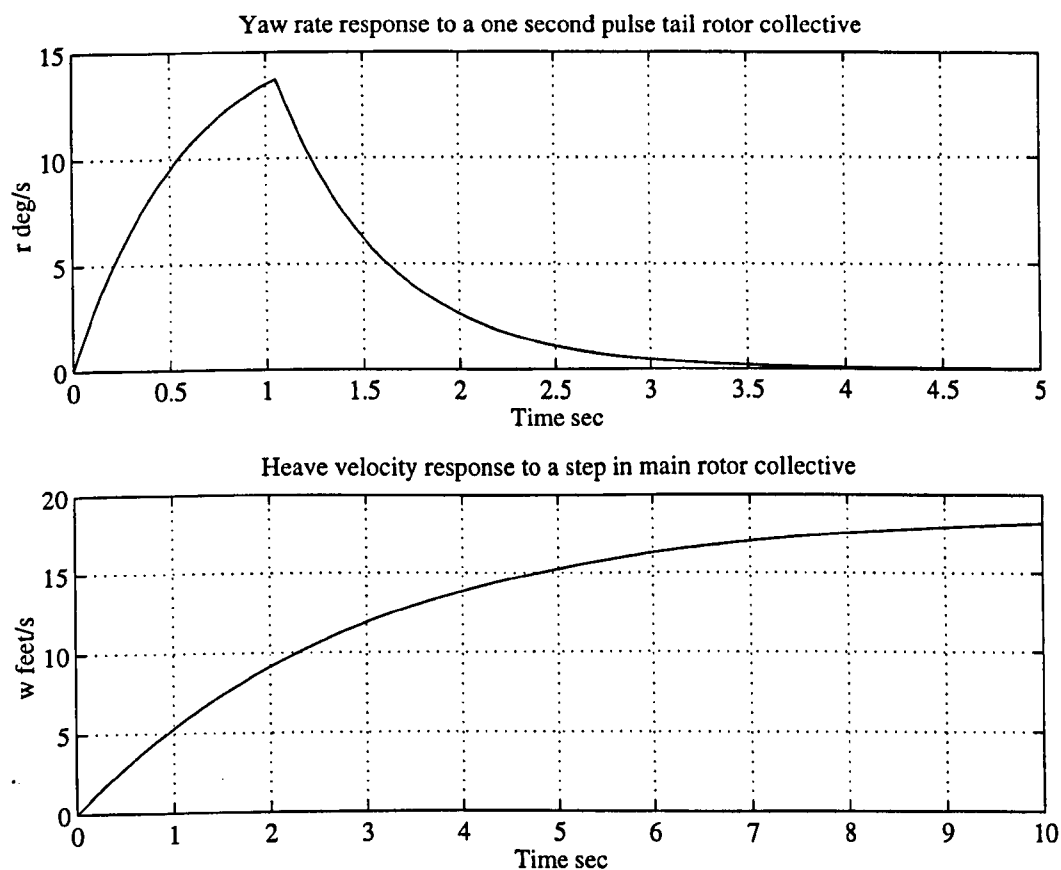


Figure 6.1.10: Yaw rate response (top) to a one second 10% pulse and heave velocity (bottom) induced by a 10% step input for an 8<sup>th</sup> order linear helicopter model with robustified state feedback control produced employing performance protection.



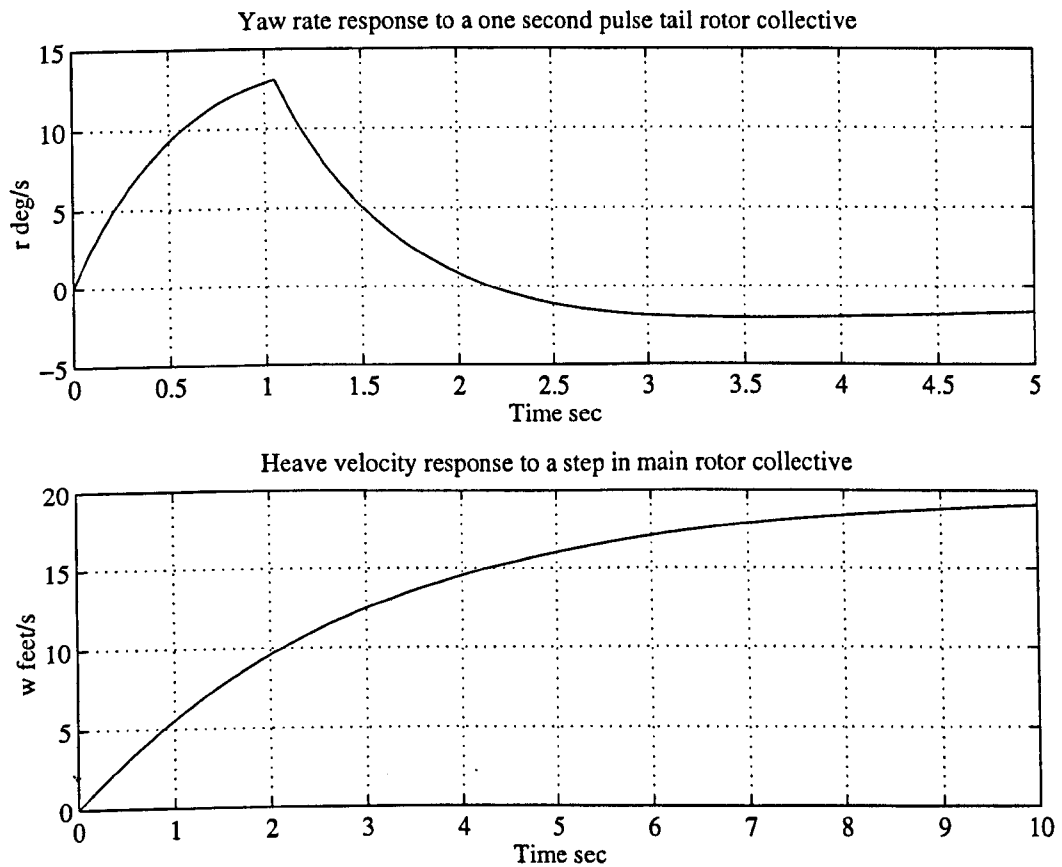


Figure 6.1.11: Yaw rate response (top) to a one second 10% pulse and heave velocity (bottom) induced by a 10% step input for an 8<sup>th</sup> order linear helicopter model with robustified state feedback control produced *without* performance protection.

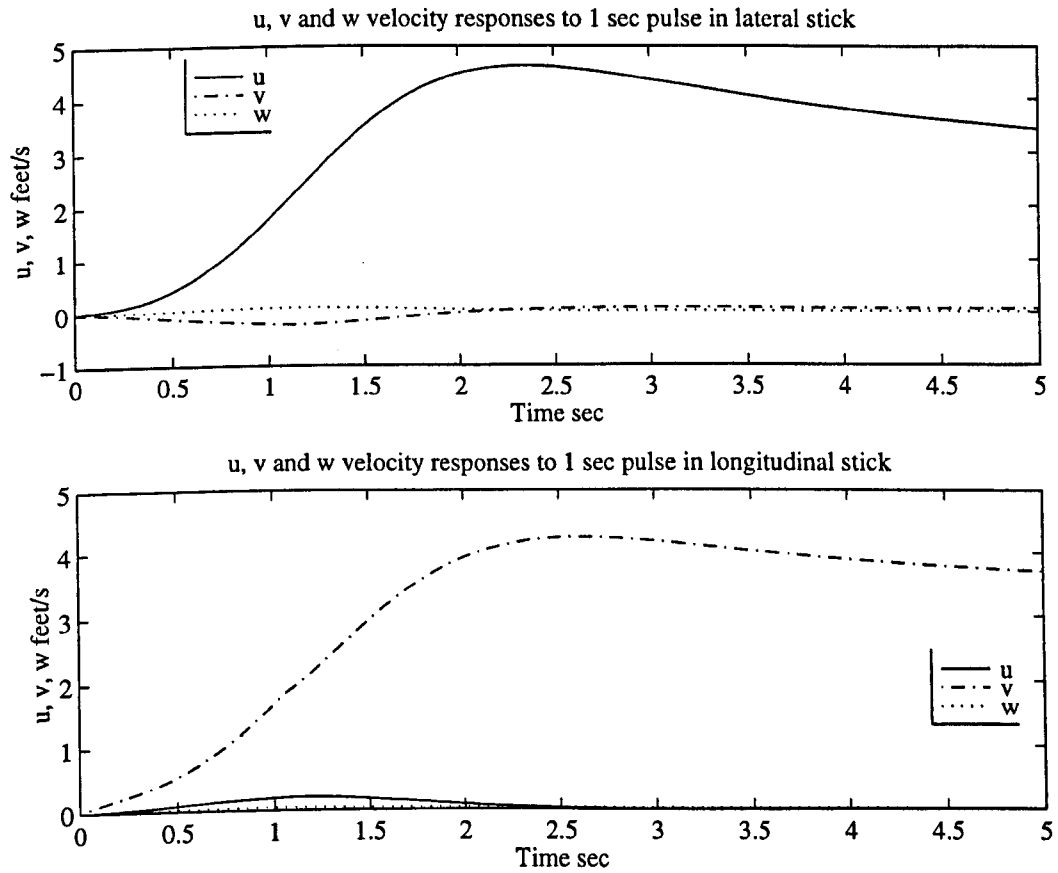


Figure 6.1.12: Linear velocity responses ( $u$ ,  $v$ ,  $w$ ) to a one second 10% pulse for an 8<sup>th</sup> order linear helicopter model with robustified state feedback control produced with performance protection.

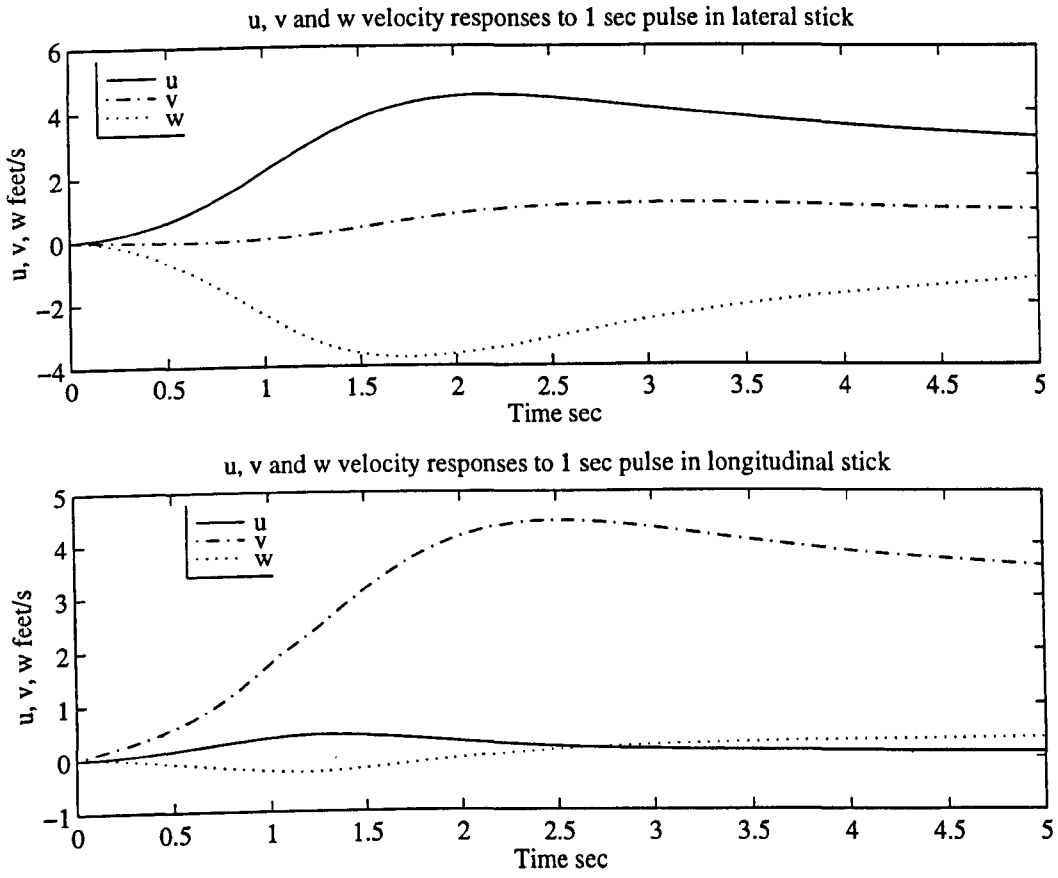


Figure 6.1.13: Linear velocity responses ( $u, v, w$ ) to a one second 10% pulse for an 8<sup>th</sup> order linear helicopter model with robustified state feedback control produced *without* performance protection.

## 6.2 An Output Feedback Control Law

The first task of the output feedback design is to decide which variables are available for measurement. Some of the variables indicated at this stage may later be removed from the design. However, initially, it is important to include as many variables as possible. For the helicopter it is common practice to measure  $p, q, r, \theta, \phi$  and, although requiring some additional estimation functions,  $\dot{h}$  is often also available. Naturally, forward airspeed is also measured ( $u$ ) but the measurement is generally very inaccurate at low air speeds making it unsuitable as a feedback variable for a hover control law. The following equation shows how  $\dot{h}$  may be derived from existing states.

$$\dot{h} = \sin(\theta)u - \cos(\theta) \sin(\phi)v - \cos(\theta) \cos(\phi)w \quad (6.2.1)$$

For the hover trim condition  $\theta = 3.4^\circ$  and  $\phi = 3.3^\circ$ , thus for the linear model  $\dot{h}$  may be approximated as follows:

$$\dot{h} \approx \begin{bmatrix} 0.057 & 0.057 & -1.0 \end{bmatrix} \begin{bmatrix} u \\ v \\ w \end{bmatrix} \quad (6.2.2)$$

Before commencing with the details of the output feedback design it worth examining the role of the now unavailable feedback variables in the state feedback solution. This can be done by seeing how the relevant gain elements modify the stability derivatives of the open loop model.

Derivative	A	BK	Derivative	A	BK
$Z_u$	0.0278	-0.0278	$Z_v$	0.0000	0.0000
$L_u$	0.1678	-0.1678	$L_v$	-0.0564	0.0564
$M_u$	0.0158	-0.0158	$M_v$	-0.0001	0.0001
$N_u$	0.0298	-0.0298	$N_v$	-0.0015	0.0015

Table 6.2.4: The change in key linear velocity stability derivatives due to state feedback.

Table 6.2.4 shows that feedback of the linear velocities is used to counteract their influence on the angular rates. Therefore without feedback of the linear velocities, it can be expected that decoupling of the velocity modes from the lateral and longitudinal modes will be difficult.

We note that with four input variables and six output variables complete assignment is possible and that 24 DoF exist. Firstly, one must decide how many stages to employ and what order to assign the eigenvectors. An important factor in this decision is the distribution of design freedom, Table 6.2.5 lists some of the possibilities.

Option	Stage 1		Stage 2		Stage 3		Retro-stage	
	Vectors	DoF	Vectors	DoF	Vectors	DoF	Vectors	DoF
1	4 right	12	4 left	4	-	-	-	-
2	5 right	15	3 left	0	-	-	1	1
3	2 left	10	6 right	6	-	-	-	-
4	3 left	15	5 right	0	-	-	1	1
5	4 right	12	2 left	2	2 right	2	-	-
6	3 right	9	3 left	6	2 right	0	1	1

Table 6.2.5: A list of some of the multistage assignment possibilities for a six output, four input, eighth order helicopter model.

For this application stages with zero DoF are best avoided. Since eigenvectors assigned in these stages are effectively prescribed by those assigned in the previous stages. Therefore to alter these vectors one must assign different vectors in the previous stages, which offers no design visibility. In this application, options one, three and five were considered.

A second important decision is the whether to perform the assignment in the state space i.e with eigenvectors or in the input and output spaces. In this case, the state space and output spaces are almost coincident. The state space additionally contains  $u, v$  and has  $w$  instead of  $\dot{h}$ . Although,  $u, v$  are not measurable outputs they are system outputs and we do wish to assign which modes appear in these outputs. Hence assignment of right eigenvectors was conducted in the state space. However, assignment of left eigenvectors was conducted in the input space.

Since we have a full set of desired right eigenvectors, a set of orthogonal desired left eigenvectors can be created by inverting the right eigenvector matrix. To generate the desired input coupling vectors the desired left eigenvectors are multiplied by an idealised input matrix, which is shown below:

$$\begin{bmatrix} u \\ v \\ w \\ p \\ q \\ r \\ \phi \\ \theta \end{bmatrix} = \begin{bmatrix} 0 & 0 & 0 & 0 \\ 0 & 0 & 0 & 0 \\ 0 & 0 & 1 & 0 \\ 1 & 0 & 0 & 0 \\ 0 & 1 & 0 & 0 \\ 0 & 0 & 0 & 1 \\ 0 & 0 & 0 & 0 \\ 0 & 0 & 0 & 0 \end{bmatrix} \begin{bmatrix} A_1 \\ B_1 \\ \theta_0 \\ \theta_t \end{bmatrix} \tag{6.2.3}$$

Next one must decide which vectors to assign in which stages. Assignment of an input coupling vector effectively determines which columns of the transfer function matrix a mode will appear. While this can ensure that a mode is excited by a single input, it may still appear in several unwanted outputs. Equally, assignment of an output coupling vector determines in which rows of the transfer function

matrix a mode will appear. Again, this can ensure a mode only appears in one output but it may be excited by inappropriate inputs. Assignment of input or output coupling vectors alone is not sufficient to guarantee complete decoupling and some experimentation with the assignment of input or output coupling vectors may be necessary to get the best results.

In this case, the right eigenvectors associated with  $p, \phi$  and  $q, \theta$  have been formulated to achieve a specific zero structure and are thus best assigned as output vectors. The eigenvectors associated with  $w$  and  $r$  are formulated to achieve decoupling and may be assigned as either input or output vectors. The right eigenvectors associated with the linear velocity modes present a problem. Ideally they would be assigned as output vectors to ensure the velocity modes only appear in the velocity outputs. However, consider the feedback output matrix ( $C$ ):

$$\begin{bmatrix} h \\ p \\ q \\ r \\ \phi \\ \theta \end{bmatrix} = \begin{bmatrix} 0.057 & 0.057 & -1.0 & 0 & 0 & 0 & 0 & 0 \\ 0 & 0 & 0 & 1 & 0 & 0 & 0 & 0 \\ 0 & 0 & 0 & 0 & 1 & 0 & 0 & 0 \\ 0 & 0 & 0 & 0 & 0 & 1 & 0 & 0 \\ 0 & 0 & 0 & 0 & 0 & 0 & 1 & 0 \\ 0 & 0 & 0 & 0 & 0 & 0 & 0 & 1 \end{bmatrix} \begin{bmatrix} u \\ v \\ w \\ p \\ q \\ r \\ \phi \\ \theta \end{bmatrix} \quad (6.2.4)$$

and the desired linear velocity eigenvectors:

$$\mathbf{v}_u^T = \begin{bmatrix} 1 & 0 & 0 & 0 & 0 & 0 & 0 & 0 \end{bmatrix} \quad (6.2.5)$$

$$\mathbf{v}_v^T = \begin{bmatrix} 0 & 1 & 0 & 0 & 0 & 0 & 0 & 0 \end{bmatrix} \quad (6.2.6)$$

It is clear that assignment of the right eigenvectors ( $\mathbf{v}_u, \mathbf{v}_v$ ) or the equivalent output vectors is ill conditioned. This is because, output feedback is being used to make the velocity modes unobservable in the measured outputs and observability is an invariant property of output feedback. As the modes become less observable, they are harder to control and the gain value magnitudes quickly explode. The lack of linear velocity feedback has obvious control implications. These are not obscured by the eigenstructure assignment technique and, indeed, have a clear interpretation. One approach to this problem is to assign the linear velocity modes as left eigenvectors. This is unlikely to achieve the desired decoupling, but will avoid an ill-conditioned problem.

Three candidate assignment options (1, 3, 5) were identified in Table 6.2.5 and all three options were briefly evaluated. Option five produced inferior results to options one and three, and was discarded. Option one was performed, assigning the modes  $p, \phi, q$  and  $\theta$  as right eigenvectors in stage one and assigning  $u, v, w$  and  $r$  as input vectors in stage two. The resulting gain matrix is given below:

$$\begin{bmatrix} A_1 \\ B_1 \\ \theta_0 \\ \theta_t \end{bmatrix} = \begin{bmatrix} 0.0082 & 0.0541 & -0.0440 & -0.0656 & -0.0371 & -0.0420 \\ 0 & -0.0410 & 0.0772 & 0.0575 & -0.0019 & 0.2626 \\ 0 & 0 & 0.0012 & -0.0002 & 0.0059 & -0.0031 \\ 0.0199 & -0.0534 & 0.0124 & 0.0183 & -0.0849 & -0.0174 \end{bmatrix} \begin{bmatrix} \dot{h} \\ p \\ q \\ r \\ \phi \\ \theta \end{bmatrix} \quad (6.2.7)$$

Figure 6.2.14 shows the roll and pitch attitude responses to a one second 10% pulse along with the usual Def-Stan template. Both comfortably meet the level one requirements. However, Figure 6.2.15 shows the corresponding on and off-axis attitudes from which it can be seen that the longitudinal motion couples very efficiently into roll.

The accompanying linear velocities depicted in Figure 6.2.16 paint a similar picture of poor cross-coupling performance.

The heave and yaw responses to a step input and one second pulse are shown in Figure 6.2.17. They show a poor steady state error in the yaw response and a divergent height mode due to cross-coupling with the linear velocities.

It is clear that, while the primary responses are acceptable, the cross-couplings require some attention.

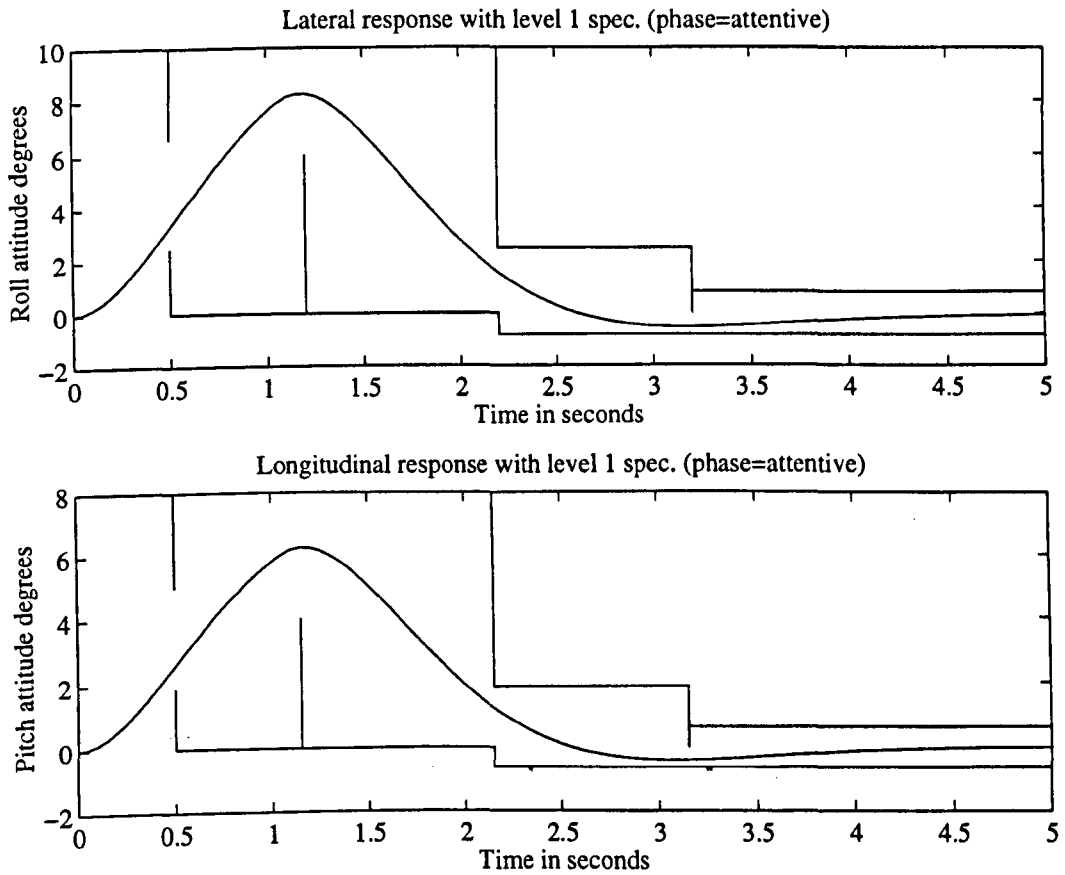


Figure 6.2.14: Roll attitude response (top) to a lateral and pitch attitude response (bottom) to a longitudinal pulse input of 10% for one second of an 8<sup>th</sup> order linear helicopter model at hover with an output feedback control law synthesized according to option *one* of Table 6.2.5.



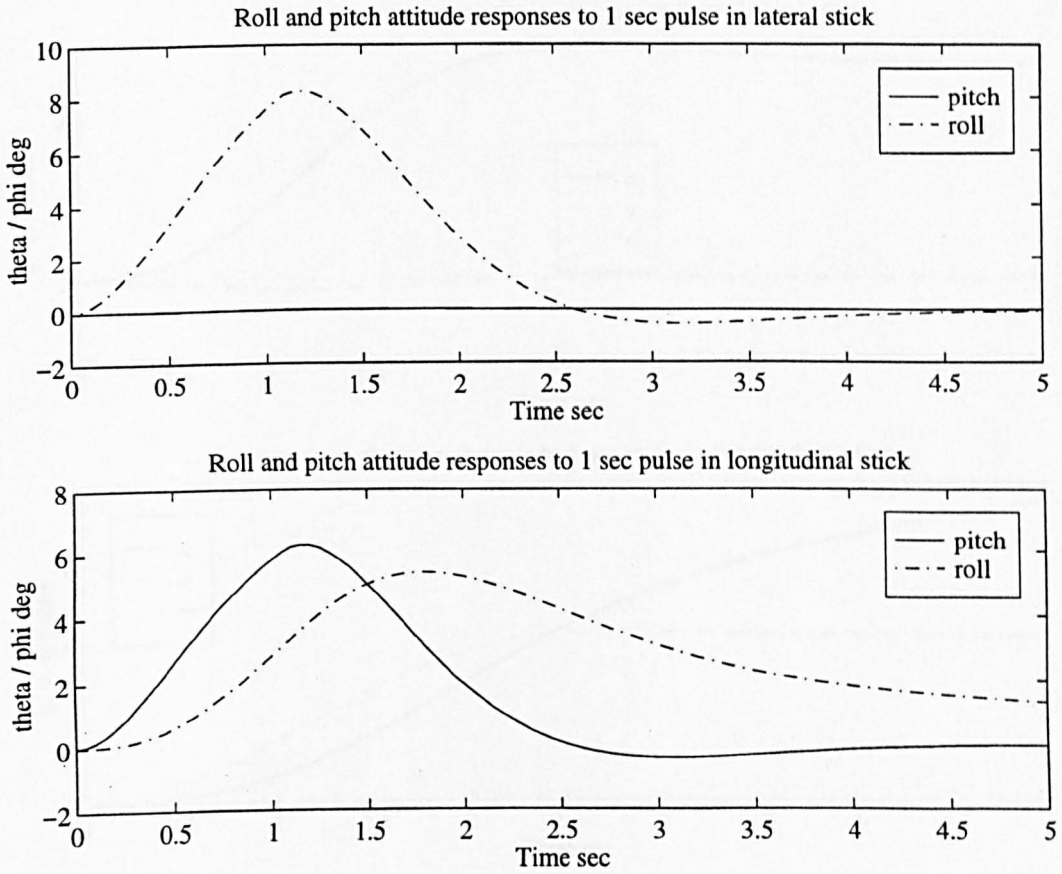


Figure 6.2.15: On and off axis attitude responses (roll and pitch) to a 10% one second lateral (top) and longitudinal (bottom) pulse input for an 8<sup>th</sup> order linear helicopter model at hover with an output feedback control law synthesized according to option *one* of Table 6.2.5.

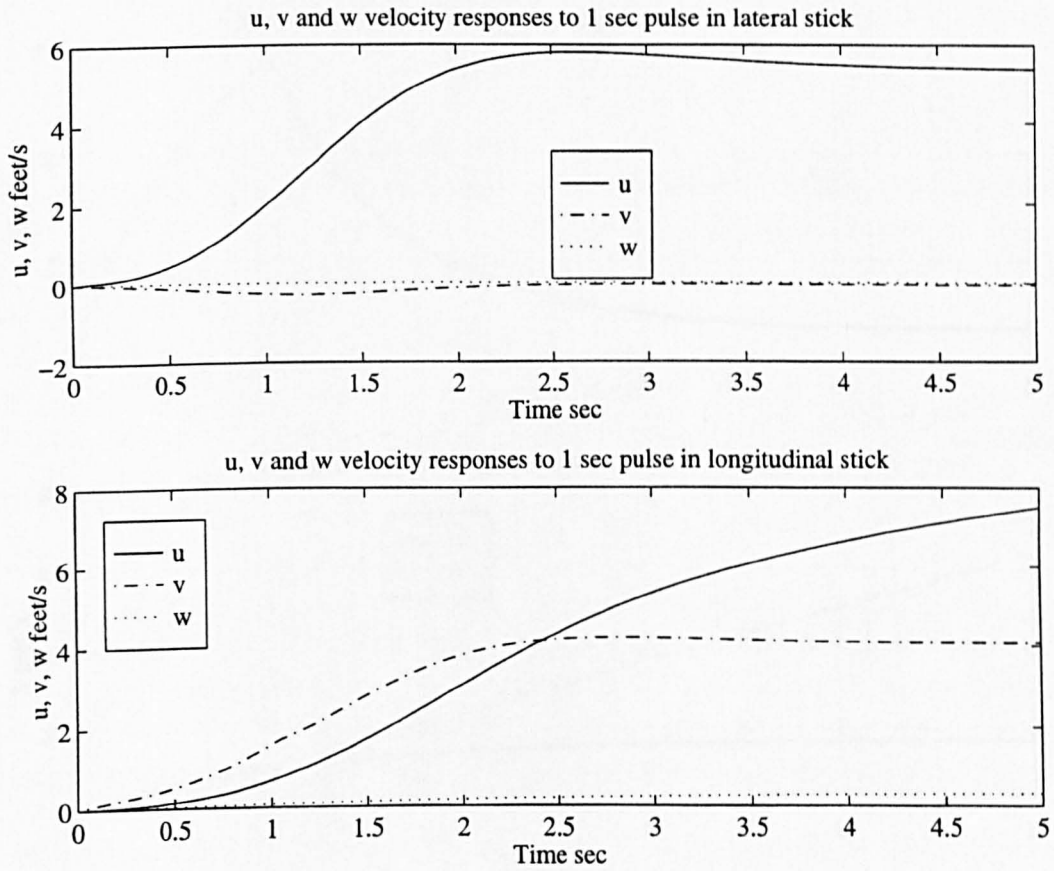


Figure 6.2.16: Linear velocity responses ( $u$ ,  $v$ ,  $w$ ) to a one second 10% pulse for an 8<sup>th</sup> order linear helicopter model with an output feedback control law synthesized according to option *one* of Table 6.2.5.

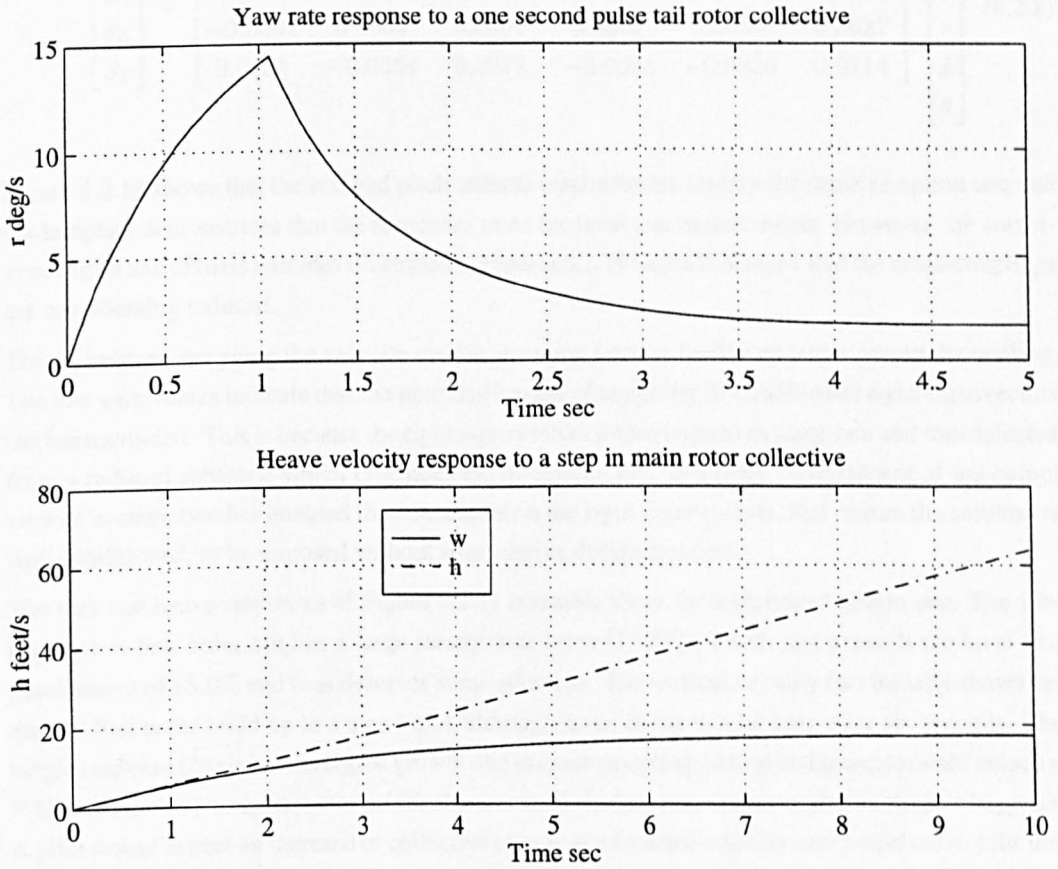


Figure 6.2.17: Yaw rate response (top) to a one second 10% pulse and heave velocity (bottom) induced by a 10% step input for an 8<sup>th</sup> order linear helicopter model with output feedback control synthesized according to option *one* of Table 6.2.5.

Assignment option three was performed, assigning the  $r, w$  modes as input vectors in stage one and assigning the remaining modes as right eigenvectors in stage two. The resulting gain matrix is shown below:

$$\begin{bmatrix} A_1 \\ B_1 \\ \theta_0 \\ \theta_t \end{bmatrix} = \begin{bmatrix} 0.0084 & 0.0534 & -0.0336 & -0.0715 & -0.0384 & -0.0031 \\ 0.0004 & -0.0403 & 0.0732 & 0.0564 & -0.0012 & 0.2435 \\ -0.0001 & 0.0004 & 0.0001 & 0.0007 & 0.0059 & 0.0027 \\ 0.0221 & -0.0554 & 0.0072 & -0.0008 & -0.0930 & 0.0714 \end{bmatrix} \begin{bmatrix} \dot{h} \\ p \\ q \\ r \\ \phi \\ \theta \end{bmatrix} \quad (6.2.8)$$

Figure 6.2.18 shows that the roll and pitch attitude responses are largely the same as option one and the template demonstrates that the responses meet the level one requirements. However, the corresponding on and off axis attitudes illustrated in Figures 6.2.19 and 6.2.20 show that the cross-couplings are considerably reduced.

This is because assigning the velocity modes as output vectors facilitates better output decoupling. The low gain values indicate that the potential hazard of assigning ill-conditioned right eigenvectors has been avoided. This is because the right eigenvectors were assigned in stage two and thus selected from a reduced subspace which precludes the ill-conditioned directions. Assignment of the output vectors in stage two has enabled the constraints on the right eigenvectors, that ensure the solution is well conditioned, to be imposed without squandering design freedom.

The yaw and heave responses of Figure 6.2.21 resemble those for assignment option one. The yaw response is first order but has a large steady state error (15.3%), which just exceeds the level two requirement of 15.0% and thus deserves some attention. The vertical velocity ( $w$ ) initially shows the desired first order build up to a step input, although some decay can be seen after six seconds. The height response ( $\dot{h}$ ) shows divergent growth due to cross-couplings into sideslip and forward velocity. Whilst these cross-couplings are undesirable it is unlikely they are as catastrophic as the plot suggests. A pilot would expect an increase in collective to induce a forward velocity and would correct for this with longitudinal stick before it dominated the response.

Part of the philosophy behind this design approach is to begin with a simple design technique, gain some experience and understanding of the problem, then progressively add embellishments to improve performance. So far, we have moved from state feedback to output feedback with simple projection. The next step is to apply iterative projection. The aim of this to trade-off the good decoupling in the longitudinal responses for a better steady state error in yaw.

The iterative projection technique was described in Section 4.5.8, but, briefly, it involves assigning each vector as a compromise between approximating the desired eigenvector and adopting a direction orthogonal to the left or right eigenvectors, as appropriate. The balance of the compromise is determined by a weighting. This implementation was based on synthesis option three of Table 6.2.5

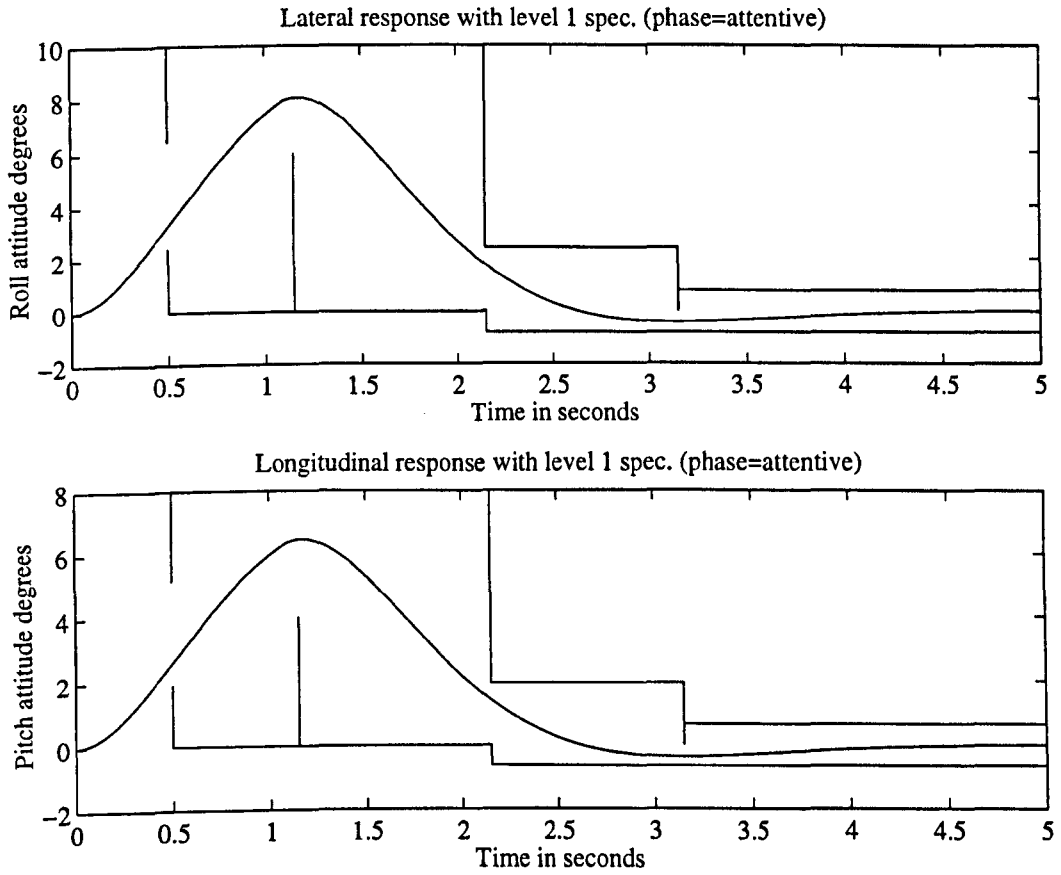


Figure 6.2.18: Roll attitude response (top) to a lateral and pitch attitude response (bottom) to a longitudinal pulse input of 10% for one second of an 8<sup>th</sup> order linear helicopter model at hover with an output feedback control law synthesized according to option *three* of Table 6.2.5.

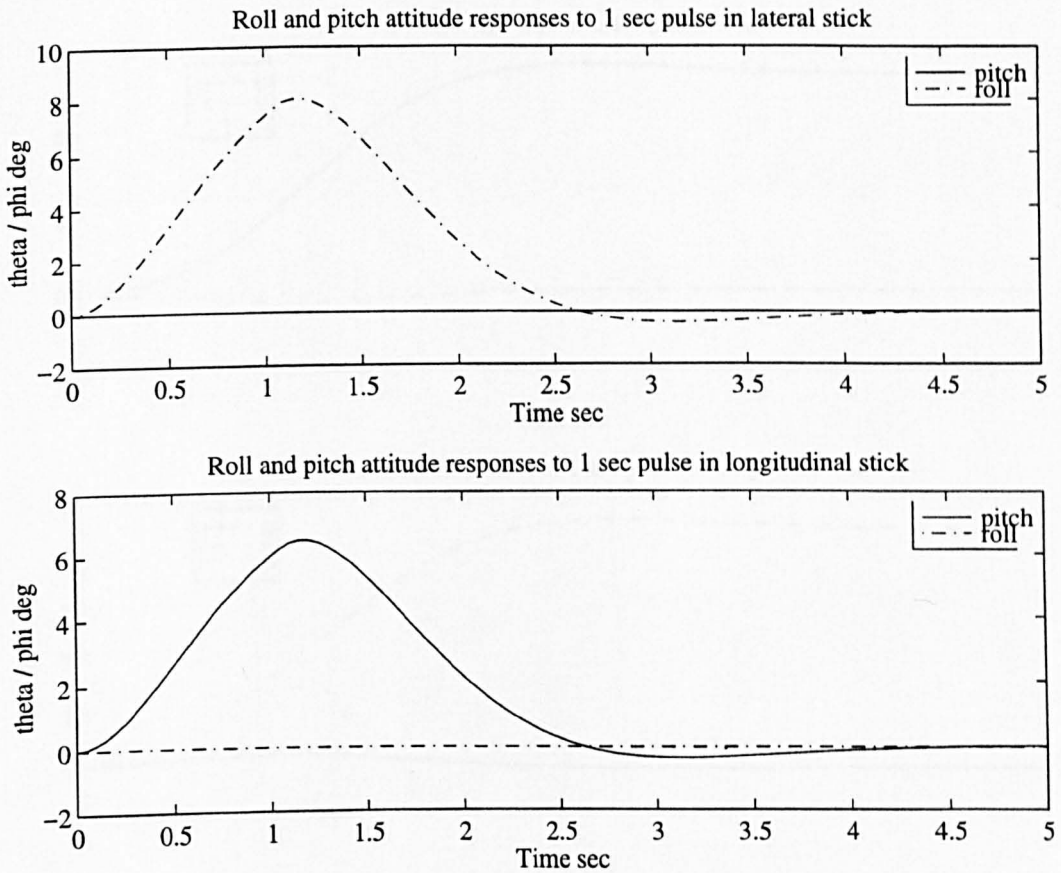


Figure 6.2.19: On and off axis attitude responses (roll and pitch) to a 10% one second lateral (top) and longitudinal (bottom) pulse input for an 8<sup>th</sup> order linear helicopter model at hover with an output feedback control law synthesized according to option *three* of Table 6.2.5.

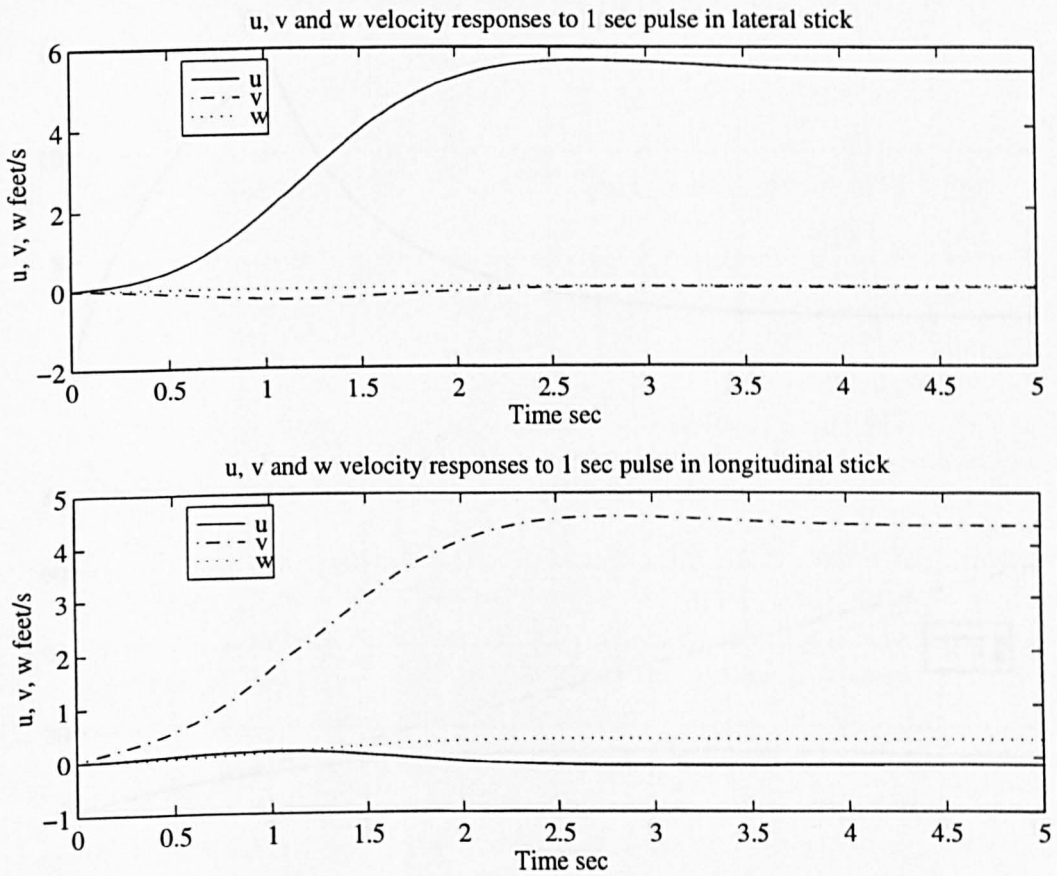


Figure 6.2.20: Linear velocity responses ( $u$ ,  $v$ ,  $w$ ) to a one second 10% pulse for an 8<sup>th</sup> order linear helicopter model with an output feedback control law synthesized according to option *three* of Table 6.2.5.

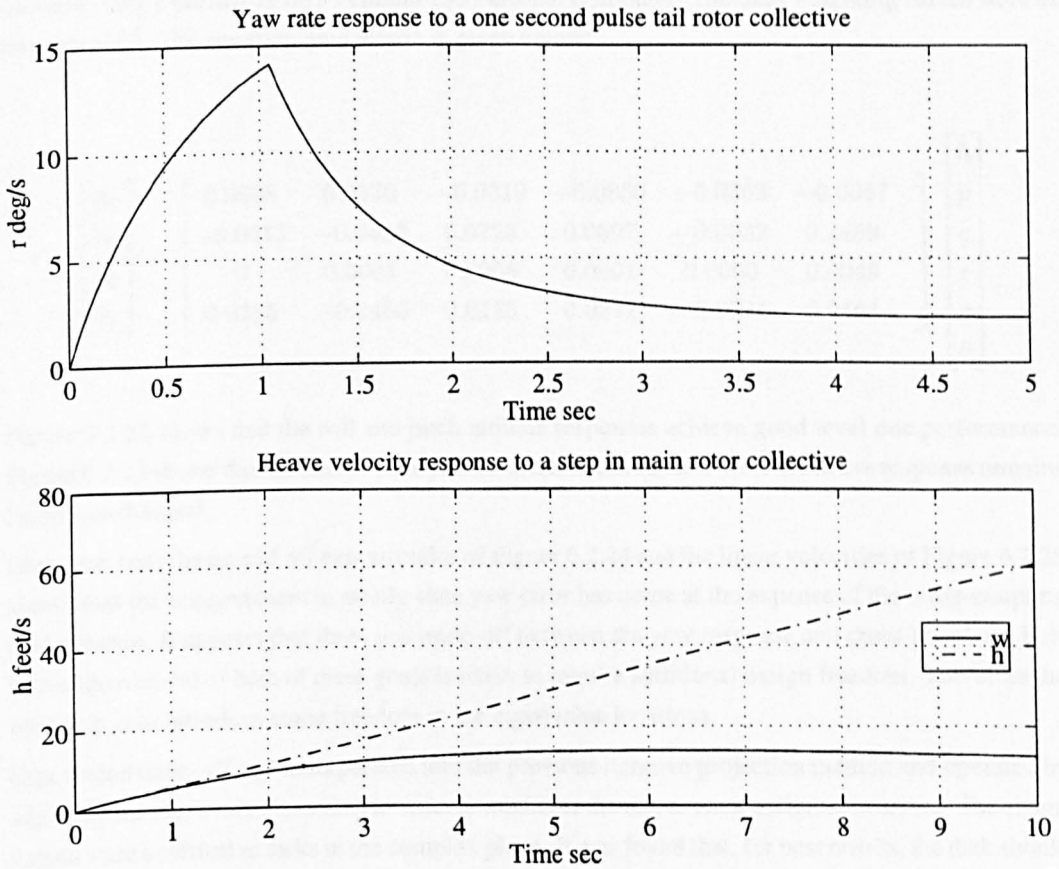


Figure 6.2.21: Yaw rate response (top) to a one second 10% pulse and heave velocity (bottom) induced by a 10% step input for an 8<sup>th</sup> order linear helicopter model with an output feedback control synthesized according to option *three* of Table 6.2.5.



and a separate weighting was used for each eigenvector. An eigenvector was deemed close enough to orthogonal if the product between it and its complementary eigenvectors was less than  $10^{-6}$ . When an eigenvector failed the orthogonality test its weighting was increased by a factor of 1.03. All the weightings were initialised with a value of  $10^{-3}$  except the left heave eigenvector which had a value of  $10^{-4}$ . A lower initial weighting value shifts the compromise more towards approximating the desired eigenvector and was found necessary for the heave mode. To avoid an ill conditioned solution and, in general, gave better results. The algorithm converged after 687 iterations which took 37.6 seconds using Matlab 4.2c on a Pentium 133 Personal Computer. The final weighting values were of the order  $10^4$ . The resulting gain matrix is given below:

$$\begin{bmatrix} A_1 \\ B_1 \\ \theta_0 \\ \theta_t \end{bmatrix} = \begin{bmatrix} 0.0098 & 0.0570 & -0.0319 & -0.0850 & -0.0362 & -0.0067 \\ -0.0013 & -0.0433 & 0.0720 & 0.0697 & -0.0032 & 0.2459 \\ 0 & 0.0001 & 0.0006 & 0.0001 & 0.0060 & 0.0049 \\ 0.0185 & -0.0466 & 0.0185 & 0.0221 & -0.0741 & 0.0663 \end{bmatrix} \begin{bmatrix} \dot{h} \\ p \\ q \\ r \\ \phi \\ \theta \end{bmatrix}$$

Figure 6.2.22 shows that the roll and pitch attitude responses achieve good level one performance. Figure 6.2.23 shows that the steady state yaw error has been reduced while the heave response remains largely unchanged.

However, both the on and off axis attitudes of Figure 6.2.24 and the linear velocities of Figure 6.2.25 shows that the improvement in steady state yaw error has come at the expense of the cross-coupling performance. It appears that there is a trade-off between the yaw response and cross-coupling. Further improvement of both of these goals is likely to require additional design freedom. Therefore the next step is to introduce some freedom in the eigenvalue locations.

Eigenvalue trade-off was incorporated into the previous iterative projection method and operated by adjusting the eigenvalue locations in order to minimise the eigenvector assignment errors. The eigenvalues were confined to disks in the complex plane. It was found that, for best results, the disk should not necessarily be centred on the ideal eigenvalue locations. For instance, the complex eigenvalues tended towards under damped solutions with the disk centred on the ideal locations. Moving the disk to left excluded these solutions and thus gave better results. The position of the linear velocity eigenvalues proved key to achieving a good trade-off between decoupling and the steady state error in yaw. They were hand placed at -0.045 for the forward speed mode and -0.043 for the side-slip mode. Table 6.2.6 summarises the radius and centre locations of the assigned eigenvalues.

The resulting gain matrix is:

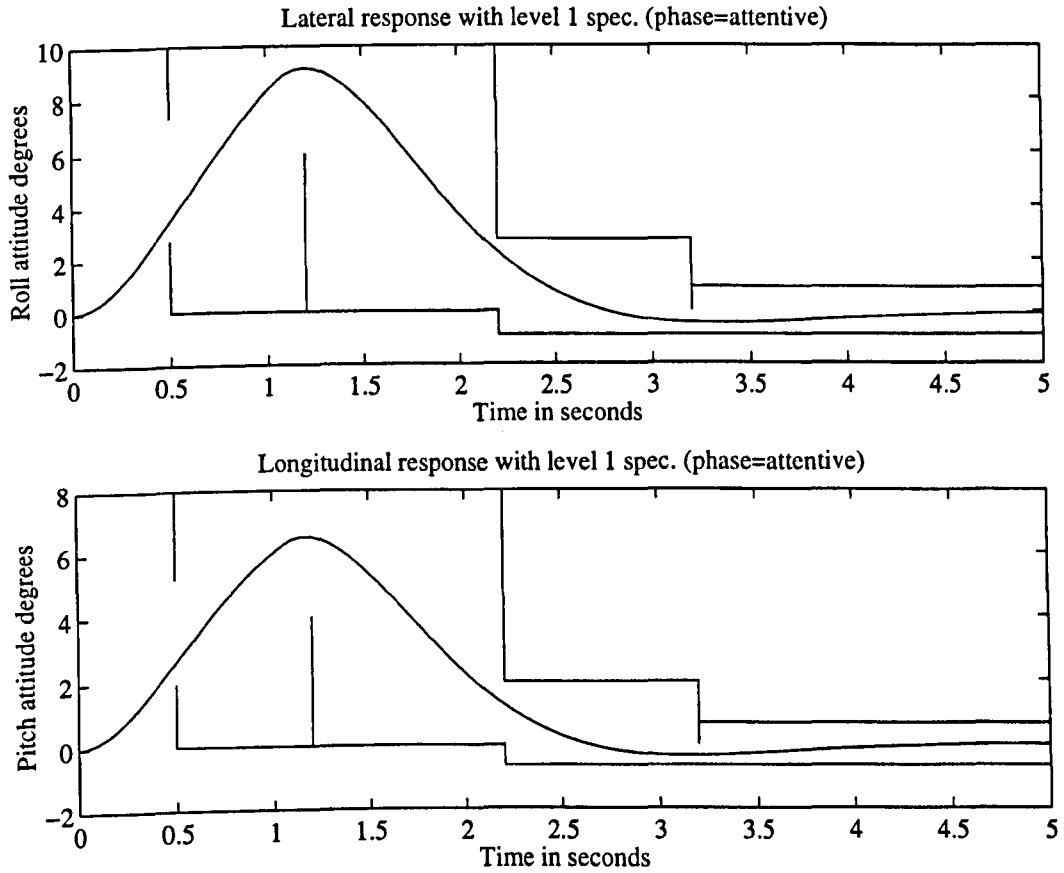


Figure 6.2.22: Roll attitude response (top) to a lateral and pitch attitude response (bottom) to a longitudinal pulse input of 10% for one second of an 8<sup>th</sup> order linear helicopter model at hover with an output feedback control law synthesized using the iterative projection algorithm of Section 4.5.8.

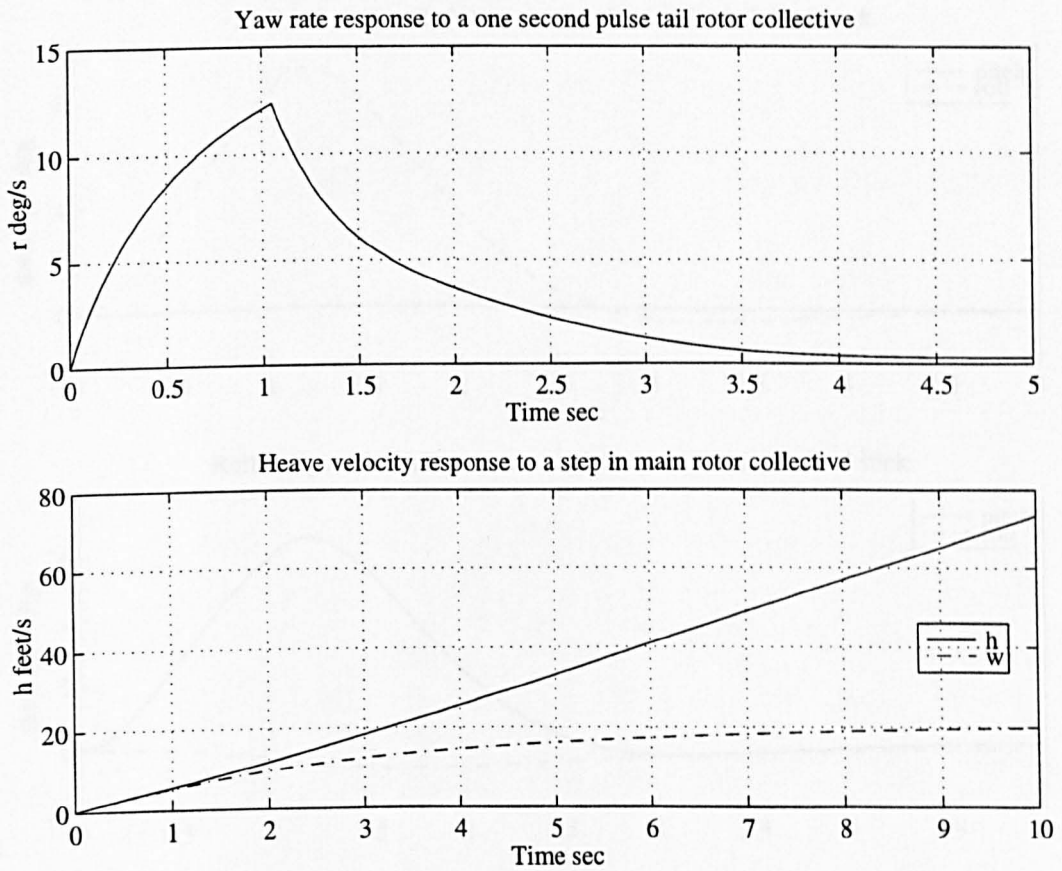


Figure 6.2.23: Yaw rate response (top) to a one second 10% pulse and heave velocity (bottom) induced by a 10% step input for an 8<sup>th</sup> order linear helicopter model at hover with an output feedback control synthesized using the iterative projection algorithm of Section 4.5.8.

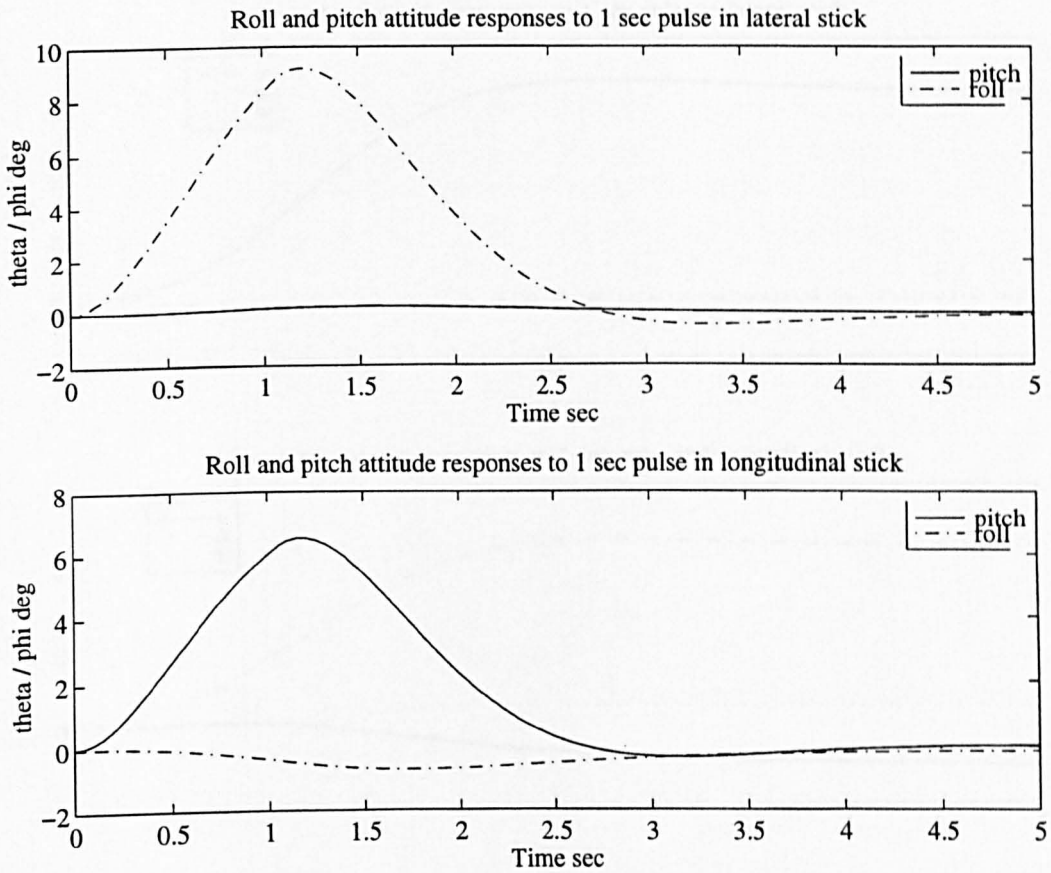


Figure 6.2.24: On and off axis attitude responses (roll and pitch) to a 10% one second lateral (top) and longitudinal (bottom) pulse input for an 8<sup>th</sup> order linear helicopter model at hover with an output feedback control law synthesized using the iterative projection algorithm of Section 4.5.8.

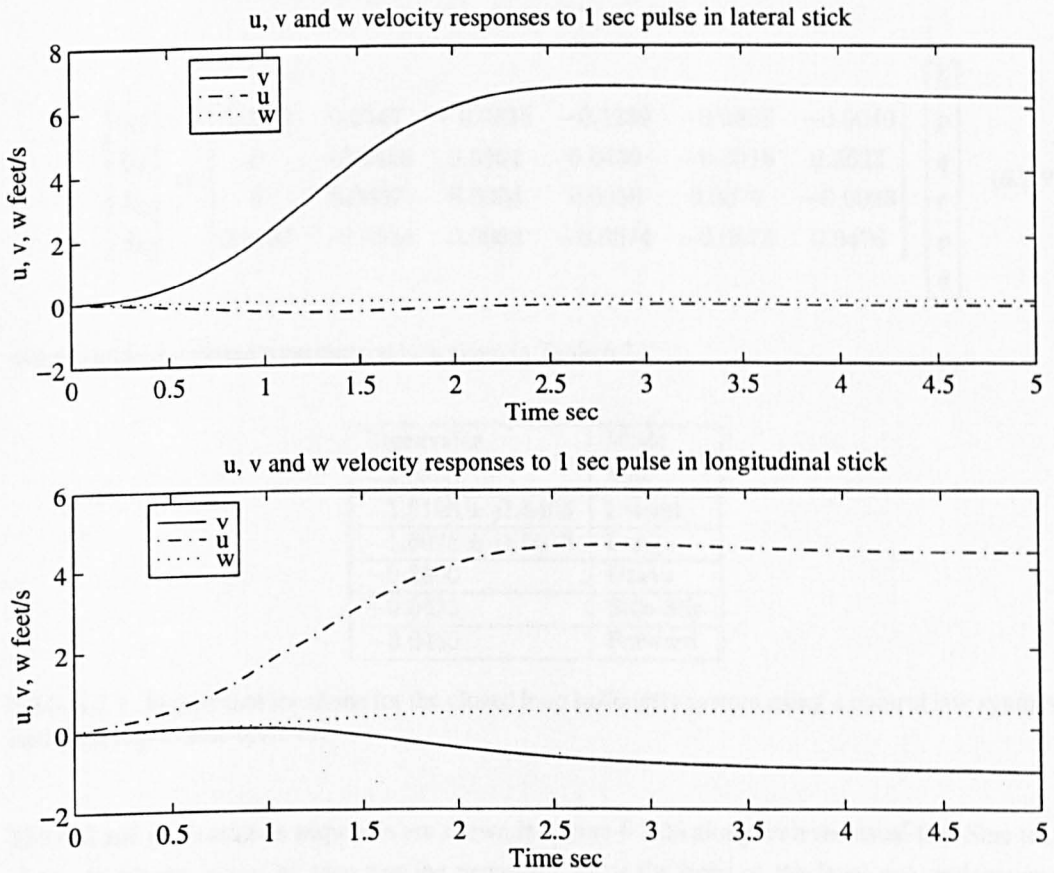


Figure 6.2.25: Linear velocity responses ( $u, v, w$ ) to a one second 10% pulse for an 8<sup>th</sup> order linear helicopter model with an output feedback control law synthesized using the iterative projection algorithm of Section 4.5.8.

Mode	Lateral	Side slip	Long.	Forward	Heave	Yaw
Centre	$-1.7 \pm j1.6$	-0.043	$-1.7 \pm j1.6$	-0.043	-0.33	-1.75
Radius	0.1	0	0.1	0	0.1	0.2

Table 6.2.6: Centre locations and radii used for the output feedback control law synthesis with eigenvalue trade-off.

$$\begin{bmatrix} A_1 \\ B_1 \\ \theta_0 \\ \theta_t \end{bmatrix} = \begin{bmatrix} 0.0079 & 0.0547 & -0.0335 & -0.1259 & -0.0408 & -0.0040 \\ 0 & -0.0406 & 0.0862 & 0.0439 & -0.0016 & 0.2623 \\ 0 & 0.0007 & 0.0003 & 0.0056 & 0.0076 & -0.0023 \\ 0.0187 & -0.0514 & 0.0088 & -0.0674 & -0.0875 & 0.0476 \end{bmatrix} \begin{bmatrix} \dot{h} \\ p \\ q \\ r \\ \phi \\ \theta \end{bmatrix} \quad (6.2.9)$$

which yields the closed loop eigenvalues given in Table 6.2.7.

Eigenvalue	Mode
-2.0500	Yaw
$-1.6196 \pm j1.5405$	Lateral
$-1.6078 \pm j1.5613$	Long.
-0.2300	Heave
-0.0433	Side-Slip
-0.0450	Forward

Table 6.2.7: Eigenvalue locations for the closed loop helicopter system using a control law synthesised with eigenvalue trade-off.

The roll and pitch attitude responses are shown in Figure 6.2.26 along with the usual Def-Stan template. In places, it can be seen that the responses are at the limit of the level one performance. However, the corresponding on and off axis attitudes illustrated in Figure 6.2.27 show that the cross-coupling between these responses is minimal.

Figure 6.2.28 depicts the yaw and heave responses. The yaw steady state error is 3.5% which comfortably meets both the level one and two requirements. The linear velocities of Figure 6.2.29 show that the decoupling is generally good.

Further improvements in performance are difficult to achieve without employing dynamic compensation. It is worth examining the robustness of the control law. Table 6.2.8 shows that the stability margins are slightly better than the initial state feedback solution but still poor.

Figure 6.2.30 shows the roll and pitch attitude responses of the 12<sup>th</sup> order helicopter model (includ-

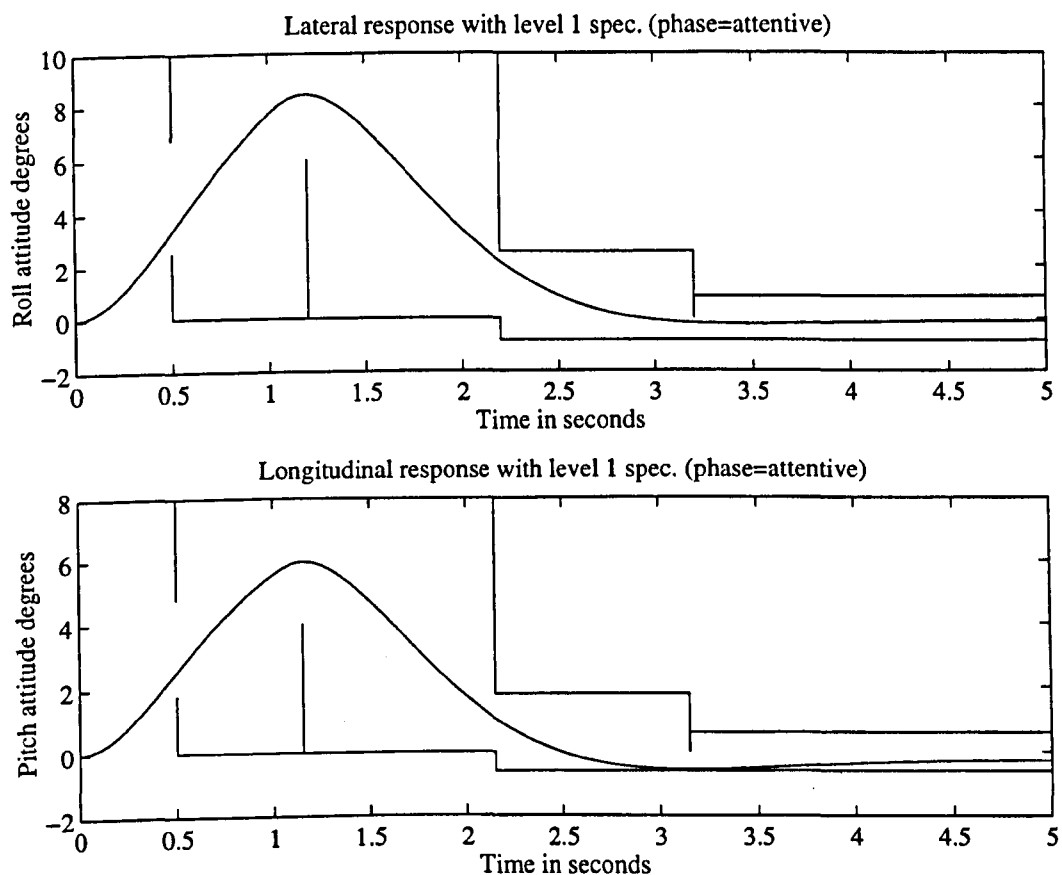


Figure 6.2.26: Roll attitude response (top) to a lateral and pitch attitude response (bottom) to a longitudinal pulse input of 10% for one second of an 8<sup>th</sup> order linear helicopter model at hover with an output feedback control law synthesized using an iterative projection algorithm employing eigenvalue trade-off.

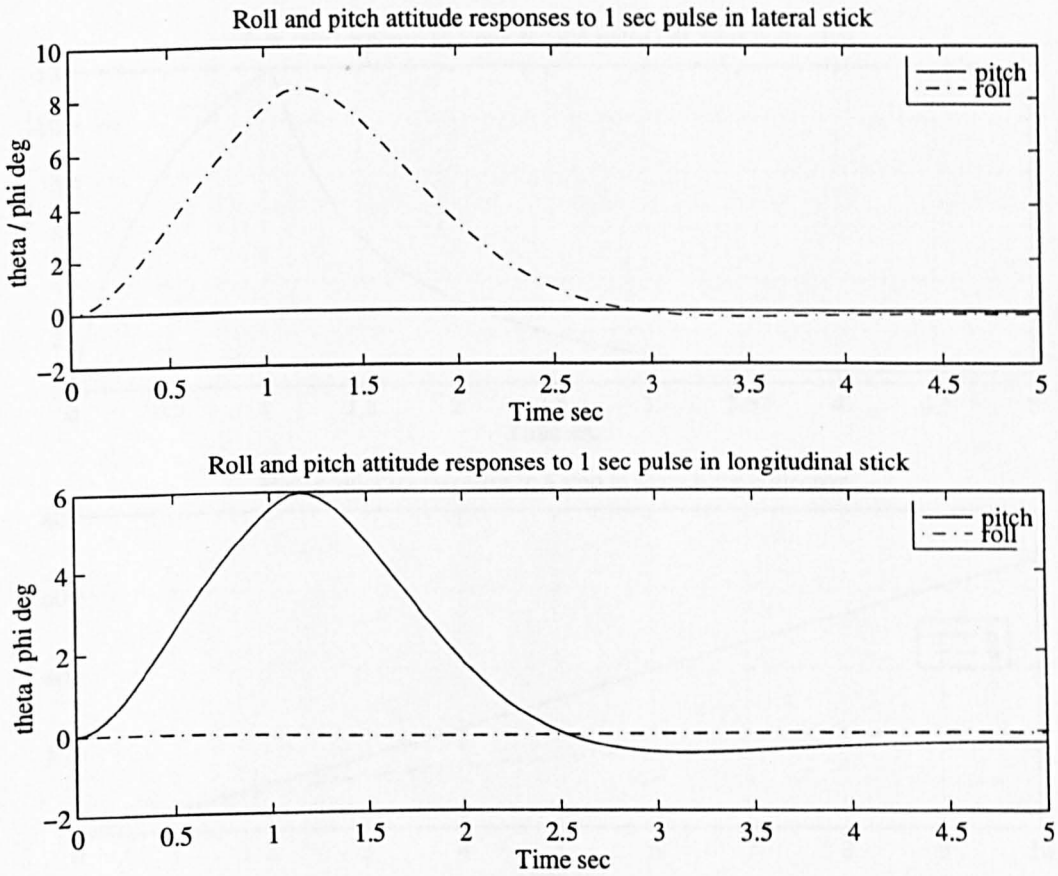


Figure 6.2.27: On and off axis attitude responses (roll and pitch) to a 10% one second lateral (top) and longitudinal (bottom) pulse input for an 8<sup>th</sup> order linear helicopter model at hover with an output feedback control law synthesized using an iterative projection algorithm employing eigenvalue trade-off.



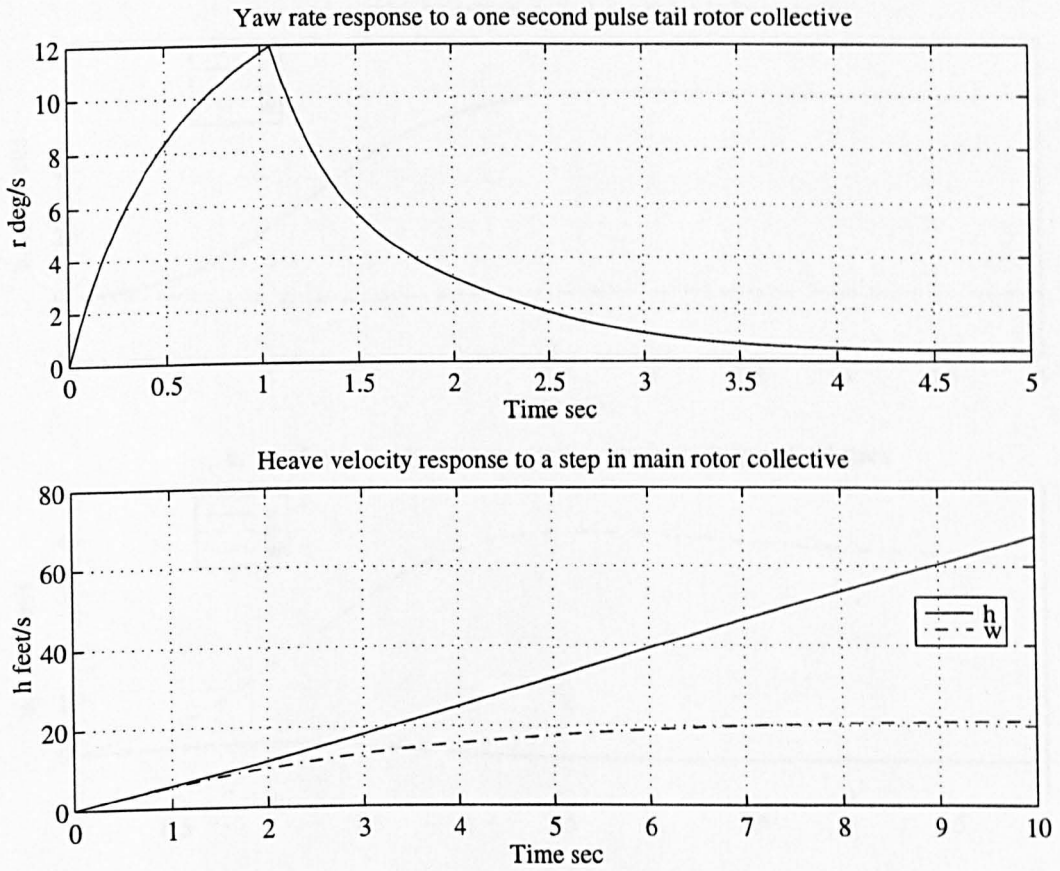


Figure 6.2.28: Yaw rate response (top) to a one second 10% pulse and heave velocity (bottom) induced by a 10% step input for an 8<sup>th</sup> order linear helicopter model with an output feedback control synthesized using an iterative projection algorithm employing eigenvalue trade-off.

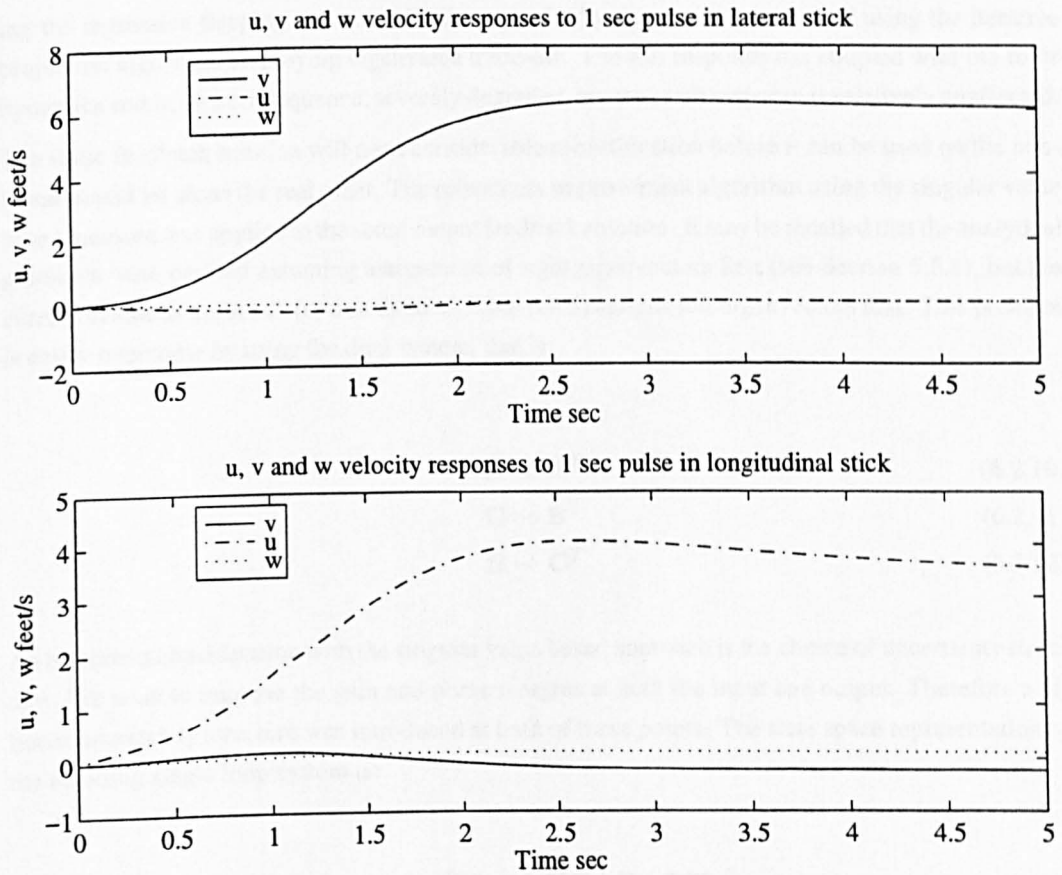


Figure 6.2.29: Linear velocity responses ( $u$ ,  $v$ ,  $w$ ) to a one second 10% pulse for an 8<sup>th</sup> order linear helicopter model with an output feedback control law synthesized using an iterative projection algorithm employing eigenvalue trade-off.

	Input	Output
Gain Margin	-0.65 dB, 0.62dB	-0.82 dB, 0.75dB
Phase Margin	-4.2°, 4.2°	-5.2°, 5.2°

Table 6.2.8: Multivariable gain and phase margins at the input and output of the closed loop helicopter system using a control law synthesised with eigenvalue trade-off.

ing the regressive flapping dynamics) with output feedback control synthesized using the iterative projection algorithm employing eigenvalue trade-off. The roll response has coupled with the rotor dynamics and is, as a consequence, severely degraded, but the pitch response is relatively unaffected. The static feedback solution will need considerable robustification before it can be used on the non-linear model let alone the real plant. The robustness improvement algorithm using the singular value based measure was applied to the static output feedback solution. It may be recalled that the analytical gradients were derived assuming assignment of right eigenvectors first (see Section 5.5.3), but the current synthesis approach (option three of Table 6.2.5) assigns left eigenvectors first. This problem is easily overcome by using the dual system, that is:

$$\mathbf{A} \mapsto \mathbf{A}^T \quad (6.2.10)$$

$$\mathbf{C} \mapsto \mathbf{B}^T \quad (6.2.11)$$

$$\mathbf{B} \mapsto \mathbf{C}^T \quad (6.2.12)$$

An important consideration with the singular value based approach is the choice of uncertainty structure. We wish to improve the gain and phase margins at both the input and output. Therefore a bilinear uncertainty structure was introduced at both of these points. The state space representation of the resulting single loop system is:

$$\mathbf{M}(s) = \left[ \begin{array}{c|cc} \mathbf{A} + \mathbf{BKC} & \mathbf{B} & \mathbf{BK} \\ \hline \mathbf{2KC} & \mathbf{I} & \mathbf{2K} \\ \mathbf{2C} & \mathbf{0} & \mathbf{I} \end{array} \right] \quad (6.2.13)$$

This structure can give a direct estimate of the gain and phase margins. However, it is very conservative since it encompasses perturbation at two loop breaking points (the input and output) whereas gain and phase margins are only defined with respect to one loop breaking point. The eigenvalues were constrained to be stable and within a radius of 0.2 from their assigned location. The optimisation was constrained to update design vectors and eigenvalues by no more than 10 percent per step. There were four steps per iteration, one each for the left and right design vectors and one each for the left and right eigenvalues. The algorithm was set to concede 20% of its robustness improvement to

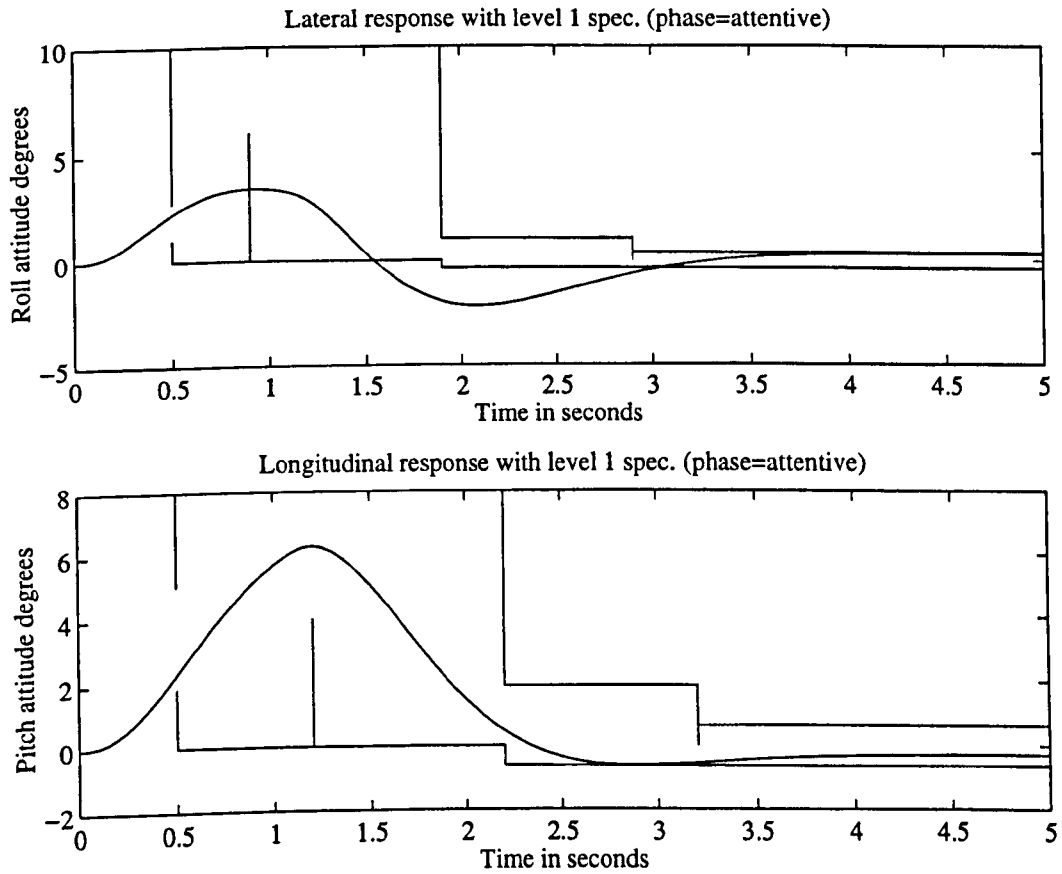


Figure 6.2.30: Roll attitude response (top) to a lateral and pitch attitude response (bottom) to a longitudinal pulse input of 10% for one second of a 12<sup>th</sup> order linear helicopter model at hover with an output feedback control law synthesized using an iterative projection algorithm employing eigenvalue trade-off.

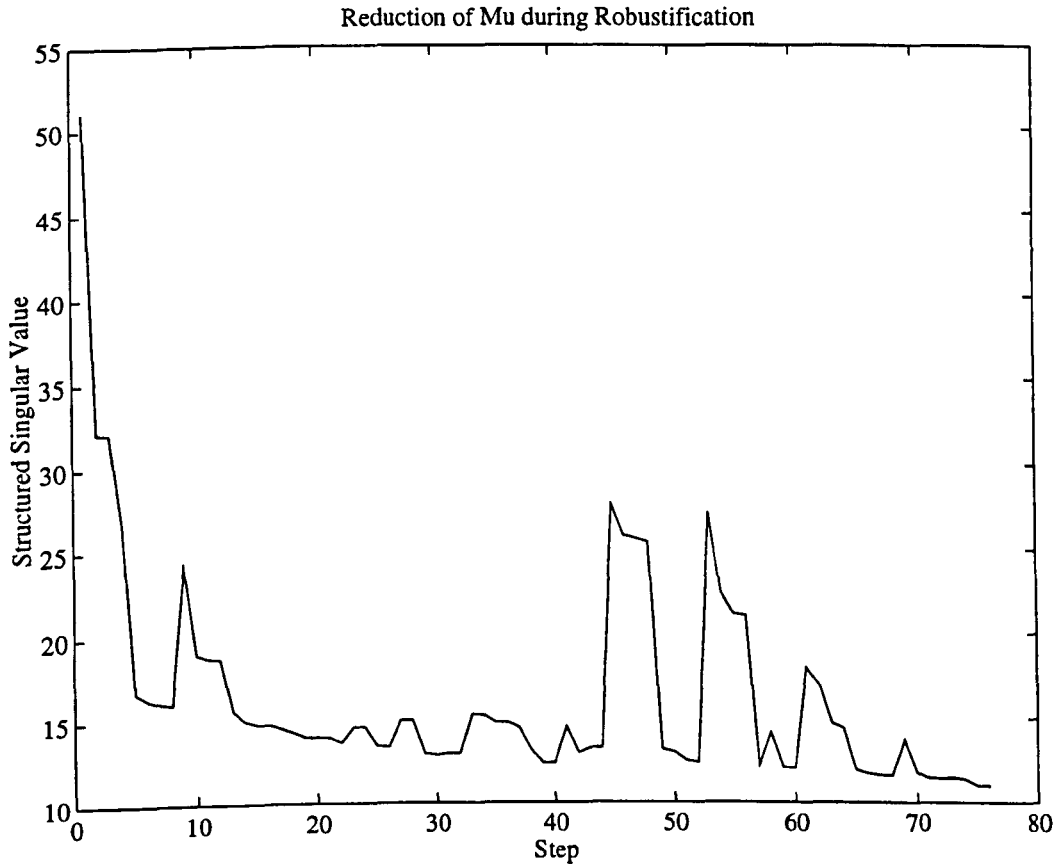


Figure 6.2.31: Convergence of the robustness improvement algorithm with the singular value based measure for an 8<sup>th</sup> helicopter model with output feedback control and a bilinear uncertainty structure at the input and output.

performance protection. However, maintaining performance proved to be an impossible task.

Figure 6.2.31 shows how the minimisation of the  $\mu$  upper bound progressed. It can be seen that initially the function decreases monotonically, but then suffers periodic increases from which it recommences the minimisation. The increases are all due to frequency jumps. That is, after minimising one peak a new peak has arisen at a different frequency. The algorithm will leap between peaks attempting to minimise them all independently. However, eventually an impasse is reached where minimising one peak causes an increase in another and vice-versa. The algorithm then becomes locked in a cycle, trying to minimise both peaks and progresses no further.

The gain matrix after 19 iteration (76 steps) is given below:

$$\begin{bmatrix} A_1 \\ B_1 \\ \theta_0 \\ \theta_t \end{bmatrix} = \begin{bmatrix} 0.0003 & 0.0433 & -0.0231 & -0.0450 & -0.0586 & -0.0049 \\ 0.0032 & -0.0421 & 0.0818 & 0.0312 & 0.0083 & 0.2576 \\ 0.0003 & 0.0095 & 0.0007 & -0.0064 & 0.0109 & 0.0396 \\ 0.0101 & -0.0669 & 0.0715 & 0.0751 & -0.1575 & 0.3176 \end{bmatrix} \begin{bmatrix} \dot{h} \\ p \\ q \\ r \\ \phi \\ \theta \end{bmatrix} \quad (6.2.14)$$

The gain and phase margins are shown in Table 6.2.9. A substantial improvement has been achieved. However, this has come at the expense of performance.

	Input	Output
Gain Margin	-3.65 dB, 3.1dB	-4.39 dB, 3.58dB
Phase Margin	-19.8°, 19.8°	-22.9°, 22.9°

Table 6.2.9: Multivariable gain and phase margins at the input and output of the closed loop helicopter system using a control law that has been optimised with respect to a singular value based robustness measure.

Figure 6.2.32 depicts the roll and pitch attitude responses along with the usual Def-Stan template and Figure 6.2.33 displays the corresponding attitude cross-coupling.

Figure 6.2.34 shows that the yaw and heave responses have not been greatly affected by the robustification but the linear velocities depicted in Figure 6.2.35 shows that the general decoupling has suffered.

For comparison robustification with respect to the time domain measure was also undertaken. Again, the optimisation was constrained to update the eigenvalues or eigenvectors by no more than 10% and 20% of the robustness improvement was conceded to performance protection. The eigenvalues were constrained to be stable and within a 0.2 radius of their initial location. A time domain uncertainty structure must be chosen and it was decided to use the non-linearity information from the linearisation. The linearisation algorithm produces three system matrices a nominal matrix plus an upper and a lower bound. The algorithm was allowed wide error tolerances ( $\epsilon_a = 0.1, \epsilon_p = 0.1$ ) to ensure a reasonable amount of uncertainty information was produced. The upper and lower bounds were processed in an identical fashion to the nominal matrix then subtracted from the nominal matrix to produce error information. The uncertainty information is given below:

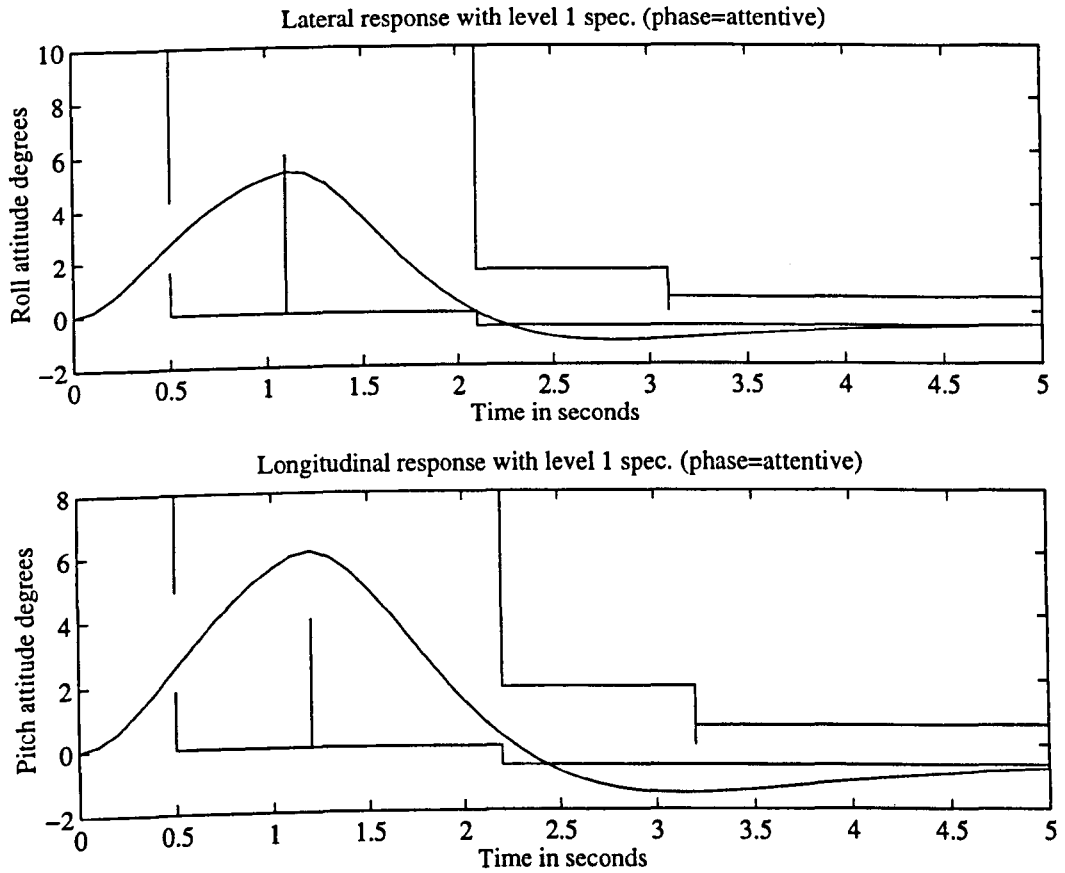


Figure 6.2.32: Roll attitude response (top) to a lateral and pitch attitude response (bottom) to a longitudinal pulse input of 10% for one second of an 8<sup>th</sup> order linear helicopter model at hover with an output feedback control law that has been optimised with respect to a singular value based robustness measure.

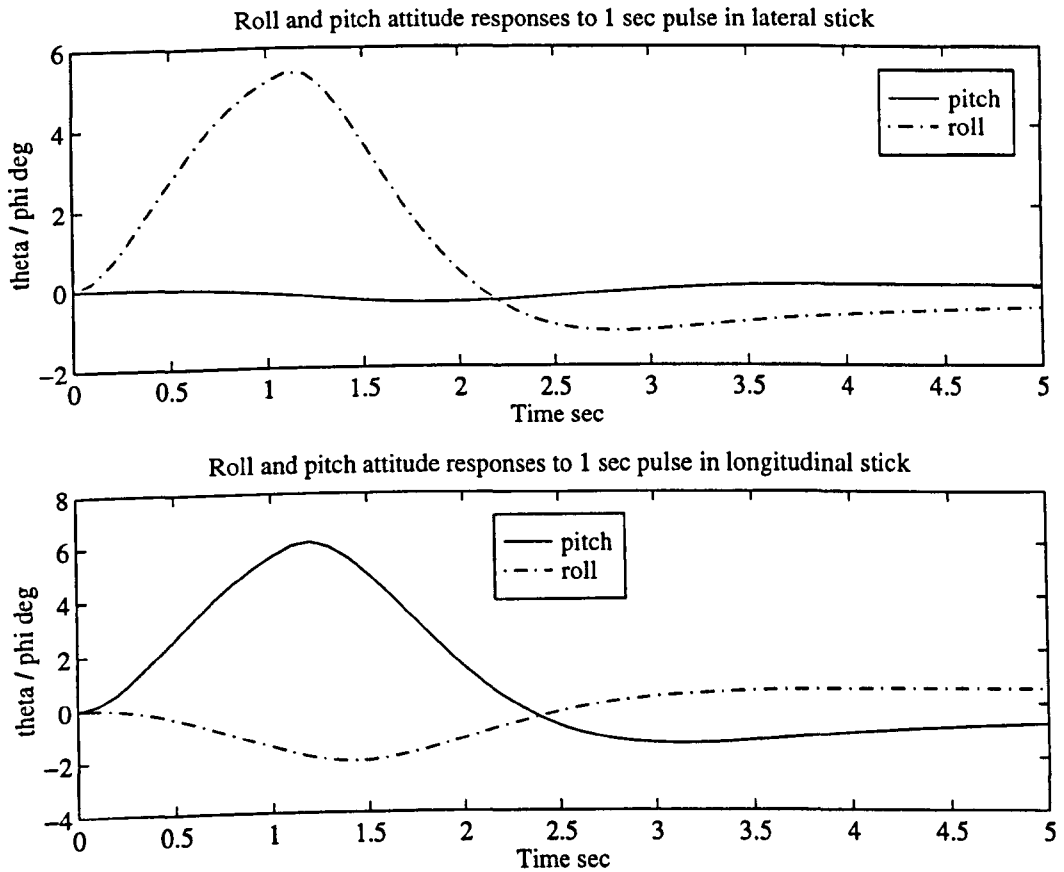


Figure 6.2.33: On and off axis attitude responses (roll and pitch) to a 10% one second lateral (top) and longitudinal (bottom) pulse input for an 8<sup>th</sup> order linear helicopter model at hover with an output feedback control law that has been optimised with respect to a singular value based robustness measure.



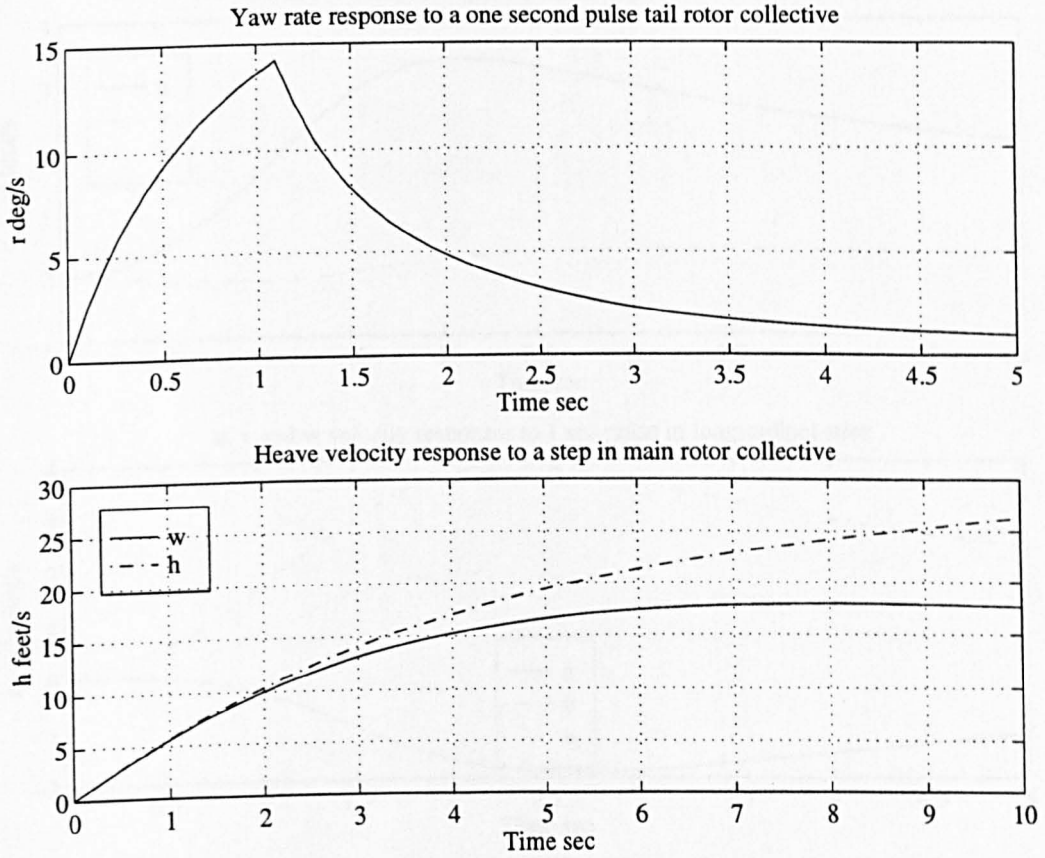


Figure 6.2.34: Yaw rate response (top) to a one second 10% pulse and heave velocity (bottom) induced by a 10% step input for an 8<sup>th</sup> order linear helicopter model with an output feedback control law that has been optimised with respect to a singular value based robustness measure.

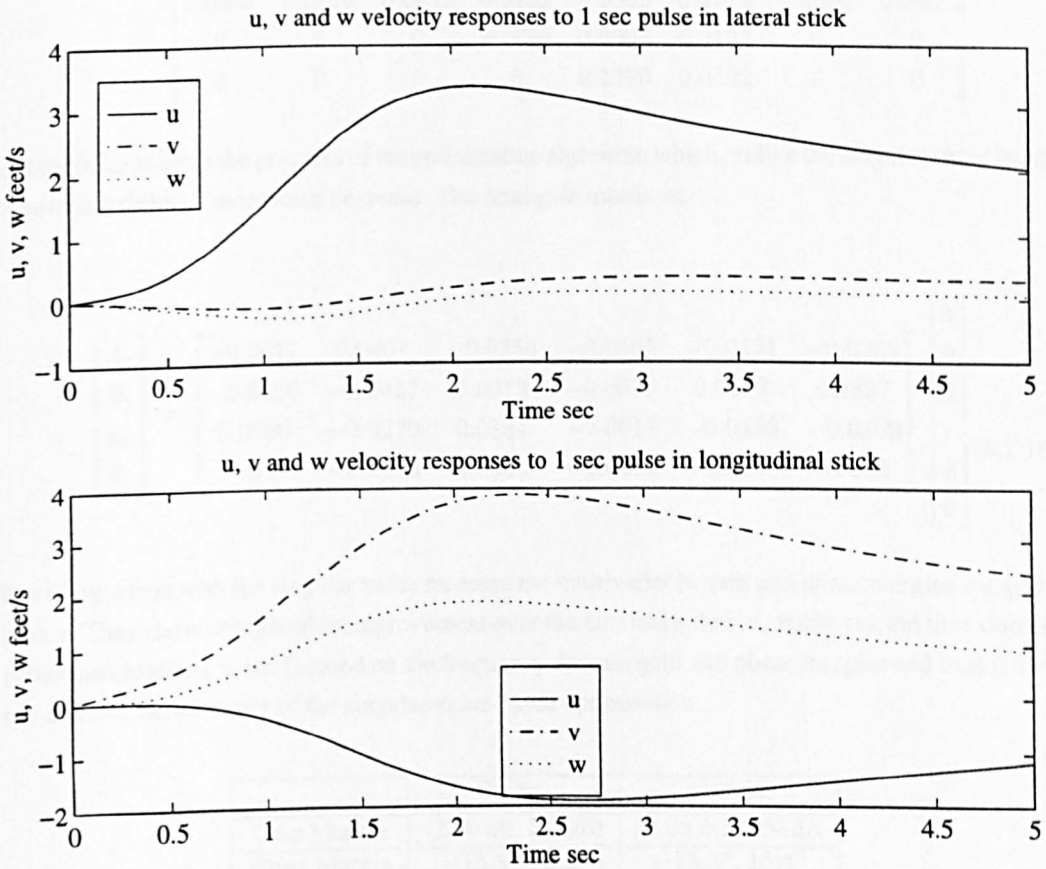


Figure 6.2.35: Linear velocity responses ( $u$ ,  $v$ ,  $w$ ) to a one second 10% pulse for an 8<sup>th</sup> order linear helicopter model with an output feedback control law that has been optimised with respect to a singular value based robustness measure.

$$\Delta A = \begin{bmatrix} 0.0046 & 0.0058 & 0.0022 & 0.0079 & 0.0360 & 0.0000 & 0.0000 & 0.0019 \\ 0.0060 & 0.0197 & 0.0058 & 0.0519 & 0.0175 & 0.0115 & 0.0019 & 0.0018 \\ 0.1059 & 0.1026 & 0.0613 & 0.0093 & 0.0038 & 0.0000 & 0.0313 & 0.0313 \\ 0.0896 & 0.0145 & 0.1219 & 1.7437 & 0.9981 & 0.0084 & 0.0000 & 0.0000 \\ 0.0067 & 0.0057 & 0.0124 & 0.1428 & 0.2082 & 0.0000 & 0.0000 & 0.0000 \\ 0.0402 & 0.0155 & 0.0650 & 0.3202 & 0.2362 & 0.0716 & 0.0000 & 0.0000 \\ 0 & 0 & 0 & 0.1795 & 0.0004 & 0.0127 & 0 & 0 \\ 0 & 0 & 0 & 0 & 0.1270 & 0.0122 & 0 & 0 \end{bmatrix} \quad (6.2.15)$$

Figure 6.2.36 shows the progress of the optimisation algorithm which, unlike the singular value based measure, exhibits a monotonic decrease. The final gain matrix is:

$$\begin{bmatrix} A_1 \\ B_1 \\ \theta_0 \\ \theta_t \end{bmatrix} = \begin{bmatrix} -0.0017 & 0.0407 & -0.0354 & -0.0495 & -0.0431 & -0.0232 \\ -0.0016 & -0.0417 & 0.0913 & -0.0378 & 0.0119 & 0.2897 \\ 0.0006 & -0.0270 & 0.0164 & -0.0015 & -0.0459 & -0.0109 \\ 0 & -0.2403 & 0.0967 & -0.0460 & -0.3888 & 0.0545 \end{bmatrix} \begin{bmatrix} \dot{h} \\ p \\ q \\ r \\ \phi \\ \theta \end{bmatrix} \quad (6.2.16)$$

For comparison with the singular value measure the multivariable gain and phase margins are given below. They show considerable improvement over the nominal solution. However, the time domain robustness measure is not focused on the frequency domain gain and phase margins and thus it does not achieve the tolerance of the singular value based optimisation.

	Input	Output
Gain Margin	-2.30 dB, 2.24dB	-2.65 dB, 2.58dB
Phase Margin	-13.3°, 13.3°	-15.4°, 15.4°

Table 6.2.10: Multivariable gain and phase margins at the input and output of the closed loop helicopter system using a control law that has been optimised with respect to a time domain robustness measure.

Figure 6.2.37 shows the roll and pitch attitude responses along with the usual Def-Stan template and Figure 6.2.38 shows the corresponding attitude cross-coupling. It can be seen that both sets of responses have suffered but that the decoupling has degraded but to a lesser extent.

Figure 6.2.39 shows that both the yaw and heave responses have been detrimentally affected by the robustification and Figure 6.2.35 depicts the linear velocities and shows that the general decoupling has also suffered.

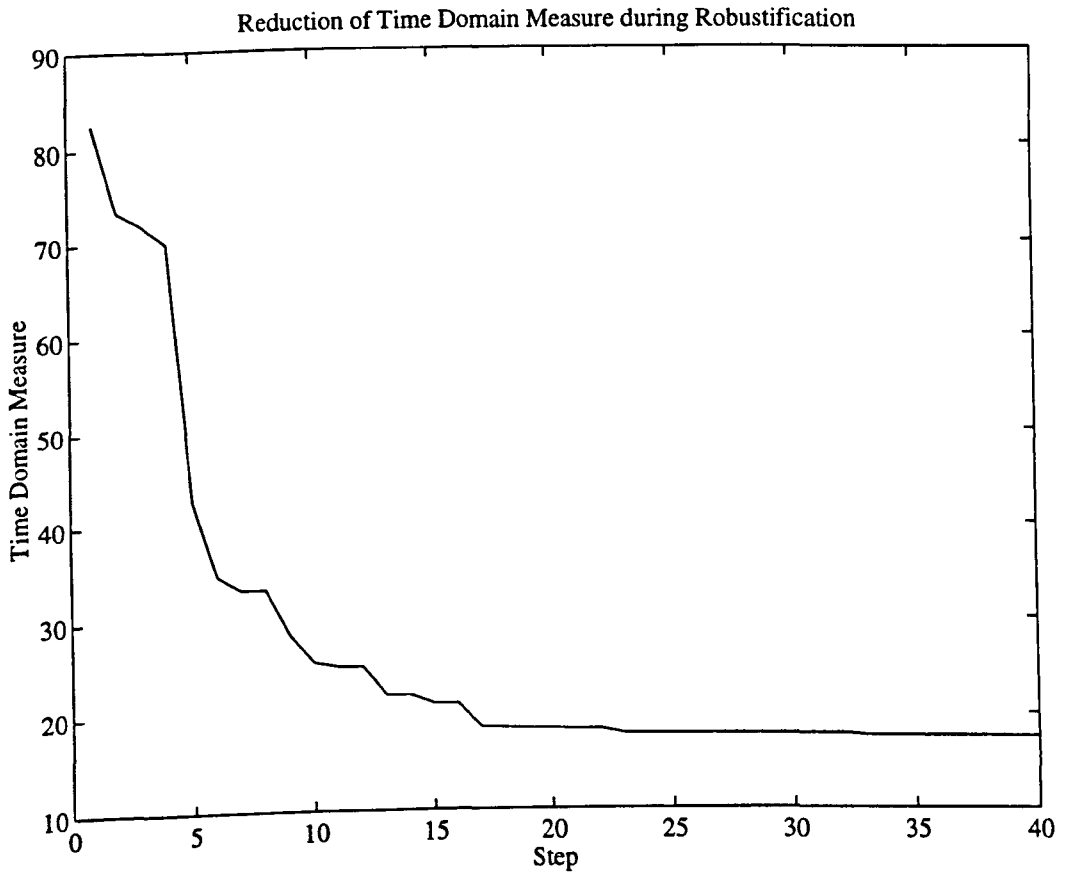


Figure 6.2.36: Convergence of the robustness improvement algorithm with the time domain measure for an 8<sup>th</sup> helicopter model with output feedback control and the uncertainty structure of Equation (6.2.15).

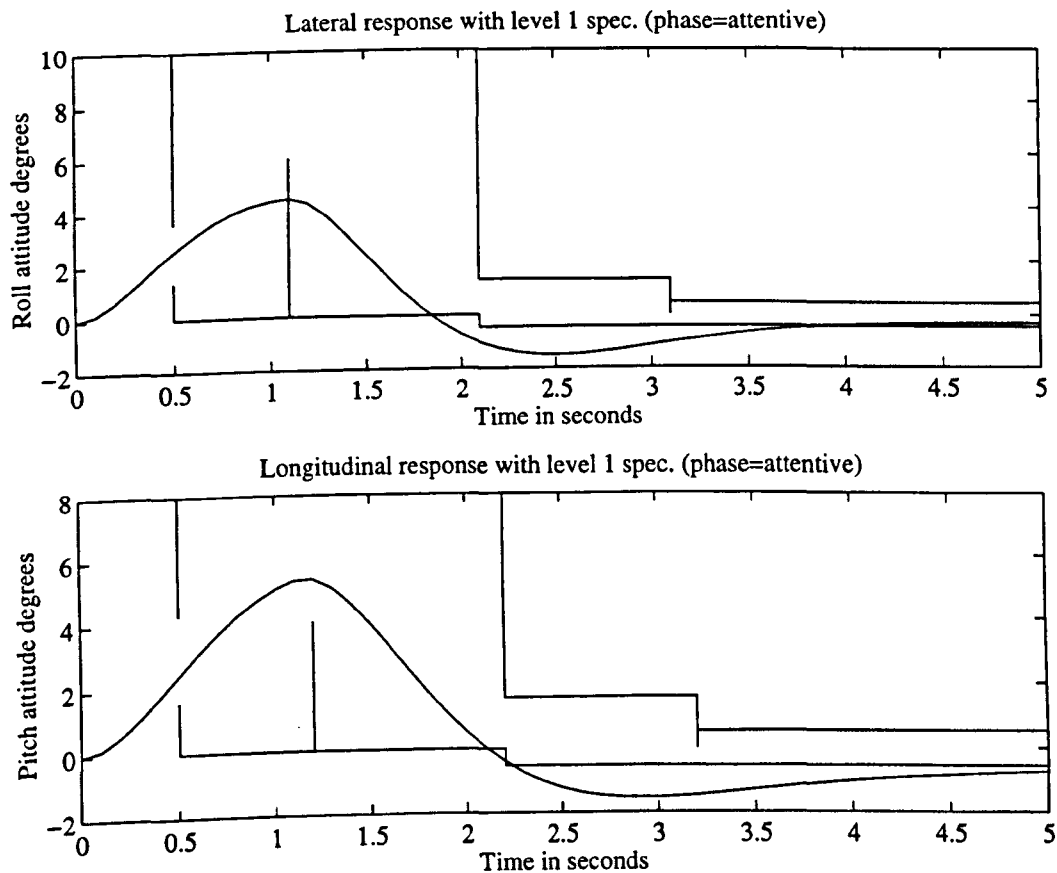


Figure 6.2.37: Roll attitude response (top) to a lateral and pitch attitude response (bottom) to a longitudinal pulse input of 10% for one second of an 8<sup>th</sup> order linear helicopter model at hover with an output feedback control law that has been optimised with respect to a time domain robustness measure.

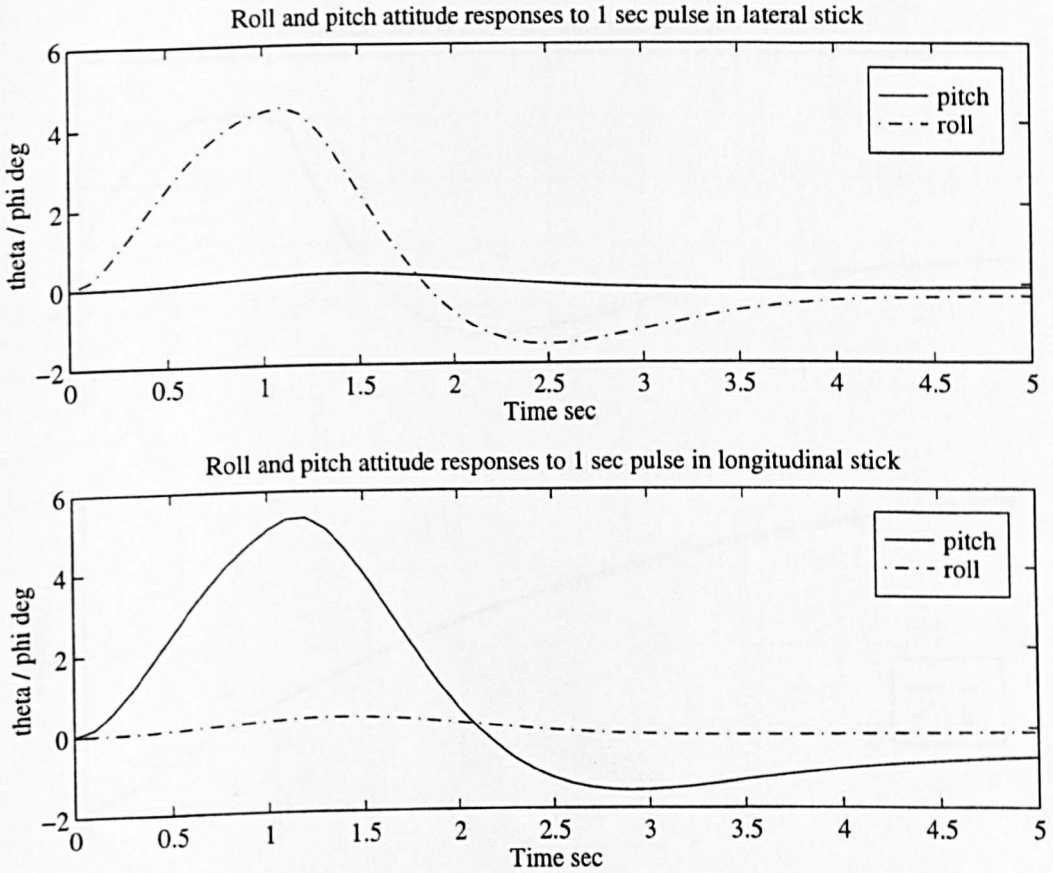


Figure 6.2.38: On and off axis attitude responses (roll and pitch) to a 10% one second lateral (top) and longitudinal (bottom) pulse input for an 8<sup>th</sup> order linear helicopter model at hover with an output feedback control law that has been optimised with respect to a time domain robustness measure.

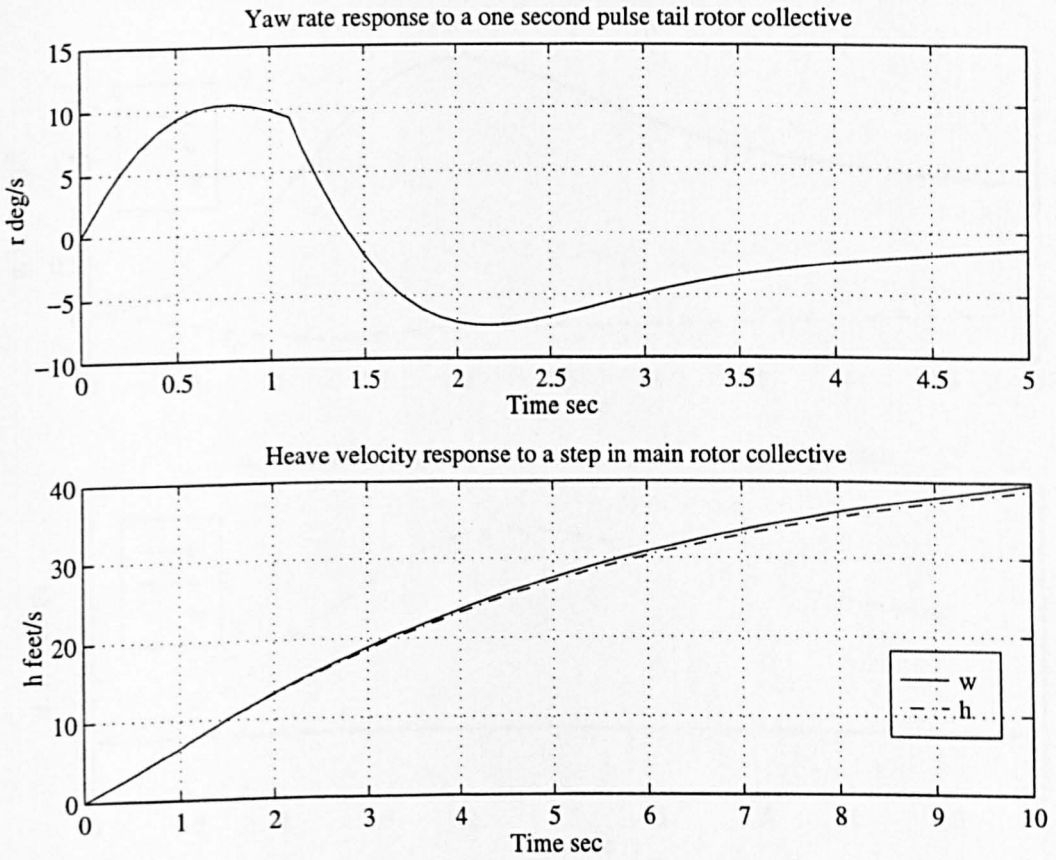


Figure 6.2.39: Yaw rate response (top) to a one second 10% pulse and heave velocity (bottom) induced by a 10% step input for an 8<sup>th</sup> order linear helicopter model with an output feedback control law that has been optimised with respect to a time domain robustness measure.

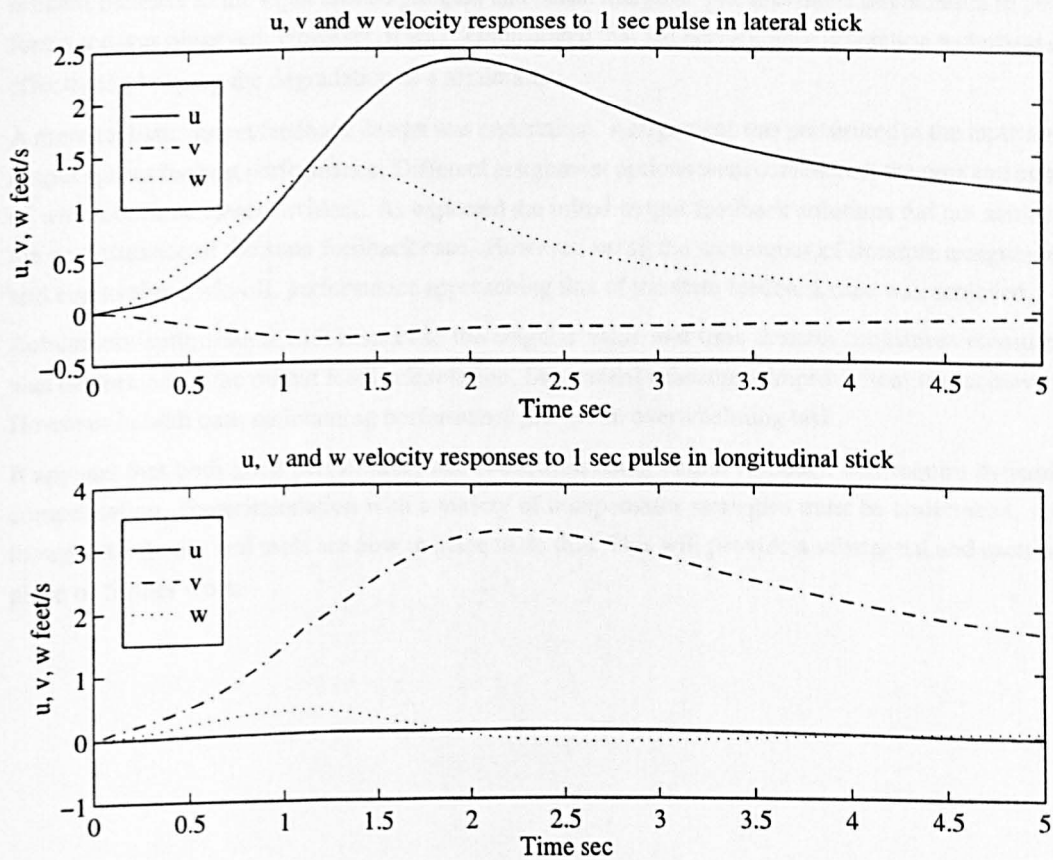


Figure 6.2.40: Linear velocity responses ( $u, v, w$ ) to a one second 10% pulse for an 8<sup>th</sup> order linear helicopter model with an output feedback control law that has been optimised with respect to a time domain robustness measure.



## 6.3 Summary

In this chapter an attitude command hover control law was designed using static feedback techniques. An initial state feedback solution showed that the desired eigenstructure derived in Section 3.5.4 concisely expresses the handling qualities performance goals. A visible link between the system eigenstructure and its performance was also demonstrated.

The robustness improvement algorithm was applied to the state feedback solution. It delivered a significant increase in the input and output gain and phase margins. The inevitable degradation in performance was observed. However, it was demonstrated that the performance protection technique is effective in keeping the degradation to a minimum.

A more realistic output feedback design was undertaken. Assignment was performed in the input and output spaces for best performance. Different assignment options were considered, the pros and cons of which became clearly evident. As expected the initial output feedback solutions did not achieve the performance of the state feedback case. However, using the techniques of iterative assignment and eigenvalue trade-off, performance approaching that of the state feedback case was achieved.

Robustness optimisation with respect to the singular value and time domain robustness measures was performed on the output feedback solution. Substantial robustness improvement was achieved. However in both case maintaining performance proved an overwhelming task.

It appears that both good performance and robustness using output feedback will require dynamic compensation. Experimentation with a variety of compensator strategies must be undertaken. Although, the theory and tools are now in place to do this. This will provide a substantial and exciting piece of further work.

# Chapter 7

## Conclusions and Further Work

### Contents

---

7.1	Conclusions	285
7.2	Contributions	287
7.3	Further Work	288

---

### 7.1 Conclusions

In the introduction it was argued that eigenstructure assignment is an appropriate technique for the design of helicopter control laws. The reasons given were:

- it provides engineering design visibility,
- there is considerable support for rapid design iteration,
- there is a straightforward relationship between the handling qualities specification and the desired eigenstructure,
- it lends itself to integrated vehicle design by using concepts familiar to both control engineers and flight dynamicists,
- controller structures are easily determined and generally simple,
- design trade-offs can easily be seen and made.

However, to exploit the benefits of eigenstructure assignment fully it should be incorporated into a suitable design methodology.

Development of such a methodology began in Chapter 2 through an understanding of vehicle dynamics. The hover case dynamics were analysed using modal techniques and a simplified system.

A reliable linearisation with useful uncertainty information was produced. This formed the basis of further development.

Chapter 3 continued development of the design methodology by examining the design objectives. The relevant criteria in the two most important handling qualities specifications (Def-Stan 00-970 and ADS 33) were examined and compared. By combining the criteria of the Def-Stan 00-970 and knowledge of the system dynamics, a desired eigenstructure was constructed. To maintain flexibility, the eigenvalues were specified as allowed regions, although ideal nominal points were also identified. The desired eigenstructure was shown to be consistent with both specifications.

With the desired eigenstructure in place, attention moved in Chapter 4 to developing an eigenstructure assignment technique that would enable the designer to achieve the best possible performance. To do this the designer needs the facility to exploit all the available design freedom. Initially, the state feedback case was considered. It was shown that improved eigenvector assignment could be achieved by introducing freedom in the eigenvalue locations. A mathematical framework for this trade-off was set up and later shown to be equally applicable to the output feedback problem. The helicopter problem requires output feedback. This was considered next. A two stage algorithm was developed, based on the sequential assignment of left and right eigenvectors. This algorithm was extended to multiple stages. It was shown how unused design freedom could be recovered and put to good use. The choice of eigenvectors in the initial stages places strong constraints on those available in subsequent stages. Therefore, selecting the optimum eigenvector in each stage alone is unlikely to lead to the best overall solution. Projection techniques were developed to combat this problem. They force the initial stages to mitigate their effect on later stages or iterate until a compromise solution is reached. These techniques enable the designer to make better use of the available design freedom. If the system states have no physical significance, the eigenvectors lose their engineering visibility. In such cases it is more appropriate to work in the input and output spaces, which implies assigning the modal coupling matrices. A technique for doing this was developed in Chapter 4. Assignment in the input and output spaces enables the engineer to make more effective use of the available design freedom. Static feedback can not always deliver the required performance and dynamic compensation must be employed. It was shown how some different approaches to dynamic compensation may be incorporated into the existing eigenstructure assignment framework. Eigenstructure assignment provides no inherent mechanism for ensuring robustness. A credible design methodology should address robustness and this is the topic of the next chapter.

Chapter 5 developed a post-assignment robustness improvement algorithm. This algorithm will improve robustness with respect to either a time domain or singular value based measure. The drawback of post-design robustness improvement is that an optimum solution, in terms of performance, can only be degraded by the adjustments made to improve robustness. However, this algorithm attempts to keep the degradation to a minimum by confining eigenvalues to allowed regions and protecting the eigenvector directions. The algorithm performs the optimisation with the same parameters used to synthesise the controller. This gives more control over the performance robustness trade-off.

A complete methodology is now in place with a powerful assignment technique, providing insightful access to all the available design freedom, a method of addressing robustness and clearly defined design objectives. In Chapter 6 the methodology was applied to design an attitude command control law for the hover case. The design example began with the state feedback case which is used to illustrate that the desired eigenstructure does embody the required performance goals. The robustness improvement algorithm was shown to deliver significant improvement in robustness and to be effective in keeping the inevitable degradation in performance to a minimum. As expected the output feedback case proved to be a more difficult problem but, using the techniques of iterative assignment and eigenvalue trade-off performance approaching that of the state feedback case was achieved. However, achieving both good performance and good robustness was not possible for the static output feedback case and it is concluded that further development would require dynamic compensation.

The author concludes that the potential of eigenstructure assignment to deliver an appropriate and effective means of designing helicopter control laws has been demonstrated. Further work is needed before the above methodology would offer a complete solution to helicopter control law design.

## 7.2 Contributions

To the best of the author's knowledge the list below describes the novel contributions of this work:

- Development of a novel algorithm that produces representative linearisations of non-linear models accompanied with useful error data and bounds on acceptable state excursions.
- Use of the Hessian form to improve the fidelity of a state space helicopter model.
- Construction of an insightful, simplified model of the helicopter hover dynamics using sensitivity analysis.
- Characterisation of all the second order systems, as a region in the complex plane, that meet the Def-Stan 00-970 response criteria, derived using analytic techniques.
- Derivation of an ideal eigenstructure that meets the Def-Stan 00-970 response criteria and is consistent with the system physics.
- Derivation of some novel proofs of sufficient conditions for complete pole assignment using static output feedback. These proofs are concise and insightful and lead directly to a two stage assignment technique.
- Derivation of novel gain equation that removes restrictions on the number of left or right eigenvectors that must be assigned and thus supports a flexible multistage assignment technique.
- Discovery that unused design freedom can exist after complete assignment and development of a method for recovering the design freedom and its utilisation in a recursive way, consistent with the original assignment approach.

- Formulation of a simultaneous eigenvalue and eigenvector assignment problem that enables a trade-off between the eigenvalue and eigenvector design objectives. An analytical solution to this problem is derived for the case of real eigenvalues.
- Development of some basic theory for assignment in the input and output spaces using the modal coupling matrices and subsequent formulation of an assignment technique.
- Development of a novel algorithm for improving robustness with respect to either of two previously non-utilised robustness measures.
- Derivation of analytic gradients between the output feedback design parameters and both of the robustness measures.
- Development of a mechanism for maintaining performance through the selection of compromise directions.

While significant contributions have been made, the design of helicopter control laws is a substantial problem and considerable opportunities exist for further work.

### 7.3 Further Work

Many suggestions for further work have been made, in context, at the end of each chapter. However, some key topics are highlighted below:

The current analytical solution to the eigenvalue trade-off algorithm is only valid for the real case. Further work is needed to extend the solution to the complex case. This not a trivial matter. A quick description of the direct approach to calculating the solution illustrates the nature of the problem. For the real case evaluation and differentiation of the cost function gives a single polynomial in one variable, the roots of which lead to the global minimum. For the complex case evaluation and differentiation gives two coupled equations in two unknowns, a general solution for this system of equations as yet does not exist. However, once found, a general subspace projection tool can be produced that minimises the following constrained optimisation:

$$J = \min_{\mathbf{f}} \|\mathbf{v}_d - \mathbf{Q}(s)\mathbf{f}\|_2^2 + w_l \|\mathbf{W}_2 \mathbf{Q}(s)\mathbf{f}\|_2^2 \quad \text{subject to} \quad |s_o - s| \leq r_d \quad (7.3.1)$$

Where the terms take their usual meaning.

An efficient computational solution to the above problem has many applications in this work. For instance:

1. Setting  $w_l = 0$  and  $r_d = 0$  is the simple projection case.

2. Setting  $w_l \mapsto \infty$  and  $r_d = 0$  provides a constrained projection.
3. Setting  $w_l \neq 0$ ,  $r_d = 0$  and  $W_2$  to the desired eigenvectors produces the sympathetic projection.
4. Setting  $r_d = 0$  and increasing  $w_l \neq 0$  in a loop with a second complementary optimisation yields the iterative projection technique.
5. Defining a radius  $r_d \neq 0$  enables eigenvalue trade-off to be performed with any of the above projection methods.

This tool subsumes conventional approaches to projection and is recommended in their place.

It was identified as part of the design example that dynamic compensation is needed to achieve both the robustness and performance goals simultaneously. The tools are in place for applying a variety of techniques for dynamic compensator design. These include full order observers, reduced order observers, feedback compensation and pre-compensation. Further work would experiment with different dynamic compensation approaches and identify a suitable strategy. An initial task would be to design a reduced order observer and verify the performance against the state feedback solution. The design example results show that robustification often causes the command tracking performance to suffer. Dynamic compensation to improve the tracking performance may also form a good early task.

Another practical topic for further work would be to apply the techniques and tools described in this thesis to a wider set of problems. The modal analysis and construction of simplified models could be repeated for different forward speeds and other trim conditions. The desired eigenstructures could be developed for rate command and translational rate command, then used to design controllers. Auto-pilot functions such as Direction Hold (DH), Height Hold (HH), Transition to Hover and so on, could also be designed.

Once some control law design experience with different response types and flight condition has been gained, a natural topic for further work is to integrate the control laws in to an AFCS. This will involve addressing issues such as gain scheduling, control law switching, bumpless transfer and anti-windup.

The robustness improvement algorithm delivers good results that certainly justify its continued development. Several opportunities for improvement exist. They include the use of quasi-newton descent directions, the development of an improved line search and the derivation of improved analytical descent directions for the time domain measure. It was observed that, while the time domain measure achieved a monotonic convergence the singular value measure suffered periodic increases due to frequency jumping. This snag is easily removed. Currently, the algorithm scans across the frequency range and identifies the dominant peak. It then calculates a descent direction with respect to that peak. The algorithm could be modified to identify a set of peaks and calculate a descent direction that will decrease all the peaks simultaneously. This does not require the derivation of any new analytical gradients. The line search algorithm will have to be modified to ensure reduction with respect to either all peaks or just the dominant peak.

Design visibility is an important issue for practising engineers. Traditionally, the engineers have adjusted the feedback gains directly and thus gained experience and a good understanding of design using these parameters. A feature of eigenstructure assignment is the bijective mapping between the gains and design parameters. That is, a set of eigenvalue and eigenvector directions can be used to calculate a unique gain matrix and, equally, the gain matrix can be transformed into a unique set of eigenvalues and eigenvector directions. It would be fruitful to develop this characteristic eigenstructure assignment into a design methodology that allows the design to be conducted in either the eigenspace or the gain space. This will further enhance visibility by enabling the designer to use the design parameters appropriate to a particular objective. Development of this design methodology will involve addressing two main issues: firstly, giving eigenvector and eigenvalues, produced by gain adjustment, a meaningful interpretation in terms of the desired eigenstructure and secondly, ensuring that compromises can be reached between adjustments made in either space.

In summary, this work represents the application of eigenstructure assignment to the rotorcraft problem. It further emphasises the true suitability of this technique to the problem domain. The tools, techniques and theory developed here are generic and reduce the practice-theory gap. They form the basis for follow on work which GKN-Westland wish to support, leading to a completely new philosophy for advanced high performance rotorcraft control system design.

# Appendix A

## Helicopter Linearisation at Hover

This appendix contains the state space linearisations, produced using the algorithm described in Section 2.3, of the non-linear helicopter model outlined in Section 2.2.1. The model has been trimmed for the hover using a Newton-Raphson technique as discussed in Section 2.2.2.

### A.1 The State Space Description

The state and input vectors are defined as follows:

$$\mathbf{x}^T \triangleq [u, v, w, p, q, r, \phi, \theta, \psi, a_{1s}, b_{1s}] \quad (\text{A.1.1})$$

$$\mathbf{u}^T \triangleq [A_1, B_1, \theta_0, \theta_t] \quad (\text{A.1.2})$$

Where the linear velocities ( $u, v, w$ ) are in feet per second, the angular rates ( $p, q, r$ ) are in radians per second and the body ( $\phi, \theta, \psi$ ), flapping ( $a_{1s}, b_{1s}$ ) and inputs ( $A_1, B_1, \theta_0, \theta_t$ ) angles are in radians. The system, input and output matrices are:



$$\mathbf{A} = \begin{bmatrix}
 -0.0044 & 0 & 0.0177 & 0 & 0.0089 & 0 & 0 & -32.12 & 0 & -32.82 & 0 \\
 0.0007 & -0.0185 & -0.0034 & -0.0697 & -0.0625 & 0.3543 & 32.06 & 0.1096 & 0 & 0 & 32.82 \\
 0.0298 & 0 & -0.3228 & 0 & -0.0534 & 0 & 1.836 & -1.914 & 0 & -2.291 & 0 \\
 0 & -0.0004 & -0.0001 & -0.0028 & 6.627 & -0.0260 & 0 & 0 & 0 & 0 & 113.0 \\
 0.0005 & 0 & -0.0021 & -1.009 & -0.0153 & 0 & 0 & 0 & 0 & 17.21 & 0 \\
 -0.0004 & 0.0086 & 0.0027 & 0.0355 & 1.246 & -0.2208 & 0 & 0 & 0 & 0 & 20.35 \\
 0 & 0 & 0 & 1.000 & -0.0034 & 0.0596 & 0 & 0 & 0 & 0 & 0 \\
 0 & 0 & 0 & 0 & 0.9984 & 0.0572 & 0 & 0 & 0 & 0 & 0 \\
 0 & 0 & 0 & 0 & -0.0573 & 1.000 & 0 & 0 & 0 & 0 & 0 \\
 0.0158 & -0.0012 & 0.0011 & -0.0131 & -1.273 & 0 & 0 & 0 & 0 & -14.06 & -2.202 \\
 0.0189 & -0.0070 & 0.0013 & -1.236 & -0.0706 & 0 & 0 & 0 & 0 & 2.202 & -14.06
 \end{bmatrix}$$

$$\mathbf{B} = \begin{bmatrix}
 0 & 0 & 17.90 & 0 \\
 0 & 0 & -1.415 & 12.89 \\
 0 & 0 & -299.4 & 0 \\
 0 & 0 & 6.723 & -0.9451 \\
 0 & 0 & -1.523 & 0 \\
 0 & 0 & 14.28 & -8.030 \\
 0 & 0 & 0 & 0 \\
 0 & 0 & 0 & 0 \\
 0 & 0 & 0 & 0 \\
 2.740 & -16.02 & 0 & 0 \\
 15.93 & 2.756 & 0 & 0
 \end{bmatrix}$$

The linearisation uncertainty information as described in Section 2.3 is:

$$\Delta A = \begin{bmatrix} 0.0011 & 0.0006 & 0.0007 & 0.0006 & 0.0006 & 0 & 0 & 0.0018 & 0 & 0 & 0 \\ 0.0006 & 0.0016 & 0.0006 & 0 & 0.0111 & 0.0137 & 0.0017 & 0.0017 & 0 & 0 & 0 \\ 0.0110 & 0.0101 & 0.0140 & 0.0110 & 0.0028 & 0 & 0.0294 & 0.0294 & 0 & 0 & 0 \\ 0 & 0 & 0.0003 & 0 & 0.0008 & 0.0010 & 0 & 0 & 0 & 0 & 0 \\ 0 & 0 & 0.0002 & 0 & 0.0025 & 0 & 0 & 0 & 0 & 0 & 0 \\ 0.0003 & 0.0001 & 0.0010 & 0 & 0.0066 & 0.0085 & 0 & 0 & 0 & 0 & 0 \\ 0 & 0 & 0 & 0 & 0 & 0 & 0 & 0 & 0 & 0 & 0 \\ 0 & 0 & 0 & 0 & 0 & 0 & 0 & 0 & 0 & 0 & 0 \\ 0 & 0 & 0 & 0 & 0 & 0 & 0 & 0 & 0 & 0 & 0 \\ 0 & 0 & 0.0001 & 0 & 0 & 0 & 0 & 0 & 0 & 0 & 0 \\ 0.0002 & 0 & 0.0003 & 0 & 0 & 0 & 0 & 0 & 0 & 0 & 0 \end{bmatrix}$$

$$\Delta B = \begin{bmatrix} 0 & 0 & 0.0527 & 0 \\ 0 & 0 & 0.0042 & 0.1453 \\ 0 & 0 & 0.8818 & 0 \\ 0 & 0 & 0.0818 & 0.0107 \\ 0 & 0 & 0.0045 & 0 \\ 0 & 0 & 0.1604 & 0.0905 \\ 0 & 0 & 0 & 0 \\ 0 & 0 & 0 & 0 \\ 0 & 0 & 0 & 0 \\ 0.1609 & 0.6853 & 0 & 0 \\ 0.9358 & 0.1178 & 0 & 0 \end{bmatrix}$$

## A.2 The Reduced Order Model State Space Description

The state space description for the reduced order helicopter model is given below:

$$\mathbf{y}^T \triangleq [u, v, w, p, q, r, \phi, \theta, \psi, a_{1s}, b_{1s}] \quad (\text{A.2.3})$$

$$\mathbf{x}^T \triangleq [u, v, w, p, q, r, \phi, \theta] \quad (\text{A.2.4})$$

$$\mathbf{u}^T \triangleq [A_1, B_1, \theta_0, \theta_t] \quad (\text{A.2.5})$$

$$A = \begin{bmatrix} -0.0337 & 0.0002 & 0.0157 & -0.4111 & 2.883 & 0 & 0 & -32.12 \\ 0.0494 & -0.0348 & 0 & -2.890 & -0.6777 & 0.3543 & 32.06 & 0.1096 \\ 0.0278 & 0 & -0.3230 & -0.0287 & 0.1473 & 0 & 1.836 & -1.914 \\ 0.1678 & -0.0564 & 0.0117 & -9.710 & 4.509 & -0.0260 & 0 & 0 \\ 0.0158 & -0.0001 & -0.0010 & -0.7938 & -1.522 & 0 & 0 & 0 \\ 0.0298 & -0.0015 & 0.0048 & -1.714 & 0.8642 & -0.2208 & 0 & 0 \\ 0 & 0 & 0 & 1.000 & -0.0034 & 0.0596 & 0 & 0 \\ 0 & 0 & 0 & 0 & 0.9984 & 0.0572 & 0 & 0 \end{bmatrix}$$

$$B = \begin{bmatrix} -0.5570 & 37.50 & 17.90 & 0 \\ 37.28 & 0.5602 & -1.415 & 12.89 \\ -0.0389 & 2.618 & -299.4 & 0 \\ 128.3 & 1.928 & 6.723 & -0.9451 \\ 0.2920 & -19.66 & -1.523 & 0 \\ 23.12 & 0.3475 & 14.28 & -8.030 \\ 0 & 0 & 0 & 0 \\ 0 & 0 & 0 & 0 \end{bmatrix} \quad (\text{A.2.6})$$

$$C = \begin{bmatrix} 1.000 & 0 & 0 & 0 & 0 & 0 & 0 & 0 \\ 0 & 1.000 & 0 & 0 & 0 & 0 & 0 & 0 \\ 0 & 0 & 1.000 & 0 & 0 & 0 & 0 & 0 \\ 0 & 0 & 0 & 1.000 & 0 & 0 & 0 & 0 \\ 0 & 0 & 0 & 0 & 1.000 & 0 & 0 & 0 \\ 0 & 0 & 0 & 0 & 0 & 1.000 & 0 & 0 \\ 0 & 0 & 0 & 0 & 0 & 0 & 1.000 & 0 \\ 0 & 0 & 0 & 0 & 0 & 0 & 0 & 1.000 \\ 0 & 0 & 0 & 0 & 0 & 0 & 0 & 0 \\ 0.0009 & 0 & 0 & 0.0125 & -0.0876 & 0 & 0 & 0 \\ 0.0015 & -0.0005 & 0.0001 & -0.0859 & -0.0187 & 0 & 0 & 0 \end{bmatrix} \quad (\text{A.2.7})$$

$$\mathbf{D} = \begin{bmatrix} 0 & 0 & 0 & 0 \\ 0 & 0 & 0 & 0 \\ 0 & 0 & 0 & 0 \\ 0 & 0 & 0 & 0 \\ 0 & 0 & 0 & 0 \\ 0 & 0 & 0 & 0 \\ 0 & 0 & 0 & 0 \\ 0 & 0 & 0 & 0 \\ 0 & 0 & 0 & 0 \\ 0.0170 & -1.143 & 0 & 0 \\ 1.136 & 0.0171 & 0 & 0 \end{bmatrix} \quad (\text{A.2.8})$$

# Appendix B

## Supporting Mathematics

### Contents

---

B.1 Proof of Matrix Lemma 4.5.3 . . . . .	296
B.2 Guaranteed Real Gain Matrix Proof . . . . .	300
B.3 Proof that the Retro-Stage Offers No Additional DoF . . . . .	302
B.4 References . . . . .	304

---

To avoid stifling the flow of the main text some of the supporting mathematics is relegated to the following appendix.

### B.1 Proof of Matrix Lemma 4.5.3

Lemma 4.5.3<sup>1</sup> forms an important part of the proof of Theorem 4.5.3 and leads to a powerful expression for the gain matrix ( $\mathbf{K}$ ). Before proving the Lemma, for completeness, let us first restate it.

#### Lemma 4.5.3

Let  $\mathbf{K} \in \mathbb{C}^{r \times m}$ ,  $\mathbf{X} \in \mathbb{C}^{m \times x}$ ,  $\mathbf{S}_1 \in \mathbb{C}^{r \times x}$ ,  $\mathbf{Y} \in \mathbb{C}^{y \times r}$  and  $\mathbf{T}_2 \in \mathbb{C}^{y \times m}$ , where  $m \geq x$  and  $r \geq y$ . Then the matrix equations:

$$\mathbf{KX} = \mathbf{S}_1 \tag{B.1.1}$$

$$\mathbf{YK} = \mathbf{T}_2 \tag{B.1.2}$$

have a consistent solution for  $\mathbf{K}$  if all the following conditions hold.

---

<sup>1</sup>To the author's knowledge the only other instance of this result is presented by Rao *et al* [RM71]. However, although the solution is identical the accompanying necessary and sufficient conditions are incorrect.

$$C1 \text{ rank}(\mathbf{X}) = x$$

$$C2 \text{ rank}(\mathbf{Y}) = y$$

$$C3 \mathbf{T}_2 \mathbf{X} = \mathbf{Y} \mathbf{S}_1$$

The general solution for  $\mathbf{K}$  is then:

$$\mathbf{K} = \mathbf{Y}^\dagger \mathbf{T}_2 + \mathbf{S}_1 \mathbf{X}^\dagger - \mathbf{Y}^\dagger \mathbf{Y} \mathbf{S}_1 \mathbf{X}^\dagger + (\mathbf{I} - \mathbf{Y}^\dagger \mathbf{Y}) \mathbf{Z} (\mathbf{I} - \mathbf{X} \mathbf{X}^\dagger) \quad (\text{B.1.3})$$

or equivalently:

$$\mathbf{K} = \mathbf{Y}^\dagger \mathbf{T}_2 + \mathbf{S}_1 \mathbf{X}^\dagger - \mathbf{Y}^\dagger \mathbf{T}_2 \mathbf{X} \mathbf{X}^\dagger + (\mathbf{I} - \mathbf{Y}^\dagger \mathbf{Y}) \mathbf{Z} (\mathbf{I} - \mathbf{X} \mathbf{X}^\dagger) \quad (\text{B.1.4})$$

where  $\mathbf{Z} \in \mathbb{C}^{y \times x}$  is a free parameter matrix that characterises the complete set of solutions.

◇◇

### Proof

The proof proceeds by first characterising all the solutions to Equation (B.1.1) and then seeking a subset of these solutions that will also satisfy Equation (B.1.2).

Examination of Equation (B.1.2) and Equation (B.1.1) quickly reveals that all solutions will satisfy:

$$\mathbf{Y} \mathbf{S}_1 = \mathbf{Y} (\mathbf{K} \mathbf{X}) = (\mathbf{Y} \mathbf{K}) \mathbf{X} = \mathbf{T}_2 \mathbf{X} \quad (\text{B.1.5})$$

$$\mathbf{Y} \mathbf{S}_1 = \mathbf{T}_2 \mathbf{X} \quad (\text{B.1.6})$$

However, meeting this condition is not enough to guarantee a solution exists. Therefore, Equation (B.1.6) is a necessary condition. A general solution [BIG74, p. 40] to Equation (B.1.1) alone will exist if and only if:

$$\text{rank} \left( \begin{bmatrix} \mathbf{S}_1 \\ \mathbf{X} \end{bmatrix} \right) = \text{rank}(\mathbf{X}) \quad (\text{B.1.7})$$

in which case the solution is:

$$\mathbf{K} = \mathbf{S}_1 \mathbf{X}^{(1)} + \mathbf{Z}_1 (\mathbf{I} - \mathbf{X} \mathbf{X}^{(1)}) \quad (\text{B.1.8})$$

Where  $\mathbf{X}^{(1)}$  is a generalised one inverse [BIG74, p. 7] that satisfies  $\mathbf{X}\mathbf{X}^{(1)}\mathbf{X} = \mathbf{X}$  and  $\mathbf{Z}_1 \in \mathbb{R}^{r \times m}$  is a free parameter that characterises the set of solutions.

Substituting the general solution of Equation (B.1.1) into Equation (B.1.2)

$$\mathbf{Y}\mathbf{K} = \mathbf{T}_2 \tag{B.1.9}$$

$$\mathbf{Y} \left( \mathbf{S}_1 \mathbf{X}^{(1)} + \mathbf{Z}_1 \left( \mathbf{I} - \mathbf{X}\mathbf{X}^{(1)} \right) \right) = \mathbf{T}_2 \tag{B.1.10}$$

$$\mathbf{Y}\mathbf{S}_1 \mathbf{X}^{(1)} + \mathbf{Y}\mathbf{Z}_1 - \mathbf{Y}\mathbf{Z}_1 \mathbf{X}\mathbf{X}^{(1)} = \mathbf{T}_2 \tag{B.1.11}$$

and invoking the necessary condition of Equation (B.1.6) gives:

$$\mathbf{T}_2 \mathbf{X}\mathbf{X}^{(1)} + \mathbf{Y}\mathbf{Z}_1 - \mathbf{Y}\mathbf{Z}_1 \mathbf{X}\mathbf{X}^{(1)} = \mathbf{T}_2 \tag{B.1.12}$$

We now seek a solution for  $\mathbf{Z}_1$  that will satisfy Equation (B.1.12). It is worth noting that examination of Equation (B.1.12) shows that  $\mathbf{Y}\mathbf{Z}_1 = \mathbf{T}_2$  is a sufficient condition for a solution. However, to find the general solution Equation (B.1.12) is rearranged into a familiar format for which the general solution is well known.

$$\mathbf{T}_2 \left( \mathbf{I} - \mathbf{X}\mathbf{X}^{(1)} \right) = \mathbf{Y}\mathbf{Z}_1 \left( \mathbf{I} - \mathbf{X}\mathbf{X}^{(1)} \right) \tag{B.1.13}$$

A solution for  $\mathbf{Z}_1$  exists if and only if

$$\text{rank} \left( \begin{bmatrix} \mathbf{Y} & \mathbf{T}_2 \left( \mathbf{I} - \mathbf{X}\mathbf{X}^{(1)} \right) \end{bmatrix} \right) = \text{rank}(\mathbf{Y}) \tag{B.1.14}$$

$$\text{rank} \left( \begin{bmatrix} \mathbf{I} - \mathbf{X}\mathbf{X}^{(1)} \\ \mathbf{T}_2 \left( \mathbf{I} - \mathbf{X}\mathbf{X}^{(1)} \right) \end{bmatrix} \right) = \text{rank} \left( \mathbf{I} - \mathbf{X}\mathbf{X}^{(1)} \right) \tag{B.1.15}$$

Examination of the general conditions above shows that, in this case, Equation (B.1.15) is always satisfied. If Equation (B.1.14) is satisfied then the general solution [BIG74, p. 39] is:

$$\mathbf{Z}_1 = \mathbf{Y}^{(1)}\mathbf{T}_2 \left( \mathbf{I} - \mathbf{X}\mathbf{X}^{(1)} \right) \left( \mathbf{I} - \mathbf{X}\mathbf{X}^{(1)} \right)^{(1)} + \mathbf{Z}_2 - \mathbf{Y}^{(1)}\mathbf{Y}\mathbf{Z}_2 \left( \mathbf{I} - \mathbf{X}\mathbf{X}^{(1)} \right) \left( \mathbf{I} - \mathbf{X}\mathbf{X}^{(1)} \right)^{(1)} \tag{B.1.16}$$

The expression  $\left( \mathbf{I} - \mathbf{X}\mathbf{X}^{(1)} \right)$  is always idempotent. It is therefore straightforward to show that:

$$\left(\mathbf{I} - \mathbf{X}\mathbf{X}^{(1)}\right) \left(\mathbf{I} - \mathbf{X}\mathbf{X}^{(1)}\right)^{(1)} = \left(\mathbf{I} - \mathbf{X}\mathbf{X}^{(1)}\right) \quad (\text{B.1.17})$$

Thus the following simplifications are afforded:

$$\mathbf{Z}_1 = \mathbf{Y}^{(1)}\mathbf{T}_2 \left(\mathbf{I} - \mathbf{X}\mathbf{X}^{(1)}\right) + \mathbf{Z}_2 - \mathbf{Y}^{(1)}\mathbf{Y}\mathbf{Z}_2 \left(\mathbf{I} - \mathbf{X}\mathbf{X}^{(1)}\right) \quad (\text{B.1.18})$$

Substituting Equation (B.1.18) into Equation (B.1.8) reveals the final solution:

$$\mathbf{K} = \mathbf{S}_1 \mathbf{X}^{(1)} + \left(\mathbf{Y}^{(1)}\mathbf{T}_2 \left(\mathbf{I} - \mathbf{X}\mathbf{X}^{(1)}\right) + \mathbf{Z}_2 - \mathbf{Y}^{(1)}\mathbf{Y}\mathbf{Z}_2 \left(\mathbf{I} - \mathbf{X}\mathbf{X}^{(1)}\right)\right) \left(\mathbf{I} - \mathbf{X}\mathbf{X}^{(1)}\right) \quad (\text{B.1.19})$$

$$= \mathbf{S}_1 \mathbf{X}^{(1)} + \mathbf{Y}^{(1)}\mathbf{T}_2 \left(\mathbf{I} - \mathbf{X}\mathbf{X}^{(1)}\right) \mathbf{Z}_2 \left(\mathbf{I} - \mathbf{X}\mathbf{X}^{(1)}\right) - \mathbf{Y}^{(1)}\mathbf{Y}\mathbf{Z}_2 \left(\mathbf{I} - \mathbf{X}\mathbf{X}^{(1)}\right) \quad (\text{B.1.20})$$

$$= \mathbf{S}_1 \mathbf{X}^{(1)} + \mathbf{Y}^{(1)}\mathbf{T}_2 - \mathbf{Y}^{(1)}\mathbf{T}_2 \mathbf{X}\mathbf{X}^{(1)} + \left(\mathbf{I} - \mathbf{Y}^{(1)}\mathbf{Y}\right) \mathbf{Z}_2 \left(\mathbf{I} - \mathbf{X}\mathbf{X}^{(1)}\right) \quad (\text{B.1.21})$$

If one begins with Equation (B.1.2) instead of Equation (B.1.1) the final solution is:

$$\mathbf{K} = \mathbf{S}_1 \mathbf{X}^{(1)} + \mathbf{Y}^{(1)}\mathbf{T}_2 - \mathbf{Y}^{(1)}\mathbf{Y}\mathbf{S}_1 \mathbf{X}^{(1)} + \left(\mathbf{I} - \mathbf{Y}^{(1)}\mathbf{Y}\right) \mathbf{Z}_2 \left(\mathbf{I} - \mathbf{X}\mathbf{X}^{(1)}\right) \quad (\text{B.1.22})$$

we see from Equation (B.1.6) that the two solutions are identical. The derivation above is summarised in the following lemma:

**Lemma B.1.1**

Let  $\mathbf{K} \in \mathbb{C}^{r \times m}$ ,  $\mathbf{X} \in \mathbb{C}^{m \times x}$ ,  $\mathbf{S}_1 \in \mathbb{C}^{r \times x}$ ,  $\mathbf{Y} \in \mathbb{C}^{y \times r}$  and  $\mathbf{T}_2 \in \mathbb{C}^{y \times m}$ . Then the matrix equations:

$$\mathbf{K}\mathbf{X} = \mathbf{S}_1 \quad (\text{B.1.23})$$

$$\mathbf{Y}\mathbf{K} = \mathbf{T}_2 \quad (\text{B.1.24})$$

have a consistent solution for  $\mathbf{K}$  if all the following conditions hold.

$$C1 \quad \text{rank} \left( \begin{bmatrix} \mathbf{S}_1 \\ \mathbf{X} \end{bmatrix} \right) = \text{rank}(\mathbf{X})$$

$$C2 \quad \text{rank} \left( \begin{bmatrix} \mathbf{Y} & \mathbf{T}_2 \left(\mathbf{I} - \mathbf{X}\mathbf{X}^{(1)}\right) \end{bmatrix} \right) = \text{rank}(\mathbf{Y})$$



$$C3 \quad T_2 X = Y S_1$$

The general solution for  $K$  is then:

$$K = Y^{(1)} T_2 + S_1 X^{(1)} - Y^{(1)} Y S_1 X^{(1)} + (I - Y^{(1)} Y) Z (I - X X^{(1)}) \quad (B.1.25)$$

or equivalently:

$$K = Y^{(1)} T_2 + S_1 X^{(1)} - Y^{(1)} T_2 X X^{(1)} + (I - Y^{(1)} Y) Z (I - X X^{(1)}) \quad (B.1.26)$$

where  $Z \in \mathbb{C}^{y \times x}$  is a free parameter matrix that characterises the complete set of solutions.

◇◇

The conditions for a solution given in Lemma 4.5.3 are more restrictive than those of Lemma B.1.1. However, for the purposes of eigenstructure assignment the conditions of Lemma 4.5.3 are more appropriate and form a natural complement to Theorem 4.5.3.

Let us consider Equation (B.1.7), recalling that  $X \in \mathbb{C}^{m \times x}$  and  $m \geq x$  it is clear that:

$$\text{rank}(X) = x \quad (B.1.27)$$

implies that:

$$\text{rank} \left( \begin{bmatrix} S_1 \\ X \end{bmatrix} \right) = x \quad (B.1.28)$$

The same argument applies to Equation (B.1.15) and if  $X$  is full rank then  $X^{(1)} = X^\dagger$  [BIG74] thus Lemma 4.5.3 is a corollary of Lemma B.1.1.

◇◇

## B.2 Guaranteed Real Gain Matrix Proof

In Section 4.5.3 it was stated that conditions C1 and C2 of Theorem 4.5.3 ensure that gain matrices calculated using the formula below are always real:

$$K = (W_2 B)^\dagger T_2 + S_1 (C V_1)^\dagger - (W_2 B)^\dagger T_2 C V_1 (C V_1)^\dagger \quad (B.2.29)$$

**Proof**

The proof proceeds by showing that conditions C1 and C2 of Theorem 4.5.3 ensure that all the complex matrices of the gain equation may be expressed as the product of a unitary complex matrix and a real matrix. It is then demonstrated, for each summand of Equation (B.2.29) in turn, that the complex elements cancel to give real products and thus a real gain matrix.

Examination of Condition C2 of Theorem 4.5.3 confirms that  $\mathbf{W}_2$  may be factorised into two full rank matrices  $(\mathbf{X}\hat{\mathbf{W}}_2)$ . Such that  $\hat{\mathbf{W}}_2 \in \mathbb{R}^{s_2 \times n}$  is real and  $\mathbf{X}$  is complex and constructed as follows:

$$\mathbf{X} = \text{diag}(\mathbf{X}_k) \quad k = 1 \dots s_2 \quad (\text{B.2.30})$$

with

$$\mathbf{X}_k = \begin{cases} 1 & \Lambda_{D2_{i,i}} \quad \text{is real, } i = 1..s_2 \\ \begin{bmatrix} \frac{1}{\sqrt{2}} & -\frac{j}{\sqrt{2}} \\ \frac{1}{\sqrt{2}} & \frac{j}{\sqrt{2}} \end{bmatrix} & \Lambda_{D2_{i,i}}, \Lambda_{D2_{i+1,i+1}} \quad \text{are a complex pair, } i = 1..s_2 \end{cases} \quad (\text{B.2.31})$$

Where  $\Lambda_{D2_{i,i}}$  is the  $i^{\text{th}}$  diagonal element of  $\Lambda_{D2}$  which is the eigenvalue associated with the left eigenvector ( $w_i$ ) or  $i^{\text{th}}$  row of  $\mathbf{W}_2$ . The construction of  $\mathbf{X}$  ensures that it is unitary and thus will satisfy  $\mathbf{X}^* \mathbf{X} = \mathbf{I}$ .

The pseudo inverse  $(\mathbf{W}_2 \mathbf{B})^\dagger$  may be calculated from a full rank factorisation [BIG74, p. 23]. The factorisation constructed above is one such factorisation and thus:

$$(\mathbf{W}_2 \mathbf{B})^\dagger = (\mathbf{X}(\hat{\mathbf{W}}_2 \mathbf{B}))^\dagger \quad (\text{B.2.32})$$

$$= (\hat{\mathbf{W}}_2 \mathbf{B})^T ((\hat{\mathbf{W}}_2 \mathbf{B})(\hat{\mathbf{W}}_2 \mathbf{B})^T)^{-1} (\mathbf{X}^* \mathbf{X})^{-1} \mathbf{X}^* \quad (\text{B.2.33})$$

$$= (\hat{\mathbf{W}}_2 \mathbf{B})^T ((\hat{\mathbf{W}}_2 \mathbf{B})(\hat{\mathbf{W}}_2 \mathbf{B})^T)^{-1} \mathbf{X}^* \quad (\text{B.2.34})$$

Since  $\mathbf{T}_2$  is constructed in an identical manner to  $\mathbf{W}_2$ , there also exists a factorisation  $\mathbf{T}_2 = \mathbf{X}\hat{\mathbf{T}}_2$  where  $\hat{\mathbf{T}}_2 \in \mathbb{R}^{s_2 \times m}$  is real and  $\mathbf{X}$  is defined above.

Thus:

$$(\mathbf{W}_2 \mathbf{B})^\dagger \mathbf{T}_2 = (\hat{\mathbf{W}}_2 \mathbf{B})^T ((\hat{\mathbf{W}}_2 \mathbf{B})(\hat{\mathbf{W}}_2 \mathbf{B})^T)^{-1} \mathbf{X}^* \mathbf{X} \hat{\mathbf{T}}_2 \quad (\text{B.2.35})$$

$$= (\hat{\mathbf{W}}_2 \mathbf{B})^T ((\hat{\mathbf{W}}_2 \mathbf{B})(\hat{\mathbf{W}}_2 \mathbf{B})^T)^{-1} \hat{\mathbf{T}}_2 \quad (\text{B.2.36})$$

which since all terms are real the result is also real.

An almost identical argument holds for the term  $S_1 (CV_1)^\dagger$ . Since this term has the same structure as the term  $(W_2 B)^\dagger T_2$ , only transposed.

Finally, we consider the term  $(W_2 B)^\dagger T_2 CV_1 (CV_1)^\dagger$ . Recalling that:

$$T_2 CV_1 = W_2 BS_1 \quad (\text{B.2.37})$$

the term may be rewritten as  $(W_2 B)^\dagger W_2 BS_1 (CV_1)^\dagger$ . This term is considered in halves. It has already been established that the portion  $S_1 (CV_1)^\dagger$  is real. Reference to Equation (B.2.34) shows that if  $W_2 B$  is expressed as  $X\hat{W}_2 B$  then the remaining portion  $(W_2 B)^\dagger W_2 B$  must also be real. Thus the term  $(W_2 B)^\dagger W_2 BS_1 (CV_1)^\dagger$  is a real matrix and hence the gain matrix ( $K$ ) is also real.

◇◇

### B.3 Proof that the Retro-Stage Offers No Additional DoF

In Section 4.5.4 it was stated that re-assigning eigenvectors in the retro-stage offers no advantage over assigning them in the initial design. Assuming that the initial design is performed using two stage assignment this statement is proved.

#### Proof

The proof proceeds by arguing that eigenvectors assigned in stage one of the initial design enjoy the maximum design freedom and thus can not be bettered. The proof then focuses on re-assignment of eigenvectors initially assigned in stage two and shows that all the allowed subspace solutions available in the retro-stage were also available in stage two of the initial design.

During stage one of the initial design, assignment enjoys the maximum design freedom for a given  $(A, B)$  or  $(A, C)$  system pair. Any assignable eigenvector must satisfy condition C1 or C2 of Theorem 4.5.3 and since these are the only restrictions that apply during stage one, it is clear that the maximum design freedom is available.

Since the stage one eigenvectors can not be bettered it is assumed that they are protected. For convenience let us assume that right eigenvectors  $(V_1)$  were assigned in stage one and thus the reduced system will satisfy:

$$0 = \tilde{C}V_1 \quad (\text{B.3.38})$$

Consider assignment of the left eigenvectors in stage two of the initial design. The allowed subspace must satisfy the augmented matrix equation below:

$$\mathbf{0} = \begin{bmatrix} \mathbf{L}_j & \mathbf{M}_j \end{bmatrix} \begin{bmatrix} \mathbf{V}_1 & \mathbf{A} - \lambda_{d_j} \mathbf{I} \\ \mathbf{0} & \mathbf{C} \end{bmatrix} \quad \text{for all } j = (s_1 + 1) \dots n \quad (\text{B.3.39})$$

Which may be expressed as two separate equations:

$$\mathbf{L}_j(\mathbf{A} - \lambda_{d_j} \mathbf{I}) + \mathbf{M}_j \mathbf{C} = \mathbf{0} \quad (\text{B.3.40})$$

$$\mathbf{L}_j \mathbf{V}_1 = \mathbf{0} \quad (\text{B.3.41})$$

Equally, the allowed subspace in the retro-stage ( $\tilde{\mathbf{L}}_j$ ) must satisfy the following equation:

$$\tilde{\mathbf{L}}_j(\tilde{\mathbf{A}} - \lambda_{d_j} \mathbf{I}) + \tilde{\mathbf{M}}_j \tilde{\mathbf{C}} = \mathbf{0} \quad (\text{B.3.42})$$

To demonstrate that there is no additional design freedom in the retro-stage we will show that all the solutions for  $\tilde{\mathbf{L}}_j$  of Equation (B.3.42) also satisfy Equation (B.3.40) and Equation (B.3.41).

Expansion of  $\tilde{\mathbf{A}}$  and a little rearrangement of Equation (B.3.42) shows that  $\tilde{\mathbf{L}}_j$  will satisfy Equation (B.3.40):

$$\tilde{\mathbf{L}}_j(\mathbf{A} + \mathbf{BKC} - \lambda_{d_j} \mathbf{I}) + \tilde{\mathbf{M}}_j \mathbf{Ncv} \mathbf{C} = \mathbf{0} \quad (\text{B.3.43})$$

$$\tilde{\mathbf{L}}_j(\mathbf{A} - \lambda_{d_j} \mathbf{I}) + (\tilde{\mathbf{L}}_j \mathbf{BK} + \tilde{\mathbf{M}}_j \mathbf{Ncv}) \mathbf{C} = \mathbf{0} \quad (\text{B.3.44})$$

Multiplication of Equation (B.3.42) by  $\mathbf{V}_1$  gives:

$$\left( \tilde{\mathbf{L}}_j(\tilde{\mathbf{A}} - \lambda_{d_j} \mathbf{I}) + \tilde{\mathbf{M}}_j \tilde{\mathbf{C}} \right) \mathbf{V}_1 = \mathbf{0} \quad (\text{B.3.45})$$

which due to Equation (B.3.38) becomes:

$$\tilde{\mathbf{L}}_j(\tilde{\mathbf{A}} - \lambda_{d_j} \mathbf{I}) \mathbf{V}_1 = \mathbf{0} \quad (\text{B.3.46})$$

and since  $\mathbf{V}_1$  are the closed loop eigenvectors:

$$\tilde{\mathbf{L}}_j \mathbf{V}_1 \Lambda_{D1} = \mathbf{0} \quad (\text{B.3.47})$$

Thus  $\tilde{\mathbf{L}}_j$  also satisfies Equation (B.3.41) which completes the proof.  $\diamond \diamond$

## B.4 References

- [BIG74] A Ben-Israel and NE Greville. *Generalised Inverses: Theory and Applications*. A Wiley-Interscience publication. John Wiley and Sons, Inc., 1974.
- [RM71] CR Rao and SK Mitra. *Generalised Inverse of Matrices and its Applications*. John Wiley and Sons, Inc., 1971.

# Appendix C

## Polynomial Matrices

### Contents

---

<b>C.1 Calculation of the Allowed Eigenvector Subspace . . . . .</b>	<b>305</b>
<b>C.2 Evaluation of the Eigenvector Cost Function . . . . .</b>	<b>309</b>
<b>C.3 References . . . . .</b>	<b>316</b>

---

Some of the techniques described in this thesis involve the manipulation of polynomial matrices. Algorithms and reliable software for the manipulation of polynomial matrices are considerably less well developed than for numerical matrix computations. This chapter considers computation of two particular problems. However, much of the theory may be used for general manipulation of polynomial matrices.

### C.1 Calculation of the Allowed Eigenvector Subspace

This section considers solving the following equation:

$$0 = \begin{bmatrix} \mathbf{A} - s\mathbf{I} & \mathbf{B} \end{bmatrix} \mathbf{N}(s) \tag{C.1.1}$$

Where  $(\mathbf{A}, \mathbf{B})$  are a controllable pair.

Duan [Dua93] proposes two symbolic methods for calculation of the solution. The first uses the Smith Canonical Form [Bar83, p319] and exploits the fact that for a controllable pair  $(\mathbf{A}, \mathbf{B})$  the matrix  $\begin{bmatrix} \mathbf{A} - s\mathbf{I} & \mathbf{B} \end{bmatrix}$  maintains full rank for all values of  $s$  [DeC89]. The Smith Canonical Form constructs two unimodular matrices<sup>1</sup>  $(\mathbf{Y}(s), \mathbf{X}(s))$  that diagonalise a given polynomial matrix, the

---

<sup>1</sup>Unimodular matrices have constant non-zero determinants. They are the units of the ring of polynomial matrices.

zeros of the diagonal matrix  $\mathbf{D}(s)$  indicate the values of  $s$  at which the given polynomial matrix loses rank. For this case the Smith Canonical Form satisfies:

$$\mathbf{Y}(s) \begin{bmatrix} \mathbf{A} - s\mathbf{I} & \mathbf{B} \end{bmatrix} \mathbf{X}(s) = \mathbf{D}(s) \quad (\text{C.1.2})$$

Since the pair  $(\mathbf{A}, \mathbf{B})$  are controllable no value of  $s$  will cause  $\mathbf{D}(s)$  to lose rank thus it follows:

$$\mathbf{Y}(s) \begin{bmatrix} \mathbf{A} - s\mathbf{I} & \mathbf{B} \end{bmatrix} \mathbf{X}(s) = \begin{bmatrix} \mathbf{I} & \mathbf{0} \end{bmatrix} \quad (\text{C.1.3})$$

The leading diagonal of  $\mathbf{D}(s)$  forms an identity matrix. The last  $r$  columns of  $\mathbf{X}(s)$  produce the  $r$  zero columns of  $\mathbf{D}(s)$ . Since  $\mathbf{Y}(s)$  is a non-singular matrix, these columns solve Equation (C.1.1). Thus we can partition  $\mathbf{X}(s)$  to extract the solution, as follows:

$$\mathbf{X}(s) = \begin{bmatrix} \mathbf{X}_1(s) & \mathbf{X}_2(s) \end{bmatrix} = \begin{bmatrix} \mathbf{X}_1(s) & \mathbf{N}(s) \end{bmatrix} \quad (\text{C.1.4})$$

where  $\mathbf{X}(s)$  is  $n + r$  by  $n + r$ ,  $\mathbf{X}_1(s)$  is  $n + r$  by  $n$  and  $\mathbf{X}_2(s) = \mathbf{N}(s)$  which are  $n + r$  by  $r$ . To apply this approach in practice an algorithm is needed to calculate the Smith Canonical Form, fortunately the general proof of this form [Mac89, GLL82, RS70] is constructive and thus may be easily converted into an algorithms.

The second approach uses the Matrix Fraction Description (MFD) [Kai80]. If all the elements of a matrix are proper rational polynomials then the matrix may be factored as  $\mathbf{X}(s)\mathbf{Y}(s)^{-1}$ . The elements of  $(s\mathbf{I} - \mathbf{A})^{-1}\mathbf{B}$  are rational polynomials. thus:

$$(s\mathbf{I} - \mathbf{A})^{-1}\mathbf{B} = \mathbf{X}(s)\mathbf{Y}(s)^{-1} \quad (\text{C.1.5})$$

$$\mathbf{0} = (\mathbf{A} - s\mathbf{I})\mathbf{X}(s) + \mathbf{B}\mathbf{Y}(s) \quad (\text{C.1.6})$$

$$\mathbf{0} = \begin{bmatrix} \mathbf{A} - s\mathbf{I} & \mathbf{B} \end{bmatrix} \begin{bmatrix} \mathbf{X}(s) \\ \mathbf{Y}(s) \end{bmatrix} \quad (\text{C.1.7})$$

Equation (C.1.7) shows that any MFD of  $(s\mathbf{I} - \mathbf{A})^{-1}\mathbf{B}$  is automatically a solution of Equation (C.1.1), explicitly we note:

$$\begin{bmatrix} \mathbf{X}(s) \\ \mathbf{Y}(s) \end{bmatrix} = \mathbf{N}(s) \quad (\text{C.1.8})$$

A convenient solution for Equation (C.1.7) can be found by inspection:

$$\mathbf{X}(s) = (s\mathbf{I} - \mathbf{A})^{-1}\mathbf{B} \quad (\text{C.1.9})$$

$$\mathbf{Y}(s) = \mathbf{I} \quad (\text{C.1.10})$$

The Smith Canonical Form and MFD approaches are both concise mathematical solutions to Equation (C.1.1). But both approaches require symbolic manipulation to perform the Smith Decomposition or matrix inversion. This presents no difficulty when working by hand or using a symbolic software package such as Maple [Hec93]. However, it is desirable to develop numerical algorithms [SPG92] that can be directly implemented in software packages such as Matlab and Octave. This requires a numerical representation of a polynomial matrix. A polynomial matrix  $\mathbf{N}(s)$  of degree  $d$  may be written as:

$$\mathbf{N}(s) = \mathbf{N}_0 + \mathbf{N}_1s + \dots + \mathbf{N}_{d-1}s^{d-1} + \mathbf{N}_ds^d \quad (\text{C.1.11})$$

Where the *degree*  $d$  is the highest power of  $s$  over all the elements of  $\mathbf{N}(s)$ ,  $\mathbf{N}_i$  is a matrix of coefficients for the indeterminate ( $s$ ) of power  $i$ . The coefficient matrices may be concatenated in to a single block coefficient matrix.

$$\mathbf{N} = [\mathbf{N}_0, \mathbf{N}_1, \dots, \mathbf{N}_{m-1}, \mathbf{N}_m] \quad (\text{C.1.12})$$

This representation is used in numerical software packages such a Matlab, where block coefficient matrices may be stored in row:

$$\mathbf{N} = [\mathbf{N}_0, \mathbf{N}_1, \dots, \mathbf{N}_{m-1}, \mathbf{N}_m] \quad (\text{C.1.13})$$

or column form:

$$\mathbf{N} = \begin{bmatrix} \mathbf{N}_0 \\ \mathbf{N}_1 \\ \vdots \\ \mathbf{N}_m \end{bmatrix} \quad (\text{C.1.14})$$

Note, that one form is not the transpose of the other since the individual coefficient matrices are not transposed. In the following development, the column representation will be used.



Addition of two polynomial matrices using the block coefficient matrix representation is straightforward. The block coefficient matrix of lower degree is padded with zeros, the two equal size matrices are then simply added. Multiplication using block coefficient form requires the construction of a matrix known as the resultant of a polynomial matrix. The resultant of a polynomial matrix  $L(s)$  is denoted  $\langle L \rangle_d$ , where  $d$  is the order of the resultant. The following recursive formula allows the resultant of a polynomial matrix to be constructed a column at a time:

$$\langle L \rangle_0 \triangleq L \tag{C.1.15}$$

$$\langle L \rangle_{i+1} \triangleq \begin{bmatrix} \langle L \rangle_i & \mathbf{0} \\ \mathbf{0} & L \end{bmatrix} \quad i = 0 \dots d \tag{C.1.16}$$

We see final form is the column representation of  $L(s)$  repeated and staggered down the main diagonal:

$$\langle L \rangle_i = \begin{bmatrix} L_0 & \mathbf{0} & \dots & \dots & \mathbf{0} \\ \vdots & L_0 & \ddots & & \vdots \\ \vdots & \vdots & \ddots & \ddots & \vdots \\ L_m & \vdots & \dots & \dots & \mathbf{0} \\ \mathbf{0} & L_m & & & L_0 \\ \vdots & \ddots & \ddots & & \vdots \\ \vdots & & \ddots & \ddots & \vdots \\ \mathbf{0} & \dots & \dots & \mathbf{0} & L_m \end{bmatrix} \tag{C.1.17}$$

Where  $L(s)$  has degree  $m$ .

If two polynomial matrices are conformable for multiplication then the block coefficient matrix of their product can be calculated directly using the resultant matrix. The order of the resultant matrix must equal the degree of the multiplying matrix.

$$X = \langle L \rangle_d N \tag{C.1.18}$$

Where  $N$  is a block coefficient matrix of degree  $d$ ,  $\langle L \rangle_d$  is an order  $d$  resultant of the polynomial matrix  $L(s)$  and  $X$  is the block coefficient matrix of their product.

Returning to the original problem, we see that solving Equation (C.1.1), requires that the product of two polynomial matrices should equal zero. Let

$$\mathbf{L}(s) = [\mathbf{A} - s\mathbf{I}, \mathbf{B}] \quad (\text{C.1.19})$$

and the block coefficient representation is:

$$\mathbf{L} = \begin{bmatrix} \mathbf{A} & \mathbf{B} \\ -\mathbf{I} & \mathbf{0} \end{bmatrix} \quad (\text{C.1.20})$$

The block coefficient form of the solution is a matrix of dimension  $r$  that spans the null space of  $\langle \mathbf{L} \rangle_d$ . Thus a numerical method for solving Equation (C.1.1) is:

1. Find minimum  $d$  such that  $\ker(\langle \mathbf{L} \rangle_d)$  has dimension  $r$ .
2. Calculate a matrix ( $\mathbf{N}$ ) that spans  $\ker(\langle \mathbf{L} \rangle_d)$ .

In fact, since both  $\mathbf{L}_0$  and  $\mathbf{L}_1$  of Equation (C.1.19) are full rank the dimension of  $\ker(\langle \mathbf{L} \rangle_d)$  is equal to the excess of columns over rows. Thus the minimum order of the resultant  $\langle \mathbf{L} \rangle_d$  which has a null space of dimension greater than or equal to  $r$  can be calculated, thus:

$$(d+1)(n+r) - ((d+1)r+n) \geq r \quad (\text{C.1.21})$$

$$d \geq \frac{n}{r} \quad (\text{C.1.22})$$

The solution in block coefficient form is:

$$\text{range}(\mathbf{N}) = \ker(\langle \mathbf{L} \rangle_d) \quad (\text{C.1.23})$$

Where the order of the resultant  $\langle \mathbf{L} \rangle_d$  is given by Equation (C.1.22). Calculation of the null space can be computed using numerically stable codes such as Singular Value Decomposition (SVD) and QR decomposition [GL83]. A memory efficient form of the algorithm that does not explicitly calculate the resultant was proposed by Wang and Davision [WD73] and implemented in Matlab by Kwakernaak [Kwa90]. A similar approach was also taken by White [Whi91].

## C.2 Evaluation of the Eigenvector Cost Function

This section details methods of evaluating the expression below, and also describes some interesting properties.

$$Jv_i = v d_i^* \left[ \mathbf{I} - \mathbf{Q}(s) (\mathbf{Q}(s)^* \mathbf{Q}(s))^{-1} \mathbf{Q}(s)^* \right] v d_i \quad (\text{C.2.24})$$

Before becoming embroiled in the details of calculating Equation (C.2.24) it is worth stating some properties of the matrix:

$$\mathcal{P}_{\mathbf{Q}} = \mathbf{Q} (\mathbf{Q}^* \mathbf{Q})^{-1} \mathbf{Q}^* \quad (\text{C.2.25})$$

A matrix of this structure is at the heart of the general least squares solution [BIG74] thus the following properties are generally applicable.

1. The matrix  $\mathcal{P}_{\mathbf{Q}}$  is known as a Projector [BIG74, p. 48], because when multiplied by an arbitrary vector ( $\mathbf{v}$ ) the result is the component in the subspace spanned by range ( $\mathbf{Q}$ ). Or in other words the projector calculates the projection of  $\mathbf{v}$  on  $\mathbf{Q}$ .
2. The matrix

$$\mathcal{P}_{\mathbf{Q}^\perp} = \mathbf{I} - \mathbf{Q} (\mathbf{Q}^* \mathbf{Q})^{-1} \mathbf{Q}^* \quad (\text{C.2.26})$$

$$\mathcal{P}_{\mathbf{Q}^\perp} = \mathbf{I} - \mathcal{P}_{\mathbf{Q}} \quad (\text{C.2.27})$$

is the orthogonal projector and calculates the component of an arbitrary vector in the space that is not in range ( $\mathbf{Q}$ ) which is known as the complement space of range ( $\mathbf{Q}$ ) and denoted<sup>2</sup>  $\mathbf{Q}^\perp$ . Thus an arbitrary vector ( $\mathbf{v}$ ) can be decomposed into the component in range ( $\mathbf{Q}$ ) and range ( $\mathbf{Q}^\perp$ ), as shown below:

$$\mathbf{v} = \mathcal{P}_{\mathbf{Q}^\perp} \mathbf{v} + \mathcal{P}_{\mathbf{Q}} \mathbf{v} \quad (\text{C.2.28})$$

The above equation is easily verified as follows:

$$\mathbf{v} = (\mathbf{I} - \mathbf{Q} (\mathbf{Q}^* \mathbf{Q})^{-1} \mathbf{Q}^*) \mathbf{v} + \mathbf{Q} (\mathbf{Q}^* \mathbf{Q})^{-1} \mathbf{Q}^* \mathbf{v} \quad (\text{C.2.29})$$

$$\mathbf{v} = \mathbf{v} \quad (\text{C.2.30})$$

---

<sup>2</sup>The use of  $\mathbf{Q}^\perp$  is a slight abuse of notation since strictly speaking one can only form the complement of a space. However,  $\mathbf{Q}^\perp$  should be interpreted as a matrix with columns that span the complement space of range ( $\mathbf{Q}$ ).

3. If the columns of  $\mathbf{X}$  form a minimal basis for the subspace  $\text{range}(\mathbf{X})$  then the projector ( $\mathcal{P}_{\mathbf{X}}$ ) onto  $\mathbf{X}$  is

$$\mathcal{P}_{\mathbf{X}} = \mathbf{X}(\mathbf{X}^*\mathbf{X})^{-1}\mathbf{X}^* \quad (\text{C.2.31})$$

4. The projectors  $\mathcal{P}_{\mathbf{Q}^\perp}$  and  $\mathcal{P}_{\mathbf{Q}}$  are idempotent matrices<sup>3</sup> that satisfy  $\mathbf{X}\mathbf{X} = \mathbf{X}$ . They are also hermitian and positive semi-definite.
5. All projectors have eigenvalues of 0 and 1 only and since  $\mathcal{P}_{\mathbf{Q}^\perp}$  and  $\mathcal{P}_{\mathbf{Q}}$  are hermitian their singular values are also 0 and 1 only.

The preceding properties have immediate consequences on the evaluation of Equation (C.2.24). Suppose that there exists  $\mathbf{F}(s)$  of maximum and full rank that satisfies:

$$\mathbf{F}(s)\mathbf{Q}(s) = \mathbf{0} \quad (\text{C.2.32})$$

then by properties 2 and 3.

$$J\mathbf{v}_i = \mathbf{v}_i^* \left[ \mathbf{F}(s)^* (\mathbf{F}(s)\mathbf{F}(s)^*)^{-1} \mathbf{F}(s) \right] \mathbf{v}_i \quad (\text{C.2.33})$$

This equality is only of benefit if a simple expression of for  $\mathbf{F}(s)$  can be found. Recalling Equation (4.3.21) and Equation (4.3.22), we note

$$(\mathbf{A} - s\mathbf{I})\mathbf{Q}(s) + \mathbf{B}\mathbf{P}(s) = \mathbf{0} \quad (\text{C.2.34})$$

Let  $\mathbf{F}$  be a matrix of maximum and full rank that satisfies:

$$\mathbf{F}\mathbf{B} = \mathbf{0} \quad (\text{C.2.35})$$

pre-multiplying Equation (C.2.34) by  $\mathbf{F}$  gives:

---

<sup>3</sup>All projectors are idempotent.

$$\mathbf{F}(\mathbf{A} - s\mathbf{I})\mathbf{Q}(s) + \mathbf{F}\mathbf{B}\mathbf{P}(s) = \mathbf{0} \quad (\text{C.2.36})$$

$$\mathbf{F}(\mathbf{A} - s\mathbf{I})\mathbf{Q}(s) = \mathbf{0} \quad (\text{C.2.37})$$

Thus an appropriate expression for  $\mathbf{F}(s)$  that satisfies Equation (C.2.32) is

$$\mathbf{F}(s) = \mathbf{F}(\mathbf{A} - s\mathbf{I}) \quad (\text{C.2.38})$$

Using Equation (C.2.33) and Equation (C.2.38) to calculate  $Jv_i$  offers considerable simplification. It obviates the need to calculate  $\mathbf{Q}(s)$  and since  $\mathbf{F}(s)$  is of lower order than  $\mathbf{Q}(s)$  subsequent manipulations are also simplified.

Evaluation of Equation (C.2.33) or Equation (C.2.24) involves the inversion of a polynomial matrix, an algorithm that uses block coefficient form has been developed by Stefandis *et al* [SPG92]. It is worth noting that the controllability of the pair  $(\mathbf{A}, \mathbf{B})$  implies that the inverse of  $(\mathbf{F}(s)\mathbf{F}(s)^*)$  exists for all  $s$  and thus the inverse of  $(\mathbf{Q}(s)^* \mathbf{Q}(s))$ , must also exist.

#### Proof

The existence of  $(\mathbf{F}(s)\mathbf{F}(s)^*)^{-1}$  can be proved by contradiction as follows:

Non-existence of  $(\mathbf{F}(s)\mathbf{F}(s)^*)^{-1}$  implies  $\det(\mathbf{F}(s)\mathbf{F}(s)^*) = 0$ . Which implies  $\mathbf{F}(s)$  is rank deficient and since  $\mathbf{F}$  is by definition full rank this implies:

$$\mathbf{F}^T \cap \ker((\mathbf{A} - s\mathbf{I})^T) = [(\mathbf{F}^T)^\perp, (\mathbf{A} - s\mathbf{I})]^\perp \neq \emptyset \quad (\text{C.2.39})$$

Recalling Equation (C.2.35) we note that  $(\mathbf{F}^T)^\perp = \mathbf{B}$ , thus

$$[\mathbf{B}, (\mathbf{A} - s\mathbf{I})]^\perp \neq \emptyset \quad (\text{C.2.40})$$

the above only holds if  $[\mathbf{B}, (\mathbf{A} - s\mathbf{I})]$  is rank deficient for some  $s$  which would imply  $(\mathbf{A}, \mathbf{B})$  are an uncontrollable pair and contradict the controllability assumption.  $\diamond\diamond$

Although, direct evaluation of  $Jv_i$  is always possible, it involves calculating an inverse then immediately collapsing it into a scalar. Intuition appeals for a more efficient approach and indeed, the following lemma shows an alternative approach can be taken.

#### Lemma C.2.1

Let  $\mathbf{Z}$  be a non-singular  $n$  by  $n$  matrix over a field  $\mathbb{F}$ , and  $\mathbf{x}^T, \mathbf{y}$  be  $n$  by 1 vectors over the same field

(F), then:

$$\mathbf{xZ}^{-1}\mathbf{y} = \frac{\det(\mathbf{Z} + \mathbf{y}\mathbf{x})}{\det(\mathbf{Z})} - 1 \quad (\text{C.2.41})$$

◇◇

**Proof**

$$\mathbf{xZ}^{-1}\mathbf{y} = (1 + \mathbf{xZ}^{-1}\mathbf{y}) - 1 \quad (\text{C.2.42})$$

$$= (\det(1 + \mathbf{xZ}^{-1}\mathbf{y})) - 1 \quad (\text{C.2.43})$$

$$= (\det(\mathbf{I}_n + \mathbf{Z}^{-1}\mathbf{y}\mathbf{x})) - 1 \quad (\text{C.2.44})$$

$$= (\det(\mathbf{Z}^{-1}\mathbf{Z} + \mathbf{Z}^{-1}\mathbf{y}\mathbf{x})) - 1 \quad (\text{C.2.45})$$

$$= \frac{\det(\mathbf{Z} + \mathbf{y}\mathbf{x})}{\det(\mathbf{Z})} - 1 \quad (\text{C.2.46})$$

◇◇

Lemma C.2.1 may be applied to either Equation (C.2.33) or Equation (C.2.24). The expressions for  $JV_i$  are as follows:

$$JV_i = \frac{\det(\mathbf{F}(s)(\mathbf{I} + \mathbf{v}\mathbf{d}_i\mathbf{v}\mathbf{d}_i^*)\mathbf{F}(s)^*)}{\det(\mathbf{F}(s)\mathbf{F}(s)^*)} - 1 \quad (\text{C.2.47})$$

$$= \frac{\det(\mathbf{Q}(s)^*(\mathbf{I} - \mathbf{v}\mathbf{d}_i\mathbf{v}\mathbf{d}_i^*)\mathbf{Q}(s))}{\det(\mathbf{Q}(s)^*\mathbf{Q}(s))} \quad (\text{C.2.48})$$

The next step in this evaluation approach is to calculate the determinant of a polynomial matrix this is achieved using a *linearization*<sup>4</sup> [GLL82]. This is an *equivalent* polynomial matrix with unity degree from which the determinant can be easily calculated.

Two square polynomial matrices ( $\mathbf{N}(s)$ ,  $\mathbf{L}(s)$ ) are called equivalent if there exist unimodular ( $\mathbf{X}(s)$ ,  $\mathbf{Y}(s)$ ) such that:

$$\mathbf{X}(s)\mathbf{N}(s)\mathbf{Y}(s) = \mathbf{L}(s) \quad (\text{C.2.49})$$

Equivalence is denoted by  $\sim$ . In the following it will be assumed that  $\mathbf{N}(s)$  is a monic matrix polynomial, that is the leading coefficient matrix ( $\mathbf{N}_d$ ) is the identity. A polynomial matrix is called regular

<sup>4</sup>This form of linearization is not to be confused with generating a first order ODE from a non-linear model.

if the leading coefficient matrix ( $\mathbf{N}_d$ ) is non-singular in which case an equivalent monic polynomial matrix can be formed by multiplying with  $\mathbf{N}_d^{-1}$ .

A linear matrix polynomial  $s\mathbf{I} - \mathbf{L}_0$  is a linearization of a monic polynomial matrix  $\mathbf{N}(s)$  if they are equivalent, that is:

$$s\mathbf{I} - \mathbf{L}_0 \sim \begin{bmatrix} \mathbf{N}(s) & \mathbf{0} \\ \mathbf{0} & \mathbf{I} \end{bmatrix} \quad (\text{C.2.50})$$

A polynomial matrix will have a set of linearisations<sup>5</sup>. A convenient linearisation is the first companion form as shown below for  $\mathbf{N}(s)$ :

$$\mathbf{L}_0 = \begin{bmatrix} \mathbf{0} & \mathbf{I} & \mathbf{0} & \cdots & \mathbf{0} \\ \mathbf{0} & \mathbf{0} & \mathbf{I} & \cdots & \mathbf{0} \\ \vdots & \vdots & \vdots & \ddots & \vdots \\ & & & \cdots & \mathbf{I} \\ -\mathbf{N}_0 & -\mathbf{N}_1 & \cdots & & -\mathbf{N}_{d-1} \end{bmatrix} \quad (\text{C.2.51})$$

The unimodular matrices ( $\mathbf{X}(s)$ ,  $\mathbf{Y}(s)$ ), that satisfy:

$$\mathbf{X}(s) \begin{bmatrix} \mathbf{N}(s) & \mathbf{0} \\ \mathbf{0} & \mathbf{I} \end{bmatrix} \mathbf{Y}(s) = s\mathbf{I} - \mathbf{L}_0 \quad (\text{C.2.52})$$

can be constructed [GLL82] such that  $\det(\mathbf{X}(s)) = \det(\mathbf{Y}(s)) = 1$ . Thus:

$$\det(\mathbf{N}(s)) = \det(s\mathbf{I} - \mathbf{L}_0) \quad (\text{C.2.53})$$

Calculating  $\det(\mathbf{N}(s))$  is reduced to finding the characteristic polynomial of  $\mathbf{L}_0$ , a task for which numerically robust algorithms [GL83] exist. Thus the numerator and denominator of Equation (C.2.47) and Equation (C.2.48) can be evaluated using a linearisation.

The application of transfer function based theory leads to an alternative computational approach. Equation (C.1.9) shows that a transfer function solution for  $\mathbf{Q}(s)$  is:

<sup>5</sup>If  $\mathbf{L}_0$  is a linearization of  $\mathbf{N}(s)$ , then any matrix similar to  $\mathbf{L}_0$  is a linearization.

$$\mathbf{Q}(s) = (s\mathbf{I} - \mathbf{A})^{-1}\mathbf{B} \quad (\text{C.2.54})$$

Applying the above definition, the product  $(\mathbf{Q}(s)^* \mathbf{Q}(s))$  is a square transfer function and thus its determinant is the quotient of the system pole and zero polynomials [Mac89, p. 46]:

$$\det(\mathbf{Q}(s)^* \mathbf{Q}(s)) = \frac{z_1(s)}{p_1(s)} \quad (\text{C.2.55})$$

Equally, this holds for the numerator determinant:

$$\det(\mathbf{Q}(s)^* (\mathbf{I} + \mathbf{v}\mathbf{d}_i\mathbf{v}\mathbf{d}_i^*) \mathbf{Q}(s)) = \frac{z_2(s)}{p_2(s)} \quad (\text{C.2.56})$$

Expressing  $\mathbf{Q}(s)$  as:

$$\mathbf{Q}(s) = \frac{\text{adj}(s\mathbf{I} - \mathbf{A})\mathbf{B}}{\det(s\mathbf{I} - \mathbf{A})} \quad (\text{C.2.57})$$

It is clear that pole polynomials  $p_1(s)$  and  $p_2(s)$  will equal one another and thus satisfy:

$$p_1(s) = p_2(s) = \det(s\mathbf{I} - \mathbf{A}) \det(s\mathbf{I} - \mathbf{A}^T) \quad (\text{C.2.58})$$

Thus the desired eigenvector cost function is the quotient of two zero polynomials:

$$\frac{\det[\mathbf{Q}(s)^* (\mathbf{I} + \mathbf{v}\mathbf{d}_i\mathbf{v}\mathbf{d}_i^*) \mathbf{Q}(s)]}{\det[\mathbf{Q}(s)^* \mathbf{Q}(s)]} = \frac{z_2(s)}{z_1(s)} \quad (\text{C.2.59})$$

For a square system  $(\mathbf{A}, \mathbf{B}, \mathbf{C})$  the zero polynomial is defined as:

$$z(s) = \det \left( \begin{bmatrix} s\mathbf{I} - \mathbf{A} & \mathbf{B} \\ \mathbf{C} & \mathbf{0} \end{bmatrix} \right) \quad (\text{C.2.60})$$

The zeros polynomials for both square and non-square systems can be calculated with numerically stable code [END82] from the state space description. Thus it only remains to derive the state space



representations, Application of a little system interconnection theory [Mac89, Dai91] gives:

$$\mathbf{Q}(s)^* \mathbf{Q}(s) = \left[ \begin{array}{cc|c} \mathbf{A} & \mathbf{0} & \mathbf{B} \\ \mathbf{I} & \mathbf{A}^T & \mathbf{0} \\ \hline \mathbf{0} & \mathbf{B}^T & \mathbf{0} \end{array} \right] \quad (\text{C.2.61})$$

and,

$$\mathbf{Q}(s)^* (\mathbf{I} + \mathbf{v}_d \mathbf{v}_d^*) \mathbf{Q}(s) = \left[ \begin{array}{cc|c} \mathbf{A} & \mathbf{0} & \mathbf{B} \\ \mathbf{I} + \mathbf{v}_d \mathbf{v}_d^* & \mathbf{A}^T & \mathbf{0} \\ \hline \mathbf{0} & \mathbf{B}^T & \mathbf{0} \end{array} \right] \quad (\text{C.2.62})$$

This method has the drawback that the transfer function is not defined if the closed and open loop poles are coincident. However, it is straightforward to implement in software packages such as Matlab and Octave where stable code for zero polynomial calculations is readily available.

### C.3 References

- [Bar83] S Barnett. *Polynomials and Linear Control Systems*. A series of Monographs and Textbooks. Marcel Dekker Inc, 1983.
- [BIG74] A Ben-Israel and NE Greville. *Generalised Inverses: Theory and Applications*. A Wiley-Interscience publication. John Wiley and Sons, Inc., 1974.
- [Dai91] RL Dailey. Lecture notes for the workshop on  $\mathcal{H}_\infty$  and  $\mu$  methods. 30th IEEE Conf. on decision and control, IEEE, Brighton, December 1991.
- [DeC89] RA DeCarlo. *Linear Systems: A State Variable Approach with Numerical Implementation*. Prentice-Hall, Inc., 1989.
- [Dua93] GR Duan. Solutions of the equation  $\mathbf{AV} + \mathbf{BW} = \mathbf{VF}$  and their application to eigenstructure assignment in linear systems. *IEEE Trans. on Automatic Control*, 38(2):276–280, February 1993.
- [END82] A Enmami-Naeini and P Van Dooren. Computation of zeros of linear multivariable systems. *Automatica*, 18(4):415–430, 1982.
- [GL83] GH Golub and CF Van Loan. *Matrix Computations*. John Hopkins University Press, 1983.
- [GLL82] I Gohberg, P Lancaster, and L.Rodman. *Matrix Polynomials*. Computer science and applied mathematics series. Academic Press, Inc., 1982.
- [Hec93] A Heck. *Introduction to Maple*. Springer-Verlag, 1993.
- [Kai80] T Kailath. *Linear Systems*. Prentice-Hall, Inc., 1980.
- [Kwa90] H Kwakernaak. Matlab macros for polynomial  $\mathcal{H}_\infty$  control system optimization. Memorandum No. 881, University of Twente, Faculty of Applied Mathematics, University of Twente, PO Box 217,7500 AE Enschede, The Netherlands, September 1990.
- [Mac89] JM Maciejowski. *Multivariable Feedback Design*. Electronic Systems Engineering. Addison Wesley, 1989.
- [RS70] HH Rosenbrock and C Storey. *Mathematics of Dynamical Systems*. Thomas Nelson and Sons Ltd, 1970.
- [SPG92] P Stefanidis, AP Papliński, and MJ Gibbard. *Numerical Operations with Polynomial Matrices: Application to Multi-Variable Dynamic Compensator Design*, volume 171 of *Lecture Notes in Control and Information Sciences*. Springer-Verlag, 1992.

- 
- [WD73] SH Wang and EJ Davison. A minimization algorithm for the design of linear multivariable systems. *IEEE Trans. on Automatic Control*, 18(3):220–225, June 1973.
- [Whi91] BA White. Assignment of eigenstructure by use of polynomial matrices. *Proc. IMECHE Journal of Systems and Control Engineering*, 205(1):207–214, 1991.